

Durham E-Theses

Morphometric Analysis of Variation in Human Proximal Long Bones Within and Between Populations

SCHULZ, ARIADNE,LUCIA

How to cite:

SCHULZ, ARIADNE,LUCIA (2018) *Morphometric Analysis of Variation in Human Proximal Long Bones Within and Between Populations*, Durham theses, Durham University. Available at Durham E-Theses Online: <http://etheses.dur.ac.uk/12681/>

Use policy

The full-text may be used and/or reproduced, and given to third parties in any format or medium, without prior permission or charge, for personal research or study, educational, or not-for-profit purposes provided that:

- a full bibliographic reference is made to the original source
- a [link](#) is made to the metadata record in Durham E-Theses
- the full-text is not changed in any way

The full-text must not be sold in any format or medium without the formal permission of the copyright holders.

Please consult the [full Durham E-Theses policy](#) for further details.

Morphometric Analysis of Variation in Human Proximal Long Bones Within and Between Populations

Ariadne Lucia Schulz

Abstract

Morphological variation and reactivity in human bone underpins many research questions in palaeopathology, osteoarchaeology, and anthropology. Studies on the post-crania primarily pertain to the cross-sectional geometry and epiphyseal or joint morphology and diaphyseal curvature. Very few studies address diaphyseal surface morphology. This study aims to quantify morphology of the epiphyses, diaphyseal surface morphology, and cross-sectional morphology of human proximal long bones in relation to interpopulation and intrapopulation variables including sex, age, childhood stress indicators, and pathology.

To provide some diversity in geography and temporality this research uses skeletons selected from the English medieval cemeteries of St. Guthlac's Priory, Hereford and Fishergate House, York, the Sudanese medieval cemetery 3-J-18 from Mis Island, and the English postmedieval cemetery Coach Lane, North Shields. Cross-sectional geometry was collected via digital sectioning of 3D scans and morphological information was collected using Geometric Morphometrics. The resulting morphological and geometric sets were compared against inter and intrapopulation variables and qualitatively compared to each other to determine which limb and what part of its proximal bone is most reactive to given variables.

Morphological variation with intra and interpopulation variables was found, and its expression varied with size, age, population, bone, and morphological or geometric set. Age and morphology vary together in both epiphyseal and diaphyseal morphology, but do not appear as related in values for cross—sectional geometry. Likewise stress indicators do vary with the morphology of the diaphysis or epiphyses but the strength of their relationship often relies on the population sampled. This suggests a wealth of impact on morphology from environment, ontogenetic trajectory and development, population affinity, health, sex, life history, and age. This research highlights variation in reactivity in different anatomical areas. Crucially, this research demonstrates the morphological plasticity of the diaphyseal surface which for some variables was very reactive and is presently largely unexamined.

Morphometric Analysis of Variation in Human Proximal Long Bones Within and Between Populations

Ariadne Lucia Schulz

Department of Archaeology
Durham University

Thesis Submitted for the Degree of Doctor of Philosophy
2016

<u>1</u>	<u>Aims and Contribution to Science</u>	27
1.1	<u>Research Questions</u>	29
1.1.1	<u>Within population variation</u>	29
1.1.1.1	<u>Sexual dimorphism and morphological variation</u>	29
1.1.1.2	<u>Age and morphological variation</u>	30
1.1.1.3	<u>Childhood stress indicators and morphological variation</u>	30
1.1.1.4	<u>Degenerative Joint Disease and morphological variation</u>	31
1.1.1.5	<u>Trauma and morphological variation</u>	31
1.1.2	<u>Between population variation</u>	31
1.1.2.1	<u>Pathological rates between populations</u>	32
1.1.2.2	<u>Comparison of interpopulation variation with variation between intrapopulation demographic groups</u>	32
1.1.2.3	<u>Comparison of intra and inter population variation</u>	33
1.1.3	<u>Morphological variation in different parts of the bone</u>	33
1.1.3.1	<u>Morphological variation between epiphyses and epiphyseal morphological variation as compared to surface morphology and cross-sectional morphology</u>	33
1.1.3.2	<u>Surface diaphyseal morphological variation as compared to epiphyseal and cross-sectional morphological variation</u>	34
1.2	<u>Thesis Structure</u>	35
<u>2</u>	<u>Background</u>	36
2.1	<u>Anatomy</u>	36
2.1.1	<u>Humeral Anatomy</u>	37
2.1.2	<u>Femoral Anatomy</u>	43
2.1.2.1	<u>Hip</u>	43
2.1.2.2	<u>Knee</u>	44
2.1.2.3	<u>Muscles of the pelvis and hip</u>	45
2.1.2.4	<u>Anterior</u>	46
2.1.2.5	<u>Medial muscles</u>	47

2.1.2.6	<u>Posterior muscles</u>	48
2.1.2.7	<u>Distal</u>	48
2.2	<u>Intrapopulation variation</u>	50
2.2.1	<u>Sex and Sexual Dimorphism</u>	50
2.2.2	<u>Age</u>	52
2.2.3	<u>The Whole Bone: Development, Mechanics, and Metabolism</u>	55
2.2.3.1	<u>Morphology</u>	58
2.2.3.2	<u>Structure</u>	59
2.2.3.3	<u>Mechanics</u>	63
2.2.3.4	<u>Bone Mineral Content, Modelling and Remodelling</u>	65
2.2.4	<u>Pathology</u>	67
2.2.4.1	<u>Developmental Stress</u>	67
2.2.4.2	<u>Degenerative Joint Disease</u>	80
2.2.4.3	<u>Osteopenic and Osteogenic Conditions</u>	87
2.3	<u>Interpopulation Variation</u>	94
2.3.1	<u>Heritable, Ancestral, or Genetic Variation</u>	95
2.3.2	<u>Phenotypic, Environmentally influenced, or Epigenetic Variation</u>	97
2.3.3	<u>Cultural or Activity Related Variation</u>	101
2.4	<u>Allometry</u>	102
3	<u>Materials and Methods</u>	107
3.1	<u>Materials</u>	107
3.1.1	<u>Coach Lane, North Shields</u>	108
3.1.2	<u>Fishergate House, York</u>	110
3.1.3	<u>St. Guthlac's Priory, Hereford</u>	112
3.1.4	<u>Sudan</u>	115
3.2	<u>Osteological Methods</u>	118
3.3	<u>Paleopathological Methods</u>	120
3.4	<u>Data Acquisition</u>	123

3.5	<u>Geometric Morphometrics (GMM)</u>	125
3.5.1	<u>Landmarks</u>	127
3.5.2	<u>Semilandmarks</u>	134
3.5.2.1	<u>Diaphyseal Semilandmarking</u>	135
3.5.2.2	<u>Cross-sectional Semilandmarking</u>	136
3.5.2.3	<u>Note on the Use of Cross-Sectional Geometry</u>	136
3.5.3	<u>Assessment of Asymmetry</u>	137
3.5.4	<u>Generalised Procrustes Analysis (GPA)</u>	140
3.5.5	<u>Error</u>	140
3.6	<u>Statistical Analysis</u>	146
3.6.1	<u>Generalised Procrustes Analysis (GPA) Principal Component Analysis (PCA)</u>	146
3.6.2	<u>Generalised Linear Model (GLM)</u>	146
4	<u>Epiphyseal Morphological Variation as Quantified by Homologous landmarks</u>	148
4.1	<u>Introduction</u>	148
4.1.1	<u>Intrapopulation Variation: Morphological Variation in the Epiphyses with Sex</u>	150
4.1.2	<u>Intrapopulation Variation: Morphological Variation in the Epiphyses with Age</u>	153
4.1.3	<u>Intrapopulation Variation: Morphological Variation in the Epiphyses with Childhood indicators of Stress</u>	153
4.2	<u>Results</u>	155
4.2.1	<u>Intrapopulation Variation</u>	177
4.2.1.1	<u>Sex</u>	177
4.2.1.2	<u>Age</u>	182
4.2.1.3	<u>Trauma and Pathology</u>	188
4.2.2	<u>Interpopulation Variation</u>	230
4.2.3	<u>Variation as seen in different parts of the bone</u>	235
4.3	<u>Discussion</u>	235
4.3.1	<u>Sex</u>	235

4.3.2	<u>Age</u>	237
4.3.3	<u>Childhood indicators of stress</u>	238
4.3.4	<u>Joint disease and Trauma and Schmorl's Nodes</u>	239
4.3.5	<u>Interpopulation Variation</u>	241
4.4	<u>Conclusion</u>	242
5	<u>Diaphyseal Morphological Variation as Quantified by Surface Semilandmarks</u>	243
5.1	<u>Introduction</u>	243
5.1.1	<u>Intrapopulation Variation: Morphological Variation in the Diaphysis with Sex</u>	246
5.1.2	<u>Intrapopulation Variation: Morphological Variation in the Diaphysis with Age</u>	248
5.1.3	<u>Intrapopulation Variation: Morphological Variation in the Diaphysis with Pathology</u> 249	
5.1.4	<u>Interpopulation Variation: Morphological Variation in the Diaphysis between Populations</u>	251
5.2	<u>Results and Preliminary Discussion</u>	252
5.2.1	<u>Intrapopulation</u>	265
5.2.1.1	<u>Sex</u>	265
5.2.1.2	<u>Age</u>	273
5.2.1.3	<u>Trauma and Pathology</u>	277
5.2.2	<u>Interpopulation</u>	305
5.3	<u>Discussion</u>	311
5.3.1	<u>Intrapopulation</u>	311
5.3.1.1	<u>Sex</u>	311
5.3.1.2	<u>Age</u>	312
5.3.1.3	<u>Pathology</u>	313
5.3.2	<u>Interpopulation</u>	315
5.4	<u>Conclusion</u>	316
6	<u>Cross-sectional semilandmarks</u>	318
6.1	<u>Introduction</u>	318

	<u>6.1.1</u>	<u>Intrapopulation Variation: Cross-Sectional Morphological Variation at Midshaft with</u>	
<u>Sex</u>			320
	<u>6.1.2</u>	<u>Intrapopulation Variation: Cross-Sectional Morphological Variation at Midshaft with</u>	
<u>Age</u>			321
	<u>6.1.3</u>	<u>Intrapopulation Variation: Cross-Sectional Morphological Variation at Midshaft with</u>	
<u>Pathology</u>			322
	<u>6.1.4</u>	<u>Interpopulation Variation: Cross-Sectional Morphological Variation at Midshaft</u>	
		<u>Between Populations</u>	323
<u>6.2</u>	<u>Results</u>		324
	<u>6.2.1</u>	<u>Intrapopulation</u>	336
	<u>6.2.1.1</u>	<u>Sex</u>	336
	<u>6.2.1.2</u>	<u>Age</u>	342
	<u>6.2.1.3</u>	<u>Trauma and Pathology</u>	346
	<u>6.2.2</u>	<u>Interpopulation</u>	371
	<u>6.2.3</u>	<u>Biomechanics</u>	377
<u>6.3</u>	<u>Discussion and Conclusion</u>		386
7	<u>Discussion and Conclusion</u>		390
<u>7.1</u>	<u>Introduction</u>		390
<u>7.2</u>	<u>Summary of results</u>		391
	<u>7.2.1</u>	<u>Within population variation</u>	392
	<u>7.2.1.1</u>	<u>Epiphysis</u>	392
	<u>7.2.1.2</u>	<u>Diaphysis</u>	393
	<u>7.2.1.3</u>	<u>Cross-Section</u>	395
	<u>7.2.2</u>	<u>Between population variation</u>	397
	<u>7.2.2.1</u>	<u>Pathological rates between populations</u>	397
	<u>7.2.2.2</u>	<u>Epiphysis</u>	402
	<u>7.2.2.3</u>	<u>Diaphysis</u>	402
	<u>7.2.2.4</u>	<u>Cross-Section</u>	403

7.2.3	<u>Morphological variation in different parts of the bone</u>	404
7.3	<u>Interpretation of Results</u>	405
7.3.1	<u>Within population</u>	405
7.3.1.1	<u>Sex and adult long bone morphology</u>	405
7.3.1.2	<u>Age</u>	407
7.3.1.3	<u>Pathologies</u>	408
7.3.2	<u>Population differences</u>	412
7.4	<u>Research Limitations</u>	415
7.4.1	<u>Sample size</u>	416
7.4.2	<u>Osteological paradox</u>	416
7.4.3	<u>What GMM does not capture</u>	419
7.4.4	<u>Number of cross-sections and ability to use morphometrics on all of them</u>	420
7.5	<u>Future Research</u>	421
7.5.1	<u>Surface morphology of articular surfaces</u>	421
7.5.2	<u>Internal architecture of the bone</u>	422
7.5.3	<u>Distal long bones</u>	423
7.5.4	<u>Robusticity and Pathology</u>	424
7.5.5	<u>Childhood Development and Ontogeny</u>	425
7.6	<u>Concluding Remarks</u>	426
8	<u>Bibliography</u>	429

Figure 2.1 Timing of development for humerus (Rho et al., 2002; Ruff & Hayes, 1982; M. Schaefer et al., 2009b).	49
Figure 2.2 Timing of development for femur (Ruff & Hayes, 1982; Schaefer et al., 2009).	50

Figure 3.1 Pictures of left humerus of CL 175 mounted on scanner for the distal partial scan on the left and the 360 degree anterior posterior scan on the right. These images captured by the NextEngine were used by the software to overlay a skin onto the ply file.	125
Figure 3.2 Humeral Landmarks and wireframes.....	129
Figure 3.3 Femoral Landmarks and wireframes.	131
Figure 4.1 PC1 and PC2 for proximal humerus homologous landmarks.	157
Figure 4.2 Shape variation of the proximal humerus.	158
Figure 4.3 Allometric regression of log CS by Shape Regression Scores for proximal humerus color coded by sex. (black = female, red = male, green = possible female, blue = possible male, cyan = unknown)	159
Figure 4.4 Allometric regression of log CS by Shape Regression Scores for proximal humerus color coded by sex. (black = 3-J-18, red = Coach Lane, green = Fishergate, blue = Hereford)	160
Figure 4.5 PC1 and PC2 for distal humerus homologous landmarks.....	163
Figure 4.6 Shape variation of the distal humerus.....	164
Figure 4.7 Allometric regression of log CS by Shape Regression Scores for distal humerus color coded by sex. (black = female, red = male, green = possible female, blue = possible male, cyan = unknown)	165
Figure 4.8 Allometric regression of log CS by Shape Regression Scores for distal humerus color coded by site. (black = 3-J-18, red = Coah Lane, green = Fishergate, blue = Hereford)	166
Figure 4.9 PC1 and PC2 for proximal femur homologous landmarks.....	168
Figure 4.10 Shape variation of the proximal femur.....	169
Figure 4.11 Allometric regression of log CS by Shape Regression Scores for proximal femur color coded by sex. (black = female, red = male, green = possible female, blue = possible male, cyan = unknown)	170

Figure 4.12 Allometric regression of log CS by Shape Regression Scores for proximal femur color coded by site. (black = 3-J-18, red = Coach Lane, green = Fishergate, blue = Hereford)	171
Figure 4.13 PC1 and PC2 for distal femur homologous landmarks.	173
Figure 4.14 Shape variation of the distal femur.	174
Figure 4.15 Allometric regression of log CS by Shape Regression Scores for distal femur color coded by sex. (black = female, red = male, green = possible female, blue = possible male, cyan = unknown)	175
Figure 4.16 Allometric regression of log CS by Shape Regression Scores for distal femur color coded by site. (black = 3-J-18, red = Coach Lane, green = Fishergate, blue = Hereford)	176
Figure 4.17 PC1 and PC2 for proximal humeral homologous landmarks by sex. (black = female, red = male, green = possible female, blue = possible male, cyan = unknown)	178
Figure 4.18 PC1 and PC2 for distal humeral homologous landmarks by sex. (black = female, red = male, green = possible female, blue = possible male, cyan = unknown)	179
Figure 4.19 PC1 and PC2 for proximal femoral homologous landmarks by sex. (black = female, red = male, green = possible female, blue = possible male, cyan = unknown)	180
Figure 4.20 PC1 and PC2 for distal femoral homologous landmarks by sex. (black = female, red = male, green = possible female, blue = possible male, cyan = unknown)	181
Figure 4.21 PC1 and PC2 for proximal humeral homologous landmarks by age. (black = 35-45 years of age, red = 45+, green = unknown, blue = 17-25, cyan = 25-35)	183
Figure 4.22 PC1 and PC2 for distal humeral homologous landmarks by age. (black = 35-45 years of age, red = 45+, green = unknown, blue = 17-25, cyan = 25-35)	184
Figure 4.23 PC1 and PC2 for proximal femoral homologous landmarks by age. (black = 35-45 years of age, red = 45+, green = unknown, blue = 17-25, cyan = 25-35)	186

Figure 4.24 PC1 and PC2 for distal femoral homologous landmarks by age. (black = 35-45 years of age, red = 45+, green = unknown, blue = 17-25, cyan = 25-35)	187
Figure 4.25 PC1 and PC2 for proximal humeral homologous landmarks by DJD and OA severity in the proximal humerus. (black = djd , red = healthy, green = mild, blue = moderate, cyan = severe, purple = unknown)	190
Figure 4.26 PC1 and PC2 for proximal humeral homologous landmarks by DJD and OA severity in the distal humerus. (black = djd , red = healthy, green = mild, blue = moderate, cyan = severe, purple = unknown)	191
Figure 4.27 PC1 and PC2 for distal humeral homologous landmarks by DJD and OA severity in the proximal humerus. (black = djd , red = healthy, green = mild, blue = moderate, cyan = severe, purple = unknown)	193
Figure 4.28 PC1 and PC2 for distal humeral homologous landmarks by DJD and OA severity in the distal humerus. (black = djd , red = healthy, green = mild, blue = moderate, cyan = severe, purple = unknown)	194
Figure 4.29 PC1 and PC2 for proximal femoral homologous landmarks by DJD and OA severity in the proximal femur. (black = djd , red = healthy, green = mild, blue = moderate, cyan = severe, purple = unknown)	196
Figure 4.30 PC1 and PC2 for proximal femoral homologous landmarks by DJD and OA severity in the distal femur. (black = djd , red = healthy, green = mild, blue = moderate, cyan = severe, purple = unknown)	197
Figure 4.31 PC1 and PC2 for distal femoral homologous landmarks by DJD and OA severity in the proximal femur. (black = djd , red = healthy, green = mild, blue = moderate, cyan = severe, purple = unknown)	199

Figure 4.32 PC1 and PC2 for distal femoral homologous landmarks by DJD and OA severity in the distal femur. (black = djd , red = healthy, green = mild, blue = moderate, cyan = severe, purple = unknown)	200
Figure 4.33 PC1 and PC2 for proximal humeral homologous landmarks by presence or absence of trauma. (black = no trauma, red = unknown, green = trauma present)	203
Figure 4.34 PC1 and PC2 for distal humeral homologous landmarks by presence or absence of trauma. (black = no trauma, red = unknown, green = trauma present).....	205
Figure 4.35 PC1 and PC2 for proximal femoral homologous landmarks by presence or absence of trauma. (black = no trauma, red = trauma present).....	207
Figure 4.36 PC1 and PC2 for distal femoral homologous landmarks by presence or absence of trauma. (black = no trauma, red = trauma present).....	209
Figure 4.37 PC1 and PC2 for proximal humoral homologous landmarks by presence or absence of LEH. (black = no LEH observed, red = not enough teeth present, green = unknown, blue = LEH observed)	211
Figure 4.38 PC1 and PC2 for proximal humoral homologous landmarks by presence or absence of CO. (black = no CO observed, red = orbitals not present, green = unknown, blue = CO observed)	212
Figure 4.39 PC1 and PC2 for distal humoral homologous landmarks by presence or absence of LEH. (black = no LEH observed, red = not enough teeth present, green = unknown, blue = LEH observed)	214
Figure 4.40 PC1 and PC2 for distal humoral homologous landmarks by presence or absence of CO. (black = no CO observed, red = orbitals not present, green = unknown, blue = CO observed).....	215
Figure 4.41 PC1 and PC2 for proximal femoral homologous landmarks by presence or absence of LEH. (black = no LEH observed, red = not enough teeth present, green = LEH observed)	217

Figure 4.42 PC1 and PC2 for proximal femoral homologous landmarks by presence or absence of CO. (black = no CO observed, red = orbitals not present, green = CO observed).....	218
Figure 4.43 PC1 and PC2 for distal femoral homologous landmarks by presence or absence of LEH. (black = no LEH observed, red = not enough teeth present, green = LEH observed)	220
Figure 4.44 PC1 and PC2 for proximal femoral homologous landmarks by presence or absence of CO. (black = no CO observed, red = orbitals not present, green = CO observed).....	221
Figure 4.45 PC1 and PC2 for proximal humeral homologous landmarks by presence or absence of Schmorl's nodes. (black = no Schmorl's nodes observed, red = not enough vertebrae present, green = unknown, blue = Schmorl's nodes observed)	223
Figure 4.46 PC1 and PC2 for distal humeral homologous landmarks by presence or absence of Schmorl's nodes. (black = no Schmorl's nodes observed, red = not enough vertebrae present, green = unknown, blue = Schmorl's nodes observed)	225
Figure 4.47 PC1 and PC2 for proximal femoral homologous landmarks by presence or absence of Schmorl's nodes. (black = no Schmorl's nodes observed, red = not enough vertebrae present, green = Schmorl's nodes observed)	227
Figure 4.48 PC1 and PC2 for distal femoral homologous landmarks by presence or absence of Schmorl's nodes. (black = no Schmorl's nodes observed, red = not enough vertebrae present, green = Schmorl's nodes observed)	229
Figure 4.49 PC1 and PC2 of proximal humeral homologous landmarks by site. (black = 3-J-18, red = Coach Lane, green = Fishergate, blue= Hereford)	231
Figure 4.50 PC1 and PC2 of distal humeral homologous landmarks by site. (black = 3-J-18, red = Coach Lane, green = Fishergate, blue= Hereford)	232
Figure 4.51 PC1 and PC2 of proximal femoral homologous landmarks by site. (black = 3-J-18, red = Coach Lane, green = Fishergate, blue= Hereford)	233

Figure 4.52 PC1 and PC2 of distal femoral homologous landmarks by site. (black = 3-J-18, red = Coach Lane, green = Fishergate, blue= Hereford)	234
Figure 5.1 Shape extreme for humeri in PC1.....	256
Figure 5.2 PC1 and PC2 visualization of variation for humeral diaphyseal morphology.....	257
Figure 5.3 Allometry regression of log CS by Shape Regression Scores for humeral diaphyseal morphology.....	258
Figure 5.4 Shape extremes for femora in PC1.	262
Figure 5.5 PC1 and PC2 visualization of variation for femoral diaphyseal morphology.....	263
Figure 5.6 Allometry regression of log CS by Shape Regression Scores for femoral diaphyseal morphology.....	264
Figure 5.7 PC1 and PC2 of humeri by sex.	267
Figure 5.8 PC1 and PC2 of femora by sex.	268
Figure 5.9 Humeral allometry by sex. (black = female, red = male, blue = possible female, green = possible male, cyan = unknown).....	269
Figure 5.10 Femoral allometry by sex. (black = female, red = male, blue = possible female, green = possible male, cyan = unknown).....	270
Figure 5.11 Shape of femora at maximum and minimum size.	271
Figure 5.12 PC1 and PC2 of humeri by age.....	274
Figure 5.13 PC1 and PC2 of femur diaphyseal surface morphology organized by age.	276
Figure 5.14 PC1 and PC2 humeri by trauma.	282
Figure 5.15 PC1 and PC2 of femur diaphyseal surface morphology organized by presence or absence of trauma.	284
Figure 5.16 PC1 and PC2 humeri by cribra orbitalia.	286

Figure 5.17 PC1 and PC2 of femur diaphyseal surface morphology organized by presence or absence of cribra orbitalia.	288
Figure 5.18 PC1 and PC2 humeri by LEH.....	290
Figure 5.19 PC1 and PC2 of femur diaphyseal surface morphology organized by presence or absence of LEH.....	292
Figure 5.20 PC1 and PC2 humeri by Schmorl's nodes.	294
Figure 5.21 PC1 and PC2 of femur diaphyseal surface morphology by presence or absence of Schmorl's nodes.	296
Figure 5.22 PC1 and PC2 humeri by DJD and OA severity at proximal epiphysis.	298
Figure 5.23 PC1 and PC2 humeri by DJD and OA severity at distal epiphysis.	300
Figure 5.24 PC1 and PC2 of femur diaphyseal surface morphology by DJD and OA severity at proximal epiphysis..	302
Figure 5.25 PC1 and PC2 of femur diaphyseal surface morphology by DJD and OA severity at distal epiphysis.....	304
Figure 5.26 Humeral diaphyseal morphological variation in PC1 and PC2 for all sites.	307
Figure 5.27 Femoral diaphyseal surface morphological variation in PC1 and PC2 for all sites. ...	308
Figure 5.28 Humeral allometry by site. (black = 3-J-18, red = Coach Lane, blue = Fishergate, Blue = Hereford).....	309
Figure 5.29 Femoral allometry by site. (black = 3-J-18, red = Coach Lane, blue = Fishergate, green = Hereford).....	310
Figure 6.1 Visualisation of PC1 and PC2 for humeral cortical shape with warp grids for PC1 extremes.	326
Figure 6.2 Visualisation of PC2 and PC3 for humeral cortical shape with warp grids for PC2 extremes.	327

Figure 6.3 Visualisation of PC2 and PC3 for humeral cortical shape with warp grids for PC3 extremes.	328
Figure 6.4 Allometry regression of log CS by Shape Regression Scores for humeral cross-sectional morphology. Warpgrids represent shape at size extremes.....	329
Figure 6.5 Visualisation of PC1 and PC2 for femoral cortical shape with warp grids for PC1 extremes.	332
Figure 6.6 Visualisation of PC2 and PC3 for femoral cortical shape with warp grids for PC2 extremes.	333
Figure 6.7 Visualisation of PC2 and PC3 for femoral cortical shape with warp grids for PC3 extremes.	334
Figure 6.8 Allometry regression of log CS by Shape Regression Scores for femoral cross-sectional morphology.....	335
Figure 6.9 PC1 and PC2 of humeral cross-sectional morphology organized by sex. (black = female, red = male, green = possible female, blue = possible male, cyan = unknown, purple = unobservable)	337
Figure 6.10 Allometry of humeral cross-sectional morphology at midshaft by sex. (black = female, red = male, green = possible female, blue = possible male, cyan = unknown, purple = unobservable)	338
Figure 6.11 PC1 and PC2 of femoral cross-sectional morphology organized by sex. (black = female, red = male, green = possible female, blue = possible male, cyan = unknown)	340
Figure 6.12 Allometry of femoral cross-sectional morphology at midshaft by sex. (black = female, red = male, green = possible female, blue = possible male, cyan = unknown)	341
Figure 6.13 PC1 and PC2 of humeral morphology organized by age. (black= 35-45 years, red = 45+ years, green = unknown, blue = 17-25 years, cyan = 25-35 years).....	343

Figure 6.14 PC1 and PC2 of femur cortices organized by age. (black= 35-45 years, red = 45+ years, green = unknown, blue = 17-25 years, cyan = 25-35 years).....	345
Figure 6.15 PC1 and PC2 of humerus cortices organized by LEH. (black = none, red = teeth not present, green = unknown, blue = LEH present)	348
Figure 6.16 PC1 and PC2 of femur cortices organized by LEH. (black = none, red = teeth not present, green = LEH).....	350
Figure 6.17 PC1 and PC2 of humerus cortices organized by cribra orbitalia. (black = none, red = orbits not present, green = unobservable, blue = cribra orbitalia present)	352
Figure 6.18 PC1 and PC2 of femur cortices organized by cribra orbitalia. (black = none, red = orbits not present, green = cribra orbitalia)	354
Figure 6.19 PC1 and PC2 of humeral cross-sectional morphology organized by DJD and OA severity at proximal joint. (black= DJD, red = healthy, green = mild, blue = moderate, cyan = severe, magenta = unknown)	356
Figure 6.20 PC1 and PC2 of humeral cross-sectional morphology organized by DJD and OA severity at distal joint. (black= DJD, red = healthy, green = mild, blue = moderate, cyan = severe, magenta = unknown)	358
Figure 6.21 PC1 and PC2 of femoral cross-sectional morphology organized by DJD and OA severity at proximal joint. (black= DJD, red = healthy, green = mild, blue = moderate, cyan = severe, magenta = unknown)	360
Figure 6.22 PC1 and PC2 of femoral cross-sectional morphology organized by DJD and OA severity at distal joint. (black= DJD, red = healthy, green = mild, blue = moderate, cyan = severe, magenta = unknown)	362
Figure 6.23 PC1 and PC2 of humeral cross-sectional morphology organized by presence or absence of trauma. (black= trauma absent red = trauma unobservable, green = trauma present)	364

Figure 6.24 PC1 and PC2 of femoral cross-sectional morphology organized by presence or absence of trauma. (black= trauma absent red = trauma present).....	366
Figure 6.25 PC1 and PC2 of humeral cross-sectional morphology organized by presence or absence of Schmorl's nodes. (black= no Schmorl's nodes, red = vertebrae not present, green = unobservable, blue = Schmorl's nodes present).....	368
Figure 6.26 PC1 and PC2 of femoral cross-sectional morphology organized by presence or absence of Schmorl's nodes. (black= no Schmorl's nodes, red = vertebrae not present, green = Schmorl's nodes present)	370
Figure 6.27 PC1 through PC3 of humeral cross-sectional morphology by site. (black = Coach Lane, red = Fishergate, green= Hereford, blue = 3-J-18)	372
Figure 6.28 Allometry of humeral cross-section at midshaft by site. (black = Coach Lane, red = Fishergate, green= Hereford, blue = 3-J-18)	373
Figure 6.29 PC1 and PC2 of femoral cross-sectional morphology by site. (black = 3-J-18, red = Coach Lane, green= Fishergate, blue = Hereford)	375
Figure 6.30 Allometry of femoral cross-section at midshaft by site. (black = 3-J-18, red = Coach Lane, green= Fishergate, blue = Hereford)	376

STATEMENT OF COPYRIGHT

The copyright of this thesis rests with the author. No quotation from it should be published without the author's prior written consent and information derived from it should be acknowledged.

ACKNOWLEDGEMENTS

I would like to herein acknowledge the many people and organizations that made the completion of this thesis possible. It being the nature of gratitude however I thoroughly expect to forget someone crucial. Firstly, no paleopathological work could be complete without access to skeletal collections and so I am very thankful to Durham University's Archaeology Department and Prof. Charlotte Roberts for allowing me access and a place to plug in the scanner. I am also very thankful to Dr. Daniel Antoine and the British Museum for allowing me access to their collections. I am also very thankful to Dr. Antoine for introducing me to chocolate sorbet. That was a welcome respite in summer. Durham University's Anthropology department also is due thanks for allowing me access to the 3D scanner without which this thesis would have been impossible. I am also grateful to both the Archaeology and Anthropology departments for granting me funds to take a course in Geometric Morphometrics again, without which I would have been lost. And of course, I am grateful to my supervisors Dr. Becky Gowland and Dr. Sarah Elton for pointing me in the right direction when I lost my way and wading through my remarkably convoluted first drafts.

Dr Tina Jacobs, Dr. Anwen Caffel, Dr. Beth Upex, Dr. Una Strand-Viðarsdóttir, and Dr. Kris (Fire) Kovarovic were also crucial in the completion of this work. Una patiently provided advice and reading after my repeated methodological failures. Beth helped me create a 3D print of a femur and consistently encouraged me in my digital madness. Anwen very gently corrected my various errors in diagnoses and misunderstandings of osteology and went out of her way regardless of her ever looming deadlines to lend a kind word and a helping hand. And she also gave me a lesson in acrobalance. Finally, Tina and Fire always had open doors and were unquenchable sources of enthusiasm. I came to them often with all manner of problems and always left feeling considerably better.

I would also be remiss if I did not thank Palace Green Library for providing me with gainful employment during my studies. My other options were busking and international man of mystery one of which I'm singularly unqualified for so I am very fortunate to have found employment in a museum and often tasked with giving historical tours (sometimes in Japanese!) of the castle and UNESCO site.

On a more personal note, I would also like to acknowledge my friends. I would like to thank Kimberly Plomp and Charlotte King for proving that there is – indeed – life after the thesis, Jo Zalea Matias and Davina Craps for sharing my love of song, dance, and minions, Michelle De Gruchy, Steph Piper and Lauren Walther for the many commiserations that must occur during postgraduate work and

for helping me maintain calm in the face of certain disaster. Special thanks must go to Ophélie Lebrasseur for being the measurement by which all happiness may be quantified, for coaching a good deal of my work, and for wholeheartedly agreeing with me on my assertion that zombies are cute. Lastly, abundant thanks must be given to my partner Denis the Menace Archibald Trouble Bouchinet whose contributions defy quantification. He has emotionally and financially supported me when I could not do so myself. He has enabled my coffee habit even though he himself does not partake. He helped me with all my numerous computer problems and even bought me extra hard drives when I ran out of space. He helped me figure out R, and he doesn't even complain when I try to bake cookies and fail miserably.

In Memoriam

During the course of my PhD I lost both my grandmothers and my mother. These are the women who informed my life and particularly my mother was very supportive of my studies. It seems only fitting that each of these women be remembered.

My mother's mother Elsie Langford was born Elsie Nelsen and grew up on a small island in the North of Wisconsin called Washington Island. The family lore is that her grandfather, Lars Peter Ottosen was born Louis of the Danish royal court as he was the illegitimate child of some king. He had been asked to command in the military but as a pacifist resisted and escaped to America only to find that country embroiled in a civil war and his English far too fluent for the conscription officers to believe he was Danish. He fled once again and found himself on the island. Elsie had numerous older brothers and sisters and recalled being annoyed with her older sister Margaret because Margaret's adventures made their parents stricter with Elsie. In the winter the lake freezes over and the snow is high, so the island children would ski and snow shoe to school. Elsie became accomplished as a cross country skier, but as an adult when someone suggested alpine skiing to her response was, "I won't throw myself off a mountain on greased sticks." Her response to golf was similar: "if I'm going to take a walk, why would I haul all that stuff with me?" Elsie lost one of her elder brothers, Norman one year on her birthday. He had been driving back with friends across the ice of the frozen lake when it gave way. All of them drowned. There is some evidence that one of Norman's friends was able to climb onto the ice before his body succumbed to hypothermia and he fell back into the lake. This event clouded her birthday for the rest of her life. As a young woman she moved to Chicago with her elder sister Margaret for work. The sisters were skilled at accountancy and so quite useful in the factories and production centres of Chicago. During WWII, Elsie worked at a factory which manufactured planes. Her co-workers wrote her

notes and poems which are collected in a journal now in my uncle's – her son's – possession. She fell in love with and married my grandfather and the pair had two children: my mother whose given name was Rebecca and my uncle Michael. Unfortunately, my grandfather was epileptic and prone to seizures. His illness – which had ended his career as a codebreaker – progressed quickly and his own sister made him move out of the house before he could accidentally hurt his own children. He died a few years later. Elsie lived then as a single mother taking her children to the Lutheran church and letting them be watched alternatively by her own mother and the Japanese neighbour that the children affectionately called Obaachan ("granny," in Japanese). At one point both Margaret and Elsie realized they had been given supervisory duties and seniority in their office without receiving a raise. Their supervisor's justification was that as women they shouldn't have one. Elsie's response to this was, "do my children's shoes cost less than yours?" She took her children to Wrigley's field for baseball and was a diehard Cubs fan. She had a little stuffed teddy bear she had named Albert and she told the children that he loved the Cubs too. She and Albert – and of course my mother and uncle – would watch the game in anticipation of the Cubs winning and them enjoying "victory berries" together. Inevitably the Cubs would lose and so they would have to have "consolation berries." In her old age she decided to move back to the island and lived there in a retirement home across the road from her childhood home. She joked that it had taken her fifty years to move across the street. Through many marriages the several families who settled on Washington Island are now all related. Elsie's cousin and close friend Carolyn was the matriarch of the Koyen clan and her son is one of the Great Lake's last commercial fishermen. Elsie then had many visitors and was known by the children of the island for her display of her collection of hundreds of angel figurines around Christmas, as well as her Snoopy Dog outside her apartment. She lived long enough to meet my brother's children, but died of complications from a stroke shortly after her 90th birthday. Her cremains are interred at Schoolhouse Beach cemetery alongside her sister, brother, parents, and now her daughter.

Anna Schulz, my father's mother, I know less about. Anna was Hungarian of Croatian descent. She lived her entire childhood in western Hungary and was from a poor farming family. She spoke Hungarian, Croatian, German, and learned Spanish and English later in life. (It is likely that she also could understand Russian, but Hungarians at the time would secretly learn Russian as a means of undermining Russian influence as the Russians did not bother to learn Hungarian and were thereby easily flouted. Most Hungarians, my grandparents included would never openly say even to family whether or not they spoke or understood Russian.) She earned a teaching degree and was possibly the first in her family to earn such a degree or certification. In the 1950s when Hungary was under control of the USSR she met

my grandfather. She kept the first picture she ever had of him throughout her life and well after he passed away she would show it to me and others and say, "look how handsome your grandfather." Their love and marriage was tested as my grandfather was in open rebellion and was the son of his town's (Sopron) mayor. The KGB arrested him sometime between 1954 (the year my father was born) and 1956 and tortured him to get to his father. His father finally died, again according to family lore, "of a broken heart," and Anna visited him in prison in her mourning clothes. One of the KGB techniques was psychological torture and so his first thought when she appeared was that his son, my father, had been killed. She had to break the news that the mourning clothes were for his father. In October of 1956 when the Hungarian revolution had its few successful weeks he escaped from prison. At that point droves of Hungarians were making for the border and the USSR had planted a minefield on the border between Hungary and Austria as well as erecting towers from which they could shoot anyone making for the border. My grandfather put in the basket of his bicycle his accordion and Anna put in the basket of her bicycle their son, my father, and they cycled across the minefield into Austria. The Austrians were good to the Hungarian refugees as they are now to the Syrians forced to make the same wild dash and they helped my family settle in Vienna. There my grandmother worked cleaning houses. The KGB was, however, relentless. They came into Vienna looking for my grandfather and when they saw him they tried to kidnap him. He shouted for help in German and the Viennese police instantly knew what was happening but told the KGB agents they had no right to harass an Austrian. They separated my grandfather from the KGB and told him they could buy him two hours to collect his family and flee. As it turned out, just as the Nazis had in the 1940s, the KGB also had a warrant for my grandfather's execution. They were on the first plane out of Europe which took them to Buenos Aires. They were desperately poor, not speaking the language at first, but Anna worked again as a cleaner and later as a teacher, and my Grandfather was able to work as a construction worker and a musician. Anna loved her life in Argentina and did not want to leave, but she loved her husband more and so agreed to move with him to Chicago. They relied on my father's English and rebuilt their life once again. Anna valued the love story she had with my grandfather more than anything and she would often say to me, "Ari-ka, you smart girl. Why you not get married? Find nice Hungarian man like grandpa." That initially angered me, but I have come to understand that for her my grandfather was the only source of stability and home in her tumultuous life. What my grandmother was really saying was that she wanted for me, happiness. In her old age she suffered a series of strokes and gradually lost each of her languages. But she was able to meet her great grandchildren and she also met my fiancé. Her appraisal of him was, "Good boy. Good

boy. You marry? You marry Ari-ka? Good boy.” She passed away just a few months after my mother and is buried next to my grandfather.

My mother was born Rebecca Kathryn, but she said that the only person she liked the saying her full name was her mother-in-law who would roll the “r” and pronounce the “ka” sound with the affection it suggests in Hungarian. So she only allowed Anna to call her that. To everyone else she was “Kathy.” My mother was a tomboy growing up constantly scraping her knees and getting dirty. Possibly for this her mother kept her red hair closely cropped. She hated that haircut and the moment she had control of her hair grew it out as long as it would grow. She and I and her mother as well had exactly the same shade of red hair and I keep a lock of hers as a memorial. Mom loved church not, I think, necessarily for the religious aspect but because it allowed her to sing. Tomboy though she was she asked to go to church and Sunday school whereas my uncle was much harder to convince. She had a beautiful voice but she would always say it was terrible and joked that I should cite my love of opera to her poor performance of lullabies. It’s actually the opposite. I love opera because she was a remarkable musician and knew to introduce me to Beethoven and Mozart at an early age. She also accompanied me to symphony choruses and when I was invited to solo for Mendelssohn’s Elijah, she was there with me. Mom was absolutely brilliant. Yet again she would always say self-deprecating things like, “will you explain it to the dumb old mommy?” This was flabbergasting because when I didn’t understand a concept it was to her I went. She was well read in both law and medicine and when I inspected her belongings after she died I found two books and a kindle on her nightstand as well as an entire library full of books. As a child she dreamed about being an astronaut, but like so many girls of the time was warned off by NASA. Then she decided she wanted to be a nurse. But she had met my father in high school and when he was offered a job at Bechtel as a Nuclear Engineer (and a position in the PhD program at Stanford which he bafflingly declined), she ended her studies a semester away from a degree in biology and followed him to California. She worked as a paralegal at first and started to gain a great knowledge of law. Then she worked for a Diabetes non-profit and then in the cardiac surgery unit of the local hospital. There she used her understanding of the law and love for medical sciences to start working on the IRB. The VA recognized her and hired her and she eventually climbed in importance enough to be asked to move to Washington DC and work at the Pentagon at a civilian rank equivalent to a full bird colonel. All this for a woman without a degree who considered herself not particularly intelligent. My mother was even happier than my father when she saw me studying for advanced degrees. As a child she had taken me aside before I was old enough to understand what it meant and made me swear to her that I would always put my career and my education ahead of any man. For her

to have succeeded as she did in life without so much as an undergraduate degree I can only imagine who she might have been if she had completed. She is now immortalised in the US regulations regarding the treatment and protection of human research subjects. Whenever I have doubt, I think to my mother's indefatigable spirit. I held my mother's memorial in the "Viking" church on Washington Island where she had done the same for her own mother two years prior and my brother buried her remains with those of her mother in the same cemetery. Hopefully I shall survive a while longer.

These women are responsible for who I am today. The world is not grown darker without them, but it is my responsibility to bear the light that they no longer can. They were all three incredible and quietly strong women. My mother was 5'11" and her mother taller still, but my little Hungarian grandmother was not even five feet tall. Still I consider them all giants. I don't know that my work will ever be as great as my mother's, and I don't know if I could survive what my grandmothers both did, but these were the women who made me and in honour of their memories I will at least try.

For my partner Denis Archibald Bouchinet

And

In loving memory of

my mother Kathryn Rebecca Schulz

my grandmother Elsie Langford

az én nagymama Anna Schulz

And

az én nagypapa Tibor Schulz

1 Aims and Contribution to Science

This research aims to determine if morphological patterns throughout the proximal long bones are explained by incidence of inter and intra population variation. Due to variable timing of modelling and remodelling in the long bones as well as altered patterns of resorption and deposition in concordance with factors like sex and age there is likely a morphological correlation between the diaphyseal surface and intrinsic and extrinsic factors. Past studies have considered similar questions on the basis of epiphyseal morphology or cross-sectional metrics (Kranioti, Bastir, et al., 2009; Shaw & Stock, 2009a, 2009b; Stevens & Viðarsdóttir, 2008), but few studies have attempted to quantify the morphology of the diaphyseal surface (Frelat et al., 2012) and none have compared cross-sectional, diaphyseal surface, and epiphyseal morphologies particularly in regards to intra and interpopulation variation.

Geometric Morphometrics (GMM) – a coordinate based system of quantitatively representing shape or form (shape with size) – is the primary methodology used to address the hypotheses posed below. The method involves placing landmarks on all included shapes and then using General Procrustes Alignment (GPA) to rotate, translate, and resize all shapes to a common centroid. Variation in the coordinates may then be compared to determine the level and degree of morphological variation. Procrustes alignment however, requires algorithmic calculations and therefore has only recently become a viable methodology in biological and archaeological studies. Algebra for GMM was thoroughly described by Bookstein (1991) and followed soon thereafter with software which increased the accessibility of the method to non-statisticians. However, the concept of describing shape mathematically without size using a coordinate system has been in place since the late 19th c. (Rohlf & Slice, 1990). This method is used in this study because unlike other forms of morphometrics applied to particularly the diaphyses, GMM provides a quantitative method of discussing morphology without the intrusion of size.

This study includes skeletons from four cemeteries: Coach Lane, North Shields, Fishergate House, York, St. Guthlac's Priory, Hereford, and 3-J-18 on Mis Island, Sudan. The first three are located in England and were selected for their homogeneity and good preservation. The Sudanese skeletal sample dates to a similar time period as Fishergate House, and Hereford cemeteries, but is from a distinct population and was chosen to counterpoint the English skeletal samples. A short description of these cemeteries and the history surrounding them may be found in sections 3.1.1 through 3.1.4.

Numerous factors determine adult skeletal morphology. These include genetic, epigenetic, pathological, environmental, and developmental factors. Specific anatomical features have been identified as heritable (for example epigenetic or non-metric traits like septal aperture and “squatter’s facet”), pathological (for example column-like morphology to the diaphysis of a long bone), or activity-related (for example expansion of the cortices and entheses with increased exercise). As early as 1881 – the date of publication for Roux’s treatise on the subject, anatomists and surgeons have been aware of the functional adaptation of bone (Roux, 1881 in Ruff, Holt, & Trinkaus, 2006; Wolff, 1986). Wolff attempted to mathematically and biomechanically quantify bony reactions, and his work became known as “Wolff’s Law.” While his more general argument remains accurate his calculations made several assumptions that have been refuted (Ruff, Holt, & Trinkaus, 2006). Roux’s less mathematical interpretation on the reactivity of bone, whilst less cited, better characterizes the phenomenon largely because he avoids characterizing the change in specific and mathematical terms (Ruff, Holt, & Trinkaus, 2006). (For further discussion on this point see section 2.2.3.)

Despite Roux’s and Wolff’s now century old observations regarding the reactivity of human bone there have been few studies particularly regarding variation in morphology of the surface diaphysis. However, many studies especially on cortical dimensions and the effects of childhood stress and nutrition on stature and skeletal development have shown that this variation must be present (Hughes-Morey, 2016; Ruff et al., 1994, 2005, 2013). This research hopes to fill the gap in the understanding of the relationship between diaphyseal morphology, life events, and population variation. This research also presents further support to studies showing post-cranial morphological variation between populations separated geographically and temporally (İşcan et al., 1998; Kranioti, Bastir, et al., 2009; Pretorius et al., 2006; Sakaue, 1998, 2004; Scholtz et al., 2010; Srivastava et al., 2013). In turn, the results of this research and the methodology developed may be applied to studies on growth, ontogeny and development, population variation, and post-cranial reactivity to environment, diet, stress and other factors. This research is not concerned with human evolution, but there are parallel applications. This research concerns itself with population and environment related morphological reactivity of the post-crania which has been shown to influence population variation, what Suzuki and colleagues (1956) would term “micro-evolution.” Additionally, as this is an archaeological study in which only dry bone was examined the relationship between morphology and variation was primary, but should not overshadow the entirety of human biology. That is, human osteological morphology may be related to inter and intra population variation, but that relationship is complex and will be mediated and enhanced

by particularly hormonal and endocrine factors which may not be immediately apparent, but are still crucial in the life of the individual, the survival of the group, and the eventual evolution of the species.

This research is useful within a wider scientific context not only due to its attention to a largely ignored aspect of human anatomy, but because it highlights the interrelatedness of inter and intra population variation in the expression of morphology. Morphological variation occurs in a consistent manner in the post-crania and is due not exclusively to genetic affiliation or environmental impact but to all those factors combined. This means that populations may to a degree be morphologically distinguished on the basis of geographical or temporal distance, and that that morphological variation is due both to the populations' genetic affinity and reactions to the outside environment, cultural practices, and life events all of which will be subject to one another in the final expression of morphology. Diaphyseal, epiphyseal, and cortical morphology are resultant of factors including pathology, age, and sex and are all mediated by genetic or ontogenetic responses. In medicine this may be applied to work on childhood nutrition, sports medicine, and geriatric care with particular emphasis on osteoarthritis and osteoporosis. For archaeology this research speaks to lifeways, cultural practices, social status and their effects on health, and may elucidate an individual's lived experience and its impact on their life and health.

1.1 Research Questions

1.1.1 Within population variation

H1: There is significant morphological variation within populations.

H0: There is not significant morphological variation within populations.

It is important to establish a baseline for morphological variation within a human population. This research question presupposes that each considered skeletal sample is largely ethnically and environmentally homogenous. That is, most individuals included in each of these cemetery populations are from similar backgrounds, largely remained in the area, and therefore experienced a similar environment. However, regardless of how homogenous these individuals may be there will still be some variation within population. The sub-questions below detail what variation is expected and why.

1.1.1.1 *Sexual dimorphism and morphological variation*

H1: Morphological variation is significantly correlated with sex.

H0: Morphological variation is not significantly correlated with sex.

Humans display moderate sexual dimorphism and our skeletons may be “sex estimated” based on primary and secondary sex characteristics (Waldron, 2009; White & Folkens, 2005). The question then is how much sexual dimorphism is present in this particular population and whether or not the morphological variation here may be separated from other morphological variation such as allometry. The level of sexual dimorphism varies between populations and though largely based on hereditary and genetic factors is also contingent upon environmental factors like health and nutrition, physical activity during childhood, natal health, and even some pathologies (İşcan et al., 1998; P. L. Walker, 2005, 2008; Wilczak, 1998). This study aims to identify and understand such patterns in relation to sexual dimorphism within each of the skeletal samples.

1.1.1.2 Age and morphological variation

H1: Morphological variation is significantly correlated with age.

H0: Morphological variation is not significantly correlated with age.

There is obvious morphological variation within an ontogenetic set, but even in a relatively static set, as here where only adults are considered, there will be morphological variation with increasing age. Age interlinks with numerous factors and therefore impacts – albeit slowly – the overall morphology of the bone. Age has an impact on an individual’s hormonal responses, their level of immunity and general health, their level of physical activity around the time of death, and the amount of time they have carried osteomorphing pathologies (Currey et al., 1996; Mays, 1996; Rho et al., 2002; Ruff & Hayes, 1982; Steckel et al., 2002; P. L. Walker, 2005).

1.1.1.3 Childhood stress indicators and morphological variation

H1: Morphological variation is significantly correlated with indicators of childhood stress.

H0: Morphological variation is not significantly correlated with indicators of childhood stress.

While purely genetic factors may have tremendous influence on morphology, numerous studies suggest that adult stature and health may be dependent on epigenetic factors *in utero* and childhood stress. Additionally, pathologies, joint development, and childhood activity influence mobility, joint surface shape, and cortical thickness. These factors however, are very inter-related. Whether they influence adult long-bone morphology in a consistent manner is as yet unknown. This study will examine

whether or not indicators of childhood stress such as cribra orbitalia, linear enamel hypoplasia (LEH), and rickets are associated with characteristic changes in adult long-bone morphology (Frost, 1999; Gowland, 2015; Hamrick, 1999; May et al., 1993; P. L. Walker et al., 2009).

1.1.1.4 Degenerative Joint Disease and morphological variation

H1: Morphological variation is significantly correlated with the severity of Degenerative Joint Disease.

H0: Morphological variation is not significantly correlated with the severity of Degenerative Joint Disease.

It is unlikely that an individual would survive long enough for degenerative joint changes experienced later in life to influence gross long bone morphology. However, if developmental, genetic, or hormonal issues cause changes to cartilaginous features thereby impacting joint fluidity and mobility, it is possible a morphological adaptation may develop. Additionally, hormonal and genetic diseases which cause osteogenic or osteopenic changes could also result in morphological variation (Kaastad et al., 2000; Linkhart et al., 1996; Vedi et al., 1996). This study will consider degenerative joint disease (DJD), osteoarthritis (OA), and Schmorl's nodes and their correlation with morphological variation.

1.1.1.5 Trauma and morphological variation

H1: Morphological variation is significantly correlated with the presence or absence of trauma.

H0: Morphological variation is not significantly correlated with the presence or absence of trauma.

Significant but survived trauma could influence mobility and activity and possibly cause wasting in the affected limb or area with adaptive hypertrophy in other parts of the body (Green Swiontkowski, 1998; Lewis, 2006; Šlaus, 2008). For this study trauma is recorded as present if healed trauma is found anywhere in the skeleton. However, limbs showing direct evidence for trauma were not included for morphological examination.

1.1.2 Between population variation

H1: There is significant morphological variation between populations.

H0: There is not significant morphological variation between populations.

GMM is a technique often used to distinguish between different skeletal populations and to identify phylogenetic differences between anatomical features of similar species (Claude et al., 2004; A.

Pearson et al., 2015; Proctor et al., 2008; Viscosi & Cardini, 2011). Therefore it is likely that some variation may occur as a result of the populations being distinct. However, three of the four skeletal samples studied are English. Due to their geographic proximity and the choice of long bones as opposed to crania for shape analysis variation between populations may be more related to environmental, temporal, pathological or socio-economic factors. It is, however, necessary to determine if variation is due to inter-population variation and if so how much variation is associated with population differences.

1.1.2.1 Pathological rates between populations

H1: There is a significant difference in the rate of pathologies between populations.

H0: There is not a significant difference in the rate of pathologies between populations.

Pathological prevalence may be used to interpret morphological variation patterns. For example, if one population shows a comparatively higher rate of childhood stress markers, that prevalence may also be relevant to the interpretation of sexual dimorphism or other morphological and metrical parameters (Karapanou & Papadimitriou, 2010; McDade et al., 2008). Alternatively, cribra orbitalia in particular may not relate to nutritional deficiencies but malaria (Gowland & Western, 2012; Smith-Guzmán, 2015). The samples studied vary in temporality, environment, climate, terrain, and socioeconomic status. It is expected that this will impact upon the prevalence and type of pathologies present in each population.

1.1.2.2 Comparison of interpopulation variation with variation between intrapopulation demographic groups

H1: Variation between intrapopulation demographic groups is greater than variation seen between populations.

H0: Variation between intrapopulation demographic groups is less than variation seen between populations.

Inter-population variation is common in human crania, but long bones are strongly influenced by sex, size and extrinsic or environmental factors for their morphology (Stevens & Viðarsdóttir, 2008; Viðarsdóttir et al., 2002a). Additionally, it may be possible that certain groups within the population show more or less inter population variation. For example, sexual dimorphism varies from group to group and may be more prevalent in some of the populations considered than in others. In those cases,

it is possible that certain subgroups of a population have greater between population variation than others. Sexual dimorphism in many populations is due to arrested or divergent ontogenetic trajectories, which means where these sexually dimorphic trajectories vary between populations, population variation may be better expressed in one sex or the other (Bulygina et al., 2006; Cobb & O'Higgins, 2007; Coquerelle et al., 2011; Velemínská et al., 2012).

1.1.2.3 Comparison of intra and inter population variation

H1: Populations are morphologically distinct.

H0: Populations are not morphologically distinct.

This final more general question is the culmination of the previous two. It is unlikely that morphological variation particularly in human long bones will be starkly succinct between or within skeletal samples. There is more likely to be a continuum of morphological variation. However, where different populations fall on that continuum relative to factors influencing inter-population variation will contextualise morphological variation as a whole.

1.1.3 Morphological variation in different parts of the bone

H1: Different parts of the bone evidence morphological variation better correlated with factors different from other parts of the bone.

H0: Morphological variation throughout the bone varies consistently with each part of the bone showing similar morphological variation to the same factors.

The basis of this question is the assumption that biological form is functionally relevant. The morphology of human long bones will have a basic genetic predetermination, but be further influenced by environment, hormones, life events, pathology and so forth. Additionally these factors will relate unevenly to different parts of the long bone due to aetiology, reactivity of the bone itself, and developmental timing (Currey, 2003; Rho et al., 2002; Ruff, 2005; Ruff et al., 2013).

1.1.3.1 Morphological variation between epiphyses and epiphyseal morphological variation as compared to surface morphology and cross-sectional morphology

H1: Epiphyseal morphological variation is distinct from all other morphological variation.

H1: Proximal and distal epiphyseal morphological variation is distinct.

H1: Epiphyseal morphological variation is distinct from surface morphological variation.

H1: Epiphyseal morphological variation is distinct from cross-sectional morphological variation.

H0: Epiphyseal morphological variation is consistent with all other morphological variation.

H0: Proximal and distal epiphyseal morphological variation is consistent.

H0: Epiphyseal morphological variation is consistent with surface morphological variation.

H0: Epiphyseal morphological variation is consistent with cross-sectional morphological variation.

Developmental timing for the epiphyses and diaphysis are different. The epiphyses of the same bone will have different developmental timings themselves (Scheuer & Black, 2000). Additionally, while the epiphyses will generally change very little after childhood, the diaphysis of a long bone can be very reactive well through adulthood (Frost, 1999; Rho et al., 2002). Therefore, the investigation of the effects of population factors on morphological variation in these different areas may suggest times in the individual's life where they were more or less vulnerable to pathology or the environment or conversely peaks of pathological assault or adverse exposure.

1.1.3.2 Surface diaphyseal morphological variation as compared to epiphyseal and cross-sectional morphological variation.

H1: Surface diaphyseal morphological variation varies differently than epiphyseal or cross-sectional morphological variation.

H0: Surface diaphyseal morphological variation varies consistently with epiphyseal and cross-sectional morphological variation.

The surface morphology of the diaphysis of the long bone has not been quantitatively studied outside of about two studies (De Groote et al., 2010; Frelat et al., 2012). There has been an assumption in the literature that cortical information is sufficient to describe the diaphysis. This may be an accurate assumption, but as there are so few studies on the surface morphology of the diaphysis it cannot yet be proven (Davies et al., 2012; Ruff, 1988, 2002; Shackelford & Trinkaus, 2002; Stock & Shaw, 2007). This study will show whether or not there is consistent morphological variation in the surface of the

diaphysis within and between populations and whether or not that variation differs qualitatively from variation seen in the epiphysis or in cross-sectional data.

1.2 Thesis Structure

The thesis will follow with a Background reviewing demographic and pathological information in the first section and background information on GMM in the second. The following chapter covers the materials and methods and includes pathology prevalence rates and error reports. The following three chapters are results chapters with discrete background and discussion sections covering each of the three morphological landmark sets. The final chapter is the general discussion and conclusion which will synthesize the results in the context of the research questions.

2 Background

The aim of this chapter is to contextualise demographic and pathological variation with morphological variation. This chapter will elucidate why pathologies were chosen and how they and other factors like sex and age might contribute to morphological variation. This chapter will also give a brief and simplified description of the theory behind GMM. The chapter is divided into three sections the first two covering intra-population and interpopulation variation respectively and the final section discussing GMM. The first section is subdivided into demographic information which includes information on the contribution of sex and age to morphology as well as a subsection on the development of bone and how intrinsic and extrinsic factors like biomechanics and bone mineral content may contribute to morphology. The second subsection under the banner of intrapopulation variation concerns pathologies. The pathology section attempts to briefly address the background of each pathology studied and explain its relationship to morphology. The comparatively brief subsequent section “Interpopulation Variation,” contextualises what variation in morphology is likely to be found between populations and provides a short background of other similar studies. The final section in this chapter discusses GMM as it is applied in this study giving a brief description of the overall method, the types of landmarks used, and discussions of error and allometry which will feature in subsequent chapters.

2.1 Anatomy

Before entering the more complex and at times theoretical domains of this literature review it is important to discuss the concrete anatomical aspects of the bones to be considered along with their development and muscle attachments. Childhood conditions regarding nutrition, body weight, and stress will directly influence the morphology of the bone (Hughes-Morey, 2016; McEwan et al., 2005; Ribot & Roberts, 1996; Ruff et al., 1994, 2013; Watts, 2015). However, population affinity and extrinsic factors may also affect developmental timing thereby indirectly influencing morphology. Figure 2.1 and Figure 2.2 give a very generalised overview of the developmental timings for the humerus and femur respectively. A more in depth discussion of bone development relevant to this thesis is available in Section 2.2.3. Bone composition

At a molecular level bone is comprised of proteins, primarily collagen and hydroxyapatite (White & Folken, 2005). The latter is comprised of calcium, phosphorus, and oxygen and hydrogen. Living bone consists of proteins, hydroxyapatite, and water the combination of which is responsible for the tensile

strength and elasticity in bones. Burr (1980) found that studies varied in the level of association between mineral density and compressive strength they reported with some studies attributing only 40-42% of compressive strength to mineral density whereas others put the rate closer to 80% (Amtmann and Schmitt, 1968 and Jurist and Foltz, 1977 in Burr, 1980). In general, a higher proportion of hydroxyapatite or bone mineral content (BMC) will result in greater elasticity but there is a threshold at which a higher BMC increases the likelihood of fracture or micro-cracks leading to fracture by making bone overly brittle (Burr, 1980; Currey et al., 1996). Human bone is distinct from bone of other animals in several key ways. Human bone has a differential rate of turnover when compared to other animals with the closest correlates being dogs and pigs (Aerssens et al., 1998). Human bone has a lower BMC than most animals and human bone is Haversian in organization (other animals particularly larger ones do have Haversian organization but they also typically have a higher BMC) leading to increased porosity which in turn may contribute to - but is not solely responsible for - lower mechanical strength (Burr, 1980).

Proteins found in the bone include osteonectin, osteocalcin, osteopontin, and particularly type I collagen (Waldron, 2009). Collagen is a fibrous protein found in various forms throughout the body. Type I collagen forms much of the matrix of the bone and it is therefore particularly crucial during modelling and remodeling. Collagen types III and V are also present in lower concentration and are responsible for fibril diameter (Viguet-Carrin et al., 2006). Additionally, collagen makes up the matrix for cartilage and comprises much of the periosteum. Osteoblasts in the process of remodeling release collagenase – an enzyme which breaks down collagen – so that they may reorganize the bony structure (Bord et al., 1996). Osteogenesis imperfecta, a pathologic condition which results in brittle bones, is due to a genetic abnormality whereby amino acids necessary for type I collagen are improperly formed. The collagen is therefore unsuitable to consistently form the matrix on which hydroxyapatite may be arranged thereby interfering with mineralization of the bone (Viguet-Carrin et al., 2006).

2.1.1 Humeral Anatomy

The humerus is the largest and most proximal bone in the human upper limb. It articulates proximally with the shoulder girdle comprised of glenoid fossa of the scapula and the clavicle. The clavicle provides the necessary platform for muscle attachments which allows for the arm to be raised upwards and is not present in many quadrupedal species. Distally, the humerus articulates with the radius and ulna whose arrangement allows for the rotation of the forearm and hand. The proximal articulation for the humerus is a ball and socket joint and therefore the humeral head is of an ovoid shape. The humeral head and anatomical neck are described by humeral landmarks one through four

(see section 3.5.1). The distal articulation may be divided into two parts: the modified ball and socket joint for the radius and the hinge joint for the ulna. The capitulum which articulates with the radial head is of ovoid shape allowing the radial head to rotate and rock over it for supination and pronation, and flexion and extension of the forearm. The trochlea and olecranon fossa articulate with the olecranon process of the ulna and allow for flexion and extension of the forearm. The capitulum does not morphologically lend itself to homologous landmarks and so is represented in this study by landmarks seventeen and twenty along the medial most edge at the midline from the plantar view and superior margin respectively and on the posterior aspect landmark twenty-four. The trochlea may be imagined as an hourglass shape and ranges from nearly cylindrical in shape to closely resembling an hourglass. In this study it is described by landmarks thirteen through sixteen as well as eighteen and nineteen and on the posterior aspect twenty-five. The olecranon fossa allows space for the olecranon process of the ulna when the arm is fully extended. (On the anterior aspect of the humerus just proximal to the capitulum and trochlea are the coronoid and radial fossae which accommodate the coronoid process of the ulna and radial head when the forearm is fully flexed.) It is largely laterally oriented and may be ovoid or triangular in shape. Here it is described by landmarks twenty-one through twenty-three which demarcate its most medial, lateral, and superior points. In data collection a fourth point demarcating the olecranon fossa's most inferior point was collected, but has been eliminated due to a relatively high rate of observer error (see section 3.5.5). In some individuals there may be a septal aperture or non-pathological hole in the olecranon fossa. The septal aperture is asymptomatic and considered a non-metric or epigenetic trait which may demonstrate genetic affinity.

The humerus plays host to a number of muscle attachments both insertion and origin. Most insertion points are positioned on the proximal portion of the bone whilst most origins are positioned more distally. Before the discussion of muscle attachments is discussed however a note should be made of the biceps brachii which entirely bypasses the humerus in terms of attachment. The long and short heads for which it is named originate at the supraglenoid tubercle of the scapula and the coracoid process respectively. The biceps brachii inserts at the radial tuberosity but also includes an aponeurosis called the aponeurosis bicipitis brachii which connects to the deep fascia of the forearm. The long head of the biceps brachii is surrounded by a synovial sheath and passes within the intertubercular groove on the anterior of the humerus. It is there bounded by the transverse humeral ligament and the tendon of the Pectoralis major which itself does insert at the humerus. The biceps brachii is partially responsible for supination of the forearm and flexion of the forearm. It is important to the morphology of the humerus due to the placement of its long head. Humeral landmark seven in this study represents the

deepest part of the intertubercular groove and will be bordered by landmarks five and eight which are meant to describe adjacent muscle attachments for the supraspinatus and subscapularis respectively, but which also contextualise the position of landmark seven (see section 3.5.1).

The muscles which attach to and originate from the humerus may be divided by muscle group. These groups are the shoulder muscles, the muscles of the chest and torso, and the muscles of the arm. The description of muscles to follow attempts to move from the proximal aspect of the humerus to the distal while maintaining the muscles in their groups. However, in some cases due to the way the muscle must act upon the bone this order cannot be maintained. The deltoideus for example inserts at about the middle of the diaphysis but will be discussed with the shoulder muscles which attach at the greater and lesser tubercles and along the crest of the lesser tubercle and before muscles from the chest which attach just proximal to it along the diaphysis.

Shoulder muscles which attach to the humerus include the subspinatus, supraspinatus, infraspinatus, teres minor, teres major and deltoidius. In this study landmarks used which refer to these muscles and attempt to morphologically describe their position are humeral landmarks five, six, eight, and nine described and diagramed in Section 3.5.1. The subspinatus originates from the subscapular fossa and inserts at the lesser tubercle of the humerus. This muscle rotates the arm medially and depending on position may aid in flexion, extension, abduction and adduction. The subspinatus also strengthens the shoulder joint by pulling the humeral head towards the glenoid fossa. The supraspinatus originates from the supraspinatus fascia and inserts into the most superior muscle attachment on the greater tubercle of the humerus. This muscle abducts the arm and strengthens the shoulder joint in a similar manner to that seen with the subspinatus. The infraspinatus originates from the infraspinatus fascia and inserts just posterior to the attachment for the supraspinatus on the greater tubercle of the humerus. As with the previous two examples this muscle strengthens the shoulder joint. The infraspinatus also rotates the arm laterally and is involved in abduction and adduction. The teres minor originates from the dorsal medial edge of the scapula near the inferior angle and inserts posterior-distally to the attachment for the infraspinatus on the greater tubercle of the humerus. This muscle in some individuals is inseparable from the infraspinatus. As with the subspinatus, supraspinatus, and infraspinatus, teres minor strengthens the shoulder joint by drawing the humerus into the capsule. The muscle is responsible for lateral rotation of the arm and some adduction. Teres major originates from the inferior angle of the scapula as well as the fibrous divide between it and teres minor and inserts into the crest of the lesser tubercle distal to teres minor's attachment. Teres major is

responsible for adduction, extension, and medial rotation. The deltoidus originates from the lateral third of the anterior of the clavicle, the lateral superior surface of the acromion and the spine of the scapula and inserts at the deltoid tuberosity of the humerus. The deltoid tuberosity is located laterally at or just proximal to the midpoint of the diaphysis. The attachment gives rise to deep fascia in the arm. The deltoideus abducts the arm and parts of the deltoideus are involved in flexion, extension, and rotation both medial and lateral. The deltoid tuberosity was not described by a landmark in this study because it is highly variable and difficult to find and because it is sufficiently far from other homologous points that it created a risk for the “Pinocchio effect,” (von Cramon-Taubadel et al., 2007). However, the deltoid tuberosity will become an important morphological factor when considering the cortices of the humerus in Chapter 6.

The latissimus dorsi and pectoralis major are two large superficial muscles originating from the back and chest respectively and inserting at the humerus. Although they are quite large and responsible for many different movements and much of the power in the arm their attachment sites are not consistently visible on the humerus. For this reason although they are likely contributory to morphological variation their contribution may only be recorded with surface semilandmarks. The latissimus dorsi is a large superficial muscle and may be imagined as an inverted triangle. It originates from the lumbar aponeurosis which is in turn attached to the spinous processes of the lower six thoracic vertebrae as well as the same of the lumbar and sacral vertebrae. It is also attached to the posterior portion of the iliac crest and the caudal ribs. It is inserted at the crest of the lesser tubercle of the humerus more proximal than the insertion point for the pectoralis major or teres major. The latissimus dorsi is responsible for extension adduction and medial rotation of the arm as well as downward and backward motion of the shoulder. The insertion point influences the shape of the intertubercular sulcus but is not consistent enough to demarcate with a homologous landmark. Its influence on morphology then must be captured with surface semilandmarks. The pectoralis major is a large superficial fan shaped muscle covering most of the superior torso. It has extensive origin points notably the ventral aspect of the sternum, the cartilage of most of the true ribs with the possible variable exclusion of ribs one and seven, the anterior sternal clavicle and the aponeurosis of the obliquus externus abdominis muscle. It inserts at the crest of the greater tubercle of the humerus. The pectoralis major is responsible for flexion, adduction, and medial rotation of the arm as well as cranial, ventral, and medial movement of the shoulder. The insertion for the pectoralis major influences the shape of the intertubercular sulcus and the distal ridge of the greater tubercle but has no homologous or near homologous point to landmark. It is therefore represented in this study by surface semilandmarks.

The coracobrachialis is delineated by *Gray's Anatomy* as a muscle of the arm (Gray, 1974 pp. 458). It originates at the coracoid process of the scapula and inserts at the medial aspect of the humeral diaphysis roughly opposite the deltoid tuberosity. The coracobrachialis is a very small muscle which shares its origin with the short head of the biceps brachii and runs parallel to it. This muscle is responsible for some flexion and abduction of the arm. As with the deltoidius, the insertion point for the coracobrachialis is too distally located to include homologous landmarks denoting its location. Additionally, because the muscle is small, its attachment location is usually near invisible on dry bone. The brachialis is the first muscle which originates from the humerus. The brachialis originates from the distal anterior surface the humerus and surrounds the inferior angle of the insertion of the deltoidius. It inserts at the tuberosity of the ulna and is responsible for flexion of the forearm. The brachialis does not create any consistently notable homologous points to be landmarked and so its impact on morphology in this study is tracked by surface semilandmarks. On the posterior proximal-lateral aspect of the humerus the lateral head of the triceps brachii originates. Its long head originates from the infraglenoid tuberosity of the scapula and the medial head originates from the posterior diaphysis of the humerus in a triangle arrangement starting proximally and medially and extending over the entire posterior surface of the diaphysis. The triceps brachii inserts at the posterior proximal portion of the olecranon. As a whole the muscle extends the forearm. The long head of the triceps brachii also helps extend and adduct the arm. The triceps does not create consistent morphological markers which may be used as homologous landmarks and so the relevant morphology of this attachment is captured with surface semilandmarks.

The brachioradialis and extensor carpi radialis longus both originate from the lateral supra condylar ridge of the humerus with the brachioradialis proximal to the extensor carpi radialis longus. The brachioradialis inserts at the styloid process of the radius and the extensor carpi radialis longus inserts at the dorsal surface of the second metacarpal. The brachioradialis flexes the forearm and the extensor carpi radialis longus extends and abducts the hand. The extensor carpi radialis brevis, extensor digitorum, extensor digiti minimi, and extensor carpi ulnaris all originate from a common tendon attached at the lateral epicondyle of the humerus. This origin is described by landmark ten. The extensor carpi radialis brevis inserts at the dorsal base of the third metacarpal and is responsible for extension of the hand. The extensor digitorum inserts at the second and third phalanges of the fingers and extends the fingers. The extensor digiti minimi joins the extensor digitorum tendon and ultimately attaches at the first phalanx of the fifth finger thereby becoming responsible for the extension of the fifth finger. The extensor carpi ulnaris and inserts into the tubercle on the medial side of the base of the fifth

metacarpal. The extensor carpi ulnaris is responsible for extension and adduction of the hand. The supinator also arises from the lateral epicondyle of the humerus and inserts into the posterior and lateral diaphyseal surface of the radius. The supinator supinates the hand. The anconeus is a small muscle which originates just distal from the distal-most attachment of the triceps brachii on the posterior lateral surface of the humerus adjacent the lateral epicondyle and inserts at the olecranon and posterior of the ulna. The anconeus is responsible for extension of the forearm. While the anconeus is located largely on the distal epicondyle it is almost continuous with the triceps brachii and therefore is inconsistently distinguished on the dry bone. It is therefore not represented in the homologous landmarks.

The pronator teres' humeral head originates just proximal to the medial epicondyle and its ulnar head originates from the ulna's coronoid process. The pronator teres inserts at the lateral aspect of the radial diaphysis and the muscle is responsible for pronation of the hand. The pronator teres along with the flexor muscles and palmaris longus may be partly responsible for the morphology of the medial epicondyle and therefore the position of homologous landmarks 11 and 12. These landmarks which denote the superior and inferior aspects of the medial epicondyle are most reflective of the position and shape of these muscles. The palmaris longus originates from the medial epicondyle and inserts into the flexor retinaculum and palmar aponeurosis. It shares a tendon with the flexors and sits between the flexor carpi ulnaris and the flexor carpi radialis. The palmaris longus is responsible for flexion of the hand. The flexor carpi radialis originates from the medial epicondyle of the humerus and inserts at the base of the second metacarpal. It is responsible for flexion of the hand and is involved in abduction of the hand. The flexor carpi ulnaris, and flexor digitorum superficialis each have two heads the humeral head of which originates from a common tendon shared with the flexor carpi radialis and palmaris longus which is attached at the medial epicondyle of the humerus. The ulnar heads originate from the olecranon and dorsal aspect of the ulna and the coronoid process and medial side of the ulna respectively. The flexor carpi ulnaris inserts at the pisiform and is connected via ligaments to the hamate and fifth metacarpal. The flexor carpi ulnaris is responsible for flexion and adduction of the hand. The flexor digitorum superficialis also has a radial head which originates from the oblique line of the radius and the muscle divides into superficial and deep aspects and gives off tendons for each finger ultimately inserting into the second phalanx of each. The flexor digitorum superficialis is responsible for flexion of the second phalanges of the fingers.

2.1.2 Femoral Anatomy

The arm and leg have a similar arrangement of joints and bones, but their function is very different in humans meaning the arrangement of muscles which may be associated with the femur will be very different than those of the humerus. This section will attempt to present them as muscle groups proceeding from insertions at the proximal aspect of the bone and culminating in distal origins. However, it will be necessary in some cases to present separate muscles as groups (such as with the case of the adductor longus, adductor brevis, and adductor magnus) and in some cases to alter the order of presentation. The goal of this section is to report the role of muscular function and anatomy in relation to osteological morphology.

As with the biceps brachii and its relationship to the humerus, several muscles of the leg entirely bypass the femur with no attachments to the bone. In the leg they are superficial muscles, but should be mentioned due to their actions within the muscle groups. The Sartorius muscle originates at the anterior superior aspect of the iliac crest and is inserted into the proximal medial tibial diaphysis. The Sartorius is responsible for flexion and lateral rotation. If the leg is flexed it helps with medial rotation. The Gracilis also bypasses the femur and is superficial. It originates at the anterior inferior margin of the pubic symphysis and is inserted at the proximal medial tibial diaphysis. The gracilis adducts the thigh, flexes the leg, and when the leg is flexed may aid in medial rotation. As these muscles bypass the femur and are sufficiently superficial – unlike the biceps brachii – to avoid having tendons cradled in any sulcus in the bone, they are not associated with any landmarks homologous or otherwise in this study.

2.1.2.1 Hip

The femur is the most proximal bone in the leg and in humans is the “longest, heaviest, and strongest bone in the body,” (White & Folkens, 2005 pp. 255) as it is responsible for supporting the weight of the torso. Much of human femoral muscular-skeletal anatomy and morphology will be related to our bipedal locomotion. As with the humerus the proximal joint - the hip - is a ball socket joint and the knee or distal joint is a hinge joint. However, anatomy of the arm preferences mobility over stability whereas in the leg, stability is more important. The articulating “socket” in the shoulder girdle was made up of the glenoid fossa, coracoid process, and clavicle which allow the arm to be easily moved in almost any direction with almost any rotation. Conversely, the hip is more restricted. The femoral head or the “ball” of the joint describes more of a sphere than did the humeral head and the acetabulum is deeper or more concave and bounded the glenoid fossa or the rest of the shoulder girdle. In this study the approximate shape of the femoral head is described by homologous femoral landmarks two, three, and

four. Femoral landmark one gives the location of the fovea capita. This bounded morphology provides greater stability in the joint and lowers the risk of injury, but it also limits mobility. While some individuals are hypermobile or certain sports like ballet and gymnastics require similar degrees of mobility in the hip as in the shoulder the hip is generally less mobile but stronger thereby able to support the individual's weight while standing, walking, running, or climbing. The human femur is notable for its valgus angle which – along with the morphology of particularly the lumbar vertebrae and spinal curvature as a whole – resolves the mechanical necessities of bipedal locomotion. The human pelvis is flared in a manner to support both the weight of the torso and the organs and so the angle of the hip, knee, and thus femur as a whole must accommodate this (Harmon, 2007; C Owen Lovejoy et al., 2002; Organ & Ward, 2006; Sylvester & Pfisterer, 2012). The mechanical and morphological requirements for bipedal locomotion balanced with requirements for parturition in relation to cranial size inform the shape of the femur as a whole, but particularly in relation to the valgus angle at the hip and knee.

In this research the fovea capitis is demarcated by femoral homologous landmark one. This depression is the attachment site for the ligamentum teres ligament which stabilises the articulation between the femoral head and acetabulum. This ligament only functions as an anchor so its relative location may be incidental to morphology, but it is a Type I homologous landmark and helps describe the morphology of the femoral head as well as its relation to the rest of the proximal femur (Gray, 1974; White & Folkens, 2000).

The iliofemorale ligament is part of the articular capsule and deserves mention due to its attachment sites. The iliofemorale ligament strengthens particularly the anterior aspect of the articulation between the femoral head and the acetabulum. It attaches on the innominate bone at the anterior inferior aspect of the iliac crest and on the femur attaches at the intertranchanteric line. No homologous landmarks are placed on the intertranchanteric line due to a lack of homologous structures, but the intertranchanteric line and the iliofemorale ligament are integral to the morphology of surrounding muscles whose attachment sites are recorded with homologous landmarks and which affect the morphology of the femoral diaphysis.

2.1.2.2 Knee

The knee like the elbow is a hinge joint but much of the morphological variation may be attributed to the requirements of bipedal locomotion. The lateral and medial epicondyles of the femur

articulate with the tibial plateau so named because it is almost flat. This is in contrast to other species of primates whose joint architecture particularly at the knee is rounder and better adapted for quadrupedal locomotion, climbing and jumping (Hamrick, 1996; Squyres & Deleon, 2015). The functionality of the knee is aided by the presence of the patella. The patella is the largest and most consistent sesamoid bone in the body and functions as an anchor for the quadriceps femoris and patellar ligament which in turn articulates with the tibial tuberosity (Gray, 1974; White & Folkens, 2000). In this study the most proximal aspect of the articulation of the femur and patella are described by landmarks fifteen, sixteen and seventeen. The remainder of the articular surface and articular border is described by landmarks twenty through twenty-six.

2.1.2.3 Muscles of the pelvis and hip

The iliopsoas muscle is comprised of the psoas major and the iliacus. The psoas minor runs alongside the psoas major originating from the last thoracic vertebra and first lumbar and inserting into the pectineal line. The psoas minor is partially responsible for flexion of the pelvis and lumbar vertebral column, but is often absent. The psoas major originates from the lumbar vertebral transverse processes and intervertebral disks as well as a series of tendons which pass between the other attachment sites along the lumbar portion of the vertebral column. The psoas major then is inserted at the lesser trochanter of the femur. This muscle along with the iliacus is responsible for flexion of the thigh, but also helps with flexion and lateral bending of the lumbar vertebral column. The iliacus originates from the iliac fossa and is inserted into the tendon of the psoas major just prior to that tendon's insertion into the lesser trochanter. The lesser trochanter of the femur is in this study demarcated by femoral homologous landmarks eleven and twelve.

The gluteus muscles especially the gluteus maximus are heavily utilised in bipedal locomotion and therefore one of the more important muscle groups to consider when discussing themes of evolution and speciation. The gluteus maximus travels in part from the gluteal line on the innominate bone to the gluteal line on the femur. In whole the gluteus maximus originates from the gluteal line and portions of the crest of the ilium as well as the posterior and inferior surface of the sacrum and coccyx. The deep fibers do insert at the gluteal line of the femur and the superficial fibers insert at the fascia lata. The gluteus maximus holds the torso upright but more directly extends and laterally rotates the leg. The gluteus medius is in part deeper than the gluteus maximus. It originates on the ilium between the crest and gluteal line from the dorsal aspect and from the gluteal line from the ventral aspect. The gluteus medius inserts at the greater trochanter of the femur. This muscle abducts the thigh and may rotate it

medially. The gluteus minimus is the deepest of the three gluteal muscles and originates from the ilium between gluteal lines and the margin of the sciatic notch. It inserts via a tendon at the greater trochanter of the femur. The gluteus minimus is responsible for medial rotation and abduction of the thigh and may also help in flexion. The greater trochanter and gluteal line are crucial attachments for the gluteal muscles and these anatomical areas are marked by homologous landmarks six and thirteen respectively.

The tensor fasciae latae originates from the anterior superior aspect of the iliac spine and inserts at the fascia lata. The tensor fasciae latae is responsible for flexion of the thigh and may aid in medial rotation. The piriformis is a deep muscle which originates at the sacrum between the foramina inferior to the second through fourth sacral vertebrae and in part from the margin of the sciatic foramen. The fibers of the piroformis insert via a tendon into the greater trochanter of the femur. The orburator internus is a very deep muscle which originates from the border of the auricular surface and superior aspect of the sciatic notch, the ischial ramus, and the rami both superior and inferior of the pubis. It extends over the obturator foramen and inserts via a tendon shared with the gemelli muscles (to be discussed below) at the greater trochanter just proximal to the trochanteric fossa. The obturator internus is responsible for lateral rotation of the thigh and may help in extension and abduction during flexion. The gemelli muscles are divided into the superior and inferior. Gemellus superior originates at the ischial spine and gemellus inferior originates at the ischial tuberosity. Both insert after blending with the tendon for the obturator internus at the greater trochanter of the femur. The gemelli are responsible for lateral rotation of the thigh. The obturator externus originates from the medial portion of the obturator foramen and rami of the pubis and ischium and inserts at the trochanteric fossa. The obturator externus is responsible for lateral rotation of the thigh. Landmark six in this study largely denotes the attachment site for the tendon for the gluteus medius as opposed to the other muscles which insert at that site, but the trochanteric fossa is marked by landmark five.

2.1.2.4 Anterior

The articularis genus is a small muscle which lies deeper than the muscles of the quadriceps femoris in particular the vastus intermedius and which originates and the distal femoral diaphysis and inserts into the synovial membrane of the knee joint. The articularis genus is responsible for proximal movement of the articular capsule. The quadriceps femoris is made up of the rectus femoris, vastus lateralis, vastus medialis, and vastus intermedius. The quadriceps femoris may also be called the quadriceps extensor as it extends the leg. It comprises most of the muscle on the anterior and both

sides of the thigh. The rectus femoris originates from two tendons the first at the anterior inferior portion of the iliac spine and the second from a sulcus just cranial to the margin of the acetabulum. The rectus femoris inserts into the base of the patella. In addition to extending the thigh, the rectus femoris also is involved in flexion. The vastus lateralis is the largest muscle in this group and originates from an aponeurosis attached to the greater tubercle, intertrochanteric line, gluteal tuberosity, and the proximal linea aspera. It inserts via a tendon that attaches to the lateral portion of the patella but also blends with the tendon of the Quadriceps femoris. The vastus medialis originates from the distal portion of the intertrochanteric line and the medial portion of the linea aspera as well as the medial portion of the supracondylar line. It inserts into the medial border of the patella and blends with the Quadriceps femoris tendon. The vastus intermedius originates from the proximal two thirds of the anterior and lateral femoral diaphysis as well as the distal portion of the intermuscular septum. It inserts into the tendon of the quadriceps femoris which in turn inserts into the base of the patella. The muscles of the Quadriceps femoris may be associated in this study with the femoral semilandmarks due to their attachment over most of the femoral diaphysis before their final insertion into the quadriceps tendon. To a degree the intertrochanteric line is captured by the edge of the surface semilandmarks as this is considered part of the margin, however, it is only indirectly associated with homologous landmarks.

2.1.2.5 Medial muscles

The pectineus originates from the pectineal line of the pubis and inserts between the lesser trochanter and linea aspera on the femur. It is responsible for flexion and adduction of the thigh along with medial rotation. In this study the insertion point is described by landmarks twelve and fourteen. The abductors – adductor longus, adductor brevis, and adductor magnus – all adduct the thigh and are also involved in medial and some lateral rotation. They all originate from the pubis with the adductor brevis and adductor magnus originating from the inferior ramus. The origin point of the adductor longus is slightly more superior and anterior and the muscle inserts at the linea aspera blending with the adjacent vastus medialis and adductor magnus. The adductor brevis inserts posterior to the insertion for the pectineus and adductor longus from the lesser trochanter to the proximal portion of the linea aspera. The adductor magnus inserts into the linea aspera as far as the adductor tubercle. The tendinous insertion for the adductor magnus is interrupted by a foramen through which the femoral blood vessels may pass. The adductor tubercle was not sufficiently robust on all individuals to assign it a homologous point, but the linea aspera should be well represented by surface semilandmarks.

2.1.2.6 Posterior muscles

The biceps femoris per its name and as with the biceps muscle in the humerus has two heads. The long head of the biceps femoris originates at the tuberosity of the ischium and the sacrotuberous ligament. The short head of the biceps femoris originates at the lateral aspect of the linea aspera (it is notable that in some cases the short head may be absent calling into question the importance of this muscle in the forming and maintenance of femoral morphology). The muscle inserts into the lateral head of the fibula and into the lateral condyle of the tibia. The tendon for the insertion of the biceps femoris splits into two to surround the fibular collateral ligament. The inferior aspect of this tendon also gives off the fascia for the lower leg. Both the semitendinosus and the semimembranosus bypass the femur with no insertion or origin on the bone. (There is a fibrous expansion which arises from the distal tendon of the semitendinosus and inserts into the lateral condyle of the femur, but it is not an insertion point for the muscle itself.) Their effect to the overall morphology of the femur then is expected to be minimal, but they will be briefly discussed if for no more than their role alongside other posterior muscles. The semitendinosus originates largely at the tuberosity of the ischium sharing the tendon with the long head of the biceps femoris. The muscle contracts into a tendon which lies medial to the popliteal triangle and inserts into the medial aspect of the tibial diaphysis. The semimembranosus does not share the tendon with the biceps femoris and semitendinosus but it does originate at the tuberosity of the ischium just superior and lateral to the tendon for the biceps femoris and semitendinosus. It then inserts into the medial posterior aspect of the medial condyle. These three muscles work together to flex the leg and the biceps femoris rotates the leg laterally during flexion where the semitendinosus and semimembranosus rotate the thigh medially during flexion. Further movement is aided by muscles discussed below. Due to their lack of femoral attachment sites no landmarks in this study may be associated with the semitendinosus or semimembranosus. The femoral attachment for the biceps femoris being the linea aspera may not be represented by homologous landmarks. Variations in morphology affected by the biceps femoris and its force on the linea aspera of the femur are therefore tracked only with surface semilandmarks applied to the diaphysis of the femur.

2.1.2.7 Distal

The gastrocnemius is a superficial muscle which originates from two heads attached to the medial and lateral condyles of the femur. The larger head attaches to the medial condyle. For both the medial and lateral head the muscle fibers extend to the inferior portion of the femoral diaphysis. The muscle inserts into a tendon shared with the soleus muscle and form the tendon calcaneus or Achilles'

tendon. The plantaris is also a superficial muscle and originates from the distal lateral portion of the linea aspera after the linea aspera divides. Its tendon runs medial to the tendon calcaneus and inserts into the calcaneus. These muscles form the calf and are responsible for extending the foot allowing for bipedal strides and also for bending of the knee when the foot is fixed. The popliteus is a deep muscle which originates from the anterior portion of a groove on the lateral femoral condyle. It inserts medially superior to the popliteal line of the tibia. The popliteus aides in flexion of the leg and when the leg is flexed rotates the tibia medially. The linea aspera once again arises as a point of origin for a muscle, but once again lends no homologous points and must be quantified with surface semilandmarks. However, the condyles and epicondyles do lend themselves to homologous points. Particularly femoral landmarks twenty through twenty-three are notable for these muscle attachments as these landmarks describe the posterior superior margin of the medial and lateral femoral condyles.

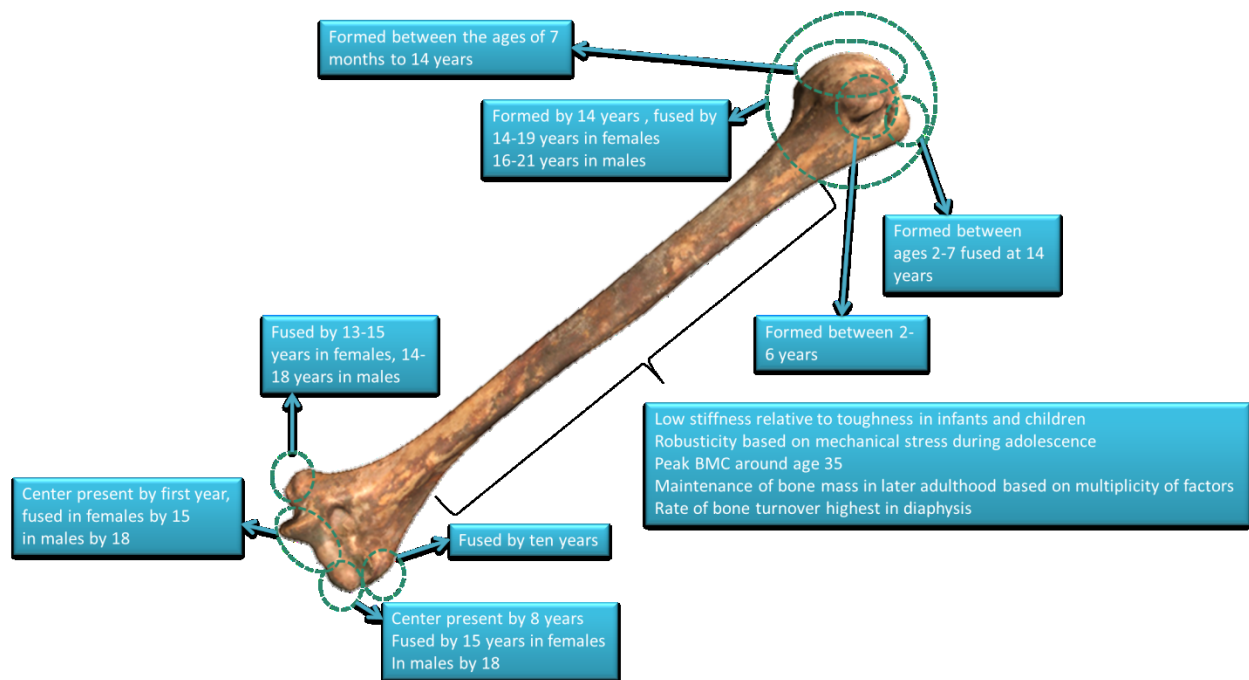


Figure 2.1 Timing of development for humerus (Rho et al., 2002; Ruff & Hayes, 1982; M. Schaefer et al., 2009b).

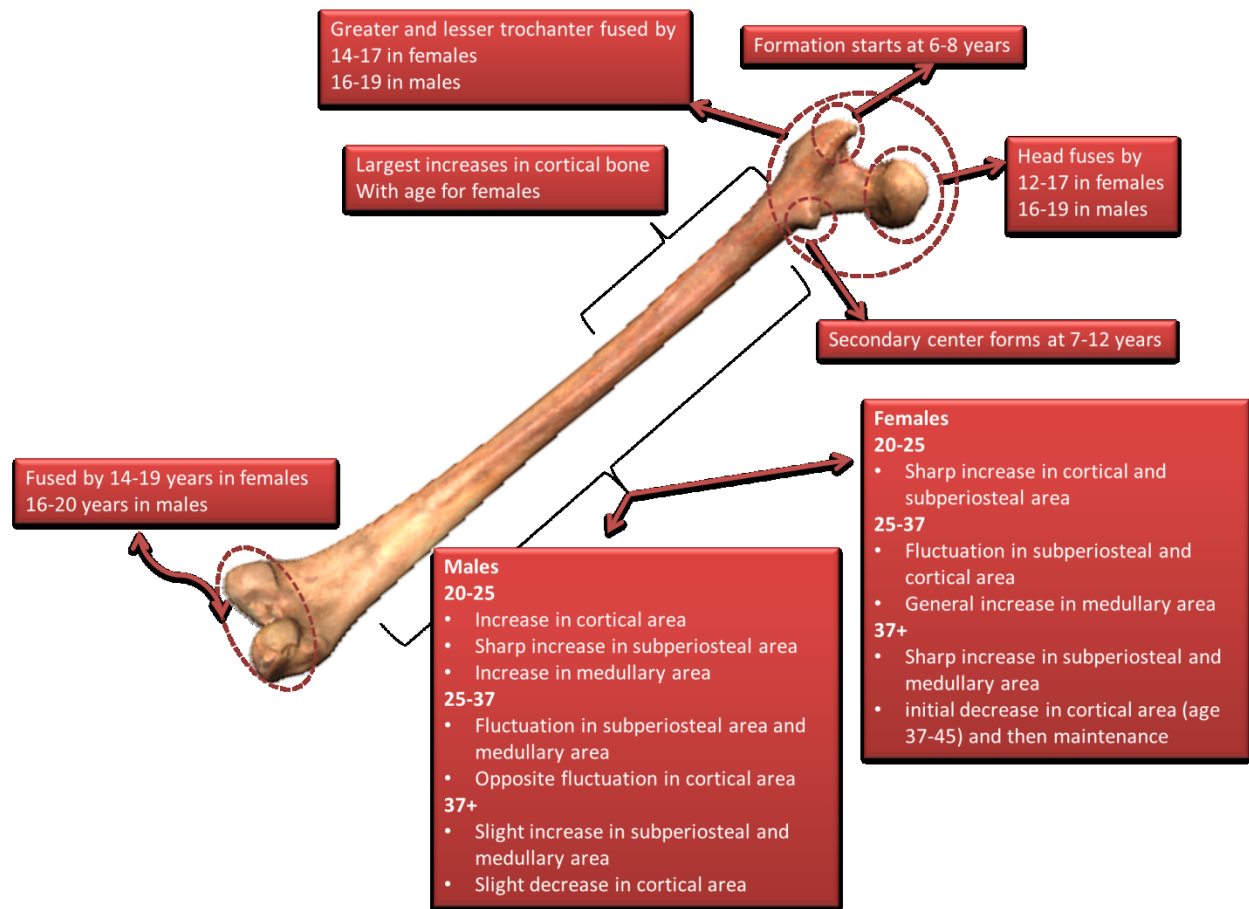


Figure 2.2 Timing of development for femur (Ruff & Hayes, 1982; Schaefer et al., 2009).

2.2 Intrapopulation variation

Intrapopulation variation and its effect on long bone morphology is the primary concern of this thesis. The following sections will attempt to summarize the relevant literature for each factor considered and explain how they may relate to morphological variation. Considerations of ancestry, heritability, and phenotypic variation in relation to climate or clinal distribution will be discussed in the following section 2.3 on interpopulation variation.

2.2.1 Sex and Sexual Dimorphism

The effects sex has on morphology may be divided into three categories: genetic effects of sex regarding primarily hormones and their effect on pelvic morphology and the rate of deposition and resorption of bone, secondary biological effects such as the difference in mechanical loading during locomotion on parts of the femur due to morphological differences in the pelvis, and cultural effects

such as sexual division of labour and sexually specific gastro-cultural practices. While these topics are distinct from one another they are also interrelated. For example, nutrition and activity levels will influence the rate of deposition and sexually specific life events such as menarche and menopause in women will drastically alter not only her biology but also her sociocultural position (Agarwal et al., 2004; Agarwal & Stout, 2004; Bilezikian et al., 2008; Brickley, 2002; Chamberlain, 2006; Eden, 1998; Hawkes, 2003; Kachel & Premo, 2012; Karapanou & Papadimitriou, 2010; Leiberman et al., 2001; Lewis, 2006; Lewis et al., 2016; Low et al., 2012; Mays, 1996, 2000, 2010, 2015b; McDade, 2003; Pálfi, 1997; Porcu et al., 1994; Post, 1971; Riis et al., 1996; Scheuer & Black, 2004; Vedi et al., 1996; Villamor et al., 2011; Waldron, 2009).

In the medical literature tremendous attention is given to osteopenic processes (see section 2.2.4.3) particularly in post-menopausal women and the assumption remains that while men may suffer bone loss due to hormonal fluctuation particularly in old age (F. H. Anderson et al., 1996) the risks for women are greater (J. B. Anderson & Garner, 1998; Eden, 1998; Karapanou & Papadimitriou, 2010; Riis et al., 1996; Vedi et al., 1996; Zeng et al., 1996). In 2004 the World Health Organization recommended that osteoporosis be diagnosed on the basis of bone mineral density (BMD) being 2.5 standard deviations or more below that expected for a young woman (*WHO scientific group on the assessment of osteoporosis at primary health care level*, 2004). Osteopenia does affect both males and females, but in modern populations is disproportionately severe in older women, and this ratio does carry over into the archaeological record (Eden, 1998; Mays, 1996). (However, in past populations some studies suggest that osteoporosis may have been more equally distributed between the sexes (Agarwal et al., 2004).) In virtually all studies remarking on osteoporosis hormonal imbalance (for females as well as males) due to life events or environment is cited as the likely culprit and hormonal therapy cited as the best therapy (F. H. Anderson et al., 1996; Eden, 1998; Kaastad et al., 2000). While the rates of subperiosteal deposition are roughly similar in females and males, and the rates of endosteal deposition actually favor females 11% versus 7% for males, the rate of endosteal resorption (or medullary expansion) for females is 39% whereas for men it is 19% (Ruff & Hayes, 1982, pp. 946). This elevated rate of averaged endosteal resorption has multiple aetiologies and is very much a product of genetic, epigenetic, and cultural factors. The primary aetiology appears to be largely due to the influence of hormones on the skeletal system. Bones are not entirely mechanical in nature and serve additionally as a reservoir for certain nutrients most notably calcium (Ruff, Holt, & Trinkaus, 2006). Life events for women including particularly parturition and lactation are initially calcium depleting. (Although, prolonged lactation has been shown to replace calcium and increase endosteal deposition (Agarwal et al., 2004). Such life events

may demand a degree of sedentism in addition to cultural expectations of activity. This could result in a situation where mechanical strain is insufficient to maintain bone deposition while biological requirements demand increased resorption (Brickley et al., 2007; Mays, 2015a). Sexual dimorphism would contribute to a diaphyseal morphological difference in that the smaller size of female long bones would impact the degree to which endosteal deposition or resorption could reasonably occur.

Location of subperiosteal and endosteal remodeling is also sexually dimorphic. Ruff and Hayes (1982) found that deposition with age in female femora and tibia occurred mostly in the proximal femur and the mid-distal shaft of the tibia whereas for males in both the femur and tibia deposition occurred mostly at midshaft. In both sexes, the second moment of area (I_{\max} : the greatest axis of the cross-section) at the midshaft increases with age. Ruff and Hayes theorise that this may be due to different patterns of mechanical strain in males and females due to different pelvic orientation, but it is noteworthy that in regards to the cross-section this fact could artificially influence results especially in studies like this where only the cross section at midshaft is considered. For a more in depth discussion of deposition and resorption refer to Section 2.2.3.

Beyond hormonal influences on the whole skeleton, female femora may have distinct morphology when compared to male femora due to the very specific obstetrical demands of human parturition. The valgus angle in females and males is likely to be variable due to the variant morphologies of the pelvis and therefore the demands of locomotion (K. M. Brown, 2015; C O Lovejoy et al., 1973; Lycett & von Cramon-Taubadel, 2013; Neubauer & Hublin, 2012; Ruff, 2005). Additionally, human sexual dimorphism includes a component of size difference and so it is likely that there will be allometric effects where shape varies with size. The variation in the valgus angle and the possible allometric effects represent the two largely consistent factors affecting morphological variation with sex (Bigoni et al., 2010; Klingenberg, 1998; Organ & Ward, 2006; Pomeroy & Zakrzewski, 2009; von Cramon-Taubadel & Lycett, 2014). It is unlikely that the valgus angle in particular will be disrupted by factors like childhood stress, bone type, age, or even population, but hormonal issues will be interrelated with any and all of these factors. Therefore, sex must be considered with each of these factors, and it should be recognized that any morphological variation seen in the skeleton due to hormones will be a function of both sex and age.

2.2.2 Age

In Bioarchaeology chronological, biological, and social age are recognized (Gowland, 2006, 2007). Social age is beyond the scope of this research, but should be considered in interpreting results.

Determining or estimating biological age in subadults is achieved by observing the developmental landmarks which have been achieved including most prominently epiphyseal union and tooth development and eruption (Brothwell, 1963; Miles, 1962, 2001; Scheuer & Black, 2000; Ubelaker, 1989). However, biological age estimation in adults is achieved largely through analysis of the degree of degeneration (Brickley & McKinley, 2004; Gowland, 2007). Degeneration occurs in a less clearly predictive manner than development at less mobile joints like the pubic symphysis, auricular surface, cranial sutures, and sternal rib ends. Skeletal changes at these joints are used to estimate broad adult age categories (e.g. young adult, middle adult, and older adult) (Brooks & Suchey, 1990; Margaret Cox, 2000; Loth et al., 1994; C O Lovejoy et al., 1985; Meindl & Lovejoy, 1985). In some populations it is also possible to use tooth wear to estimate age (Brothwell, 1989). However, Miles (1962, 2001) cautions that although age estimation using tooth wear is a reliable system, the rate of wear is not always consistent between populations and therefore should be reassessed for each population especially those with varying dietary habits.

In this study, age was estimated using epiphyseal union particularly of the clavicle, and degree of degeneration at the pubic symphysis, and auricular surface. A fuller discussion of aging techniques can be found in Section 3.2. Cranial sutures were not used because of the high degree of interobserver and intraobserver error shown in that method of age estimation (Mays, 2015b; Miles, 2001). Sternal ribs ends were also not used to estimate age due to the taphonomic damage in several of the collections as well as the curation of the skeletons making identification of the fourth rib difficult to impossible (İşcan et al., 1984, 1985). Tooth wear was not used in age estimation because the study included diverse populations with varying diets and because none of the populations had an established standard to which tooth wear could be compared (Miles, 1963)(Brothwell, 1963; Miles, 1962, 2001).

Archaeologically reported age ranges become increasingly inclusive in older age, the last category often reported as some variant of “over 50 years” or “45+”. Aside from being imprecise, this can present statistical and demographic problems. Gowland (2007) underscores the mismatch between epigraphic or historical reports of age and those skeletal and explains how taphonomic effects, statistical issues, and the sociocultural perception of age may influence a demography. Gowland (2007) and Samworth and Gowland (2007) demonstrate how the application of Bayesian statistics may correct for statistical errors in mortality profiles but caution that all statistical models for adjusting mortality profiles require assumptions specific to the skeletal sample in question.

Human longevity particularly that of post-menopausal women could be largely responsible for or symbiotic with our neurological evolution. Post-menopausal women are unable to produce additional offspring and therefore take fewer resources, but are still able to contribute. This means they may make up for and provide for daughters who are temporarily unable to contribute resources due to pregnancy (Hawkes, 2003). However with our current methods of estimating biological age, these critical individuals disappear or at least, detail is lost. Besides the attraction to the middle, aging of skeletons is dependent upon the taphonomic survival of the pubic symphysis and auricular surface both of which are made up of cancellous bone which degrades easily. Older individuals are especially vulnerable to taphonomic erasure due to their lower bone mineral content (BMC) (Gowland, 2007).

Some of the pathologies considered in this study are specific to advanced age. Several of the publications on osteoporosis use some variation on the terminology “age related bone loss” to describe osteopenia which does not comfortably fit the diagnostic threshold of osteoporosis, and osteoarthritis is largely considered, if not due to wear or microtrauma, a vagary of age (Agarwal et al., 2004; Brickley, 2002; Jurmain, 1980, 1999; Mays, 1996; Weiss & Jurmain, 2007). Degeneration of joint capsules is noted as a signifier of advanced age, but so is an increase in prevalence of enthesal changes (Cardoso & Henderson, 2010; C. Y. Henderson, 2009). In fact, Cardoso and Henderson noted that the only correlation that could be found for enthesal changes was age. In the context of ossification of cartilaginous tissue as indicative of age, this is highly suggestive that pathologies and conditions such as enthesal changes and osteoarthritis have less to do with activity patterns than they do factors such as age. (For further discussion of enthesal changes refer to Section 2.2.4.3.2.)

Demonstrating the interrelatedness of hormones and age on pathology and potentially morphology, Jurmain (1999) notes that women maintain a lower rate of osteoarthritis until the onset of menopause at which point the prevalence of OA in women well overtakes that of men pointing to a hormonal aetiology for this particular pathology. Additionally, for osteoporosis, both Agarwal and colleagues (Agarwal et al., 2004) and Mays (1996) separately observe that the rate of bone loss increases around menopause, but does not substantially change thereafter. Several studies have concentrated on sexual difference in prevalence of such pathologies as indicative of distribution of labour or sexual difference in diet or activity patterns (J. B. Anderson & Garner, 1998; Bridges, 1989b, 1991; Lovell, 1994) but if the impact of changing hormones in men and women contributes to a sudden but not maintained prevalence in pathological conditions then age and the appearance of age may have a more hormonal explanation.

While the epiphyses of the long bones do not completely fuse until late adolescence or early adulthood their morphology does seem to be dictated by environment, health, weight, and activity during childhood (Drapeau & Streeter, 2006; Frost, 1999; Hamrick, 1999). Unlike the points of articulation, diaphyseal particularly cross-sectional morphology appears to retain plasticity into adulthood with the rate of deposition and resorption for each part of each bone largely determined in late adolescence or early adulthood with a peak in bone mineral density occurring in the mid-thirties (Drapeau & Streeter, 2006; Rabey et al., 2015; Rho et al., 2002; Ruff, 2005; Ruff, Holt, & Trinkaus, 2006; Wallace et al., 2012). Sub-periosteal and endosteal deposition and resorption in the diaphyses of long bones appears to be dependent on numerous intrinsic and extrinsic factors and particularly sensitive to mechanical strain, but in general the loci of deposition or resorption is age dependent (Ruff, Holt, & Trinkaus, 2006). In childhood subperiosteal deposition and endosteal resorption are dominant (Frost, 1999; Trinkaus et al., 1994). In adolescence and through early adulthood deposition occurs more prominently on the endosteal surface. Finally in the fourth decade, the process usually reverses with medullary expansion or endosteal resorption becoming the predominant characteristic of cross-sectional morphology (Trinkaus et al., 1994). This means that particularly cross-sectional and surface morphology of the diaphysis should be age dependent even in adults.

Age cannot be separated completely from factors like sex, development and pathology and vice versa. All of these factors however influence morphology of the long bone at the time of death as well as the expression and survivability of various pathologies. The following sections therefore will continue to reference age and its impact on morphology.

2.2.3 The Whole Bone: Development, Mechanics, and Metabolism

The now widely known “Wolff’s law” is the underpinning theory of biomechanics. Based on his 1892 publication studies continue to be published using Wolff’s work as a theoretical and sometimes even mathematical basis (Biewener et al., 1996; Boyle & Kim, 2011b; Bridges, 1991; Chen et al., 2010; Currey, 2003; De Groote et al., 2010; Drapeau & Streeter, 2006; Frassica et al., 1997; Frost, 1994, 1999, Jang & Kim, 2008, 2010; Lieberman et al., 2004; Marchi, 2015; Mays, 2001; O’Higgins et al., 2012; Özener, 2010; Pomeroy & Zakrzewski, 2009; Rabey et al., 2015; Ruff et al., 1994; Sofaer-Derevenski, 2000; Sparacello & Pearson, 2010; Weiss, 2005; Wilczak, 1998). Wolff observed that bones react when force is applied to them. Building upon the work of previous academics particularly in regards to the internal structure of the bone Wolff set out to mathematically predict forces enacted on the bone and bone’s “functional adaptation,” to them with some emphasis on the internal structure (Wolff, 1986).

Wolff's impact has been legendary but recent studies question to a degree the mechanical applicability of Wolff's original work and some of his assumptions as well as the interpretation of the theory of "functional adaptivity" in many publications. This has led to some humorous phrases like, "who's afraid of the big bad Wolff," (Ruff, Holt, & Trinkaus, 2006) with the counterpoint of "a Wolff in sheep's clothing," (Barak et al., 2011) but the critiques of the perhaps over interpretation involved in some activity reconstruction or especially occupational markers research is warranted.

As Ruff and colleagues commented, the difficulty in applying Roux's and particularly Wolff's laws is that bones, particularly long bones are multifunctional (Ruff, Holt, & Trinkaus, 2006). Neither Roux nor Wolff set out to create a scientific "law," and in neither case do their observations constitute a law, but their writing continues to be relevant causing the larger osteological community to commonly refer to the observable phenomenon of morphological and structural osseous modification in reaction or relation to activity and loading as either Roux's or Wolff's law. Roux observed structural and morphological variation in loaded versus unloaded human bone and posited that the bone adapted to adequately and ideally mollify mechanical stress on the bone. The classic interpretation of Wolff's law and his own writing on it ignore all but the structural and mechanical functions of bones. His biomechanical analysis of bone was mathematically peerless but offered no rumination on bones as serving a metabolic or developmental function. Roux's law is more malleable as he did not delve into the physics involved and simply made the observation that forces acting on bones may alter the morphology of the bone (Roux, 1881 and Wolff, 1986 in Ruff, Holt, & Trinkaus, 2006). Later analysis of this concept show that the basic interpretation of Roux's and Wolff's laws – that osseous morphology may vary and adapt with loading – is generally correct. However, there are numerous stipulations. Osseous adaptation is dependent upon the type of loading; Shaw and Stock show in their study large variation on the morphology and index of cortices for semi-professional athletes in swimming, field hockey, cricket, long-distance running, and controls (Shaw & Stock, 2009a, 2009b). Other authors show that some types and duration of loading – particularly running – may even have a deleterious effect (Bourrin et al., 1994, Li et al., 1991, Ma et al., 2010; 2011, and Matsuda et al., 1986 in Wallace et al., 2012). Additionally, the area of the bone or type of bone that is most reactive to biomechanical loading is also variable. Roux in particular observed osseous reaction in cancellous bone and Wolff also addresses this area. Other authors also suggest morphological variation with mechanical loading in enthesal changes (Zumwalt, 2006) and general morphology (Rabey et al., 2015). There is also debate on when in an individual's life their bones are most susceptible to morphological reorganization on the basis of biomechanical loading with numerous authors supporting the view that most morphological organization of the long bone

occurs during childhood and adolescence, and other authors suggesting that morphological reaction to loading continues throughout adulthood (Frost, 1994, 1999; Hamrick, 1999; O. M. Pearson & Lieberman, 2004; Rabey et al., 2015; Ruff, Holt, & Trinkaus, 2006; Shaw & Stock, 2009b).

Long bones in particular have three main functions: structural, mechanical, and metabolic (Bilezikian et al., 2008; Confavreux et al., 2009; Currey, 2003; Lee et al., 2007; Lee & Karsenty, 2008; O. M. Pearson & Lieberman, 2004; Rho et al., 2002; Wallace et al., 2012; Wei & Ducky, 2010). Roux and Wolff's laws primarily concern themselves with the former two with Wolff attempting to create very specific equations for how bone would react to the forces exerted upon it. Wolff's error was attempting to create a simplified set of equations describing very specific phenomena (Ruff, Holt, & Trinkaus, 2006). This background section on biomechanics will also focus primarily on the structural and mechanical function of bones, but the metabolic role can impact shape and function and therefore will also be addressed. This subject is complex and difficult to represent in a linear fashion especially where shape is paramount. Each of these factors is interrelated in such a way that they will consistently influence one another. To reflect this but illustrate the concept in written form I will first address bone shape and potential events during which shape might be altered at a gross or microscopic level. I will then cover the three main functions of bone: structural, mechanical, and metabolic as it pertains to biomechanics and shape, and then I will visit upon modelling and remodeling.

One set of definitions must be made before continuing as differences exist with respect to the use of specific terminology between the various subdisciplines of anthropology and archaeology. In biomechanics "stress" and "strain" here carry special meaning. Stress in a biomechanical sense is loading and is a function of force over area. Strain is the amount of deformation (Bilezikian et al., 2008; Currey, 2004; Currey et al., 1996; Frassica et al., 1997; Harrigan & Hamilton, 1992; Lieberman et al., 2001; Lieberman et al., 2004; Rho et al., 2002). A dependent term, "elasticity" describes the moment where the stress does not continue to increase without a significant increase in strain. Elasticity is often described in terms of Young's modulus or the ratio of compressive stress over longitudinal strain (Currey, 2003, 2004; Currey et al., 1996; Jacobs et al., 1995; Jang & Kim, 2008; O'Higgins et al., 2011; Parr et al., 2012; Reilly & Currey, 2000; Rho et al., 2002). This ratio was developed for mechanical rather than biomechanical purposes and therefore it is useful to remember that while the human skeleton does have a very important mechanical and structural component, its other biological functions or lack of adaptation will prevent it from being described in its entirety in biomechanical terms.

2.2.3.1 Morphology

This thesis attempts to address the entirety of long bone morphology and address the possibly variable morphological reaction of different parts of the long bone to intrinsic and extrinsic factors. By necessity the shape consideration of the bone are split into three main parts: the epiphyses, the diaphysis, and the cross-section. Each of these sections however impact the mechanical and structural integrity of the others and the bone shape as a whole will theoretically change with any sort of physical, metabolic, or hormonal impact on any part of the bone. Therefore, shape variation should be consistent across the entire bone. Furthermore, the final shape of the bone at death may be impacted by numerous factors the most obvious being intrinsic factors like sex and heritance.

Currey states that it is reasonable to consider bone to be a material whose mechanical properties are determined by factors other than the phylogenetic status of the animals from which specimens came” (Currey, 2004: pp. 549). That is, while population affinity is a factor, interpopulation variation is likely also impacted by environment and within species morphological variation may be primarily or even exclusively dictated by environmental factors. Between species with different locomotive behaviours different femoral cross-sectional morphology is evidenced (Currey, 2003) and this is reflected in exclusively human studies as well where athletes and even different kinds of athletes show different cross sectional morphologies (Shaw & Stock, 2009a, 2009b). In experimental studies on sheep and pigs where the animals could be exercised in a controlled manner, loading created a morphological but not material change in long bones (Currey, 2003; Lieberman et al., 2004; Zumwalt, 2005, 2006). The close relationship of morphology – particularly but by no means exclusively cross-sectional morphology – and loading is widely recognized (De Groote, 2011a; Drapeau & Streeter, 2006; Lieberman et al., 2001; Marchi, 2015; Rabey et al., 2015; Rhodes & Knüsel, 2005; Ruff, 2000, 2002; Schwartz et al., 2013; Stock & Pfeiffer, 2004; Wallace et al., 2012; Yamanaka et al., 2005).

As hinted above mechanical and structural integrity are due largely to shape, but also to mineralization. Different bones may have different levels of mineralization and this will change through life (Agarwal, 2008; Agarwal et al., 2004; Bilezikian et al., 2008; Currey, 2003; Currey et al., 1996; Gowland, 2007; Haduch et al., 2009; Rho et al., 2002). There is a genotypic basis for the initial bone mineral content (BMC). Currey (2003) uses the example of newborn atlas deer and human infants. Newborn deer will be required to move with the herd very shortly after birth, therefore their long bones must support them and they are born with a higher level of BMC than human neonates. Currey describes these varying levels of mineralization as “stiffness” and “toughness.” Atlas deer being cursorial

animals have stiff highly mineralised bones which will support their weight as they begin to run immediately after birth whereas human infants have tough bones with lower mineralization which cannot immediately support their weight, but are less likely to form micro-cracks. Unlike shape, mineralization does not change with loading, but is important from a structural and mechanical vantage as stiffer bones are able to support more weight, but tougher bones are better able to resist fatigue damage and therefore remodeling (Currey, 2004; Martin, 2003; Reilly & Currey, 2000; Zioupos et al., 1996, 2008). Currey goes so far as to say that a bone's functionality depends on the dual factors of "bone material, and arrangement of this material in space – the size and shape of the bone," (Currey, 2003: pp. 1487).

Morphology according to much of the previous biomechanical literature is paramount. Section 2.2.3.4 will discuss the metabolic function of bones, but the emphasis on morphology in the above citations and many other past publications is warranted. If Wolff's law or – as Ruff and colleagues (2006) prefer – Roux's law is accurate then morphology as quantified in this study will in some way reflect extrinsic factors due to the plasticity of bone.

2.2.3.2 Structure

Shape and structure are closely interrelated as they allow the bone to be supportive. The ability of the bone to support weight is dependent on its stiffness (high BMC) while its resistance to failure is dependent on its toughness (low BMC). Put simply the more a bone can bend the less likely it is to break but also the less likely it is to be able to support loads without bending. Currey shows a positive relationship between the "tension in bending" or elasticity and calcium content in bone as well as an inverse relationship between calcium content and strain at failure (2004). Rather unsurprisingly, strain has been shown to decrease with increasing elasticity (Les et al. 2002 in Currey, 2004) and there is a positive relationship between ultimate stress and elasticity (Currey, 2004). Therefore the ability of a bone to function structurally as load bearing without failing under strain is linked to the level of mineralization of the bone. However, as noted in the introduction to this section not all features of bone are adaptive, the general structure and microstructure will change with intrinsic factors like age and remodelling, and extrinsic factors like maternity, pathology, or poor nutrition can cause structural changes to the bone.

While the bone may not be mineralised to the ideal level of adaptivity for its total function including biomechanics, structure, and metabolic, there is a theoretical ideal level of mineralization or

balance of stiffness and toughness for each bone (Currey, 2003) although, bones may operate effectively well outside of the ideal. Structure, and structural integrity, is also dictated by the arrangement of osteons. In an ideal system, osteons in long bones will be arranged longitudinally, but this is not always the case particularly in subadults (Rho et al., 2002). Additionally, while different species and even bones in the same individual might have different levels of mineralization or arrangement of osteons simply for the adaptive purpose of that bone in the system, mineralization and osteon arrangement appear to differ between different parts of the same bone (Rho et al., 2002). Both the level of mineralization and the arrangement of osteons change with age and this will be covered in slightly more detail at the end of this section.

Bone's ability to neither bend under loading nor break is due to its level of elasticity or measure by Young's modulus. As mentioned in the introduction to this subsection, elasticity is a measure of the degree to which a substance can withstand stress without significant strain. Currey shows that "strain tends to be less in the stiffer bone ... the relationship is tighter when Ca is the independent variable," (Currey, 2004: pp. 553). This is all logical, however as previously noted, mineralization and osteonal arrangement is not consistent throughout the bone. Rho and colleagues in fact, find a "clear and consistent difference between the stiffness of the bone in the osteons and the surrounding interstitial bone," (Rho et al., 2002: pp. 193). This means that the ability of a bone to support loads or stress is dependent upon its stiffness which is in turn dictated by the arrangement and number of osteons. In spite of previous protestations that bones may not be perfectly adaptive particularly in their structure and mineralization, Currey mentions firstly that bone strength is largely consistent over a wide range of different species and there is little to no possibility of reasonably increasing the strength or elasticity of the bone over what it already has (Currey, 2003). (While this is undoubtedly accurate, see below for a brief mention of the metabolic effects of parturition). With osteons and osteonal arrangement being the source of stiffness in a bone, ideally the bone will only experience one major source of loading or stress (Reilly & Currey, 2000). Therefore stiffness and elasticity of the bone as a whole will be dependent upon the arrangement of osteons and interstitial bone, in vivo loading which may determine the arrangement particularly of the secondary osteons, and age dictating whether the individual has yet lived long enough to have secondary osteons or has experienced metabolic effects which would alter either the arrangement of osteons or the BMC (Rho et al., 2002).

The arrangement of bone's microstructure as well as its overall structure, and its alteration with age and loading are of particular importance to the structure of the bone. Before addressing the very

pertinent microstructure a few general comments on the morphology of the overall structure of the long bone are warranted. One of the major criticisms of Wolff's law has to do with his treatment of bone as a simple cylinder (Ruff, Holt, & Trinkaus, 2006). In fact, a long bone consists of cancellous bone, and trabecular bone and the argument could be made that subchondral bone is also distinct from these two forms of bone. Trabecular and cancellous bone in particular have very different densities and will react differently to stress events both physical and metabolic or hormonal. Osteopenia may be observed as the relative widening of gaps in the trabecular structure (Agarwal et al., 2004) as well as the thinning of cortical bone in metacarpals (Mays, 1996). However, cortical bone also appears to be remarkably reactive to various types of loading (Stock & Pfeiffer, 2004). All of these changes in bone would affect its structure and structural integrity and in fact, archaeologically osteoporosis is not diagnosed until a structural failure has occurred (Brickley & McKinley, 2004). Beyond the types of bone, long bones are anisotropic or, stated as a tautology, long bones are long. This means that ideally all structures within the long bone will also be longitudinally oriented. But that is not always the case. Generally, in adult bones osteons are arranged longitudinally with Haversian canals therefore running parallel to the length of the bone, but Volkmann's canals must run transversely (Currey, 2003) and to a degree so must canaliculi. Likewise lamellae, while typically ideally oriented given the necessities of osteons, do form around the lacunae which causes force to be directed not straight on, but around this "flow" of lamellae (Currey, 2003). To conflate the microstructural issues there is no guarantee that secondary osteons will always be ideally oriented and in fact usually interrupt the existing lamellar structure (Currey, 2003). Unsurprisingly then, interstitial bone will be stiffer than osteonal bone (Rho et al., 2002), but will have a non-linear structure through which forces may be directed. Elasticity in bone is also higher longitudinally (Reilly and Burstein, 1975 in Currey, 2003). Currey points out that the various microstructural voids in bone will then act as "stress-concentrating" and be in turn somewhat relieved by the previously mentioned lamellar flow as it redirects forces (Currey, 2003: pp. 1489); however, there does not seem to have been an attempt to quantify the stress and strain as it varies based on the microstructure of the bone. The other assumption often made and certainly made by Wolff (Ruff, Holt, & Trinkaus, 2006) is that bones, particularly human bones are hollow. This is only partly accurate. Human bones are not solid (unlike those of alligators and manatees which do have almost solid long bones), but the medullary cavity is filled with marrow which depending on age will be either hemopoietic or fatty (Currey, 2003; P. L. Walker et al., 2009). A cylinder would be stiffer than solid bone, but because of the fatty marrow they are not and probably have different structural values than if they were truly hollow. However, fat is considerably less dense than bone. Currey also notes in this observation that birds and pterodactyls

have tremendously thin cortices and their medullary cavities in some cases is filled with gas (Currey, 2003). Curry remarks that the fat stored in the medullary cavity is not used until the “final stages of starvation” (2003: pp. 1492) and that therefore suggests that the relative thickness of the cortex of the long bones in various species is adaptive to their means of locomotion. The very thick boned animals mentioned are aquatic and might need the almost solid bones to resolve issues of neutral buoyancy. Humans and other mammals with fatty marrow in relatively large medullary cavities are terrestrial and would require some weight for effective locomotion whereas animals which fly like birds, bats and flying foxes, and pterodactyls would need bones which can support the musculature necessary to move their wings, but would not significantly alter their weight and then the power that they would need to take flight.

Much of bone’s structure is dependent on age and life events. General trends point to peak bone strength, elasticity, and recovery for young to middle adults and a steady decline thereafter. Subadult bone will be tougher than adult bone and BMC will increase until thirty-five years of age in humans and decrease thereafter (Rho et al., 2002). Optimal BMC or elasticity has not been pinpointed and may vary between individuals as studies variously indicate a decrease or increase in elasticity with age (Rho et al., 2002). Rho and colleagues note that there “may be a point of optimum mineralisation whereby when a certain mineralisation threshold is exceeded bone becomes weaker,” which may explain the dissonance between studies regarding the stiffness of bone with age (Rho et al., 2002: pp. 189). Furthermore, bone stiffness changes with age in both the osteonal and interstitial areas (Rho et al., 2002). Further to the point noted two paragraphs above regarding the position of secondary osteons, Currey notes that fibrolamellar orientation changes with growth and may not necessarily be oriented in advantageously to direct force around voids (Currey, 2003). This could be a factor on why subadult bone tends to be tougher but not stiffer. If continued growth means an increasing patchwork of fibrolamellar bone it may be more adaptive for BMC to increase after growth is complete. Complicating the overall picture females experience metabolic stresses on their bones from parturition and arguably for normal reproductive cycles. This can result in a general thinning of cortices in females, but some studies suggest in humans the effects may be somewhat offset by extended breast-feeding (Agarwal et al., 2004; Currey, 2003). Finally, while it is clear that BMC is not altered with loading the microstructure, particularly in the process of remodelling, is. As structure impacts “stiffness” and “toughness,” it will impact the bone’s functionality or ability to bear weight. Here morphology may be understood as a concession to microstructural realities as the bone reacts to intrinsic and extrinsic pressures. The relevance of this discussion to this thesis is that while it can be argued that the main function of bone is structural, the

multiplicity of biological functions which maintain bone and in which bone participates mean that morphology cannot be understood as purely biomechanical. The internal microscopic structure of bone is crucial to its development and maintenance, but cannot be better than optimal. That is, the arrangement of the microstructure will never be perfectly ideal due to the process of resorption and deposition. BMC while crucial to structural integrity is dictated by other biological processes and beam theory as it relates to bones is undermined due to the consistent presence of bone marrow. Therefore, microstructure and the body's ability to maintain that structure will have continual effects on gross morphology whether due to catastrophic failure in the form of a fracture or to maintenance of the ideal levels of "stiffness" and "toughness" through BMC.

2.2.3.3 *Mechanics*

It is very difficult to divide structure and mechanics as the structure will speak to how mechanically effective the bone will be. Many of the points touched on above directly impact the mechanics of human bone. Elasticity is dependent on the bone being mineralised to have "higher yield stress" (Currey, 2004: pp. 553). Additionally, it is noted above that osteonal and interstitial bone vary in their microstructure and as hardness is an important factor in mechanics it is important to note that the nanoindentation values of both are different with osteonal sites being harder than interstitial bone (Rho et al., 2002). When applying these measures to bones it is important to remember that while variation in hardness or stiffness at the micro level may not have large variation, there is some variation – bones are not homogenous in their mechanical and structural properties, bone may not be set up to be ideally adaptive, and loading – while it will generally be mainly along the length of the bone - may involve tension, compression, and torsion (Currey, 2003; Rho et al., 2002). Additionally, Hoffer and colleagues found that hardness may be unrelated to age, sex, or even body mass and concludes that the mechanical qualities of bone are more due to the organization and tissue mass of the bone (Hoffer et al. 2000 in Rho et al., 2002). Thus the position and organization of osteons mentioned above is paramount and porosity could undermine the integrity of the bone (Currey, 2004).

Biomechanical models particularly Wolff's tend to assume that bone is ideally adapted to its structural and mechanical function. However, as stated at the opening of this section, bone must also be able to remodel and contribute to the metabolism. The microstructure of bone is heterozygous with varying levels of "toughness" and "stiffness" in the osteonal and interstitial bone dependent upon the age of the osteons and the ratio of calcium and water. This promotes elasticity and allows for growth

and development but also creates a matrix where secondary osteons often cut through the lamellae altering the level of structural integrity. However, cells are adaptive to the force exerted on them (Currey, 2003, 2004; O. M. Pearson & Lieberman, 2004; Ruff, Holt, & Trinkaus, 2006). On a macro level, this can influence the shape and relative size of the joint surfaces as children with higher body mass developed larger joint surfaces particularly in their knees (Frost, 1999); however, it will also influence the organization of bone on a cellular and material level (Currey, 2003). This is partially an evolutionary adaptive trait as shown previously with the relative stiffness or toughness of newborn atlas deer as compared to newborn humans, but there is also an ontological effect where strain or loading causes the bone to react materially and morphologically to the particular situation of the individual (Currey, 2003). It is notable however that the morphological change is small, which for this study suggests that morphological differences may not be detectable in conjunction with the various factors which could be associated with different levels of loading. Currey (2003) notes that bone is adaptive to loading at a cellular level with increased mineralization and in a later publication he correlates mineralization with elasticity (Currey, 2004). However Rho and colleagues (2002) caution that increased or excessive mineralization may lead to localised damage – micro-cracks - which would undermine the structural integrity (Martin, 2003; Reilly & Currey, 2000; Zioupos et al., 2008). Additionally, due to its inconsistent turnover rate the bony matrix consists of both old and young tissues. Older tissues are generally stiffer with higher mineralization and younger tissues generally tougher and more resistant to micro-cracks (Grynpas, 1993 in Rho et al., 2002). This leads further credence to the idea that there would be a peak level of mineralization or stiffness relative to toughness around the age of thirty as by that age enough tissue would be old enough to be mineralised but the bone would still have a high enough turnover rate to avoid hypermineralization. The level of mineralization and arrangement of osteons and lamellae tends to be mechanically adaptive, but not in a consistent or readily quantifiable sense. The arrangement of bone in general meets and responds to the various loading necessities of the individual, but long bones in a mechanical or structural sense do not appear to be perfectly efficient adaptations to their usage. One must consider the assertion that evolution is not always adaptive, but in the case of bone especially there are other factors at play and some of those shall be discussed below.

2.2.3.4 Bone Mineral Content, Modelling and Remodelling

As suggested previously, bone grows, and while its primary function is mechanical and structural, it also serves metabolic purposes and particularly in humans is subject to growth and repair. This subsection will attempt to cover the metabolic aspect of bone as well as modelling and remodeling.

Hinted but not explicitly stated in previous sections is the fact that the initial modelling of bone is “probably rather uncoordinated,” (Currey, 2003: pp. 1487). Remodeling is the replacement of that bone in a more organized sequence which should leave the total bone mass intact but does directionally reorganize the bone. Human infant and juvenile skeletons are replete with woven bone which in adults would indicate healing in response to a pathological process, but in subadults simply implies growth. Modelling involves the layering of woven and lamellar bone (which may be referred to as fibrolamellar or plexiform bone). This type of bone is very resistant to transverse loading, but not yet ideally organized for locomotion and the sorts of loadings that will be enacted upon the bones in adolescence and adulthood (Currey, 2003). Fibrolamellar bone is so oriented – or more correctly lacking in orientation – not due to expected loadings but rather because woven bone may be quickly laid down as a matrix over which lamellar bone may grow. Remodeling of the bone will then create Haversian systems more aligned to loading and thus more adapted to locomotion and normal loading. This form of remodeling has small to no metabolic impact. The bone is not being destroyed to introduce calcium or other minerals into the bloodstream because the bone mass remains largely unchanged with secondary remodeling (Currey, 2003). I will touch on instances where remodeling is undertaken for metabolic purposes in subsequent paragraphs. It should be noted here that if a child experiences malnutrition during growth, growth may be suspended. Extreme forms of malnutrition and multigenerational effects of malnutrition specifically in relation to linear enamel hypoplasia (LEH), cribra orbitalia, and B₁₂ deficiencies are discussed below, but here it is notable that temporary cessation of growth in the long bones can lead to the creation of Harris lines or medial-lateral lines of increased bone density near the epiphysis of a long bone. This increased bone density could possibly be a result of dead osteocytes not being replaced and therefore remaining hypermineralised in that location (Mays, 1985, 1995; McEwan et al., 2005; Nowak & Piontek, 2002). Fibrolamellar bone and remodeled bone have varying levels of resistance to mechanical forces and remodeling is a slow process which starts at the midshaft and radiates outwards over time. This means in children, the same bone can easily be remodeled near the center and fibrolamellar at the proximal and distal extremes. Recalling that in humans, young bone is typically more “tough” than “stiff,” the effect of remodeling and loading can lead to “creep” or

deformation of the bone due to low but persistent mechanical stress (Currey, 2003; O. M. Pearson & Lieberman, 2004; Zioupos et al., 1996). Once again it is necessary to note the distinct but close relationship normal growth and remodeling has with possible childhood stresses such as, in this case, rickets. While every child at risk for creep may not have rickets, a severe vitamin D deficiency would certainly cause greater risk by preventing normal mineralization (Brickley et al., 2005, 2007; Haduch et al., 2009; Ives & Brickley, 2014; Whyte & Thakker, 2013).

Secondary remodeling is not specific to humans but is largely specific to mammals and birds (and is seen in large reptiles) (Currey, 2003). Primary remodeling will orient osteons advantageously and continual iterations of remodeling will generally not alter this arrangement. However, remodeling is reactive to strain on the bone and so the arrangement of bone microstructure will change particularly at entheseal sites (however, gross morphology of the enthesis is not related to activity (Nolte & Wilczak, 2012; Rabey et al., 2015; Zumwalt, 2006)). This allows for the bone to alter itself in size or shape without weakening the muscle attachments (Currey, 2003). This change in the orientation of the bone is pertinent for growth and the resulting migration of the attachment sites, but it is also interesting in the context of variations in cortical thickness for different athletes (Shaw & Stock, 2009a, 2011) as it allows for the muscle attachment to remain consistent and appropriately strong regardless of remodeling of the endosteal or periosteal surface. In humans, growth involves an initial instance of remodeling where osteons are adaptively organized, but subsequent remodeling continually occurs often in areas of trauma, high strain, or where cell death has occurred. Assuming this process is consistent, bone remains “stiff” enough to support weight, but still “tough” enough to avoid fracture during routine activities. When remodeling is no longer balanced however, bone may become structurally flawed resulting in fracture from hypermineralization. There is some slight suggestion that remodeling occurs primarily in response to damage or cell death as humans are one of the few mammals that continually experience remodeling and in some mammals – notably artiodactyls like the atlas deer noted before – can have incomplete remodeling where an adult cross-section contains both remodeled and fibrolamellar bone (Biewener et al., 1996; Currey, 2003; Frost, 1999; O. M. Pearson & Lieberman, 2004; Ruff, Holt, & Trinkaus, 2006). Additionally, the anterior and posterior aspects of the cortices of radii of horses experience differing levels of remodeling and different arrangement of osteons due to mainly tensile forces on the anterior and compressive forces on the posterior (Currey, 2003). In humans, entheseal changes may in some cases be considered enthesopathies where their proliferation is due to trauma or a hormonal issue causing increased osteogenesis (Cardoso & Henderson, 2010; Havelková et al., 2011; J. Rogers et al., 1997; Samsel et al., 2014). Abnormally high rates of osteogenesis usually corresponds with

hypermineralization and potentially cell death, so it is possible that remodeling initially occurs due to strains on the bone from the muscle, but continues due to hormonal imbalances or an excess of trauma. This could and does occasionally lead to a situation where an individual's osteogenesis becomes pathological, but the reaction of bone remodeling specifically to strain and potentially trauma means that the reorganization of osteons will only occur in relation to strain on the bone. Remodelling can react to cell death (Gawri et al., 2014; Peng et al., 2003; W. Wilson, 2005) and there may be osteons which interrupt the lamellar flow, but the orientation will remain mechanically anisotropic (Currey, 2003; Winet, 1996).

2.2.4 Pathology

The morphology of human long bones is influenced by conditions within a normal non-pathological range simply due to the reactivity of bone. Therefore, when conditions exceed the normal threshold it is reasonable to assume that further morphological impact may occur in different parts of the bone. Additionally, the relationship may involve positive feedback in that if the morphology of the bone or joint is altered due to adverse conditions this may put the individual at greater risk for degenerative pathologies like osteoarthritis or osteoporosis which may further impact the morphology of the bone. This section will detail various pathologies included in the study and provide background for why they may be correlated with adult long bone morphology.

2.2.4.1 Developmental Stress

Biological stress is defined as a disruption of biological homeostasis. In bioarchaeology particularly recently there has been much concern that the term is overused, too generally applied, and conflated with "health" (Klaus, 2014; Reitsema & McIlvaine, 2014; Temple & Goodman, 2014). Concerns regarding the logical implications or applications of stress indicators have been brought up in literature as classic and relatively early as the "Osteological Paradox," (Wood et al., 1992). Despite these issues, the term stress is still widely used in Bioarchaeology, but DeWitte and Stojanowski (2015) optimistically note the increasing contextuality of its usage. DJD, OA, and Schmorl's nodes have been used to argue that a population is "stressed" or that one subsection of a population is more stressed than another (Angel et al., 1987; Bridges, 1994; Lovell, 1994; Novak & Šlaus, 2011). Such studies usually term the relationship as physical or activity related stress, but this still conflates the term with biological and for these studies, mechanical stress as well. Mechanical stress may well be a factor, and certainly, where loss of biological homeostasis whether momentary or prolonged causes the overproduction of cortisol thereby hormonally weakening cartilage or promoting overstimulation of the immune system stress

strictly defined could be related to these degenerative changes. However, in this thesis these degenerative issues are dealt with apart from stress. Stress here is considered biological stress serious enough to cause the formation of cribrous lesions in the ocular orbits or linear enamel hypoplasia (LEH). The assumption is that individuals with these stress indicators would have experienced disruption long enough and acute enough to cause lasting health issues which may later effect development of skeletal morphology as well as influence metabolic processes to the point where they would also affect resorption and deposition to the point of distinctive morphological variation.

There is mounting evidence to suggest that nutritional and immune deficiencies are intergenerational. That is, they are not specific to the individual. A single short instance of famine for one person may cause deleterious health effects in their children and even grandchildren (Gowland, 2015). Nutritional and pathological insults in an individual may be temporally isolated and even skeletally determined with the relative position of LEH (Hillson, 2005a; Hillson & Bond, 1997), arguably the position of Harris lines (Mays, 1985, 1995), and the development of the neural canal (Watts, 2015). However susceptibility to nutritional, pathological, and even psychological assaults is present – due to epigenetic effects – from the time of the development of the ovum in the mother. Therefore, adaptability to stress in a maternal line may be influenced by the health of the grandmother.

In the cemeteries used for this study, familial relation was unclear. However, with the exception of Coach Lane all cemeteries considered to span several centuries of use and so it is reasonable to assume that some of the individuals buried there may have been descendants of other individuals in the same cemetery. While skeletal signs of stress are specific to the individual, given the important role of epigenetic transfer of susceptibility, individuals considered here are not discrete, but viewed as a trend.

In addition to the fairly transparent effects of pathology and nutritional deficiency, these stressors and others including psychological stress from, for example, physical or emotional abuse, hierarchical status, or racial tension may trigger immune responses. As Watts (2015) points out a single instance or several discrete instances of cortisone secretion is merely adaptive and maintains biochemical homeostasis when the body is assaulted by psychological or physical stress. In short term and isolated instances, cortisol is an anti-inflammatory hormone which, in addition to others, helps break down glucose and maintain homeostasis. She warns however that maintained or repeated triggering of cortisol secretion leads to exhaustion. At this point the body, or more specifically cell receptors, lose their sensitivity to cortisol and like hormones impeding the immunological response and requiring the production of more anti-inflammatory hormones for a response. This not only impedes

maintenance of homeostasis, but has deleterious immunological and neurological effects. The immune system must produce more hormones to maintain itself leading to heightened susceptibility to pathology and possible disruption of development.

Hormonal disruptions or imbalances in turn wreak numerous assaults on the skeleton including arrested or impeded growth of long bones (Lewis et al., 2016; McEwan et al., 2005; Watts, 2015), impeded growth of the joints (Frost, 1999; Hamrick, 1999), increased risk of infection, rickets (Whyte & Thakker, 2013), and increased risk of arthroses including osteoarthritis and rheumatoid arthritis (Craps, 2015; Jurmain, 1999; Reginato & Olsen, 2002; Weiss & Jurmain, 2007). Many of these assaults on the physiological system may be synthesized into the “Barker Hypothesis.” The “Barker Hypothesis” is an observation put forth by David T. P. Barker which proposes that diverse morbidity and mortality in adults may be due to heterogeneous factors during the individual’s development *in utero* and in infancy and childhood. Barker observed that individuals with low birth weight or individuals who gained weight rapidly in infancy had a higher risk particularly for cardiac disease and type II diabetes. He suggests an epigenetic trigger where birth weight and size (even where the ovum is donated by another woman) is dependent on uterine conditions. This prevents the obstetric complication of a small woman attempting to give birth to large baby, but it also means that the developing foetus will be physiologically adjusted to the environment signaled by the uterine conditions and, particularly if the mother was malnourished during pregnancy or chronically malnourished, redirect available resources towards the brain to the possible detriment of other tissues developing concurrently. This last ensures survival and protects neurological development, but leads to less developed muscle, less insulin resistance, fewer cells in organ tissues particularly the kidneys, higher risk of osseous fracture, and reduced stature. Regarding both type II diabetes and reaction to the stress hormone cortisol, the developing infant is physiologically primed for an environment in which resources are scarce. A matching environment at birth and infancy will perpetuate and consolidate these developmental hurdles, but a mis-matched environment may cause the individual to physiologically overcompensate leading to obesity, insulin resistance, and a weakened immune system (Barker, 2003, 2004; Cooper et al., 2002). The “thrifty gene” theory originally was largely coalesced by Neel’s (1962) observations on the prevalence of non-insulin dependent diabetes mellitus (NIDDM). His thesis was that the genetic predisposition to develop NIDDM although detrimental in societies with dietary stability was adaptive and therefore selected for in societies with dietary uncertainty. NIDDM causes insulin sensitivity in muscle cells and adipose creation and retention which in societies where dietary uncertainty and high degrees of physical labour are the norm would lead to better metabolic efficiency and therefore better survival and a reproductive advantage. However

in societies where there is dietary stability and high degrees of physical labour are not the norm, NIDDM leads to obesity and type II diabetes (Bindon & Baker, 1997; Neel, 1962). The “thrifty gene” interacts particularly with the Barker hypothesis at NIDDM and obesity. According to Barker’s hypothesis, the “thrifty gene” may in fact be epigenetic and triggered by nutritional stress *in utero* and during infancy and early childhood. Conceptually, it can be extended to explain variation in stature and limb ratios for severely malnourished children (Vercellotti et al., 2014).

All stress indicators in this study have multifactorial aetiologies. However, a sufficiently stressed individual is at risk of falling into a continual positive feedback loop of stress. Sufficient physiological, nutritional, or even psychological stress may lead to lowered immune response leading to anti-inflammatory response and heightened cortisol response. Over time and repeated activation, the threshold rises and stress becomes cumulative. Additionally, if the low status or nutritional deficiency is generational in nature, the individual may already have an epigenetically triggered weakened or more reactive immune system (Watts, 2015). With overstimulation or lack of resources the immune system which is meant to be the body’s defense against all assaults, becomes an attacker itself (Sicotte et al., 2008). However, indicators of childhood stress particularly those observed on adults need not be interpreted as exclusively deleterious (DeWitte & Stojanowski, 2015; Temple & Goodman, 2014). Adults with childhood stress indicators survived the incident. While it was possible that these individuals were more susceptible than others to extrinsic factors they may also have been healthier or exposed to less stress than individuals who died as children. It follows however that stresses which disrupt development enough to cause skeletal childhood stress indicators may also influence long bone morphology.

2.2.4.1.1 Cribra orbitalia

Cribra orbitalia is a raised and porotic lesion on the ocular orbit. It is often conflated with or considered related to porotic hyperostosis and both are caused by hypertrophy of the cranial vault marrow (D. Ortner & Putschar, 1981; Smith-Guzmán, 2015; Stuart-Macadam, 1987b, 1989). However, although it appears to show similar aetiologies or co-morbidities the precise relationship between the two lesions is not yet entirely understood (Gowland & Western, 2012; P. L. Walker et al., 2009). In paleopathology presence of this lesion is usually associated with anaemias. Originally, cribra orbitalia and porotic hyperostosis were attributed to genetic anaemias such as thalassaemia and sicklaemia (Stuart-Macadam, 1987b). But the paleopathological literature primarily that of Stuart-Macadam associates them now with all anaemias including iron-deficiency and megaloblastic (Gowland & Western, 2012; Stuart-Macadam, 1987a, 1987b, 1992; Sullivan, 2005; P. L. Walker et al., 2009; Wapler et

al., 2004). In the last two decades, *cribra orbitalia* has also been shown to be a symptom of numerous other physiological stresses including malaria (Gowland & Western, 2012; Smith-Guzmán, 2015), parasites (Sullivan, 2005; P. L. Walker et al., 2009), drug use, and certain kinds of cancer (Sullivan, 2005; Schier, 1995 in P. L. Walker et al., 2009), as well as more cultural or psychological stresses like sex, and status (Sullivan, 2005; P. L. Walker et al., 2009). In all of these cases, a form of anaemia is the likely cause for the *cribra orbitalia*, but the precise aetiologies of the underlying cause of the anaemia is highly variable. Sex has also been shown to be relevant in that women generally retain less iron than men regardless of diet and have high iron B_{12} and folic acid costs in menarche, maternity, and lactation, but gender also impacts culinary habits and availability of resources (Koehler et al., 2012; Sullivan, 2005; P. L. Walker et al., 2009). Some cultures may allocate resources based on sex or age often leaving the elderly, very young, or females of all ages with less than their male counterparts (May et al., 1993; Somerville et al., 2015). Religion or cultural standards of beauty may also impact individuals in a psycho-cultural manner causing children and adolescents to receive more or less food or where resources are in abundance, intentionally choose to eat, fast, or practice vegetarianism or veganism (C. J. Adams, 2006; Thomas, 2016; Wright & Adams, 2015).

Food selection is also a possible cause of *cribra orbitalia*. A fundamental change in dietary practice occurs with agriculture where grains or carbohydrates become a much larger part of the diet or are more abundant than animal proteins (Armelagos et al., 2011; Cucina et al., 2006; Sullivan, 2005; P. L. Walker et al., 2009). Similarly, strict vegetarians may not have access to appropriate amounts of vitamin B_{12} and folic acid which occur mostly in animal proteins. A fetal or intergenerational consequence is also in effect here as foetuses which are not exposed to sufficient prenatal B_{12} may have trouble fighting infection in later life. Additionally, B_{12} is stored in an adult liver, but an infant or foetus is only developing those stores. Thus, B_{12} deficiency in the mother by choice or circumstance may not have obvious or immediate impacts on her body, but can easily result in lower immune response, diarrhoea, and neurological consequences in the infant (P. L. Walker, 1986). Prolonged breastfeeding in absence of other foods may also lead to malnutrition as the infant will only receive what nutrients the mother does. Weaning may also be fraught certainly in times of famine where weaning foods are nutritionally poor, but also in cultures where weaning foods are not nutritious (Katzenberg et al., 1996). In such circumstances the presence of *cribra orbitalia* is not only reflective of their childhood nutrition, but their mother's health and the culture in which they were weaned as well.

However, prosperity is not a guard against megaloblastic anaemia acquired from lowered vitamin B₁₂ levels. Food selection besides vegetarianism may also include a macrobiotic diet which can restrict animal proteins or particularly refined foods. Over-processing of some cereals can also lead to malnutrition creating a situation where potentially, a person of very high status eating the best foods available on a daily basis may suffer from malnutrition simply because the staple cereal was processed until most of the vitamins were removed. Middle or high status people may also select a diet which distinguishes them from lower status individuals, but is lacking in essential nutrients (Sullivan, 2005).

Diet selection may also increase risk of parasitism as parasites which inhibit the absorption of B₁₂ are particularly common in certain fish (Sullivan, 2005). Parasitism is not dependent only on diet and vectors for infection include, living conditions, crowding, and hygienic practices. Regardless of status in a particularly crowded urban environment such as Medieval York or the pueblos there is high probability of exposure to and accidental ingestion of parasites. In both urban environments it was often common practice to pile refuse on the street and allow human or animal waste to remain in the open and close to water supplies (Sullivan, 2005; P. L. Walker et al., 2009). People, particularly those of low status lived in very close proximity such that even those of high status who may have been able to afford cleaner or larger housing would have suffered some exposure to parasites. As mentioned before, the parasite aetiology has multiple biological mechanisms. Parasites can prevent absorption of nutrients particularly folic acid, B₁₂, and iron. They can also trigger an immune response which can result in anaemias and taxing of the hormonal system as well as diarrhoea which effectively flushes nutrients. Finally, parasites can also cause intestinal bleeding creating a very direct cause of anaemia both iron deficiency and megaloblastic.

Stuart-Macadam showed in a series of radiographs that in severely anemic children seven typical diagnostic osteological changes will occur. These changes include, “hair on end” pattern of trabeculation; 2) outer table thinning or disappearance; 3) texture changes; 4) diploic thickening; 5) orbital roof thickening; 6) orbital rim changes; and 7) frontal sinus development,” (1987a: pp. 511-512). Expansion of the diploe in the cranial vault is triggered as a last resort of the immune system by the sustained early destruction of red blood cells (RBC). If RBC destruction exceeds RBC production the body will attempt to correct it by causing the marrow which produces the RBC to become hypertrophic. Therefore, a megaloblastic anaemia would lead to cribra orbitalia, but iron-deficiency anaemia which simply lowers the production of RBC might not directly result in cribra orbitalia (P. L. Walker et al., 2009). However, megaloblastic anaemias are still resultant of malabsorption or deficiencies in crucial

vitamins like B₁₂ and folic acid (P. L. Walker et al., 2009). The possibility of co-morbidity is high as the aetiologies are similar. With the exception of the invasion of soft-tissues into the diploe prolonged anemic episodes have similar effects particularly on the immune system. Iron deficiency anaemia may be specifically triggered by the immune system to limit sources of iron to a pathogen or neoplasm. If the iron is already bound on a molecular level, the pathogen cannot access it. However, prolonged anemic episodes weaken the immune system's responsiveness causing higher activation thresholds and therefore higher costs (Sullivan, 2005).

Cribra orbitalia will develop in children and adolescents as a symptom of sustained megaloblastic anaemia as RBC is produced in the cranial vault and long bones during development, but in adults the production of RBC occurs in the axial skeleton sternum and vertebrae (Sullivan, 2005). Stuart-Macadam found no cribra orbitalia in individuals younger than six months old, the greatest frequency of severe lesions in children aged from six months to two years, severe cribra orbitalia lesions only in children between six months and fourteen years and statistically significantly less cribra orbitalia lesions overall in adults (Stuart-Macadam, 1985, 1989). The likely physiological reason for the decrease in lesion frequency in adults and children is size of the medullary cavity. The medullary cavities of very young children (under four years) are entirely filled with hemopoietic (red) marrow. With age and development, the medullary cavity will enlarge and the space unused by the hemopoietic marrow will be filled by fatty (yellow) marrow. With age and size therefore the likelihood of extramedullary erythropoiesis or diploic expansion disrupting compact bone decreases because hemopoietic marrow may simply displace fatty marrow within the medullary cavity (Smith-Guzmán, 2015; Stuart-Macadam, 1985, 1989; Sullivan, 2005). Additionally, there is some evidence that anaemias may present as a "cribrous syndrome" not restricted to the orbitals (Djuric et al., 2008; Smith-Guzmán, 2015). While the relationship between specifically cribra orbitalia and cranial vault porotic hyperostosis remains under scrutiny (Gowland & Western, 2012; D. Ortner & Putschar, 1981; Stuart-Macadam, 1987b, 1989) there is some suggestion that porotic hyperostosis is a similar expression of anaemia – clearly sharing the same aetiology – but occurring later in life. Smith-Guzman goes so far to suggest that anaemias in adults produce cribrous lesions around the epiphysis of the humeral and femoral head as well as in the axial skeleton (2015). Stuart-Macadam points to a progression of porotic hyperostosis from the frontal bone, to the parietals and finally to the occipital with age and noting that the most diploic expansion is expressed in the parietal bones (Stuart-Macadam, 1985, 1987b, 1989).

Adults – as examined in this study – will have healed or healing cribra orbitalia and this study did not attempt to quantify other cribrous lesions or cranial vault hyperostosis (Stuart-Macadam, 1985; and Walker 1985;1986 in P. L. Walker et al., 2009). However, even in this issue there is some dissent. Stuart-Macadam (1985) theorises that cribra orbitalia occurs exclusively in subadults and therefore studies of cribra orbitalia should include only children. Certainly other studies have reported an age bias in cribra orbitalia (Sullivan, 2005; P. L. Walker et al., 2009). The rates and severity decrease with age as the lesions heal. However, Sullivan (2005) found active lesions in adults. She theorises that perhaps childhood anemic episodes cause a hypertrophic expansion of the marrow into the diploe and crucially the soft tissues remain there into adulthood. This means a slower rate of healing than might otherwise be expected, but it also means that in subsequent anemic episodes that same hemopoietic marrow may be repeatedly activated despite the developmental anatomical shift in centers for RBC production. Other research also suggests that while cribra orbitalia must at least originate from anaemia at a very young age, adults experiencing anemic events might develop porotic hyperostosis or other lesions (Sullivan, 2005). However in a recent study on cribrous lesions in individuals who suffered from malaria, Smith-Guzman noted that cribrous lesions on the humerus and femur were associated with young people whereas cribra orbitalia lesions appeared on people of all ages (2015). This likely has to do with remodelling, but as an alternative explanation she explains that where hemopoietic marrow to be hypertrophic at or around the time of metaphyseal fusion then a cortical defect may result causing these porous lesions and by way of marrow hypertrophy, directly relate them to megaloblastic anaemia. Supporting the general consensus that cribra orbitalia develops exclusively during childhood it is notable that the demographic for cribra orbitalia lesions does not skew towards women. Adult women are more physiologically and culturally stressed for nutrition, and yet there is not a significant difference between the sexes for the prevalence or severity of cribra orbitalia lesions (Stuart-Macadam, 1985, 1989; Sullivan, 2005). This probably results from the fact that the cultural and physiological causes of nutritional stress for women occur largely after the age of four when most cribra orbitalia lesions are believed to have formed.

Cribra orbitalia or like symptoms is also not the exclusive domain of anaemia. Trauma, infection, and diseases like scurvy will also produce similar lesions. Macroscopically similar lesions may occur due to inflammation (Gowland & Western, 2012; Wapler et al., 2004). However, particularly in the case of anaemia, the disruption to growth and development may be considered substantial and can be expected to impact that individual's adult health and longevity as discussed above. It is possible that some of that disruption may translate into morphological variation.

2.2.4.1.2 Linear Enamel Hypoplasia (LEH)

As with the rest of Section 2.2.4.1 this section addresses the possible correlation between long bone morphology and developmental stress (1.1.1.3). Linear enamel hypoplasia (LEH) forms during infancy and childhood, but is relevant in studies of adults because it speaks to the general stress of the population and both the Barker and “thrifty gene” hypotheses (Armstrong et al., 2009).

LEH appears as a linear striation running parallel to the crown of the tooth and is caused by a disruption to amelogenesis in the secretory stage (Goodman & Armstrong, 1985; Watts, 2015). A second kind of enamel disruption called enamel hypocalcification may occur during the maturation stage of amelogenesis and appears as a line on the tooth of a different color than the surrounding enamel similar to LEH but lacks the diagnostic indentation of LEH (Armstrong et al., 2009). These disruptions – the first in matrix formation and the second in calcification – are similar in pathogenesis likely chemically resulting from increased cortisone (Watts, 2015) but different in timing and are likely often counted together as enamel hypoplasias. Numerous factors may lead to hypoplasias including local trauma, congenital abnormalities, malnutrition, overfeeding, psychological stress, infectious disease, metabolic disruption, and possibly weaning (Armstrong et al., 2009; Goodman & Armstrong, 1985; Goodman & Rose, 1990; Hillson, 2005a; Hillson & Bond, 1997; Katzenberg et al., 1996). As a result of this very diverse pathogenesis, LEH is considered non-specific, but is a good indicator of episodes of health stress (Šlaus, 2008).

While LEH and cribra orbitalia are both indicators of childhood stress they have some key differences in their aetiology and frequency. For one, LEH is more likely to be preserved than cribra orbitalia. There are two reasons for this. LEH occurs in enamel and is therefore virtually indelible both in during the individual’s life (barring severe attrition or tooth loss) and in the archaeological record as enamel is largely resistant to taphonomic processes (Armstrong et al., 2009). The bones of the cranium are more likely to degrade than the teeth. Additionally, there is some evidence suggesting that cribra orbitalia may remodel or heal later in life assuming the hemopoietic marrow recedes (Sullivan, 2005). The second reason for the prevalence of LEH over cribra orbitalia is the threshold for both of these indicators. Certain teeth are very sensitive to any form of disruption during the second and third stages of amelogenesis and will react to relatively slight insults by either lowered secretion or lowered calcification. Conversely, cribra orbitalia only occurs when malnutrition (via infection, diarrhea, or poor nutrition) is so severe that hemopoietic marrow must exceed its bounds and enter the trabecular bone. Cribra orbitalia is only likely to be triggered up to the age of four years and requires severe stress

whereas LEH may be triggered as long as tooth crowns are forming (arguably as late as 16 years) and has a very low threshold (Armélagos et al., 2009; Hillson, 2005b; Hillson et al., 1998; Hillson & Bond, 1997). This means that while we can expect to see both LEH and cribra orbitalia in severely stressed individuals, the absence of cribra orbitalia does not necessarily suggest a lower level of stress. Additionally, depending on timing, weaning culture, and the health of the mother, prolonged breast-feeding may protect an infant from adverse conditions. If a child is breastfed until about four years of age they may still be malnourished particularly if the mother is in poor health, trying to prevent future pregnancies, or offsetting the allocation of other foods to the infant via breastfeeding. The child may thereby develop LEH in their adult dentition, but escape hemoblastic anaemia (Katzenberg et al., 1996). Therefore, the interpretation of these two stress indicators must be considered complimentary.

Presence or absence of LEH may also affect the mortality profile and could be indicative of social class and sex related responses to stress. Firstly, it should be noted that in some studies (Šlaus, 2000) LEH will be more prevalent in subadults, however, as it is a permanent condition it will be present whether or not the individual survives childhood. A higher prevalence in children may be attributed to the osteological paradox (that is, non-survivors were less healthy, had more stress, and died younger) (Wood et al., 1992). This requires a different interpretation than for cribra orbitalia. There are higher rates of CO in subadults and young adults and this could to a degree be the osteological paradox, but cribra orbitalia affects an area of the skeleton which could remodel over time provided the hemopoietic marrow recedes. For LEH to disappear from the archaeological record the affected individual would have to either experience antemortem tooth loss or attrition or carious lesions severe enough to obscure the defect. Presence of LEH is associated with early mortality. The rate of LEH is higher in subadults, but even among adults those with LEH tend to die younger than those without it or with fewer incidents of LEH (Boel et al., 2007; Duray, 1996; Goodman & Armélagos, 1985; Watts, 2015). LEH is associated with morbidity particularly cardiovascular complaints (Armélagos et al., 2009). For this study this is significant in that the age profiles and morbidity prevalences are likely related, and the effect of a stress indicator on adult morbidity and mortality may also speak to long bone morphology and ontogeny. Beyond the age component however, Watts (2015) points out a further significant trend in intrapopulation variation for the prevalence of LEH. She argues – building upon Goodman's (Goodman, 1991) assertion that effective levels of stress are influenced by social, cultural, and ecological factors – that LEH is more prevalent in lower status individuals and more prevalent in females than males (also found in (Šlaus, 2000)). This points to a socioeconomic hierarchy wherein individuals in good socioeconomic standing are better equipped to insulate themselves and their children from stress

than individuals of lower status. In their study of malnourished Guatemalan children May and colleagues (1993) found that girls experiencing illness or stress were allocated fewer resources than their male counterparts in similar situations. The dichotomy was severe enough to suggest that sick girls were not only receiving less nutrition than sick boys but that resources were being allocated away from them to healthier children. In this case the entire demographic has a low socioeconomic status, but girls – particularly sick girls – are put at the bottom of the socioeconomic ladder and allocated resources last. There are serious implications here for social justice, but this also illustrates the compounding effect of socioeconomic status on stress and consequently stress indicators. The difference in expression of LEH between populations and within populations could, in some cases, indicate differences in socioeconomic status.

It is also noteworthy that teeth do not equally express LEH. Watts (2015) quoted the vulnerable age window for the formation of LEH to be between one and six years, but there continues to be crown development until about sixteen years of age. Goodman and Armelagos (1985) however, explain that the expression of LEH depends on numerous factors some of which are epigenetic. They conclude that a tooth whose size and developmental timing is strictly defined genetically is more likely to have LEH than a tooth being formed under looser genetic controls. The incisors and canines are very sensitive to disruption partially because amelogenesis occurs for those teeth during early childhood when the individual is more likely to become increasingly susceptible to environmental insults and partially because the genetic control on the anterior dentition is stricter than for premolars and molars. This matches very well with the “thrifty gene” hypothesis or the idea that an individual’s physiological system will reallocate energy to vital systems when stressed and therefore curtail or arrest development of anything not immediately essential. Molars and premolars may still express LEH, but many studies do not consider them because the spacing of perikymata in molars varies widely (Hillson, 2005b)..

Childhood stress indicators are therefore important to this study in that they may be linked to the Barker hypothesis and the “thrifty gene” hypotheses. It is widely supported that childhood stress affects long bone growth and cortical robusticity as well as adult morbidity and mortality, but it remains to be seen how that pertains to long bone morphology.

2.2.4.1.3 Residual Rickets and Osteomalacia

Residual rickets and osteomalacia are very rare in this study and do not constitute a significant proportion of the examined demographic. However, individuals diagnosed with residual rickets (none in the selected skeletal set were found with osteomalacia) were not excluded from the study and so a brief discussion on these conditions is warranted. Residual rickets and osteomalacia were considered and the former recorded because of their pronounced effect on long bone morphology. Their presence also speaks to the general health and wellbeing of the populations in question. Were it more common in the populations considered it would certainly pertain to intrapopulation morphological variation.

Rickets and osteomalacia occur due to improper calcification or mineralization of the bone due to a deficiency in vitamin D. Vitamin D can be found in low quantities in eggs, oily fishes, and dairy products, but is more correctly a prohormone and primarily produced via cutaneous exposure to sunlight (Brickley et al., 2007; Ives & Brickley, 2014; Roberts & Manchester, 2010). The prevalence of rickets may be influenced by latitudinal position, but also by socio-economic status and cultural practices. Vitamin D production or absorption may also be impeded by certain genetic conditions, diets high in phytates (certain phytates will bind to calcium and zinc lowering the absorption of vitamin D), as well as intestinal malabsorption due to short bowel syndrome or pancreatic disease (Roberts & Manchester, 2010; Whyte & Thakker, 2013). Low vitamin D causes low absorption of calcium and phosphorus which in turn causes a fault in osteoids and bone with reduced rigidity (Brickley et al., 2007; Ives & Brickley, 2014; Schattmann et al., 2016). As a result, children with low vitamin D can experience warping of their softened bones due only to weight bearing activities such as walking. Adults may experience osteomalacia which, similar to rickets, involves failure of the osteoids to properly mineralise resulting in lack of organization at pseudo-fractures which usually present as bony calluses about the axial skeleton especially at the scapula and pelvis, and may present as flattening at the proximal femur (Ives & Brickley, 2014). Once rickets is no longer active – osteoids are mineralizing properly – cortical bone will form at the site of any pseudo-fractures and the disease is classified as residual (Brickley et al., 2005; Ives & Brickley, 2014). The alteration in morphology may be retained into adulthood. Particularly in infants with malnourished mothers, osteomalacia may be exacerbated by low dietary calcium (Brickley et al., 2007; Roberts & Manchester, 2010).

Historically, rickets and osteomalacia are rare until the postmedieval period when cultural practices particularly in Europe kept children, particularly children of wealthy households indoors (Brickley et al., 2007; Roberts & Manchester, 2010). In Britain during the industrial revolution the

socioeconomic profile of rickets transformed from a disease affecting the wealthy to one affecting the working class as children began working during daylight hours in factories. Cod liver oil was recommended to counteract the deficiency, but while helpful, does not contain enough vitamin D to make up for lack of exposure to sunlight (Roberts & Manchester, 2010).

Certain morphological changes are typical of osteomalacia and rickets. Rickets may result in severe bending and even folding as body weight during locomotion in either crawling or walking slowly deforms the soft under-mineralised bone (Brickley et al., 2007; Roberts & Manchester, 2010). This may be accompanied by some microfracture particularly visible radiographically or a “pseudofracture” where the bone is bent but fails to fracture as there is no disunion. However, in the case of a pseudofracture, remodeling is triggered but usually only results in the further deposit of unmineralised osteoids and cartilage (Ives & Brickley, 2014). Rickets and osteomalacia often have comorbidity with osteoporosis due in part to low dietary calcium and a failure of nutrients to properly bind (Whyte & Thakker, 2013). This often leads to a sparser trabeculae (D. Ortner & Putschar, 1981). However there are further morphological changes. Ortner and Putschar (1981) describe a thickening of the midshaft and at the growth plates due to an excess of unmineralised osteoids and cartilage which cannot be resorbed. In long bones the result is what they call a column like shape to long bones with “cup-shaped depression of the metaphyseal areas” and a “rachitic rosary” at the osteochondral junction of the ribs (D. Ortner & Putschar, 1981; pp. 274). The term “rachitic rosary” is also used to describe the swelling at the metaphysis of the wrists in infants (Whyte & Thakker, 2013). Roberts and Manchester similarly describe the metaphyseal morphology of rickets as trumpet-like due again to the excess of unmineralised cartilage (2010; pp. 237). Brickley and colleagues describe a proximal flattening in the femoral diaphysis, but remark that in the populations examined for their 2007 article the orientation of that flattening is slightly different than the associated flattening found in other populations (Brickley et al., 2007). An attempt at medical intervention or simply natural healing of a bone with rickets could also appear radiographically in the form of a thickened cortex (Brickley et al., 2007). When considering residual rickets however it is important to remember that adults who have since recovered will have had time for their bones to remodel and possibly morphologically correct. Therefore, while the populations examined in this study had a very low prevalence rate of residual rickets it is possible that individuals considered healthy in fact suffered from rickets that would not be visible without a radiograph or had rickets and subsequently recovered enough that the morphological change is no longer apparent.

Rickets and osteomalacia are included here because of their possible influence on long bone morphology and because they speak to the general health of the population. However, while these conditions may be indicative of or related to poor diet, infectious disease, and crowding they are dissimilar in aetiology from cribra orbitalia and enamel hypoplasia. The latter two are largely even primarily influenced by nutrition whereas the relationship of nutrition to rickets and osteomalacia is almost negligible. Additionally, the populations considered for this study had very low rates of rickets – which generally conforms to the wider context. Cribra orbitalia and enamel hypoplasia occur with reasonable frequency whilst residual rickets is relatively rare. (This last could be a result of taphonomic effects as individuals with osteomalacia or rickets are likely to have unmineralised and osteoporotic bone which may not survive in the archaeological record and their bones are more likely to break postmortem (Brickley et al., 2007).) Considering, however, that mild residual rickets is difficult to detect without radiographs and that successful remodeling will likely have occurred by adulthood, some morphological “noise” could possibly be attributed to undetected residual rickets.

2.2.4.2 Degenerative Joint Disease

2.2.4.2.1 Osteoarthritis (OA)

Osteoarthritis (OA) has been recorded in early hominins (Trinkhaus, 1983 in Roberts & Manchester, 2010)) as well as a dinosaur (Karch and McCarthy, 1960 in Roberts & Manchester, 2010). It remains very common in modern populations and although not lethal has a very real impact.

There has been much debate about proper terminology regarding OA because of its diverse aetiologies. Because *-itis* implies inflammation Larsen (1997) recommended calling it osteoarthroses suggesting instead that it results from continued wear and tear. However, recently clinical studies especially have found evidence that inflammation is central to the aetiology of OA (Finnegan et al., 2014; Laiguillon et al., 2014; Shin et al., 2014; Weiss & Jurmain, 2007; Willett et al., 2014). Meanwhile the term Degenerative Joint Disease (DJD) was presented as an alternative broader category which includes but is not limited to OA. The term Osteoarthritis will be used here with Degenerative Joint Disease used as a generalised term meaning joint arthroses which cannot be suitably diagnosed.

OA is classified as a neuromechanical joint disease which on its surface classifies OA as a primarily biomechanical pathology. However, the aetiologies for OA are complex. Synovial joints or diarthroses are bordered *in vivo* by cartilaginous material. The joint capsule consists of synovial fluid in the synovial cavity which acts as a cushion for the articular highly lubricated hyaline cartilage. The

cartilage itself is made up of chondrocytes suspended in and perpetually repairing an extracellular matrix consisting of collagen and chondroitin sulfate (Frost, 1999; Hamrick, 1999). OA initially appears as damage to or thinning of the cartilage. Subchondral osseous involvement at this stage might consist of porosity and possibly osteophytes. Eburnation will occur when part or all of the cartilage has been destroyed and the bones contact and erode each other with movement of the joint.

Several authors complain of lack of consistency and accuracy when archaeologically recording joint disease (Jurmain, 1999; Roberts & Manchester, 2010; Waldron & Rogers, 1991). Various arthroses including but not limited to OA have been combined in some studies. Additionally, they note that there has been some lack of consistency in recording methodologies and argue for the adoption of Rogers and Waldron's (1989) method. This method diagnoses OA only where eburnation is present or when eburnation is not present, when two of the following are present: marginal osteophytes, surface osteophytes, pitting on the joint surface, or deformation of the joint contour (J. Rogers & Waldron, 1989; Waldron & Rogers, 1991). The Waldron and Rogers method of recording acts on a binary where OA is either present or not present, but other methods such as the Buikstra Ubelaker (1994) method – cited by Jurmain and colleagues (2012) as the most widely used criteria for diagnosing OA – are ordinal. The issue of inter and intraobserver error still exists and is likely inflated by using an ordinal rather than binary system. However, this study is interested in morphological variation with increasing severity of OA, therefore, the ordinal Buikstra and Ubelaker system was selected over the considerably safer binary methods.

The recording of OA in archaeology is based on bony changes primarily in diarthrodial joints, but also amphiarthrodial. To understand why these bony changes are indicative of OA it is important to understand the specific way these changes occur. Porosity has been argued to be unrelated to OA by Rothschild (1997; Weiss & Jurmain, 2007) who could find no relationship between porosity and OA. However, other authors theorise that especially where the cartilage is damaged and supply of nutrients interrupted capillaries form in the subchondral bone to allow for osteocyte migration (Klaus et al., 2009; Laiguillon et al., 2014) Osteophytic formation is due to auto-immune response to inflammation. When cartilage is damaged or fibrous capsules ruptured the resulting inflammation will trigger osteophytic growth (Klaus et al., 2009; Laiguillon et al., 2014; Roberts & Manchester, 2010; Siebelt et al., 2014). Comparatively the aetiology of eburnation is simple. Once subchondral bone is denuded bone contact eventually wears down the surface creating a polished or eburnated joint.

Activity, injury, and stress have been repeatedly linked to the aetiology for OA but cannot be classified as the only causes (K. R. Brown et al., 2008; Gawri et al., 2014; Siebelt et al., 2014). Age has been put forth by many authors as an aetiology (Jurmain, 1980; Mays, 2001; Molnar et al., 2011; Weiss & Jurmain, 2007). However, Jurmain observed the association with a higher rate of OA after menopause in women compared to men of the same age suggesting a hormonal component (Jurmain, 1977, 1999). Additionally, Larsen observes a higher rate of OA in populations in colder environments where metabolism of vitamin D would be more difficult and in obese women who – besides suffering added biomechanical stress to their knees – would also produce much more oestrogen than normal women, normal men, and obese men (1997). These arguments are underscored by a literature of medical documentation and research where endocrine involvement catalyses the destruction of cartilage (Grenier et al., 2014; Laiguillon et al., 2014; Reginato & Olsen, 2002; Shin et al., 2014; Siebelt et al., 2014; Willett et al., 2014). The genesis of these hormonal or endocrinal responses is often linked to age, injury, or inflammation, but the responses themselves are more biochemical than biomechanical.

Attempts to discern a pattern of OA affected joints that can suggest specific activity patterns have been numerous (K Kennedy, 1989) but ultimately unsuccessful (Jurmain et al., 2012). Extending from an argument first put forth by Merbs (1983) Lovell states, “individuals performing the same task may do so differently as far as the mechanics of the activity are concerned, whether due to personal factors such as age, height, weight, handedness, reference or pain threshold, or to other factors like training and experience” (1994). Simply, Individual variation and the diverse aetiology of OA compound to make assumption of activity patterns from OA alone impossible. However, OA often results from continued use after an abnormality is present (D. Ortner & Putschar, 1981). So while it is overly specific to assume a specific activity from OA patterning, general levels of activity and biomechanical stress may be discerned and even healed trauma may result in localised OA.

Presence of OA in a cemetery population is often used alongside nutritional health to determine general levels of stress. Disparities in prevalence of OA is further used evidentially to support hypotheses of division of labour by socio-economic status, age, sex or any other possible cultural divisions. There are merits, but also endemic problems with both of these uses of OA prevalence statistics. OA generally increases with age (Leiberman et al., 2001; Molnar et al., 2011; Weiss & Jurmain, 2007) and as stated previously, with continued use after an abnormality is present (D. Ortner & Putschar, 1981). Micro-traumas borne by the cartilage and subchondral bone could constitute such abnormalities meaning that OA would become present in a population where insufficient rest time

occurred after loading. Moreover many studies cite excessive exercise or loading as a possible aetiology for OA. Pálfi found high levels of OA and microtrauma in the joints of medieval male Magyar skeletons consistent with injuries and skeletal changes found in other populations known for equestrianism (Larsen, 1997; Pálfi, 1992, 1997; Wentz & Grummond, 2009). Similarly, populations historically known to have experienced an increased amount of stress seem to show an increase in OA prevalence rates. Although urbanized populations typically do not show OA until after the age of 30 (Larsen, 1997, p. 163), urban African American skeletons from the first half of the 19th century show higher rates of OA than contemporary rural populations suggesting heavy manual labour (Angel et al., 1987; Parrington & Roberts in Larsen, 1997). Likewise, the very stressed postmedieval Croatian population studied by Novak and Šlaus exhibits high levels of OA alongside a high mortality rate for young adults (Novak & Šlaus, 2011; Šlaus, 2000). Bridges and Knüsel both use the prevalence of OA to determine social or sexual division of labour and the prevalence rates are convincing (Bridges, 1994; Knüsel et al., 1997). Additionally, some clinical studies suggest that increased exercise may damage the cartilaginous matrix and lead to OA. Siebelt and colleagues found that mechanically stressing a joint where the cartilaginous matrix had been chemically depleted will exacerbate OA (Siebelt et al., 2014).

However, other authors found no positive correlation between increased biomechanical stress and OA prevalence and some suggested that exercise – albeit not excessive – may even reduce rates of OA. Both Frost and Hamrick separately acknowledge the usefulness of the right amount of biomechanical stress in strengthening the histological and morphological structure of epiphyses in subadults (Frost, 1999; Hamrick, 1999). Knüsel, though acknowledging in previous studies that OA may be indicative of too much stress notes that habitual activity does not lead to OA (Knüsel et al., 1997, p. 481) and while Jurmain prior to publishing *Stories of the Skeleton* linked OA and stress (Jurmain, 1977) he later clarified his position by explaining that the link is tenuous (Jurmain, 1999).

Age is a central question in this study for its relation to production of hormones and thereby maintenance of long bone morphology, however these and other related reasons cause a slight relationship between age and OA prevalence. DJD in amphiarthrodial joints, and change to the joints very similar to the markers for OA is used bioarchaeologically in age estimations (Buikstra & Ubelaker, 1994). There also seems to be some disagreement in the literature about just how related OA is to age (Mays, 2015b; Weiss & Jurmain, 2007). Very likely OA is not directly related to age and in fact presents as a result of continued long term damage coupled with hormonal changes both of which would accumulate with age.

Generally, a correlation is seen with OA and age (Jurmain, 1977; Larsen, 1997; Weiss & Jurmain, 2007) (but see (Knüsel et al., 1997, p. 483)). However, there is never a clear pattern. Larsen stipulates that OA is not usually seen before the age of 30 in urban populations, but the pattern does not hold for rural populations or populations with high levels of manual labour (Larsen, 1997). Jurmain says that although there is a correlation with age there is a higher level of correlation with population which supports a more genetic or activity related aetiology for OA (Jurmain, 1977). Jurmain and Weiss do note the positive correlation between OA and age in adulthood, but stipulate that it is a result of diagnosis in bioarchaeology. In bioarchaeology, per suggestions by Waldron and Rogers, OA is diagnosed by the presence of eburnation or the presence of both porosity and osteophytes (Waldron & Rogers, 1991). However, even Waldron and Rogers noted the association of osteophytes with the aging process: a phenomenon well represented by the clinical literature and noted by Jurmain and Weiss (Waldron & Rogers, 1991; Weiss & Jurmain, 2007). Additionally, the surest way of precisely aging an individual especially past the age of 50 is by histologically determining the amount of osteon remodelling (D. Ortner & Putschar, 1981). Jurmain and Weiss show that marginal osteophytes can occur without OA and are more securely correlated with old age than OA (Weiss & Jurmain, 2007). While reduction of the joint space or cartilage health cannot be determined *post mortem* the use of especially marginal osteophytes as a diagnostic criteria for OA may be misleading. This may be linked to the discussion of bone's microstructure in subsection 2.2.3.2 as changing an inconsistent rates of remodelling will be influenced by OA and therefore possibly alter the biomechanical effectiveness of the bone leading to a morphological change.

OA affects both amphiarthrodial and diarthrodial joints. Amphiarthrodial joints are cushioned with very thick fibrocartilage which contains both collagen I and collagen II. This, aside from the mechanical necessities of bone and muscle, makes them not immobile joints, but less mobile and more stable than diarthrodial joints. For diarthrodial joints hyaline cartilage collagen is 90% Type II (Jurmain, 1999, p. 20). This cartilage is very thin at 2-5 mm allowing for good joint articulation and unlike other connective tissues is hypocellular. Chondrocytes are suspended in a cartilaginous extracellular matrix to repair damage, but typically are very separate only being found in groups during mitosis. The cells produce sulfated-glycosaminoglycans which set the cartilage's fixed-charge density which allows cations and water to enter the extracellular matrix and create the necessary hydrostatic pressure (Siebelt et al., 2014). Hyaline cartilage is primarily 68-78% water which allows it to compress by 40% (Jurmain, 1999).

The anatomy of the joint and interaction of cartilage and bone is very efficient, however in the event of injury, inflammation, or chemical imbalance recovery is difficult. Frost and Hamrick both note that there is an ideal level of strain that promotes growth without degrading cartilage (Frost, 1999; Hamrick, 1999). In fact, without some level of activity Frost theorises that natural repair and regeneration of the cartilage wherein old cartilage is destroyed and areas with some strain are repaired, cartilage will degenerate via the body's natural repair processes (Drapeau & Streeter, 2006; Frost, 1999). Chondrocytes will repair damage and react to stress, but as noted previously cartilage is hypocellular and the health of the extracellular matrix is critical to the maintenance of the cartilage.

Macroscopically, the extracellular matrix is hydrostatic so that it may equally distribute force across the joint surface. As long as force remains under a certain threshold, no one part of the cartilage or joint surface will be adversely affected. However, this only holds for about 16 hours and some force (Frost, 1999; Gawri et al., 2014). The cartilage will dehydrate with use after which they will become less efficient at distributing force and may become subject to damage. If severe damage to the cartilage occurs, synovial fluid may leak out of the joint capsule and damage the subchondral bone (Frost, 1999). However, pathogenesis is uncertain as some studies have shown damage to the subchondral bone may precede cartilage degeneration (Radin, 1982 in Larsen, 1997). Joint surface porosity, often used with the appearance of osteophytes to diagnose OA may be a vascular invasion of the subchondral bone in order to rehydrate malnourished cartilage (Weiss & Jurmain, 2007) or to heal the subchondral bone itself (Winet, 1996). Porosity rarely occurs at the site of greatest pressure to the joint or of eburnation and so is considered secondary.

Damage and degeneration may be observed microscopically as well. Cartilage is hypovascular as well as hypocellular and so chondrocytes must regulate the extracellular matrix chemically via positive and negative feedback loops. Once the chondrocytes themselves are put under undue strain, they will release cytokines which promote inflammation. Besides promoting inflammation, the cytokines also bind to Toll-Like Receptors (TLR) due to their chemical similarity to extracellular proteins on certain bacteria. The TLR produce more cytokines to create a positive feedback loop promoting inflammation and cause the upregulation of several genes associated with inflammation (Gawri et al., 2014). Gawri and colleagues were able to reproduce increased cytokine and upregulation of genes in chondrocytes subjected to strain at low frequency and with rest periods. Their methods even resulted in apoptosis. Therefore, once the extracellular matrix is damaged enough to cause mechanical strain on the

chondrocytes, cartilage degeneration from the process of inflammation is almost inevitable (Gawri et al., 2014).

OA has diverse aetiology relating in part to chemical imbalance, hormonal change, age, and activity levels. All of these factors have or likely have impact on long bone morphology. Additionally, DJD and OA, particularly when painful, could cause a behavioural alteration in movement resulting in morphological changes in the diaphysis and cross-sectional geometry. Conversely, the morphology of the long bone could predispose an individual to OA by making injury more likely. Therefore there are several ways in which DJD and OA could be linked with morphological variation in proximal long bones.

2.2.4.2.2 Schmorl's Nodes

Schmorl's nodes are often mentioned alongside spinal arthritis due to their association with abnormalities in the intervertebral disc. However, they may also be associated with trauma or micro-traumas resulting from excessive physical stress. Schmorl's nodes are a herniation of the intervertebral disk into the vertebral body. In archaeological studies they have been associated with high levels of physical stress (e.g. heavy lifting), and bipedalism (Bridges, 1989a; Klaus et al., 2009; Knüsel et al., 1997; Lovell, 1994; Novak & Šlaus, 2011; Robb, 1998; Šlaus, 2000; Sofaer-Derevenski, 2000; Weiss, 2005; Wentz & Grummond, 2009). However, Schmorl's nodes appear in non-human great apes (Jurmain, 1999) suggesting they might appear for reasons other than biomechanical stress. Schmorl's nodes do not increase in prevalence with age and they may decrease (Novak & Šlaus, 2011). This last may suggest either that Schmorl's nodes may occur and heal with age or that those represented with Schmorl's nodes were not healthy individuals who died young.

The aetiology of Schmorl's nodes is usually linked to herniation of the intervertebral disc and the condition is linked to back pain. Peng and colleagues (2003) found that histologically, the formation of Schmorl's nodes may be due to herniation of the intervertebral disc directly, but could also be due to osteonecrosis and sclerosis of the surface of the vertebral body following damage to the fibrocartilage. They liken this pathogenesis to avascular necrosis of the femoral head, but as noted in the OA section (sub-section 2.2.4.2.1), damage to the cartilage often results in varying levels of osteonecrosis and damage to the underlying bone. What is different here is that this necrosis occurs in the absence of vascularization whereas in OA porosity likely results from subchondral vascularization. Similarly, rupture of the annulus fibrosis will result in vertebral osteophytes (Novak & Šlaus, 2011; Roberts & Manchester, 2010). These conditions are each similar in their histological aetiologies but vary in their pathogenesis.

While vertebral osteophytes and various arthroses including OA increase in prevalence and severity with age, Schmorl's nodes sometimes have the opposite relationship with age. This suggests that they may result from morphology and stresses already present in human physiology. Plomp and colleagues (2012a) were able to associate the morphology of affected vertebrae to the severity of the Schmorl's node. In a later paper they were able to associate the size and morphology of the vertebral pedicles to the severity of Schmorl's nodes in the lumbar vertebrae (Plomp, Roberts, et al., 2015). They hypothesise that the morphology of the affected vertebrae was less suited than their healthy counterparts to distribute compressive loads suffered as a result of bipedal locomotion. This is due in part to the shape of the vertebral body itself but also the size of the pedicles which would be able to "buttress" the spine. This underscores Bridges (1994) observation that – due to spinal curvature – certain areas of the spine and individual vertebrae may be subject to greater mechanical loading than others. This culminated in Plomp and colleagues (2015) paper which associates the presence or absence of Schmorl's nodes with the morphological evolutionary adaption to bipedal locomotion. They conclude that while it is possible for vertebrae to remodel in response to stress and pathology the morphology observed is likely the cause of the Schmorl's Node. Humans with vertebrae more adapted to bipedal locomotion are less likely to suffer Schmorl's Nodes.

Schmorl's Nodes then are a stress indicator for adults, but one that relies on an underlying morphology and is associated with bipedal locomotion and possibly over-exertion. If they may be associated with stress particularly stress related to walking and lifting they could be generally associated with morphological variation in the proximal long bones. Specifically, Schmorl's nodes may be associated with robusticity particularly in the diaphysis and cross-sectional geometry. Additionally, Plomp's use of GMM as a method was critical for her discovery of the biomechanical aetiology of Schmorl's nodes. This is because the morphology would be difficult to see using other metric methods and almost impossible to quantify. This study hopes to make similar use of GMM with the acknowledgement that particularly diaphyseal shape may only be quantified via this methodology.

2.2.4.3 Osteopenic and Osteogenic Conditions

2.2.4.3.1 Osteopenic Pathologies and Fractures

Osteoporosis is the advanced form of osteopenia and continues to be a health risk today (*WHO scientific group on the assessment of osteoporosis at primary health care level*, 2004). Osteopenia is simply low bone mass or "poverty of the bone" whereas osteoporosis is a 30% reduction that is likely to lead to related fractures (Roberts & Manchester, 2010). These fractures are common as the individual's

bones have become thin and brittle enough to make them more susceptible to fracture even with normal use. The disease generally results from an imbalance in osteoblastic and osteoclastic activity (O. M. Pearson & Lieberman, 2004; Roberts & Manchester, 2010). Osteoporosis may be primary meaning that it is unrelated to any other condition, or secondary meaning that there is another condition causing it. Primary osteoporosis is divided into Type I and Type II. Type I is the most common and occurs in women within 15 to 20 years of menopause due to the replacement of oestradiol with oestrone. Type II osteoporosis is also known somewhat pejoratively as “senile osteoporosis,” because it occurs well after menopause and is caused by decreased activity of the kidneys and thus low metabolism of vitamin D (Larsen, 1997; Roberts & Manchester, 2010). However, as diagnosis of osteoporosis and osteopenia relies on a reduction of bone mass they are technically impossible to diagnose based on skeletal remains alone unless that individual’s previous bone mass is known. Individual variation means that what would be an osteopenic bone in one person may be healthy and normal in another. In archaeology, osteoporosis is usually diagnosed through compression or “cod-fish” fractures in the vertebrae (Brickley & McKinley, 2004). However, in a living population individuals may be diagnosed without the presence of fractures. If imaging like CT or MRI scans shows a significant change in cortical thickness, the individual may be diagnosed with osteoporosis. Similar techniques have been applied to cemetery populations, however as these populations are deceased only under rare occasions may there be a baseline image with which to compare the final result. (However, it is acceptable to diagnose osteopenia by establishing a baseline of bone mass for the age, sex, and population affinity of the individual in question (Roberts & Manchester, 2010).) Additionally, deceased populations are susceptible to diagenesis which may mimic osteopenia (Agarwal et al., 2004; Mays, 1996). Thus individuals exhibiting osteopenia or osteoarthritis will be underrepresented in a cemetery population.

As finding osteoporosis in archaeological or cemetery populations is difficult, several methods have been attempted. Agarwal and colleagues (Agarwal et al., 2004) took photographs of sectioned vertebrae and which they then visually manipulated so that they could view only the connectivity of the trabecular bone. This allowed them to count trabecular “nodes” and then estimate bone loss or comparative connectivity within a population. They note that with imaging techniques their method is theoretically clinically applicable. Certainly it is also applicable to other cemetery populations whether by sectioning or imaging, but it is not simple and where the sectioning technique is applied, it is also destructive. On the other hand it provides a remarkably quantifiable and accurate picture of trabecular connectivity and therefore bone density and strength.

Other studies (Mays, 1996) have adopted an older but effective clinical cortical index. Mays measured the thickness of the of the medullary cavity and total width of the second metacarpal and applied the formula

$$\text{cortical index} = \frac{\text{total bone width} - \text{medullary width}}{\text{total bone width}} \times 100$$

Like osteoarthritis, osteoporosis is typically associated with old age. In modern populations it is largely considered an ailment of post-menopausal women. However, there are several problems with this generalization. Osteoporosis affects women and men. In Archaeological populations women do not even always have a higher rate of apparent bone loss than men (Agarwal et al., 2004; Mays, 1996). Secondly, there is little evidence to show that it is a disease of the aged more than the aging. That is, loss in cortical density is apparent in older adults – just pre to peri-menopausal – but cortical density does not decrease significantly after that point (Agarwal et al., 2004; Frost, 1999; Mays, 1996). And finally, there is mounting evidence that childhood health and nutrition may be a better indicator of later osteopenia than even hormonal changes during adulthood (Frost, 1999; Karapanou & Papadimitriou, 2010; Mays, 1996).

The endosteum is laid down immediately prior to puberty and its health and thickness are dependent upon factors such as nutrition, general health, and physical activity at and in the years prior to puberty (Drapeau & Streeter, 2006; Frost, 1999). Poor nutrition during childhood is widely recognized by the World Health Organization as a major health issue impacting immune response, bone strength, stature, and health of offspring (World Health Organization UNICEF, 2003). Because of its clear effect on the bone, particularly the inner table childhood nutrition is a major factor in later presentation of osteopenia and osteoporosis.

Other contributory factors may occur after puberty and after attainment of adulthood. For the most part these are hormonal fluctuations, but adult bone strength may still be compromised by poor nutrition. Calcium intake via diet or supplement is popularly considered a foil to the gradual thinning of cortices and trabeculae however there is some evidence to suggest that high calcium intake in adulthood does not significantly alter the osteopenic process. Dietary calcium is useful in deterring bone mass loss and Anderson (1995) recommends that after 25 women and men ingest 800mg of calcium a day. However she also recommends that adolescents and young adults age 11-25 take in an additional 400mg of calcium daily (Anderson, 1995: p. 270). Calcium can also block the absorption of iron and in

turn contribute to anaemia. However, while intentionally ingesting calcium may not be particularly useful for adults, proper nutrition is still paramount as malnutrition eventually leads to an increase in osteoclastic activity without accompanying osteoblastic activity (McEwan et al., 2005; O. M. Pearson & Lieberman, 2004). Additionally, if calcium is not present in the diet, necessary calcium will be leached from the bones. In adults, most of the observable change in this last case has come from the inner table of the bone as in adulthood bone is absorbed from the endosteum and deposited periosteally (Larsen, 1997).

Other dietary habits are crucial to the formation of bone. Vitamin D is the most obvious contributor and has been discussed in subsection 2.2.4.1.3. Lack of vitamin D either from milk or metabolised from exposure to UV leads to hypocalcaemia and hypophosphatemia (Anderson, 1995). As both calcium and phosphate are integral parts of the bone structure, having low levels of them would obviously impede deposition of new bone or formation of bone in juveniles. Less obviously, there is some evidence that a high protein diet may lead to osteopenic problems. Individuals with high protein intake have urinary output high in calcium (Stini, 1990 in Roberts & Manchester, 2010). High protein intake may impede calcium absorption but it is entirely possible in this last case that the calcium in the urine is simply dietary calcium which was too abundant to be absorbed.

In regards to the last point and as Roberts and Manchester point out, it seems logical that if high protein intake results in less absorption of calcium and more calcium in the urine, then hunter gatherer groups with high protein intake would show higher frequencies of osteoporosis than agriculturists whose diet would be based more heavily on cereals (2010 p. 244). However, that does not seem to be the case. Roberts and Manchester then theorise that perhaps the exercise involved in the hunter-gatherer lifestyle might counteract the calcium loss from a high protein diet. But as they argue agriculturalists seem to have more osteoarthritis which suggests they had a comparable if not higher workload to hunter-gatherers. Roberts and Manchester conclude the argument with the thought that osteoporosis has a very complex aetiology and should be considered alongside other stress markers (Roberts & Manchester, 2010).

Crucially for adults, osteoblastic activity increases with weight-bearing activities. The results may be subtle as with increased cortical thickness or obvious as with the formation of more robust enthesal changes. Thus an active adult is more likely to have a slower rate of bone mass loss than an inactive adult. Factoring in weight, heavy individuals are more likely to have better bone mass than light or underweight individuals simply because they are bearing more weight and thus placing more strain on

their bones which respond with osteoblastic activity (Agarwal et al., 2004; Kohrt et al., 1997; Shanb & Youssef, 2014; Vainionpää et al., 2005).

Much has already been said in regard to the balance of osteoblasts and osteoclasts. Osteoclasts are necessary to free up nutrients, remove damaged bone, and allow for the bone to be remodelled. However, osteoclasts work faster than osteoblasts and their ratio to osteoblasts increases with the individual's age. Nishida and colleagues found that with age there is a decline in osteoprogenitor cells which developed into osteoblasts (Nishida et al., 1999 in O. M. Pearson & Lieberman, 2004). Further unbalancing the system aged cortical bone has fewer lacunae which allows for more micro-cracks and weakness.

Hormonal contributions to osteoporosis may be oft overstated but are still deserving of note. As seen above, archaeological populations show a relatively equal amount of osteopenia and osteoarthritis among both females and males (Agarwal et al., 2004; Mays, 1996). Modern populations, especially modern Western populations show more women with osteoporosis than men. The dichotomy is usually explained at least in part by increased life span. However as stated above, osteopenic decline peaks around menopause, but does not continue at that rate in later life. Additionally, it may be somewhat fallacious to claim that modern populations have greater longevity than archaeological ones simply because age estimation using standard techniques caps at 50 years of age. As discussed in subsection 2.2.2 it is clear based on historical and epigraphic documentation that many individuals from around the world during different time periods lived well past 50 years (Gowland, 2007). Menopause has recently been hailed as part of our species' evolutionary adaption as it frees an adult woman from potential pregnancy and allows her to gather resources for their children – who may be pregnant - and grandchildren who are presumably not yet fully prepared to contribute resources (Hawkes, 2003). Menopause has been shown to have been historically stable regarding when in a woman's lifespan it occurs (Hawkes, 2003; Kachel & Premo, 2012). These two ideas taken together suggest that despite our difficulty in age estimation many past peoples well exceeded 50 years of age.

Menopause and the onset of menopause are linked with an increase in severity of osteopenia and osteoporosis, but other events such as parity and lactation are contributory. During pregnancy and initial lactation osteoclastic activity exceeds osteoblastic activity in order to provide nutrients for the foetus and then for the neonate and infant (Agarwal et al., 2004; Mays, 2000, 2010). Some studies, however show that extended lactation leads to recovery (Agarwal et al., 2004; López et al., 1996). This means that number of pregnancies and time between pregnancies can contribute to a decline in bone

mass (P. H. Henderson et al., 2000; Mays, 2010). Pearson and Lieberman (2004) point out that oestrogen in normal doses increases osteoblastic and chondroblastic activity, but they do not specify if they are referring to oestrone, oestradiol, or oestriol. The distinction is crucial as prior to menopause and outside of pregnancy, oestradiol is the primary oestrogen. Likely, this is the oestrogen that upregulates osteoblastic activity and thus prevents osteopenic decline. However, oestrone is the oestrogen common after menopause and thus may well be related with osteoporosis. Likewise, oestriol is produced during pregnancy, and while it is neuroprotective specifically chemically protecting the fat sheaths around the axons of neurons, it may be responsible for the osteoclastic activity which frees up calcium for metabolic use by mother and foetus (Sicotte et al., 2008).

Hormonal involvement in bone shape especially where osteopenia is considered becomes immediately circular. Alterations in hormonal expression can cause weight gain or loss (Kaastad et al., 2000). As shown above, low weight is contributory to osteopenia simply because the bone is not bearing enough weight to cause formation of more bone. But aside from that simple relationship, hormones regulate the uptake of calcium and other nutrients. Depending on hormonal levels, calcium uptake from dietary sources may be raised or lowered. If it is lowered, calcium will be leached from bones to balance the system. Additionally, the hormonally influenced weight gain could contribute to further release of oestrogen as fat and oestrogen production are linked. Kaastad and colleagues (2000) found that rats whose ovaries were surgically removed gained more weight and had higher bone mass than control rats. Somewhat conversely but pointing to the importance of hormonal balance, young active women who stop menstruating due to low body fat ratios experience a significant loss in bone mass (Kriener, 1995 in Larsen, 1997). It is important to note that Kriener was researching with women engaged in extreme cardio-vascular exercise regimens rather than weight bearing activities.

Multiple traumas are associated with osteoporosis. Most notable for archaeology is the 'cod-fish vertebrae' or compression fracture of the vertebrae mentioned above. However, other traumas are common and include hip fractures, rib fractures, wrist fractures –probably from falls (Colles' fracture being the most diagnostic), and notably spondylolysis (Bridges, 1989b; Merbs, 2002; Roberts & Manchester, 2010). The former three are relatively self-explanatory: with the weakening of the bone, less impact is required to cause the bone to fracture so a relatively innocuous bump or stumble could result in a broken bone. However, spondylolysis is more typically associated with heavy labour or activity. It is a fracture or an agenesis of the *pars interarticularis*. It is typically associated with young individuals with high levels of physical activity. However, it does also occur in older women and in these

cases, Bridges (1989b) associates the fracture with osteoporosis suggesting that comparatively light physical activity was sufficient to fracture the bone in its weakened state. It should also be noted that kyphosis or ‘dowager’s hump’ are particularly diagnostic of osteoporosis and result from compression fractures in the thoracic and lumbar vertebrae (Agarwal et al., 2004; Brickley, 2002; Roberts & Manchester, 2010). However, many individuals presenting with osteoporosis or osteopenia may also have degenerative joint disease or osteoarthritis with osteophytic action. Differential rates of remodelling in different parts of the skeleton or even the same bone allow for individuals to have this co-morbidity. Resorption of the endosteum may occur simultaneously with the formation of osteophytes at the joint margin and vascularization of the subchondral bone.

2.2.4.3.2 Enteseal Changes

Enteseal changes are formative or lytic alterations to the fibrous or fibrocartilaginous enthesis (Cardoso & Henderson, 2010; Samsel et al., 2014). They have multiple aetiologies some of which are pathological but also may occur in healthy individuals. In the past they were considered activity related change, but several authors have since debated the veracity of that interpretation (Cardoso & Henderson, 2010; Jurmain et al., 2012; Niinimäki, 2011; Weiss, 2003; Weiss et al., 2012). Individuals designated as “bone formers” will have advanced enteseal changes (Mays, 2015a, 2015b; J. Rogers et al., 1997) and the development of enteseal changes may be due to a genetic predisposition for spondyloarthropathies (Samsel et al., 2014).

Enteseal changes form due to auto-immune response, but the pathogenesis for the autoimmune response is debatable and probably varies case by case. The fibrocartilaginous entheses near the epiphyses are the most prone to injury or in fact enteseal change (Cardoso & Henderson, 2010). Whereas the longer entheses along the diaphyses may be entirely fibrous the fibrocartilaginous entheses feature a gradation of mineralised tissue which is mechanically necessary to dissipate loads, but also could be culpable in hyperossification at the site. Ossification is a result of cytokine related inflammation similar to that seen for the formation of vertebral osteophytes, OA, and Schmorl’s nodes (Samsel et al., 2014). This points towards an auto-immune aetiology for many of these pathologies which could have a greater and more global chemical and metabolic effect. Auto-immune response may be triggered by a genetic predisposition, bacterial infection, injury, or bacterial infection triggered by injury (Samsel et al., 2014).

Past literature has suggested that micro-traumas may exacerbate the entheses enough to cause the formation of an enteseal change and have therefore linked enteseal changes to activity related

change and sexual division of labour (Churchill & Morris, 1998; Havelková et al., 2011; Wilczak, 1998). Peterson (1998) and many other authors attempted to link enthesal changes at certain muscle sites to activities like spear throwing, bow pulling, grinding and so forth. Pálfi (1992) uses the dual presence of enthesal changes and OA to argue that only the males in his study of medieval Magyar were routinely mounted. Hawkey (1998) in her evaluation of an impaired male used the presence of enthesal changes to attempt to reconstruct his decreasing mobility as the disease progressed. Havelková and colleagues (2011) do briefly touch on the problematic nature of using enthesal changes to reconstruct activity and Weiss (2003) was one of the first to very clearly call into question the validity of this approach. The major unravelling of this approach occurred as a result of work by Henderson, Jurmain, Niinimäki and Weiss who observed that enthesal changes were almost invariably related to size, age, and sex (Cardoso & Henderson, 2010; Jurmain et al., 2012; Niinimäki, 2011; Weiss et al., 2012).

Enthesal changes are not formally recorded in this study but their presence was noted and where they occur with spinal arthropathies the individual is classified as having an osteogenic bone type. Particularly in the context that they may denote genetic predisposition for spondyloarthropathies they are interesting to this study in that they represent a different kind of immune response than is likely to be seen in osteopenic or normal individuals. They are likely to have an effect on morphology both directly in that the enthesal changes could subtly alter the epiphyseal shape and because if they are strongly linked to auto-immune response there may be slight alterations to the morphology of the rest of the bone.

2.3 Interpopulation Variation

Interpopulation variation here refers to variation between populations which is consistent enough to statistically delineate populations. It is therefore not exclusively heritable. In particular, climate variation may contribute to morphological variation and activity levels or nutritional practices which are consistent within the population may contribute to a phenotypic expression which distinguishes the population from others to varying degrees. Manica and colleagues (2007) while arguing for the out of Africa interpretation of human evolution present their data with corrections for clinal variation. Japanese skulls from the prehistoric Jōmon through the modern show considerable morphological variation particularly during the Kamakura period despite having a relatively stable population with little admixture. While considering an evolutionary component, many authors attribute this to changes in diet over time (Kamegai et al., 1982; Suzuki et al., 1956). It is possible, as discussed

above, for diet, activity level, and pathology to cause morphological variation at an individual or intrapopulation level, however when these factors are consistent throughout a population – as is often the case for clinal variation – then while morphology may not be strictly heritable it does speak to interpopulation variation.

Interpopulation variation may be inferred from genetic, epigenetic or non-metric traits, metrics particularly craniometrics, and from a cultural perspective practices like cranial deformation or tooth ablation which leave lasting marks on the skeleton (Hanihara, 1992, 1996, 2000, 2008, Hanihara & Ishida, 2001, 2009; Herrera et al., 2014; Manica et al., 2007; Relethford & Harpending, 1994). GMM has been used particularly with cranial-facial features to show interpopulation variation, but other authors have shown that interpopulation variation is also apparent in the morphology of long bones most notably the humerus (Claude et al., 2004; Harvati, 2009; İşcan et al., 1998; Ponce de León & Zollikofer, 2001; Proctor et al., 2008) (also see (T. L. Rogers, 2009; Vance & Steyn, 2013) for sexual dimorphism in the distal humerus). This research is not solely interested in interpopulation variation, but it must be discussed in order to show the degree of morphological variation with intrapopulation variation.

2.3.1 Heritable, Ancestral, or Genetic Variation

Several hypotheses and sub-hypotheses exist for the evolution of *Homo sapiens*. These include the Out of Africa theory which is divided into several possible sub-hypotheses for timing, number of migrations, and degree of interrelatedness with other hypotheses and the parallel evolution theory. Presently, the hypothesis backed by the most evidence is the Out of Africa theory. This is relevant here because if humans evolved from a single stock in Africa, then African particularly East, sub-Saharan diversity is greatest with all other populations decreasing in diversity the further removed from Africa they become (Hanihara, 1996, 2008; Harvati, 2009; Manica et al., 2007; Relethford, 2009, 2010). This study includes a selection of individuals from medieval Sudan and a selection of individuals from medieval and postmedieval England. Presumably the Sudanese population should exhibit more diversity than the English populations. Additionally, this theory points to the primacy of variation within populations rather than between populations as observed in particular by Relethford (Relethford, 2009; Relethford & Harpending, 1994).

Based on genetic and craniometrics data most authors conclude that the high degree of among group diversity shown in East sub-Saharan African populations as compared to the progressive relative lower degree of among group diversity shown radiating outward from East Africa indicates a series of genetic “bottlenecks” as modern humans spread out of Africa and further throughout the world

(Hanihara, 2008; Manica et al., 2007; Relethford & Harpending, 1994). Manica and colleagues show that 19-25% of heritable variation in craniometrics measurements may be related to the distance of the population from Africa (Manica et al., 2007 pp. 246). Relethford and Harpending (1994) are echoed by Hanihara (2008) in his statement that the diminishing rate of within group variation with distance from Africa points to a lower effective population at divergence as well as relatively recent divergence. Relethford and Harpending (1994) additionally comment that populations in Europe, South East Asia and the Americas evidence lower phenotypic variations in comparison to East African populations which additionally suggests not only a smaller population at the time of divergence, but also less long range gene flow. These populations were relatively isolated genetically and therefore evidence less within group variation. Conversely, the high within group variation evidenced by the East African populations suggest that their initial population was much larger and more diverse and also maintained this size and diversity over time. There are two pertinent points to take away from this discussion of the origin of modern humans. For one, interpopulation variation is partially described by and dependent upon intrapopulation variation and variation within the Sudanese population is likely to be greater than variation within the English populations and may contribute to between population variation.

Genetic within group variation however does not preclude between group variation. Relethford (2009) stressed that most variation occurs within populations, but that populations could be delineated with genetic and phenotypic information (Relethford, 2010; Relethford & Harpending, 1994; Relethford & Lees, 1982). Often this amounts to genetic “distance” or how far populations are from one another (this is imperfectly related to geographical distance as it has to do with the duration and level of admixture). Genetic traits are heritable, and phenotypic traits have a degree of heritability. Therefore, phenotypic traits which are more heritable like craniometrics and epigenetic traits are useful lines of evidence for determining within and between group variation as well as genetic distance between populations.

GMM has obvious applications in evaluating within and between group variation in terms of shape and this has been performed by Baab, McNulty, and Rohlf (2012) in order to demonstrate phylogenetic variation in shape. Similarly, Viðarsdóttir and colleagues (2002a) used GMM to demonstrate craniofacial and ontogenetic variation between populations. Baab, McNulty, and Rohlf (2012) were concerned with demonstrating the usefulness of applying morphological quantification to studies in phylogenetic variation, and therefore parenthetically showed the relationship between cranial shape and genetic distance. They also underlined the importance of modularity and ontogeny in evolution as well

as touching on the impact of functional morphology. All of their observations were applied to variation between species as opposed to within a species as is the case for this study as well as previous studies mentioned in this section, however some of these observations particularly ontogeny and genetic distance in relation to cranial morphology are applicable here. Viðarsdóttir and colleagues (2002a) expand on these themes directly applying analysis of craniofacial morphology to within and between group variation including an analysis of ontogeny. They found that infant and juvenile craniofacial morphology is already sufficiently distinct to classify individuals by population, but ontogeny is further population specific. Both ontogeny and craniofacial morphology are heavily although not exclusively heritable, but these studies demonstrate the notable impact of genetics on phenotype and the usefulness of morphology in determining population affinity. However, both studies also note the influence of various non-genetic factors on morphology. These factors are arguably more expressed in post-cranial morphology and will be discussed in the following sections. Regardless of the degree of impact from heritable or environmental factors, crania have been shown to be morphologically consistent enough that populations may be defined via a GMM studies of the cranium and mandible (Hennessy et al., 2004; Hennessy & Stringer, 2002; Humphries et al., 2015).

2.3.2 Phenotypic, Environmentally influenced, or Epigenetic Variation

The previous section nearly conflated craniometrics and epigenetic particularly dental epigenetic traits with genetic affinity and heritability. These traits are phenotypic rather than genetic. However, osteoarchaeology must largely rely on phenotypic traits to determine genetic affinity and heritability. This section will discuss where problems may arise and why it is possible with some caution to consider some phenotypic traits as largely heritable or indicative of genetic affinity.

Living conditions, environment, and diet have been shown to have a likely impact on morphology in some cases in excess of genetic expression. Rethethford (2009) attempted to determine how well linked craniometrics and geographic distance were and he found that not only are geographic and morphometric distance almost perfectly predictive of one another, but metrics could be used to correctly classify people within their geographical groups at almost any level of specificity. (In the same publication he cautions that most morphological variation occurs within rather than between populations.) However, he also found three outliers specifically the Beirut, the Greenland Inuits, and Peruvians. The Peruvian population was closer craniometrically to surrounding populations than expected which he theorised was a result of very quick migration. That is the population had not been isolated long enough from the surrounding populations to evidence a more specific morphological

signature. The other two outliers in this context are more pertinent because both the population from Beirut and the Greenland Inuits lived in very cold environments. Other authors have noted a correlation between phenotypic and clinal variation (Cardini, Jansson, et al., 2007; Hanihara, 1996, 2008; Manica et al., 2007; Relethford, 2010) and some have noted that specific environments such as cold environments or islands may through diet, temperature and other factors influence phenotype (Bindon & Baker, 1997; Millien et al., 2006). Manica and colleagues (2007) suggest that in general terms the likely causes of clinal variation are minimum and maximum temperature and precipitation. However, regardless of the role climate plays in phenotype, these populations remain distinct. While it is important to explore the effect of climate on morphology in relation to heritability and genetics, studying inter and intra population variation on a phenotypic level is acceptable here due to the low probability of any individual or group of individuals having migrated from far enough away to disturb the general morphological trends of the populations in question. While this section is concerned primarily with between population variation it is notable that Relethford (2010) as well as Hanihara and Ishida (2009) both note that while their regionally diverse populations may be delineated, there is more within group variation than between group variation.

This argues that phenotypic traits are sufficient in determining genetic affinity and heritability but still has not addressed whether or not phenotypic traits of any sort are strictly heritable. Unfortunately, the answer is complicated. Climate effects are likely to be relatively constant for individuals with genetic affinity. When observing phenotypic traits like epigenetic markers on teeth and craniometrics it is important to note that while these are effective in delineating populations, they are not strictly heritable. Teeth and craniometrics give useful phenotypic data when investigating variation particularly between populations (Ruff, 1994). Hanihara (2008) explains that epigenetic traits on teeth as heritable markers is supported by twin studies but also points out the consistency of environmental pressures in all population studies of epigenetic and metric traits (Relethford & Harpending, 1994; Relethford & Lees, 1982). The obvious should also be stated; while identical twins and even fraternal twins are closely genetically related, twins also share at least a uterine environment. A study of craniometrics and dentition of various temporally separated Japanese populations showed significant variation between the populations in spite of them having very limited admixture (Kamegai et al., 1982). When discussing morphology or epigenetic traits while heritability is a factor population variation may be dependent on climate to a sizeable degree. However, while questions of heritability in relation to epigenetic traits is relevant for determining the relationship between genotype and phenotype it is less relevant when discussing variation between and within populations because the environment for these

groups may be assumed to be relatively stable. Metrics and epigenetic traits may be assumed, within a geographical, cultural, and temporal context to be reasonable surrogates for genotype.

This use of epigenetic traits as largely heritable is underscored in the use of dental epigenetic traits to support the Out of Africa theory briefly outlined in the previous section. Dental traits in sub-Saharan East Africa show a level of variability that is unmatched outside of Africa (Hanihara, 2008) and has been maintained at least from the Predynastic through the Christian era. Distance from Africa is largely predictive of the level of variability and type of dental epigenetic traits in most populations. If either dental epigenetic traits were not good indicators for population variation or if the Out of Africa theory was partially or completely incorrect (for example if there had been multiple largely contemporaneous origins or if there had been multiple waves of anatomically modern humans out of Africa), this worldwide variation in epigenetic dental traits would likely not evidence as it has with a generally smooth and progressive loss of diversity (Hanihara, 2008; Relethford, 2009; Relethford & Harpending, 1994; Relethford & Lees, 1982).

The same stipulations which apply to dental epigenetic traits apply with craniometrics. I have above argued that epigenetic traits may with certain caveats be interpreted as surrogates for heritability where DNA may not be readily studied because they have been shown to follow expected patterns for migration and genetic diversity and they generally match well with genetic data. Craniometrics have successfully been used to delineate human populations, but it must be again stressed that there is generally more variation within populations than between and that a population's craniometrics may drastically change without any or significant genetic admixture due to factors which may include temperature, diet, and stress (Kamegai et al., 1982; Relethford, 2009, 2010; Relethford & Harpending, 1994). With that understood craniometrics within GMM has frequently been used to determine intra and infraspecies population affinity (Hennessy et al., 2004; Hennessy & Stringer, 2002; Humphries et al., 2015; Viðarsdóttir et al., 2002a). Of particular note Viðarsdóttir and colleagues showed that not only were craniometrics a reliable means of determining population affinity, but infant craniofacial complexes were sufficiently determinant to be correctly classified regardless of ontogenetic trajectory, but that ontogenetic trajectory was also a function of population affiliation (Viðarsdóttir et al., 2002b).

With the understanding of the relationship between population variation, craniometrics, and epigenetic traits in mind it is logical to assume that long bones and the rest of the post-crania may exhibit some population specific morphological variation. Studies to be discussed subsequently have found correlation in morphology of post-cranial elements and population. The question becomes how

much of morphology in the post-cranial skeleton is a result of population affinity and how much is a result of more individual factors like sex, age, pathology, and activity level. Harmon (2007, 2009) in her study of early hominin hips quantified the morphology of bipedal locomotion in primates. In this case populations actually refer to species or nearly speciated hominins but the relationship between functional morphology and genetic affinity is clear: shape may be dictated by both ecology and genetic affinity, but neither will be entirely determinate of shape and genetic affinity does have strong influence on morphology. Anderson and Trinkaus (1998) and Pujol and colleagues (2016) attempted to better define the relationship between hip morphology and ontogeny, and population affinity, sexual dimorphism, and activity at adolescence in humans and came to similar conclusions. In general they found that particularly in relation to the femoral angle the primary correlation and likely causation was activity level during adolescence. Both studies found a small degree of sexual dimorphism and considered the possibility of population related morphological variation (Anderson and Trinkaus (1998) went so far as to divide the sample by population and latitude), but on the basis of their evidence they both concluded that the variation present was more likely the result of activity and loading at adolescence (Pujol et al., 2016).

The patterns of sexual dimorphism particularly in long bones may also be population dependent (Green & Curnoe, 2009; Kranioti, Bastir, et al., 2009; Patriquin et al., 2003; Pretorius et al., 2006; Robinson & Bidmos, 2009; Sakaue, 2004; Srivastava et al., 2013; P. L. Walker, 2008). İşcan and colleagues (1998) researched several populations' trends of sexual dimorphism in long bones they found that different measures were more predictive of sex in different populations and different populations showed a slightly different arrangement of metrics in the long bones. In their study the populations included were Thai as South East Asian, and Japanese and Chinese as East Asian. Chinese tended to have on average longer bones but with smaller epiphyses and less sexual dimorphism. Japanese were shorter but clustered largely with Chinese, and Thai showed a bit more robusticity particularly in the epiphyses but shorter bones overall. This underscores the usefulness of known sex and age skeletal collections, but in contrast Stevens and Viðarsdóttir (2008) using the Terry collection showed that the morphology of the knee was not well correlated with different populations and in fact bore more correlation with urban or suburban life

Phenotypic variation between populations clearly exists, but is dependent upon and interrelated with additional factors including sex, clinal variation, and "economic" variation (or physical activity and nutrition specifically in mid to late adolescence). Phenotypic variation also varies in how

genetically predetermined it is based on what area of the body is examined. Dental and cranial traits appear to be highly heritable, with post-cranial traits being more susceptible to other factors. However, interpopulation variation is not dependent on whether or not a specific metric or non-metric trait is heritable, just if it is consistent. That is even if phenotypic traits are largely dictated by environment, diet, and physical activity, they remain relevant in the discussion of interpopulation variation if they are consistent enough within one population to delineate that population from another.

2.3.3 Cultural or Activity Related Variation

In some cases, populations intentionally or unintentionally modify themselves to in performance of their cultural belonging or their status within their own culture. This appeared very rarely in the populations examined in this study, but should be briefly noted. In some cases cranial modification is used to advertise the status or identity of an individual. This modification must be performed at infancy and so refers to the status and culture of the parents rather than the individual themselves. In later life many populations practice tooth ablation for various reasons. Jōmon populations practiced tooth ablation to demonstrate endogamic or exogamic practices. Other populations use tooth ablation as a rite of passage to demonstrate the individual is of a certain age, and still others engage in the practice for cosmetic reasons (Temple et al., 2011). This modification may be performed with some level of autonomy from the individual with the modification as it must be performed in adulthood.

The skeleton and teeth may also be modified unintentionally in response to cultural or subsistence practices. Artificial but accidental modifications to the teeth may occur with pipe smoking, clutching other items like nails in the teeth, or softening fibers along the teeth thus creating grooves. Another probably largely accidental skeletal modification is the warping of the ribs due to corsetry. These unintentional modifications may provide information on the individual's status and daily life and sometimes may demarcate them as part of a specific population.

Activity, particularly daily activity that may refer to subsistence practices may also have an effect on the skeleton. Several studies in the previous section mentioned morphological variation in either the hip (specifically the angle of the femoral neck) or the knee in relation to either "economic activity," or rural or urban environment (J. Y. Anderson & Trinkaus, 1998; Stevens & Viðarsdóttir, 2008). In this case there may often be some correlation between morphology and sex pointing possibly to sexual division of labour or less mobility for certain groups of people. Additionally, geology or subsistence practices may lead to a higher or lower rate of trauma in a given population. In this study general demographic studies of the Mis Island population show a higher rate of trauma. There are many possible causes for

this but one likely suggestion is that this population worked with large domesticates and relied on them in agriculture as well as for meat and dairy products. The high rate of trauma may be consistent enough to be considered interpopulation variation (Edwards, 2004; Ginns, 2007).

Diet may also be used to confirm an individual's relationship to a given population. This idea is the general basis of stable isotope testing which can demonstrate where an individual was at certain points in their life by the chemical signature left in their tissues by food and water consumed at those points. This sort of testing may also identify individuals from outside a population or individuals who are not native to the area in which they are interred. Additionally, diet and specifically dietary deficiencies may also help place individuals. Epidemics or famines and sometimes low level parasitic infection may ignore status and affect all members of a population simultaneously. For example, when populations initially alter their subsistence techniques to agriculture they often experience an initial decline in general health due to the reliance on cereal grains over proteins combined with periods of food scarcity (Blom et al., 2005; Eerkens et al., 2014; Somerville et al., 2015; Sullivan, 2005; P. L. Walker, 1986). When dietary effects such as this are so widespread interpopulation variation may be a function of diet.

2.4 Allometry

Allometry is. "the study of size and its consequences," (Mitteroecker et al., 2013a), but GMM via the Procrustes method attempts to eliminate size, rotation, and translation so that objects – in this case biological objects – may be compared. Here it is crucial to define the difference between size, shape, and form. Size may be used in classical morphometrics to good effect as it measures objects by ratio, length, width, distance and so on. Shape in a mathematical sense however has no size. Form consists of both size and shape and is therefore a useful concept to at least consider in a GMM study as in most biological sets size has at least some impact on morphology. GMM, the primary method in this study, has the capacity to ignore size. However, while morphology features largely in each of the research questions considered for this study, morphology may also be dependent upon size. For example, this study includes both females and males and two population sets (those being English and Sudanese). Whilst it is possible that sexual dimorphism and interpopulation variation may be represented exclusively by shape or possibly not even be present, the influence of size – if present – must be considered as it may pertain to ontogeny, biomechanics, and any other number of contributory factors.

There are two methods or schools for implementing study of allometry. They are the Gould-Mosimann school and the Huxley-Jolicoeur school. The Gould-Mosimann school is the method used primarily in GMM and conceptualises allometry as covariation of shape and size. As is done throughout this study using the Gould-Mosimann, shape variables (Procrustes shape variables) are regressed against size (Centroid Size) (Mitteroecker et al., 2013a). The Huxley-Jolicoeur method makes the first principle component an allometric trajectory. This is implemented in GMM through the use of form space. The critical difference in these two methodologies or conceptualisations is that the central component of the Gould-Mosimann school is that shape may vary with size but is not dependent on it and in the Huxley-Jolicoeur school shape and size are co-dependent (Klingenberg, 2016). Swiderski (2003) demonstrated through an ontogenetic analysis of shape variation in mandibular morphology of fox squirrels that using methods where size and shape are conflated (e.g. linear measurements) overestimated the allometric effect. Allometry was still present in his example when using GMM, but to a lesser degree. With this in mind, the Huxley-Jolicoeur school is still useful particularly in studies of ontogeny but may also allow for a multivariate approach to allometry simply by dedicating the first Principal Component (PC) of a Principal Component Analysis (PCA) to size (D. C. Adams et al., 2013).

There are three main types of allometric studies: ontogenetic, evolutionary, and static (Baab, McNulty, et al., 2012; Klingenberg, 2016; Mitteroecker et al., 2013b). Each of these often overlaps into others as studies on static allometry will frequently examine adults from different species and evolutionary allometry is often interested in heterochrony and ontogenetic allometric trajectories will inform intra and inter-population and species variation (Baab, McNulty, et al., 2012; Klingenberg & Zimmermann, 1992; McNulty, 2012; Mitteroecker, Gunz, Weber, et al., 2004; Rozzi et al., 2005; Shea, 1989; Viðarsdóttir et al., 2002b; Viðarsdóttir & Cobb, 2004; Zollikofer & Ponce de León, 2004). This study is of largely contemporaneous adults from the same species so all allometry examined here will be static.

Ontogenetic trajectory concerns the very dramatic changes in shape and size which occur with growth. Another concept which applies to all allometry but is easiest to explain in the context of human development is positive versus negative allometric trajectories. Here allometry is expressed as a regression either with shape and size or with two different size variables in this case head size versus limbs and torso. The possibilities are negative allometric variation, isometry, and positive allometric variation. If babies just grew proportionally and adults had the same relative limb lengths and head to body ratios as infants but were just larger, that would be isometry. (In his study of the long bones of

neosauropod dinosaurs, Bonnan (2007) observed an allometric trajectory very close to isometry and concluded that particularly in the case of *Brachiosaurus* these animals had reached the upper limit of possible allometric change.) The growth of limbs through childhood and adolescence however represents positive allometry because they are lengthening relative to the head and torso and therefore a regression of these two sizes would be greater than 1. The growth of the human head from infancy through adulthood however represents negative allometry because it is not growing considerably relative to the torso and limbs and so a regression there would be less than 1. Human hominid and primate cranial ontogeny is central to studies interested in the relationship between growth and speciation (Leigh, 2006; McNulty, 2006; McNulty, 2012; Mitteroecker, Gunz, Bernhard, et al., 2004; Ponce de León & Zollikofer, 2001; Rozzi et al., 2005; Shea, 1983, 1989; Viðarsdóttir & Cobb, 2004; Zollikofer & Ponce de León, 2004). Ontogenetic trajectories defined by allometry, are so integral in the determination of adult shape that McNulty and colleagues (2006) were able to give the Taung child fossil skull the adulthood he or she never had.

Evolutionary allometry is closely linked to ontogenetic allometry and usually concerns shape and size change with rates and timing of development or evolutionary heterochrony (Klingenberg, 1998; Klingenberg & Zimmermann, 1992; McNulty, 2012). This means that morphology in speciation can often be understood as a species taking on the childlike form (paedomorphism) or the super developed form (peramorphism) of a closely related or ancestor species (Klingenberg, 1998; Shea, 1989). Based on the brain and cranial vault size for humans relative to other hominids an argument has been made for humans being – at least where the cranium is concerned – paedomorphic relative to extinct hominids. Based just on the size of the cranial vault that follows, but the argument has also been made that the human brain itself does not demonstrate the same level of neotony and is only different in that certain neurological structures are more developed than those for extinct hominids (Falk, 1980; Shea, 1989). A similar argument exists for the evolutionary morphological relationship between chimpanzees and bonobos (Lieberman et al., 2007). Conversely, Cardini and Elton (2008a) found that evolutionary variation within the guenon clade corresponds closely with allometric trajectories. Usually when discussions of evolutionary heterochronic morphology break down it is due to variance in ontogenetic trajectories within the same species. For example, bonobo cranial morphology is in many ways relatively paedomorphic to chimpanzee cranial morphology but additional variation in ontogenetic trajectories also contribute to cranial morphological inter-species variation (Lieberman et al., 2007). There is also within species variation where in particular sexual dimorphism may be in part understood as an ontogenetic trajectory that was arrested earlier in one sex than the other. However, this too is not

always fully explained by allometry. Guenons, as Cardini and Elton (2008b) show, display sexual dimorphism on an almost entirely allometric trajectory. Sexual dimorphism in this clade is based almost entirely on size. Cobb and O'Higgins (2007) show that this is not the case for great apes which more commonly share an ontogenetic trajectory until the eruption of the second permanent molars and then diverge.

When not considering ontogenetic trajectories the allometric variation evidenced in some species' sexual dimorphism is static allometry. Static allometry is allometry within or between populations or species where all individuals are adults or at the same developmental stage. This study is comprised exclusively of adults and therefore all allometry observed may be classed as static (Baab, McNulty, et al., 2012; Klingenberg, 1998; Shea, 1989). Static allometric variation in this study is most likely to occur linked to sexual dimorphism or interpopulation variation.

Where allometry is robust it is possible to represent shape variation with a single PC, usually PC1, as one axis and CS as the other as Viðarsdóttir and colleagues demonstrated (Viðarsdóttir et al., 2002b). Klingenberg and Zimmermann, evaluated allometry by plotting shape statistics in a single PC against logarithmically transformed measurements. They showed that by using Common Principle Components Analysis (CPCA) which considers all eigenvectors of morphological variation the Common Principle Components (CPC) could be plotted against CS producing similar results as where the PC1 is plotted against CS (Klingenberg & Zimmermann, 1992). (The Klingenberg and Zimmermann method of using CPCA summarizes eigenvectors for all sets meaning that the set with the strongest signal can overpower the other sets. This is then an appropriate method for studies where most variation is truly in the first PC or in examples of evolutionary or static allometry where there is little difference in shape variation between sets, but in a set where shape varies more diversely, this technique may obscure the lesser signals (1992).) However with more powerful programs now available, Mitteroecker and colleagues warn that this method applied less robustly than in the above example could lead to misunderstandings of the data as a single PC is by its nature a data reduction technique and so does not represent the total shape variation of the set. They instead suggest that the "allometric shape score" or the vector of regression coefficients might be a better method and that statistical tests for allometry should be multivariate rather than based on only one PC (Mitteroecker et al., 2013a). The tests for allometry in this study follow that guidance.

Because form and shape differ with the addition (or lack of subtraction) of another variable they must be represented in different but similar spaces. Shape space has been discussed above. Form space

is similarly a Euclidean approximation of the Procrustes distance between forms following the Huxley-Jolicoeur school. However, there are different methods for arriving at form. Possibly the simplest is to simply eliminate the portion of Procrustes fitting that involves size. Objects are translated and rotated, but not scaled. Mitteroecker and colleagues (Mitteroecker et al., 2013a; Mitteroecker, Gunz, Bernhard, et al., 2004) suggest a more explicit method of representing size in studies of form is by “augmenting the Procrustes shape coordinates with the natural logarithm of centroid size ... as an additional variable” (Mitteroecker et al., 2013a).

One last note regarding allometry and size within the context of this study must be made. This study utilises a relatively small sample size. When subdividing among populations in particular the sample size is further reduced. Cardini and Elton (2007) show that small samples of around ten may produce accurate size means and shape variance, but standard deviation of size is very large and the shape mean very inaccurate until the sample reaches and exceeds forty and thirty individuals respectively. This poses difficulty when subdividing by site. The entire sample together is large enough to avoid these issues, but subdivision while possible should be undergone with an eye towards the statistical issues surrounding sample size.

3 Materials and Methods

This chapter provides details regarding the skeletons examined for this study and explains the methodology employed. Section 3.1 will detail the composition of the sample, 3.2 will detail the osteological methods used to obtain the demographic information and section 3.3 will explain the palaeopathological methods. Justification for the use of left antimeres is provided in section 3.5.3. Sections 3.4 and 3.6 deal with the various applications of Geometric Morphometrics (GMM) used in this study and the subsequent quantitative analysis.

3.1 Materials

The sample comprises a selection of adult skeletons from the Coach Lane site from North Shields, UK (N = 50, 1711-1857) (Langthorn, n.d.), the Fishergate House York, UK (N = 27, 10th to 16th c. AD) (Holst, 2005), the St. Guthlac's Priory, Hereford, UK, (N = 12, 12th to 16th c. AD) (Roberts, n.d.) and cemetery 3-J-18 from Mis Island, Sudan (N = 36, 7th to 16th c. AD). All four populations were selected for availability and preservation. This study required in addition to standard skeletal recording, 3D scanning. While the scanner used was portable each bone took about one and a half hours to scan and a power source. Therefore, selection of sites was also based on access to a lab and substantial allocation of bench time. Ideally, further populations can and should be added to this research. This study is on morphology of the whole proximal long bone, therefore only individuals with a complete and well preserved left humerus or femur were included. No element which scored above Grade 2 on Brickley and McKinley's surface erosion criteria (2004) could be included. A fifth site was excluded because only a few adults from the site scored below Grade 2. Tibiae, ulnae, and radii were originally intended to be included in this study however, due to their size and shape they could not reliably and efficiently be digitally rendered with the equipment available at the time. (Humeri and femora take 1.5 to 2 hours each to 3D scan and are usually rendered without misalignments. When the same methodology was applied to distal elements the scanning time was roughly the same, but misalignments which severely misrepresented morphology were common. Future research can include these using white light techniques.)

With the exception of 3-J-18 which was included as counterpoint, all sites are from England and two are from the North of England. Therefore, population variation between sites is assumed to stem from temporal trends rather than spatial/environmental differences. Using the methods outlined by Brickley and McKinley (2004), individuals were assigned to one of five categories of biological sex: female, probable female (?female), unknown, probable male (?male), and male. Age and sex

distributions by sex are illustrated by population in Table 3.1, Table 3.5, Table 3.9, and Table 3.13. Age estimation was based on the methods outlined by Brooks and Suchy (1990) and Lovejoy and colleagues (1985) and following Scheuer and Black (2000) the medial flake of the clavicle was also observed. Ages range from as young as 17 to over 45 years and are divided into four categories: young adult (17-25), young mature adult (25-35) middle mature adult (35-45), and old mature adult (45+). Many skeletons presented with pathologies and tables of some of the pathologies are also detailed in their respective sections. Each section also includes a table on DJD and OA severity by epiphysis. (In some cases due to damage only one epiphysis from a given bone could be included.)

3.1.1 Coach Lane, North Shields

North Shields is located near the mouth of the River Tyne appropriately on the north side. The river meanders and so the precise location of Coach Lane, North Shields is just west of the mouth of the river and North-West of South Shields. Coach Lane is the most recent of the sites included in this study and its cemetery was in use from about 1711-1857 AD. During this period, North Shields was urban and relatively crowded. Similar to many cities in England during the Industrial Revolution, it was a busy centre for industries including salt, coal, and lime production or transport and also hosted roperies, tanneries and other work and production concerning the shipping industry (Craps, 2015). By the early 18th c. North Shields had become crowded and had fallen into disrepair. To alleviate this, a new town was planned around the location of the Coach Lane cemetery (Craps, 2015). Some of those buried at Coach Lane may be from the older more crowded town, but others may have had better living conditions.

This cemetery belonged to the Society of Friends more commonly known as “Quakers.” In life, the Quakers were likely reasonably integrated into society in all but worship, and separated from the rest of the community only in death. Bodies were interred in a supine position in wooden coffins with iron hinges and brackets. Quaker beliefs involve the integration of people of differing socioeconomic status and encouragement of charity. Consequently, very few grave goods accompany the deceased, although a pair of gold engraved cufflinks was recovered from one of the burials. The presence of hinges on the coffins also suggests that there was some sort of funerary display of the body before interment (Gaimster, 2011). Coach Lane consists of 245 discrete burials overall (162 of which were age estimated to have been over 18 at time of death) and 87 charnel contexts (Langthorn, n.d.).

Table 3.1 Coach Lane individuals by sex and age.

Coach Lane	Sex	Age			
		18-25	25-35	35-45	45+
Total	50	6	11	9	22
Female	20	1	3	4	12
% of pop.	40.00%	2.00%	6.00%	8.00%	24.00%
Male	28	5	8	5	10
% of pop.	56.00%	10.00%	16.00%	10.00%	20.00%
Unknown	2	0	0	0	0
% of pop.	4.00%	0.00%	0.00%	0.00%	0.00%

Table 3.2 Coach Lane childhood stress indicators.

Coach Lane	Cribra Orbitalia			LEH		
	CO present	CO absent	orbitals not present	LEH present	LEH absent	teeth not present
Total	14	31	5	40	5	5
Female	9	11	0	17	3	0
% of pop.	18.00%	22.00%	0.00%	34.00%	6.00%	0.00%
Male	5	20	3	23	2	3
% of pop.	10.00%	40.00%	6.00%	46.00%	4.00%	6.00%
Unknown	0	0	2	0	0	2
% of pop.	0.00%	0.00%	4.00%	0.00%	0.00%	4.00%

Table 3.3 Coach Lane trauma and Schmorl's nodes.

Coach Lane	Trauma		Schmorl's Nodes		
	Trauma Present	Trauma Absent	Schmorl's Nodes Present	Schmorl's Nodes Absent	Vertebrae not present
Total	8	42	33	12	5
Female	3	17	11	7	2
% of pop.	6.00%	34.00%	22.00%	14.00%	4.00%
Male	5	23	21	5	2
% of pop.	10.00%	46.00%	42.00%	10.00%	4.00%
Unknown	0	2	1	0	1
% of pop.	0.00%	4.00%	2.00%	0.00%	2.00%

Table 3.4 Coach Lane DJD by element.

Coach Lane	DJD Severity				
	Healthy	DJD	Mild OA	Moderate OA	Severe OA
Proximal Humerus	29	16	0	2	8
Distal Humerus	31	18	1	1	4
Proximal Femur	28	7	1	2	12
Distal Femur	27	12	2	1	8

3.1.2 Fishergate House, York

Fishergate House cemetery was in use from circa 900AD to 1500 and therefore constitutes one of the medieval English sites. It is located in the North of England in the city of York. This site is relatively close to the River Ouse. York was one of the walled medieval castle cities and a political, ecclesiastical, and trade center although arguably of lesser status than the city of Durham due to its Palatine.

To recover expenses accrued during the Hundred Years War tax by individual was implemented. When the rates were adjusted, taxes were levied by church and street. St. Helen's – the church with which Fishergate House cemetery belongs – had the lowest tax rate and is therefore likely the church of choice for the poorest citizens of York. In contrast, separated by a wall found during the excavation the Gilbertine monks at the priory of St. Andrews likely enjoyed a much gentler more privileged life (Ashby & Spall, 2005; Goldberg, 1992).

Fishergate House was in use for some six hundred years. During this time York was variously a Viking settlement, invaded by the Normans, subject to “the Black Death,” experienced a peasant revolt, and economic boom and bust (Palliser, 2014). Therefore, generalizations about York are not likely to apply to all the individuals from Fishergate House included in this study. Assuming those interred in the cemetery lived close by, they would have lived in close vicinity to the River Ouse which would have provided fish, but may also have been a vector for parasites and pathogens. Sullivan in her study of cribra orbitalia in the neighboring cemetery cites both nutritional stress and parasite load as possibly pathogenesis. She comments that York was several times royally condemned for its poor sanitation and that parasite load for all residents would have been high, but likely higher among the most economically disadvantaged (Sullivan, 2005). Palliser (1973, pp. 45-46) also cites conditions that would have incubated disease such as the practice of emptying chamber pots and discarding “butcher's offal” directly onto streets cleaned only by scavenging pigs. According to the Domesday Book, by the Norman invasion of 1066 AD over 9,000 people resided in York and other contemporary sources place the figure at a (likely

inflated) 30,000 (Palliser, 2014). In addition, studies of sinusitis on this population suggest a relatively high level of crowding or pollution (Holst puts the rate of sinusitis at 49%, King and Henderson put it at 55% and Roberts puts it at 72%) (Holst, 2005; King & Henderson, 2014; Roberts, 2007). York's population slumped from an estimated 12,000 to 8,000 in the mid-16th c. but was repopulated within a century (Palliser, 1973). Due to the crowding and poor sanitation York's population fluctuated heavily with the plagues which swept through Europe from the 13th through the 16th c. At the end of the 16th c. York was hit particularly hard as evidenced by the number of last wills executed, the deaths of city officials, and the precipitous drop in population both from mortality and flight (Palliser, 1973).

York also suffered three major invasions particularly in the early history of this cemetery. Danish Vikings invaded in 867 AD and 1016 AD, and Normans invaded in 1066 AD. The Domesday book suggests some level of depopulation in the vicinity of York around the time William the Conqueror garrisoned there, but Palliser (2014) points out that this may have just been a disruption of agriculture and trade leading to lower output in the wake of the Norman invasion.

As with Coach Lane there are few grave goods to be found at Fishergate House including only a scallop shell, a buckle and a ring, here likely due to socioeconomic status. Most are buried supine and extended and are oriented east to west. They were interred for the most part in shrouds although some coffins were used. Children are buried throughout the cemetery but are concentrated in the northern portion (Ashby & Spall, 2005). The cemetery has yielded some 244 individuals including 152 adults (Holst, 2005), however those selected for use in this study had to have minimal taphonomic damage and a complete left humerus or left femur.

Table 3.5 Fishergate House individuals by sex and age.

Fishergate House	Sex	Age			
		18-25	25-35	35-45	45+
Total	27	5	3	5	14
Female	13	1	2	1	9
% of pop.	48.15%	3.70%	7.41%	3.70%	33.33%
Male	14	4	1	4	5
% of pop.	51.85%	14.81%	3.70%	14.81%	18.52%
Unknown	0	0	0	0	0
% of pop.	0.00%	0.00%	0.00%	0.00%	0.00%

Table 3.6 Fishergate House childhood stress indicators.

Fishergate House	Cribra Orbitalia			LEH		
	CO present	CO absent	orbitals not present	LEH present	LEH absent	teeth not present
Total	3	24	0	17	10	0
Female	1	12	0	11	2	0
% of pop.	3.70%	44.44%	0.00%	40.74%	7.41%	0.00%
Male	2	12	0	6	8	0
% of pop.	7.41%	44.44%	0.00%	22.22%	29.63%	0.00%
Unknown	0	0	0	0	0	0
% of pop.	0.00%	0.00%	0.00%	0.00%	0.00%	0.00%

Table 3.7 Fishergate House trauma and Schmorl's nodes.

Fishergate House	Trauma		Schmorl's Nodes		
	Trauma Present	Trauma Absent	Schmorl's Nodes Present	Schmorl's Nodes Absent	Vertebrae not present
Total	10	17	18	9	0
Female	4	9	6	7	0
% of pop.	14.81%	33.33%	22.22%	25.93%	0.00%
Male	6	8	12	2	0
% of pop.	22.22%	29.63%	44.44%	7.41%	0.00%
Unknown	0	0	0	0	0
% of pop.	0.00%	0.00%	0.00%	0.00%	0.00%

Table 3.8 Fishergate House DJD by element.

Fishergate House	DJD Severity				
	Healthy	DJD	Mild OA	Moderate OA	Severe OA
Proximal Humerus	11	13	4	2	1
Distal Humerus	9	15	4	1	2
Proximal Femur	11	4	3	4	3
Distal Femur	7	7	2	3	5

3.1.3 St. Guthlac's Priory, Hereford

St. Guthlac's Priory is also medieval being in use from the 1143 to 1539AD (Gaimster & O'Connor, 2006). In this collection there are some 37 individuals 31 of which are adults (Roberts, n.d.). However, once again this study could only include a small fraction of those individuals as illustrated in the tables

provided. The site was discovered and excavated when the County Hospital was built. Most individuals in the cemetery are adult males and are believed to be the Benedictine Monks belonging to the priory (Gaimster & O’Conor, 2006).

St. Guthlac’s Priory was attested in about 1000 AD but is likely to have been founded earlier (Barrow, 1999). For much of the medieval period the priory oversaw the day to day execution of tasks in their area, but by the late 14th c. their responsibilities and privileges were curtailed (Dohar, 1987). The monks likely lived in some measure of privilege and comfort and in some cases took their comfort to excess (“Short Notices,” 1908). They would be the least likely of the English populations to show signs of childhood stress, malnutrition, or to suffer from a high parasite load. They are however, likely to suffer from caries, and more likely to have DISH due to their some of their purportedly excessive diets. Those interred here remain at risk for trauma, infectious disease, osteoarthritis, and osteoporosis. However due to their privileged lifestyles pathologies and disorders resulting from stress and physical activity are less prevalent than in some of the other populations. The cemetery was not exclusive to monks and requests for internment of notable women do exist (D. Walker, 1964). Female skeletons from Hereford are included in this study.

The initial excavation showed a neat plan in the cemetery with burials arranged in columns and rows. However, later excavations revealed multiple grave cuts possibly suggesting different phases of use (Christie, 2002). The burials are oriented northwest to Southeast rather than properly East to West. Coffins were more frequent here and there are several deviant burials which include a burial in a stone cist, a burial with stone headrests or pillows and burials on beds of mortar or lime. There is also one individual buried with a “mortuary chalice.” While the cemetery is includes mostly men, women and children are distributed throughout (Gaimster & O’Conor, 2006).

Table 3.9 Hereford individuals by sex and age.

Hereford	Sex	Age			
		18-25	25-35	35-45	45+
Total	12	1	3	4	4
Female	5	0	2	2	1
% of pop.	41.67%	0.00%	16.67%	16.67%	8.33%
Male	4	1	1	1	1
% of pop.	33.33%	8.33%	8.33%	8.33%	8.33%
Unknown	3	0	0	1	2
% of pop.	25.00%	0.00%	0.00%	8.33%	16.67%

Table 3.10 Hereford childhood stress indicators.

Hereford	Cribra Orbitalia			LEH		
	CO present	CO absent	orbitals not present	LEH present	LEH absent	teeth not present
Total	2	10	0	4	8	0
Female	1	4	0	1	4	0
% of pop.	8.33%	33.33%	0.00%	8.33%	33.33%	0.00%
Male	1	3	0	2	2	0
% of pop.	8.33%	25.00%	0.00%	16.67%	16.67%	0.00%
Unknown	0	3	0	1	2	0
% of pop.	0.00%	25.00%	0.00%	8.33%	16.67%	0.00%

Table 3.11 Hereford trauma and Schmorl's nodes.

Hereford	Trauma		Schmorl's Nodes		
	Trauma Present	Trauma Absent	Schmorl's Nodes Present	Schmorl's Nodes Absent	Vertebrae not present
Total	1	11	8	4	0
Female	0	5	3	2	0
% of pop.	0.00%	41.67%	25.00%	16.67%	0.00%
Male	1	3	4	0	0
% of pop.	8.33%	25.00%	33.33%	0.00%	0.00%
Unknown	0	3	1	2	0
% of pop.	0.00%	25.00%	8.33%	16.67%	0.00%

Table 3.12 Hereford DJD by element.

Hereford	DJD Severity				
	Healthy	DJD	Mild OA	Moderate OA	Severe OA
Proximal Humerus	7	1	1	1	0
Distal Humerus	6	3	1	0	0
Proximal Femur	5	2	0	0	1
Distal Femur	4	2	2	0	0

3.1.4 Sudan

The Sudanese population included in this research comes from site 3-J-18 of Mis Island at the 4th Cataract of the River Nile. This site is medieval (7th c. AD to 1500 AD) and the church with which they are associated is architecturally similar to those of the “Type 4 Late Christian” style (Ginns, 2006). Several cemeteries were discovered on Mis Island many dating to the medieval period and most with good to excellent preservation including many naturally wholly or partially mummified individuals. (Here preservation was so good that where elements are excluded it is usually due to that element still having soft tissue attached.) This site includes fifty-six adults, fourteen adolescents and twenty-six children, infants, or neonates. They are buried in extended positions but in a variety of different orientations. Often their hands are positioned over their pelvis. They were often buried in shrouds bound with cords binding the body for inhumation.

While the church and cemeteries on Mis Island are well preserved and archaeologically catalogued, Medieval Nubia offers comparatively sparse sites or records. Much of the architecture, particularly of Middle and Upper Nubia was timber and so did not preserve. Medieval Nubia was generally Christian starting with the conversion of the elite in the 6th c. and echoed in the relative simplicity of their ensuing mortuary practices as well as the rise in monasteries (Edwards, 2004; Welsby, 2002). Nubia was initially divided into three kingdoms: Nobadia in the north or Lower Nubia, Makuria in Middle Nubia and Alodia or Alwa in the south or Upper Nubia. Nobadia and Makuria unified and the military conqueror took on the religion – Monophysitism under the Patriarch of Alexandria – of the conquered, but the practices and lifestyle of the religion are difficult to determine. Offering a hint, in 1203 or 1204 a “Nubian ruler” did a pilgrimage to Jerusalem and Constantinople and was allowed by the Crusaders to visit chapels in the latter city dedicated specifically to Nubian Christians. However, the Catholics were largely as intolerant of Coptic Christians and other Christians as they were of Muslims (Welsby, 2002).

Whilst records of Nubia in Nubia may not have survived, those in the Muslim and Arab worlds did. More fortunately while the Muslims especially the Egyptians were in an almost constant state of raid and invasion mostly with Makuria, their historians were apparently generally impartial with descriptions of all involved (Welsby, 2002). It should be noted however that the bulk of the earliest histories are from roughly the 9th c. but they record as early as the 6th c. (Edwards, 2004). It is notable that Alodia – the kingdom to which the individuals in this study would have belonged - particularly its capital Soba was in ruins by the time the Ottoman Turks arrived in the 1560s.

A *Baqt* existed between the Makurians and the Egyptians and is essential to Nubian history as it establishes some understanding of the resources and lifeways of the region. The *Baqt* was established in the mid 7th c. after the seizure of Old Dongola (the capital at the time). At the time it was formed the Egyptians were essentially in an orderly retreat and so whilst the *Baqt* is termed as tribute demanded of “infidels” it is not as one sided as that would seem. The Egyptians were tasked with paying the Makurians in grain, horses, textiles and other goods and the Makurians were tasked with paying the Egyptians some 442 slaves to various authorities (Edwards, 2004; Welsby, 2002). That the Egyptians were paying in foodstuffs, livestock, and textiles and the Nubians in people suggests that Makuria in particular was unable to supply the sort of grains, beers, wines, or materials that Egypt might have found useful or exotic. A Makurian embassy at one point did bring a giraffe, but at no point on record did Egypt attempt to demand large wild animals. The demand of slaves and subsequent failure to fill that demand suggests that Makuria involved itself in raids with relative frequency (all records indicate that not only did they raid frequently but they were considered remarkably accurate archers) and that their population density was not high enough to provide a failsafe (Edwards, 2004; Welsby, 2002). This should not suggest that any of the Nubian kingdoms suffered from food insecurity relative to Egypt as palaeobotanic results show the presence of sorghum, bulrush millet, some hulled barley, and grapes and figs. The contemporary source Al-Aswari observed that the staple crop used for bread and beer was a grain called “dhurra.” He also notes very large herds of cattle and the high consumption of beef (Edwards, 2004; Welsby, 2002). Interestingly, salt is not noted in the historical records and the only nearby sources may not have been mined (Welsby, 2002). Soba also sported what is known archaeologically as “Soba ware” which is a ceramic intricately decorated on a black or brown slip. Other glasses and ceramics from as far as Iran were found in Soba suggesting at least some level of trade.

Nubia appears –due to the level of irrigation - to be more rural in nature. Nubians may have experienced raids with relative frequency and in fact, this is born out in the relative frequency of trauma (although that could be equally well explained by falls in a geologically rough environment or from raising cattle). They seem to have had good access in general to foodstuffs, although their proximity to the Nile whilst allowing for agriculture and fishing would also be a vector for disease particularly parasites and malaria. If their diet was focused on meat consumption as Al-Aswari reports there could be a higher incidence of heart-disease, gout, and DISH, but it would offset dietary lack of vitamin B₁₂ and iron. There is no indication that the Sudanese individuals wore excessive clothing or remained inside throughout the day and therefore it is unlikely that they would have suffered from vitamin D deficiencies without an additional genetic or pathological vector. This would also reduce the rate of

auto-immune disorders like Ankylosing Spondylitis, Multiple Sclerosis, and inflammatory bowel disease (Samsel et al., 2014). There is some indication that exposure to cook fires increased the rate of sinusitis but whether that rate is comparable to populations experiencing urban pollution is yet unknown. There were several incidents of low harvest years in the medieval period. Like Europe the Sudan experienced several very cold years in the opening of the first millennium including one incident in 1011AD when ice was reported in the Nile. Patriarchs of Alexandria Joseph (831-849AD) and Gabriel (1121-1149AD) also reported droughts and “pestilences.” There are also low flood years reported in 1373 and 1450 which would have resulted in lower crop yields and possibly some food insecurity (Edwards, 2004).

Table 3.13 3-J-18 individuals by sex and age.

3-J-18	Sex	Age			
		18-25	25-35	35-45	45+
3-J-18	34	10	9	8	7
Female	18	6	4	3	5
% of pop.	52.94%	17.65%	11.76%	8.82%	14.71%
Male	15	3	5	5	2
% of pop.	44.12%	8.82%	14.71%	14.71%	5.88%
Unknown	1	1	0	0	0
% of pop.	2.94%	2.94%	0.00%	0.00%	0.00%

Table 3.14 3-J-18 childhood stress indicators.

3-J-18	Cribra Orbitalia			LEH		
	CO present	CO absent	orbitals not present	LEH present	LEH absent	teeth not present
3-J-18	11	23	0	16	18	0
Female	8	10	0	7	11	0
% of pop.	23.53%	29.41%	0.00%	20.59%	32.35%	0.00%
Male	3	12	0	9	6	0
% of pop.	8.82%	35.29%	0.00%	26.47%	17.65%	0.00%
Unknown	0	1	0	0	1	0
% of pop.	0.00%	2.94%	0.00%	0.00%	2.94%	0.00%

Table 3.15 3-J-18 trauma and Schmorl's nodes.

3-J-18	Trauma		Schmorl's Nodes		
	Trauma Present	Trauma Absent	Schmorl's Nodes Present	Schmorl's Nodes Absent	Vertebrae not present
3-J-18	11	23	9	25	0
Female	6	12	5	13	0
% of pop.	17.65%	35.29%	14.71%	38.24%	0.00%
Male	5	10	4	11	0
% of pop.	14.71%	29.41%	11.76%	32.35%	0.00%
Unknown	0	1	0	1	0
% of pop.	0.00%	2.94%	0.00%	2.94%	0.00%

Table 3.16 3-J-18 DJD by element.

3-J-18	DJD Severity				
	Healthy	DJD	Mild OA	Moderate OA	Severe OA
Proximal Humerus	11	2	0	0	0
Distal Humerus	11	1	0	1	0
Proximal Femur	4	8	0	0	0
Distal Femur	9	1	0	1	1

3.2 Osteological Methods

Only adults were included in this study. Delineation of adulthood was determined by epiphyseal union of the long bones (Buikstra & Ubelaker, 1994; M. Schaefer et al., 2009b). Individuals whose epiphyses had fused but who still retained an epiphyseal scar were included because the areas of interest were not morphologically interrupted by the scar. The age range in this study is therefore 17 to over 45 years.

Table 3.17 Estimated age ranges and abbreviations.

Age Range	Abbreviation	Extended Form
17-25	ya	Young Adult
25-35	mya	Mature Young Adult
35-45	mma	Mature Middle Adult
45+	moa	Mature Old Adult

Age ranges are provided in Table 3.17. Age ranges follow Brickley and McKinley (2004) and Buikstra and Ubelaker (1994). Age was estimated based on the condition of the undamaged pubic

symphyseal face and auricular surfaces (Brooks & Suchey, 1990; Margaret Cox, 2000; C O Lovejoy et al., 1985). When the individual was believed to fall into either the young adult or mature young adult categories the epiphyseal union of the medial clavicle was used to make the delineation (Scheuer & Black, 2000). Individuals who are clearly adult but could not be aged due to missing or damaged elements were categorized as “unknown.” These methods for aging were selected because they are easily replicable and widely accepted by the scientific community. However, aging techniques were applied without reference to the population. This was done to maintain consistency and techniques which are extremely variable between populations such as tooth wear were not included for age estimation. However, Marquez Grant (2015) specifically cautions against the wide application of age estimation techniques. (Error data was not collected for age estimation in this study, however all populations examined have been or are in the process of being thoroughly documented and it is therefore possible to compare age data.) Age ranges were kept deliberately wide due to rates of observer error recorded in the age estimation of adult remains (Chamberlain, 2006; Hunter & Cox, 2005; Osborne et al., 2004; Samworth & Gowland, 2007).

Table 3.18 Estimated sex categories and abbreviations.

Sex Category	Abbreviation
Female	f
Possible female	?f
Unknown/indeterminate	uk
Possible male	?m
Male	m

Sex was divided into five categories as shown in Table 3.18. Sex was estimated using the sciatic notch, the inferior pubic ramus, sacral alia and curvature, iliac shape, supraorbital ridges, mastoid process, mandibular ramus, mental eminence, gonial angle, nuchal crest, glabella, and frontal and parietal bossing where available (Brickley & McKinley, 2004; Buikstra & Ubelaker, 1994; Mays & Cox, 2000; White & Folkens, 2000). Where available, pelvic morphology was preferentially used over cranial and mandibular indicators. Available intact anatomical indicators of sex were evaluated on a scale of one through five with one being the most feminine and five the most masculine. The average score of for the pelvic features was given as the individual’s sex. In cases where pelvic morphology was unavailable or indeterminate cranial and mandibular indicators were used. When cranial and mandibular indicators gave opposite scores from pelvic indicators the certainty of the sex of the

individual was downgraded by one degree. For example if an individual's pelvic score was five and their cranial and mandibular score was one they would have been recorded as a possible male.

3.3 Paleopathological Methods

The presence or absence of Linear Enamel Hypoplasia (LEH), Cribra Orbitalia (CO), Schmorl's Nodes (SN), and trauma were recorded. Techniques and rationale for inclusion may be found below.. Severity of OA was recorded following Buikstra and Ubelaker (1994). Table 3.19 details the delineation of DJD and OA presence, absence and severity. Presence of only porosity or only marginal osteophytes was noted as Degenerative Joint Disease (DJD), but not OA. Following Buikstra and Ubelaker's methods the scores were divided into rankings of "mild," "moderate," and "severe." If both porosity and osteophytes were scored at or lower than 1.2 and 3.2 respectively and covered less than half of the margin and joint surface then OA was classified as mild. If any of the conditions for mild OA were exceeded, but no eburnation or surface osteophytes were present and only up to 66% of the joint surface or margin was affected then the OA was classified as moderate. If either eburnation or surface osteophytes were present the joint was classed as having severe OA (Jurmain, 1999; Larsen, 1997; D. Ortner & Putschar, 1981; Weiss & Jurmain, 2007). These categories were chosen because they may easily be collapsed into "healthy" "DJD" and "OA" to compare to other studies, but also in this form allow for a continuum of DJD and OA severity to compare with morphology.

Table 3.19 Categories and descriptions Joint Disease scoring.

Joint Disease Category	Buikstra and Ubelaker Score	Description
Healthy	No higher than 1.1 and 2.1 for osteophytes and 3.1 and 4.1 for porosity	Minimal or no porosity or marginal osteophytes
DJD	Clear 1.1 and 2.1 or higher or 3.1 and 4.1 or higher but not both	Either porosity or marginal osteophytes, but not both
Mild OA	Both 2.1 and 4.1 with basic scores no higher than 1.2 and 3.2.	Porosity and marginal osteophytes, but not severe and not covering more than 33% of joint surface and margin
Moderate OA	Both 2.1-2.2 and 4.1-4.2 with any score which exceeds "mild" but does not become "severe."	Porosity and marginal osteophytes over up to 66% of the joint surface and margin
Severe OA	1.3 or higher with a score of 2.3 and marginal osteophytes or 3.3 with a score of 4.3 and clear porosity or any higher score including eburnation (5.1-5.3) or surface osteophytes (7.1, 7.2)	Eburnation, surface osteophytes, or both porosity and marginal osteophytes over 66% of the joint surface and margin

Trauma was recorded as present or absent regardless of location or severity and prevalence is reported by individual. Standard procedures were followed for noting trauma and location and type were noted (Brickley & McKinley, 2004). All suspected trauma was closely examined to ensure it was not post-mortem and any injuries that showed no evidence of healing were excluded. Perimortem trauma was noted as such, but as this research is concerned with morphological change and a skeleton would not have time to adapt to lethal trauma perimortem trauma was statistically considered “no trauma.” Trauma included blunt force, sharp force, fractures, and muscle injuries which resulted in partial ossification of the tendon. Ribs and vertebrae were carefully examined for fractures as their rate of post mortem breakage is quite high. When no indication could be found to confirm that the trauma had been survived it was recorded as “no trauma.”

Schmorl’s nodes were recorded as present or absent. All available vertebral bodies were examined. When ovoid depressions appeared on the vertebral body in one or more vertebrae they were recorded as Schmorl’s nodes. Vertebral bodies with potential Schmorl’s nodes were examined with a magnifying glass to confirm that the suspected lesion was not post mortem damage. Schmorl’s nodes are associated with trauma and mechanical stress with possible exacerbation from other pathological conditions, including neoplastic disease (K. R. Brown et al., 2008; Jurmain, 1999; Larsen, 1997; D. Ortner & Putschar, 1981; Peng et al., 2003; Plomp et al., 2012b; Roberts & Manchester, 2010). Schmorl’s Nodes were included because they have been associated with morphology of the vertebral arch and due to their association with physical activity, stress, and trauma (Peng et al., 2003; Plomp et al., 2012a; Plomp, Roberts, et al., 2015; Plomp, Viðarsdóttir, et al., 2015; Wentz & Grummond, 2009). While it was not expected that presence or absence of Schmorl’s nodes could explain morphology, their prevalence in the populations studied as well as their association with stress, trauma, and morphology inspired their inclusion in this study. Their prevalence rate is reported by individual.

Cribriform orbitalia was classed as either present or absent. Cribriform orbitalia may be scored for severity using Stuart-Macadam’s (1985, 1991) methods, but the purpose of this study was simply to identify individuals with evidence of health stress during early childhood. The superior aspect of the orbital was inspected for porosity, raised bone, and outgrowth of the trabecular structure. Due to the size of these lesions most orbitals were inspected in good ambient light with a magnifying glass but where the severity classification for cribriform orbitalia would normally be “light” the orbitals were inspected for healed or slightly raised bone around the foramina with a magnifying glass and a small torch was moved

around to show whether or not the observed porosity was likely cribra orbitalia (thereby raising small shadows adjacent to the porosity) or taphonomic damage (lacking shadows). Where any cribrous lesion regardless of severity was found to be present on the superior aspect of the orbitals, whether bilateral or not was classed as “present” for the category “cribra orbitalia,” (Larsen, 1997; D. Ortner & Putschar, 1981; Roberts & Manchester, 2010). The scholarly consensus is that cribra orbitalia are symptomatic of severe childhood anaemia although whether it is iron deficiency or hemoblastic anaemia or both which cause the lesions is debated in the literature (Blom et al., 2005; Gowland & Western, 2012; Stuart-Macadam, 1987a, 1987b; Sullivan, 2005; P. L. Walker et al., 2009; Wapler et al., 2004). Cribra orbitalia was recorded to determine what permanent effects if any severe childhood stress might have on the adult appendicular skeletal morphology.

Linear Enamel Hypoplasia (LEH) was included in this study as an indicator of childhood stress. Hillson (2005a) and in particular Hillson and Bond (1997) show that LEH likely represents a discrete interruption in growth. Only furrow-form enamel hypoplasia was recorded. Molars were excluded due to the range of spacing in their perikymata. As most studies do not include molars for this reason and the author was inexperienced in recording LEH it was deemed efficient to avoid complication in this respect. Teeth with carious lesions were also excluded. Individuals with less than two teeth suitable for recording were recorded as having no available teeth. The available incisors, canines, and premolars of each individual were examined with a magnifying glass and with a small strong torch to show whether or not shadows appeared. LEH was only recorded as present if two or more teeth had furrow-form enamel hypoplasia. (Brown striae were not recorded as LEH) (Armélagos et al., 2009; Goodman & Armélagos, 1985; Hillson, 2005a; Hillson & Bond, 1997; May et al., 1993; Roberts & Manchester, 2010; Šlaus, 2000). Prevalence is reported by individual and not tooth because the point of recording LEH in this study was to determine if the individual had any childhood stress rather than to determine when or how often growth was interrupted.

Hillson (Hillson, 2005a) recommends the use of at least some microscopic examination of LEH and in the interest of time and efficiency that was not undertaken in this study. Additionally, radiographs were not taken and so Harris lines and actual endosteal thickness were not assessed. Radiographs of all individuals in all sites was not possible and while Harris lines give valuable information regarding cessation of growth, they may be resorbed whereas LEH is permanent and cribra orbitalia is not believed to heal well (Garn & Baby, 1969; Larsen, 2002).

Several conditions which have the potential to alter bone morphology and some whose diagnosis is dependent on altered bone morphology were recorded during the course of this research. This includes residual rickets which originally was included as one of the indicators of childhood stress, osteoporosis, Hansen's disease, and a possible case of neoplastic disease. In all of these cases only a few individual's – or for neoplastic disease only one individual – showed symptoms of the respective pathologies and in initial testing were not statistically morphologically distinct from the rest of their population. Additionally, these pathologies were largely population specific. No Hansen's disease was recorded in any individual outside of 3-J-18. As these pathologies may interact with other IVs but did not appear to disrupt mean shape individuals with them were not excluded from the study. (Agarwal, 2008, 2016; Agarwal et al., 2004; Angel et al., 1987; Larsen, 1997, 2002; D. J. Ortner & Mays, 1998; D. Ortner & Putschar, 1981; Pinhasi & Mays, 2007; Roberts & Manchester, 2010; Soler, 2012; Waldron, 2009). Other conditions were recorded in brief where noted but will not appear in this study. These include caries, periodontal disease, ankylosing spondylitis, diffuse idiopathic skeletal hyperostosis, and arachnoid granulations. Other pathologies like rheumatoid arthritis and osteochondritis dissecans which would be interesting to this study did not appear on any individual with elements which were sufficiently intact to enter into the study.

Intraobserver error was assessed for the OA scoring. Error was assessed by randomly selecting 30% of the original sample to be re-evaluated for severity of OA. This aspect of palaeopathological recording used ranking as opposed to presence or absence and therefore has the greater potential for error. Intraobserver error was recorded when results differed by two orders, where the order of rankings is "healthy," "DJD," "mild," "moderate," "severe". For example, if the original record denoted an individual as "healthy" and the second analysis recorded the same individual as having "DJD," it was not considered an error, whereas if it had been "mild," "moderate," or "severe" it would have been. On this basis I have errors in 28.75% of the total. This remarkably high error rate underscores Jurmain's insistence on using only presence or absence in recording OA (1999). Despite the high rate of error this study does use ordered rankings of severity for DJD and OA to attempt to show morphological variation with increasing severity.

3.4 Data Acquisition

Digital 3D ply files were created by scanning long bones with a NextEngine™ 3D Scanner and processed in scan Scanstudio ("NextEngine Scan Studio HD: Scan, Align, Fuse, Polish and Export Version 1.3.2," 2010). The NextEngine is an active surface scanner (meaning it produces its own light and creates

a surface model of polygons), but scans must be trimmed, aligned and fused after capture (Davies et al., 2012; Errickson et al., 2014). When possible, all divisions of scans were collected in a single session to reduce movement of the turntable and ensure good alignment. Scans were aligned with an accuracy of at least 0.005 inches and fused at 0.5 inch resolution. The scans were inspected for holes at landmark sites and when the digital surface was complete enough to ensure landmarking would not be interrupted the NextEngine software was used to fill any further holes and create a “watertight” ply file. This version was then oriented in ScanStudio using the method outlined in Ruff (2002) which involves rotating and fixing the scan on set axes. This was saved as a .xml file which were then sectioned using the software AsciiSection developed by Davies and colleagues (2012) to create the cortical sections and measurements. Images of the scans were captured by the scanner and scanning software (See Figure 3.1).



Figure 3.1 Pictures of left humerus of CL 175 mounted on scanner for the distal partial scan on the left and the 360 degree anterior posterior scan on the right. These images captured by the NextEngine were used by the software to overlay a skin onto the ply file.

3.5 Geometric Morphometrics (GMM)

Many morphometric studies employ linear measurements or measurements based on size. These may be quickly and easily obtained over large samples and measurements are standardized (Buikstra & Ubelaker, 1994). Additionally, size is crucial to many research questions particularly those concerning stature or proportion. However, morphometric measurements which include size may not be translated to shape. Whilst these measurements include information on form – or shape including size – the size information may not be removed to create meaningful shape information. Thus, when relying on linear or sized based morphometric measurements one must always consider size. Geometric Morphometrics (GMM) conversely, considers shape without size (although see section 2.4).

GMM is coordinate based. Shape is defined by landmarks (to be defined in Sections 3.5.1 and 3.5.2.) chosen to best represent shape variation for the particular research question. (However, researchers may choose to base their coordinate locations on existing standards for metric measurements. This allows for repeatability, and also allows for comparison to morphometric studies which used linear rather than coordinate system of measurement.) Landmarks therefore, define the shape to be studied and hold no intrinsic size information (Slice, 2005; Zelditch et al., 2004). Once all landmark sets for the data set exist they may be Procrustes adjusted to fit each other using Generalised Procrustes Analysis (GPA). GPA scales, rotates, and translates all shape objects in the data set. If size is considered it may be reintroduced using Centroid Size (CS) – as done in this study – or GPA may be performed without scaling shape objects to the mean size (Mitteroecker et al., 2013a). The Procrustes adjusted shapes may then be compared to one another.

In the process of GPA, a centroid for each shape will have been calculated as well as an average shape for each set. The variation of each shape from the average will be the Procrustes residual or shape score. These may be regressed against size as is the case for much of the allometry performed in subsequent chapters. However, morphology may vary in a multiplicity of ways. The coordinates or landmarks selected will to a degree dictate what morphological variation will be detected in the study underscoring the importance of choosing landmarks which appropriately represent the research question (Viscosi & Cardini, 2011). Shape variation may be imagined as a cloud of points each representing an individual shape set in multidimensional shape space or Kendall's space on the basis of their directional variation from the mean shape (D. C. Adams et al., 2004; Viscosi & Cardini, 2011). Principal Components Analysis (PCA) identifies the percentage of each eigenvector of variation. Returning to the cloud analogy, if the cloud is elliptical the first Principal Component (PC) will be along its longest axis and represents the greatest shape variation. Shape variation may be visually represented by plotting PCs in two to three dimensions. A potential distortion does present itself at this juncture in that Kendall's shape space is curved and statistical analysis of shape residuals assumes Euclidean distances. The distances from the mean are actually projections from shape space to a tangential plane thereby resolving the issue of non-Euclidean geometry. For non-biological studies of morphology where variation is greater distortion in the process of projection would require correction, but in biology virtually all shape variation even for studies involving multiple species is small enough that the issue of distortion is not present (Kendall, 1989; Viscosi & Cardini, 2011). With morphology now quantitatively represented it may be incorporated into a number of statistical tests.

This study is primarily concerned with morphology and how it varies with other intrinsic and extrinsic factors. A morphological method like GMM where shape may be quantitatively represented but which allows for the exclusion or inclusion of size is therefore critical. Previous studies have investigated long bones using GMM in order to link morphology to factors like sex, phylogeny and population (Bacon, 2000; Bonnan, 2007; De Groote, 2011a; Kranioti, Bastir, et al., 2009; Kranioti, Vorniotakis, et al., 2009; Kranioti & Michalodimitrakis, 2009; Milne et al., 2009; Pujol et al., 2016). With few exceptions (De Groote et al., 2010; Frelat et al., 2012), diaphyseal shape is usually discussed in the context of cross-sections which is appropriate for a multiplicity of research questions especially those concerned with activity and robusticity, but may not represent the entire morphology of the diaphysis (Drapeau & Streeter, 2006; Ruff, 2005; Shaw & Stock, 2009a, 2009b; Stock & Shaw, 2007). Beyond morphological variation with intrinsic and extrinsic factors, this study also asks whether the shape of the epiphyses, diaphysis, or cross-sections better represents morphological variations with these factors. GMM is the only method with which these questions might be addressed and has the added benefit of allowing for the consideration of size without requiring it.

3.5.1 Landmarks

Bookstein warns that “homologous” is simply absence of as he terms it “heterology,” (Bookstein, 1991 pp. 62-63). That is, objects must be similar enough to one another to be comparable. Bookstein uses the example of comparing a human mandible to fish mandible. These two things are both mandibles, but they are so morphologically and functionally different that comparing them will show morphological variation, but it will not be meaningful. Homologous landmarks may be understood as landmarks which possess the least amount of difference or as Lele and Richtmeier put it “unambiguous correspondence between forms being compared” (2001b; pp. 19). Like Bookstein (1991), Lele and Richtmeier (2001b) only accept homogeneity if all biological shapes stem from a common ancestor therefore being in close phylogenetic proximity. Therefore, they posit that members of the same species would by default have homologous structures.

Homologous landmarks are typically divided into a hierarchy of three types a quick reference for which is provided in Table 3.20. Semilandmarks, which shall be discussed in the following section, are often considered the fourth “Type” of landmark with landmarks described in descending order of their homology. As suggested above the primary concern of homology in biological studies is related to phylogenetics. Type I landmarks are therefore considered the most homologous because they are

evolutionary in nature, will occur only once and are defined by “the strongest (local) evidence,” (O’Higgins, 2000a; pp. 106). Type II landmarks may be functionally homologous but need not be developmentally so. Bookstein uses the example of the tips of teeth and O’Higgins adds the tip of a wing for birds or mammals (Bookstein, 1991; O’Higgins, 2000b). Type III landmarks are the least homologous. O’Higgins (2000a) describes them as deficient in at least one dimension and Lele and Richtmeier (2001b) term them “fuzzy landmarks,” and suggest that the best way to obtain them would be to landmark each specimen with them several times and obtain the average. Bookstein simply describes Type III landmarks as extrema whose loci are determined by anatomical structures but are often the farthest from or centroids of that structure (1991). To obtain a reasonable representation of shape this study did include Type III landmarks. However, intraobserver error testing showed that the landmarking error was reasonable as further explained in section 0.

Table 3.20 Definition of types of homologous landmarks (Bookstein, 1991; Lele & Richtsmeier, 2001a).

	Definition	Example from literature
Type I	Intersection of tissues	Nuclei of a neuron, eye of a vertebrate
Type II	Maxima of curvature	Tips of claws and teeth or bony processes
Type III	Extrema	The outwardmost bossing of the left frontal cranial bone

Homologous landmarks once obtained require no manipulation at the individual level and may immediately be subjected to the Procrustes method after which they are considered shape coordinates as they no longer refer to their original object, but to the Procrustes adjusted shape of that object (K. Schaefer & Bookstein, 2009). They are not dependent on other landmarks in the set and therefore landmarks found to display error unrelated to morphological variation may be deleted without compromising the integrity of the set as a whole. Depending on the methodology used it may not even be necessary to obtain all homologous landmarks in one sitting. If, as in this study, computer renderings are the “shape” in question rather than the bone itself homologous points could be added to the overall set. Best practice however, was followed in this study and all landmarks to be considered as a set were collected together at once.

Twenty-five homologous landmarks were placed on each humerus, chosen to adequately describe the shape, be visible on digital objects and avoid areas that are frequently subject to taphonomic destruction. . The full humeral landmark set is detailed in Figure 3.2 and Table 3.21 and the

full femoral landmark set is detailed in Figure 3.3 and Table 3.22. Three dimensional homologous landmarks were collected with *IDAV 3D Landmark Editor* and GPA was performed in the *R* package “Geomorph,” (D. C. Adams & Otárola-Castillo, 2013b)

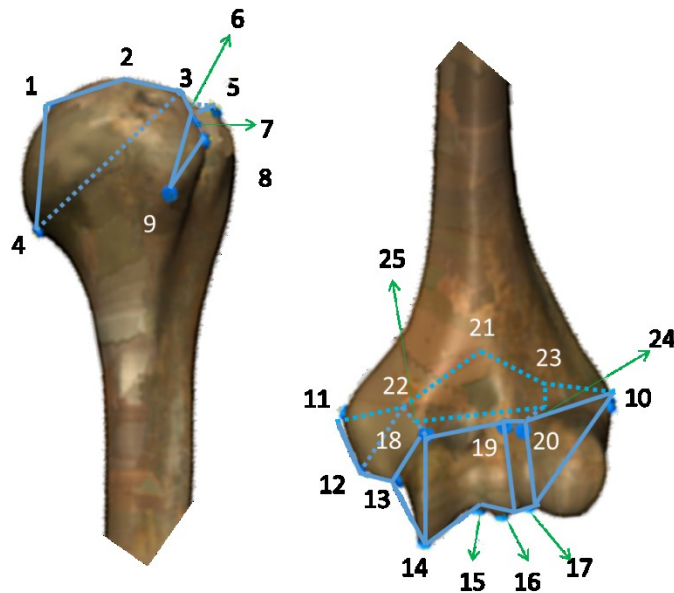


Figure 3.2 Humeral Landmarks and wireframes

Table 3.21 Humeral Landmarks

Humeral Landmark Number	Description	Landmark Set	Type
1	Most superior-medial point of the humeral head	Proximal Humerus	Type III
2	Most superior point of the humeral head at the midline	Proximal Humerus	Type III
3	Most superior point on the border of head and neck at the midline	Proximal Humerus	Type II
4	Most inferior point on the border of head and neck at the midline	Proximal Humerus	Type II
5	Most anterior point of the mm. supraspinatus attachment	Proximal Humerus	Type II

6	Most posterior point of the mm. supraspinatus attachment	Proximal Humerus	Type II
7	Deepest most superior point of the intertubercular groove	Proximal Humerus	Type II
8	Most superior point of the subscapularis on the lesser tubercle attachment	Proximal Humerus	Type II
9	Most inferior point of the subscapularis on the lesser tubercle attachment	Proximal Humerus	Type II
10	Most lateral point of lateral epicondyle	Proximal Humerus	Type II
11	Most superior-medial point of medial epicondyle	Distal Humerus	Type II
12	Most inferior medial point of medial epicondyle	Distal Humerus	Type II
13	Most superior point of the border of the medial epicondyle and the trochlea at the midline from the inferior aspect	Distal Humerus	Type II
14	Most inferior-medial point of trochlea	Distal Humerus	Type III
15	Most superior point of the trochlea at midline from the inferior aspect	Distal Humerus	Type III
16	Most inferior-lateral point of trochlea at midline	Distal Humerus	Type II
17	Most superior point at the midline of the border of the trochlea and the capitulum from the inferior aspect	Distal Humerus	Type II
18	Most superior-medial point of trochlea from anterior aspect	Distal Humerus	Type I
19	Most superior-lateral point of the trochlea from anterior aspect	Distal Humerus	Type I
20	Border of trochlea,	Distal Humerus	Type I

	diaphysis, and capitulum from anterior aspect		
21	Most superior point of the olecranon fossa	Distal Humerus	Type II
22	Most medial point of the olecranon fossa	Distal Humerus	Type II
23	Most lateral point of the olecranon fossa	Distal Humerus	Type II
24	Most lateral-superior point on posterior aspect of the border of the trochlea and diaphysis	Distal Humerus	Type II
25	Most medial-superior point on posterior aspect of the border of the trochlea and diaphysis	Distal Humerus	Type II

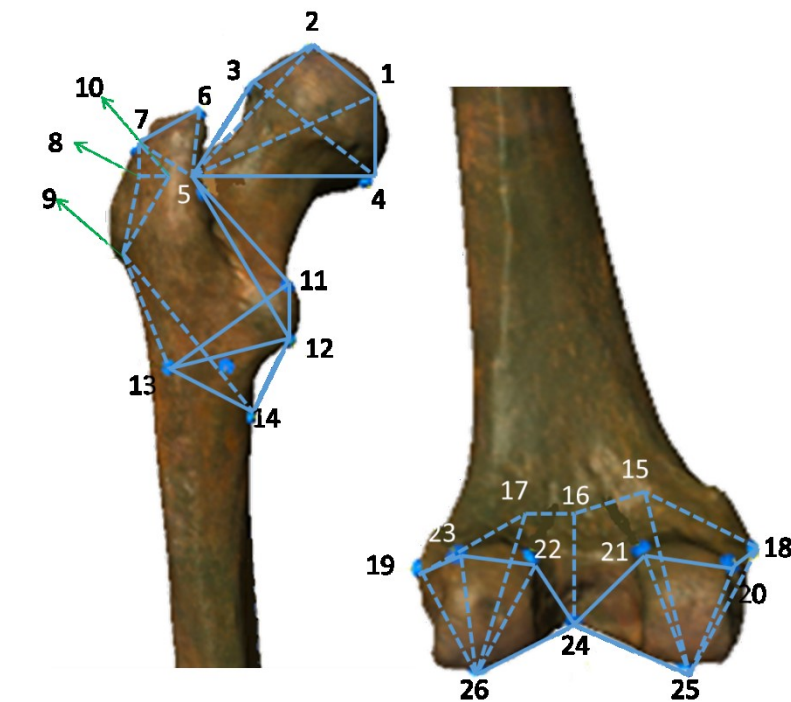


Figure 3.3 Femoral Landmarks and wireframes.

Table 3.22 Femoral Landmarks

Femoral Landmark Number	Description	Landmark Set	Type
1	Fovea Capita	Proximal Femur	Type I
2	Most superior point of the femoral head	Proximal Femur	Type III
3	Superior border of	Proximal Femur	Type II

	head and neck at midline		
4	Inferior border of head and neck at midline	Proximal Femur	Type II
5	Deepest point of the trochanteric fossa	Proximal Femur	Type II
6	Most superior- medial point of the mm. gluteus medius attachment	Proximal Femur	Type II
7	Most inferior-lateral point of the mm. gluteus medius attachment	Proximal Femur	Type II
8	Most superior point of the mm. gluteus minimus attachment	Proximal Femur	Type II
9	Most inferior point of the mm. gluteus minimus attachment	Proximal Femur	Type II
10	Most superior point of the fossa described by the intersection of the greater trochanter, the anterior intertrochanteric line, and the mm. gluteus minimus attachment site	Proximal Femur	Type II
11	Most superior point of the mm. psoas major attachment	Proximal Femur	Type II
12	Most inferior point of the mm. psoas major attachment/ Intersection of inferior portion of lesser trochanter and pectineal line	Proximal Femur	Type I
13	Superior edge of gluteal line	Proximal Femur	Type I
14	Intersection of pectineal and spiral lines	Proximal Femur	Type I
15	Most superior point	Distal Femur	Type II

	of anterior border of lateral condyle with diaphysis		
16	Most inferior point of anterior border of condyles and diaphysis	Distal Femur	Type II
17	Most superior point of anterior border of medial condyle with diaphysis	Distal Femur	Type II
18	Most medial point of medial epicondyle	Distal Femur	Type II
19	Most lateral point of lateral epicondyle	Distal Femur	Type II
20	Most superior-medial point of posterior medial condyle	Distal Femur	Type II
21	Most superior-lateral point of posterior medial condyle	Distal Femur	Type II
22	Most superior-medial point of posterior lateral condyle	Distal Femur	Type II
23	Most superior-lateral point of posterior lateral condyle	Distal Femur	Type II
24	Most anterior point of border at junction of posterior condyles	Distal Femur	Type II
25	Most posterior point of protuberance making up most inferior projection of medial condyle	Distal Femur	Type III
26	Most posterior point of protuberance making up most inferior projection of lateral condyle	Distal Femur	Type III

3.5.2 Semilandmarks

The necessity of semilandmarks and the initial algebra supporting their implementation was addressed in Bookstein's "Orange Book" (1991). Additional theoretical work on semilandmarks specifically has continued to the present day with publications on the math and theory of semilandmarks including Gunz, Mitteroecker, and Bookstein, (Gunz et al., 2005a), Gunz and Mitteroecker (2013), and McCane (2013) and studies featuring more application of semilandmarks including Frelat and colleagues (2012) and Perez, Bernal, and Gonzalez (2006). However, implementation of the technique particularly on large samples has been difficult. Most applications of semilandmarks have featured not a three dimensional surface but a two dimensional curve (Bulygina et al., 2006; Gonzalez et al., 2009; González et al., 2007; Mitteroecker, Gunz, Weber, et al., 2004; Plomp et al., 2012a).

Biological homogeneity is already less exact than true homogeneity from a mathematical perspective, but such concessions are necessary to describe biological morphology (Bookstein, 1991; Gunz et al., 2005a; Zelditch et al., 2004). Semilandmarks are not homologous, but together describe structures which may not be adequately described by homologous points. For example, in this study homologous points alone are used to describe the morphology of the epiphyses. This leads to an odd situation where a disease like OA, which has a diagnostic criteria of changes in the contour of the joint surface, will not necessarily be noticed using a morphological method. To capture joint contour using GMM semilandmarks would be crucial. Semilandmarks on both curves and surfaces rely on bordering homologous points (Gunz et al., 2005a). When the borders and surface or curve is described the semilandmarks may be algorithmically slid along that surface or curve to best describe it (Bookstein, 1991; Gunz et al., 2005a). This process as Gunz, Mitteroecker, and Bookstein explain is very similar to the Least Squares method used in Procrustes adjustment where the best fit is determined based on what arrangement least disrupts the global average (Gunz et al., 2005a).

Despite difficult methodology, surface semilandmarks potentially contain more pertinent information particularly in regards to intrapopulation variation in comparison to homologous points. This is because surface semilandmarks on the diaphysis are able to capture a complexity of shape that would be lost due to the requirements of homology in homologous landmarks.

Semilandmarks were used in this research in two ways. The primary use was in a semilandmark mesh around the diaphyses of the long bones to capture the morphology of a somewhat complex and varying shape largely devoid of homologous points. The second utilization of landmarks was to define a

circle or more correctly a “curve” around the midpoint of the diaphysis approximating cortical circumference on the outer table.

Diaphyses do not have homologous points – with the exception of the highly variable nutrient foramen – and thus are infrequently addressed in shape studies. However, using semilandmarks diaphyseal shape may be adequately described (Frelat et al., 2012; Gunz & Mitteroecker, 2013; McCane, 2013; Mitteroecker & Gunz, 2009; Perez et al., 2006). Following Mitteroecker and Gunz (2009) and Gunz and Mitteroecker (2013) this study used semilandmark mesh surfaces. Semilandmarks in curves were placed on a plane tangential to the curve (Mitteroecker & Gunz, 2009) and slid based on a resistance fit (Perez et al., 2006; Rohlf & Slice, 1990) so it is useful (although Gunz and Mitteroecker (2013) note, not algebraically necessary) to place a homologous landmark at the border of the curves. For this reason and to accommodate R scripts, semilandmark meshes in this study will be bordered on either end by anchoring homologous landmarks.

3.5.2.1 Diaphyseal Semilandmarking

Semilandmarking of the diaphysis was largely automated. After obtaining sets of homologous landmarks as outlined in Section 3.5.1 the sets were depleted to contain only “border” landmarks (the homologous landmarks bordering the curve to define the lines tangential to curvature). A list of border landmarks is provided in Table 3.23 below. The compiled ply files were then digitally colored using MeshLab (Cignoni & Ranzuglia, 2014) black and white with black demarcating the epiphysis, and white the diaphysis. An arbitrary individual was chosen as atlas and the ply and semilandmarks were combined in R (“R Development Core Team. 2008. R: a language and environment for statistical computing. R Foundation for Statistical Computing,” n.d.). One-hundred surface semilandmarks were automatically placed at even intervals in the defined space. (It should be noted that the use of one-hundred surface semilandmarks brings the number of variables (k) to one-hundred and twelve for humeri and one-hundred and thirteen for femora well exceeding the number of observations (n). In more “general” statistical inquiries for k may not exceed n , but Gunz, Mitteroecker and Bookstein (2005a) dismiss the issue for anthropological questions where dimension reduction techniques like PCA are used.) The rest of the sample was iteratively registered using the colored ply files and individual border landmark sets for each individual. Once all individuals were entered semilandmarks were slid using the thin plate spline (TPS) bending energy technique (Gunz et al., 2005a; Gunz & Mitteroecker, 2013). After sliding, the semilandmarks were considered homologous and subjected to GPS and then PCA and allometry tests as

normal. (This technique and the script to execute it was designed and written by Dr. Emma Sherratt at UCL for the “geomorph” package in *R* and is her intellectual property.)

Table 3.23 Border and non-border homologous points.

	Border Landmarks	Non-border Landmarks
Proximal humerus	4,7,8,9	1-3,5,6,
Distal humerus	10,11,18-23	12-17,24,25
Proximal femur	8,9,12,13	1,2,3,4,5,6,7,10,11,14
Distal femur	15-23	24,25,26

3.5.2.2 Cross-sectional Semilandmarking

The methodology for cross-sectional data acquisition largely follows Ruff (2002) and the same orientations used here for humeri and femora are illustrated in the appendix of that work. Humeri and femora 3D scans were first oriented in the CAD toolbox of NextEngine Scan Studio (“NextEngine Scan Studio HD: Scan, Align, Fuse, Polish and Export Version 1.3.2,” 2010) by the criteria outlined in Ruff (2002) and saved to an .xyz file. The resulting oriented scans were then put through AsciiSection (Davies et al., 2012) which digitally sectioned them to create cross-sectional outlines along the diaphysis. The sections were then landmarked in tpsDig (Rohlf, 2015). For humeri the most extreme point of the deltoid tuberosity was used as a homologous landmark and 19 semilandmarks were placed evenly and in a clockwise rotation around the rest of the cross section. (Cross-sections were intentionally taken at 50% for the purpose of including the deltoid tuberosity however Ruff (2002) suggests taking the midsection of the humerus at 40% for cross-sectional geometry. As a result some studies will not be comparable with this one.) For femora two homologous landmarks were used at the start and the end of the curve. These two homologous points were the extremities of the linea aspera which in the cross sectional image often appear as sharp corners. The remaining 18 semilandmarks were placed evenly in a clockwise rotation around the image. Using the tps software suite and the Geomorph package in *R* the curve was defined, the landmarks slid and fixed, and as usual GPA was performed (D. C. Adams & Otárola-Castillo, 2013a).

3.5.2.3 Note on the Use of Cross-Sectional Geometry

This study will include a brief analysis of the cross-sectional geometry of the observed individuals (see section 6.2.3 for results). This is to demonstrate what cross-sectional geometry may show relative

to cross-sectional morphology. Using AsciiSection (Davies et al., 2012), cross-sectional geometry for the available left humeri and femora were calculated. AsciiSection also provided images of the cross-sections for landmarking in tpsDig (Rohlf, 2015). Following Stock and Shaw (2007), the program estimated total area (TA), I_x or the length of the x axis, I_y or the length of the y axis, I_{max} or the largest diameter, and I_{min} or the shortest diameter. From this, J was calculated by summing I_{max} and I_{min} and I_x/I_y . (J is average bending rigidity and may be calculated by summing two ideally perpendicular axes. Most studies will use $J = I_x + I_y$ because J is meant to be the sum of any two perpendicular axes, but this study will use $J = I_{max} + I_{min}$ as, while these axes may not always be perpendicular, they are likely to be and the purpose of J in this study is to determine covariance of IVs with shape residuals and here metric calculations so the perpendicularity of the axes used here is less important than the sum of extrema.) Mean and standard deviation for each property are provided by sex and population (See Table 6.25, Table 6.26, Table 6.27, and Table 6.28.). Cross-sectional geometry is a longer standing means of understanding morphometrics in the context of variation but one which includes size. Applying geometric techniques and GMM techniques to the same questions allows the two to be evaluated on usefulness to the question at hand. It is expected that some factors will be more reflective of variation in shape and others will be more reflective of variation in form (size and shape). Additionally, while GMM does allow shape estimation via warp grid deformation or estimation of shape based on the position in shape space, geometric properties are directly reflective of the sort of shape variation they evince. That is, if one geometric property shows variation with one of the factors tested it is immediately clear what kind of shape variation is occurring whereas with GMM it is clear that shape variation exists but in what way is not immediately obvious.

The calculation of cross-sectional geometry is meant to provide some context to robusticity and structural integrity. It can extend into questions of ontogeny, degeneration, sex and division of labour, and nutrition, but research questions for cross-sectional geometric methodology are usually concerned with subsistence, population differences, sexual dimorphism in a very specific sense, and handedness. This exercise will help determine whether or not these same values may be useful indicators of pathologies or stress.

3.5.3 Assessment of Asymmetry

Left humeri and femora were preferred for this study but in some individuals taphonomic concerns forced the exclusion of the left element. In such cases the right antimeres was scanned for

inclusion. However, as noted in numerous studies (Benjamin M. Auerbach & Ruff, 2006; Benítez et al., 2014; Bridges, 1994; Klingenberg et al., 2002; Klingenberg & McIntyre, 1998; Rhodes & Knüsel, 2005; Shaw & Stock, 2009a; Sofaer-Derevenski, 2000; Steele, 2000; Stirland, 1998; Stock & Pfeiffer, 2004; Weiss, 2005; Wilczak, 1998) humans often display directional asymmetry often due at least in part to handedness (Nolte & Wilczak, 2012; Peterson, 1998; Shaw & Stock, 2009a, 2009b). To ensure variation was not driven by directional asymmetry a small test of paired humeri and paired femora was conducted.

Individuals with complete or nearly complete homologous landmark sets for either the humerus or femur were selected so that their paired antimeres could be compared. The homologous points for each element were divided into the proximal and distal landmark sets the distribution of which may be seen in Table 3.24. The landmark sets were imported into MorphoJ and a Procrustes fit was performed to register them. The Centroid Size (CS) was exported to Microsoft Excel and a paired t-test was performed at 0.05 confidence to compare right and left CS for each landmark set.

Table 3.24 Number of individuals included in asymmetry analysis by site. The difference in numbers between proximal and distal landmark sets is due to taphonomic damage.

	Proximal Humerus	Distal Humerus	Proximal Femur	Distal Femur
Coach Lane	22	25	8	18
Fishergate	6	6	7	7
Hereford	2	2	1	1
Total	30	33	16	26

For the paired t-test, H_0 was “there is no difference between the CS of right and left landmark sets” and H_1 was “there is difference between the CS of right and left landmark sets.” Therefore if the p-value is greater than 0.05 then we must accept H_0 . Results of the t-test may be found in Table 3.25. The p-value for each set is less than 0.05 thus CS is not comparable in antimeres as there is directional asymmetry in all sets.

Table 3.25 Results of paired t-test. All p-values are less than .05.

	p-value	Result
Proximal Humerus	0.044444899	Reject H_0
Distal Humerus	0.00083	Reject H_0
Proximal Femur	0.019956	Reject H_0
Distal Femur	1.33899E-05	Reject H_0

To test the level of asymmetry of shape following Klingenberg (2015) an ANOVA was performed for each set of landmarks in MorphoJ. Results are shown in Table 3.26, Table 3.27, Table 3.28, and Table 3.29. Here as well shape between humeral and femoral antimeres showed directional asymmetry at a 95% level of confidence for all homologous landmark sets. Therefore, antimeres cannot be reasonably substituted in this study.

Table 3.26 Shape vs. Side ANOVA for Proximal Humerus.

Proximal Humerus Shape, Procrustes ANOVA							
Effect	Sum of Squares	Mean of Squares	df	F	P (param.)	Pillai tr.	P (param.)
Individual	0.57367457	0.000989094	580	2.29	<.0001	12.6	<.0001
Side	0.03261211	0.001630605	20	3.78	<.0001	0.72	0.3359
Ind * Side	0.25033582	0.000431614	580	Infinity	NaN		
Residual	0	0	20				

Table 3.27 Shape vs. Side ANOVA for Distal Humerus.

Distal Humerus Shape, Procrustes ANOVA:					
Effect	Sum of Squares	Mean of Squares	df	F	P (param.)
Individual	0.496384	0.000352545	1408	2.07	<.0001
Side	0.028944	0.000657824	44	3.7	<.0001
Ind * Side	0.239539	0.000170127	1408		

Table 3.28 Shape vs. Side ANOVA for Proximal Humerus

Proximal Femur Shape, Procrustes ANOVA:					
Effect	Sum of Squares	Mean of Squares	df	F	P (param.)
Individual	0.309617	0.000503	615	2.13	<.0001
Side	0.018682	0.000456	41	1.93	0.0006
Ind * Side	0.145244	0.000236	615		

Table 3.29 Shape vs. Side ANOVA for Distal Femur.

Distal Femur Shape, Procrustes ANOVA:					
Effect	Sum of Squares	Mean of Squares	df	F	P (param.)
Individual	0.39401	0.000543	725	1.52	<.0001
Side	0.078727	0.002715	29	7.59	<.0001
Ind * Side	0.259148	0.000357	725		

3.5.4 Generalised Procrustes Analysis (GPA)

Generalised Procrustes Analysis (GPA) is a standard statistical method within GMM wherein all shapes in the data set are adjusted to eliminate size, rotation, and translation ideally so that the only variation is morphology (Baab, McNulty, et al., 2012; Bookstein, 1991; McCane, 2013; Mitteroecker & Gunz, 2009; O'Higgins & Jones, 1998; Rohlf & Slice, 1990; Swiderski, 2003; Viscosi & Cardini, 2011; Zelditch et al., 2004). The centroid is calculated using the sum of squares formula and centroid size is determined by taking the square root of the sum of squares (Bookstein, 1991; Zelditch et al., 2004). To scale all the shapes in the set one must simply subtract each coordinate from the average for that coordinate and divide it by the square root of the squared sum of coordinates or the mean centroid. Once all shapes in the data set are aligned they may be analysed based on their directional divergence from the mean morphology.

After integration of the landmarks into the appropriate sets, the coordinates were adjusted using GPA in *R*. For tests of asymmetry and intraobserver tests only homologous points were used and so GPA was performed in MorphoJ ("MorphoJ, version 1.06b," n.d.).

Most results in this study are given in shape space. However, humans are sexually dimorphic and therefore it is likely that there may be variation of size with shape. Therefore, allometric results are presented in all chapters by regressing the shape score against the logirhythm of the centroid size. In biology size and shape may covary and allometry as a regression of the log CS against shape gives important insight into morphology (Mitteroecker et al., 2013a). Where allometry is considerable form space can be a useful means of visualising it. Form space is simply shape space which includes size. Form space may be found by simply not eliminating size during Procrustes fitting or it may be calculated by "augmenting the Procrustes shape coordinates with the natural logarithm of centroid size," (Mitteroecker et al., 2013a; Mitteroecker, Gunz, Bernhard, et al., 2004). Form space, like shape space is a Euclidean representation of morphometric distance between individuals while using dimension reduction techniques, but unlike shape space it is based on CS. As the centroid is the arithmetic mean, a non-biological object with no landmarks unusually distant from the centroid would have isotropic variation and so any non-isotropic variation may be considered shape difference (Mitteroecker et al., 2013a).

3.5.5 Error

Three major types of error exist for a landmark study such as this one. They are precision, repeatability, and observer error. Repeatability is dependent on precision as shall be elucidated below.

Observer error may be split into inter-observer error and intra-observer error. In this study only Intraobserver error is applicable because landmark data was collected only by the author.

Precision is the measure of variability between measurements of the same specimen taken by the same observer and includes instrument as well as observer error (Lele & Richtsmeier, 2001b). Ideally, no variability in landmark coordinates would exist. For studies using a Microscribe or other such digitizing hardware instrument error may include zeroing and minor shifts to the table and specimen where it is anchored. For this study, three dimensional laser scans were digitized using computer software and so instrument error should be only the precision with which the original scan data was obtained. Precision for the NextEngine Desktop Scanner is advertised at 0.05 inches, but this is variable between different scans and is also in imperial measures. Following Lele and Richtsmeier (2001b pp. 41-42), to determine the actual precision for scans, the scans must be compared in multiple instances. Eight humeri and eight femora were selected for a second scanning. Landmarks were placed twice on the new scan and the original scan creating four sets of landmarks for each specimen. By creating sets of landmarks on two different digital objects the instrument may be measured for precision against itself in multiple instances. Additionally the landmarks taken on each scan may be compared to each other to ensure that the error represented is based on the variation of the scan rather than observer error. Once intraobserver error is removed what error remains is instrument error (Table 3.32). Instrument error in this study is always less than 1%.

To quantify intraobserver error, total landmark error was averaged. This was found by calculating the distance from each coordinate to the centroid of the given observation. The mean and standard deviation of the distances from centroid were found for each landmark and then the difference between each observation at the landmark and the mean were calculated. Following Singleton (2002), the percent deviation from the mean was found by dividing the mean of the difference from mean distance from the centroid by the mean distance from the centroid for each landmark. For every landmark this value approached 0%, suggesting very small intraobserver error. Following Cardini and Elton (2008a) the coefficient of variation (CV) was calculated for each landmark. The averaged CV for each landmark is given in Table 3.30. (Number of landmarks vary because those with high error were removed.).

Table 3.30 Averaged coefficient of variation. Landmarks over 3% are shaded light grey and those over 5% are shaded in dark grey.

Humeral Landmark Error			Femoral Landmark Error	
Landmark			Landmark	
1	2.41%		1	0.45%
2	1.78%		2	1.21%
3	2.11%		3	1.63%
4	0.74%		4	1.34%
5	1.68%		5	3.75%
6	2.59%		6	1.55%
7	3.15%		7	1.60%
8	1.97%		8	1.60%
9	2.37%		9	1.34%
10	0.52%		10	2.79%
11	0.78%		11	3.30%
12	1.72%		12	5.24%
13	1.77%		13	1.89%
14	1.57%		14	1.46%
15	2.97%		15	2.92%
16	2.46%		16	2.03%
17	1.32%		17	0.26%
18	4.00%		18	0.37%
19	2.37%		19	0.39%
20	2.50%		20	0.37%
21	2.79%		21	0.26%
22	11.68%		22	0.18%
23	2.37%		23	0.18%
24	3.10%		24	0.18%
25	2.23%		25	0.23%
26	3.57%		26	0.15%
			27	0.24%
			28	0.17%
Average	2.56%			1.32%

Table 3.31 Average error by landmark set.

	Average Error by Set	Average Error by Set after removing outliers
Proximal Humerus	2.09%	2.09%
Distal Humerus	2.81%	2.26%
Proximal Femur	2.13%	1.83%
Distal Femur	0.25%	0.25%

Table 3.32 Final average CV for each set subtracted from average CV for multiple observations of two scans of the same element to provide instrument error.

			Instrument Error
F34 left humerus	proximal	1.89%	-0.2%
	distal	0.18%	-2.08%
F39 left humerus	proximal	1.66%	-0.43%
	distal	0.17%	-2.09%
F39 right humerus	proximal	2.56%	0.47%
	distal	0.17%	-2.09%
F49 right humerus	proximal	2.42	0.33%
	distal	0.19	-2.07%
F34 right femur	proximal	2.79%	0.96%
	distal	0.23%	-0.02%
F39 right femur	proximal	1.94%	0.11%
	distal	0.31%	0.06%
F49 right femur	proximal	1.83%	0.00%
	distal	0.18%	-0.07%
F186 left femur	proximal	1.72%	-0.11%
	distal	0.16%	-0.09%

Repeatability refers to the “ratio of the precision of a particular measure to the biological differences among specimens (Kohn and Cheverud, 1992 in Lele & Richtsmeier, 2001b pp. 37). Lack of, or low repeatability caused the elimination of some landmarks for this study. Based on the coefficient of variation averaged across all elements, landmarks and observations intraobserver error is 2.56% and 1.32% for the humerus and femur respectively (Table 3.31). Landmark variability changed from individual to individual possibly due to individual variation or scan resolution but over the entire set sampled for precision, only one landmark on each element was especially problematic. The humerus landmark 22 (the most distal aspect of the olecranon fossa) had an error of 11.68%. This may be due to the almost featureless appearance of the posterior aspect of the trochlea. Similarly, landmark 12 on the femur showed 5.24% error. This landmark denotes the approximate distal limit of the quadratus femoris attachment, but is rarely robust and so difficult to find. Humeral landmark 22 and femoral landmarks 11 and 12 have been removed from analysis due to their high rate of error.

Observer error is predictably more variable than instrument error. Landmarks were originally selected on the basis of being representative, as a group, of the shape of the bone and having anatomical significance. However, lack of homologous placement or feasibility in determination of landmark location on three dimensional scans in a pilot study caused the elimination of numerous landmarks. Once the final landmark set had been determined, intraobserver error on this landmark set was assessed by landmarking five humeri

and five femora three times a day over the course of three days. A Procrustes ANOVA was performed in MorphoJ with “side” set to first or third observation. Results for humeri are given in Table 3.33 and Table 3.34 and results for femora are given in Table 3.35 and

Table 3.36, and indicated that there was no difference in shape or centroid size between the two sets of observations.

Table 3.33 ANOVA results of intraobserver error for proximal humerus.

Centroid size:

Effect	SS	MS	df	F	P (param.)
Individual	792.9395	198.234867	4	483.05	<.0001
Side	0.010687	0.010687	1	0.03	0.8796
Ind * Side	1.641518	0.410379	4	2.55	0.0712
Residual	3.221314	0.161066	20		

Shape, Procrustes ANOVA:

Effect	SS	MS	df	F	P (param.)	Pillai tr.	P (param.)
Individual	0.227774	0.002847171	80	12.85	<.0001		
Side	0.006522	0.00032612	20	1.47	0.1155		
Ind * Side	0.01773	0.00022163	80	1.87	<.0001	2.93	0.9594
Residual	0.047285	0.000118211	400				

Centroid size:

Effect	SS	MS	df	F	P (param.)
Individual	1793.027	448.256853	4	1004.27	<.0001
Side	0.371935	0.371935	1	0.83	0.413
Ind * Side	1.785404	0.446351	4	3.52	0.0249
Residual	2.536837	0.126842	20		

Shape, Procrustes ANOVA:

Effect	SS	MS	df	F	P (param.)
Individual	0.168418	0.001026939	164	18.77	<.0001
Side	0.003942	9.61356E-05	41	1.76	0.0072
Ind * Side	0.008974	5.47201E-05	164	1.34	0.0057
Residual	0.033457	4.08007E-05	820		

Table 3.34 ANOVA results of intraobserver error for distal humerus.

Centroid size:

Effect	SS	MS	df	F	P (param.)
Individual	792.9395	198.234867	4	483.05	<.0001
Side	0.010687	0.010687	1	0.03	0.8796
Ind * Side	1.641518	0.410379	4	2.55	0.0712
Residual	3.221314	0.161066	20		

Shape, Procrustes ANOVA:

Effect	SS	MS	df	F	P (param.)	Pillai tr.	P (param.)
Individual	0.227774	0.002847171	80	12.85	<.0001		
Side	0.006522	0.00032612	20	1.47	0.1155		
Ind * Side	0.01773	0.00022163	80	1.87	<.0001	2.93	0.9594
Residual	0.047285	0.000118211	400				

Table 3.35 ANOVA results of intraobserver error for proximal femur.

Centroid size:

Effect	SS	MS	df	F	P (param.)
Individual	458.0229	458.022931	1	1353828	0.0005
Side	5.065348	5.065348	1	14972.19	0.0052
Ind * Side	0.000338	0.000338	1	0	0.9842
Residual	6.506546	0.813318	8		

Shape, Procrustes ANOVA:

Effect	SS	MS	df	F	P (param.)
Individual	0.072356	0.001764789	41	19.87	<.0001
Side	0.00279	6.80409E-05	41	0.77	0.8013
Ind * Side	0.003641	8.88073E-05	41	2.56	<.0001
Residual	0.011371	3.46666E-05	328		

Table 3.36 ANOVA results of intraobserver error for distal femur.

Centroid size:

Effect	SS	MS	df	F	P (param.)
Individual	53.43152	53.431521	1	24.48	0.127
Side	3.703646	3.703646	1	1.7	0.4168
Ind * Side	2.182747	2.182747	1	0.02	0.8917
Residual	3004.332	115.551227	26		

Shape, Procrustes ANOVA:

Effect	SS	MS	df	F	P (param.)
Individual	0.040385	0.001392574	29	13.64	<.0001
Side	0.003497	0.00012059	29	1.18	0.3287
Ind * Side	0.002962	0.000102121	29	0.4	0.9982
Residual	0.192807	0.000255712	754		

3.6 Statistical Analysis

3.6.1 Generalised Procrustes Analysis (GPA) Principal Component Analysis (PCA)

GPA is a method of removing size, rotation, and translation from shape objects in order to consider them as entirely morphological. GPA provides “Procrustes coordinates” which are coordinates of each objects adjusted per above. These may be used to calculate Centroid Size (CS) the mean Procrustes shape for the set, and determine the distance of any given shape object from the mean object. For the purposes of biological sets however allometry – the variation of shape with size – may be present particularly in sexual dimorphism. Allometry was determined in this study by regressing the Procrustes Residuals (distance from the mean Procrustes shape) against $\log(\text{CS})$ following Mitteroecker and colleagues (2004).

After GPA, PCA was performed using the R statistical package. PCA is a dimension reduction technique which provides visualizations which were used to assess the Euclidean distance between individuals and also determines the type and weight of morphological variation.

3.6.2 Generalised Linear Model (GLM)

To determine whether or not variation is present between groups the most obvious choice would have been ANOVA or MANOVA. However, the strict interpretation of both these tests requires that Independent Variables (IVs) not be continuous. This means using ANOVA or MANOVA variables could only be tested against size or shape rather than both at once. To circumvent this problem the very similar statistical method GLM was chosen. GLM allows for continuous IVs and does not order variables allowing for interactions to be efficiently tested.

GLM analysis was performed in the R (“R Development Core Team. 2008. R: a language and environment for statistical computing. R Foundation for Statistical Computing,” n.d.) using the package “Geomorph” and the function *procD.lm()* (D. C. Adams & Otárola-Castillo, 2013a). The linear model allows for Independent Variables (IVs) to be continuous rather than categorical. The function in R is also specifically designed to allow for Procrustes residuals to be used without altering their array. The Procrustes linear model functions similarly to ANOVA and requires the same assumptions of homogeneity and discrete IVs (no individual can occupy two categories in an IV at once), the function refers to itself as an ANOVA and the results may be interpreted similarly. For cross-sectional geometric values, ANOVA and the post-hoc test Tukey’s HSD were conducted by using the R functions *aov()* and

TukeyHSD(). GLM and ANOVA used throughout this study are type III as they use the “marginal” Sum of Squares (SS) method. This means that the fit is random as opposed to ordered, making the inclusion of interactions for IVs more efficient. Additionally, the F-values are not used to compute P-values as to do so would assume the number of observations is greater than the number of variables. A greater number of variables than observations is permissible provided appropriate statistical tests are chosen (Gunz et al., 2005a; Slice, 2005). For the data set as a whole, observations do exceed variables, but if subdivided by site variables will exceed observations, so these methods were chosen as they may be consistently applied regardless of the subdivision of the dataset.

GLM tests were conducted using shape as the DV and the variable to be tested as the IV along with size and sex as interactions. Size and sex are included in each test because they are likely to influence the expression of each variable considered, and because allometry and sexual dimorphism create enough morphological variation to assume that some conditions or pathologies may express differently on individuals of different sex or size. Without considering size and sex concurrently, variation specific to these factors and the factor tested for would appear random. Biomechanical properties already incorporate size information; therefore, interactions were less necessary. In the ANOVA tests each cross-sectional geometric value was considered the DV and each variable (e.g. sex, age, pathological status) was considered the IV.

For the analysis of cross-sectional geometry alone Type III ANOVAs were used. Cross-sectional geometric dimensions and measurements are based on linear and area measurements and so size is already incorporated. Therefore, it was possible to restrict the IVs to non-continuous or categorical statistics. A Type III ANOVA was used so that as with the GLM analysis interactions could be considered simultaneously. ANOVA tests were also performed in *R* using the *aov()* function.

4 Epiphyseal Morphological Variation as Quantified by Homologous landmarks

4.1 Introduction

In this chapter I will quantify and explain the patterns found in the populations in regards to how shape defined by homologous landmarks at the proximal and distal epiphyses of the humerus and femur relates to various aspects of inter and intra population variation. This thesis attempts to address morphological variation in relation to intrapopulation variation including sex, age, indicators of childhood stress, presence or absence of joint disease, and presence or absence of trauma as well as interpopulation variation and variation within the different areas of the bone. This section will be primarily concerned with intrapopulation variation leaving interpopulation and variation within the bone to subsequent pertinent chapters. Here I will focus only on results from the homologous landmark set.

Previous GMM studies on long bones use primarily homologous landmarks (Bacon, 2000; Bonnan, 2004; Bonnan et al., 2008; Harmon, 2007; Kranioti, Bastir, et al., 2009; Kranioti, Vorniotakis, et al., 2009; Kranioti & Michalodimitrakis, 2009; Milne et al., 2009; Stevens & Viðarsdóttir, 2008) and while homologous landmarks may not be as morphologically descriptive as semilandmarks, they are easier to apply, are not subject to the “sliding” function, and may be compared to more previous studies. Homologous landmarks were used to consider the morphology of the proximal and distal epiphyses of the left humerus and femur. Landmarks were chosen to correspond as closely as possible with previous studies (Bacon, 2000; Harmon, 2007; Kranioti, Bastir, et al., 2009; Stevens & Viðarsdóttir, 2008) and adequately describe the shape of the epiphysis. For this analysis the epiphyses of each bone were considered separately. This was necessary because no homologous landmark could be consistently placed on the diaphysis and the length of the long bones would require artificial affine deformation along the y axis during Procrustes alignment. No shape information would be preserved by considering both epiphyses as a set, and without significant arithmetic intervention (see Frelat et al., 2012) signal disrupting distortion would be introduced at the very first step of the analysis (Von Cramon-Taubadel et al., 2007; J. A. Walker, 2000).

In addition to the possibility of comparing results with other studies, the consideration of the epiphyses via homologous landmarks is useful from an aetiological or theoretical standpoint. One of the

primary considerations in intrapopulation variation particularly for this study is sexual dimorphism. Morphology of the epiphyses particularly of the femur should be indicative of sex. To allow for both parturition and bipedalism female and male pelves must have different shapes and orientations which in turn would alter the shape and orientation of the femur at both the proximal and distal epiphysis. It is possible that at least some compensation occurs in the relative rotation of the diaphysis, but considering relative timing of metaphyseal ossification with puberty it would seem likely that some quantifiable morphological variation might occur in the epiphyses of the femur. Additionally, contrary to expectations, there is evidence to suggest that the medial epicondyle of the distal humerus is oriented consistently differently in males and females (İşcan et al., 1998; Kranioti, Bastir, et al., 2009; Kranioti & Michalodimitrakis, 2009; Sakaue, 2004).

Age is the second consideration for variation within a population, but is unlikely to have any impact on epiphyseal morphology as represented by homologous landmarks. This is because the individuals selected for this study are all adults and therefore ontogenetically static. They will not evidence any development in the joint or epiphysis and while they may evidence degeneration particularly in the joint, such degeneration is multifactorial having to do not only with age but also with trauma, hormone involvement, activity or sedentism, pathology, and nutrition. Additionally, age in adults is less likely to consistently affect an epiphyseal shape than it is the diaphyseal shape or cross section due to the timing and pattern of osseous remodeling (Agarwal et al., 2004; Frost, 1999; Jang & Kim, 2008).

Conversely, the third consideration in intrapopulation variation is childhood stress which – if chondral and epiphyseal development are dependent on biomechanical loading in childhood – has a greater likelihood of influencing epiphyseal morphology. Epiphyseal development and finally fusion respectively occur during childhood and adolescence (Frost, 1999; Scheuer & Black, 2000). There is considerable evidence to show that stature and long bone length and robusticity are affected by childhood stress and particularly nutrition (Bogin, 1999). It is therefore reasonable to assume that morphology of the epiphyses as expressed in adult form may be linked to presence or absence of childhood stress markers.

Joint morphology may be altered by pathology – for example enthesal changes or osteophytes indicative of osteoarthritis or degenerative joint disease can alter the morphology of the peri-articular area. While enthesal changes may occur anywhere there is a cartilaginous junction, degenerative joint disease may only occur at the joint. Slightly more obtusely, the epiphyses operate biomechanically in

part as the ends of levers. An alteration in their shape would alter mobility and conversely an alteration in mobility could conceivably alter the epiphyseal morphology. Finally, and most crucially, the size and shape of a joint particularly a weight bearing joint has been shown to be at least somewhat related to developmental factors and weight (Frost, 1999; Stevens & Viðarsdóttir, 2008). Particularly the valgus angle – which has been implicated as indispensable to bipedalism may be impacted by joint morphology.

The last subsection or contributor to intrapopulation variation is trauma. As with age it is unlikely that trauma will bear tremendous influence on the morphology of the epiphysis due to timing of development and remodeling. Unless an injury is extremely severe and alters locomotion and is timed well with joint or epiphyseal development it is unlikely to affect the morphology of the epiphysis itself. Additionally, trauma heals and remodels. It is possible that trauma could disrupt an individual's development by altering their biomechanical loading, but presumably after or even during recovery the individual would return to their normal activities which would once again trigger reactive remodeling with weight bearing activities (Drapeau & Streeter, 2006; Schwartz et al., 2013).

The second research question that may be considered here is that of interpopulation variation. While the field of morphometrics is frequently invoked to determine geographical origin studies on morphological variation in both humans and animals as it correlates with between group variation such studies are usually concerned with cranial and cranio-facial variation. However, there is some interpopulation variation in post-crania. İşcan and colleagues show that different areas of the humerus show morphological variation between populations (1998). Similarly, Stevens and Viðarsdóttir (2008) show a weak correlation between the morphology of the distal femur and an urban or rural environment. By knowing whether or not significant variation occurs between groups we can know if populations may be considered together – morphological variation represents only factors such as sex, age or pathology – or if morphological variation between groups is sufficient enough to obscure the effects of such factors.

4.1.1 Intrapopulation Variation: Morphological Variation in the Epiphyses with Sex

Humans are moderately sexually dimorphic and in both forensic and paleopathological studies elements of the postcrania particularly the pelvis are used in sexual identification. The rate of success of identifying male and female skeletal remains via the qualitative methodology has been reported to be as high as 95-100% (Krogman and İşcan, 1986 in Kranioti, Bastir, et al., 2009). However, archaeologically and forensically the crania and pelvic girdle may be damaged, fragmentary, or missing. To combat this,

numerous studies have assessed sexual dimorphism in other elements of the post-crania including the scapula, humerus, radius and ulna, metacarpals, metatarsals, calcaneus, tibia, femur, and even the patella (Gonzalez et al., 2009; González et al., 2007; Introna Jr et al., 1998; İçcan et al., 1998; Kranioti, Bastir, et al., 2009; Kranioti, Vorniotakis, et al., 2009; Kranioti & Michalodimitrakis, 2009; Sakaue, 2004; Scholtz et al., 2010). The rate of success and the measurement by which the most sexual dimorphism is evident varies, but some degree of sexual dimorphism is usually discernable particularly in the long bones. To a degree this is expected. Being sexually dimorphic humans have different developmental trajectories based on their reaction to their levels of oestrogens and testosterone. For example, cortical development seems to be higher in male adolescents than it is in female adolescents (Ruff, 2005; Ruff et al., 1994). Males are typically larger than females and so may possibly require a slightly different arrangement of muscle attachments, articular surface, epicondylar breadth, or relative size of epiphysis to diaphysis. Finally, and as mentioned previously, female humans have the singular complication of being required to physiologically resolve bipedalism and parturition of offspring with comparatively large crania. Logically, the compromise of the valgus angle in relation to a widened pelvis would influence the morphology of femur in some consistent way. Some authors also suggest an occupational component partially due to sexual division of labour and partially due to the fact that a different biomechanical system would produce slightly different biomechanical requirements for the execution of the same task (Meyer et al., 2011; Molnar et al., 2011; Novak & Šlaus, 2011; Robb, 1998; Sparacello et al., 2011b; Stock & Pfeiffer, 2004; Wilczak, 1998).

Counter-intuitively many studies find that while certain morphological aspects of the femur are sexually dimorphic, the humerus, for the populations studied, may be even more so (İçcan et al., 1998; Kranioti & Michalodimitrakis, 2009; Sakaue, 2004). This is often considered to be a result of sexual division of labour or robusticity. Kranioti and colleagues (2009) found that for their population of Cretan individuals the best indicator of sexual dimorphism in the humerus was the proximal head. Kranioti and colleagues used radiographs and placed two-dimensional homologous landmarks on both the proximal and distal outlines of the humeral epiphyses. Their results showed that the position and size of the greater tubercular was best correlated with sex. In a similar vein Bašić and colleagues showed that the humeral measurement that correlated best with females was maximum head diameter (2013).

Other studies found a greater epicondylar breadth in the distal humerus when comparing males to females (Robinson & Bidmos, 2009; Sakaue, 2004) and Kranioti and colleagues found the shape of the female distal humerus tends to be more square and the male distal humerus tends to be more

rectangular (2009). Other studies have similarly cited epicondylar widths in the distal humerus as sexually dimorphic although the rate of accuracy for identification seems to vary with the population (Albanese et al., 2005; Boldsen et al., 2015; İşcan et al., 1998). Kranioti and colleagues also noted that the trochlea was relatively larger in males and the capitulum relatively larger in females. Mills, İşcan and colleagues and Sakaue (İşcan et al., 1998; Sakaue, 2004) noted that the articular surface was sexually dimorphic. Interestingly, previous studies did note a relative size difference within the bone between the sexes. Both İşcan and colleagues and Sakaue noted that the female humerus tends to have a long diaphysis with small epiphyses while the male humerus tends to have a long diaphysis with relatively large epiphyses. They explain that this would make for higher robusticity which certainly could be deemed sexually dimorphic due to testosterone levels especially at adolescence.

Most studies agreed that the humerus was more sexually dimorphic than the femur or tibia, but sexual dimorphism was observed and could be used to classify individuals as male or female. In the lower limb Sakaue (2004) found that the proximal epicondylar breadth of the tibia is a better indicator of sex than any variations in the femur. Where the knee was found to be particularly sexually dimorphic most authors attributed it as I have to activity and weight during development and crucially adolescence. In this case and in contrast to the humerus, occupational stress would be less impactful because the femur and tibia are weight bearing. Additionally, the dimorphism here concerns the orientation of the articular surface itself pointing biomechanically at bipedalism and body weight during development of the joint. Studies of knees in other primates show that the knee is particularly susceptible to morphological variation with mode of locomotion, so for human knees to vary due to weight during development seems reasonable (Hamrick, 1996; Yamanaka et al., 2005).

As noted in the background chapter, sexual dimorphism is population dependent. This holds true in a more general sense for pelvic and cranial markers of sexual dimorphism and for the degree of sexual dimorphism, but for long bones which presumably have a more multifactorial morphological developmental trajectory, manifestations of long bone sexual dimorphism in one population will not consistently be the best indicators of sexual dimorphism in other populations (İşcan et al., 1998). This problem of population specificity is addressed by Albanese and colleagues who created a universal methodology for metric sex estimation specifically concerning long bones (2005).

In this study sex estimation was performed on each skeleton (methodology may be found in Section 3.2). Landmarks were taken and shape assessed using methods explained in Section 3.5. Then using the R package “Geomorph,” sexual dimorphism was assessed using GLMs (D. C. Adams & Otárola-

Castillo, 2013b). That is the shape score determined sexual dimorphism of the individual elements, but determination of sex was based on standard estimation methods. Results for the effect of sex on morphological variation in the proximal and distal epiphyses may be found in Section 4.2.1.1.

4.1.2 Intrapopulation Variation: Morphological Variation in the Epiphyses with Age

Despite the tremendous role development appears to play on epiphyseal morphology, in this study epiphyseal morphology is not likely correlated with age (Frost, 1999; Hamrick, 1999). This is simply because this study only included adults. Development of epiphyses and thus period of the human lifespan wherein the epiphyses might morphologically change ends at about seventeen or eighteen years of age and there is no real alteration with age outside of incidents of trauma or corrosive arthroses. As this study included no children or adolescents change in the homologous landmarks of the epiphyses with age is unlikely. However, while the epiphyses may not significantly remodel after adulthood there is a chance that the diaphysis may. Cortical bone is laid down in adolescence (Kaastad et al., 2000; Lieberman et al., 2004; O. M. Pearson & Lieberman, 2004; Ruff, 2000, 2002, 2005, Ruff et al., 1994, 2013; Ruff & Hayes, 1982; Shaw & Stock, 2009a; Šlaus, 2000), but it is possible that activity or degeneration with age may change the shape of the diaphysis. Regardless, it is expected that the epiphyses quantified in this study would not be morphologically altered by age alone. Results for the effect of age on morphological variation in the proximal and distal epiphyses may be found in Section 4.2.1.2.

4.1.3 Intrapopulation Variation: Morphological Variation in the Epiphyses with Childhood indicators of Stress

The question of morphological variation with presence or absence of childhood indicators of stress is not as obvious as the previous question on age. Childhood indicators of stress in this study included cribra orbitalia often linked to severe megaloblastic anaemia in very young children and LEH. Both of these indicators are developmentally specific and will only occur in reaction to various stress during childhood. As joints osteologically and cartilaginously form during childhood and adolescence it would be reasonable to presume that contemporary stress might alter their morphology. Conversely, the human immune system will react to stress during development and may postpone development, but simultaneously an excess particularly of cortisol, which is released by the body to attempt to maintain homeostasis, will damage the synovial capsule of joints (Frost, 1999; Gowland, 2015; Hamrick, 1999).

The presence of cribra orbitalia in an adult skeleton points to an anemic episode during early childhood. Cribra orbitalia only develops in young children (Stuart-Macadam, 1985) and is theorised to be resultant of anaemias stemming either from genetic causes or from infectious disease or malnutrition

with multiple possible aetiologies (Stuart-Macadam, 1987b; P. L. Walker et al., 2009; Wapler et al., 2004). Cribra orbitalia is relatively uncommon in Northern Europe particularly in areas where malaria is not present (Gowland & Western, 2012; Smith-Guzmán, 2015) because historically the Northern European diet especially for children and the lower economic echelons involves copious amounts of dairy. Walker and colleagues suggest that low vitamin C either due to dietary deficiencies or loss during diarrhoea could exacerbate cribra orbitalia-like lesions either via co-morbidity or by inhibiting absorption of B₁₂ (P. L. Walker et al., 2009). However, regardless of the exact cause for cribra orbitalia and similar lesions to form there must be either a genetic anaemia or prolonged severe malnutrition or malabsorption occurring before the individual reaches four or five years of age when their medullary cavities are large enough to compensate for hypertrophy of hematopoietic marrow (Stuart-Macadam, 1985; P. L. Walker et al., 2009). The immune system would be triggered likely repeatedly in the mitigation of the resultant anaemia and such over stimulation would almost necessarily lead to long term detrimental immunological and even neurological effects (Gowland & Western, 2012; J. A. Walker, 2000). Additionally Smith-Guzman linked cribra orbitalia with “cribrous lesions” around the articular surface of the long bones (Smith-Guzmán, 2015). Other studies have remarked on an alteration of trabecular structure with anaemia and mention that cavities in the cancellous bone will connect to surface porosities presumably due to marrow hypertrophy (Gowland & Western, 2012; Stuart-Macadam, 1987a, 1987b, 1989). This alteration in the trabeculae and cancellous bone would seem likely to alter the morphology of the epiphysis.

Linear enamel hypoplasia (LEH) is less severe than cribra orbitalia and has even been linked to emotional stress but is more frequently linked to malnutrition or episodes of infection (Herring et al., 1998; Hughes-Morey, 2016; Katzenberg et al., 1996; McEwan et al., 2005; Temple, 2014; Watts, 2015). As adult dentition develops, if a stressful episode occurs enamel deposition will be disrupted. After the episode subsides, enamel deposition will resume as normal. By tracking the rate of development of adult dentition and the position of LEH, it is possible to determine when in an individual's life they experienced episodes of infection, malnutrition, or general stress (Hillson, 2005a; Hillson & Bond, 1997). LEH may form at any time during the formation of deciduous and permanent dentition and so is less age restrictive than cribra orbitalia (Hillson (2005b) gives methodologies for determining the timing of stress based on the position of LEH relative to the crown of the tooth). Enamel deposition is also more sensitive to stressful events and there is no chance of remodeling. Thus, LEH is a permanent indicator of non-specific childhood stress. As with cribrous lesions the presence of LEH would indicate stress during development and crucially stress which may be contemporary with the formation of the epiphyses.

The effects of malnutrition or severe stress in young children have been documented in numerous studies and publications and shown to lead to cardiovascular complications, transgenerational poor health, immune deficiencies, Type II Diabetes, and crucially here an alteration in the metrics of the long bones (Armstrong et al., 2009; Goodman & Armstrong, 1985; Goodman & Rose, 1990; Gowland, 2015; McEwan et al., 2005; Sorensen et al., 2009). Malnourished populations consistently show a different osteometric arrangement in comparison to their healthy counterparts which might suggest a developmental alteration in the morphology of the long bones due to nutritional stress. However, the homologous landmarks in this study might not reflect any such relationship. There are good reasons for this. Firstly, the joint itself may be compromised but not morphologically altered in the event of severe malnutrition or it may alter only within the normal range. While stressed individuals might have even consistent morphological variation it may not be extreme enough to be considered abnormal or even necessarily indicative of poor health. Secondly, the populations sampled here were not very heterogeneous and very little severe stress is present. There may not be any severely affected individuals or such individuals may not have lived to adulthood. Finally, all the cemeteries sampled in this study were used over the course of at least a century and it is very possible that the intergenerational factor is in play. That is, many of the individuals in these cemeteries may be directly related to one another and so a grandmother in poor health may be morphologically very similar to the adult children of her daughter. Results for the effect of childhood stress on morphological variation in the proximal and distal epiphyses may be found in Section 4.2.1.3.3.

4.2 Results

Ninety-five percent of all shape variance in the proximal humerus is described by twelve principal components (PCs) and all variance is described in 20 PCs as shown in Table 4.1. A visualization of shape variation in PC1 and PC2 may be seen in Figure 4.1, and humeral proximal epiphyseal morphological change along PC1 and relative to the mean shape is available in Figure 4.2. Allometric results by sex available in Figure 4.3 and Table 4.2 show that there is allometry present, but it is not related to sex and sex does not explain morphology. Allometric results for the proximal humeral epiphysis by site available in Figure 4.4 and Table 4.3 show that the allometry may also not be related to site, but site does explain morphology.

Table 4.1 Variance by PC for Proximal Humerus Homologous landmarks

PC	Standard Deviation	Proportion of Variance	Cumulative Proportion
1	0.05922	22.3720%	22.3720%
2	0.05352	18.2730%	40.6450%
3	0.04709	14.1480%	54.7940%
4	0.03986	10.1340%	64.9280%
5	0.03271	6.8280%	71.7560%
6	0.02978	5.6580%	77.4140%
7	0.02771	4.8990%	82.3130%
8	0.02582	4.2550%	86.5680%
9	0.02335	3.4780%	90.0450%
10	0.02086	2.7770%	92.8230%
11	0.01724	1.8970%	94.7190%
12	0.01391	1.2350%	95.9540%
13	0.01323	1.1170%	97.0710%
14	0.01106	0.7810%	97.8520%
15	0.009986	0.6360%	98.4880%
16	0.008767	0.4900%	98.9790%
17	0.007784	0.3870%	99.3650%
18	0.007391	0.3480%	99.7140%
19	0.005163	0.1700%	99.8840%
20	0.004267	0.1160%	100.0000%

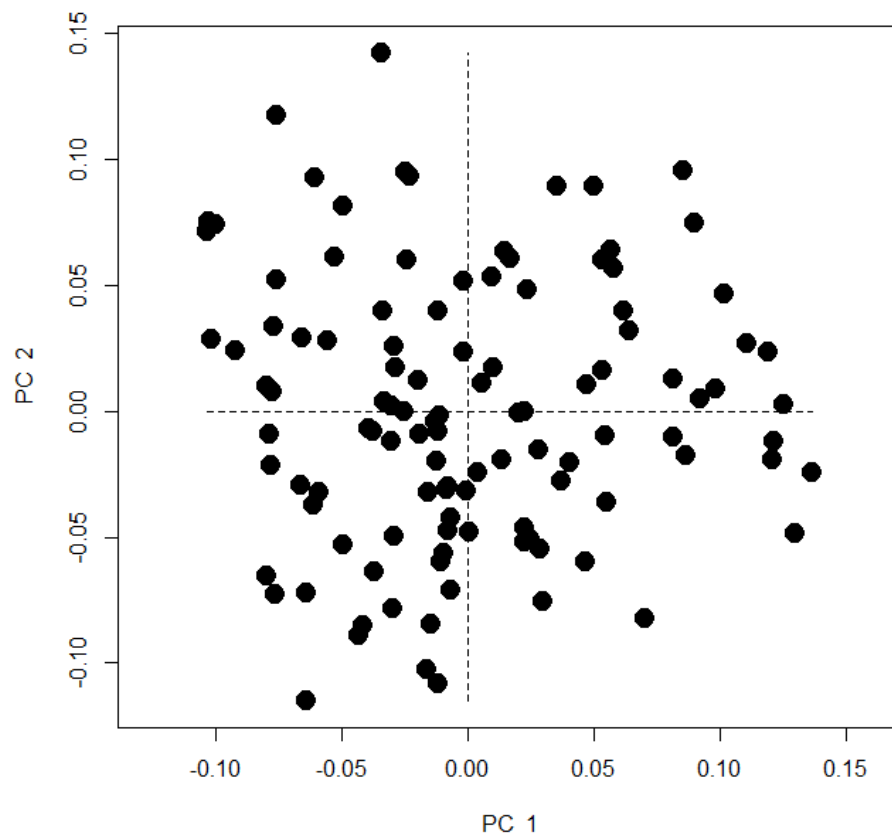


Figure 4.1 PC1 and PC2 for proximal humerus homologous landmarks.

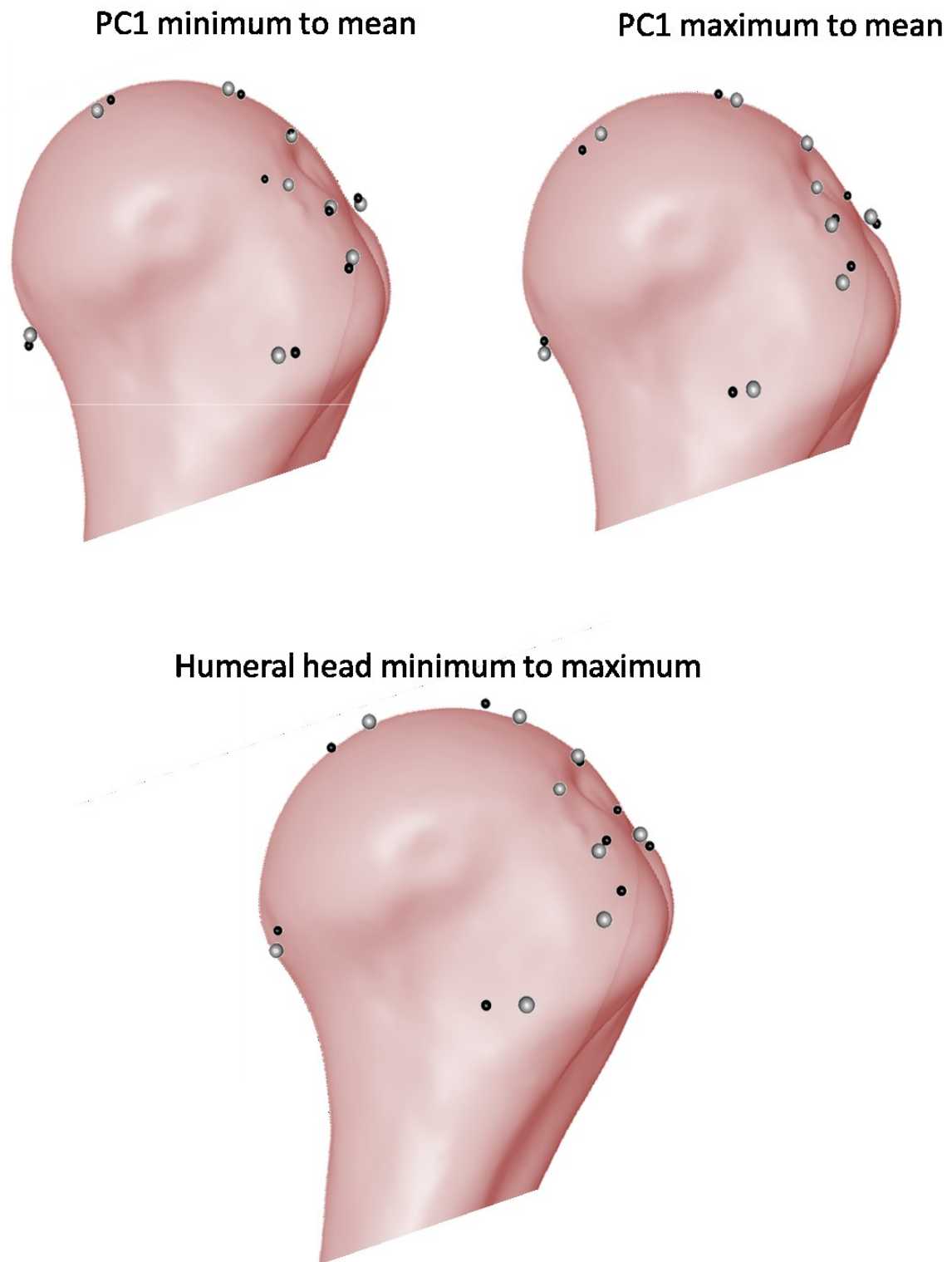


Figure 4.2 Shape variation of the proximal humerus.

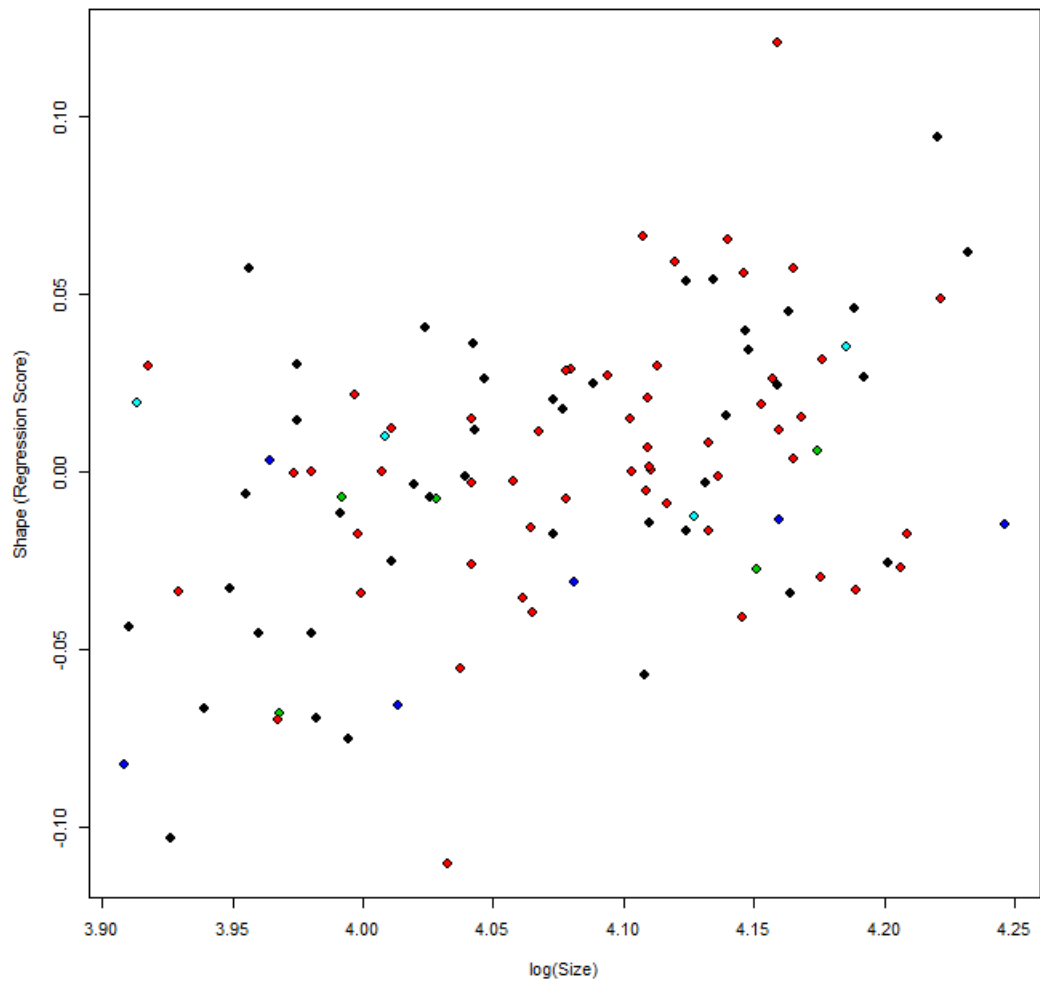


Figure 4.3 Allometric regression of log CS by Shape Regression Scores for proximal humerus color coded by sex. (black = female, red = male, green = possible female, blue = possible male, cyan = unknown)

Table 4.2 Homogeneity of Slope Test and Type I Sum of Squares and Cross products for proximal humeral epiphysis by sex.

Homogeneity of Slopes Test							
	Df	SSE	SS	Rsq	F	Z	Pr(>F)
Common Allometry	105	1.6202					
Group Allometries	101	1.5564	0.063832	0.037024	1.0356	0.49615	0.314

Type I (Sequential) Sums of Squares and Cross-products							
	Df	SS	MS	Rsq	F	Z	Pr(>F)
log(size)	1	0.03111	0.031111	0.018045	2.0162	1.65256	0.042
sex	4	0.07275	0.018187	0.042194	1.1786	0.78299	0.22
Residuals	105	1.62024	0.015431				
Total	110	1.7241					

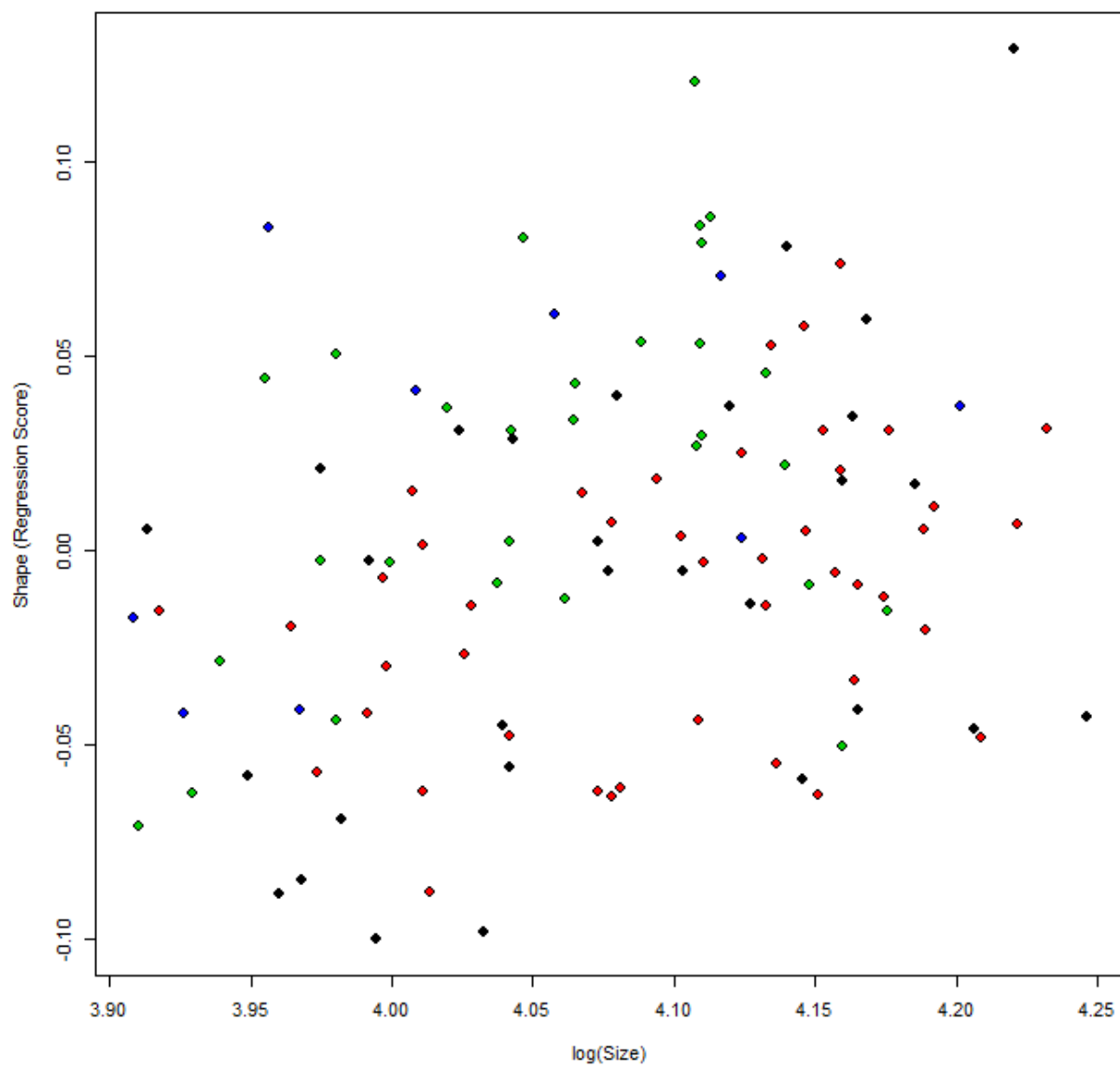


Figure 4.4 Allometric regression of log CS by Shape Regression Scores for proximal humerus color coded by sex. (black = 3-J-18, red = Coach Lane, green = Fishergate, blue = Hereford)

Table 4.3 Homogeneity of Slope Test and Type I Sum of Squares and Cross products for proximal humeral epiphysis by site.

Homogeneity of Slopes Test							
	Df	SSE	SS	Rsqr	F	Z	Pr(>F)
Common Allometry	106	1.4852					
Group Allometries	103	1.4459	0.03931	0.022801	0.9334	0.44016	0.324

Type I (Sequential) Sums of Squares and Cross-products							
	Df	SS	MS	Rsqr	F	Z	Pr(>F)
log(size)	1	0.03111	0.031111	0.018045	2.2204	1.8486	0.022
Site	3	0.20778	0.06926	0.120515	4.9431	5.7886	0.001
Residuals	106	1.48521	0.014011				
Total	110	1.7241					

Ninety-five percent of all shape variance in the distal humerus is described by twenty-six principal components (PCs) and all variance is described in forty-one PCs as shown in Table 4.4. A visualization of shape variation in PC1 and PC2 may be seen in Figure 4.5 and humeral distal epiphyseal morphological change along PC1 and relative to the mean shape is available in Figure 4.6. Allometric results by sex available in Figure 4.7 and Table 4.5 show that size does explain shape, but it is not related to sex, and shape of the proximal humerus is not explained by sex. Allometric results for the distal humeral epiphysis by site available in Figure 4.8 and Table 4.6 show that site does explain morphology about as well as size, but site is still not the cause of allometric variation.

Table 4.4 Variance by PC for Distal Humerus Homologous landmarks

PC	Standard Deviation	Proportion of Variance	Cumulative Proportion
1	0.04573	18.3310%	18.3310%
2	0.03475	10.5860%	28.9170%
3	0.02949	7.6210%	36.5380%
4	0.02846	7.0970%	43.6340%
5	0.02617	6.0010%	49.6350%
6	0.02345	4.8220%	54.4570%
7	0.02179	4.1620%	58.6190%
8	0.02097	3.8540%	62.4730%
9	0.02027	3.6020%	66.0750%
10	0.02004	3.5200%	69.5950%
11	0.01881	3.1000%	72.6940%
12	0.01798	2.8350%	75.5290%

13	0.01665	2.4310%	77.9600%
14	0.01617	2.2920%	80.2520%
15	0.01582	2.1920%	82.4450%
16	0.01484	1.9300%	84.3740%
17	0.01386	1.6830%	86.0570%
18	0.01322	1.5320%	87.5880%
19	0.01291	1.4600%	89.0480%
20	0.0119	1.2410%	90.2890%
21	0.01164	1.1870%	91.4770%
22	0.01068	0.9990%	92.4760%
23	0.0104	0.9490%	93.4250%
24	0.009441	0.7810%	94.2060%
25	0.009074	0.7220%	94.9270%
26	0.008831	0.6830%	95.6110%
27	0.008349	0.6110%	96.2220%
28	0.008141	0.5810%	96.8030%
29	0.007991	0.5600%	97.3620%
30	0.007406	0.4810%	97.8430%
31	0.006768	0.4010%	98.2450%
32	0.006393	0.3580%	98.6030%
33	0.00601	0.3170%	98.9190%
34	0.005145	0.2320%	99.1510%
35	0.004888	0.2090%	99.3610%
36	0.004503	0.1780%	99.5390%
37	0.004089	0.1470%	99.6850%
38	0.003822	0.1280%	99.8130%
39	0.003091	0.0840%	99.8970%
40	0.002685	0.0630%	99.9600%
41	0.002134	0.0400%	100.0000%

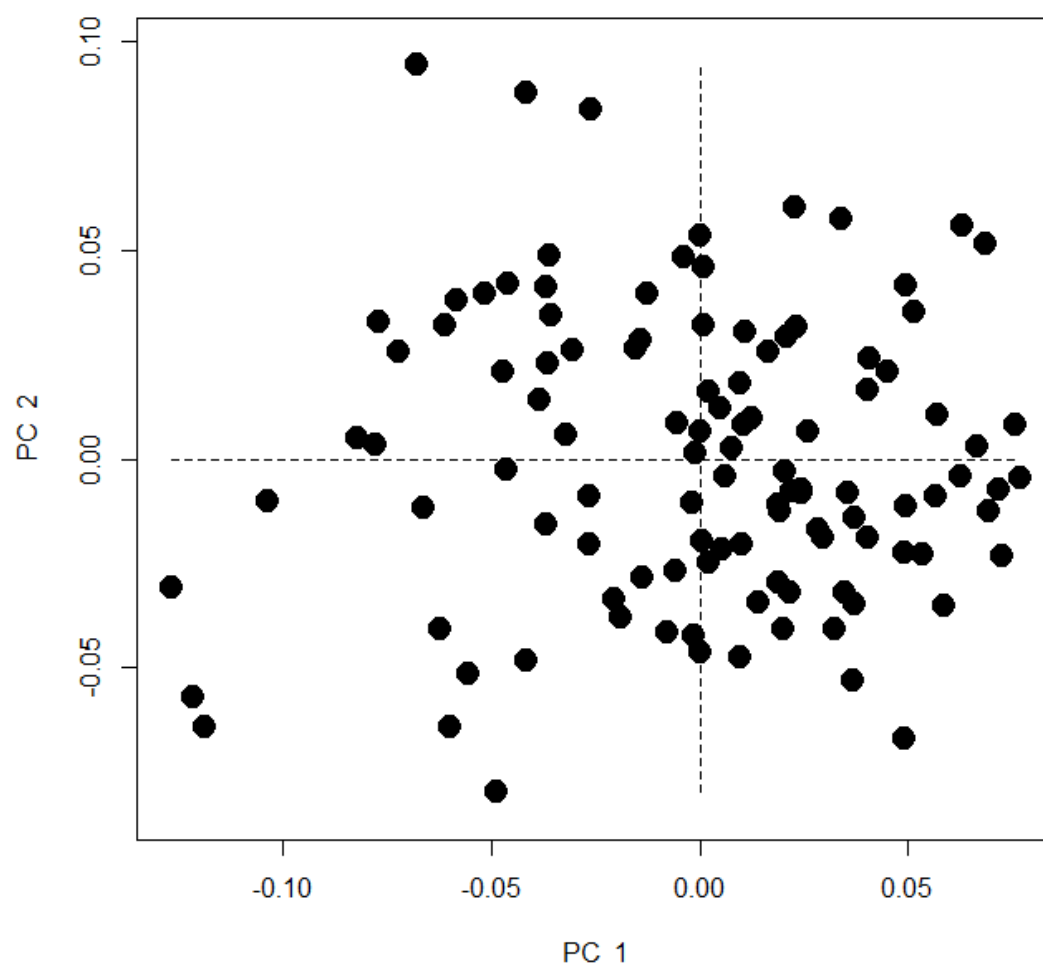
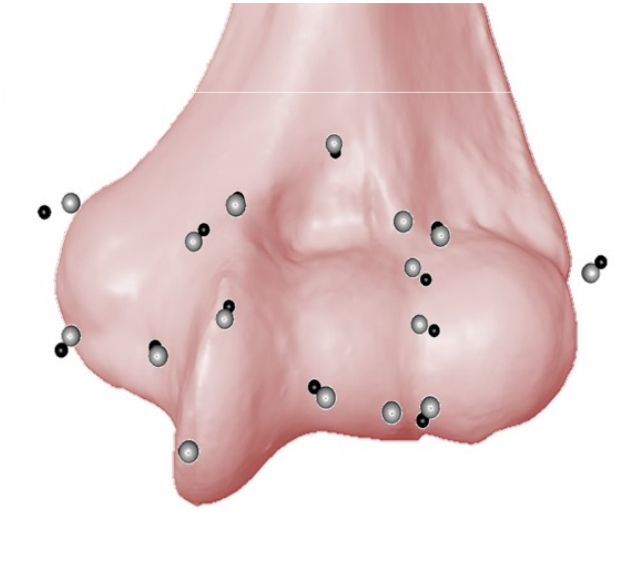
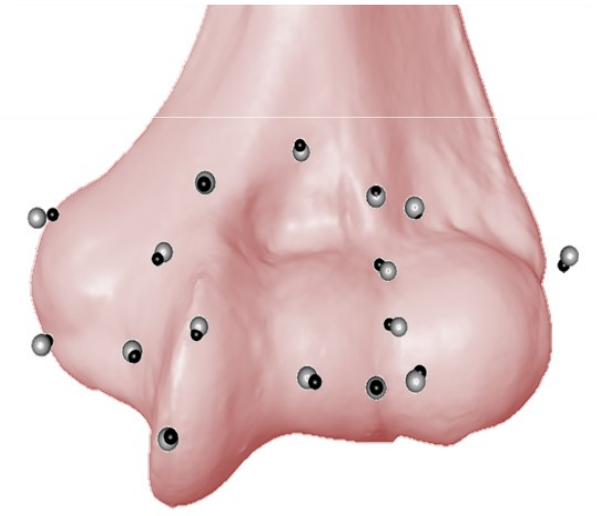


Figure 4.5 PC1 and PC2 for distal humerus homologous landmarks.

PC1 minimum to mean



PC1 maximum to mean



Distal Humerus minimum to maximum

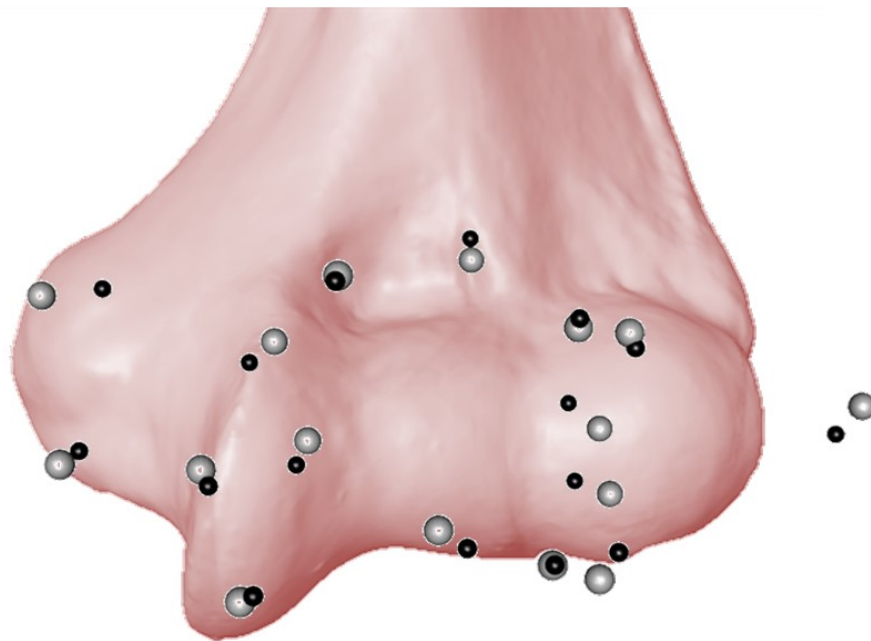


Figure 4.6 Shape variation of the distal humerus

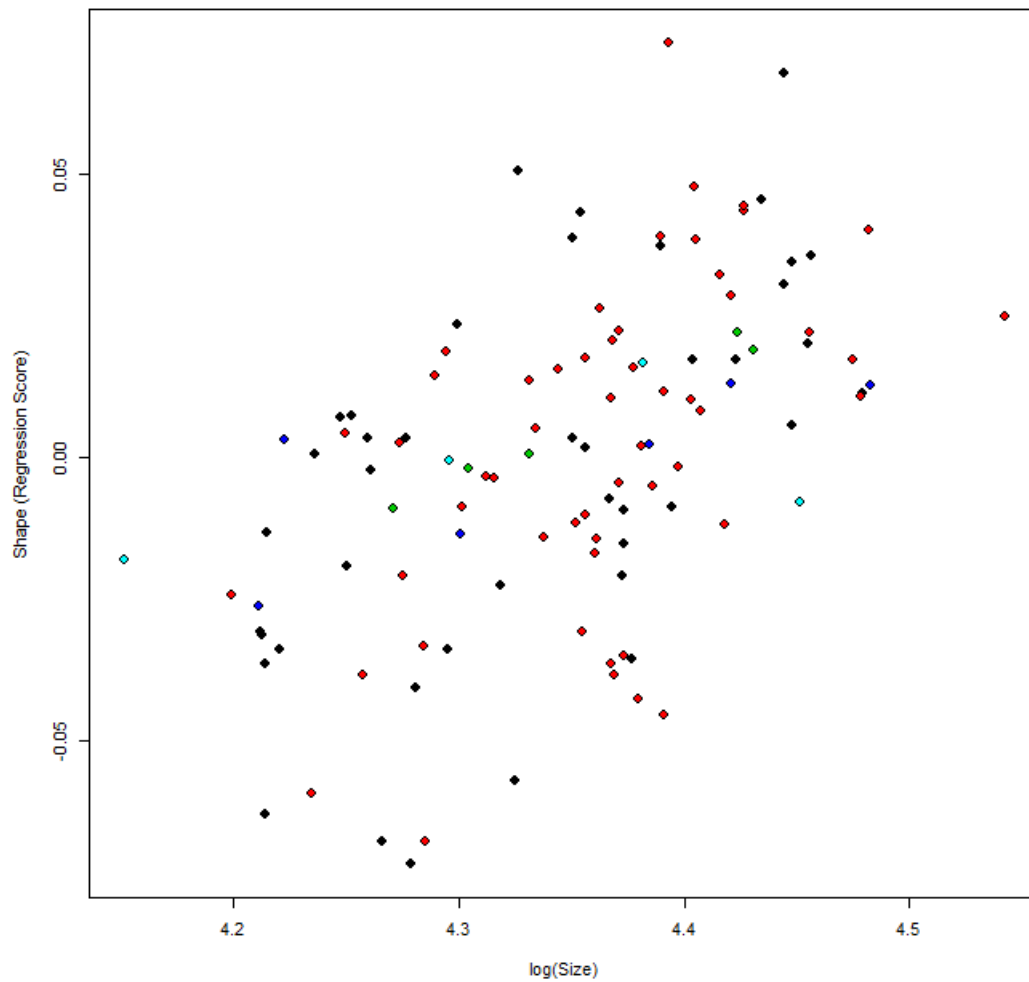


Figure 4.7 Allometric regression of log CS by Shape Regression Scores for distal humerus color coded by sex. (black = female, red = male, green = possible female, blue = possible male, cyan = unknown)

Table 4.5 GLM Procrustes shape residuals compared to log(CS) for distal humerus by sex.

Homogeneity of Slopes Test							
	Df	SSE	SS	Rsq	F	Z	Pr(>F)
Common Allometry	105	1.1868					
Group Allometries	101	1.1458	0.040983	0.032654	0.9031	-0.18047	0.543

Type I (Sequential) Sums of Squares and Cross-products							
	Df	SS	MS	Rsq	F	Z	Pr(>F)
log(size)	1	0.02773	0.027727	0.022092	2.4531	2.85275	0.003
sex	4	0.04053	0.010134	0.032297	0.8966	-0.35034	0.632
Residuals	105	1.18679	0.011303				
Total	110	1.25505					

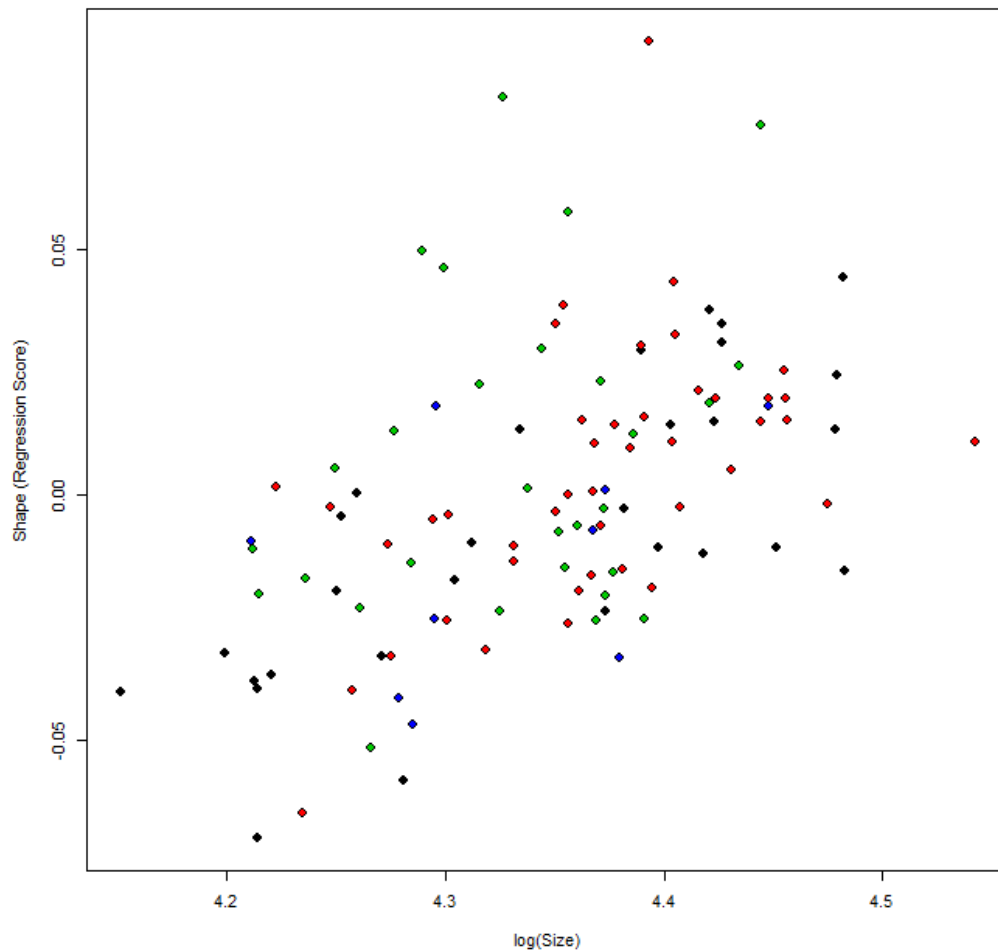


Figure 4.8 Allometric regression of log CS by Shape Regression Scores for distal humerus color coded by site. (black = 3-J-18, red = Coah Lane, green = Fishergate, blue = Hereford)

Table 4.6 GLM Procrustes shape residuals compared to log(CS) for distal humerus by site.

Homogeneity of Slopes Test							
	Df	SSE	SS	Rsq	F	Z	Pr(>F)
Common Allometry	106	1.0997					
Group Allometries	103	1.0686	0.03115	0.024819	1.0008	0.69505	0.238

Type I (Sequential) Sums of Squares and Cross-products							
	Df	SS	MS	Rsq	F	Z	Pr(>F)
log(size)	1	0.02773	0.027727	0.022092	2.6726	3.1105	0.001
site	3	0.1276	0.042534	0.10167	4.0997	6.9479	0.001
Residuals	106	1.09972	0.010375				
Total	110	1.25505					

Ninety-Five percent of all variance in the homologous landmarks shape set of the proximal femur was described in twenty-two PCs with total shape variance described in thirty-five. This is illustrated in Table 4.7. Objects are charted along PC1 and PC2 in Figure 4.9 and shape change of the proximal femur along PC1 relative to mean shape is available in Figure 4.10. Figure 4.11 and Table 4.8 give allometric results by sex. Allometry was present but not due to sex, and sex does not explain morphology. Figure 4.12 and Table 4.9 give allometric results by site and show that allometry is present but again is not related to the IV, but the IV of site does explain morphology.

Table 4.7 Variance by PC for Proximal Femur Homologous landmarks

PC	Standard deviation	Proportion of Variance	Cumulative Proportion
1	0.04689	14.9330%	14.9330%
2	0.04016	10.9510%	25.8840%
3	0.03791	9.7590%	35.6430%
4	0.03638	8.9860%	44.6290%
5	0.0322	7.0430%	51.6720%
6	0.03019	6.1900%	57.8620%
7	0.02733	5.0730%	62.9350%
8	0.02521	4.3140%	67.2490%
9	0.02466	4.1300%	71.3790%
10	0.02319	3.6530%	75.0320%
11	0.02144	3.1210%	78.1530%
12	0.02004	2.7260%	80.8790%
13	0.01907	2.4690%	83.3490%
14	0.01748	2.0740%	85.4230%
15	0.01704	1.9730%	87.3960%
16	0.01567	1.6670%	89.0630%
17	0.01463	1.4530%	90.5160%
18	0.0136	1.2550%	91.7720%
19	0.01304	1.1550%	92.9270%
20	0.01154	0.9050%	93.8310%
21	0.01142	0.8860%	94.7170%
22	0.01076	0.7860%	95.5040%
23	0.01038	0.7320%	96.2350%
24	0.009796	0.6520%	96.8870%
25	0.009679	0.6360%	97.5230%
26	0.008479	0.4880%	98.0110%
27	0.007668	0.3990%	98.4100%
28	0.007248	0.3570%	98.7670%
29	0.006815	0.3150%	99.0820%

30	0.006319	0.2710%	99.3540%
31	0.005676	0.2190%	99.5720%
32	0.004878	0.1620%	99.7340%
33	0.004403	0.1320%	99.8660%
34	0.003626	0.0890%	99.9550%
35	0.002575	0.0450%	100.0000%

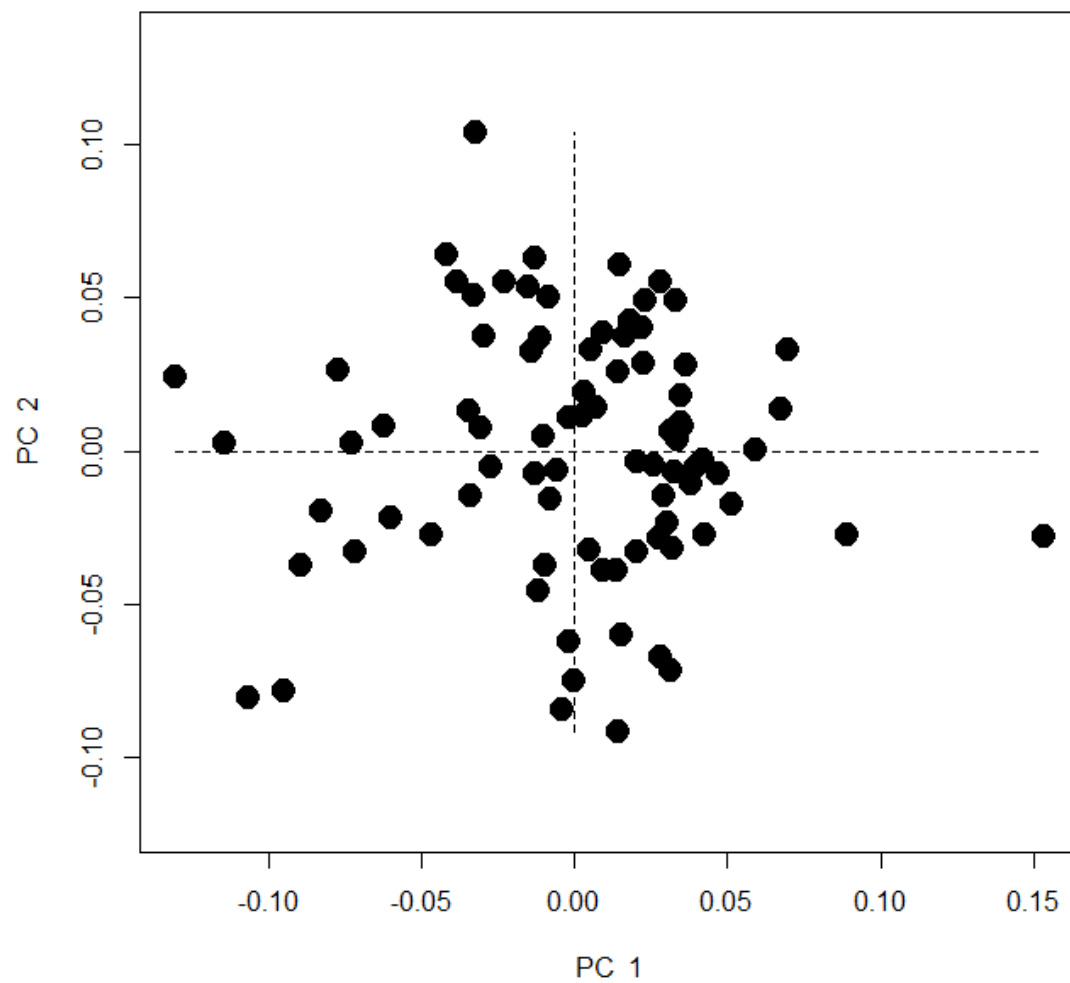


Figure 4.9 PC1 and PC2 for proximal femur homologous landmarks.

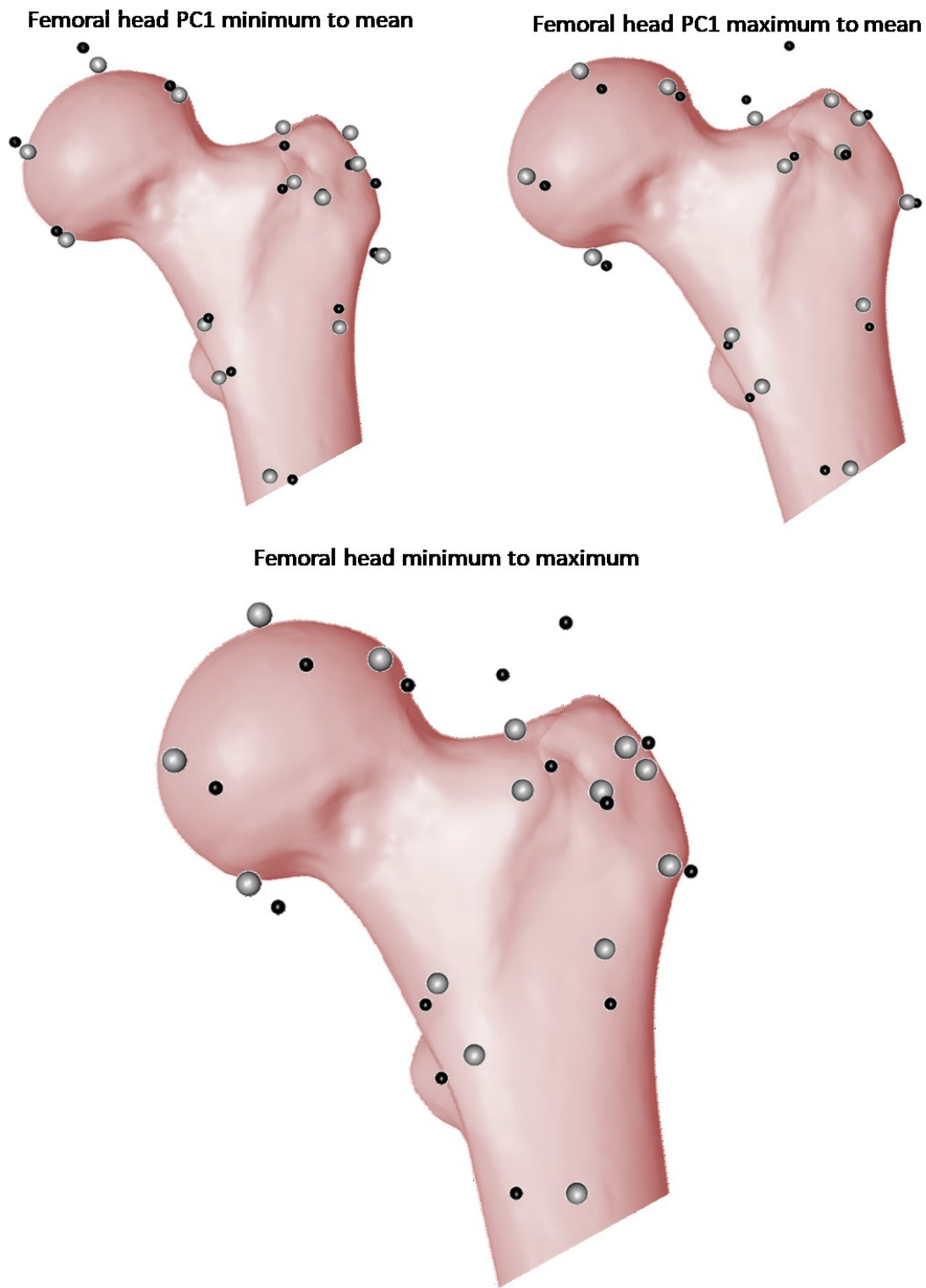


Figure 4.10 Shape variation of the proximal femur.

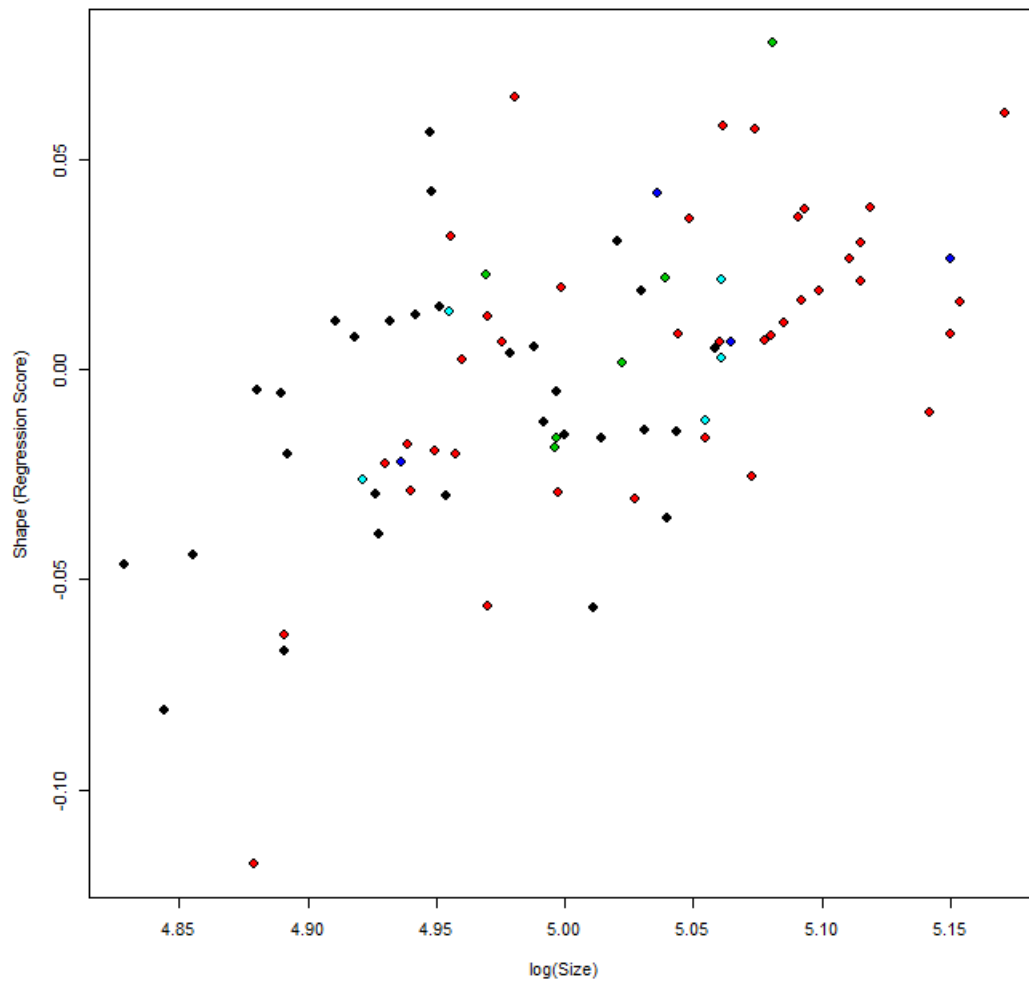


Figure 4.11 Allometric regression of log CS by Shape Regression Scores for proximal femur color coded by sex. (black = female, red = male, green = possible female, blue = possible male, cyan = unknown)

Table 4.8 GLM Procrustes shape residuals compared to log(CS) for proximal femur by sex.

Homogeneity of Slopes Test							
	Df	SSE	SS	Rsqr	F	Z	Pr(>F)
Common Allometry	77	1.1132					
Group Allometries	73	1.0551	0.058118	0.048131	1.0052	0.56441	0.282

Type I (Sequential) Sums of Squares and Cross-products							
	Df	SS	MS	Rsqr	F	Z	Pr(>F)
log(size)	1	0.03482	0.034816	0.028834	2.4082	2.72677	0.001
sex	4	0.05944	0.014861	0.049228	1.0279	0.42661	0.334
Residuals	77	1.11323	0.014458				
Total	82	1.20749					

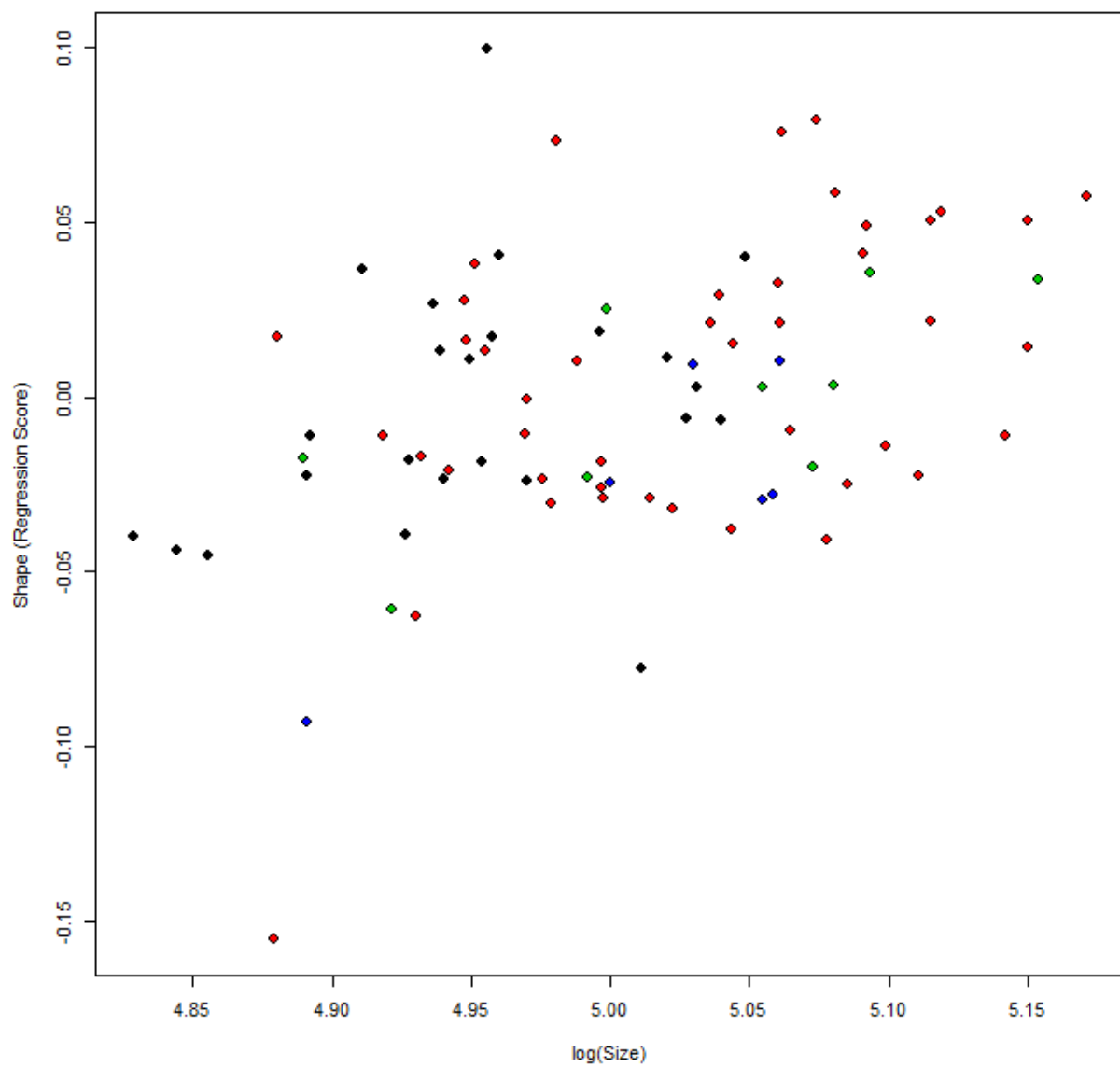


Figure 4.12 Allometric regression of log CS by Shape Regression Scores for proximal femur color coded by site. (black = 3-J-18, red = Coach Lane, green = Fishergate, blue = Hereford)

Table 4.9 GLM Procrustes shape residuals compared to log(CS) for proximal femur by site.

Homogeneity of Slopes Test							
	Df	SSE	SS	Rsq	F	Z	Pr(>F)
Common Allometry	78	1.0873					
Group Allometries	75	1.0549	0.032453	0.026877	0.7691	-0.64262	0.724

Type I (Sequential) Sums of Squares and Cross-products							
	Df	SS	MS	Rsq	F	Z	Pr(>F)
log(size)	1	0.03482	0.034816	0.028834	2.4976	2.8295	0.001
site	3	0.08536	0.028452	0.070689	2.041	3.6214	0.001
Residuals	78	1.08732	0.01394				
Total	82	1.20749					

Ninety-five percent of variation in the homologous landmarks of the distal femur is described in sixteen PCs. Total variation is described in twenty-nine PCs. This may be seen in Table 4.10. Individual shapes are plotted by PC1 and PC2 in Figure 4.13 and a visualization of shape changes along PC1 relative to the mean shape is available in Figure 4.14. Allometry by sex is plotted in Figure 4.15 and results are given in Table 4.11. Allometry is present but not related to sex and sex does not explain morphological variation. Allometry by site is plotted in Figure 4.16 and results are shown in Table 4.12. Allometry in the distal femur is also not related to site, but site does explain morphological variation.

Table 4.10 Variance by PC for Distal Femur Homologous landmarks

PC	Standard deviation	Proportion of Variance	Cumulative Proportion
1	0.09797	44.1800%	44.1800%
2	0.04638	9.8990%	54.0790%
3	0.0395	7.1800%	61.2600%
4	0.03564	5.8470%	67.1060%
5	0.03062	4.3150%	71.4220%
6	0.02966	4.0490%	75.4710%
7	0.02846	3.7290%	79.2010%
8	0.02542	2.9740%	82.1740%
9	0.02278	2.3890%	84.5630%
10	0.02097	2.0240%	86.5870%
11	0.02004	1.8490%	88.4350%
12	0.01987	1.8170%	90.2530%
13	0.01765	1.4340%	91.6860%
14	0.01727	1.3730%	93.0590%
15	0.01542	1.0940%	94.1530%
16	0.01391	0.8910%	95.0440%
17	0.0131	0.7900%	95.8400%
18	0.01278	0.7510%	96.5860%
19	0.01114	0.5710%	97.1570%
20	0.01056	0.5130%	97.6700%
21	0.009617	0.4260%	98.0950%
22	0.008899	0.3650%	98.4600%
23	0.008227	0.3120%	98.7710%
24	0.007947	0.2910%	99.0620%
25	0.007785	0.2790%	99.3410%
26	0.007056	0.2290%	99.5700%
27	0.006268	0.1810%	99.7510%
28	0.005491	0.1390%	99.8900%
29	0.004892	0.1100%	100.0000%

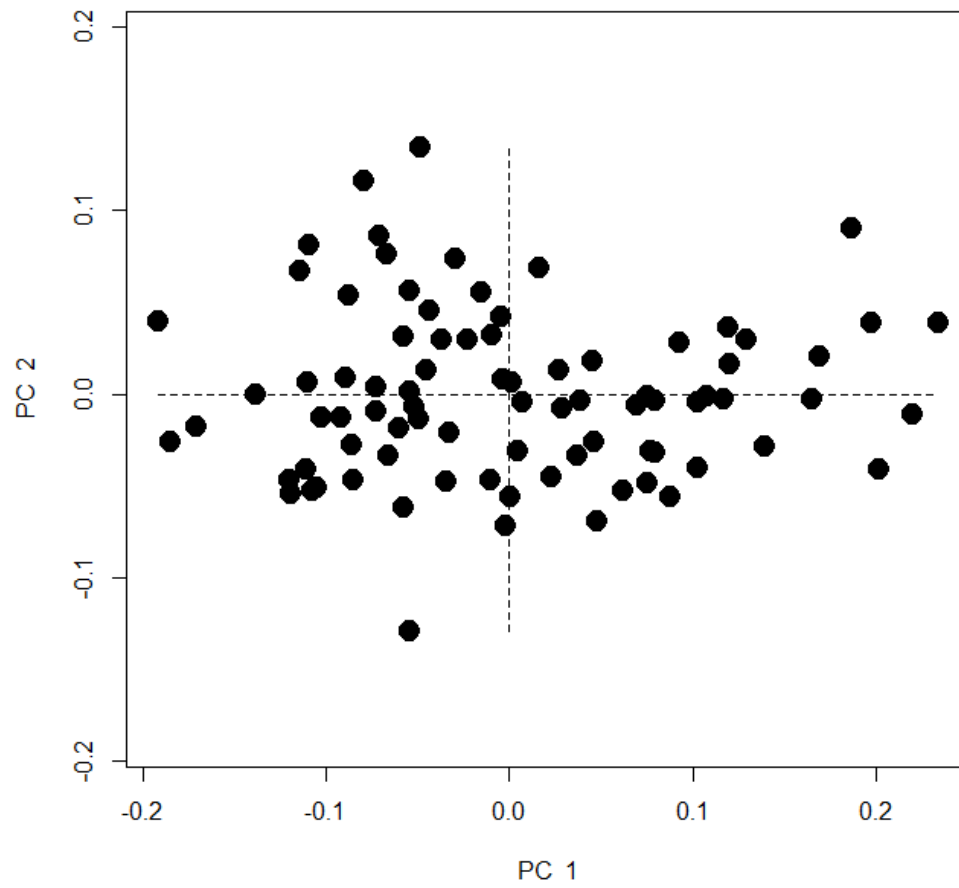


Figure 4.13 PC1 and PC2 for distal femur homologous landmarks.

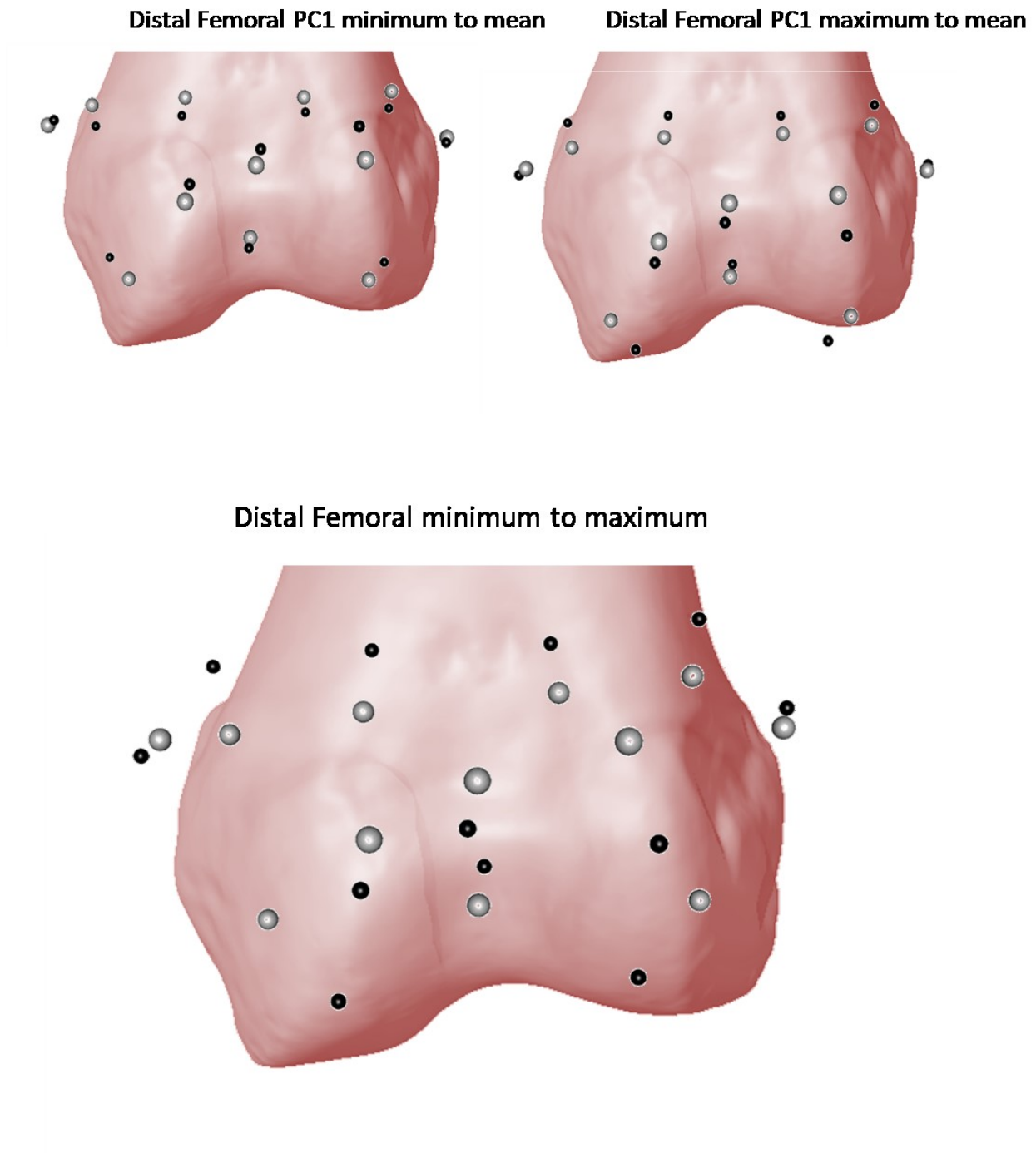


Figure 4.14 Shape variation of the distal femur.

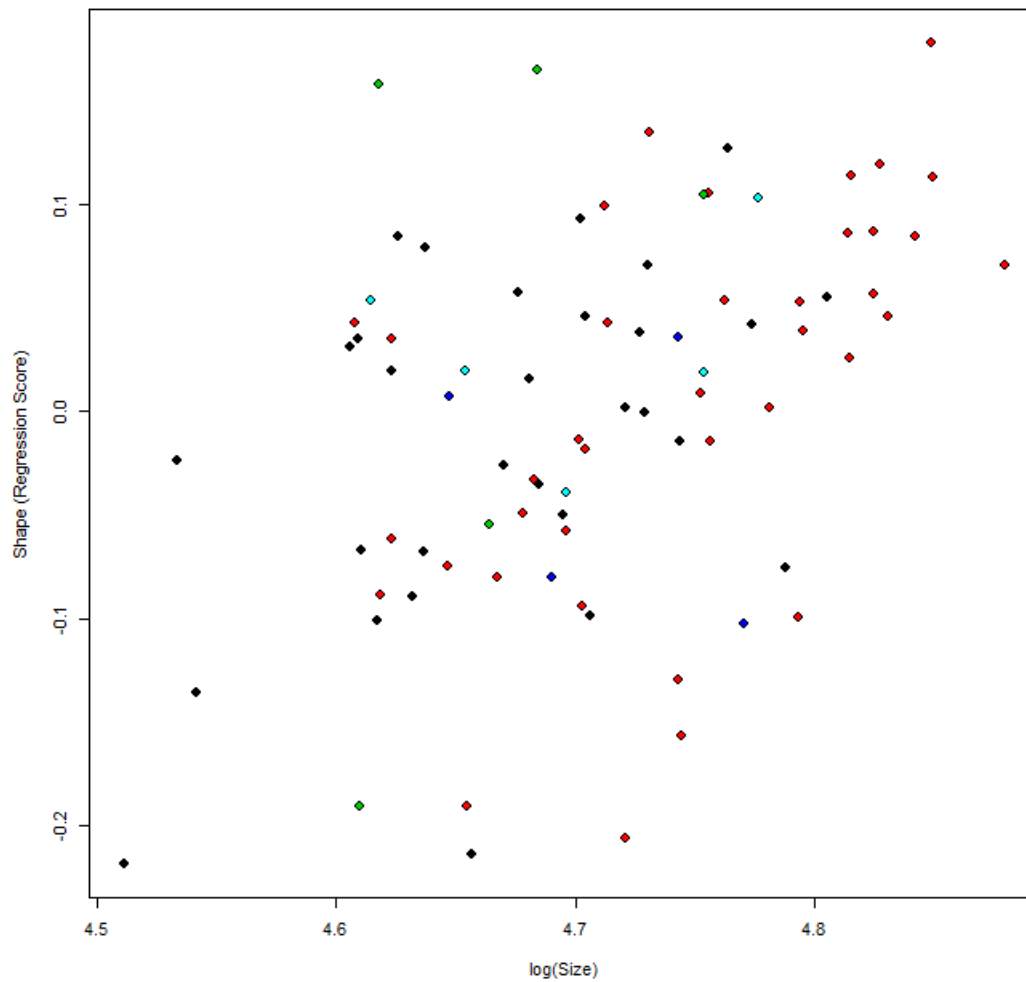


Figure 4.15 Allometric regression of log CS by Shape Regression Scores for distal femur color coded by sex. (black = female, red = male, green = possible female, blue = possible male, cyan = unknown)

Table 4.11 GLM Procrustes shape residuals compared to log(CS) for distal femur by sex.

Homogeneity of Slopes Test							
	Df	SSE	SS	Rsq	F	Z	Pr(>F)
Common Allometry	77	1.5618					
Group Allometries	73	1.4857	0.076113	0.042724	0.9349	0.32944	0.367

Type I (Sequential) Sums of Squares and Cross-products							
	Df	SS	MS	Rsq	F	Z	Pr(>F)
log(size)	1	0.13277	0.132765	0.074524	6.5455	3.6279	0.001
sex	4	0.08691	0.021729	0.048787	1.0712	0.6303	0.249
Residuals	77	1.56183	0.020284				
Total	82	1.78151					

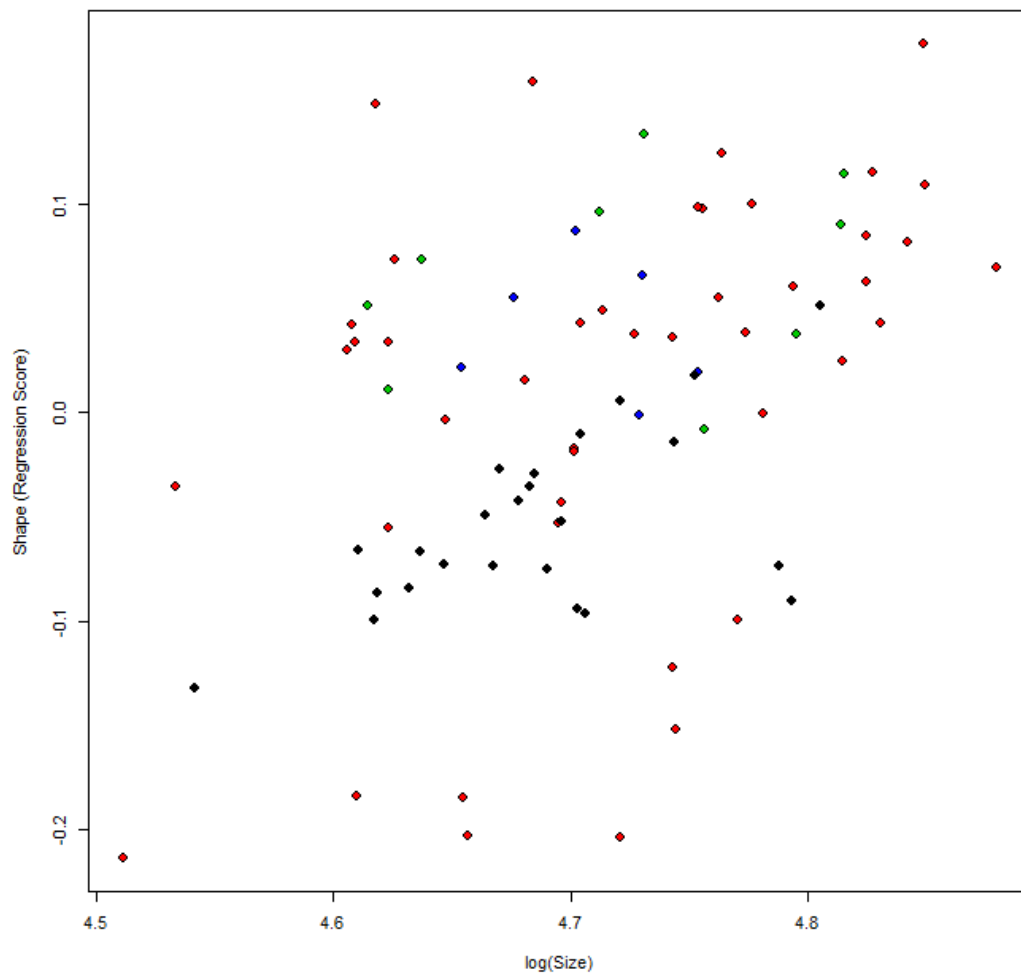


Figure 4.16 Allometric regression of log CS by Shape Regression Scores for distal femur color coded by site. (black = 3-J-18, red = Coach Lane, green = Fishergate, blue = Hereford)

Table 4.12 GLM Procrustes shape residuals compared to log(CS) for distal femur by site.

Homogeneity of Slopes Test							
	Df	SSE	SS	Rsq	F	Z	Pr(>F)
Common Allometry	78	1.4176					
Group Allometries	75	1.3808	0.036832	0.020675	0.6669	-0.41703	0.638

Type I (Sequential) Sums of Squares and Cross-products							
	Df	SS	MS	Rsq	F	Z	Pr(>F)
log(size)	1	0.13277	0.132765	0.074524	7.3049	3.8243	0.001
site	3	0.23111	0.077036	0.129726	4.2386	4.6489	0.001
Residuals	78	1.41764	0.018175				
Total	82	1.78151					

4.2.1 Intrapopulation Variation

Regarding the first hypothesis regarding variation within populations based on the IVs chosen for this research there is some variation. Neither the morphology of the proximal nor the distal humerus are uniquely described by any of the IVs in this study. Their morphology is explained by combinations of IVs. The morphology of the proximal femoral epiphysis is uniquely explained both by Schmorl's nodes and by DJD severity in both the proximal and distal femur. The morphology of the distal femur is also uniquely explained by Schmorl's nodes but not by DJD severity. This section will give further detail on intrapopulation IVs in relation to epiphyseal morphology.

4.2.1.1 Sex

Figure 4.17 through Figure 4.20 show individual shapes for the proximal humeral epiphysis, the distal humeral epiphysis, the proximal femoral epiphysis, and the distal femoral epiphysis plotted along PC1 and PC2 and are colour coded by sex. Table 4.13 through Table 4.16 give the results for GLMS of each shape set by sex. Sex did not uniquely explain shape for any of the epiphyses. However, as can be seen in the section on interpopulation variation (section 4.2.2) sex can explain the morphology of the proximal humerus when combined with size, and it can explain proximal femoral epiphyseal morphology when combined with either size or site.

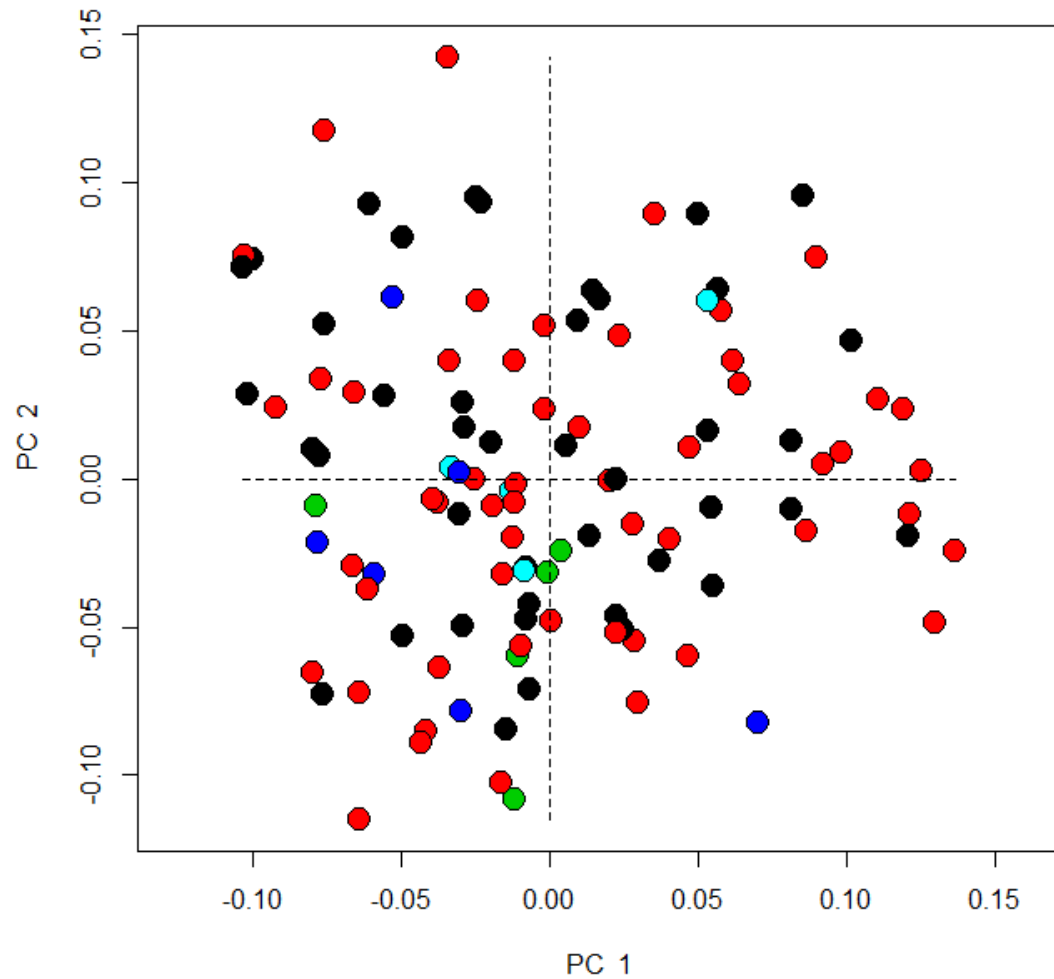


Figure 4.17 PC1 and PC2 for proximal humeral homologous landmarks by sex. (black = female, red = male, green = possible female, blue = possible male, cyan = unknown)

Table 4.13 GLM of proximal humeral morphology by sex.

	Df	SS	MS	Rsq	F	Z	Pr(>F)
Csize	1	0.03057	0.030566	0.017729	1.9818	1.61456	0.05
sex	4	0.07309	0.018271	0.04239	1.1847	0.80078	0.212
Csize by sex	4	0.06269	0.015673	0.036363	1.0162	0.42018	0.343
Residuals	101	1.55775	0.015423				
Total	110	1.7241					

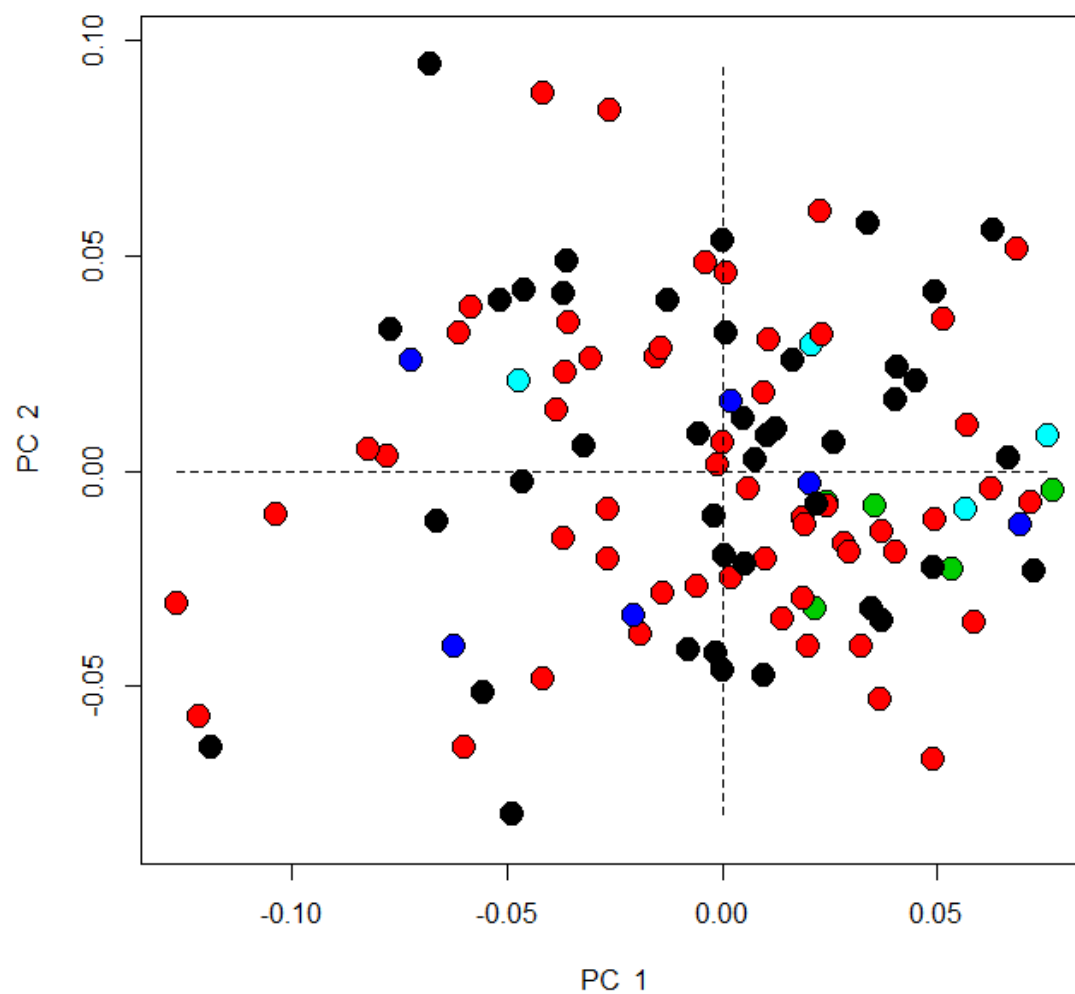


Figure 4.18 PC1 and PC2 for distal humeral homologous landmarks by sex. (black = female, red = male, green = possible female, blue = possible male, cyan = unknown)

Table 4.14 GLM of distal humerus morphology by sex.

	Df	SS	MS	Rsqr	F	Z	Pr(>F)
Csize	1	0.02775	0.027748	0.022109	2.4452	2.83301	0.004
sex	4	0.04057	0.010143	0.032326	0.8938	-0.36511	0.637
Csize by sex	4	0.04056	0.010141	0.032319	0.8936	-0.23104	0.562
Residuals	101	1.14617	0.011348				
Total	110	1.25505					

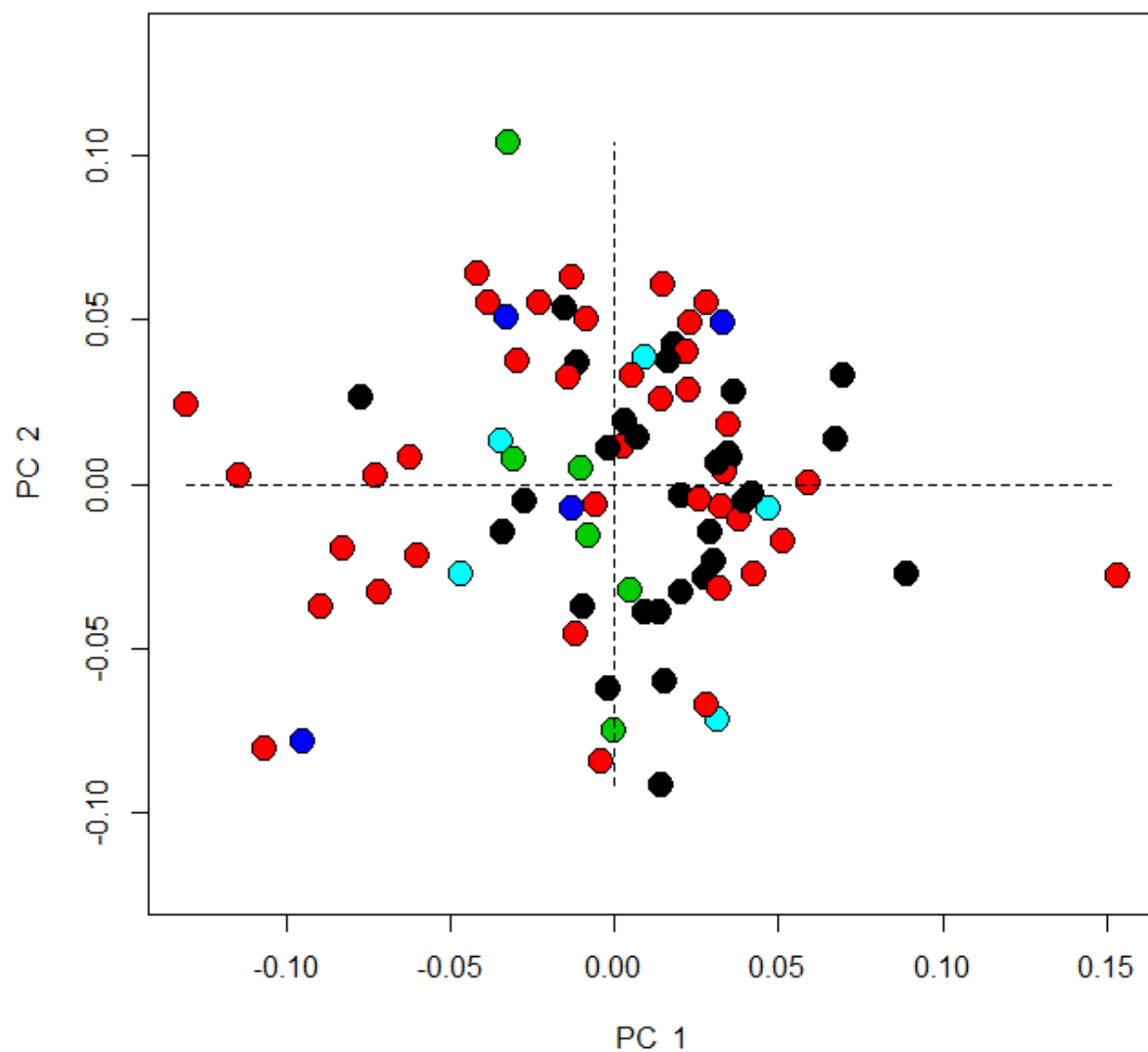


Figure 4.19 PC1 and PC2 for proximal femoral homologous landmarks by sex. (black = female, red = male, green = possible female, blue = possible male, cyan = unknown)

Table 4.15 GLM of proximal femur morphology by sex.

	Df	SS	MS	Rsqr	F	Z	Pr(>F)
Csize	1	0.03399	0.033989	0.028149	2.3502	2.66842	0.002
sex	4	0.05965	0.014911	0.049396	1.0311	0.43732	0.33
Csize by sex	4	0.05813	0.014532	0.048141	1.0049	0.55857	0.29
Residuals	73	1.05573	0.014462				
Total	82	1.20749					

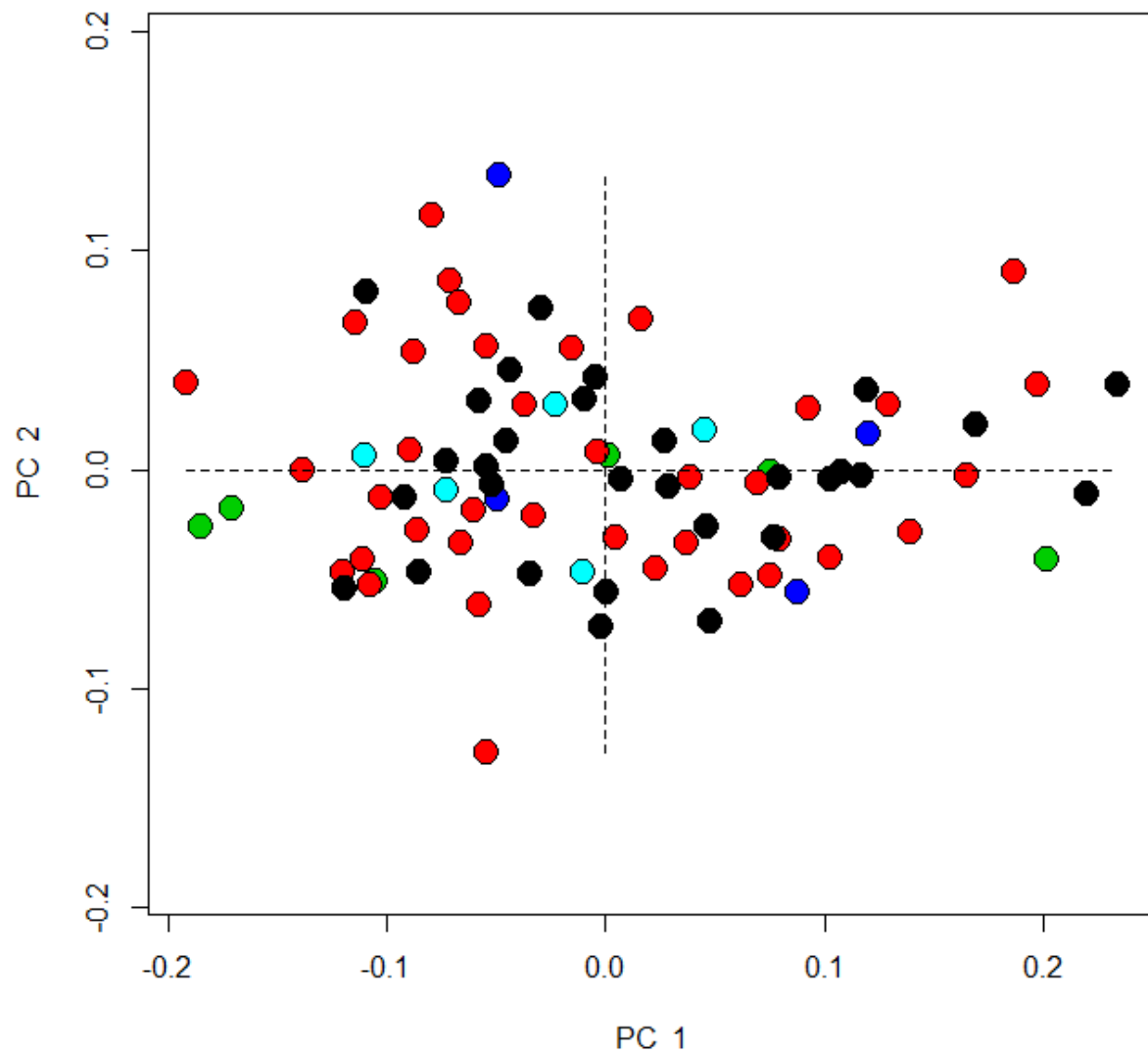


Figure 4.20 PC1 and PC2 for distal femoral homologous landmarks by sex. (black = female, red = male, green = possible female, blue = possible male, cyan = unknown)

Table 4.16 GLM of distal femur morphology by sex.

	Df	SS	MS	Rsq	F	Z	Pr(>F)
Csize	1	0.13421	0.134209	0.075334	6.5972	3.6505	0.001
sex	4	0.08748	0.02187	0.049105	1.0751	0.6444	0.247
Csize by sex	4	0.07476	0.01869	0.041965	0.9187	0.2769	0.388
Residuals	73	1.48506	0.020343				
Total	82	1.78151					

4.2.1.2 Age

PC plots by age of the proximal and distal humeral and femoral epiphyseal shapes are given in Figure 4.21 through Figure 4.24 and results for GLMs may be found in Table 4.17 through Table 4.20. Age did not uniquely explain any morphological variation seen in any of the epiphyseal shapes. However proximal humeral morphology could be explained at a confidence of 0.05 by age combined with site and size. At a higher confidence ($p < 0.01$), proximal humeral morphology was explained by age combined with size and sex and age combined with size, site, and sex. Distal humeral morphology was explained strongly ($p < 0.01$) by age combined with size and site and by age combined with site and sex. Distal humeral morphology was also explained at 0.05 confidence by age combined with size and sex. The proximal femoral epiphyseal shape was not uniquely explained by age, but when age was combined with almost any other IV or set of IVs they explained morphology at a confidence level of 0.01. Distal femoral morphology was strongly ($p < 0.01$) explained by age combined with sex. It was also explained at a lower confidence ($p < 0.05$) by age combined with site and size and age combined with size, site and sex.

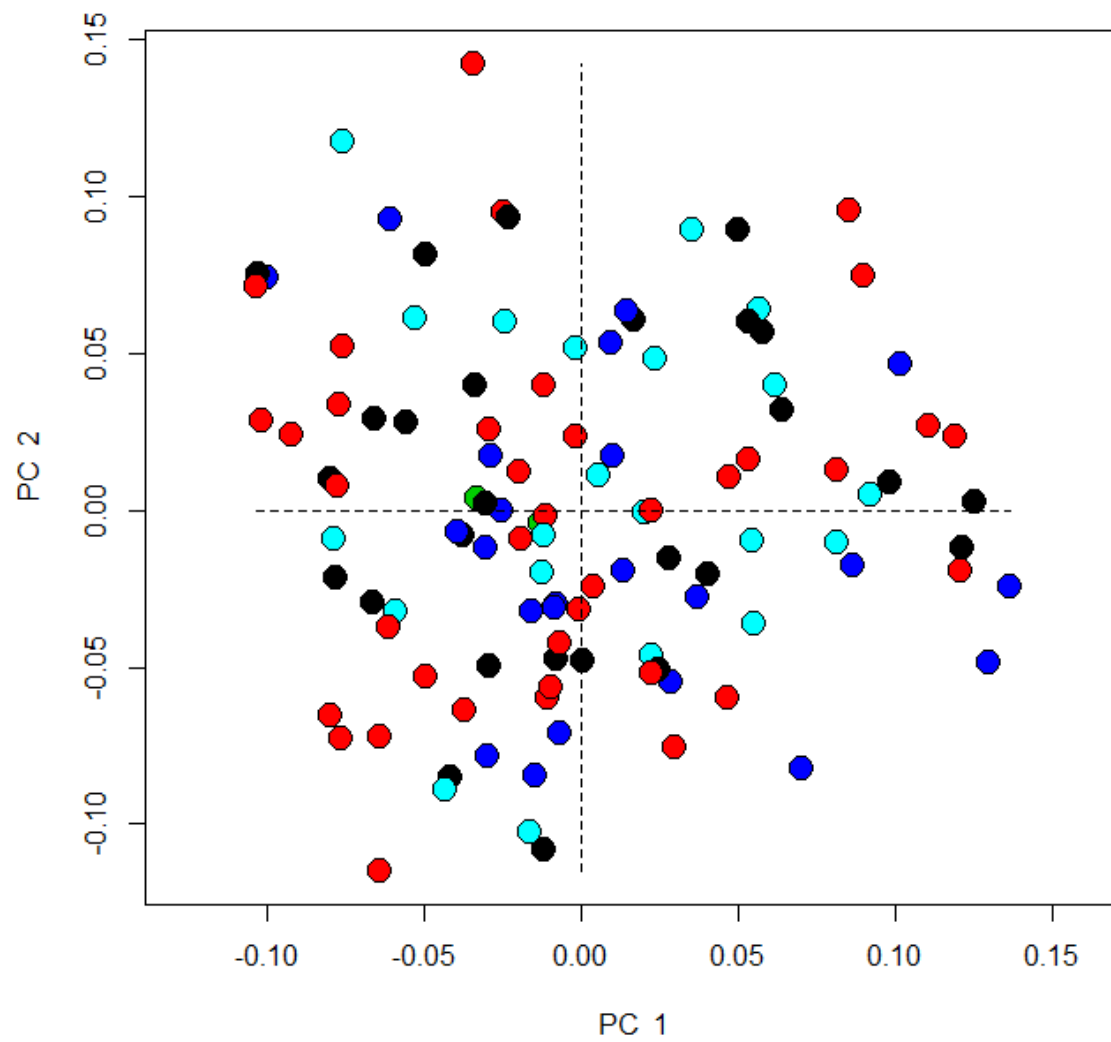


Figure 4.21 PC1 and PC2 for proximal humeral homologous landmarks by age. (black = 35-45 years of age, red = 45+, green = unknown, blue = 17-25, cyan = 25-35)

Table 4.17 GLM of proximal humerus morphology by age.

	Df	SS	MS	Rsqr	F	Z	Pr(>F)
Csize	1	0.03057	0.030566	0.017729	1.9837	1.5981	0.049
site	3	0.20712	0.069039	0.120131	4.4805	5.32	0.001
sex	4	0.06955	0.017386	0.040337	1.1284	1.1103	0.133
Age	4	0.05548	0.013871	0.032181	0.9002	0.4402	0.313
Csize by site	3	0.04831	0.016104	0.028022	1.0451	1.1363	0.12
Csize by sex	4	0.04835	0.012087	0.028041	0.7844	0.2275	0.416
site by sex	8	0.07831	0.009789	0.045423	0.6353	-0.649	0.734
Csize by Age	3	0.0357	0.0119	0.020706	0.7723	0.5653	0.283
site by Age	8	0.10669	0.013336	0.06188	0.8655	1.4318	0.068
sex by Age	6	0.07892	0.013153	0.045772	0.8536	1.5541	0.06
Csize by site by sex	3	0.03969	0.013229	0.023018	0.8585	1.5688	0.058
Csize by site by Age	7	0.08467	0.012096	0.04911	0.785	1.8648	0.032
Csize by sex by Age	3	0.05366	0.017885	0.031121	1.1607	2.8533	0.003
site by sex by Age	6	0.05183	0.008638	0.030062	0.5606	0.9022	0.18
Csize by site by sex by Age	2	0.04188	0.020939	0.02429	1.3589	2.4278	0.005
Residuals	45	0.69339	0.015409				
Total	110	1.7241					

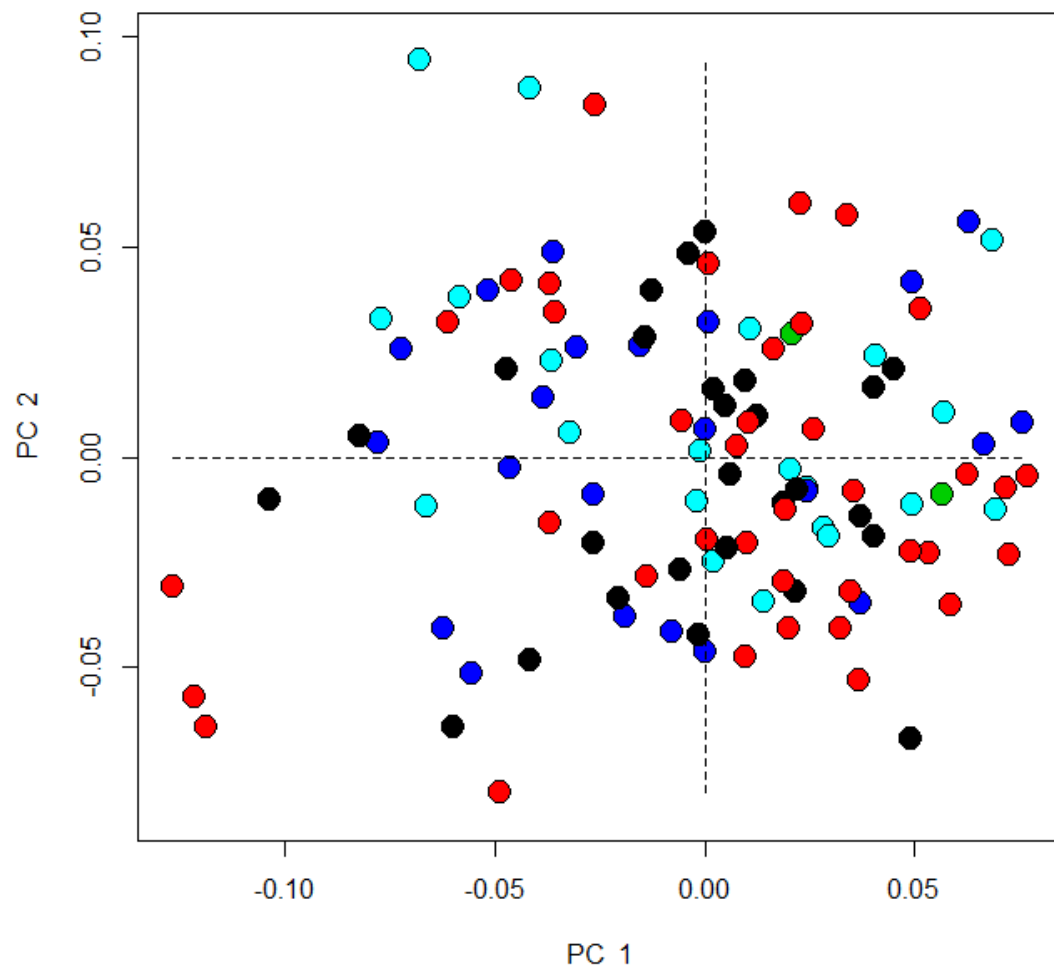


Figure 4.22 PC1 and PC2 for distal humeral homologous landmarks by age. (black = 35-45 years of age, red = 45+, green = unknown, blue = 17-25, cyan = 25-35)

Table 4.18 GLM of distal humerus morphology by age.

	Df	SS	MS	Rsqr	F	Z	Pr(>F)
Csize	1	0.02775	0.027748	0.022109	2.3929	2.7311	0.008
site	3	0.12729	0.04243	0.101422	3.659	6.0571	0.001
sex	4	0.03267	0.008169	0.026034	0.7044	-1.0219	0.843
Age	4	0.04234	0.010584	0.033733	0.9127	0.4459	0.324
Csize by site	3	0.02772	0.00924	0.022086	0.7968	-0.0437	0.513
Csize by sex	4	0.04447	0.011119	0.035437	0.9588	0.9766	0.161
site by sex	8	0.06638	0.008298	0.05289	0.7155	-0.2248	0.568
Csize by Age	3	0.03345	0.01115	0.026652	0.9615	1.5347	0.063
site by Age	8	0.07303	0.009129	0.058192	0.7873	0.9493	0.169
sex by Age	6	0.04846	0.008077	0.038613	0.6965	0.6897	0.24
Csize by site by sex	3	0.03756	0.012521	0.02993	1.0798	2.6363	0.007
Csize by site by Age	7	0.04937	0.007053	0.039335	0.6082	0.554	0.266
Csize by sex by Age	3	0.03262	0.010875	0.025994	0.9378	2.2586	0.016
site by sex by Age	6	0.07096	0.011827	0.056542	1.0199	3.0427	0.003
Csize by site by sex by Age	2	0.01913	0.009566	0.015244	0.8249	1.481	0.064
Residuals	45	0.52183	0.011596				
Total	110	1.25505					

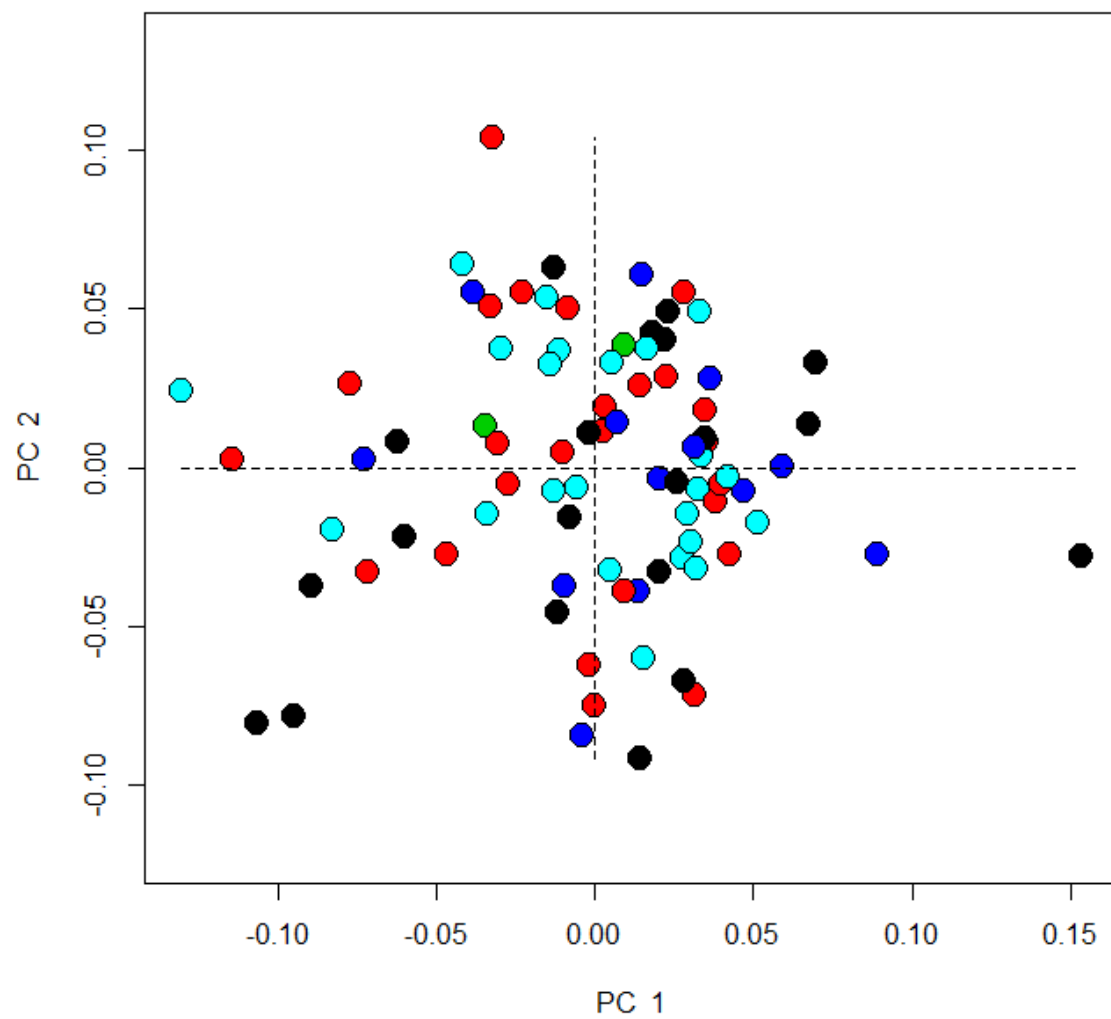


Figure 4.23 PC1 and PC2 for proximal femoral homologous landmarks by age. (black = 35-45 years of age, red = 45+, green = unknown, blue = 17-25, cyan = 25-35)

Table 4.19 GLM of proximal femur morphology by age.

	Df	SS	MS	Rsqr	F	Z	Pr(>F)
Csize	1	0.03399	0.033989	0.028149	2.533	2.8357	0.001
Site	3	0.08567	0.028558	0.070952	2.1282	3.5752	0.001
sex	4	0.05318	0.013295	0.044043	0.9908	0.5698	0.275
Age	4	0.04829	0.012072	0.039992	0.8997	0.2808	0.382
Csize by site	3	0.03641	0.012137	0.030154	0.9045	0.4762	0.325
Csize by sex	4	0.07025	0.017561	0.058175	1.3087	2.5056	0.009
site by sex	5	0.08666	0.017333	0.071771	1.2917	2.8973	0.002
Csize by Age	4	0.05867	0.014667	0.048587	1.093	2.4246	0.008
site by Age	6	0.08366	0.013943	0.069282	1.0391	2.9978	0.003
sex by Age	5	0.07279	0.014558	0.060281	1.0849	3.421	0.001
Csize by site by sex	1	0.01517	0.015175	0.012567	1.1309	2.2441	0.009
Csize by site by Age	5	0.06164	0.012327	0.051046	0.9187	2.959	0.002
Csize by sex by Age	3	0.02482	0.008275	0.020558	0.6166	1.4826	0.057
site by sex by Age	3	0.05038	0.016794	0.041723	1.2515	3.9944	0.001
Csize by site by sex by Age	2	0.03677	0.018384	0.030449	1.37	2.553	0.001
Residuals	29	0.38914	0.013419				
Total	82	1.20749					

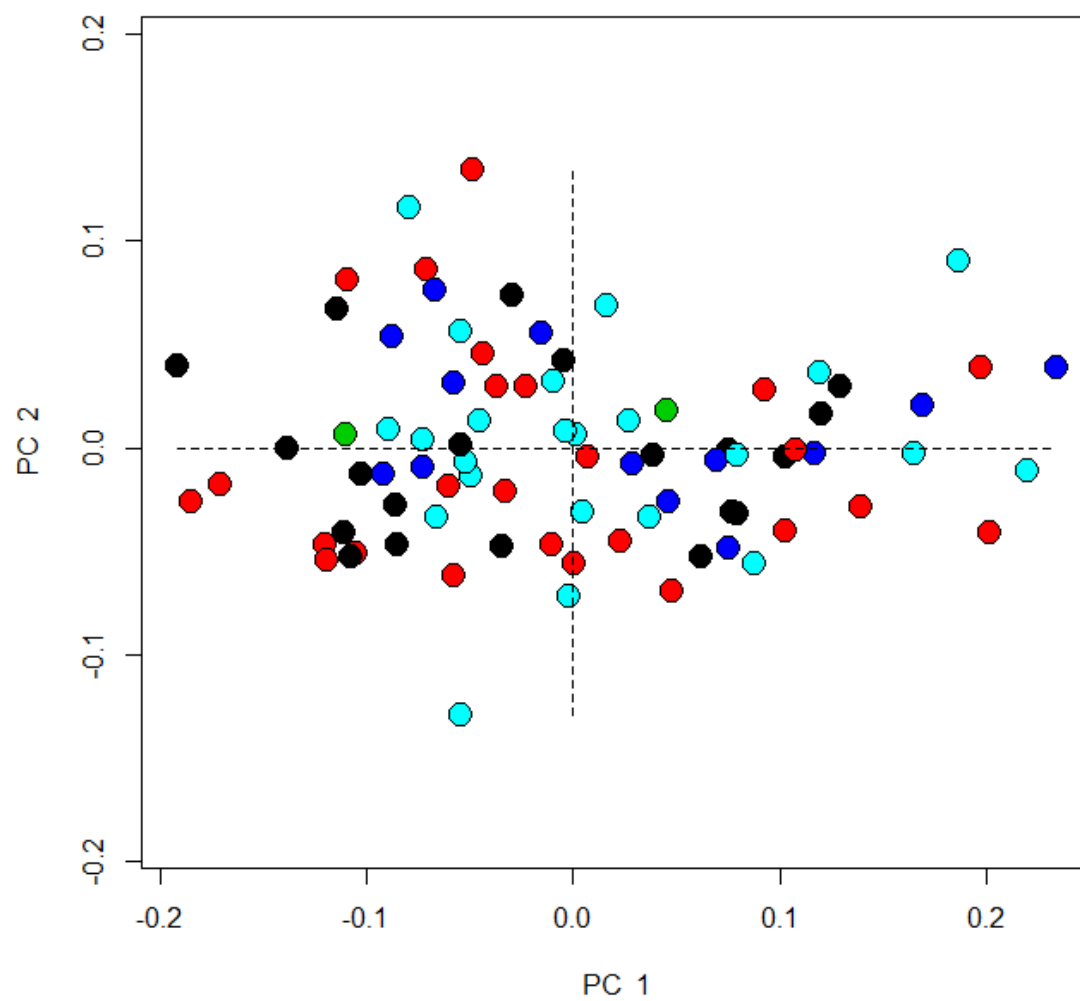


Figure 4.24 PC1 and PC2 for distal femoral homologous landmarks by age. (black = 35-45 years of age, red = 45+, green = unknown, blue = 17-25, cyan = 25-35)

Table 4.20 GLM of distal femur morphology by age.

	Df	SS	MS	Rsqr	F	Z	Pr(>F)
Csize	1	0.13421	0.134209	0.075334	6.6263	3.581	0.001
site	3	0.23011	0.076705	0.129168	3.7872	4.1568	0.001
sex	4	0.07326	0.018315	0.041122	0.9043	0.544	0.271
Age	4	0.04588	0.01147	0.025754	0.5663	-0.8393	0.8
Csize by site	3	0.03577	0.011923	0.020078	0.5887	-0.487	0.677
Csize by sex	4	0.08058	0.020146	0.045233	0.9947	1.1863	0.133
site by sex	5	0.07068	0.014136	0.039673	0.6979	0.2918	0.384
Csize by Age	4	0.07678	0.019195	0.043098	0.9477	1.3622	0.09
site by Age	6	0.12822	0.021369	0.071971	1.0551	2.0438	0.028
sex by Age	5	0.11422	0.022844	0.064113	1.1279	2.5241	0.004
Csize by site by sex	1	0.01154	0.011543	0.006479	0.5699	0.7059	0.239
Csize by site by Age	5	0.06229	0.012457	0.034962	0.615	1.0743	0.143
Csize by sex by Age	3	0.05884	0.019614	0.033029	0.9684	2.1928	0.011
site by sex by Age	3	0.04052	0.013507	0.022746	0.6669	1.5326	0.068
Csize by site by sex by Age	2	0.03125	0.015624	0.01754	0.7714	1.8319	0.034
Residuals	29	0.58736	0.020254				
Total	82	1.78151					

4.2.1.3 Trauma and Pathology

Trauma and pathology – with the exception of indicators of childhood stress – were not expected to have great effect on the morphology of the epiphyses. Results ran counter to expectations. LEH and CO when combined with other factors could sometimes explain morphology, but femoral epiphyseal shape was uniquely explained by the presence or absence of Schmorl's nodes and the severity of DJD. Results for trauma and pathology and how they relate to epiphyseal morphology are elucidated below.

4.2.1.3.1 Degenerative Joint Disease and Osteoarthritis

DJD severity from both the proximal and distal articular surfaces was compared to both epiphyseal shapes for that limb. Graphs and GLM results for the proximal humerus are available in Figure 4.25 and Figure 4.26 and Table 4.21. The results for the distal humerus may be found in Figure 4.27, Figure 4.28, and Table 4.22. Results for the proximal femoral epiphysis can be seen in Figure 4.29 and Figure 4.30 with GLMs in Table 4.23. Distal femoral results are reported in Figure 4.31, Figure 4.32, and Table 4.24. Neither the proximal nor distal humeral shape were uniquely explained by DJD severity

in either joint alone, but when combined with other IVs including size, sex, and site, along with DJD severity their morphology was explained. The proximal femoral epiphyseal shape was uniquely explained by DJD severity in the proximal femur at a confidence level of 0.05, but was also explained by DJD in the distal joint at a confidence level of 0.01. Other IVs combined with DJD severity in either epiphysis were also able to explain morphology of the proximal femoral epiphysis. The distal femoral epiphysis was only explained by DJD severity when that IV was combined with other IVs.

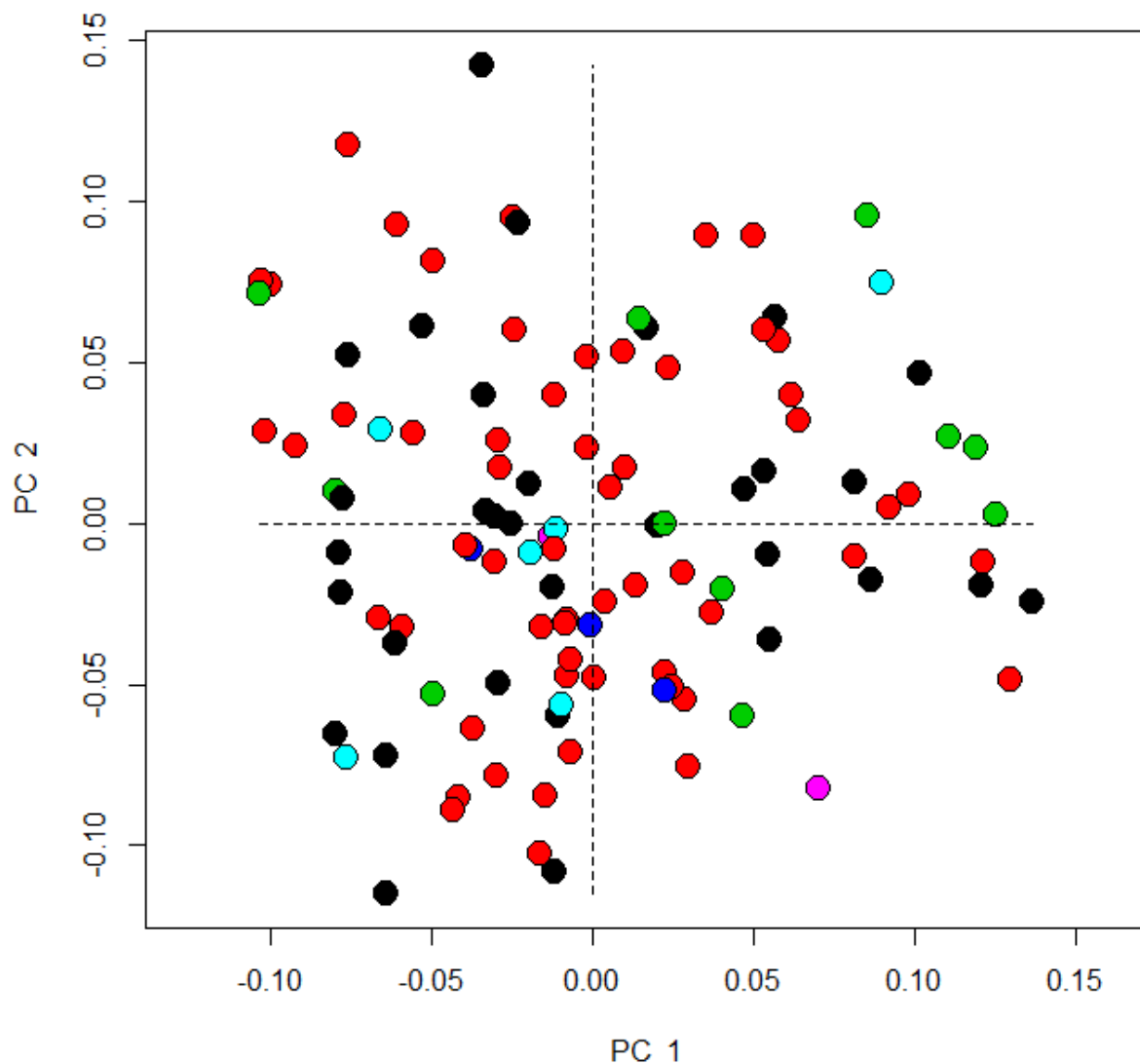


Figure 4.25 PC1 and PC2 for proximal humeral homologous landmarks by DJD and OA severity in the proximal humerus. (black = djd , red = healthy, green = mild, blue = moderate, cyan = severe, purple = unknown)

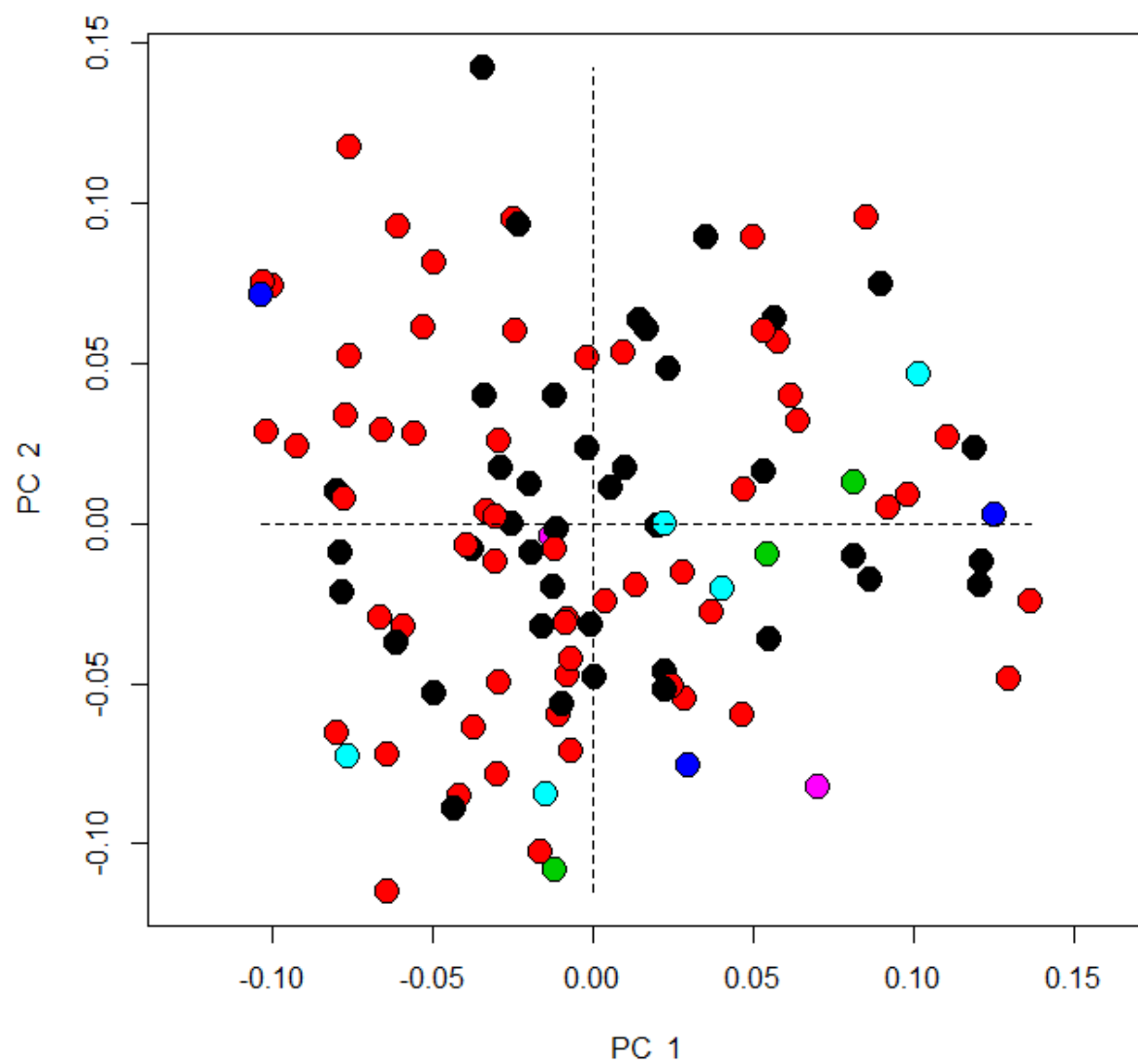


Figure 4.26 PC1 and PC2 for proximal humeral homologous landmarks by DJD and OA severity in the distal humerus. (black = djd , red = healthy, green = mild, blue = moderate, cyan = severe, purple = unknown)

Table 4.21 GLMs of proximal humerus morphology by proximal degenerative joint disease and distal degenerative joint disease.

	Df	SS	MS	Rsqr	F	Z	Pr(>F)
Csize	1	0.03057	0.030566	0.017729	2.0564	1.6695	0.036
site	3	0.20712	0.069039	0.120131	4.6449	5.4368	0.001
sex	4	0.06955	0.017386	0.040337	1.1697	1.2709	0.105
proxOA	5	0.05637	0.011274	0.032696	0.7585	-0.2513	0.609
Csize by site	3	0.04683	0.015612	0.027165	1.0503	1.1167	0.137
Csize by sex	4	0.05417	0.013542	0.031419	0.9111	0.8099	0.209
site by sex	8	0.09842	0.012303	0.057085	0.8277	0.7227	0.233
Csize by proxOA	4	0.06921	0.017303	0.040145	1.1641	2.1855	0.015
site by proxOA	8	0.09273	0.011591	0.053785	0.7799	1.1107	0.128
sex by proxOA	5	0.06517	0.013034	0.037801	0.8769	1.6581	0.041
Csize by site by sex	2	0.03178	0.015891	0.018434	1.0692	2.1069	0.016
Csize by site by proxOA	4	0.03922	0.009805	0.022748	0.6597	0.9419	0.188
Csize by sex by proxOA	2	0.02064	0.010318	0.01197	0.6942	0.9238	0.187
site by sex by proxOA	2	0.01814	0.009069	0.01052	0.6101	0.6664	0.278
Csize by site by sex by proxOA	1	0.02155	0.021549	0.012499	1.4498	2.2769	0.007
Residuals	54	0.80263	0.014864				
Total	110	1.7241					

	Df	SS	MS	Rsqr	F	Z	Pr(>F)
Csize	1	0.03057	0.030566	0.017729	2.2216	1.8304	0.024
site	3	0.20712	0.069039	0.120131	5.0179	5.7172	0.001
sex	4	0.06955	0.017386	0.040337	1.2637	1.5905	0.053
distOA	5	0.07693	0.015385	0.044618	1.1182	1.4447	0.07
Csize by site	3	0.04307	0.014358	0.024983	1.0436	1.1455	0.137
Csize by sex	4	0.05059	0.012647	0.029342	0.9192	0.9265	0.176
site by sex	8	0.09097	0.011372	0.052766	0.8265	0.7438	0.232
Csize by distOA	4	0.07676	0.019189	0.04452	1.3947	2.7224	0.006
site by distOA	7	0.08939	0.01277	0.051849	0.9282	1.8855	0.029
sex by distOA	2	0.02987	0.014937	0.017327	1.0857	1.7976	0.028
Csize by site by sex	3	0.0386	0.012868	0.022391	0.9353	1.8597	0.037
Csize by site by distOA	3	0.03609	0.01203	0.020932	0.8743	1.7186	0.038
Csize by sex by distOA	1	0.0225	0.022505	0.013053	1.6357	2.3539	0.003
site by sex by distOA	2	0.03191	0.015953	0.018505	1.1595	2.2877	0.007
Csize by site by sex by distOA	2	0.03219	0.016094	0.01867	1.1698	2.0936	0.01
Residuals	58	0.798	0.013759				
Total	110	1.7241					

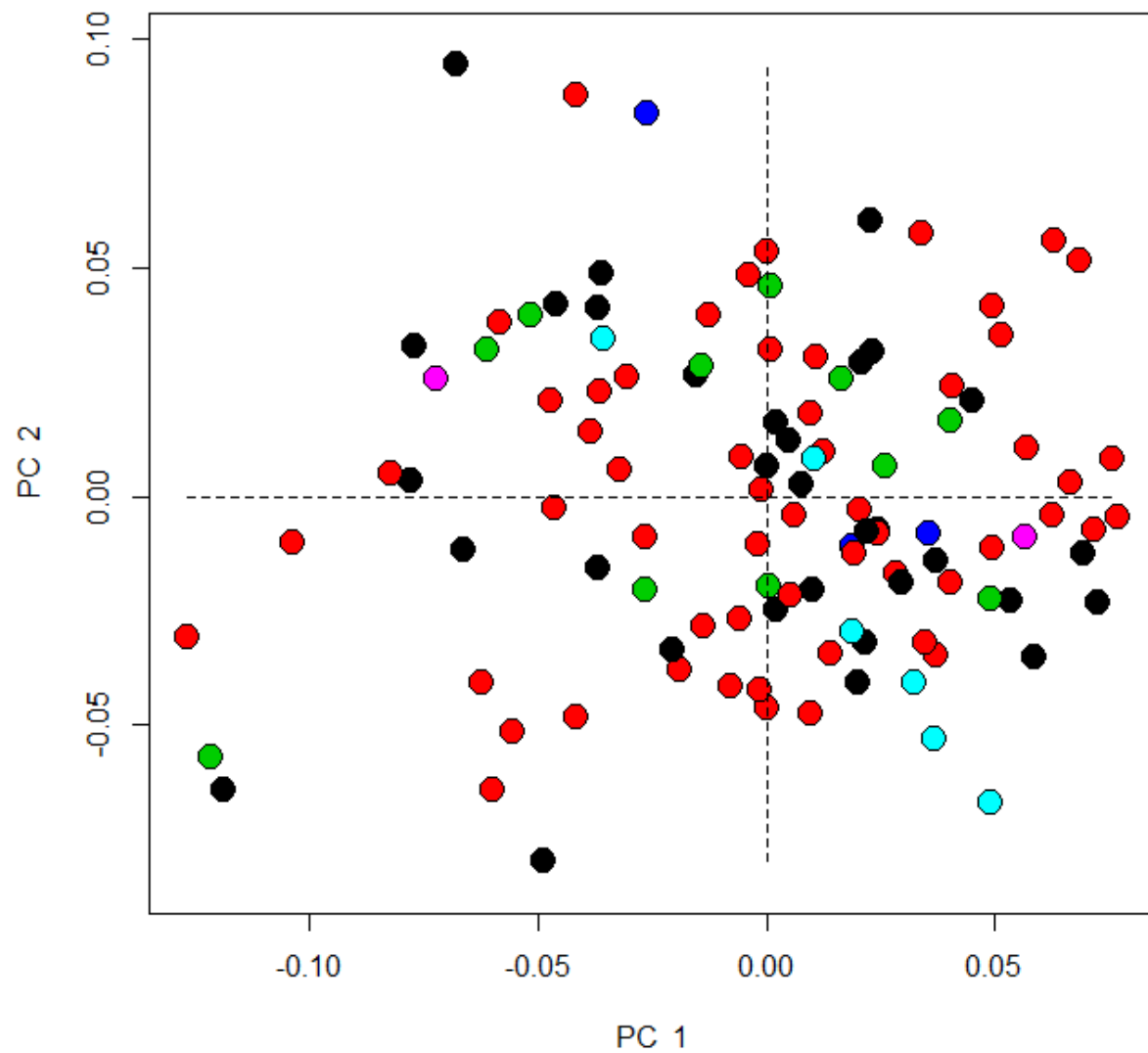


Figure 4.27 PC1 and PC2 for distal humeral homologous landmarks by DJD and OA severity in the proximal humerus. (black = djd , red = healthy, green = mild, blue = moderate, cyan = severe, purple = unknown)

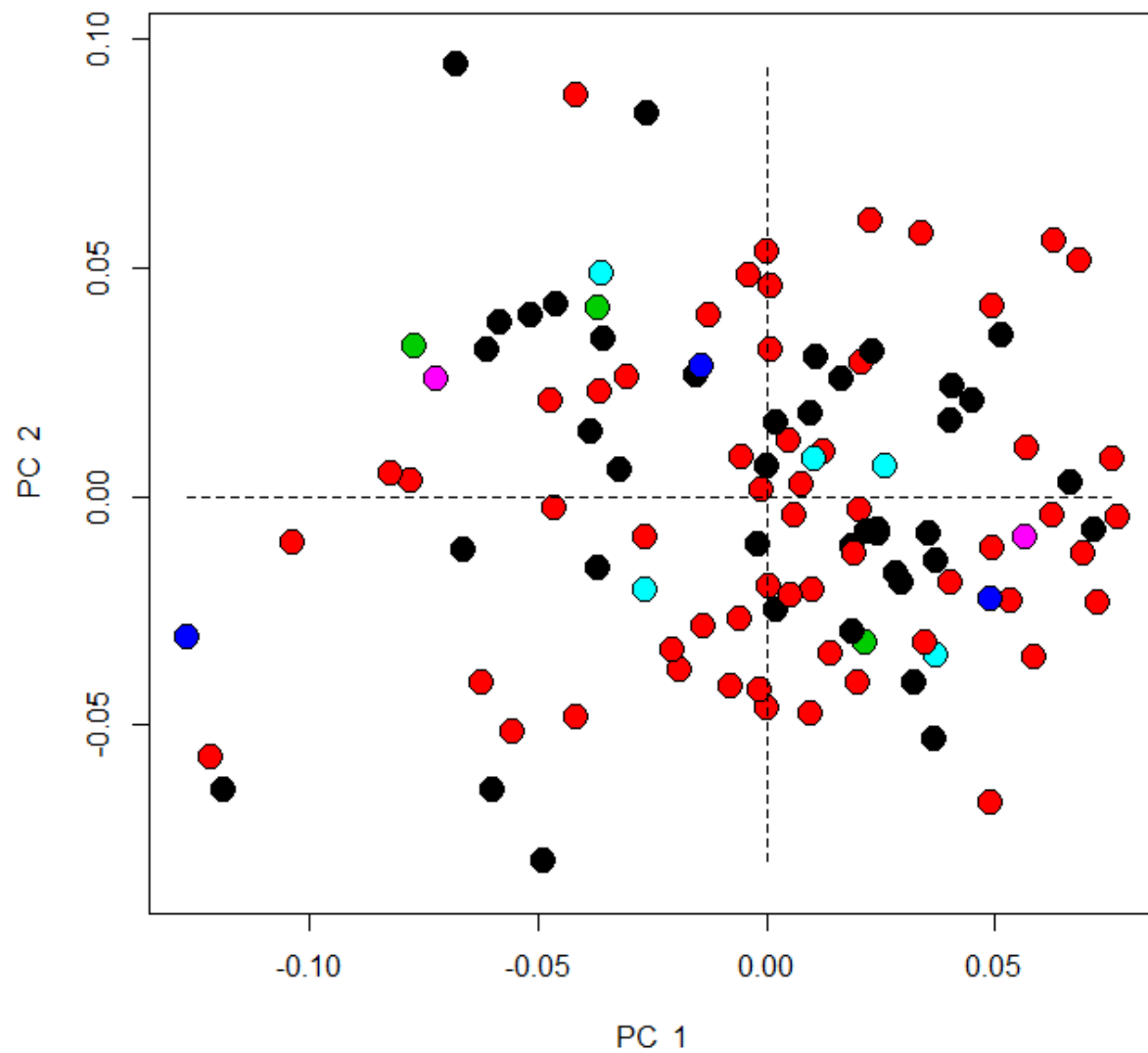


Figure 4.28 PC1 and PC2 for distal humeral homologous landmarks by DJD and OA severity in the distal humerus. (black = djd , red = healthy, green = mild, blue = moderate, cyan = severe, purple = unknown)

Table 4.22 GLMs of distal humerus morphology by proximal degenerative joint disease and distal degenerative joint disease.

	Df	SS	MS	Rsq	F	Z	Pr(>F)
Csize	1	0.02775	0.027748	0.022109	2.6355	3.0231	0.001
site	3	0.12729	0.04243	0.101422	4.03	6.5661	0.001
sex	4	0.03267	0.008169	0.026034	0.7758	-0.5367	0.718
proxOA	5	0.04332	0.008665	0.034519	0.823	-0.095	0.512
Csize by site	3	0.03016	0.010053	0.02403	0.9548	0.7968	0.206
Csize by sex	4	0.04494	0.011236	0.03581	1.0672	1.5177	0.076
site by sex	8	0.07915	0.009894	0.063068	0.9398	1.3442	0.095
Csize by proxOA	4	0.03324	0.00831	0.026486	0.7893	0.687	0.232
site by proxOA	8	0.08298	0.010373	0.06612	0.9852	2.2045	0.017
sex by proxOA	5	0.05092	0.010183	0.040568	0.9672	2.1361	0.016
Csize by site by sex	2	0.02512	0.012559	0.020014	1.1929	2.8115	0.003
Csize by site by proxOA	4	0.04558	0.011395	0.036316	1.0823	3.0181	0.002
Csize by sex by proxOA	2	0.03458	0.017291	0.027554	1.6423	3.1549	0.001
site by sex by proxOA	2	0.01559	0.007795	0.012422	0.7404	1.3067	0.092
Csize by site by sex by proxOA	1	0.01321	0.013211	0.010526	1.2548	2.2801	0.007
Residuals	54	0.56854	0.010528				
Total	110	1.25505					

	Df	SS	MS	Rsq	F	Z	Pr(>F)
Csize	1	0.02775	0.027748	0.022109	2.585	2.9678	0.004
site	3	0.12729	0.04243	0.101422	3.9528	6.5414	0.001
sex	4	0.03267	0.008169	0.026034	0.761	-0.6305	0.743
distOA	5	0.04541	0.009082	0.036182	0.8461	0.1142	0.446
Csize by site	3	0.02535	0.00845	0.020199	0.7872	-0.0574	0.519
Csize by sex	4	0.04618	0.011545	0.036796	1.0755	1.5434	0.07
site by sex	8	0.07682	0.009602	0.061208	0.8946	1.0589	0.147
Csize by distOA	4	0.04081	0.010201	0.032513	0.9504	1.4009	0.093
site by distOA	7	0.0716	0.010229	0.057049	0.9529	2.1135	0.027
sex by distOA	2	0.01503	0.007514	0.011974	0.7	0.6058	0.26
Csize by site by sex	3	0.03532	0.011775	0.028146	1.097	2.5078	0.01
Csize by site by distOA	3	0.03714	0.012379	0.029589	1.1532	2.7277	0.008
Csize by sex by distOA	1	0.00653	0.006535	0.005207	0.6088	0.5222	0.307
site by sex by distOA	2	0.01907	0.009536	0.015197	0.8884	1.7042	0.048
Csize by site by sex by distOA	2	0.02549	0.012746	0.020312	1.1874	2.1051	0.023
Residuals	58	0.62258	0.010734				
Total	110	1.25505					

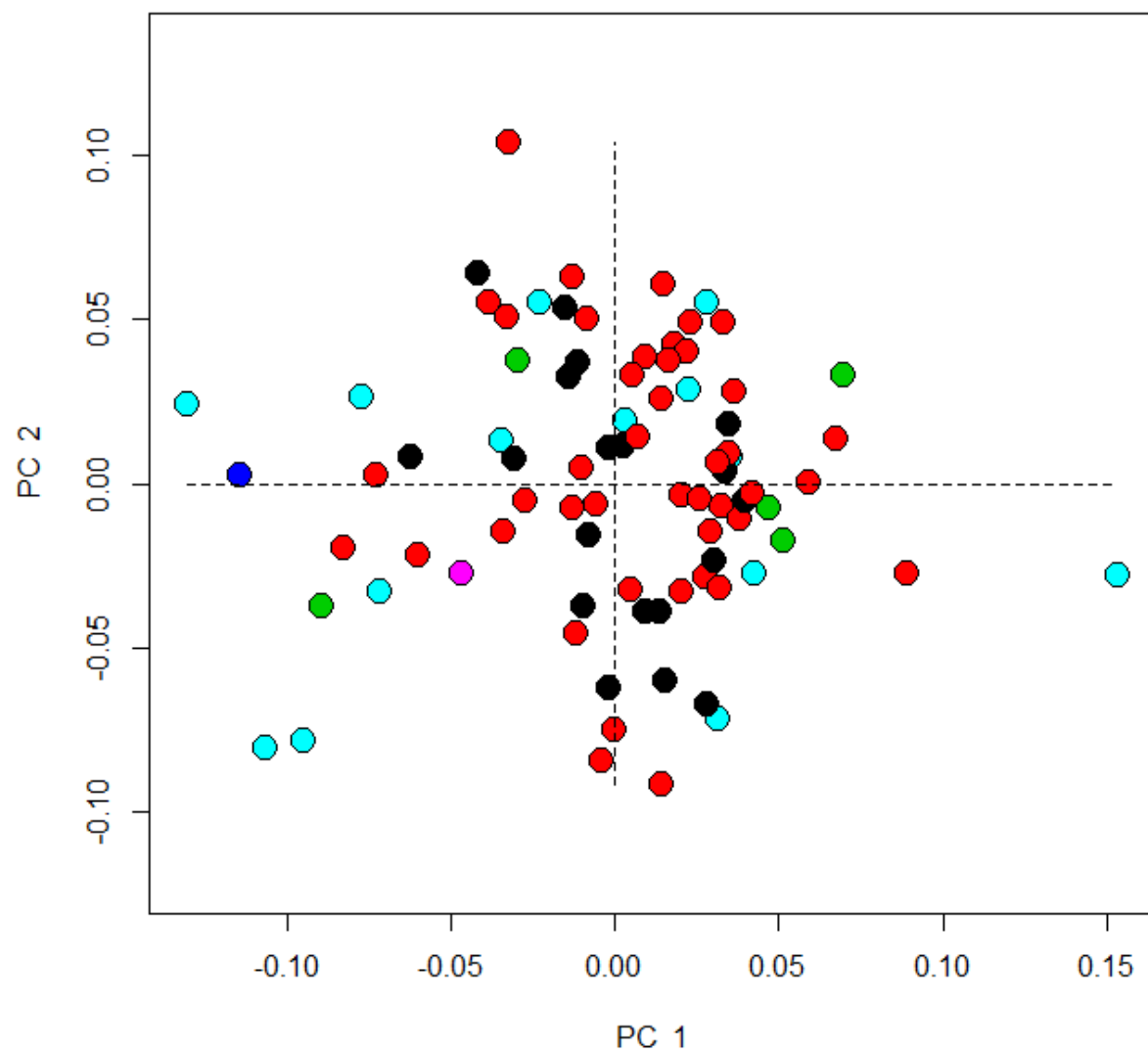


Figure 4.29 PC1 and PC2 for proximal femoral homologous landmarks by DJD and OA severity in the proximal femur. (black = djd , red = healthy, green = mild, blue = moderate, cyan = severe, purple = unknown)

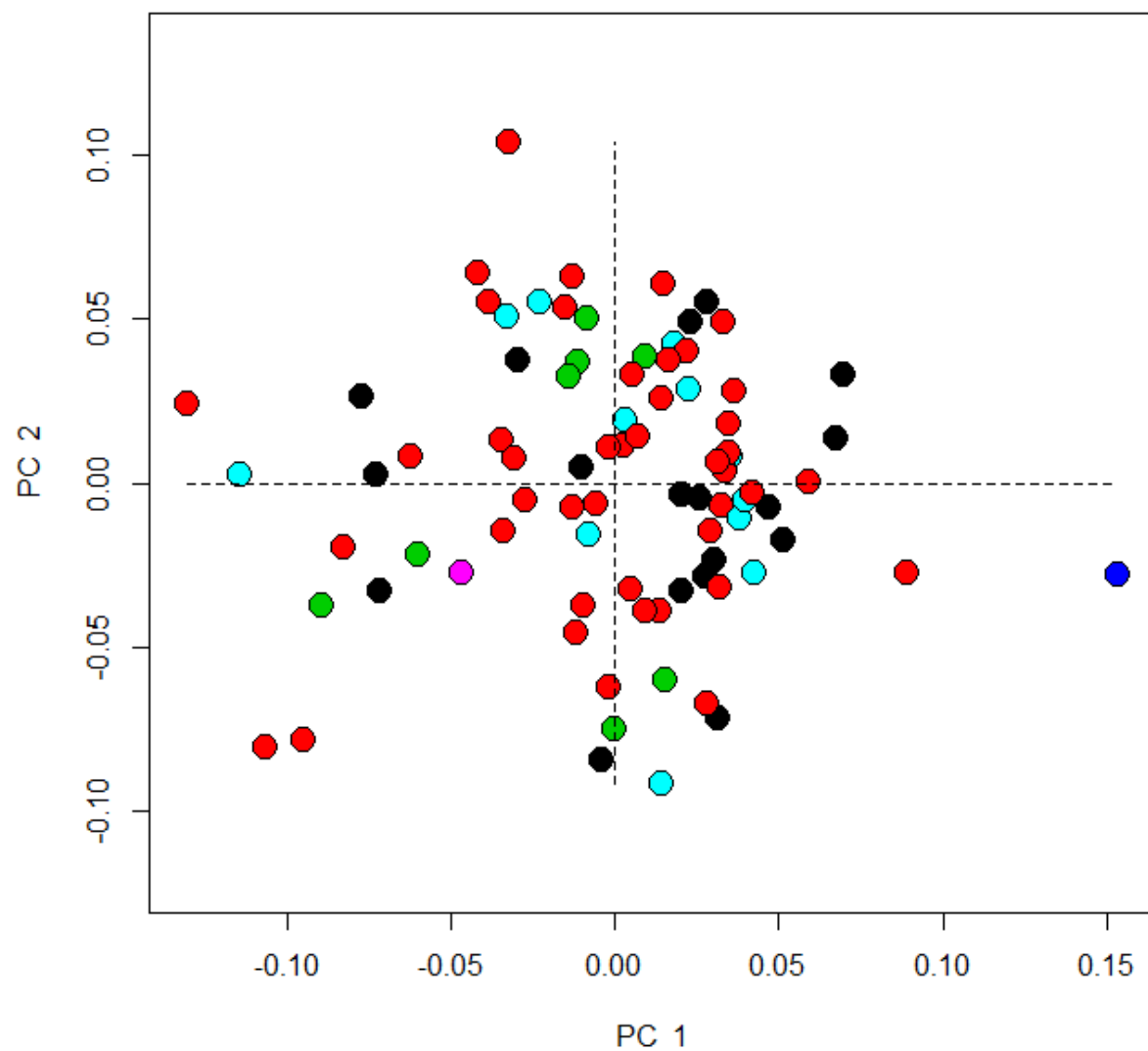


Figure 4.30 PC1 and PC2 for proximal femoral homologous landmarks by DJD and OA severity in the distal femur. (black = djd , red = healthy, green = mild, blue = moderate, cyan = severe, purple = unknown)

Table 4.23 GLMs of proximal femoral morphology by proximal degenerative joint disease and distal degenerative joint disease.

	Df	SS	MS	Rsq	F	Z	Pr(>F)
Csize	1	0.03399	0.033989	0.028149	2.6135	2.9649	0.001
site	3	0.08567	0.028558	0.070952	2.1959	3.829	0.001
sex	4	0.05318	0.013295	0.044043	1.0223	0.7632	0.231
proxOA	5	0.08569	0.017138	0.070966	1.3178	2.3049	0.013
Csize by site	3	0.03343	0.011144	0.027686	0.8569	0.4555	0.325
Csize by sex	4	0.06596	0.016489	0.054622	1.2679	2.5374	0.009
site by sex	6	0.0999	0.016651	0.082737	1.2803	3.343	0.001
Csize by proxOA	3	0.044	0.014665	0.036435	1.1276	2.5122	0.007
site by proxOA	5	0.08238	0.016476	0.068223	1.2669	3.6869	0.001
sex by proxOA	5	0.07254	0.014507	0.060072	1.1155	3.6072	0.001
Csize by site by sex	1	0.0081	0.008104	0.006711	0.6231	0.9477	0.17
Csize by site by proxOA	1	0.00871	0.008706	0.00721	0.6694	1.1524	0.118
Csize by sex by proxOA	2	0.02639	0.013196	0.021858	1.0147	2.3452	0.005
site by sex by proxOA	1	0.01072	0.010717	0.008875	0.824	1.859	0.032
Csize by site by sex by proxOA	1	0.01565	0.015649	0.01296	1.2033	1.3169	0.02
Residuals	37	0.48119	0.013005				
Total	82	1.20749					

	Df	SS	MS	Rsq	F	Z	Pr(>F)
Csize	1	0.03399	0.033989	0.028149	2.4236	2.705	0.001
site	3	0.08567	0.028558	0.070952	2.0363	3.3175	0.001
sex	4	0.05318	0.013295	0.044043	0.948	0.3406	0.364
distOA	5	0.11069	0.022137	0.091667	1.5785	3.1087	0.001
Csize by site	3	0.03418	0.011393	0.028306	0.8124	0.2912	0.399
Csize by sex	4	0.06382	0.015955	0.052852	1.1376	2.207	0.013
site by sex	6	0.09203	0.015339	0.076218	1.0937	2.717	0.002
Csize by distOA	3	0.03906	0.01302	0.032347	0.9284	1.9022	0.028
site by distOA	8	0.10217	0.012771	0.08461	0.9106	2.4705	0.006
sex by distOA	5	0.06616	0.013231	0.054788	0.9435	2.9626	0.002
Csize by site by sex	2	0.01608	0.008042	0.01332	0.5734	0.9887	0.162
Csize by site by distOA	2	0.02655	0.013275	0.021987	0.9466	1.816	0.025
Csize by sex by distOA	2	0.01592	0.007959	0.013183	0.5675	0.9969	0.159
site by sex by distOA	1	0.00848	0.008477	0.00702	0.6045	1.1187	0.134
Csize by site by sex by distOA	1	0.01074	0.010744	0.008897	0.7661	1.5237	0.057
Residuals	32	0.44878	0.014024				
Total	82	1.20749					

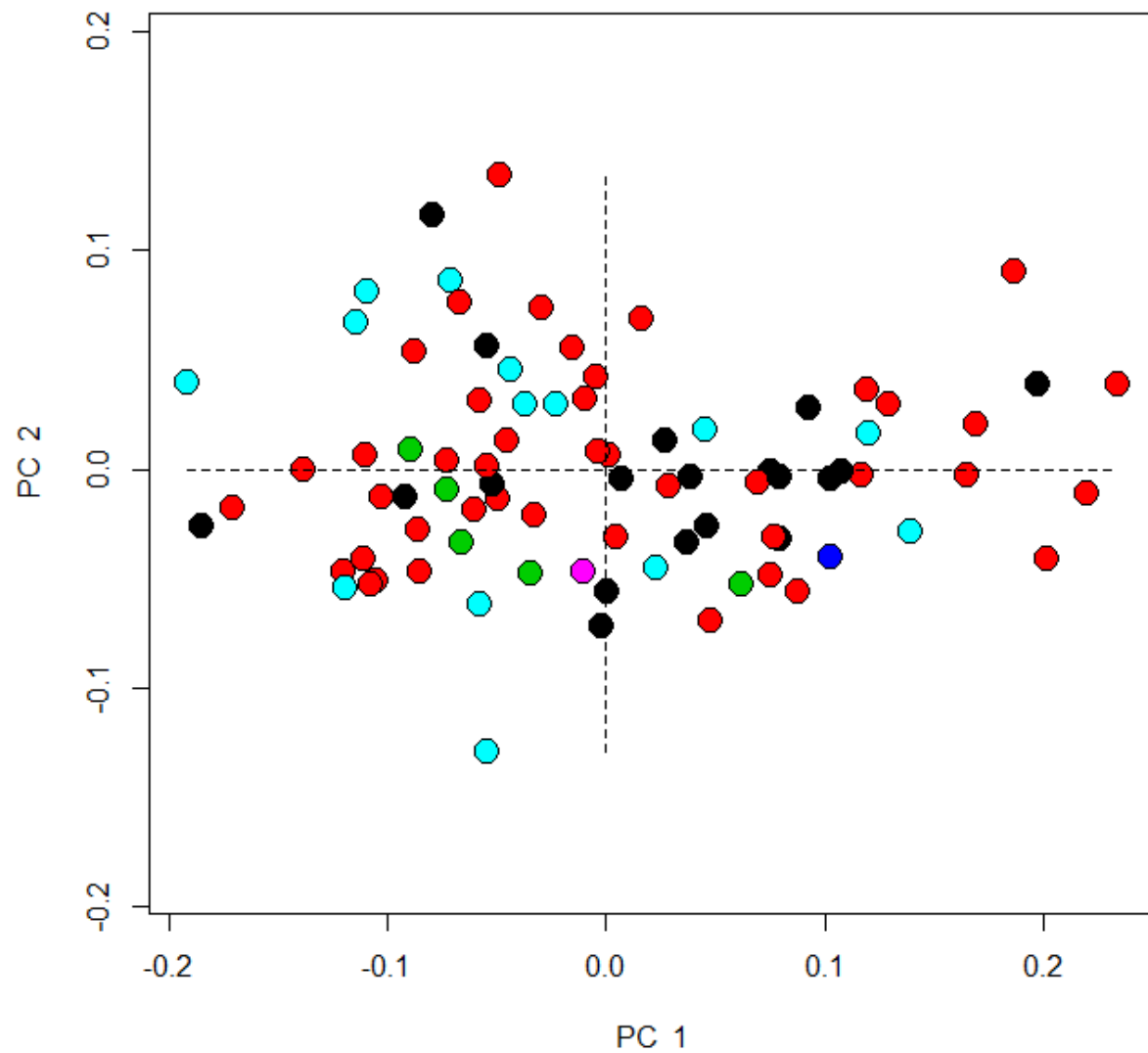


Figure 4.31 PC1 and PC2 for distal femoral homologous landmarks by DJD and OA severity in the proximal femur. (black = djd , red = healthy, green = mild, blue = moderate, cyan = severe, purple = unknown)

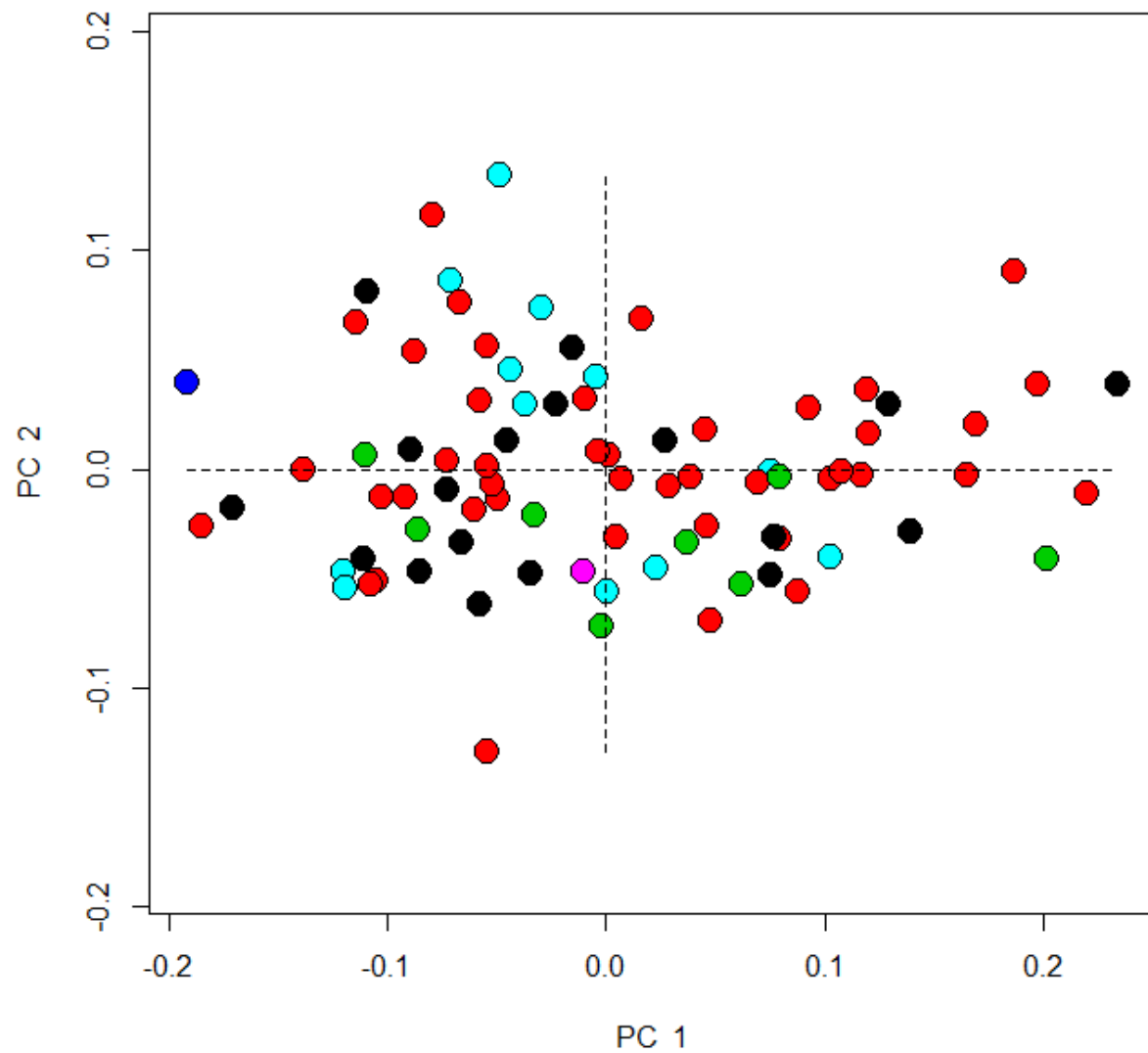


Figure 4.32 PC1 and PC2 for distal femoral homologous landmarks by DJD and OA severity in the distal femur. (black = djd , red = healthy, green = mild, blue = moderate, cyan = severe, purple = unknown)

Table 4.24 GLMs of distal femoral morphology by proximal degenerative joint disease and distal degenerative joint disease.

	Df	SS	MS	Rsqr	F	Z	Pr(>F)
Csize	1	0.13421	0.134209	0.075334	6.7745	3.6452	0.001
site	3	0.23011	0.076705	0.129168	3.8719	4.2475	0.001
sex	4	0.07326	0.018315	0.041122	0.9245	0.6478	0.235
proxOA	5	0.08359	0.016718	0.046921	0.8439	0.5566	0.302
Csize by site	3	0.03307	0.011025	0.018565	0.5565	-0.5659	0.704
Csize by sex	4	0.08138	0.020345	0.04568	1.0269	1.3886	0.092
site by sex	6	0.07946	0.013243	0.044601	0.6685	0.2405	0.406
Csize by proxOA	3	0.06803	0.022677	0.038188	1.1447	1.9847	0.033
site by proxOA	5	0.08118	0.016236	0.045567	0.8195	1.369	0.095
sex by proxOA	5	0.07867	0.015734	0.04416	0.7942	1.5836	0.052
Csize by site by sex	1	0.02621	0.026205	0.014709	1.3228	2.1295	0.021
Csize by site by proxOA	1	0.01413	0.014128	0.00793	0.7131	1.0546	0.157
Csize by sex by proxOA	2	0.04104	0.02052	0.023036	1.0358	1.9968	0.03
site by sex by proxOA	1	0.00486	0.004859	0.002727	0.2453	-0.5113	0.688
Csize by site by sex by proxOA	1	0.01931	0.019314	0.010841	0.9749	1.5773	0.058
Residuals	37	0.733	0.019811				
Total	82	1.78151					

	Df	SS	MS	Rsqr	F	Z	Pr(>F)
Csize	1	0.13421	0.134209	0.075334	6.369	3.5038	0.002
site	3	0.23011	0.076705	0.129168	3.6401	4.0543	0.001
sex	4	0.07326	0.018315	0.041122	0.8691	0.3993	0.323
distOA	5	0.08755	0.017509	0.049142	0.8309	0.3788	0.353
Csize by site	3	0.0259	0.008632	0.014536	0.4096	-1.4573	0.939
Csize by sex	4	0.07508	0.018769	0.042143	0.8907	0.8977	0.186
site by sex	6	0.07791	0.012985	0.043731	0.6162	-0.113	0.553
Csize by distOA	3	0.05985	0.019951	0.033596	0.9468	1.3741	0.097
site by distOA	8	0.17676	0.022095	0.099221	1.0486	2.3669	0.008
sex by distOA	5	0.07047	0.014095	0.039559	0.6689	1.1762	0.121
Csize by site by sex	2	0.02224	0.011119	0.012483	0.5277	0.6079	0.274
Csize by site by distOA	2	0.02855	0.014275	0.016026	0.6775	1.1319	0.14
Csize by sex by distOA	2	0.0237	0.011851	0.013304	0.5624	0.7988	0.203
site by sex by distOA	1	0.01131	0.011312	0.00635	0.5368	0.8599	0.199
Csize by site by sex by distOA	1	0.01029	0.010295	0.005779	0.4885	0.667	0.247
Residuals	32	0.67431	0.021072				
Total	82	1.78151					

4.2.1.3.2 Individuals with trauma versus unaffected individuals

PC charts for proximal and distal humeral morphology considered by trauma may be found in Figure 4.33 and Figure 4.34 with GLM results in Table 4.25 and Table 4.26. PC charts for proximal and distal femoral morphology as effected by trauma may be seen in Figure 4.35 and Figure 4.36 with GLM results in Table 4.27 and Table 4.28. Trauma did not uniquely explain proximal or distal epiphyseal shape in either the humerus or femur. When trauma was combined with size it explained proximal humeral morphology at a confidence level of 0.05 and when combined with both size and site, trauma explained proximal humeral morphology at a confidence level of 0.01. Distal humeral morphology was explained with statistical confidence ($p < 0.05$) by trauma combined with site and sex and with strong statistical confidence ($p < 0.01$ when trauma was combined with size, site and sex. Proximal femoral morphology was explained at a confidence level of 0.05 by trauma when combined with both size and sex and at a p -value of 0.01 when trauma was combined with site, when it was combined with sex or when it was combined with both site and sex. The distal femoral morphology was explained by size and trauma together and by trauma combined with site and sex at a p -value of 0.05.

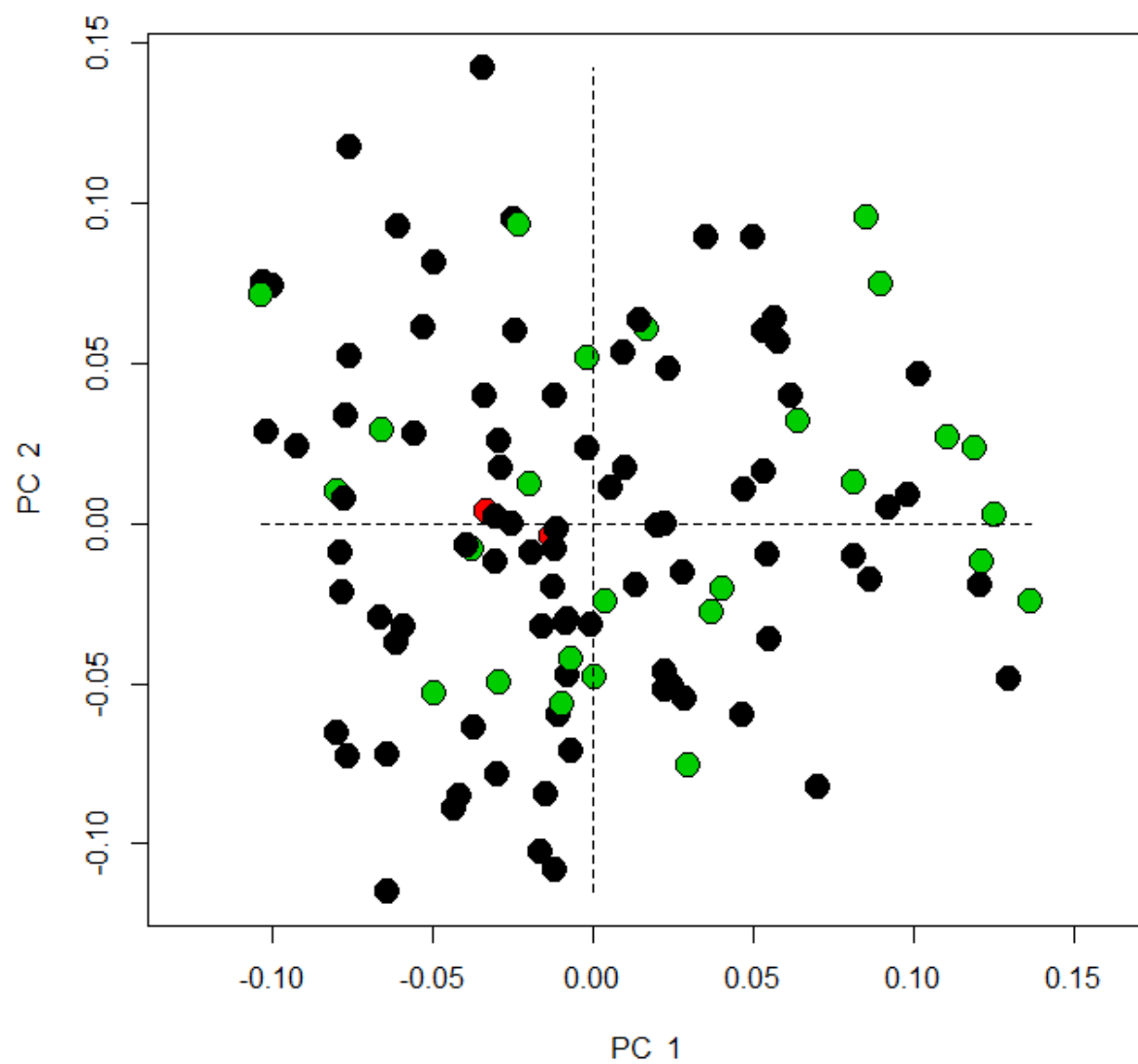


Figure 4.33 PC1 and PC2 for proximal humeral homologous landmarks by presence or absence of trauma. (black = no trauma, red = unknown, green = trauma present)

Table 4.25 GLM of proximal humerus morphology by presence or absence of trauma.

	Df	SS	MS	Rsq	F	Z	Pr(>F)
Centroid Size	1	0.03057	0.030566	0.017729	2.1368	1.7549	0.029
site	3	0.20712	0.069039	0.120131	4.8262	5.6485	0.001
sex	4	0.06955	0.017386	0.040337	1.2154	1.4423	0.077
Trauma	2	0.02296	0.01148	0.013317	0.8025	0.0838	0.473
Csize by site	3	0.05052	0.016841	0.029304	1.1773	1.4939	0.069
Csize by sex	4	0.0531	0.013275	0.030798	0.928	0.8176	0.217
site by sex	8	0.07475	0.009343	0.043355	0.6532	-0.6194	0.727
Csize by Trauma	1	0.02434	0.024342	0.014119	1.7017	2.0806	0.019
site by Trauma	3	0.03556	0.011853	0.020624	0.8286	0.6871	0.249
sex by Trauma	2	0.03014	0.015071	0.017483	1.0536	1.4103	0.071
Csize by site by sex	3	0.04209	0.01403	0.024412	0.9808	1.5155	0.07
Csize by site by Trauma	2	0.0413	0.02065	0.023955	1.4436	2.4334	0.008
Csize by sex by Trauma	1	0.01669	0.016693	0.009682	1.167	1.5126	0.07
site by sex by Trauma	2	0.0202	0.0101	0.011717	0.7061	0.6213	0.275
Csize by site by sex by Trauma	2	0.01818	0.009088	0.010542	0.6353	0.4391	0.337
Residuals	69	0.98704	0.014305				
Total	110	1.7241					

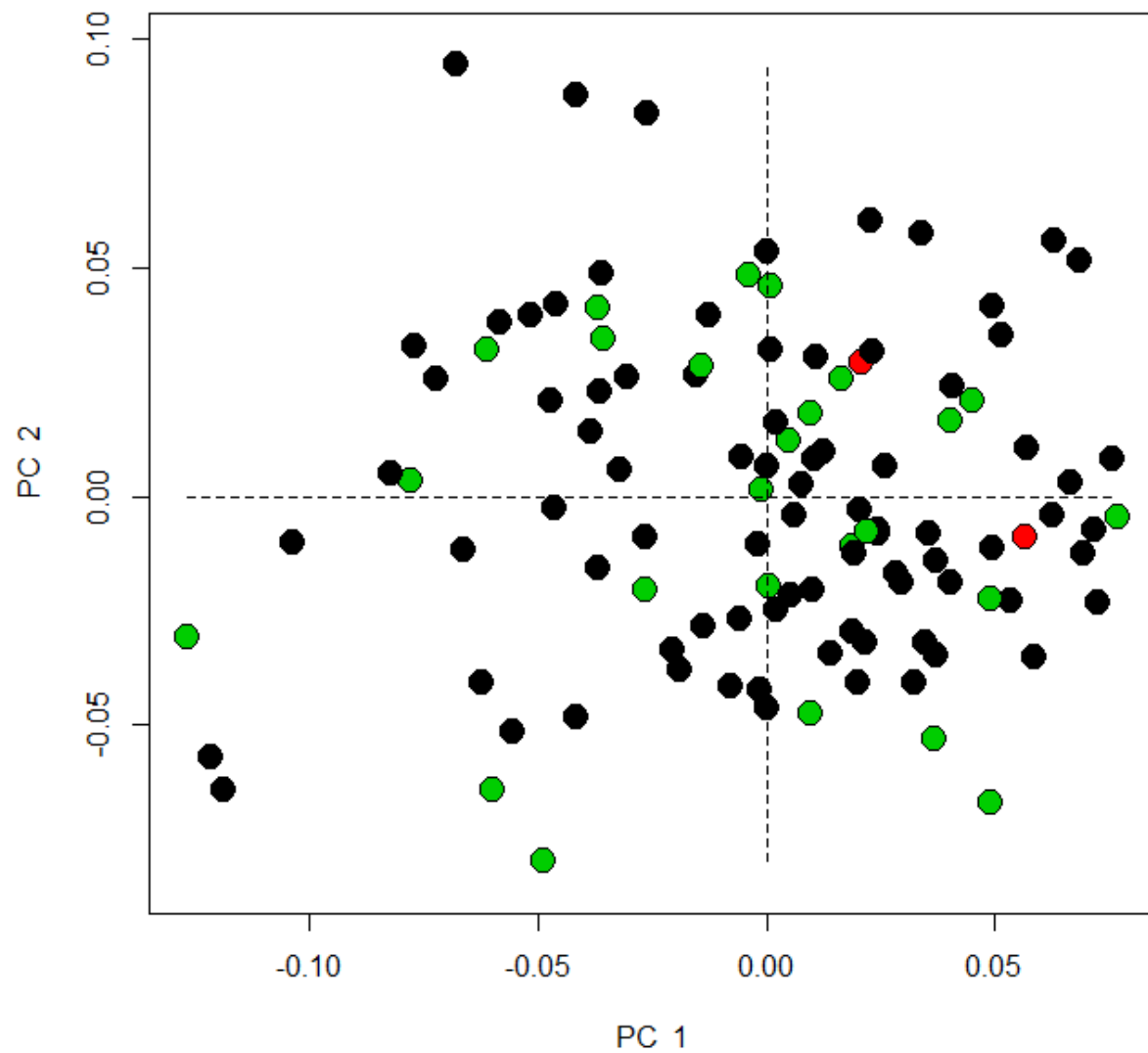


Figure 4.34 PC1 and PC2 for distal humeral homologous landmarks by presence or absence of trauma. (black = no trauma, red = unknown, green = trauma present)

Table 4.26 GLM of distal humerus morphology by presence or absence of trauma.

	Df	SS	MS	Rsqu	F	Z	Pr(>F)
Csize	1	0.02775	0.027748	0.022109	2.6313	3.0353	0.002
site	3	0.12729	0.04243	0.101422	4.0235	6.6896	0.001
sex	4	0.03267	0.008169	0.026034	0.7746	-0.5637	0.726
Trauma	2	0.02306	0.011531	0.018375	1.0934	1.0677	0.133
Csize by site	3	0.02891	0.009638	0.023038	0.9139	0.4933	0.304
Csize by sex	4	0.04675	0.011688	0.03725	1.1083	1.6381	0.057
site by sex	8	0.06853	0.008566	0.054603	0.8123	0.4025	0.333
Csize by Trauma	1	0.01124	0.01124	0.008956	1.0658	1.3742	0.088
site by Trauma	3	0.03072	0.010239	0.024476	0.971	1.3552	0.084
sex by Trauma	2	0.01875	0.009375	0.01494	0.889	1.0241	0.142
Csize by site by sex	3	0.03734	0.012447	0.029751	1.1803	2.3166	0.017
Csize by site by Trauma	2	0.01083	0.005413	0.008626	0.5133	-0.6347	0.747
Csize by sex by Trauma	1	0.00854	0.008538	0.006803	0.8096	0.8056	0.206
site by sex by Trauma	2	0.02895	0.014473	0.023063	1.3724	2.5305	0.01
Csize by site by sex by Trauma	2	0.02609	0.013043	0.020784	1.2368	2.4636	0.009
Residuals	69	0.72764	0.010546				
Total	110	1.25505					

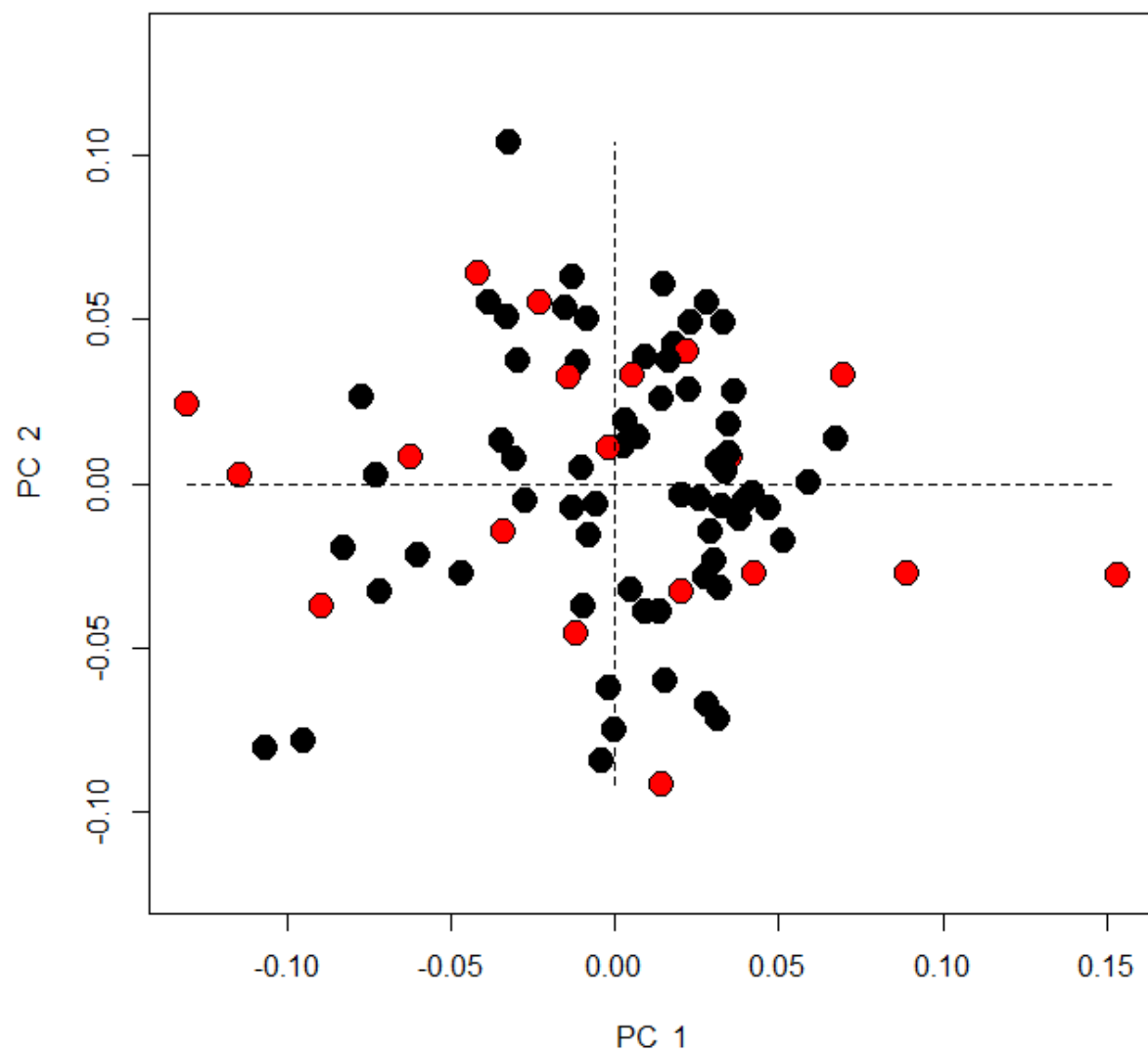


Figure 4.35 PC1 and PC2 for proximal femoral homologous landmarks by presence or absence of trauma. (black = no trauma, red = trauma present)

Table 4.27 GLM of proximal femur morphology by presence or absence of trauma.

	Df	SS	MS	Rsqr	F	Z	Pr(>F)
Csize	1	0.03399	0.033989	0.028149	2.517	2.8503	0.001
site	3	0.08567	0.028558	0.070952	2.1148	3.6587	0.001
sex	4	0.05318	0.013295	0.044043	0.9846	0.5773	0.292
Trauma	1	0.01143	0.011426	0.009463	0.8462	0.108	0.463
Csize by site	3	0.03357	0.01119	0.027801	0.8286	-0.0351	0.511
Csize by sex	4	0.06768	0.016921	0.056052	1.253	2.1981	0.017
site by sex	6	0.10145	0.016908	0.084014	1.2521	2.8158	0.005
Csize by Trauma	1	0.00515	0.005146	0.004262	0.3811	-1.3248	0.905
site by Trauma	2	0.04197	0.020983	0.034755	1.5539	3.3033	0.001
sex by Trauma	1	0.02055	0.02055	0.017019	1.5218	2.6141	0.005
Csize by site by sex	3	0.04283	0.014278	0.035474	1.0573	2.0901	0.02
Csize by site by Trauma	2	0.01708	0.008542	0.014148	0.6325	0.3835	0.345
Csize by sex by Trauma	1	0.0152	0.0152	0.012588	1.1256	1.8644	0.024
site by sex by Trauma	1	0.01924	0.019241	0.015934	1.4248	2.6106	0.008
Csize by site by sex by Trauma	1	0.01032	0.010322	0.008548	0.7643	1.0473	0.139
Residuals	48	0.64818	0.013504				
Total	82	1.20749					

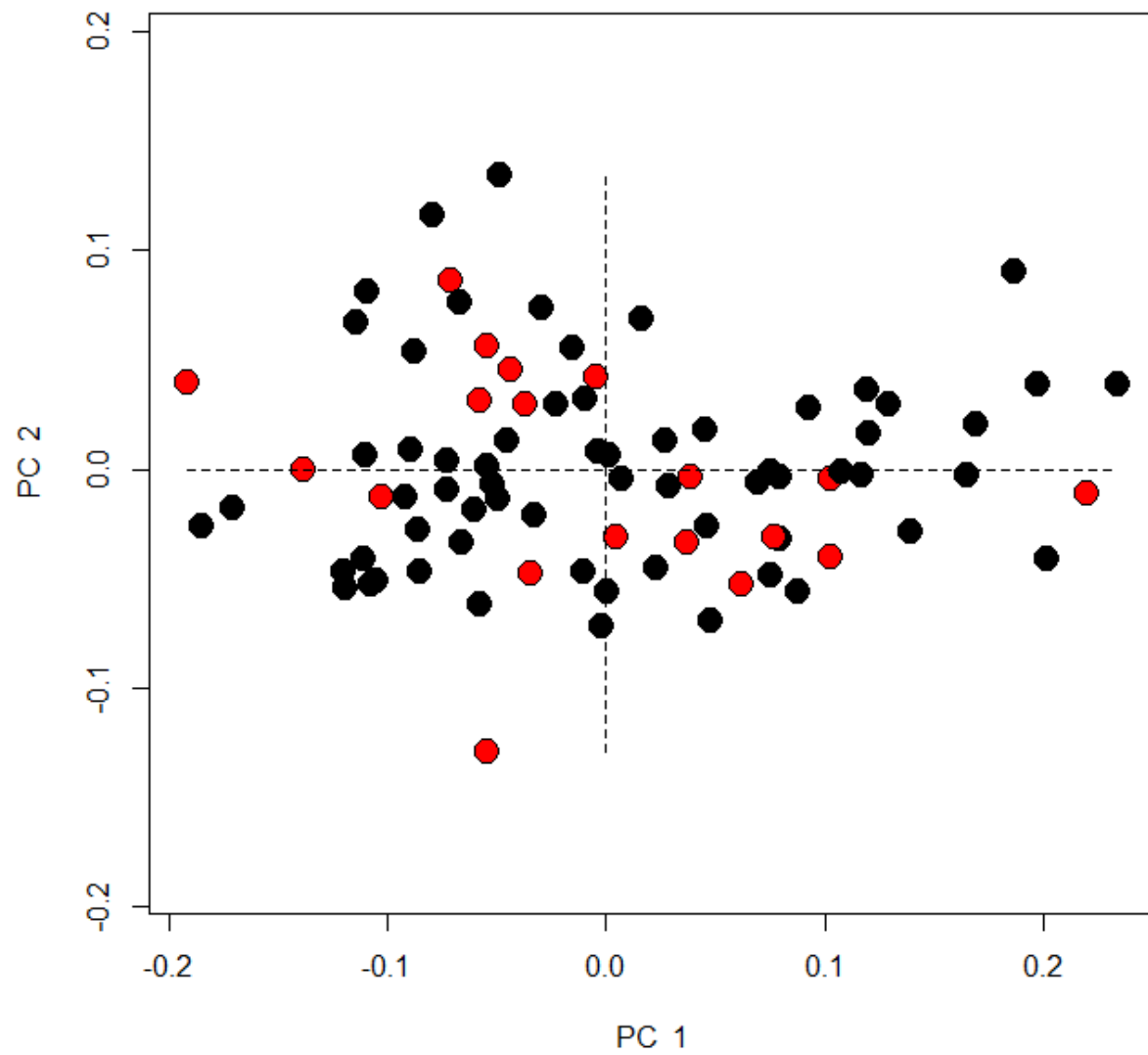


Figure 4.36 PC1 and PC2 for distal femoral homologous landmarks by presence or absence of trauma. (black = no trauma, red = trauma present)

Table 4.28 GLM of distal femur morphology by presence or absence of trauma.

	Df	SS	MS	Rsq	F	Z	Pr(>F)
Csize	1	0.13421	0.134209	0.075334	7.0694	3.762	0.001
site	3	0.23011	0.076705	0.129168	4.0404	4.4585	0.001
sex	4	0.07326	0.018315	0.041122	0.9647	0.7854	0.203
Trauma	1	0.01048	0.010484	0.005885	0.5522	-0.3514	0.628
Csize by site	3	0.03663	0.012211	0.020562	0.6432	-0.3609	0.618
Csize by sex	4	0.07916	0.01979	0.044434	1.0424	1.3082	0.101
site by sex	6	0.08075	0.013459	0.045329	0.709	0.2334	0.388
Csize by Trauma	1	0.03447	0.034475	0.019351	1.8159	2.2483	0.015
site by Trauma	2	0.03681	0.018404	0.020661	0.9694	1.2371	0.118
sex by Trauma	1	0.02208	0.022084	0.012396	1.1633	1.6408	0.065
Csize by site by sex	3	0.04714	0.015712	0.026458	0.8276	1.1213	0.14
Csize by site by Trauma	2	0.01944	0.009718	0.01091	0.5119	0.0194	0.465
Csize by sex by Trauma	1	0.0202	0.020196	0.011337	1.0638	1.4248	0.089
site by sex by Trauma	1	0.02498	0.024983	0.014024	1.316	1.7415	0.047
Csize by site by sex by Trauma	1	0.02053	0.020531	0.011524	1.0815	1.5813	0.073
Residuals	48	0.91125	0.018984				
Total	82	1.78151					

4.2.1.3.3 Individuals with developmental stress indicators versus unaffected individuals

The shape of the proximal humerus in and its relationship with indicators of childhood stress may be found in Figure 4.37 for LEH, Figure 4.38 for CO with results for both GLMs in Table 4.29. Results for the distal humerus are found in Figure 4.39 and Figure 4.40 and GLMs are compiled in Table 4.30. The proximal femoral epiphyseal morphology and its relationship with childhood stress is illustrated in Figure 4.41 and Figure 4.42, while GLMs are reported in Table 4.31. The distal femur's results may be found in Figure 4.43 and Figure 4.44 with results from the GLMs in Table 4.32. Neither LEH nor CO could uniquely explain humeral or femoral epiphyseal morphology. When stress indicators were combined with other IVs they were able to explain the morphologies observed.

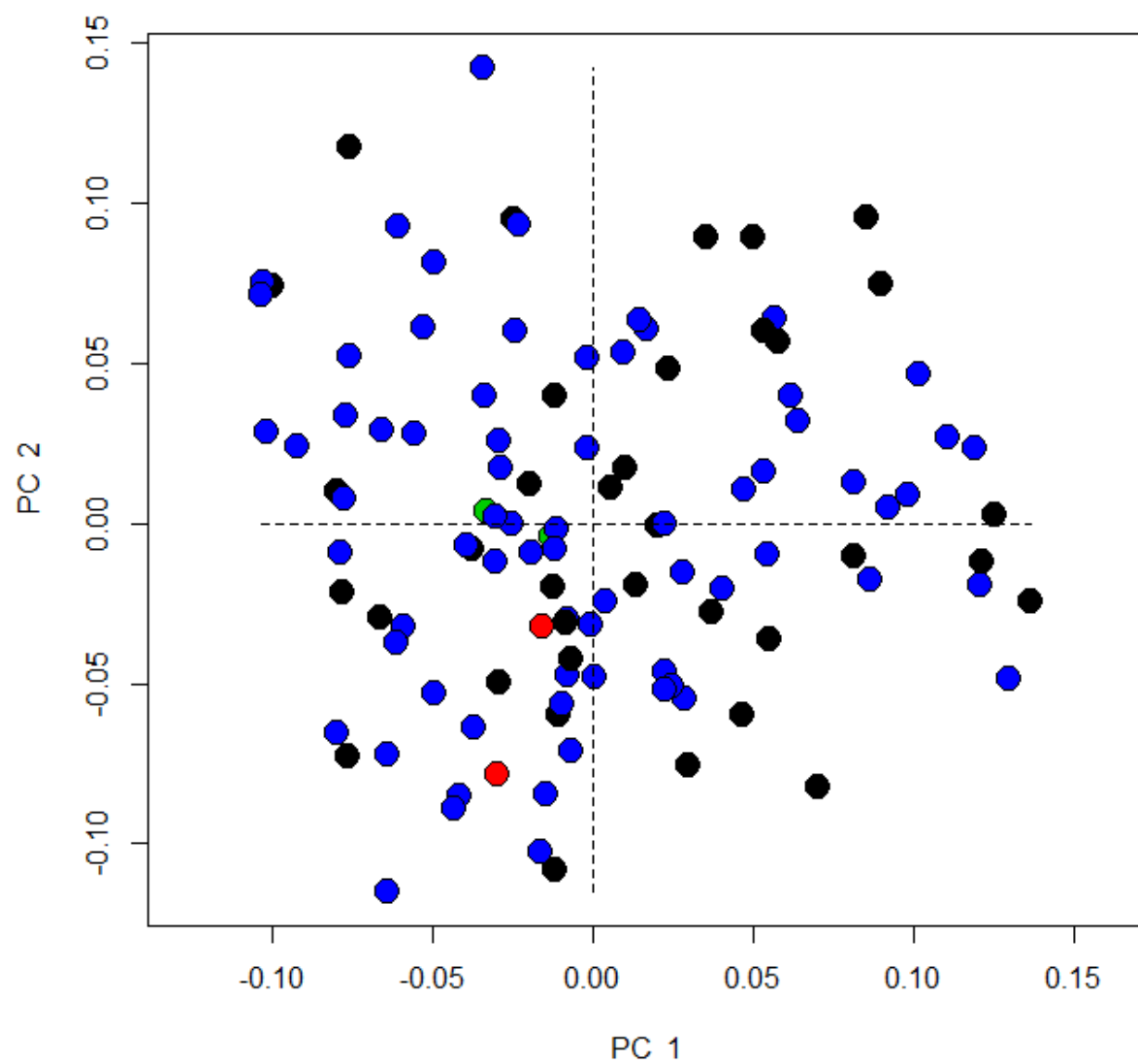


Figure 4.37 PC1 and PC2 for proximal humeral homologous landmarks by presence or absence of LEH. (black = no LEH observed, red = not enough teeth present, green = unknown, blue = LEH observed)

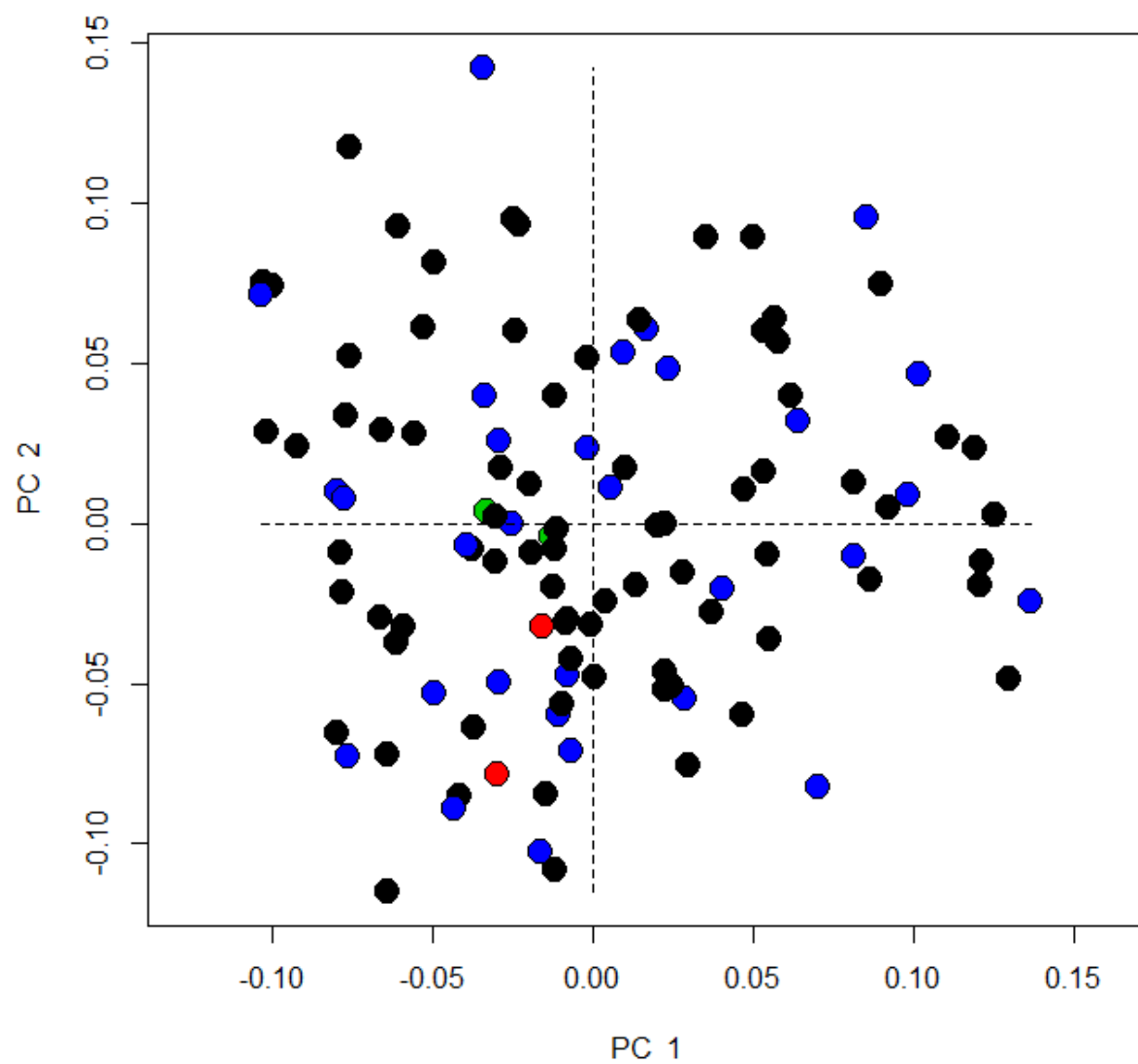


Figure 4.38 PC1 and PC2 for proximal humoral homologous landmarks by presence or absence of CO. (black = no CO observed, red = orbitals not present, green = unknown, blue = CO observed)

Table 4.29 GLM of proximal humerus morphology by presence or absence LEH and CO.

	Df	SS	MS	Rsqr	F	Z	Pr(>F)
Csize	1	0.03057	0.030566	0.017729	2.055	1.678	0.038
site	3	0.20712	0.069039	0.120131	4.6417	5.5203	0.001
sex	4	0.06955	0.017386	0.040337	1.1689	1.2782	0.105
LEH	3	0.03652	0.012174	0.021184	0.8185	0.1066	0.462
Csize by site	3	0.05077	0.016924	0.029449	1.1379	1.394	0.092
Csize by sex	4	0.05303	0.013257	0.030757	0.8913	0.7089	0.242
site by sex	8	0.07009	0.008761	0.040654	0.5891	-1.1242	0.86
Csize by LEH	2	0.01928	0.00964	0.011182	0.6481	-0.0404	0.532
site by LEH	3	0.04776	0.015921	0.027703	1.0704	1.6423	0.062
sex by LEH	2	0.03527	0.017636	0.020459	1.1857	1.7789	0.036
Csize by site by sex	4	0.04495	0.011237	0.02607	0.7555	0.744	0.224
Csize by site by LEH	3	0.02311	0.007703	0.013404	0.5179	-0.4106	0.667
Csize by sex by LEH	1	0.01153	0.011526	0.006686	0.775	0.8001	0.233
site by sex by LEH	2	0.02851	0.014255	0.016536	0.9584	1.5514	0.051
Csize by site by sex by LEH	2	0.02926	0.01463	0.016971	0.9836	1.5726	0.056
Residuals	65	0.96679	0.014874				
Total	110	1.7241					

	Df	SS	MS	Rsqr	F	Z	Pr(>F)
Csize	1	0.03057	0.030566	0.017729	2.1881	1.8053	0.022
site	3	0.20712	0.069039	0.120131	4.9421	5.7245	0.001
sex	4	0.06955	0.017386	0.040337	1.2446	1.5295	0.061
CO	3	0.04378	0.014593	0.025393	1.0447	0.9287	0.172
Csize by site	3	0.04728	0.015761	0.027425	1.1282	1.3864	0.082
Csize by sex	4	0.0518	0.012951	0.030046	0.9271	0.8603	0.198
site by sex	8	0.06762	0.008453	0.039221	0.6051	-0.9968	0.829
Csize by CO	2	0.02959	0.014797	0.017165	1.0592	1.2747	0.102
site by CO	3	0.03713	0.012377	0.021536	0.886	1.0478	0.149
sex by CO	2	0.02996	0.01498	0.017377	1.0723	1.4569	0.066
Csize by site by sex	4	0.05812	0.01453	0.033709	1.0401	1.9973	0.019
Csize by site by CO	2	0.04352	0.021759	0.025241	1.5576	2.8782	0.002
Csize by sex by CO	1	0.01039	0.010387	0.006025	0.7436	0.6527	0.276
site by sex by CO	2	0.03058	0.015291	0.017738	1.0946	1.9311	0.024
Csize by site by sex by CO	2	0.04511	0.022554	0.026163	1.6145	3.1445	0.001
Residuals	66	0.92199	0.01397				
Total	110	1.7241					

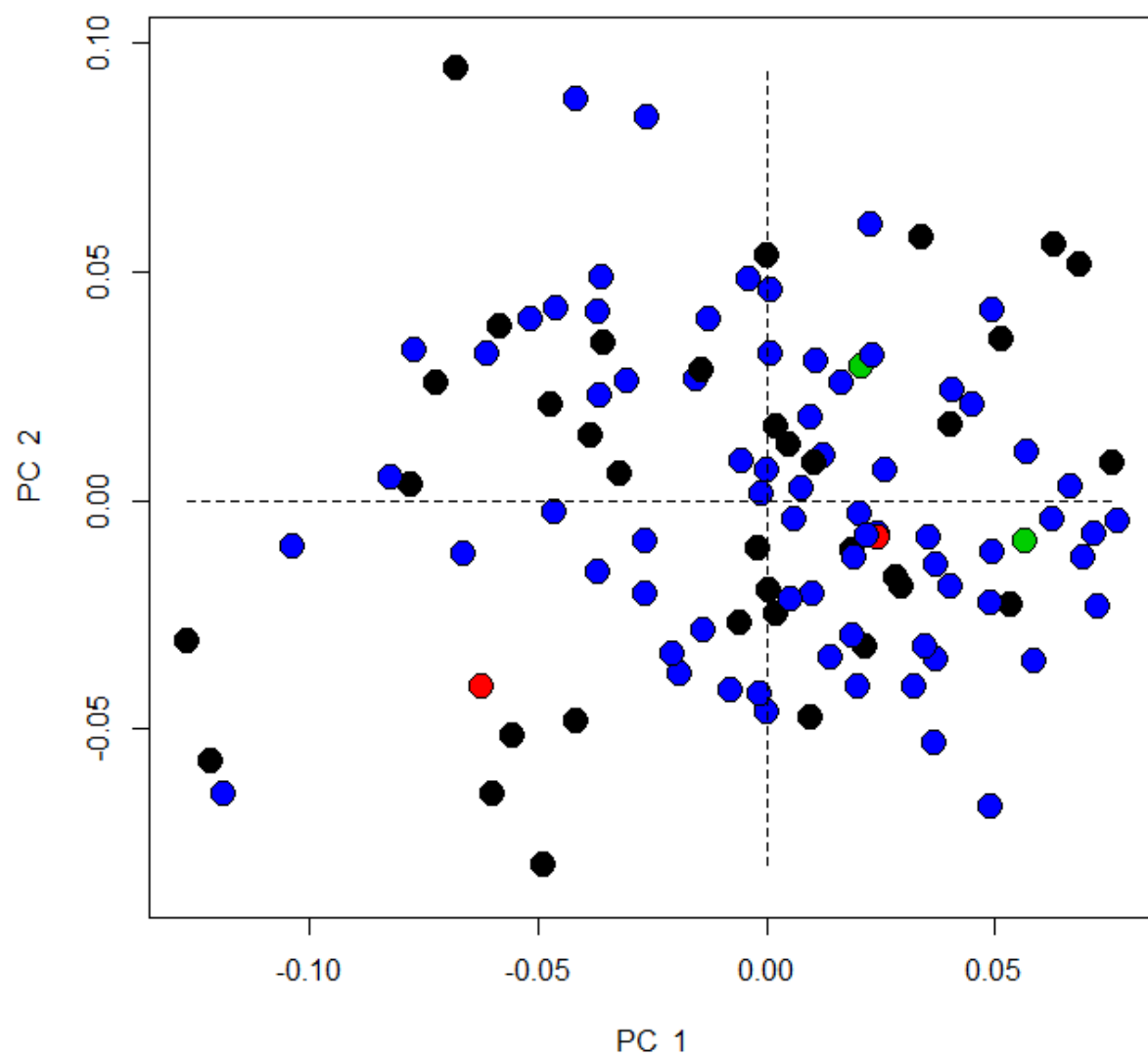


Figure 4.39 PC1 and PC2 for distal humoral homologous landmarks by presence or absence of LEH. (black = no LEH observed, red = not enough teeth present, green = unknown, blue = LEH observed)

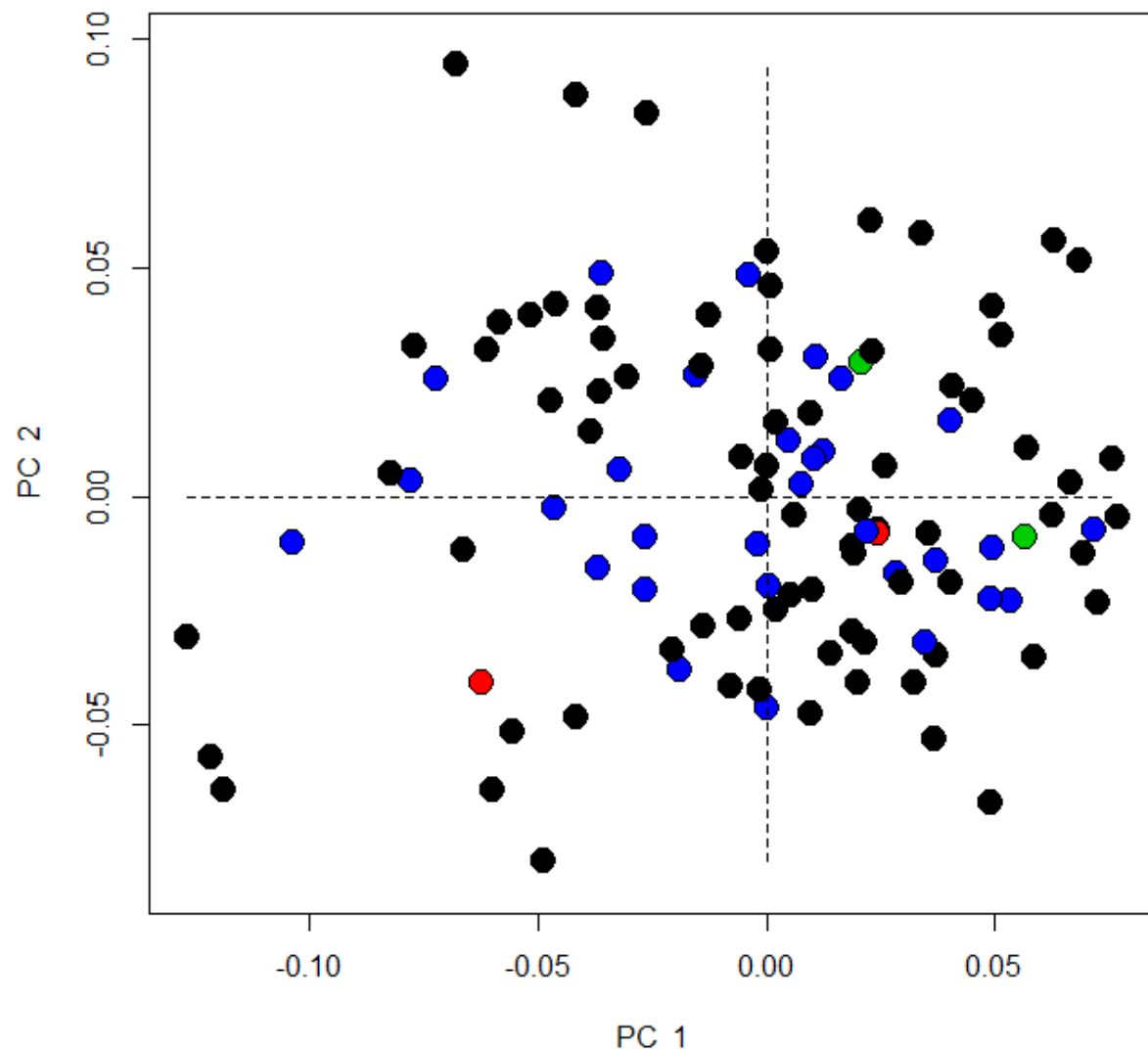


Figure 4.40 PC1 and PC2 for distal humoral homologous landmarks by presence or absence of CO. (black = no CO observed, red = orbitals not present, green = unknown, blue = CO observed)

Table 4.30 GLM of distal humerus morphology by presence or absence LEH and CO.

	Df	SS	MS	Rsqr	F	Z	Pr(>F)
Csize	1	0.02775	0.027748	0.022109	2.6179	2.9982	0.001
site	3	0.12729	0.04243	0.101422	4.003	6.6028	0.001
sex	4	0.03267	0.008169	0.026034	0.7706	-0.5764	0.714
LEH	3	0.02633	0.008776	0.020979	0.828	-0.0096	0.49
Csize by site	3	0.03163	0.010544	0.025203	0.9947	0.9282	0.183
Csize by sex	4	0.04856	0.01214	0.038692	1.1454	1.8295	0.038
site by sex	8	0.06385	0.007982	0.050877	0.753	-0.0211	0.49
Csize by LEH	2	0.02662	0.01331	0.02121	1.2557	1.9563	0.037
site by LEH	3	0.03793	0.012643	0.03022	1.1927	2.4391	0.007
sex by LEH	2	0.01837	0.009186	0.014639	0.8667	1.0646	0.138
Csize by site by sex	4	0.0416	0.0104	0.033145	0.9811	2.0372	0.029
Csize by site by LEH	3	0.03238	0.010793	0.025799	1.0182	2.1154	0.022
Csize by sex by LEH	1	0.01386	0.013864	0.011046	1.308	2.2136	0.012
site by sex by LEH	2	0.01824	0.009122	0.014536	0.8606	1.5964	0.051
Csize by site by sex by LEH	2	0.01899	0.009494	0.01513	0.8957	1.5143	0.058
Residuals	65	0.68897	0.0106				
Total	110	1.25505					

	Df	SS	MS	Rsqr	F	Z	Pr(>F)
Csize	1	0.02775	0.027748	0.022109	2.489	2.8573	0.003
site	3	0.12729	0.04243	0.101422	3.806	6.4209	0.001
sex	4	0.03267	0.008169	0.026034	0.7327	-0.8464	0.8
CO	3	0.02371	0.007903	0.01889	0.7089	-0.691	0.755
Csize by site	3	0.02928	0.00976	0.023329	0.8754	0.2903	0.377
Csize by sex	4	0.04758	0.011894	0.037909	1.0669	1.4315	0.074
site by sex	8	0.06192	0.00774	0.049335	0.6943	-0.5401	0.685
Csize by CO	2	0.02085	0.010427	0.016616	0.9353	0.9319	0.157
site by CO	3	0.02647	0.008824	0.021092	0.7915	0.5761	0.26
sex by CO	2	0.01565	0.007825	0.01247	0.7019	0.2921	0.382
Csize by site by sex	4	0.03766	0.009416	0.030009	0.8446	1.1036	0.135
Csize by site by CO	2	0.0182	0.009099	0.0145	0.8162	0.9258	0.185
Csize by sex by CO	1	0.01369	0.013688	0.010906	1.2278	1.7574	0.04
site by sex by CO	2	0.01761	0.008805	0.014031	0.7898	0.9505	0.17
Csize by site by sex by CO	2	0.01895	0.009473	0.015096	0.8498	1.2205	0.121
Residuals	66	0.73578	0.011148				
Total	110	1.25505					

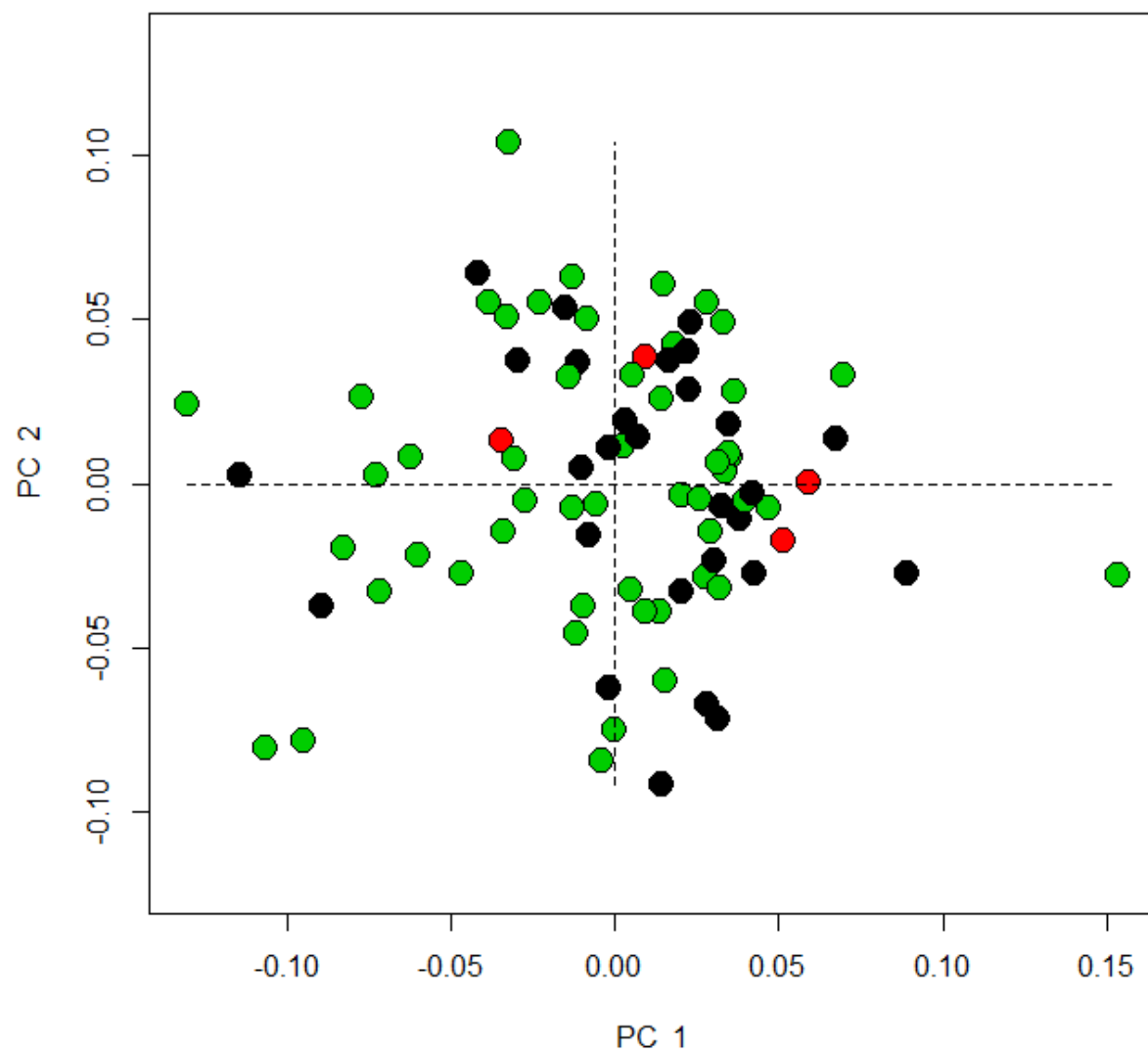


Figure 4.41 PC1 and PC2 for proximal femoral homologous landmarks by presence or absence of LEH. (black = no LEH observed, red = not enough teeth present, green = LEH observed)

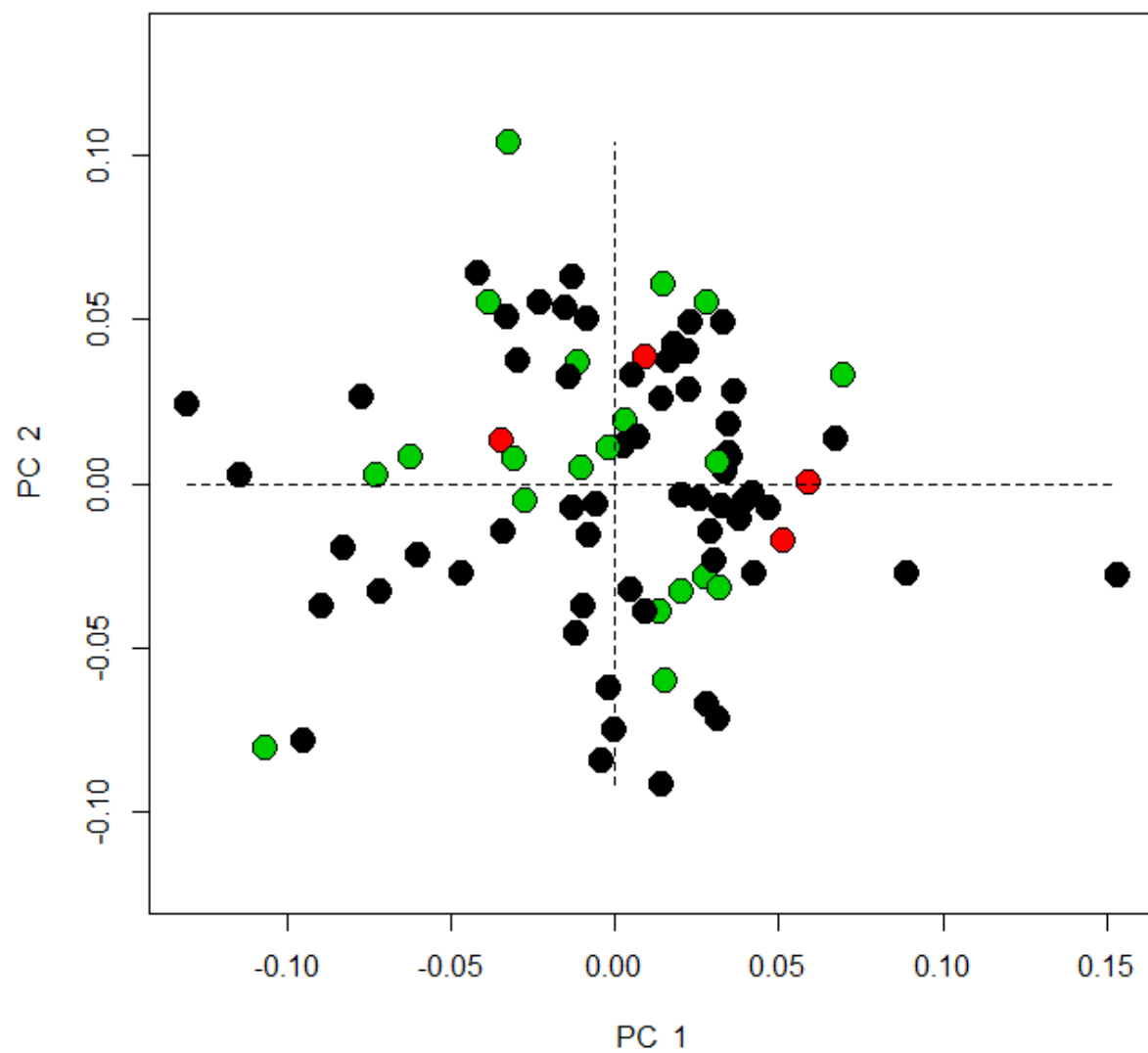


Figure 4.42 PC1 and PC2 for proximal femoral homologous landmarks by presence or absence of CO. (black = no CO observed, red = orbitals not present, green = CO observed)

Table 4.31 GLM of proximal femoral morphology by presence or absence LEH and CO.

	Df	SS	MS	Rsqr	F	Z	Pr(>F)
Csize	1	0.03399	0.033989	0.028149	2.4257	2.7492	0.001
site	3	0.08567	0.028558	0.070952	2.0381	3.4964	0.001
sex	4	0.05318	0.013295	0.044043	0.9489	0.3901	0.345
LEH	2	0.02517	0.012586	0.020846	0.8982	0.3459	0.367
Csize by site	3	0.03689	0.012297	0.030553	0.8776	0.2769	0.379
Csize by sex	4	0.06774	0.016936	0.056103	1.2087	2.0692	0.02
site by sex	6	0.10248	0.01708	0.084869	1.219	2.7945	0.002
Csize by LEH	2	0.03451	0.017257	0.028584	1.2316	2.3162	0.007
site by LEH	3	0.04482	0.014941	0.037121	1.0663	2.3073	0.011
sex by LEH	3	0.03474	0.011581	0.028774	0.8265	1.3909	0.085
Csize by site by sex	2	0.02095	0.010474	0.017348	0.7475	1.0728	0.134
Csize by site by LEH	2	0.01719	0.008593	0.014232	0.6132	0.4619	0.323
Csize by sex by LEH	1	0.0133	0.013303	0.011017	0.9494	1.4548	0.063
site by sex by LEH	1	0.00762	0.007618	0.006309	0.5437	0.2939	0.404
Csize by site by sex by LEH	1	0.0127	0.012702	0.01052	0.9065	1.4589	0.068
Residuals	44	0.61652	0.014012				
Total	82	1.20749					

	Df	SS	MS	Rsqr	F	Z	Pr(>F)
Csize	1	0.03399	0.033989	0.028149	2.4278	2.747	0.001
site	3	0.08567	0.028558	0.070952	2.0398	3.4784	0.001
sex	4	0.05318	0.013295	0.044043	0.9497	0.3841	0.359
CO	2	0.02406	0.012028	0.019922	0.8591	0.1493	0.434
Csize by site	3	0.03483	0.01161	0.028845	0.8293	0.0092	0.486
Csize by sex	4	0.06754	0.016884	0.05593	1.206	2.0098	0.019
site by sex	6	0.10099	0.016832	0.083637	1.2023	2.7018	0.002
Csize by CO	2	0.02009	0.010046	0.01664	0.7176	0.4275	0.322
site by CO	2	0.02365	0.011823	0.019583	0.8445	0.8812	0.198
sex by CO	2	0.0267	0.013351	0.022113	0.9536	1.5741	0.054
Csize by site by sex	3	0.03614	0.012046	0.029928	0.8604	1.3523	0.087
Csize by site by CO	1	0.01682	0.01682	0.013929	1.2014	2.2189	0.015
Csize by sex by CO	2	0.02517	0.012587	0.020849	0.8991	1.3849	0.077
site by sex by CO	1	0.01695	0.016945	0.014033	1.2103	2.0445	0.018
Csize by site by sex by CO	1	0.01171	0.011708	0.009696	0.8363	1.2903	0.093
Residuals	45	0.63001	0.014				
Total	82	1.20749					

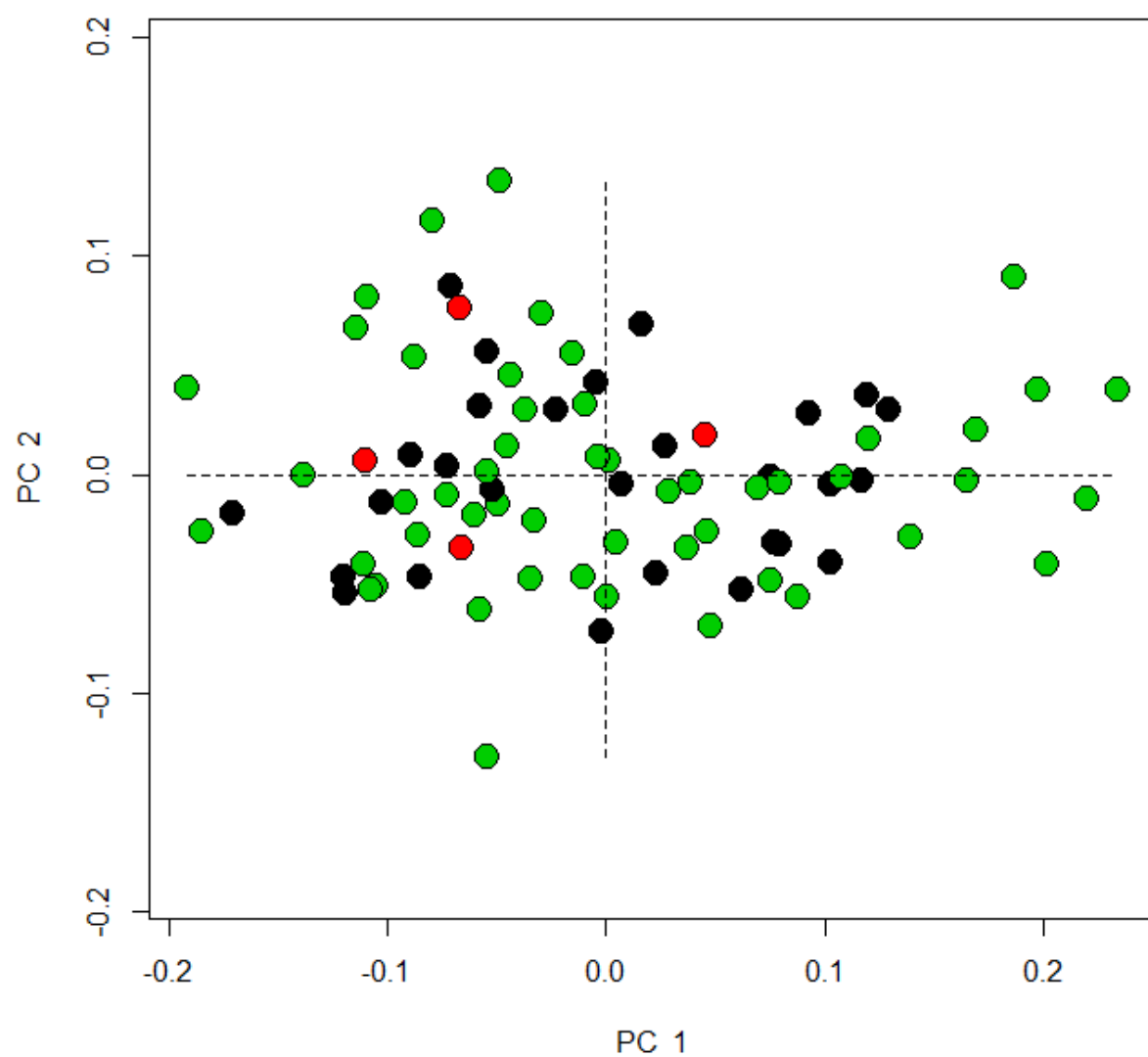


Figure 4.43 PC1 and PC2 for distal femoral homologous landmarks by presence or absence of LEH. (black = no LEH observed, red = not enough teeth present, green = LEH observed)

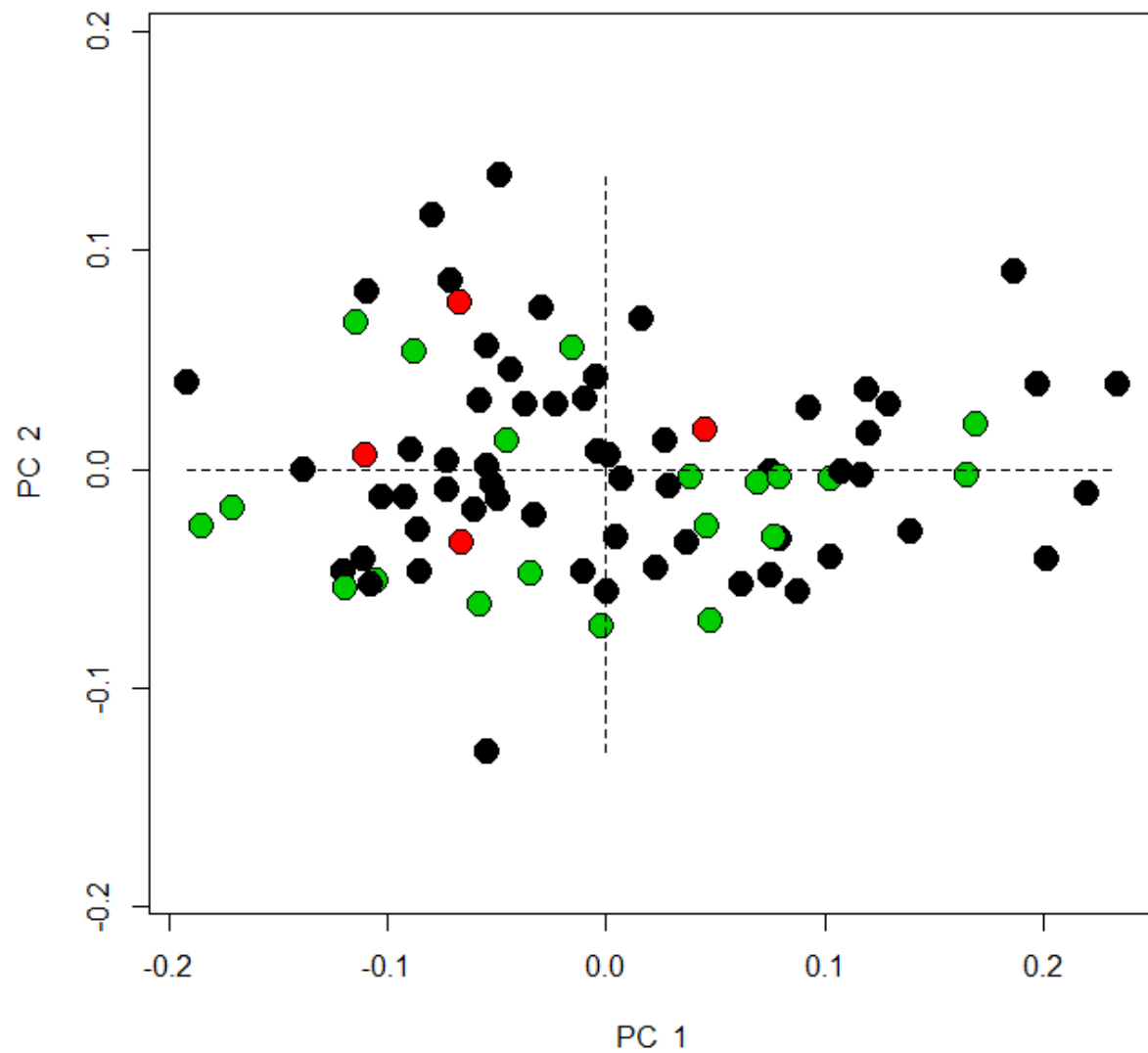


Figure 4.44 PC1 and PC2 for proximal femoral homologous landmarks by presence or absence of CO. (black = no CO observed, red = orbitals not present, green = CO observed)

Table 4.32 GLM of distal femoral morphology by presence or absence LEH and CO.

	Df	SS	MS	Rsqr	F	Z	Pr(>F)
Csize	1	0.13421	0.134209	0.075334	7.0046	3.727	0.001
site	3	0.23011	0.076705	0.129168	4.0034	4.392	0.001
sex	4	0.07326	0.018315	0.041122	0.9559	0.7403	0.21
LEH	2	0.02521	0.012606	0.014153	0.658	-0.1575	0.551
Csize by site	3	0.03949	0.013162	0.022165	0.687	-0.1264	0.537
Csize by sex	4	0.07874	0.019686	0.044201	1.0275	1.3305	0.1
site by sex	6	0.09105	0.015175	0.051107	0.792	0.6759	0.249
Csize by LEH	2	0.03184	0.015922	0.017874	0.831	0.8596	0.185
site by LEH	3	0.08815	0.029384	0.049482	1.5336	2.7166	0.003
sex by LEH	3	0.05164	0.017213	0.028985	0.8984	1.2929	0.107
Csize by site by sex	2	0.04623	0.023116	0.025951	1.2065	2.1288	0.018
Csize by site by LEH	2	0.02372	0.011858	0.013313	0.6189	0.6541	0.24
Csize by sex by LEH	1	0.01137	0.011369	0.006382	0.5934	0.616	0.274
site by sex by LEH	1	0.00761	0.007605	0.004269	0.3969	-0.0773	0.503
Csize by site by sex by LEH	1	0.00584	0.005842	0.00328	0.3049	-0.4594	0.676
Residuals	44	0.84304	0.01916				
Total	82	1.78151					

	Df	SS	MS	Rsqr	F	Z	Pr(>F)
Csize	1	0.13421	0.134209	0.075334	7.3059	3.7925	0.001
site	3	0.23011	0.076705	0.129168	4.1756	4.5357	0.001
sex	4	0.07326	0.018315	0.041122	0.997	0.8837	0.18
CO	2	0.027	0.0135	0.015156	0.7349	0.1354	0.39
Csize by site	3	0.04068	0.013559	0.022833	0.7381	0.0836	0.443
Csize by sex	4	0.07774	0.019436	0.043638	1.058	1.4155	0.086
site by sex	6	0.08813	0.014688	0.049469	0.7996	0.7339	0.231
Csize by CO	2	0.04037	0.020186	0.022662	1.0989	1.4483	0.074
site by CO	2	0.03452	0.017258	0.019374	0.9395	1.2219	0.121
sex by CO	2	0.08526	0.042631	0.047859	2.3207	3.2869	0.002
Csize by site by sex	3	0.05234	0.017447	0.029379	0.9497	1.7352	0.047
Csize by site by CO	1	0.01039	0.010387	0.005831	0.5654	0.512	0.302
Csize by sex by CO	2	0.03798	0.018991	0.02132	1.0338	1.8757	0.038
site by sex by CO	1	0.01314	0.013137	0.007374	0.7151	0.9983	0.168
Csize by site by sex by CO	1	0.00974	0.009741	0.005468	0.5303	0.4566	0.317
Residuals	45	0.82664	0.01837				
Total	82	1.78151					

4.2.1.3.4 Schmorl's Nodes

Humeral proximal and distal epiphyseal morphology (illustrated in Figure 4.45 and Figure 4.46 respectively) could not be uniquely explained by the presence or absence of Schmorl's nodes although in both cases when combined with other IVs morphology was explained. (See Table 4.33 for the GLM for the proximal humerus and Table 4.34 for the GLM for the distal humerus.) Femoral distal and proximal morphology (See Figure 4.47 and Figure 4.48) was uniquely explained by Schmorl's nodes with confidence at 0.05 for the proximal epiphysis and 0.01 for the distal epiphysis. Schmorl's nodes combined with the other IVs also could explain femoral epiphyseal morphology (See Table 4.35 and Table 4.36).

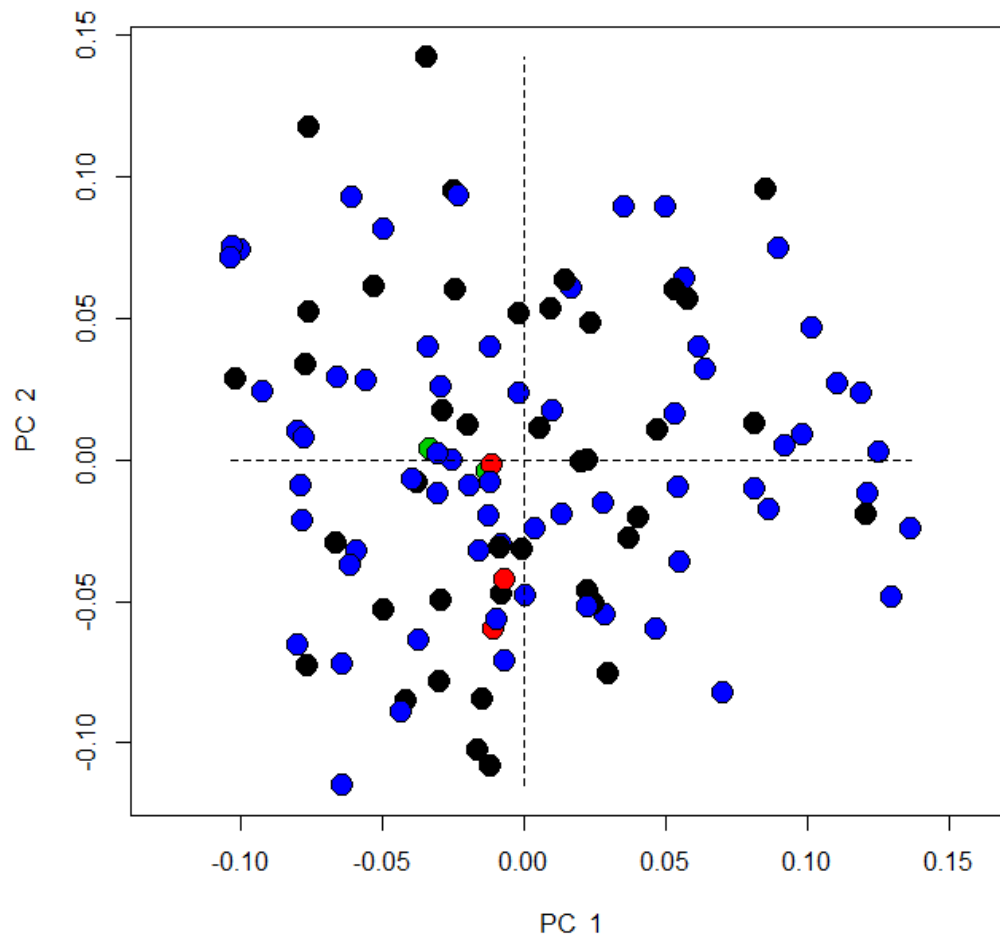


Figure 4.45 PC1 and PC2 for proximal humeral homologous landmarks by presence or absence of Schmorl's nodes. (black = no Schmorl's nodes observed, red = not enough vertebrae present, green = unknown, blue = Schmorl's nodes observed)

Table 4.33 GLM of proximal humerus morphology by presence or absence Schmorl's nodes.

	Df	SS	MS	Rsqr	F	Z	Pr(>F)
Csize	1	0.03057	0.030566	0.017729	2.2172	1.8281	0.023
site	3	0.20712	0.069039	0.120131	5.0079	5.754	0.001
sex	4	0.06955	0.017386	0.040337	1.2612	1.5842	0.06
Schmorl's nodes	3	0.03469	0.011564	0.020122	0.8388	0.2061	0.43
Csize by site	3	0.04638	0.015459	0.026899	1.1213	1.3391	0.094
Csize by sex	4	0.05308	0.013269	0.030786	0.9625	0.9933	0.158
site by sex	8	0.07902	0.009877	0.04583	0.7164	-0.112	0.554
Csize by Schmorl's nodes	2	0.03132	0.015659	0.018165	1.1359	1.4976	0.063
site by Schmorl's nodes	3	0.03317	0.011055	0.019237	0.8019	0.6659	0.25
sex by Schmorl's nodes	4	0.06799	0.016996	0.039433	1.2329	2.203	0.013
Csize by site by sex	3	0.04352	0.014506	0.025242	1.0523	1.9087	0.026
Csize by site by Schmorl's nodes	2	0.03041	0.015205	0.017638	1.1029	1.8959	0.017
Csize by sex by Schmorl's nodes	1	0.01843	0.018427	0.010688	1.3366	1.9044	0.027
site by sex by Schmorl's nodes	2	0.05193	0.025963	0.030117	1.8833	3.1901	0.001
Csize by site by sex by Schmorl's nodes	1	0.01709	0.017085	0.00991	1.2393	1.9275	0.022
Residuals	66	0.90987	0.013786				
Total	110	1.7241					

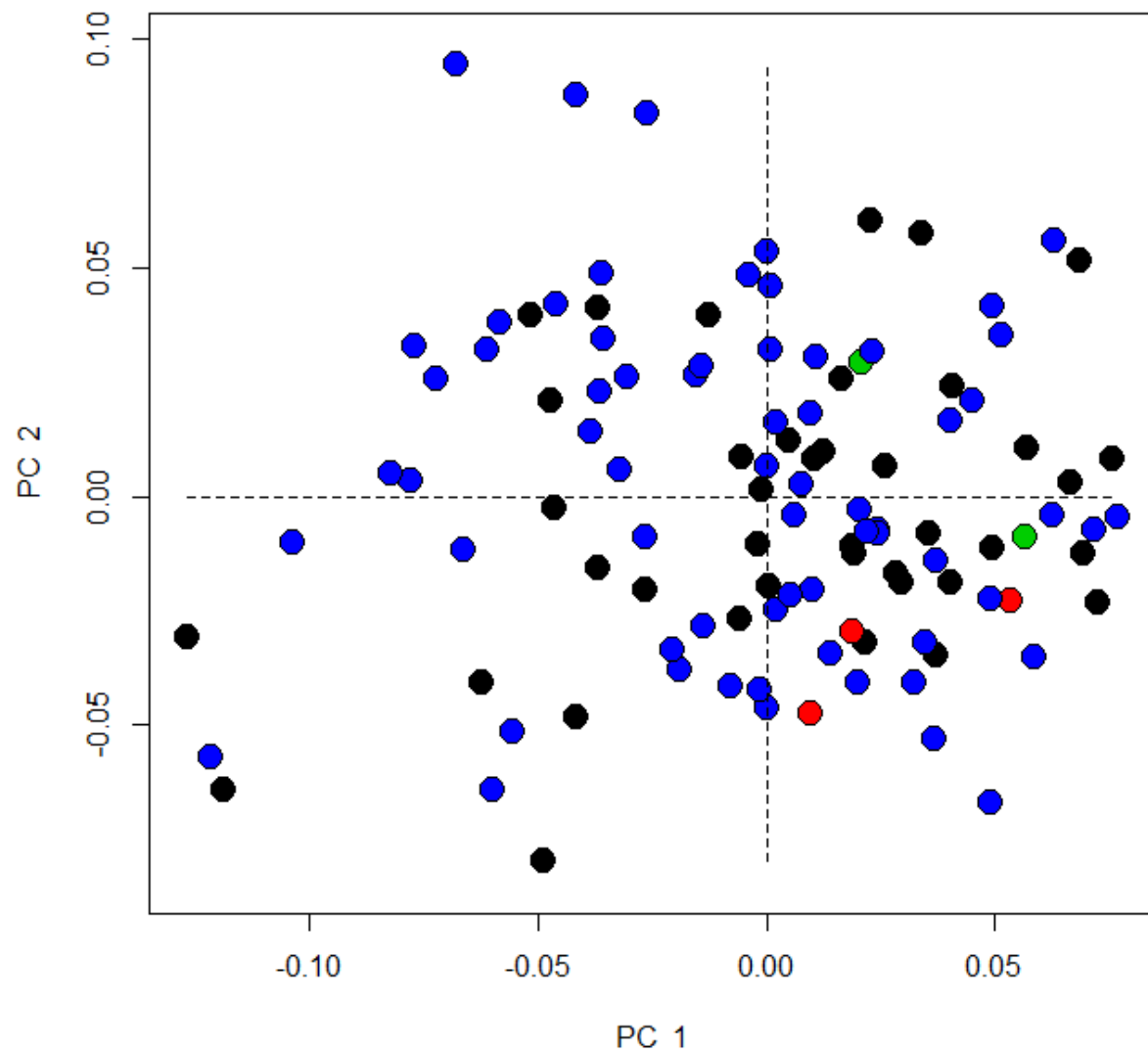


Figure 4.46 PC1 and PC2 for distal humeral homologous landmarks by presence or absence of Schmorl's nodes. (black = no Schmorl's nodes observed, red = not enough vertebrae present, green = unknown, blue = Schmorl's nodes observed)

Table 4.34 GLM of distal humerus morphology by presence or absence Schmorl's nodes.

	Df	SS	MS	Rsqr	F	Z	Pr(>F)
Csize	1	0.02775	0.027748	0.022109	2.6164	3.003	0.003
site	3	0.12729	0.04243	0.101422	4.0007	6.6541	0.001
sex	4	0.03267	0.008169	0.026034	0.7702	-0.5741	0.728
Schmorl's nodes	3	0.02821	0.009404	0.022479	0.8867	0.2843	0.386
Csize by site	3	0.02871	0.00957	0.022875	0.9023	0.4683	0.311
Csize by sex	4	0.04977	0.012442	0.039654	1.1731	1.9386	0.028
site by sex	8	0.06766	0.008458	0.053914	0.7975	0.3437	0.34
Csize by Schmorl's nodes	2	0.02619	0.013097	0.020871	1.2349	1.9457	0.036
site by Schmorl's nodes	3	0.03345	0.01115	0.026651	1.0513	1.7688	0.043
sex by Schmorl's nodes	4	0.03679	0.009199	0.029317	0.8673	1.227	0.111
Csize by site by sex	3	0.03166	0.010553	0.025226	0.9951	1.8136	0.047
Csize by site by Schmorl's nodes	2	0.02196	0.010981	0.017498	1.0354	2.0912	0.024
Csize by sex by Schmorl's nodes	1	0.01079	0.010794	0.0086	1.0177	1.5825	0.054
site by sex by Schmorl's nodes	2	0.02029	0.010146	0.016168	0.9566	1.8511	0.04
Csize by site by sex by Schmorl's nodes	1	0.01187	0.011871	0.009458	1.1193	1.317	0.058
Residuals	66	0.69997	0.010606				
Total	110	1.25505					

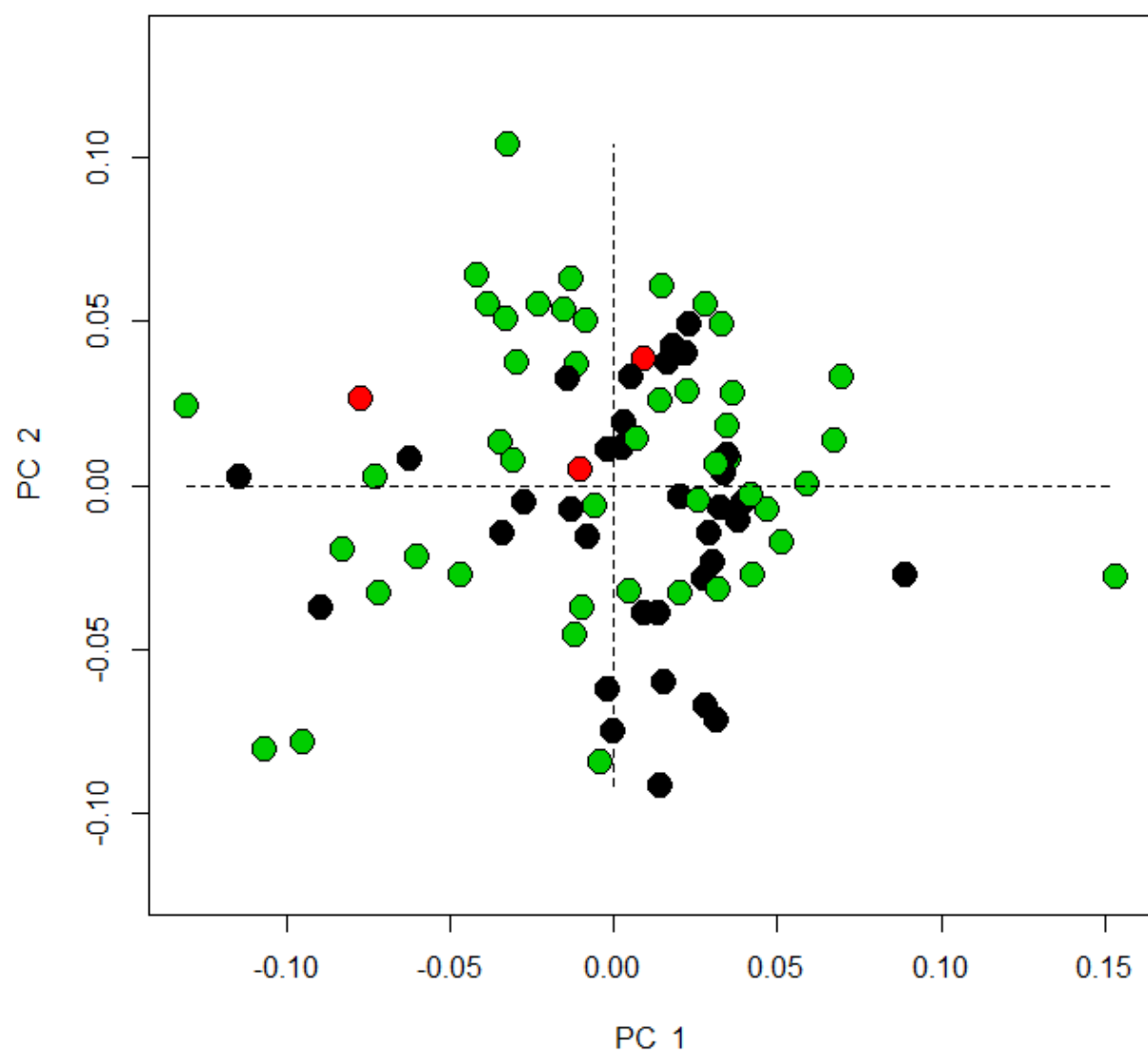


Figure 4.47 PC1 and PC2 for proximal femoral homologous landmarks by presence or absence of Schmorl's nodes. (black = no Schmorl's nodes observed, red = not enough vertebrae present, green = Schmorl's nodes observed)

Table 4.35 GLM of proximal femoral morphology by presence or absence Schmorl's nodes.

	Df	SS	MS	Rsqr	F	Z	Pr(>F)
Csize	1	0.03399	0.033989	0.028149	2.4499	2.783	0.001
site	3	0.08567	0.028558	0.070952	2.0584	3.5289	0.001
sex	4	0.05318	0.013295	0.044043	0.9583	0.4354	0.331
Schmorl's nodes	2	0.03819	0.019096	0.03163	1.3764	1.9044	0.025
Csize by site	3	0.03775	0.012583	0.031263	0.907	0.4678	0.309
Csize by sex	4	0.0767	0.019176	0.063524	1.3822	2.7783	0.003
site by sex	6	0.08687	0.014478	0.07194	1.0435	2.0362	0.025
Csize by Schmorl's nodes	2	0.0322	0.016099	0.026665	1.1604	2.1774	0.015
site by Schmorl's nodes	3	0.03523	0.011744	0.029178	0.8465	1.3622	0.092
sex by Schmorl's nodes	3	0.03838	0.012792	0.031781	0.922	1.6863	0.043
Csize by site by sex	2	0.0169	0.008452	0.014	0.6092	0.3365	0.372
Csize by site by Schmorl's nodes	1	0.01163	0.011632	0.009633	0.8384	1.1959	0.106
Csize by sex by Schmorl's nodes	1	0.01242	0.012424	0.010289	0.8955	1.4103	0.078
site by sex by Schmorl's nodes	1	0.01566	0.015665	0.012973	1.1291	2.136	0.014
Csize by site by sex by Schmorl's nodes	1	0.00838	0.008377	0.006938	0.6038	0.476	0.32
Residuals	45	0.62433	0.013874				
Total	82	1.20749					

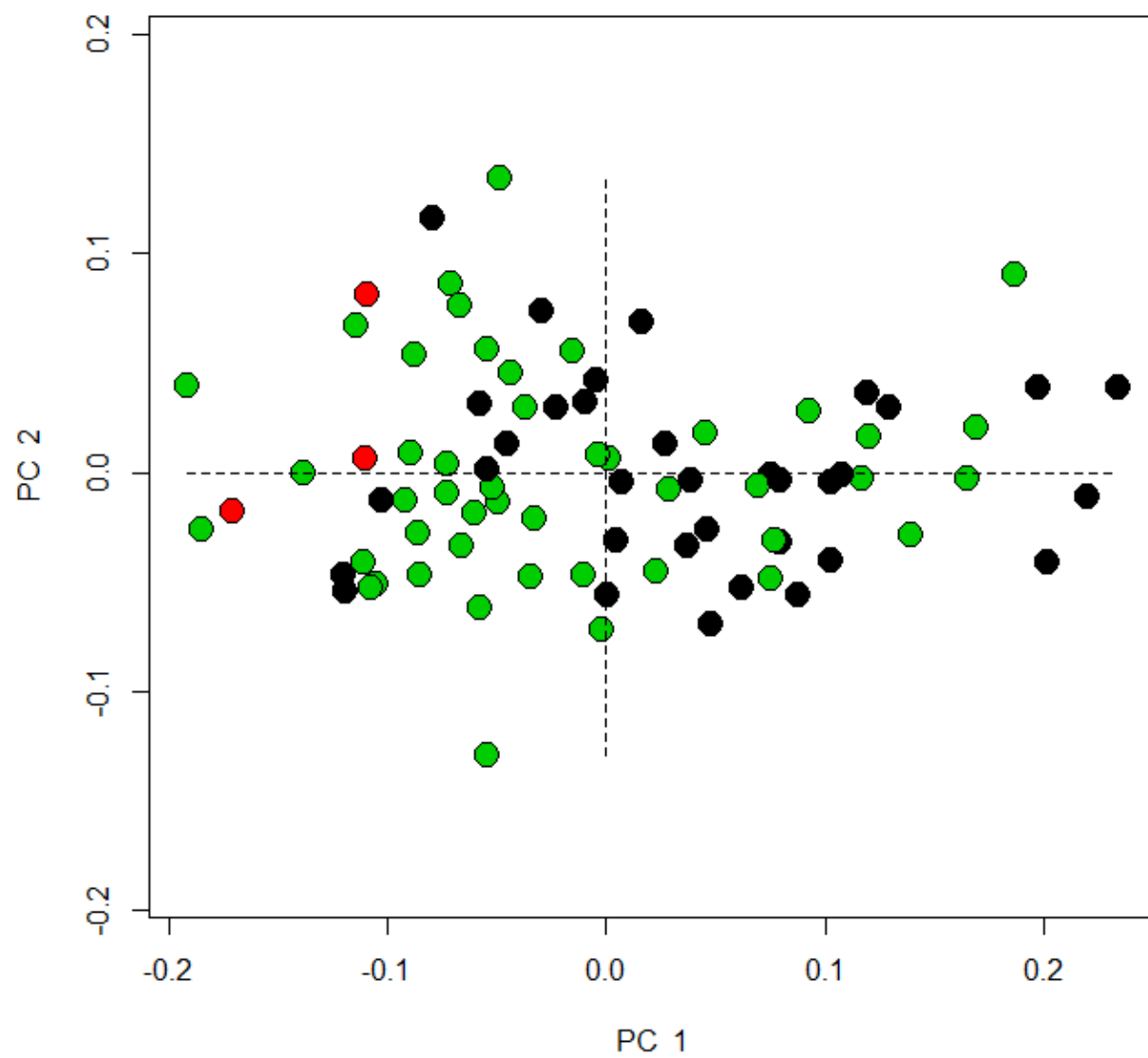


Figure 4.48 PC1 and PC2 for distal femoral homologous landmarks by presence or absence of Schmorl's nodes. (black = no Schmorl's nodes observed, red = not enough vertebrae present, green = Schmorl's nodes observed)

Table 4.36 GLM of distal femoral morphology by presence or absence Schmorl's nodes.

	Df	SS	MS	Rsqu	F	Z	Pr(>F)
Csize	1	0.13421	0.134209	0.075334	7.2835	3.7788	0.001
site	3	0.23011	0.076705	0.129168	4.1628	4.4903	0.001
sex	4	0.07326	0.018315	0.041122	0.9939	0.8626	0.187
Schmorl's nodes	2	0.07164	0.035822	0.040215	1.9441	2.4207	0.008
Csize by site	3	0.04605	0.015351	0.025851	0.8331	0.543	0.284
Csize by sex	4	0.09024	0.022561	0.050656	1.2244	2.0496	0.026
site by sex	6	0.08215	0.013692	0.046113	0.7431	0.6594	0.242
Csize by Schmorl's nodes	2	0.02561	0.012803	0.014373	0.6948	0.5399	0.276
site by Schmorl's nodes	3	0.03463	0.011542	0.019437	0.6264	0.41	0.332
sex by Schmorl's nodes	3	0.06416	0.021387	0.036015	1.1607	2.0027	0.029
Csize by site by sex	2	0.03514	0.017572	0.019727	0.9536	1.6205	0.058
Csize by site by Schmorl's nodes	1	0.02483	0.024831	0.013938	1.3476	1.9757	0.029
Csize by sex by Schmorl's nodes	1	0.012	0.012001	0.006736	0.6513	0.7863	0.212
site by sex by Schmorl's nodes	1	0.01649	0.016491	0.009257	0.8949	1.4099	0.09
Csize by site by sex by Schmorl's nodes	1	0.01179	0.011785	0.006615	0.6396	0.7362	0.243
Residuals	45	0.82919	0.018426				
Total	82	1.78151					

4.2.2 Interpopulation Variation

The second hypothesis is concerned with variation between populations. From this sample of humeral and femoral epiphyseal morphology the null hypothesis that there is not variation between the populations is rejected. All epiphyseal morphologies are explained uniquely and with a confidence level at 0.01 by site. Plots of PC1 and PC2 for the proximal and distal humerus by site are found in Figure 4.49 and Figure 4.50 and results for their GLMs are found in Table 4.37 and Table 4.38. The chart for the proximal femoral epiphysis by site is Figure 4.51 and the same for the distal femur is Figure 4.52 with their respective GLMs to be found in Table 4.39 and Table 4.40.

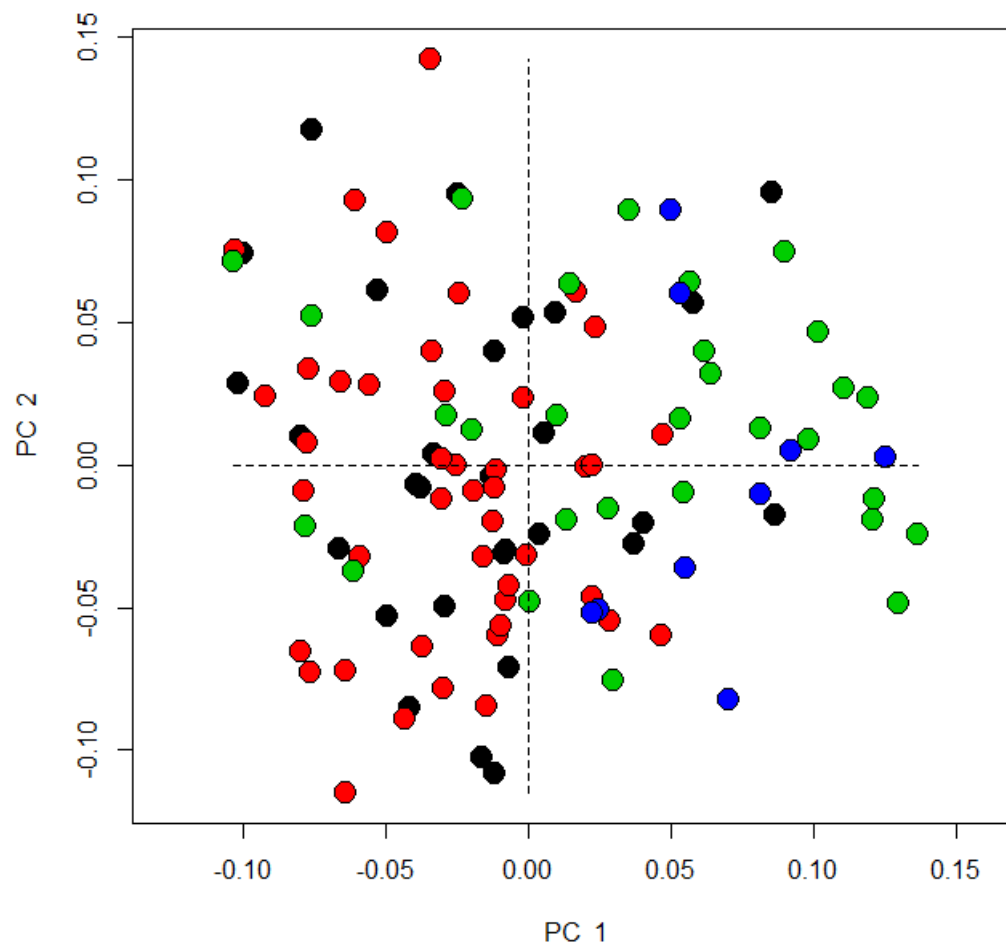


Figure 4.49 PC1 and PC2 of proximal humeral homologous landmarks by site. (black = 3-J-18, red = Coach Lane, green = Fishergate, blue= Hereford)

Table 4.37 GLM of proximal humerus morphology by site.

	Df	SS	MS	Rsq	F	Z	Pr(>F)
Csize	1	0.03057	0.030566	0.017729	2.1755	1.7986	0.026
site	3	0.20712	0.069039	0.120131	4.9138	5.7262	0.001
sex	4	0.06955	0.017386	0.040337	1.2375	1.5236	0.066
Csize by site	3	0.04456	0.014853	0.025844	1.0571	1.0422	0.161
Csize by sex	4	0.05933	0.014832	0.034412	1.0557	1.2531	0.094
site by sex	8	0.08041	0.010051	0.046637	0.7154	-0.2408	0.604
Csize by site by sex	4	0.06641	0.016603	0.038521	1.1817	2.0804	0.02
Residuals	83	1.16616	0.01405				
Total	110	1.7241					

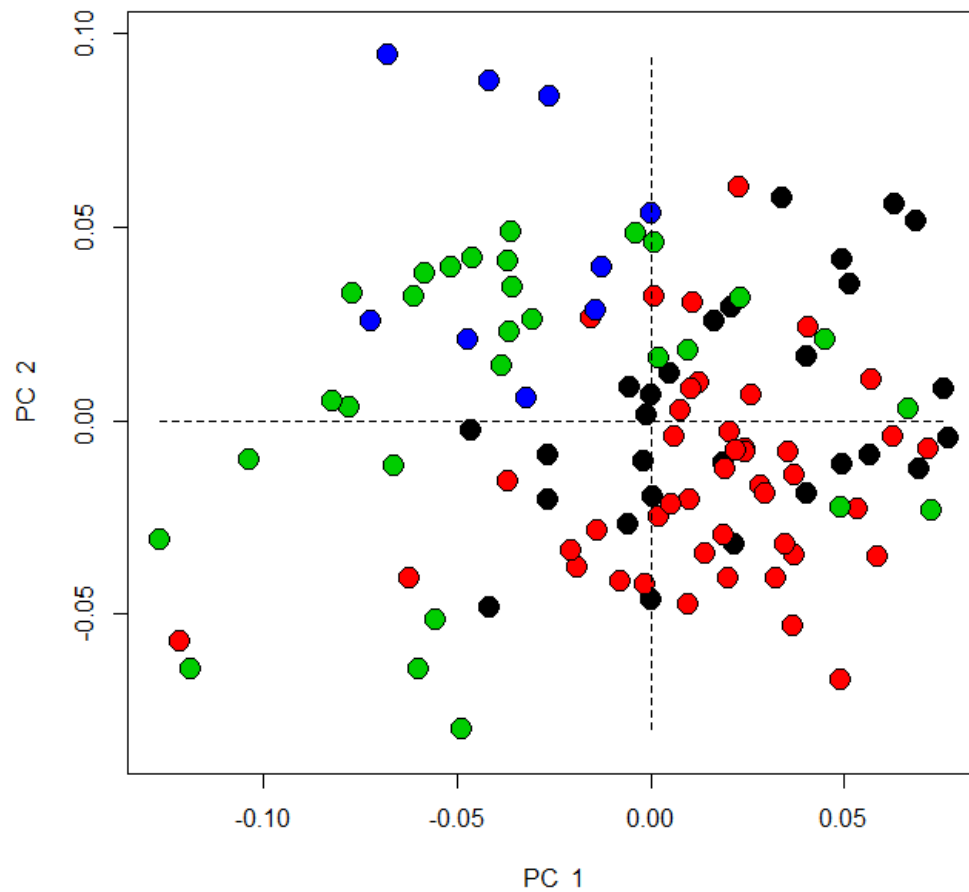


Figure 4.50 PC1 and PC2 of distal humeral homologous landmarks by site. (black = 3-J-18, red = Coach Lane, green = Fishergate, blue= Hereford)

Table 4.38 GLM of distal humerus morphology by site.

	Df	SS	MS	Rsqr	F	Z	Pr(>F)
Csize	1	0.02775	0.027748	0.022109	2.6132	3.0122	0.001
site	3	0.12729	0.04243	0.101422	3.9959	6.7269	0.001
sex	4	0.03267	0.008169	0.026034	0.7693	-0.6028	0.737
Csize by site	3	0.02837	0.009458	0.022607	0.8907	0.2838	0.374
Csize by sex	4	0.04583	0.011459	0.03652	1.0791	1.3892	0.084
site by sex	8	0.07095	0.008868	0.056528	0.8352	0.4075	0.311
Csize by site by sex	4	0.04085	0.010214	0.032552	0.9619	1.2703	0.106
Residuals	83	0.88133	0.010618				
Total	110	1.25505					

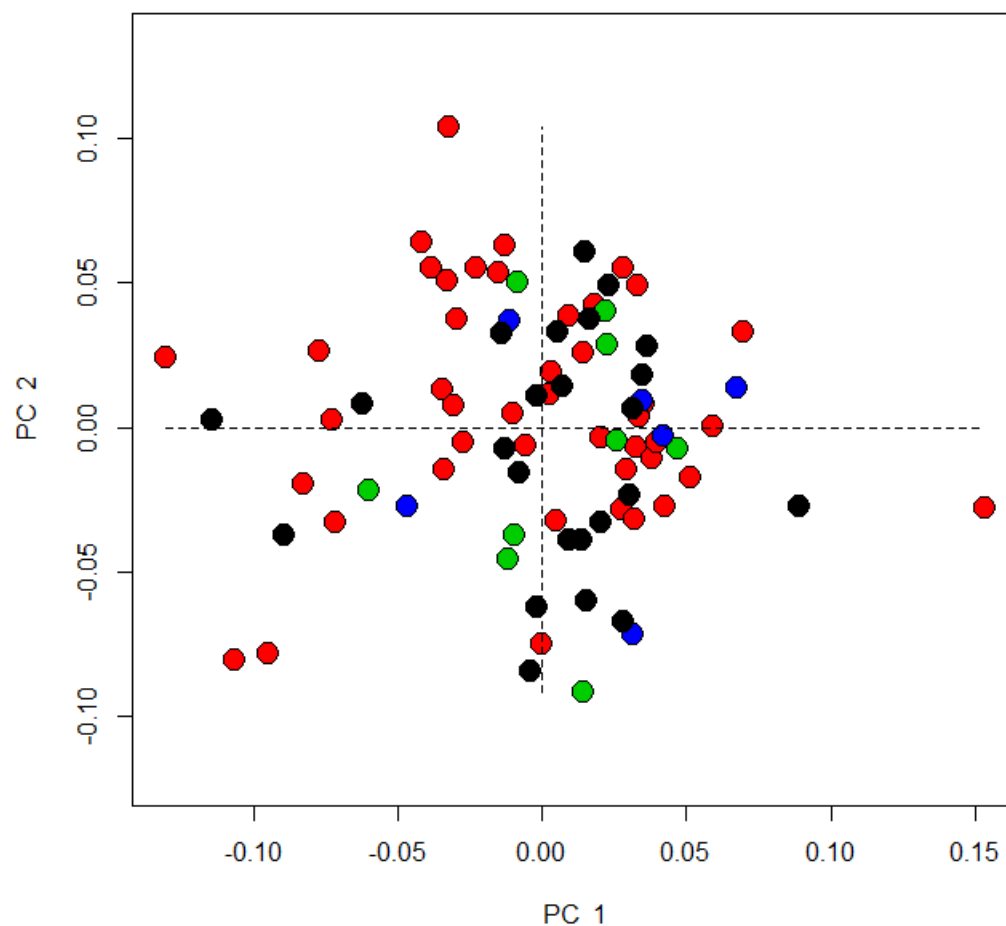


Figure 4.51 PC1 and PC2 of proximal femoral homologous landmarks by site. (black = 3-J-18, red = Coach Lane, green = Fishergate, blue= Hereford)

Table 4.39 GLM of proximal femoral morphology by site.

	Df	SS	MS	Rsq	F	Z	Pr(>F)
Csize	1	0.03399	0.033989	0.028149	2.4744	2.8174	0.001
site	3	0.08567	0.028558	0.070952	2.0791	3.6382	0.001
sex	4	0.05318	0.013295	0.044043	0.9679	0.5024	0.309
Csize by site	3	0.03322	0.011073	0.027512	0.8062	-0.2041	0.577
Csize by sex	4	0.06768	0.016919	0.056046	1.2317	2.0775	0.02
site by sex	6	0.10111	0.016852	0.083739	1.2269	2.6729	0.003
Csize by site by sex	3	0.03594	0.011982	0.029768	0.8723	0.98	0.168
Residuals	58	0.79669	0.013736				
Total	82	1.20749					

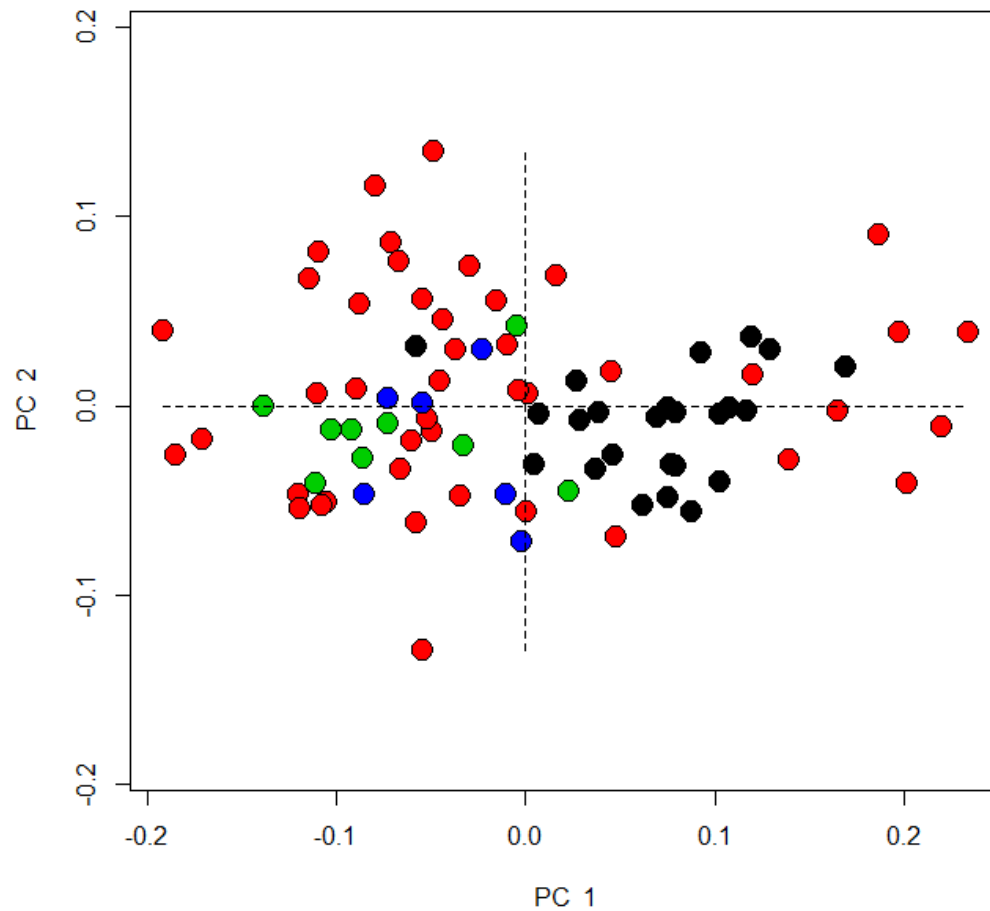


Figure 4.52 PC1 and PC2 of distal femoral homologous landmarks by site. (black = 3-J-18, red = Coach Lane, green = Fishergate, blue= Hereford)

Table 4.40 GLM of distal femoral morphology by site.

	Df	SS	MS	Rsq	F	Z	Pr(>F)
Csize	1	0.13421	0.134209	0.075334	7.0912	3.7615	0.001
site	3	0.23011	0.076705	0.129168	4.0528	4.4785	0.001
sex	4	0.07326	0.018315	0.041122	0.9677	0.7979	0.198
Csize by site	3	0.03817	0.012725	0.021428	0.6723	-0.2496	0.568
Csize by sex	4	0.07914	0.019785	0.044424	1.0454	1.3079	0.11
site by sex	6	0.08125	0.013542	0.045609	0.7155	0.2334	0.391
Csize by site by sex	3	0.04764	0.01588	0.026741	0.839	0.9105	0.184
Residuals	58	1.09772	0.018926				
Total	82	1.78151					

4.2.3 Variation as seen in different parts of the bone

Variation in the humeral epiphyses could only be related to a combination of IVs or site alone. In contrast both the proximal and distal femoral epiphyses showed morphological variation uniquely explained by not only site but also Schmorl's nodes. The proximal femoral epiphysis also could be uniquely morphologically explained by both proximal and distal DJD severity. This makes the proximal femoral epiphysis the most closely related to the IVs examined in this study.

4.3 Discussion

It was expected that site would impact epiphyseal morphology. That prediction was shown to be accurate. Most to all other predictions made in the opening of this chapter were essentially proved wrong. Indicators of childhood stress were expected to have the greatest impact on epiphyseal morphology due to their contemporary timing in development and Schmorl's nodes and DJD severity and OA were added without expecting positive results. However, the only intrapopulation IVs which could uniquely explain morphological variation were DJD severity and the presence and absence of Schmorl's nodes.

4.3.1 Sex

Sex did not uniquely explain humeral or femoral epiphyseal morphology, but the morphology of the proximal humerus and femur were explained by sex and site together. Sex also helped explain morphologies when combined with other IVs. Firstly, it is notable that sex is best able to explain morphology when paired with site underscoring that sexual dimorphism varies between populations (İşcan et al., 1998; Patriquin et al., 2003, 2005; Robinson & Bidmos, 2009; P. L. Walker, 2008). Secondly, sexual dimorphism is seen largely in the proximal epiphysis for both the humerus and femur. A discussion of all the epiphyses and how they could express sexual dimorphism will follow.

While the humeral head is not usually considered a predominate indicator of sexual dimorphism morphological aspects of the proximal humerus have been shown to be sexually dimorphic. Kranioti and colleagues showed that perhaps the best indicator of sex in the humerus for their population of contemporary individuals from Crete was the relative size of the greater tubercle which was more pronounced in women than in men (2009). They suggest that a possible aetiology is the sexually dimorphic development of the supraspinatus muscle. This is likely a contributing factor to sexual dimorphism evidenced here. The greater tubercle and intertubercular sulcus are part of the rotator cuff and play host to numerous other muscle attachments including the infraspinatus and teres major and

teres minor. Additionally, the intertubercular sulcus exists to cradle the tendon for the long head of the biceps brachii. The supraspinatus muscle is important to the development of sexual dimorphism in the relative pronouncement of the greater tubercle of the proximal humerus and it is part of a suite of musculature which could also contribute to the morphological variation associated with sexual dimorphism. In fact, due to the possible involvement of the intertubercular sulcus and the relative size and use of the muscles another likely contributor to morphological variation would be the biceps. If the argument for sexual division of labour as contributory to sexual dimorphism were to be inferred (İşcan et al., 1998; Kranioti, Bastir, et al., 2009; Ruff, 2005) then the structurally delicate but large biceps brachii which is primarily responsible for the flexion of the forearm would likely show and cause some sexual dimorphism. Relative hypertrophy of the biceps' long head could explain the sexual dimorphism seen in the relative position of the intertubercular sulcus. Additionally, the relative shape of the intertubercular sulcus may reflect either the general orientation of the torso and shoulder or the relative depth of the humeral head.

Sexual dimorphism was not found in the distal humerus in this study, but it has been evident in other studies. Two studies found the olecranon fossa and medial epicondyle as consistent indicators of sexual dimorphism even before complete fusion of the medial epicondyle (T. L. Rogers, 2009; Vance & Steyn, 2013). Rogers (2009) describes the female olecranon fossa as ovoid and M-L oriented and the male olecranon fossa as triangular. Vance and Steyn (2013) who performed a GMM analysis on the distal humerus, explain that the triangular appearance of the male olecranon fossa is due to the superior point of the fossa being more superior in males than females. The difference between the analysis here and Vance and Steyn's conclusions could be due simply to variation in sexual dimorphism between populations. Another explanation however, is the choice of landmarks in each study. This underscores the importance in GMM of choosing landmarks appropriate to the research question. Vance and Steyn (2013) used two-dimensional landmarks and were specifically interested in the olecranon fossa whereas this study took a more generalised approach and use three dimensional landmarks. Using the same landmarks may have produced similar results. However, here and for Rogers (2009) and Vance and Steyn (2013) the olecranon fossa is sexually dimorphic.

The proximal femur when site was considered did show some sexual dimorphism. Anderson and Trinkaus (1998) did not find sexual dimorphism in the angle of the femoral neck. The valgus angle is necessary for bipedal locomotion and were it to be disrupted by an especially wide pelvis in females or an especially narrow pelvis in males it would have to be mitigated with angle, shaft rotation, or more

likely some combination of both. Previous studies have frequently found particularly allometric sexual dimorphism in the proximal femur but most state that sexual dimorphism is more consistent in the distal femur (Alunni-Perret et al., 2008; Mall et al., 2000; Sakaue, 2004; Stevens & Viðarsdóttir, 2008). This study did not find that allometry explained sexual dimorphism, but when size and sex were considered together they did explain proximal femoral morphology.

The distal femur in was not very sexually dimorphic in this study. A possible reason for this is that the knee is weight bearing and develops during adolescence possibly before the individual has expressed their adult weight. Differential development in females and males may favor females with bigger knees simply because as children and adolescents females are larger or about the same size as males although their joint development is timed slightly earlier than that of their male counterparts (M. Schaefer et al., 2009a). The lack of variation in the distal femoral epiphysis relative to the proximal suggests that there must be corresponding morphological variation likely in the diaphysis to resolve the valgus angle.

4.3.2 Age

Development of epiphyses and thus the period of the human lifespan wherein the epiphyses might morphologically change ends in early adulthood and literature indicates no real alteration with age outside of incidents of trauma or erosive arthroses (Drapeau & Streeter, 2006; Frost, 1999; Hamrick, 1996). As this study included no children or adolescents under the age of seventeen and determined by epiphyseal fusion, it was expected that there would be no consistent change in the homologous landmarks of the epiphyses with age. This expectation was fulfilled in that age never uniquely explained epiphyseal shape. However, when interactions were considered morphological variation did correlate with age in all elements.

Particularly in the proximal femoral epiphysis age when grouped by size or sex did seem to explain morphological variation. It is puzzling that the epiphyseal morphology should vary with age in a set of adults however the proximal distal divide may offer clues as to why this is happening. For both the humerus and femur the distal epiphysis forms and fuses prior to the proximal epiphysis with some areas being moderately incomplete potentially into an individual's early twenties (Scheuer & Black, 2000). Additionally, epiphyseal fusion and formation varies temporally between females and males with females completing development earlier. There is also some speculation that for craniofacial morphology the female ontogenetic trajectory may be arrested to become paedomorphic rather than diverging in some cases of sexual dimorphism (O'Higgins & Jones, 1998). Whether the same ontogenetic

trajectories exist in the post-crania is uncertain but possible. Along the same line of reasoning, populations which are smaller in stature tend to reach maturity more swiftly than those which are tall (Millien et al., 2006). When this is adaptive it may relate to availability of resources and sexual maturity, but it may also simply be a byproduct of growth. If an individual is genetically predetermined to be tall and there are no major physiological insults then they may enjoy a longer period of growth. For someone who is predisposed to be short they may grow at the same rate as a taller individual, but simply stop growing earlier. As the proximal epiphyses are more related to shape variation than the distal epiphyses it is possible this shape variation represents the last phase of development.

Other possibilities for the variation of shape with age when related to sex and size include disease process in particular osteopenia and osteogenic processes. Osteopenia would first and most severely affect the trabeculae of the bone located in the epiphysis. Conceivably the outer table of bone might then be altered to adapt to the weakening trabecular bone. Likewise with osteogenic conditions enthesal changes and possibly osteophytes could alter the morphology of the epiphysis. Both of these conditions are sex and age linked which could possibly explain the link between age, sex, and shape. To explain size in this context one must consider the architecture of the bone as well as the size and strength of the surrounding soft tissues. The larger the bone the more stable its physical architecture and the less malleable its epiphyseal morphology. Additionally, whilst the details of both Roux and Wolff's theories are still debated their general veracity is not and bone is reactive (O. M. Pearson & Lieberman, 2004; Ruff, Holt, & Trinkaus, 2006). The larger the muscle and weight of the person the more robust the bone and its muscle attachment sites will be thus potentially altering morphology over time.

4.3.3 Childhood indicators of stress

Neither LEH nor CO could explain morphologies for any of the epiphyses studied. However, when interactions were considered for size, site, or sex then indicators of childhood stress could explain epiphyseal morphology.

Rates of LEH and cribra orbitalia are variable between the two population sets. Cribra orbitalia is more prevalent in the Sudanese population. Given the distribution of correlation with morphological variation it is possible that the pathogenesis of cribra orbitalia is relevant in reference to morphological variation. The Sudanese population was more likely than any of the English populations to be exposed to malaria and given historical reports on Sudanese diet (rich in animal protein and therefore B₁₂ and iron) malaria is the most likely cause of cribra orbitalia for the Sudan (Edwards, 2004; Stuart-Macadam, 1985; P. L. Walker et al., 2009; Wapler et al., 2004). In the English populations malaria is less likely due to the

colder climate suggesting that cribra orbitalia in those populations was due more to severe dietary stress, malabsorption, or loss of nutrients via diarrhoea (Gowland & Western, 2012). Other parasites may also be responsible, but given the crowded and often unsanitary conditions particularly for the individuals interred at Coach Lane and Fishergate cemeteries the most likely cause of cribra orbitalia would be nutritional stress possibly exacerbated by chronic diarrhoea. This could explain the relative prevalences of CO, and also accounts for why CO may explain the morphology of the proximal humerus and femur when paired with site.

The situation is however reversed for LEH. This may again pertain to differential pathologies or stressful events shaping LEH as LEH has diverse aetiologies particularly when compared to cribra orbitalia. The rate of Hansen's disease for the Sudan was anecdotally higher than that of the English populations and it is further possible that other pathogens were more prevalent in the Sudan. Unfortunately, because LEH has such diverse aetiologies speculation on this point is less useful. It is notable that prevalence rates for LEH in females and males for both population sets are reversed. Only 38.9% of Sudanese females showed LEH compared to 60% of males and in the English populations 72.1% of females had LEH whereas only 63.4% of males did. This may suggest some cultural effect like preferential distribution of food or exposure to pathogens or stress due to expectations of work and play even for children. Alternatively there may have been a bias within the data collection itself as many of the teeth from 3-J-18 were broken. The difference could also be due to environmental effects or even population related ontogenetic effects.

4.3.4 Joint disease and Trauma and Schmorl's Nodes

Trauma did not uniquely explain morphology for any of the epiphyses but joint disease and the presence or absence of Schmorl's nodes both were able to explain morphological variation in the proximal femur, and Schmorl's nodes could also uniquely explain morphology in the distal femur. If the individual survived long enough, while joint disease is permanent and degenerative, the trauma may have largely remodeled. Trauma severe enough to alter locomotive patterns would probably also entail a period of immobility. There might be cortical wasting, but immobility could prevent sympathetic injury and therefore any remodeling to uninjured areas to compensate for the impact in mobility. Furthermore, the trauma would have had to be timed so that the individual was young enough that their epiphyses were still morphologically susceptible to influence and the individual would have had to have died after the morphological change occurred but before the trauma itself was fully healed.

Novak and Šlaus (2011) demonstrated that Schmorl's nodes may heal, meaning they may not readily appear in older individuals and may not have the necessary impact on mobility to alter epiphyseal morphology. Wentz and Grummond (2009) observed Schmorl's nodes in a young Scythian male and theorised they, in conjunction to trauma to his calcanei, were due to frequent mounting and dismounting. Pálfi's (1992) work seems to support this in part as he found considerable arthritis in joints associated with horseback riding among primarily the males in a population of 10th c. Hungarians. Pálfi also found enthesal changes for attachments associated with the pectoral muscles, but severe osteological changes were reserved for the males in his population. This could mean that female bone is less likely to react morphologically – which could obscure results in a study like this where male and female results are frequently pooled. Further to this study, the individuals with severe appreciable osteoarthritic and enthesal changes would have spent their entire adult life mounted. Pálfi's population and nomadic horse people in general may represent an extreme in mobility and robusticity not seen in agricultural or sedentary populations. Conversely, Hawkey (1998) conducted an osteobiography on an impaired individual whose arthritis was severe enough to prevent him from walking. Exacerbating if not causing his immobility, this individual had severe enthesal changes suggesting that although he was, as Hawkey suggests, largely immobile and this is likely reflected in his cortices, it may not have been reflected in his epiphyseal morphology.

It seems that this morphological variation explained by Schmorl's nodes and DJD severity has to do with mobility and locomotion as the hip and the knee are weight-bearing and their anatomy is crucial to bipedal locomotion. Timing of these IVs is disparate and does not overtly correspond with development of the epiphyses (M. Schaefer et al., 2009a). Schmorl's nodes are most common in young adults and DJD and OA are degenerative pathologies which can effect children but are more commonly seen in adults with increasing age (Jurmain, 1999; Šlaus, 2000). There is evidence that joints, especially in the legs, develop during preadolescence in response to body weight (Drapeau & Streeter, 2006; Frost, 1999; Hamrick, 1996, 1999). So particularly where DJD and OA are considered related to compounding lifetime stress epiphyseal shape and DJD could be considered symptomatic of the same underlying problem that being poor health and poor nutrition in childhood (Klaus et al., 2009). Similarly, if Plomp and colleagues (2015) are correct regarding their "Ancestral shape hypothesis," and individuals are predisposed to Schmorl's nodes based on the shape of their vertebrae then either those same individuals may have similar genetically predetermined morphology to their hips and knees or the impact of the differently shaped vertebrae would be sufficiently continuous from such a young age that their epiphyseal morphology is affected.

4.3.5 Interpopulation Variation

Epiphyseal morphology showed interpopulation variation in all elements examined in this chapter. Sex when paired with site only explained proximal femoral morphology. Morphological variation between populations is well documented (Alunni-Perret et al., 2008; Benjamin Miller Auerbach, 2008; Relethford, 2009, 2010; Relethford & Harpending, 1994; Stevens & Viðarsdóttir, 2008). That epiphyseal morphology would be dictated at least in part by population is not surprising. Developmental timing of the ossification of the epiphyses also suggests that their morphology is genetically predetermined to some extent and population dependent (Frost, 1999; M. Schaefer et al., 2009a). Particularly in context of the results regarding childhood stress disorders which develop closest to concurrently with the epiphyses yet have little effect on their shape there must be a strong genetic component to epiphyseal shape. This likely comes at the cost of other developmental processes like longitudinal growth of the bone or cortical development and deposition (Mays, Ives, et al., 2009). However, it is widely accepted in bioarchaeology and forensic sciences that sex estimation must occur within the context of population because sexual dimorphism is population dependent (Bulygina et al., 2006; İşcan et al., 1998; Patriquin et al., 2003, 2005; Robinson & Bidmos, 2009; P. L. Walker, 2008). The epiphyses of the femur are the last to completely form and fuse completely onto the diaphysis, but the distal epiphysis generally completes development later than the proximal epiphysis. Additionally, the final stages of development in the humeral epiphyses also occur during adolescence. These are however gross interpretations of the epiphyses including all parts at once. They may demonstrate ontogenetic modularity that allows for the proximal femoral epiphysis to be more morphologically sensitive to sex. Alternatively, there may be indications of sexual dimorphism in the epiphyses that the landmarks chosen for this study were unable to show. While site did not help to explain why sexual dimorphism is not appearing in this set, it did have a strong showing. R^2 values were over 10% for all but the proximal femur and morphological variation by site dominated the first PC.

4.4 Conclusion

Morphological variation in the epiphyses did not generally behave as predicted. Site was expected to explain morphological variation and did. However sex, which should have had some impact, did not. The most interesting result from this chapter is that Schmorl's nodes and the severity of DJD could explain femoral epiphyseal morphology in spite of the fact that both Schmorl's nodes and DJD or OA would form after epiphyseal shape was fully developed.

5 Diaphyseal Morphological Variation as Quantified by Surface Semilandmarks

5.1 Introduction

This chapter investigates the relationship between the morphology of the surface of the diaphysis and inter and intrapopulation variation. As with the homologous epiphyseal landmarks, these data will be used to illustrate the relationship between morphology and intrapopulation variation including sex, age, indicators of childhood stress, presence or absence of joint disease, and the presence or absence of trauma. This addresses the first hypothesis regarding within population variation, and the second hypothesis regarding variation between populations. The final hypothesis regarding morphological variation in different parts of the bone will be left to the Discussion chapter (Section 7) once morphological variation for all parts of the bone have been reported.

This thesis attempts to expand upon and quantify concepts from Wolff's and Roux's laws. I am examining whether relationships exist between shape and factors like sex, age, and pathology. This concept of bone reacting to stressors has been proven repeatedly and is used frequently in the archaeological and evolutionary anthropological literature to discuss such subjects as lifestyle (Ruff, 2000; Ruff et al., 1994; Shaw & Stock, 2009a; Sparacello et al., 2011b; Sparacello & Marchi, 2008; Stock & Pfeiffer, 2004), handedness (Shaw & Stock, 2009b; Stock et al., 2013; L. A. B. Wilson & Humphrey, 2015), stress (Drapeau & Streeter, 2006; Ruff et al., 1994; Schwartz et al., 2013), and sexual division of labour (Bridges, 1989a; Ruff, 2005). In the previous chapter I showed that intrinsic and extrinsic factors may be related to epiphyseal morphology, but the relationship is usually not strong and usually only appears when other factors are considered. For example, LEH alone may not be related to epiphyseal morphology, but if the individual's sex is also considered a relationship does exist in the proximal epiphyses. I also discussed that this is probably a result of the development of the epiphysis and the relative amount of impact of muscle strain on it. The diaphysis, however, is very different and theoretically is continually impacted by strain, stress, pathology, hormonal change with age, nutrition and so forth. Cross-sectional studies have proven some level of correlation between age, sex, and activity level and cross-sectional morphology, and here I will quantify the same in regards to surface diaphyseal morphology (See Section 5.2.1 for results in intrapopulation variation and Section 5.2.2 for results on interpopulation variation).

Diaphyseal morphology or in fact total bone morphology is usually discussed in terms of beam theory (Lieberman et al., 2004; Shaw & Stock, 2009a; Stock & Pfeiffer, 2004; Yamanaka et al., 2005). Beam theory treats the bone as a cylindrical shape to which standard mechanics may be applied to determine factors such as bending resistance and strength. Cross-sectional data is closely tied to beam theory in that beam theory suggests that cross-sectional morphology will change in response to various strains on the bone to avoid fracture at certain “moments” of the bone. There are several issues with the necessary assumptions in beam theory which may be summed up as follows: beam theory assumes that the bone is cylindrical in shape which it is not, beam theory also assumes that the sole purpose of the bone is mechanical which as previously discussed ignores bone as a metabolic organ, and finally, beam theory assumes that morphological variation exists solely to mediate strains and avoid fracture. These concerns aside, beam theory does highlight the necessity of considering the morphology of the entire bone and addresses both axial and torsional strain (Ruff, 2000). Whilst cortical studies have been remarkably effective at determining reliable correlation between morphology and many demographic factors considered here – elucidated fully in the first two research questions – cross sectional morphology even where multiple sections of the diaphysis are considered does not describe the morphology of the diaphysis in its entirety. By comparing the correlations between morphological variation of the diaphyseal surface with population, age, sex, pathology and the variation of the cross-sectional morphology this study will examine whether or not the whole morphology of the diaphysis is consistently changed with the variables in question to a greater or lesser degree than that of the cross-section.

The first intrapopulation variable to be considered is sex. Sexual dimorphism, particularly in the femur may be represented by torsion in the diaphyseal curvature. The torsion of the femur resolves the valgus angle at both the proximal and distal epiphyses. This torsion would be almost impossible to capture with homologous points: it could only be represented by the relative position of the proximal and distal epiphyses which, due to their distance from one another, would be subject to mathematical distortion during Procrustes adjustment and therefore be less reliable. But from a biomechanical standpoint this resolution of the valgus angle is fundamental to human bipedalism and reproduction. In contrast it could be argued that the humeral diaphysis might be less sexually dimorphic as any sexual dimorphism in this area would be secondary and due primarily to general robusticity and hormonal effects. However, the diaphysis of adults is morphologically sensitive to any number of environmental effects. Robusticity or general size and musculature may have an additive effect particularly on the

morphology of the humeral diaphysis which – in addition to being unrelated to parturition – is also not loaded for locomotion.

The second intrapopulation variable to be considered is age. The more plastic and reactive nature of the diaphysis in adults, particularly when compared to the very static epiphyses may also show more morphological diversification with age. While the epiphyseal morphology would be predetermined for life at a point during childhood or adolescence (Drapeau & Streeter, 2006; Frost, 1999; Hamrick, 1999), the diaphysis continues to remodel throughout adulthood and can be very reflective of environmental conditions and lifestyle. While health in adolescence and early adulthood does seem to have a large influence on cortical thickness and morphology, peak BMC is not reached until well into adulthood (Lieberman et al., 2004; Niinimäki, 2011; Rhodes & Knüsel, 2005; Ruff et al., 1994; Stock et al., 2013; Zumwalt, 2006). Age also has a variety of secondary effects. As stated repeatedly, the severity of osteopenia is primarily age related and osteogenic conditions are more likely to increase in prevalence and severity with age (Agarwal & Stout, 2004; Jurmain et al., 2012). Additionally, the older the individual the longer any pathology or environmental condition will potentially have to alter the morphology of the bone. This means that hormonal changes and changes in activity levels are more likely to be reflected with age in the morphology of the diaphysis.

By the same rationale however childhood indicators of stress – with the exception of rickets – are less likely to consistently influence diaphyseal morphology. This addresses the third variable relating to intrapopulation variation. If the plasticity of the diaphysis is sensitive to lifestyle, nutritional, and hormonal changes throughout childhood and adulthood then morphology is likely to continually remodel since the incident of childhood stress. The conditions necessary for childhood indicators of stress such as low marrow capacity or enamel formation are ontological and so only occur early in an individual's life. In contrast, diaphyseal remodeling continues throughout. This is in direct opposition to what was expected for the epiphyses, but contrary to expectations, the epiphysis showed little morphological variation consistent with indicators of childhood stress. Two notes should be made here. Firstly, in cases of extreme childhood stress and malnutrition morphological variation, particularly allometric variation in the diaphysis would be expected due to repeated interruptions in growth (McDade et al., 2008). Secondly, cribra orbitalia and LEH have diverse aetiologies and may not be exclusively linked to malnutrition but rather also to infection, parasite load, genetic disease, psychological stress and so forth (Gowland, 2015; Gowland & Western, 2012; Sullivan, 2005; P. L. Walker et al., 2009). However, as noted previously whilst childhood health may have a more profound effect on

the epiphysis it does have some effect on the diaphysis, particularly on the cortical architecture. Depending on precisely the mode of endosteal and subperiosteal deposition on bone with age, childhood stress could easily be responsible for the basis of diaphyseal morphology which continues regardless of deposition and resorption into adulthood or is erased at some point during adulthood due to the variation in remodeling with age. This is emphasized in cases of residual rickets. The bone will remodel, but deformations may persist through adulthood.

It is also possible that so called “degenerative” pathologies, or pathologies acquired later in life may have an effect on the diaphyseal morphology. This is the fourth variable considered within the question of intrapopulation variation. Some pathologies or conditions which have an osteogenic or osteopenic component are even expected to correspond with morphological variation. For example, an older individual with vertebral compression fractures likely suffers from osteopenia or even osteoporosis and should evidence thinning in their cortex which may be evidenced in the general shape of the diaphysis. An individual with DISH, AS, or possibly just OA might have a higher number and severity of enthesal changes and for these individuals, musculature may be affected by the disease. These factors could easily alter the diaphyseal morphology of the humerus and femur. However, it is also possible that even if these changes are occurring, the variation will be inconsistent. That is, individuals with osteopenic or osteogenic pathologies may show morphological variation distinguishing them from the unaffected population but not distinguishing by pathology. Variation resulting from pathology could also interact with robusticity, lifestyle, and environment in such a way that such changes do not distinguish the individual even from the normal range of morphological variation.

Lifestyle, environment, and nutrition should have much more clear effects on the diaphyseal morphology meaning that there should be some interpopulation variation in morphology. The populations sampled in this study do not have a great temporal divide, but are all from distinct towns and cities (particularly the Sudanese individuals), and there is also some difference in the demographics between the skeletal samples. These populations are likely to have experienced different environments, levels of crowding, daily activities, and pathological load and therefore may be expected to have morphological variation in the very plastic long bone diaphysis consistent with their population differences.

5.1.1 Intrapopulation Variation: Morphological Variation in the Diaphysis with Sex

Sexual dimorphism in long bone diaphyseal morphology - results for which may be found in Section 5.2.1.1 with discussion in Section 5.3.1.1 - may be broken up into three different components,

those being the direct effects of hormones on morphology, the indirect effects of how muscle and bone size may influence bone remodeling thereafter, and the far more cultural effect of sexual division of labour (this latter point deserved mention but is far beyond the scope of this thesis).

The rates and location of osteoblastic and osteoclastic activity are heavily influenced by hormones. The female life cycle particularly in regards to menarche, maternity, lactation and menopause are often cited as particularly important for the regulation of bone remodeling (Bridges, 1989a; Rho et al., 2002). While there may be somewhat complimentary patterns in male hormonal flux males do not experience pregnancy and arguably have a less pronounced “andropause,” or lessening of hormonal activity with age and therefore have less metabolic demands on their skeletal structure (Agarwal et al., 2004; Kaastad et al., 2000). The rate of remodeling or deposition and resorption is dependent on age and hormones (Ruff, Holt, & Trinkaus, 2006) which means particularly for females it may be tied heavily to hormonal flux during life events like maternity. Females and males have been shown to have the same amount of subperiosteal deposition, but females seem to have more resorption (Ruff & Hayes, 1982). Additionally, Ruff and Hayes (1982) have shown that the position in the bone of subperiosteal deposition seems to be sex specific as well, at least in the femur with females putting down more bone in the proximal femur and males putting down more bone –and losing less – at midshaft. This sexually dimorphic difference in location should be present in the diaphyseal surface semilandmark results, but it will probably be more notable in the cross-section at midshaft results.

Hormonal influence aside sexual dimorphism will cause different forces to act on slightly different areas of the bone due to differences in bone size and muscle size and strength (Ruff, Holt, & Trinkaus, 2006). This issue becomes very difficult to separate from hormonal influence on deposition and resorption because the two are very closely related, and because cell responsiveness – or the amount of strain needed to trigger osteoblastic activity – is largely dependent on previous strain and bone shape and form (Ruff, Holt, & Trinkaus, 2006). An example of the very complicated relationship between bone morphology, hormones, and size can be seen in the complexity surrounding enthesal changes. Enthesal changes can change the morphology of the diaphysis and the epiphysis. However, they are multifactorial in cause. The general consensus is that enthesal changes will occur with greater frequency and severity in older males (Cardoso & Henderson, 2010; Foster et al., 2014; Jurmain et al., 2012; Nolte & Wilczak, 2012; Rabey et al., 2015). Nolte and Wilczak (2012) found that enthesal changes were more sexually dimorphic than linear metrics. However, in a previous study Wilczak (1998) also found that there was no sexual dimorphism in enthesal changes on the humeral head for the

individuals included. She notes however, that in her 1998 study the age ranges were such that the males might not have been old enough to evidence sexual dimorphism in enthesal changes. Other literature suggests that enthesal changes are sometimes pathological or can simply arise from significant use of the muscle (Cardoso & Henderson, 2010; C. Y. Henderson, 2009; Jurmain et al., 2012). However, particularly in the last case significant use of the muscle would also be determined by preexisting conditions such as size of the bone and size and strength of the muscle.

Use of the muscle and therefore robusticity of the bone are also influenced by culture. Numerous studies have cited a sexual division of labour as a possible contributing factor to differences in bone shape and form or asymmetry particularly in the humerus (Bridges, 1989a; Sparacello & Marchi, 2008; Stock et al., 2013; Stock & Pfeiffer, 2004). Asymmetry is of particular use when studying sexual division of labour because although labour may be divided the type of labour may cause a higher or lower degree of asymmetry. For example, Bridges (1989a) showed that agricultural Amerindians could be differentiated from earlier hunter gatherers because the females showed less humeral asymmetry. This was not because females were doing less labour and, in fact, it could be argued that agriculturalism required more physical labour than before, but the tasks these women were engaging in employed both of their arms relatively equally. Stock and colleagues (2013) had similar observations when comparing the relative asymmetry rates of 18th c. British populations, Medieval British populations, several hunter-gatherer populations, and, chimpanzees. Their results showed a high degree of sexual dimorphism and asymmetry in the latter two groups with significantly less in the former groups. This study does not address asymmetry and so it is expected that some of these patterns will not be present, however the placement of strain does matter and so sexual division of labour could influence diaphyseal morphology.

For this study, the reason for sexual dimorphism is less important than its presence or absence. Given previous studies, the presence or absence of sexual dimorphism in medieval and postmediaeval populations is likely due to the first two factors noted here. That is, sexual dimorphism would be a result of sex hormones and the secondary characteristics resulting from the influence of those hormones.

5.1.2 Intrapopulation Variation: Morphological Variation in the Diaphysis with Age

This study includes only adults with fused epiphyses. In the previous chapter, it was shown that this focus on adults resulted in little variation in the morphology of the epiphyses, but as noted in Section 4.1.2, the diaphysis continually remodels throughout life and its plasticity is more likely to morphologically alter with age in addition to a variety of other factors. However, the equipment and software necessary to conduct studies with three dimensional surface semilandmarks has only recently

become available. Therefore, very few studies have been conducted on the morphology of the diaphyseal surface of long bones and so most literature cited in this chapter will in fact concern cross-sectional morphology, curvature, or at best 2D morphology.

Trinkaus and colleagues (1994) describe the development of the adult diaphysis as its departure from the juvenile cross-sectional circle morphology to a more adult ovoid morphology. They also note that childhood development and nutrition should influence and even be predeterminate of future cortical deposition (Trinkaus et al., 1994). (It is notable however that in this case the deposition is endosteal rather than sub-periosteal and there is some dissent in the literature about when in an individual's life and where sub-periosteal versus endosteal deposition or resorption occur (Mays, Ives, et al., 2009; O'Neill & Ruff, 2004; Ruff et al., 1994; Ruff & Hayes, 1982; Sparacello & Pearson, 2010).) Ruff and colleagues (Ruff, Holt, & Trinkaus, 2006) expand on Roux's law (more popularly considered Wolff's law) by saying that the history of the bone – most pertinently the loading history – matters. This is supported by studies of juvenile rates in which the loading of their bones during growth changed their morphology (Ruff, Holt, & Trinkaus, 2006). Furthermore Ruff and colleagues (2006) and numerous other authors (Lieberman et al., 2004; Mays, Ives, et al., 2009; Niinimäki, 2012; Rhodes & Knüsel, 2005; Stock & Pfeiffer, 2004) have noted that while asymmetry is found in the humeri of all competition level tennis players regardless of the age they began playing, those who started younger have more asymmetry.

During adulthood diaphyseal growth continues particularly in early adulthood. Early adulthood is when the diaphysis is most sensitive to strain, but deposition and resorption will occur at different sites and at different rates dependent on age and hormones (Ruff, Holt, & Trinkaus, 2006). Although most subperiosteal deposition appears to occur before adulthood the bone will adjust to different levels of strain and as suggested in the previous section, enthesal changes which could alter the morphology of the diaphysis occur more frequently in older males (Nolte & Wilczak, 2012).

5.1.3 Intrapopulation Variation: Morphological Variation in the Diaphysis with Pathology

While factors like age and sex are likely to play a large role in determining diaphyseal morphology, pathologies may also have an effect. As mentioned earlier, childhood stress (rickets aside) is not likely to have a significant effect on diaphyseal morphology unless it was so severe as to alter the length of the long bones. This is simply because childhood stress would not be entirely concurrent with the development of the diaphysis. If the individual experienced an instance of malnutrition or disease as a child but that incident was not prolonged or severe, then while it might result in traces such as cribra orbitalia or LEH, it may not affect the diaphyses, simply because these remodel frequently and to a

greater degree in adolescence and early adulthood (Ruff & Hayes, 1982). However, other pathologies are very likely to alter diaphyseal morphology either directly with hormonal alterations that would cause an altered rate of deposition or resorption, or indirectly by redistributing the location of strain on the bone as the individual attempts to compensate for the pathology or trauma.

Conversely, Barker (2004) observed that LEH prevalence was positively correlated with heart disease. Other authors have shown that childhood stress influences metric measurements usually shown in the length of the bone and other aspects of the individual's health (Armstrong et al., 2009; Blom et al., 2005; Boldsen, 2007; McEwan et al., 2005; Schug & Goldman, 2014; Šlaus, 2000; Watts, 2015). These effects include endocrinal, hormonal, metabolic, and cardiovascular consequences which may even persist for generations (Gowland, 2015). Studies of individuals with severe childhood stress show thinner than usual cortices or less optimal BMC (McEwan et al., 2005; Rho et al., 2002; Sparacello et al., 2016). This could translate to morphological variation in the diaphysis.

Diaphyses remodel throughout an individual's life (Drapeau & Streeter, 2006; Lewis, 2006; Waldron, 2009). If childhood stresses impact adult diaphyseal morphology then degenerative diseases and trauma should also explain the morphology to some degree as well. There is also the possibility that diaphyseal morphology causes or is coincidental to particularly degenerative diseases. If diaphyseal structure causes excessive wear to cartilaginous joints then osteoarthritis or degenerative joint disease may be related to diaphyseal morphology. This appears to be an entirely biomechanical consequence, but there could also be a hormonal or endocrinal aspect where resorption and deposition is altered at the same time as excessive cortisol release damages or thins cartilage.

Schmorl's nodes are theorised by Peng and colleagues (2003) to be caused by herniated intervertebral disks. They are also observed most prevalently on younger adults which would suggest that particularly where Schmorl's nodes are present on older or middle aged individuals there should also be some alteration in the morphology of the femoral diaphysis because the pain of a herniated intervertebral disk would interrupt or alter movement. In middle aged and older adults there would be enough time for the femoral diaphysis to reshape to account for the alteration in movement. Conversely, in this scenario it is possible particularly in older individuals that their injury – the herniation – has reasonably healed and they have returned to normal patterns of movement. Plomp and colleagues' (2012a; 2015) theory on the aetiology of Schmorl's nodes might also suggest that femoral diaphyseal morphology might be particularly relevant, but as they theorise that the morphology of the vertebrae and neural arch are most indicative of the presence or absence of Schmorl's nodes it is also possible that

a particular skeletal morphology might also be present in other elements not due to biomechanical or traumatic interference but to genetic predisposition.

Incidents of trauma could conceivably be relevant or irrelevant to all manner of biomechanical response. Depending on severity, location, level of healing of the injury prior to death, and the individual's particular pain tolerance trauma is expected to have varying effects on the diaphyseal morphology.

5.1.4 Interpopulation Variation: Morphological Variation in the Diaphysis between Populations

As the diaphysis continually remodels, it is more likely to show interpopulation variation than the epiphyses due to additive effects of environment and activity if not genetic affinity. Lovejoy and colleagues (2003) assert that the morphology of the diaphysis is determined at a very young age and need only be altered in adulthood to avoid failure. Other authors suggest that diaphyseal morphology will be primarily determined by activity or strain (Bridges, 1989a; Ruff, Holt, & Trinkaus, 2006; Shackelford & Trinkaus, 2002; Shaw & Stock, 2009a). The English populations studied here are likely to represent individuals who experienced very similar lifestyles and shared genetic affinity. Therefore assuming their lifestyles and environment or even terrain were just slightly different could cause interpopulation variation to be represented in diaphyseal morphological variation. Particularly Fishergate and Hereford, the two English medieval populations from which skeletons were included, are likely to be similar in lifestyle and activity. The Sudanese individuals should be different from the English jointly due to their geographical distance and the very different environment. However, Coach Lane is also likely to be less similar to the other two English populations as it is temporally distinct. It is rational to assume that the Sudanese population will most clearly differentiate itself from the other populations, that Coach Lane may distinguish itself somewhat from Hereford and Fishergate, but that the latter two will be largely similar despite being relatively far apart and from very disparate socio-economic backgrounds.

Activity levels, subsistence patterns, and pathogen loads are all somewhat different for the four represented populations. While there will be some difference in environment for the English populations, the environment for Sudanese population will be the most different due in particular to terrain and temperature. Roux's and Wolff's laws both state – albeit with different levels of specificity and biomechanical accuracy – that forces acting upon the bone will alter the morphology of the bone. This has been repeatedly proven true with numerous studies particularly on cortical morphology but

also with studies on subjects such as femoral, radial and ulnar curvature (De Groote, 2011a, 2011b; Shackelford & Trinkaus, 2002; Yamanaka et al., 2005). Taking this theory one step further, if an individual is born, raised, lives, and then dies in one place and their activities throughout their life remain relatively constant, then their bone morphology may be considered reflective of the community in which they lived both geographically and temporally as those dictate activity and lifeways.

Genetic affinity may have some effect on the morphology of the diaphysis, but even if the English populations consistently pool away from the Sudanese population the most likely explanation for this morphological distinction will be cumulative environmental, health, and biomechanical effects.

5.2 Results and Preliminary Discussion

For a general review of methods please see Chapter 3. For a more specific discussion of the methods utilised here refer to Section 3.5.2.1. In this section all figures and analysis will refer to the same data set. Therefore, while PC and allometry figures will be provided multiple times to visualise variation, PC tables will only be provided once.

For humeri, ninety-five percent of variance is described in the first forty-nine PCs with ninety-nine percent of variance described in the first eighty-one PCs (Table 5.1). All variation is described in one hundred and ten PCs.

Table 5.1 Variance by PC for humerus surface semilandmarks.

	Standard deviation	Proportion of Variance	Cumulative Proportion
PC1	0.01259	27.4190%	27.4190%
PC2	0.008918	13.7590%	41.1780%
PC3	0.006639	7.6260%	48.8040%
PC4	0.006185	6.6180%	55.4220%
PC5	0.004992	4.3100%	59.7320%
PC6	0.004531	3.5510%	63.2840%
PC7	0.004292	3.1860%	66.4700%
PC8	0.003879	2.6030%	69.0730%
PC9	0.003324	1.9110%	70.9850%
PC10	0.003123	1.6870%	72.6720%
PC11	0.002911	1.4660%	74.1380%
PC12	0.00268	1.2420%	75.3800%
PC13	0.002604	1.1740%	76.5530%
PC14	0.002542	1.1180%	77.6710%
PC15	0.002515	1.0950%	78.7660%

PC16	0.002468	1.0540%	79.8200%
PC17	0.00239	0.9880%	80.8080%
PC18	0.002294	0.9100%	81.7180%
PC19	0.002248	0.8740%	82.5920%
PC20	0.002202	0.8390%	83.4310%
PC21	0.002018	0.7050%	84.1360%
PC22	0.001997	0.6900%	84.8260%
PC23	0.001921	0.6390%	85.4650%
PC24	0.001898	0.6230%	86.0880%
PC25	0.001838	0.5850%	86.6730%
PC26	0.001818	0.5720%	87.2450%
PC27	0.001789	0.5540%	87.7990%
PC28	0.001742	0.5250%	88.3230%
PC29	0.001665	0.4800%	88.8030%
PC30	0.001654	0.4730%	89.2760%
PC31	0.001574	0.4290%	89.7050%
PC32	0.001557	0.4190%	90.1240%
PC33	0.001526	0.4030%	90.5270%
PC34	0.001508	0.3940%	90.9210%
PC35	0.001467	0.3720%	91.2930%
PC36	0.001436	0.3570%	91.6500%
PC37	0.001425	0.3520%	92.0020%
PC38	0.001379	0.3290%	92.3300%
PC39	0.001337	0.3090%	92.6400%
PC40	0.0013	0.2920%	92.9320%
PC41	0.001289	0.2870%	93.2190%
PC42	0.001275	0.2810%	93.5010%
PC43	0.001218	0.2570%	93.7580%
PC44	0.001206	0.2510%	94.0090%
PC45	0.001194	0.2460%	94.2550%
PC46	0.001155	0.2310%	94.4860%
PC47	0.001129	0.2210%	94.7070%
PC48	0.001122	0.2180%	94.9250%
PC49	0.001103	0.2100%	95.1350%
PC50	0.001075	0.2000%	95.3350%
PC51	0.00107	0.1980%	95.5330%
PC52	0.001037	0.1860%	95.7190%
PC53	0.001025	0.1820%	95.9010%
PC54	0.001015	0.1780%	96.0790%
PC55	0.0009892	0.1690%	96.2480%
PC56	0.0009824	0.1670%	96.4150%

PC57	0.0009448	0.1540%	96.5700%
PC58	0.000933	0.1510%	96.7200%
PC59	0.0009211	0.1470%	96.8670%
PC60	0.0009102	0.1430%	97.0100%
PC61	0.0008951	0.1390%	97.1490%
PC62	0.0008725	0.1320%	97.2810%
PC63	0.0008633	0.1290%	97.4100%
PC64	0.0008566	0.1270%	97.5370%
PC65	0.0008279	0.1190%	97.6550%
PC66	0.0008237	0.1170%	97.7730%
PC67	0.0008054	0.1120%	97.8850%
PC68	0.0007815	0.1060%	97.9900%
PC69	0.000768	0.1020%	98.0920%
PC70	0.0007595	0.1000%	98.1920%
PC71	0.0007429	0.0950%	98.2880%
PC72	0.0007279	0.0920%	98.3790%
PC73	0.0007107	0.0870%	98.4670%
PC74	0.0006914	0.0830%	98.5490%
PC75	0.0006708	0.0780%	98.6270%
PC76	0.0006639	0.0760%	98.7040%
PC77	0.0006521	0.0740%	98.7770%
PC78	0.0006449	0.0720%	98.8490%
PC79	0.0006277	0.0680%	98.9170%
PC80	0.0006274	0.0680%	98.9850%
PC81	0.0005899	0.0600%	99.0460%
PC82	0.0005804	0.0580%	99.1040%
PC83	0.0005662	0.0550%	99.1590%
PC84	0.0005615	0.0550%	99.2140%
PC85	0.000539	0.0500%	99.2640%
PC86	0.0005315	0.0490%	99.3130%
PC87	0.0005185	0.0470%	99.3590%
PC88	0.0005108	0.0450%	99.4050%
PC89	0.0005063	0.0440%	99.4490%
PC90	0.000499	0.0430%	99.4920%
PC91	0.0004902	0.0420%	99.5340%
PC92	0.0004726	0.0390%	99.5720%
PC93	0.0004586	0.0360%	99.6090%
PC94	0.0004528	0.0350%	99.6440%
PC95	0.0004421	0.0340%	99.6780%
PC96	0.0004317	0.0320%	99.7100%
PC97	0.0004106	0.0290%	99.7390%

PC98	0.000403	0.0280%	99.7670%
PC99	0.0003952	0.0270%	99.7940%
PC100	0.0003814	0.0250%	99.8200%
PC101	0.0003761	0.0240%	99.8440%
PC102	0.0003641	0.0230%	99.8670%
PC103	0.0003523	0.0210%	99.8890%
PC104	0.0003371	0.0200%	99.9080%
PC105	0.0003264	0.0180%	99.9270%
PC106	0.0003183	0.0180%	99.9440%
PC107	0.0003022	0.0160%	99.9600%
PC108	0.0002983	0.0150%	99.9750%
PC109	0.0002783	0.0130%	99.9890%
PC110	0.0002549	0.0110%	100.0000%

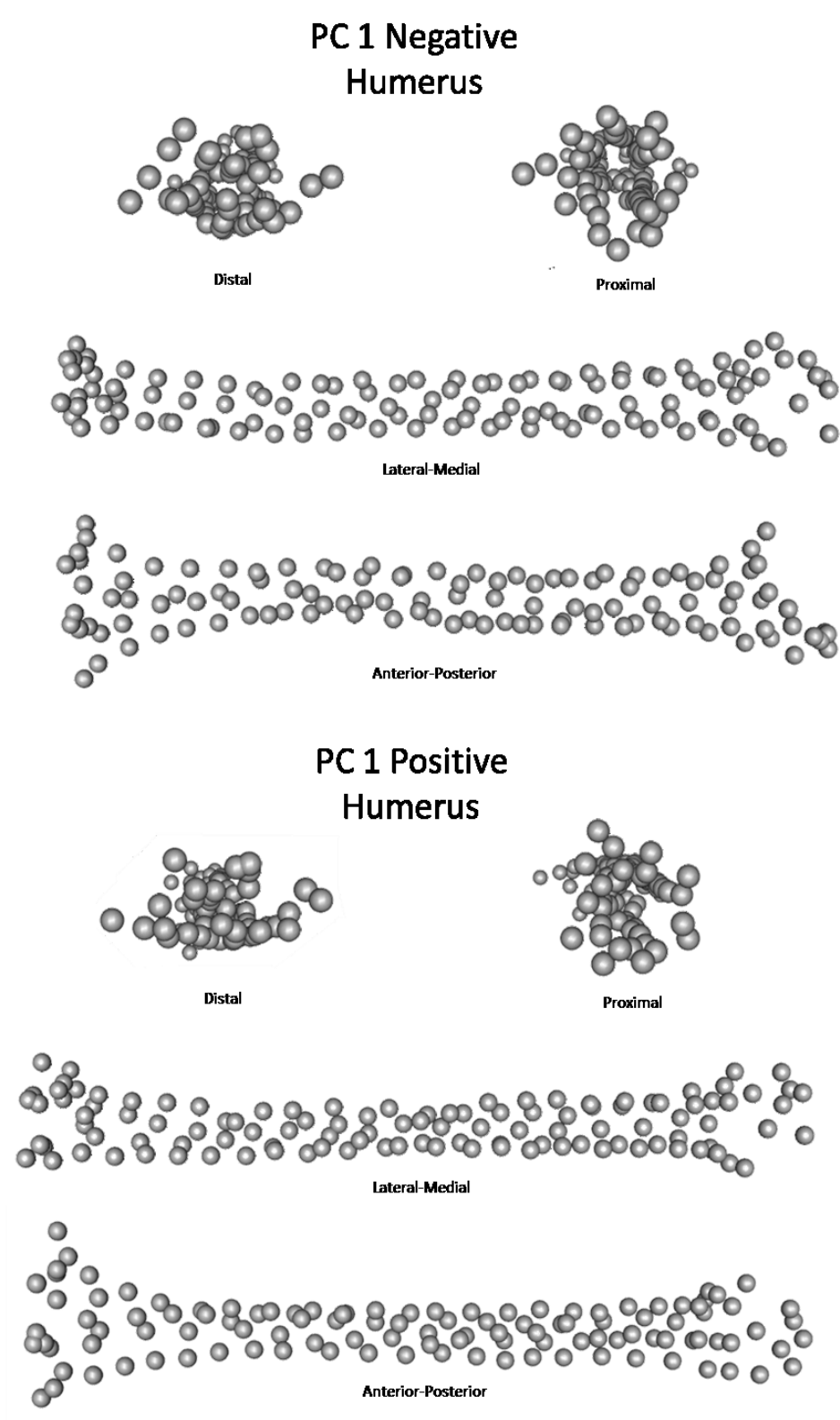


Figure 5.1 Shape extreme for humeri in PC1.

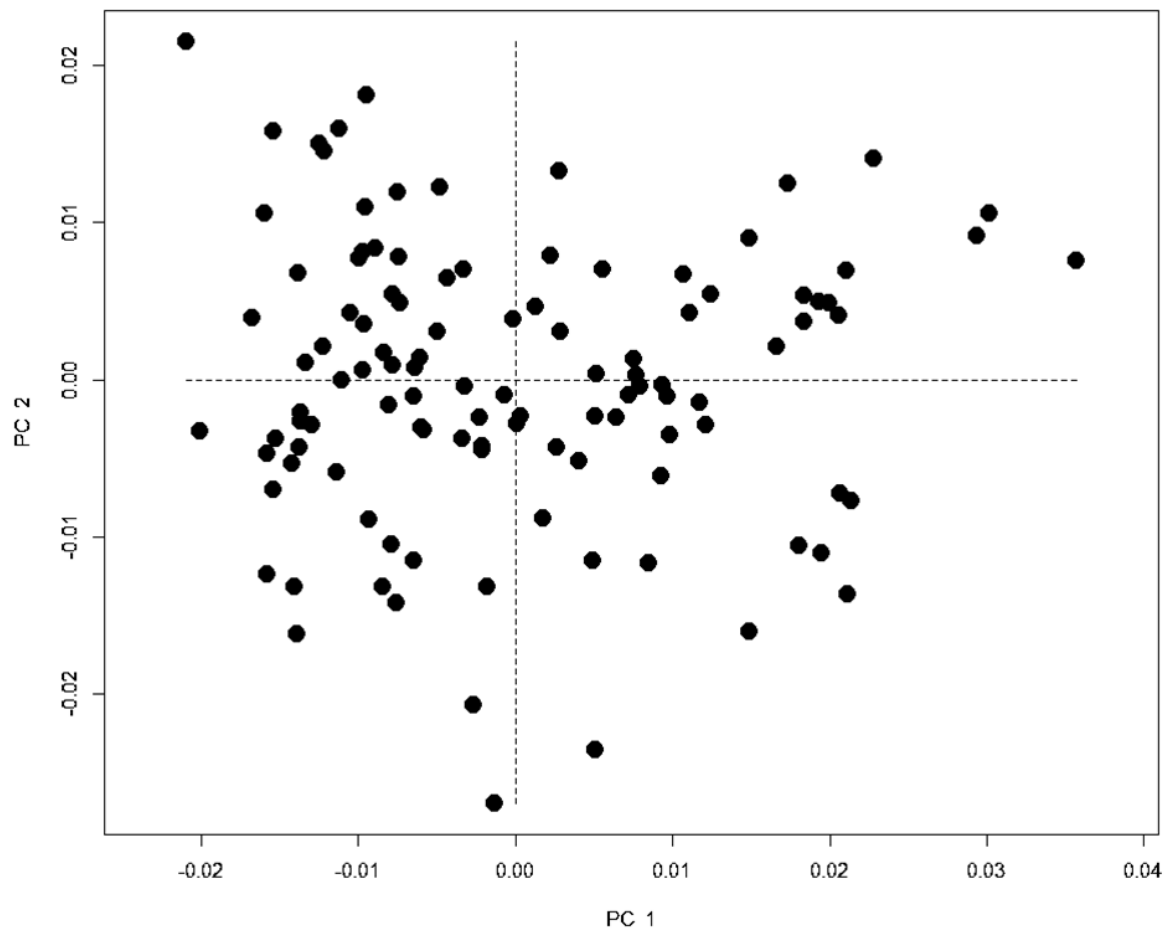


Figure 5.2 PC1 and PC2 visualization of variation for humeral diaphyseal morphology.

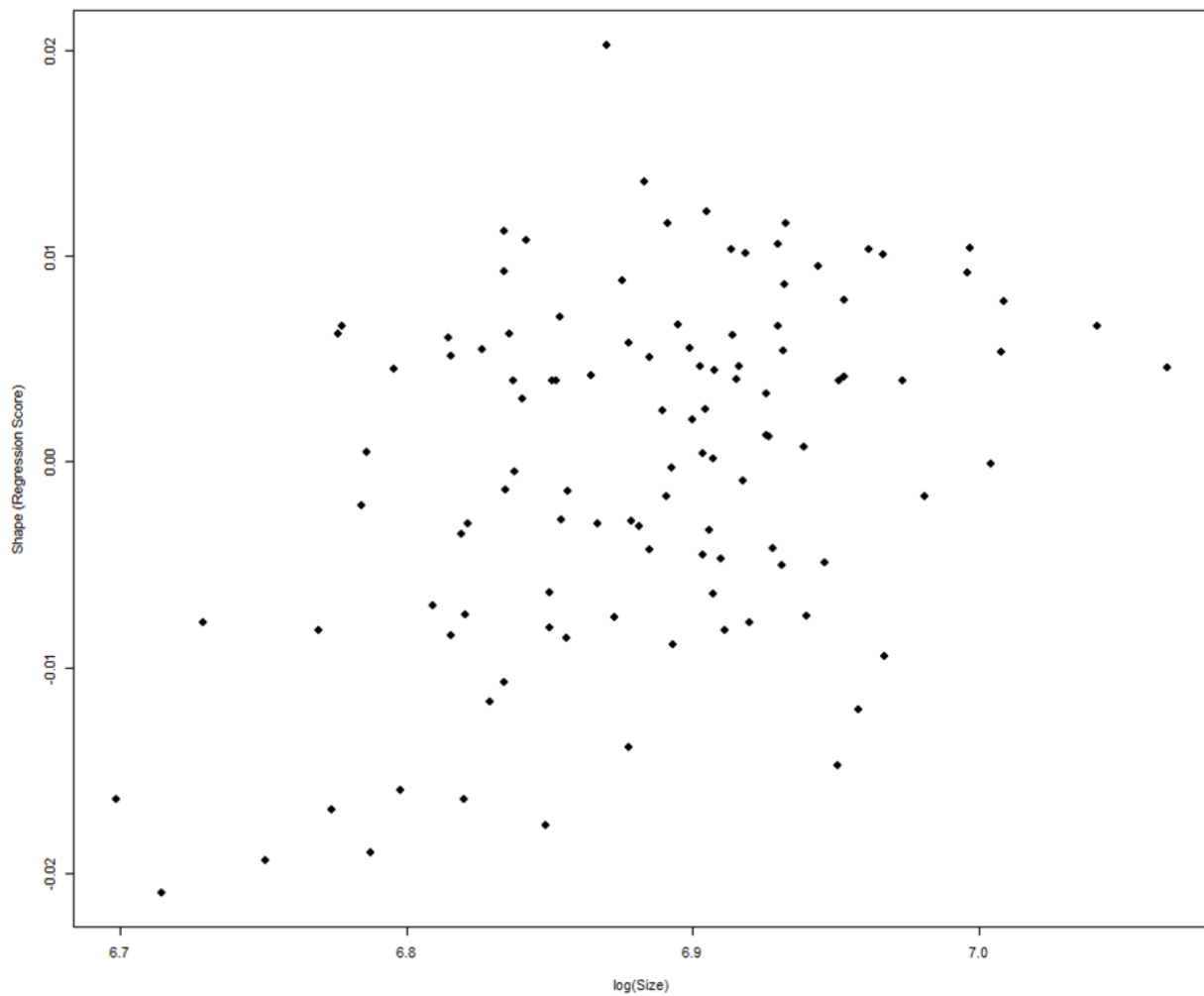


Figure 5.3 Allometry regression of log CS by Shape Regression Scores for humeral diaphyseal morphology.

Table 5.2 GLM Procrustes shape residuals compared to log(CS) for humeral diaphyseal morphology.

	Df	SS	MS	Rsq	F	Z	Pr(>F)
log(size)	1	0.001262	0.00126227	0.019853	2.2078	2.0235	0.031
Residuals	109	0.062319	0.00057174				
Total	110	0.063582					

As seen in Figure 5.1 there is some visually discernable morphological variation at the extremes of PC1. In general the shape at the positive extreme of PC1 appears more gracile than the negative extreme. From the medial-lateral view the positive extreme exhibits more tapering at the midshaft. Also viewed from the medial-lateral view the negative extreme shows more curvature in the posterior distal diaphysis. Viewed from the anterior-posterior view the distal portion of the diaphysis appears more

laterally oriented in relation to the distal epiphysis in the positive shape extreme. The negative shape extreme also shows more definition or curvature along the mid to proximal lateral aspect of the diaphysis. From the distal aspect the positive shape extreme is wider and less curved or ovoid than the negative shape extreme. The idea that PC1 in this case represents at least to some degree shape variation with size or allometry is supported as shape variation is statistically significantly explained by size variation and the R squared value is – for the purposes of this data set – high. (See Figure 5.3 and Table 5.2).

In femora, ninety-five percent of all variation was described in the first thirty-four PCs; ninety-nine percent of all variation was described in the first fifty-four percent. All variance is described in sixty-nine PCs. A full breakdown of variance may be found in Table 5.3.

Table 5.3 Variance by PC for femur surface semilandmarks.

	Standard deviation	Proportion of Variance	Cumulative Proportion
PC1	0.01077	25.5150%	25.5150%
PC2	0.007651	12.8800%	38.3950%
PC3	0.005897	7.6510%	46.0460%
PC4	0.005663	7.0570%	53.1030%
PC5	0.004468	4.3920%	57.4950%
PC6	0.004104	3.7060%	61.2000%
PC7	0.004049	3.6080%	64.8080%
PC8	0.003647	2.9270%	67.7360%
PC9	0.003554	2.7800%	70.5150%
PC10	0.003445	2.6120%	73.1270%
PC11	0.003198	2.2500%	75.3770%
PC12	0.002925	1.8830%	77.2600%
PC13	0.002835	1.7680%	79.0280%
PC14	0.002612	1.5010%	80.5290%
PC15	0.002543	1.4230%	81.9520%
PC16	0.00244	1.3100%	83.2620%
PC17	0.002384	1.2500%	84.5130%
PC18	0.002241	1.1060%	85.6180%
PC19	0.002141	1.0090%	86.6270%
PC20	0.00204	0.9160%	87.5430%
PC21	0.002037	0.9130%	88.4560%
PC22	0.00191	0.8030%	89.2590%
PC23	0.001877	0.7760%	90.0340%
PC24	0.001713	0.6460%	90.6800%
PC25	0.001631	0.5850%	91.2650%

PC26	0.001592	0.5580%	91.8230%
PC27	0.001522	0.5100%	92.3330%
PC28	0.001502	0.4960%	92.8290%
PC29	0.001441	0.4570%	93.2860%
PC30	0.001407	0.4360%	93.7210%
PC31	0.001378	0.4180%	94.1390%
PC32	0.001361	0.4080%	94.5470%
PC33	0.001268	0.3540%	94.9010%
PC34	0.001253	0.3460%	95.2460%
PC35	0.001227	0.3320%	95.5780%
PC36	0.001161	0.2970%	95.8740%
PC37	0.00113	0.2810%	96.1550%
PC38	0.001095	0.2640%	96.4190%
PC39	0.001057	0.2460%	96.6650%
PC40	0.001032	0.2340%	96.8990%
PC41	0.001011	0.2250%	97.1240%
PC42	0.0009677	0.2060%	97.3300%
PC43	0.0009315	0.1910%	97.5210%
PC44	0.000917	0.1850%	97.7060%
PC45	0.0008999	0.1780%	97.8840%
PC46	0.0008784	0.1700%	98.0540%
PC47	0.0008586	0.1620%	98.2160%
PC48	0.0008395	0.1550%	98.3710%
PC49	0.0007873	0.1360%	98.5080%
PC50	0.0007804	0.1340%	98.6420%
PC51	0.0007421	0.1210%	98.7630%
PC52	0.0007352	0.1190%	98.8820%
PC53	0.0007137	0.1120%	98.9940%
PC54	0.0007046	0.1090%	99.1030%
PC55	0.0006749	0.1000%	99.2030%
PC56	0.0006316	0.0880%	99.2910%
PC57	0.0006162	0.0840%	99.3750%
PC58	0.0006023	0.0800%	99.4550%
PC59	0.0005612	0.0690%	99.5240%
PC60	0.0005572	0.0680%	99.5920%
PC61	0.0005324	0.0620%	99.6550%
PC62	0.0005171	0.0590%	99.7130%
PC63	0.0004881	0.0520%	99.7660%
PC64	0.000458	0.0460%	99.8120%
PC65	0.0004476	0.0440%	99.8560%

PC66	0.0004422	0.0430%	99.8990%
PC67	0.0004238	0.0400%	99.9390%
PC68	0.0004138	0.0380%	99.9760%
PC69	0.0003278	0.0240%	100.0000%

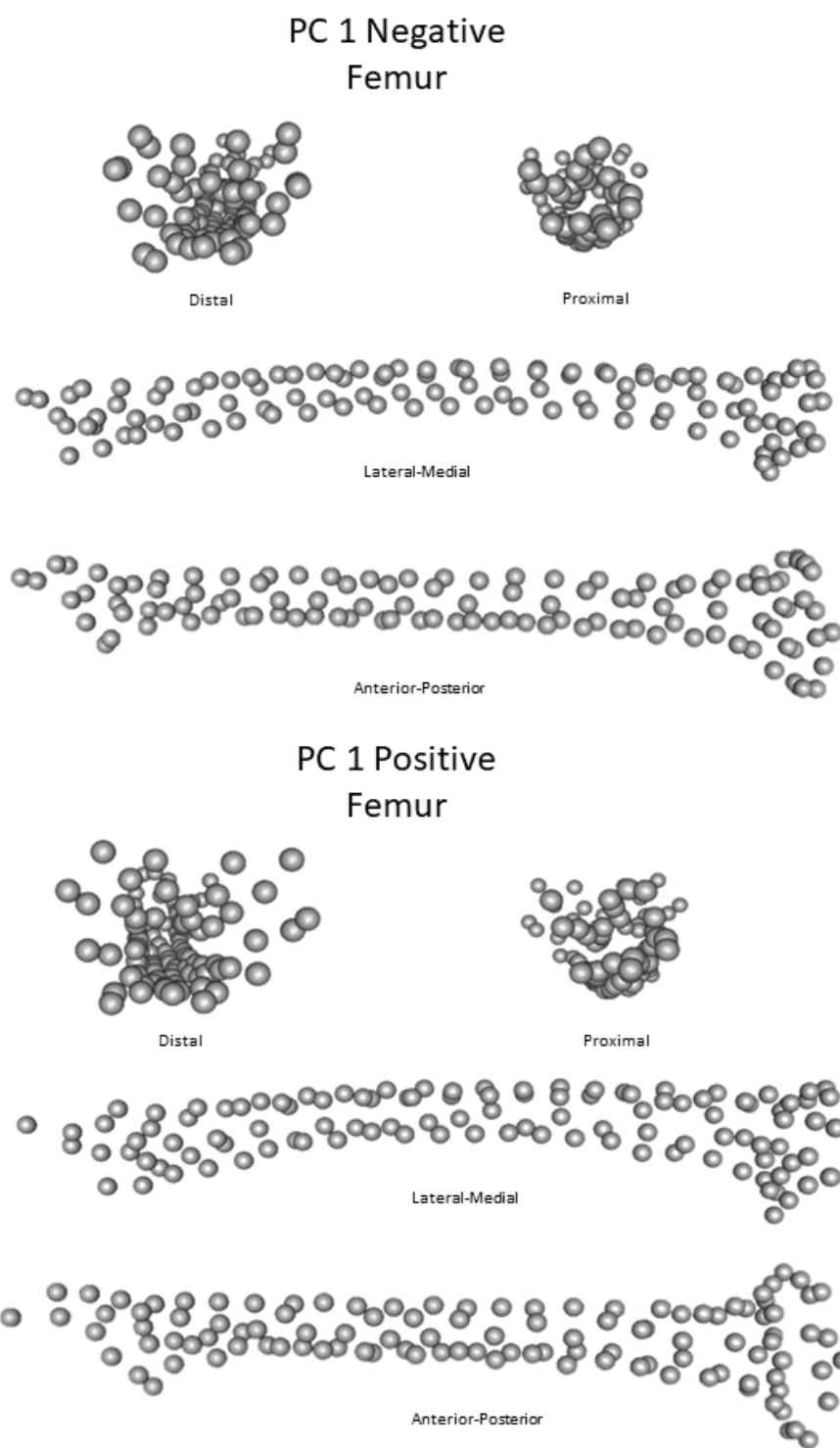


Figure 5.4 Shape extremes for femora in PC1. .

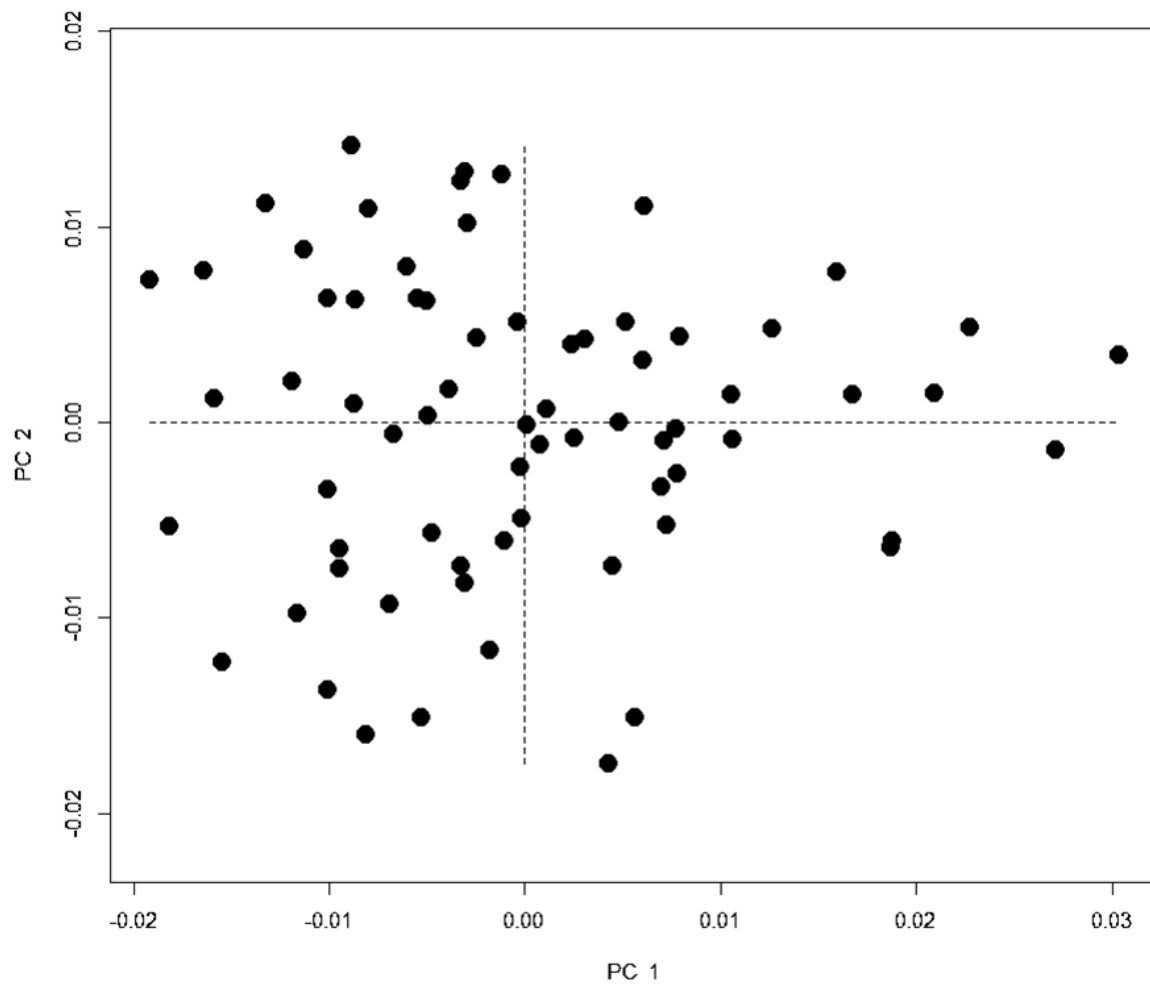


Figure 5.5 PC1 and PC2 visualization of variation for femoral diaphyseal morphology.

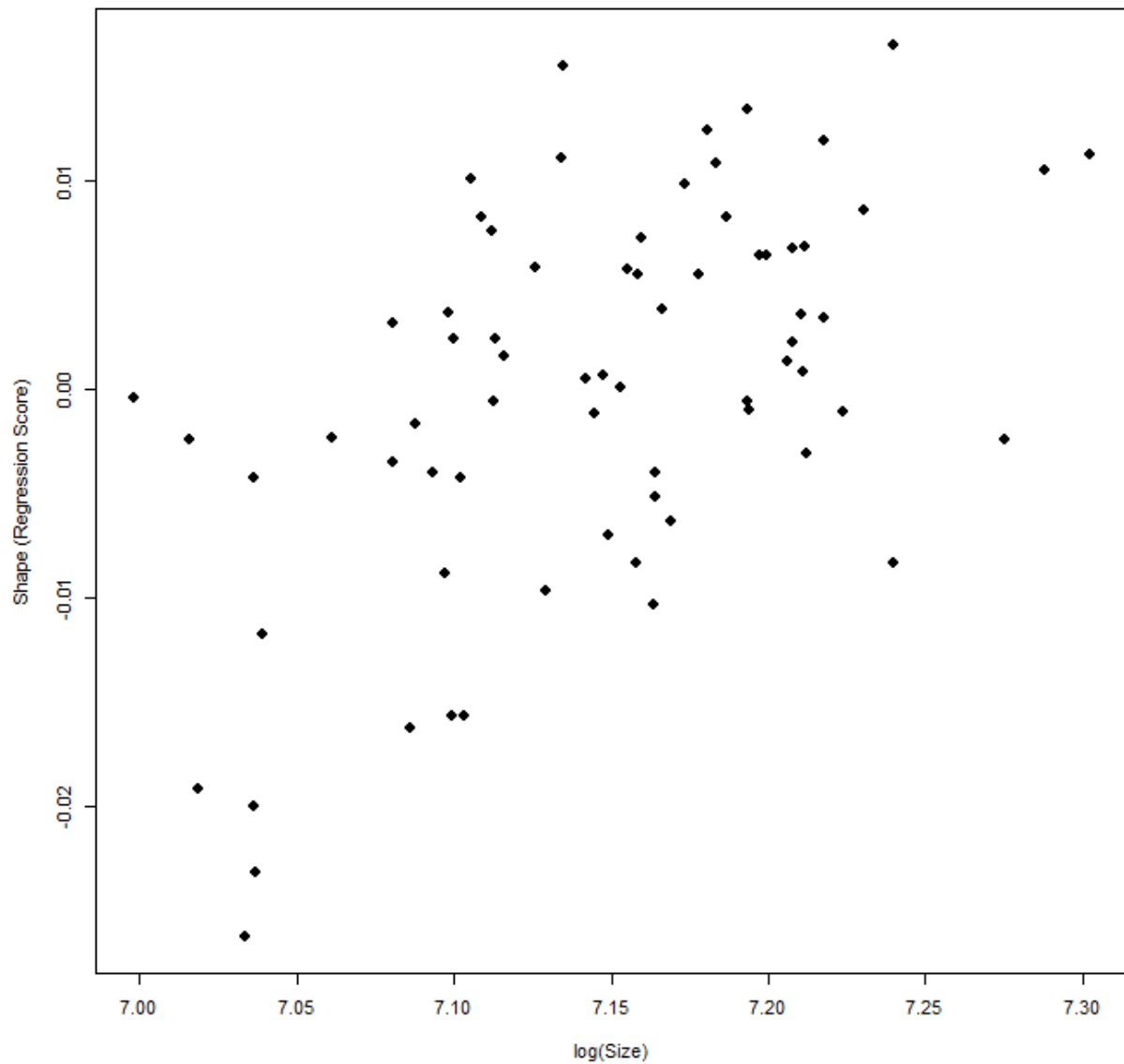


Figure 5.6 Allometry regression of log CS by Shape Regression Scores for femoral diaphyseal morphology.

Table 5.4 GLM Procrustes shape residuals compared to log(CS) for femoral diaphyseal morphology.

	Df	SS	MS	Rsq	F	Z	Pr(>F)
log(size)	1	0.0017347	0.00173471	0.05532	3.9821	3.7775	0.001
Residuals	68	0.0296227	0.00043563				
Total	69	0.0313574					

As was seen with the humeral surface morphology the positive and negative extremes in PC1 for femoral morphology seem to pertain to gracility and robusticity. This does not necessarily mean that the

variation pertains to allometry although based on Figure 5.6 and Table 5.4 allometry is present. The negative shape extreme for the femur features a slender diaphysis with a comparatively lower degree of curvature when viewed from the lateral-medial aspect (See Figure 5.4). From the anterior-posterior aspect it is clear that the positive shape extreme exhibit more expansive epiphyses. In particular, the lateral epicondyle is less obtusely placed relative to the diaphysis in the positive shape extreme suggesting a larger distal epiphysis. When viewed from the distal aspect it also appears that the size of the distal epiphysis would be relatively larger than that of the negative shape extreme relative to their respective diaphyses. Similarly the area covered in the positive extreme shape for the proximal epiphysis appears greater and more robust when compared to that of the negative extreme. The view from the proximal aspect also shows greater flaring towards the epiphysis in the positive shape extreme, but it is not as pronounced as that seen in the distal view.

5.2.1 Intrapopulation

5.2.1.1 Sex

Little to no morphological variation is apparent in shape space for humeral surface variation. Females and males overlap almost entirely in PC1 and PC2. However, as shown in Table 5.5, the GLM model was significant with size, site, and the interaction of site and sex as uniquely significant. For size at an alpha equal to 0.05 the results for centroid size as an independent variable against Procrustes shape variables are $F(1,83) = 2.50, p < .05, R^2 = .019$. Site set at an alpha of 0.05 was $F(3,83) = 8.13, p < .01, R^2 = .19$. For the interaction between sex and site at an alpha equal to 0.05 $F(8,83) = 1.16, p < .01, R^2 = .07$. This suggests a correlation between sexual dimorphism and population meaning not that sex does not influence humeral surface morphology but that it does not uniquely influence it. Sexual dimorphism influences shape by site. When allometry is considered, dimorphism is not apparent. Figure 5.9 plots the humeral natural logarithm of centroid size against shape. (The logarithm of CS is used to ensure that the scaling remains isotropic (Mitteroecker et al., 2013a). For a review of methodology and background see Section 2.4 and 3.5.2.1.) A Homogeneity of Slopes test (Table 5.7) was conducted with a significance of .05% and the null hypothesis that the slopes were parallel was accepted. A further ANOVA with randomized residual permutation (1000 iterations) was used and found at 0.05 significance there is allometry but it does not pertain to sexual dimorphism.

Figure 5.11 shows the shape extremes at minimum and maximum size. These are similar to those seen in the shape extremes in PC1 found in Figure 5.1. In both shape extremes there is curvature in the posterior distal portion of the diaphysis as viewed from the medial lateral perspective and neither

extreme shows a diaphysis which exhibits significantly more tapering than the other. Additionally, while the minimum shape extreme does show slight lateral displacement of the distal diaphysis relative to the shape maximum the difference is not as notable as in the PC1 positive shape extreme. Morphology for the humeral surface is statistically explained by size, but there is demonstrably more to it than simple allometry.

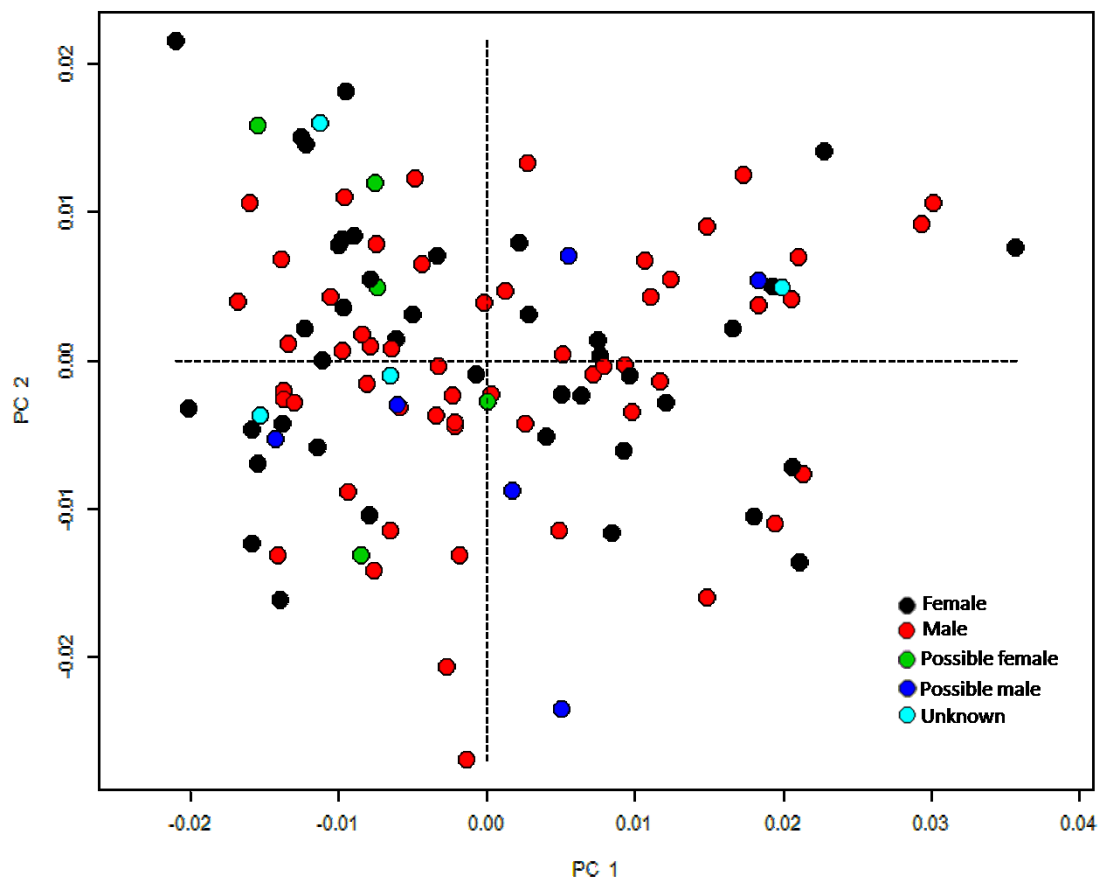


Figure 5.7 PC1 and PC2 of humeri by sex.

Table 5.5 GLM with interactions of humeral diaphyseal surface morphology by size, site, and sex.

	Df	SS	MS	Rsqr	F	Z	Pr(>F)
Centroid Size	1	0.001207	0.0012067	0.018979	2.4992	2.3071	0.021
Site	3	0.011779	0.0039263	0.185254	8.1317	8.1267	0.001
Sex	4	0.001581	0.0003953	0.024868	0.8187	0.2547	0.398
Centroid Size x Site	3	0.001311	0.0004368	0.020612	0.9048	0.8578	0.189
Centroid Size x Sex	4	0.001617	0.0004042	0.025432	0.8372	0.6395	0.275
Site x Sex	8	0.004471	0.0005589	0.070322	1.1575	2.9363	0.003
Centroid Size x Site x Sex	4	0.001541	0.0003853	0.024242	0.7981	0.9977	0.158
Residuals	83	0.040075	0.0004828				
Total	110	0.063582					

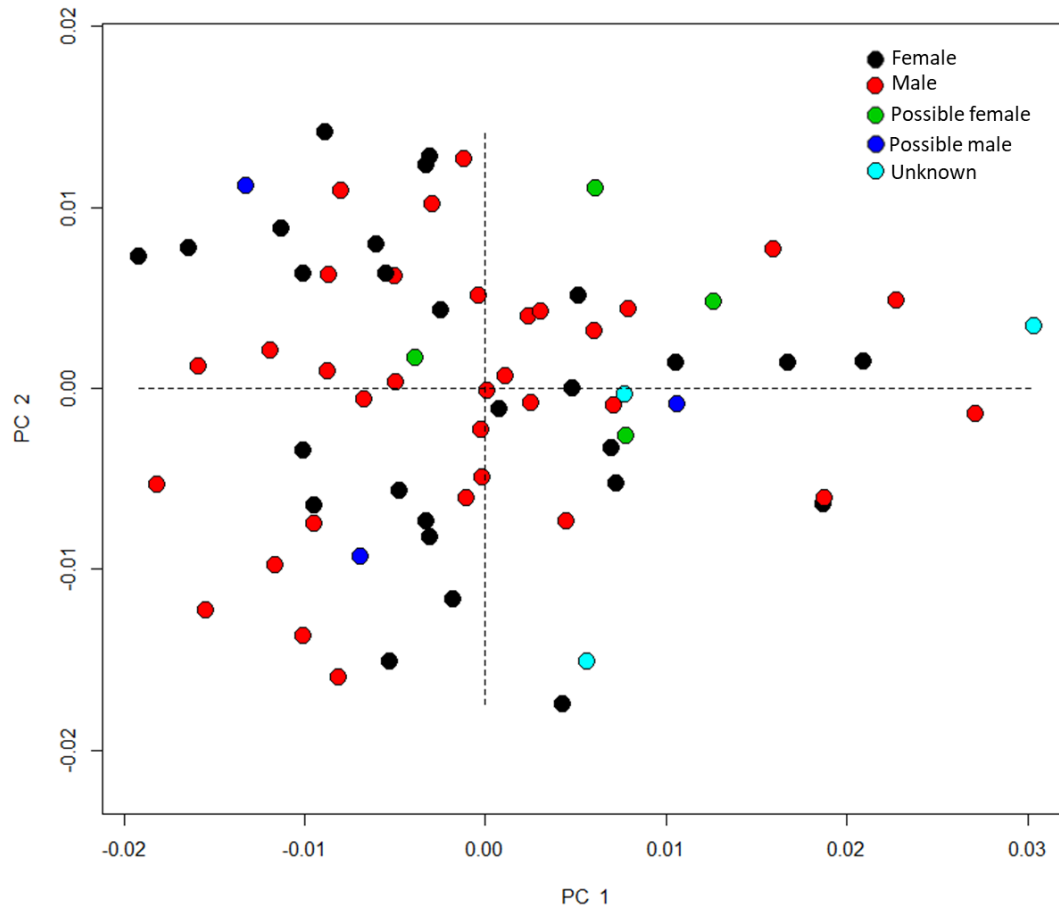


Figure 5.8 PC1 and PC2 of femora by sex.

Table 5.6 GLM with interactions of femoral diaphyseal surface morphology by size, site, and sex.

	Df	SS	MS	Rsqr	F	Z	Pr(>F)
Centroid Size	1	0.0016903	0.00169029	0.053904	4.4158	4.0078	0.001
Site	3	0.0037406	0.00124686	0.119289	3.2573	5.1879	0.001
Sex	4	0.0019723	0.00049307	0.062896	1.2881	2.0327	0.025
Centroid Size x Site	3	0.0009557	0.00031856	0.030477	0.8322	0.381	0.349
Centroid Size x Sex	4	0.0014552	0.00036381	0.046408	0.9504	1.1829	0.123
Site x Sex	5	0.0023932	0.00047865	0.076321	1.2504	2.7378	0.004
Centroid Size x Site x Sex	2	0.0011592	0.00057958	0.036966	1.5141	3.1218	0.003
Residuals	47	0.017991	0.00038279				
Total	69	0.0313574					

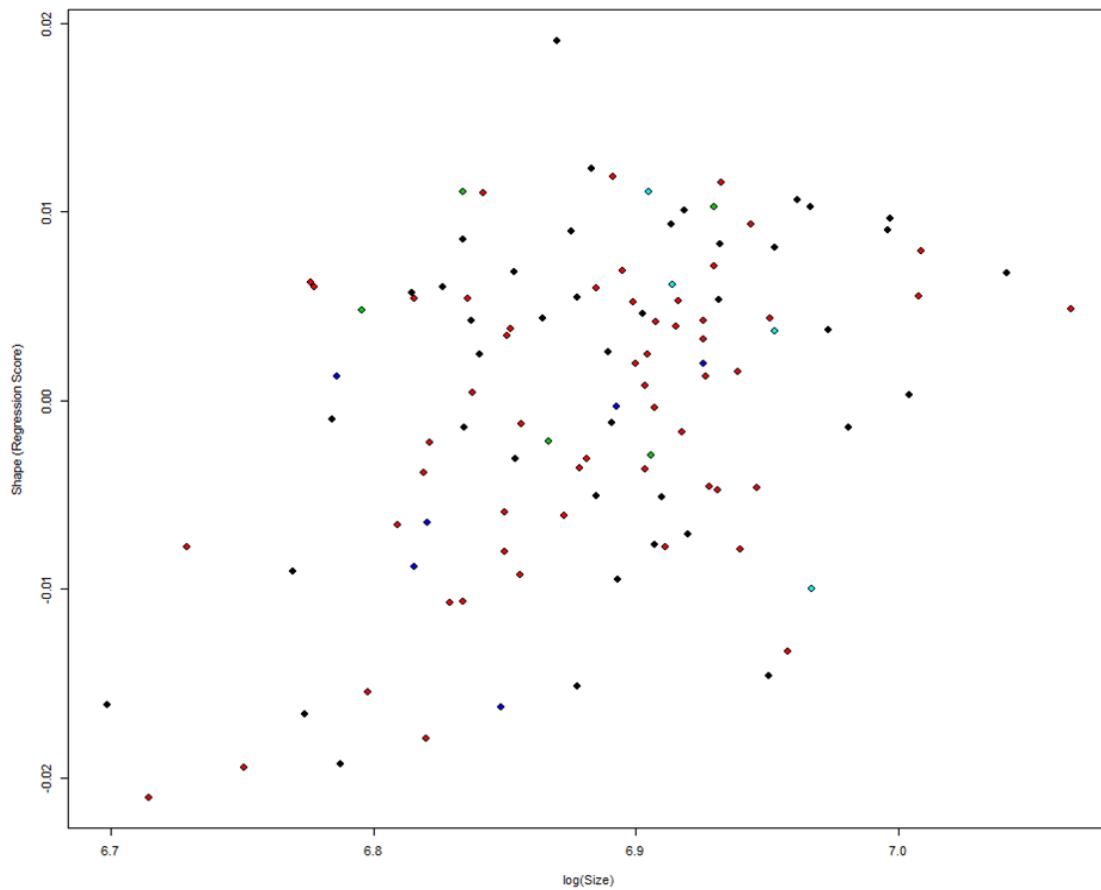


Figure 5.9 Humeral allometry by sex. (black = female, red = male, blue = possible female, green = possible male, cyan = unknown)

Table 5.7 Homogeneity of Slopes Test and ANOVA results (1000 iterations) for humeri.

Homogeneity of Slopes Test							
	Df	SEE	Sum of Squares	Rsqr	F	Z	Pr(>F)
Common Allometry	105	0.060407					
Group Allometries	101	0.058233	0.0021739	0.034191	0.9426	0.062326	0.466

Type I (Sequential) Sums of Squares and Cross-products							
	Df	Sum of Squares	Mean Square	Rsqr	F	Z	Pr(>F)
log(size)	1	0.001262	0.00126227	0.019853	2.1941	2.00812	0.032
Sex	4	0.001913	0.00047821	0.030085	0.8312	-0.58116	0.706
Residuals	105	0.060407	0.0005753				
Total	110	0.063582					

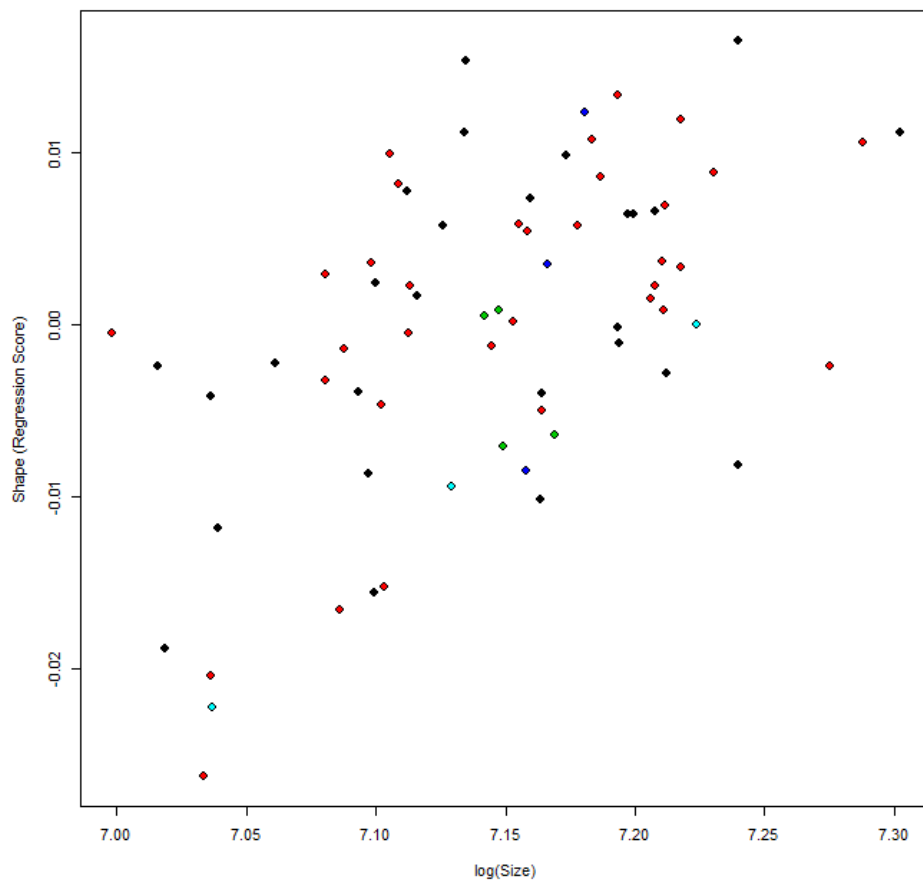


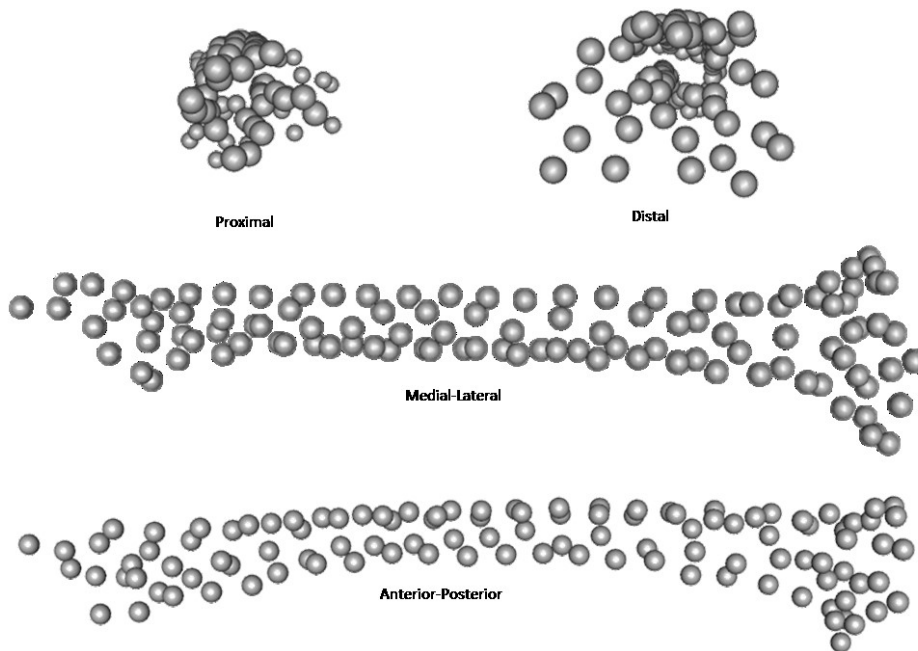
Figure 5.10 Femoral allometry by sex. (black = female, red = male, blue = possible female, green = possible male, cyan = unknown)

Table 5.8 GLM Procrustes shape residuals compared to log(CS) for femoral diaphyseal morphology by sex.

Homogeneity of Slopes Test							
	Df	SEE	Sum of Squares	Rsqr	F	Z	Pr(>F)
Common Allometry	64	0.027327					
Group Allometries	60	0.025314	0.0020137	0.064217	1.1932	1.4417	0.084

Type I (Sequential) Sums of Squares and Cross-products							
	Df	Sum of Squares	Mean Square	Rsqr	F	Z	Pr(>F)
log(size)	1	0.0017347	0.00173471	0.05532	4.0626	3.831	0.001
Sex	4	0.0022954	0.00057385	0.073201	1.3439	1.6913	0.049
Residuals	64	0.0273273	0.00042699				
Total	69	0.0313574					

Shape at minimum size
Femur



Shape at maximum size
Femur

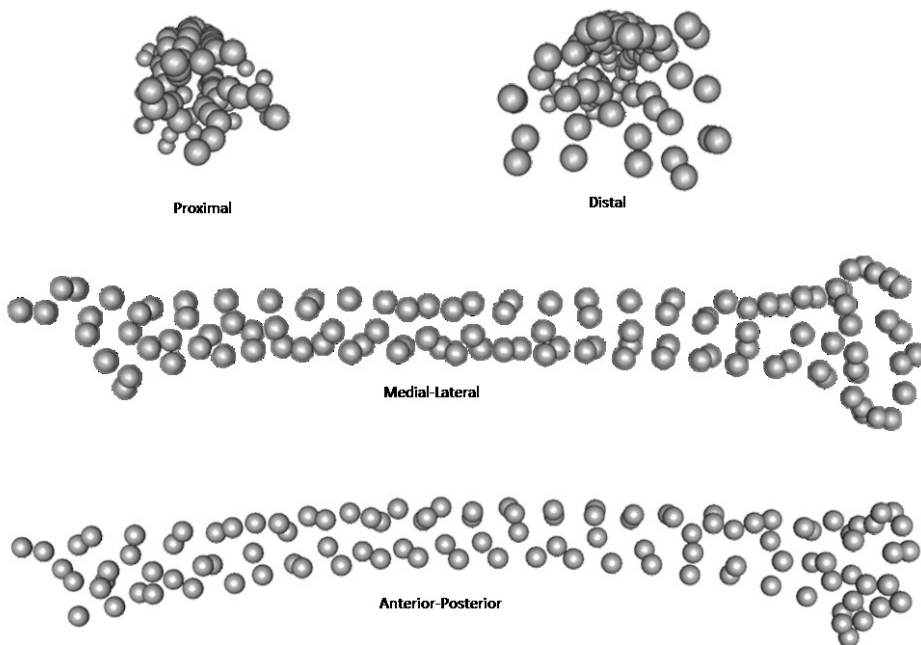


Figure 5.11 Shape of femora at maximum and minimum size.

Femoral size and shape behave similarly to the humerus particularly in regards to sex. As with humeri, shape alone shows no division in the PC visualizations between females and males and so the overlap of shapes is largely complete as seen in Figure 5.8. However, when size is taken into account female and male femora are clearly divergent in morphology. Table 5.8 and Figure 5.10 respectively give results for an allometry test of femoral diaphyseal morphology including sex. For the femur the size varies strongly ($p < 0.01$) with shape. When sex is considered with size the relationship to shape is less strong, but still statistically significant.

Shape diagrams at maximum and minimum size are provided in Figure 5.11. Surface morphology variation in the femur by size has many of the features observed for the positive and negative shape extremes in PC1, but they are not observed in the same sets. As viewed from the medial-lateral view the minimum shape extreme appears to have the most gracile diaphysis but the curvature of the diaphysis is roughly equal to that seen in the maximum extreme shape. Additionally, when observing from the anterior-posterior views the maximum extreme shape appears to have the most slender diaphysis. Interestingly, the relative position of the lateral epicondyle is not notable in either the maximum or minimum shape extreme and the minimum size extreme appears to have the largest epiphyses.

Results of the GLM for femoral surface morphology as explained by site, sex, centroid size, and interactions of the three are provided in Table 5.6. For size at an alpha equal to 0.05 the results for centroid size as an independent variable against Procrustes shape variables are $F(1,47) = 4.42$, $p < .01$, $R^2 = .054$. With site as the independent variable at an alpha equal to 0.05, $F(3,47) = 3.26$, $p < .01$, $R^2 = .119$. For sex as the independent variable with the alpha equal to 0.05, $F(4,47) = 1.29$, $p < .05$, $R^2 = .063$. When site and sex are considered together at an alpha equal to 0.05, $F(5,47) = 1.25$, $p < .01$, $R^2 = .076$. When centroid size, site, and sex are considered together at an alpha equal to 0.05, $F(2,47) = 1.51$, $p < .01$, $R^2 = .037$. Unlike with humeral surface morphology here sex does uniquely explain some of the shape variation. Site and centroid size both uniquely explain shape variation but size considered with site and size considered with sex do not uniquely explain variation. Because site and sex considered together and size, site, and sex considered together seem to explain variation it is likely that centroid size is correlated with site and sex and therefore can only uniquely explain femoral shape variation when considered alone or when combined with both site and sex.

5.2.1.2 Age

Figure 5.12 and Figure 5.13 are visualizations in the first two PCs organized by age group. There is no clear separation of the age groups in either humeri or femora and this remains the case in the lower PCs. However, GLM tests were conducted using shape of the humerus (Table 5.9) and femur (Table 5.10) respectively as the dependent variable (DV) and size, sex, and age group as the IV.

For humeral surface morphology age group may not uniquely explain variation. However, when site and age are considered together at an alpha of 0.05 then $F(8,45) = 1.06$, $p < .01$, $R^2 = .066$. Similarly, when sex and age are considered together at alpha = 0.05, $F(6,45) = 0.96$, $p < .01$, $R^2 = .045$. Other significant results are reported in Table 5.9 when centroid size is also considered with site and age or sex and age. Results are also significant when all IVs are considered together. Age group then likely covaries with site and sex and to a small degree with size. Age does influence humeral surface morphology but on a trajectory determined by factors including size, population, and sex.

When considering femoral surface morphology if alpha were equal to 0.10 rather than 0.05, age group would be a statistically significant explanation of shape variation. As seen in Table 5.8 $F(4,17) = 1.06$, $p < .10$, $R^2 = .058$. However, setting the alpha at 0.05 if centroid size and age group are considered together for centroid size and age group considered together $F(3,17) = 0.91$, $p < .05$, $R^2 = .037$. Similar significant and very significant values are reported when age group is considered with size, sex, and site. This means that although age group only weakly explains shape variation alone, it interacts with other predictors to provide a better statistical explanation of observed variance. Age group in femora covaries to some degree with size, site, and sex.

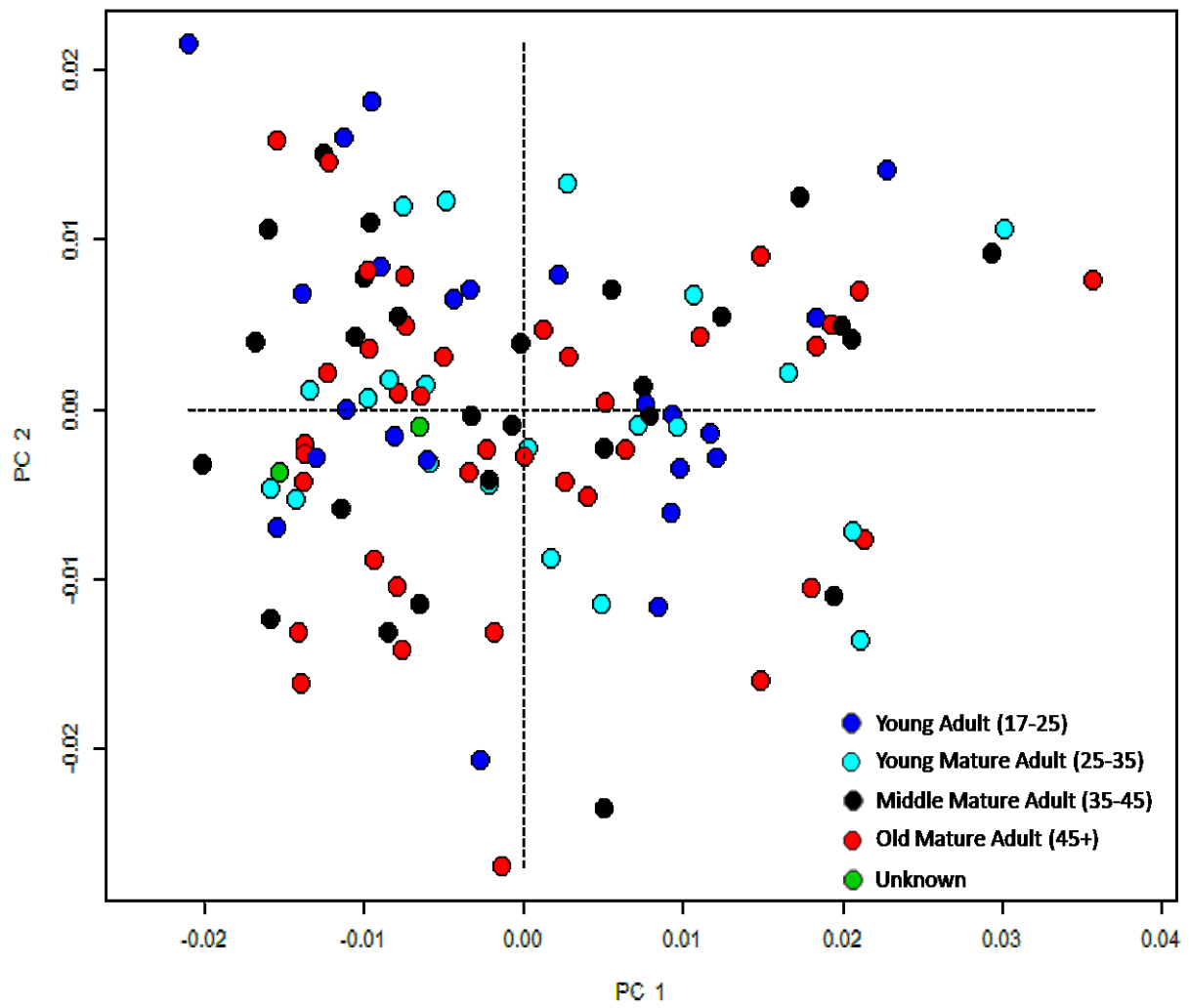


Figure 5.12 PC1 and PC2 of humeri by age.

Table 5.9 GLM with interactions of humeral diaphyseal surface morphology by size, site, sex, and age.

	Df	SS	MS	Rsqr	F	Z	Pr(>F)
Centroid Size	1	0.001207	0.0012067	0.018979	2.4247	2.2087	0.021
Site	3	0.011779	0.0039263	0.185254	7.8891	7.7867	0.001
Sex	4	0.001581	0.0003953	0.024868	0.7942	0.0711	0.477
Age Group	4	0.001609	0.0004023	0.025309	0.8084	0.3079	0.379
Centroid Size x Site	3	0.001297	0.0004324	0.020404	0.8689	0.7466	0.223
Centroid Size x Sex	4	0.001567	0.0003919	0.024653	0.7874	0.457	0.324
Site x Sex	8	0.004687	0.0005859	0.073715	1.1772	3.0142	0.004
Centroid Size x Age Group	3	0.001288	0.0004292	0.020253	0.8625	1.4139	0.075
Site x Age Group	8	0.004202	0.0005252	0.066081	1.0553	3.7312	0.001
Sex x Age Group	6	0.002877	0.0004795	0.045253	0.9636	3.1706	0.001
Centroid Size x Site x Sex	3	0.0012	0.0003999	0.01887	0.8036	2.0006	0.019
Centroid Size x Site x Age Group	7	0.00306	0.0004371	0.048127	0.8783	3.4162	0.001
Centroid Size x Sex x Age Group	3	0.001196	0.0003986	0.018807	0.8009	2.4935	0.007
Site x Sex x Age Group	6	0.002731	0.0004552	0.042952	0.9146	3.7892	0.001
Centroid Size x Site x Sex x Age Group	2	0.000905	0.0004527	0.01424	0.9096	2.3183	0.008
Residuals	45	0.022396	0.0004977				
Total	110	0.063582					

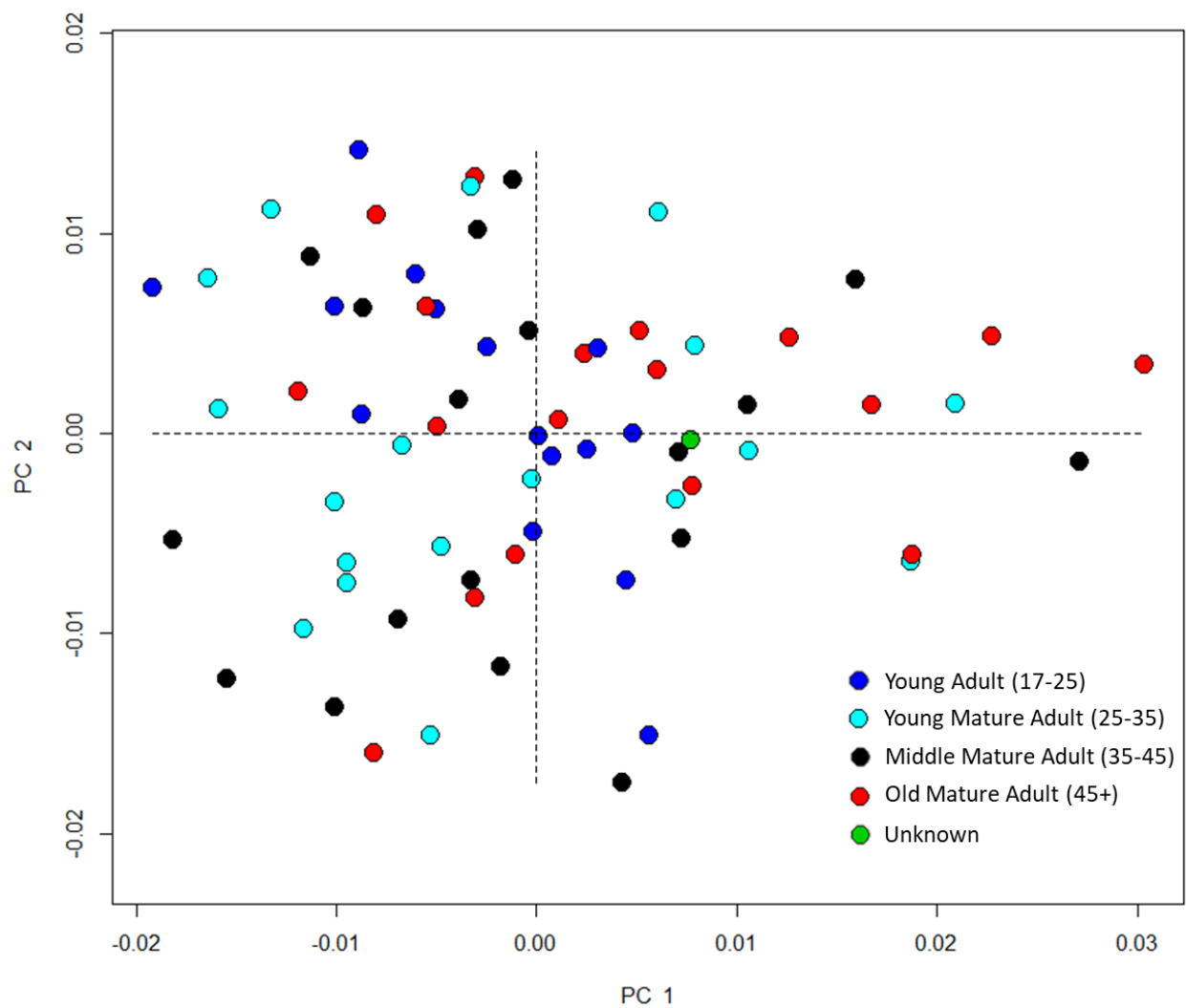


Figure 5.13 PC1 and PC2 of femur diaphyseal surface morphology organized by age.

Table 5.10 GLM with interactions of femoral diaphyseal surface morphology by size, sex, and age.

	Df	SS	MS	Rsqr	F	Z	Pr(>F)
Centroid Size	1	0.0016903	0.00169029	0.053904	3.9401	3.5484	0.001
Site	3	0.0037406	0.00124686	0.119289	2.9065	4.2016	0.001
Sex	4	0.0019723	0.00049307	0.062896	1.1494	1.3281	0.096
Age Group	4	0.0018125	0.00045314	0.057803	1.0563	1.4318	0.096
Centroid Size x Site	3	0.0009608	0.00032027	0.030641	0.7466	0.2077	0.411
Centroid Size x Sex	4	0.00166	0.00041499	0.052937	0.9674	1.3456	0.087
Site x Sex	4	0.0015358	0.00038395	0.048978	0.895	1.404	0.089
Centroid Size x Age Group	3	0.0011728	0.00039093	0.037401	0.9113	1.7945	0.046
Site x Age Group	6	0.0019686	0.0003281	0.06278	0.7648	1.6226	0.056
Sex x Age Group	4	0.0014853	0.00037132	0.047366	0.8656	2.3041	0.016
Centroid Size x Site x Sex	2	0.0007879	0.00039395	0.025126	0.9183	2.4429	0.009
Centroid Size x Site x Age Group	5	0.0019036	0.00038073	0.060708	0.8875	3.1788	0.001
Centroid Size x Sex x Age Group	3	0.000781	0.00026035	0.024908	0.6069	1.8099	0.039
Site x Sex x Age Group	4	0.0014776	0.00036941	0.047123	0.8611	3.1064	0.002
Centroid Size x Site x Sex x Age Group	2	0.0011154	0.00055769	0.03557	1.3	3.2102	0.001
Residuals	17	0.0072929	0.00042899				
Total	69	0.0313574					

5.2.1.3 Trauma and Pathology

The morphology of the femoral diaphysis was more slightly more sensitive to nutritional stress than the humeral diaphysis. As previously, the PC visualizations gave no clear pattern and despite correlations between morphology and incidence of pathology there did not seem to be grouping in shape space.

There was a very low prevalence of trauma particularly in the English sites (for population level trauma prevalences refer to Table 7.3). The Sudanese site had a higher incidence of trauma perhaps due to the geology of the area or perhaps owing to their subsistence practices relying heavily on cattle. As seen in Figure 5.14 humeri of individuals who had signs of trauma did not visibly vary or cluster. As seen in Figure 5.15, the femora of individuals with trauma also do not fall outside of the normal bounds for their population or truly cluster together. GLMs were used to test variance. Shape was the DV and size, sex, site, and trauma the IVs.

When considering humeral surface morphology trauma did not uniquely explain variance. (See Table 5.11) However, when size and trauma were considered together at an alpha of 0.05, $F(1,69) = 1.24$, $p < .05$, $R^2 = 0.01$. When sex and trauma are considered together at an alpha of 0.05, $F(2,69) = 1.10$, $p < .05$, $R^2 = 0.02$. When site and trauma are considered together at an alpha of 0.05, $F(3,69) = 1.48$, $p < .01$, $R^2 = 0.03$. When centroid size is added to the interactions the R^2 value drops again but for centroid size with sex and trauma still remains statistically significant ($F(1,69) = 1.74$, $p < .01$, $R^2 = 0.01$). When site, sex, and trauma are considered together without centroid size at an alpha of 0.05, $F(2,69) = 0.88$, $p < .05$, $R^2 = 0.01$. And when site, sex, trauma, and centroid size are all considered together at an alpha of 0.05 $F(2,69) = 1.06$, $p < .01$, $R^2 = 0.02$. This suggests that trauma does not influence humeral morphological shape alone, but interacts with size, population, and sex. The morphological expression of trauma is dependent on these multiple factors.

Trauma did not uniquely explain femoral surface morphology. But as with humeral surface morphology when other IVs were combined with trauma they did explain the DV with statistical significance. When site and trauma were considered together at an alpha of 0.05, $F(2,36) = 2.76$, $p < .01$, $R^2 = 0.07$. When size, site, and trauma were considered together and alpha was equal to 0.05, $F(2,36) = 0.93$, $p < .05$, $R^2 = 0.02$. When site, sex, and trauma were considered together at an alpha of 0.05, $F(2,69) = 0.85$, $p < .05$, $R^2 = 0.02$. For femoral morphology population and size seemed to impact how trauma could influence morphology, but sex does not seem to be a factor. This is in contrast with humeral morphology where sex could be linked with how trauma affected morphology.

LEH does not uniquely explain humeral morphology. Site and LEH explain humeral morphology (alpha = 0.05, $F(3,65) = 0.92$, $p < .05$, $R^2 = 0.02$). When sex and LEH are considered together when the alpha is 0.05, $F(2,65) = 1.13$, $p < .05$, $R^2 = 0.02$. When size, LEH, and site are considered together and the alpha is 0.05, $F(3,65) = 1.65$, $p < .01$, $R^2 = 0.04$. However, when site, sex, and LEH were considered together and when all four IVs were considered together they could only explain morphological variation if the alpha were equal to 0.10. This suggests that both site and sex covary to a degree with LEH, but along different trajectories. It further suggests that the trajectory where site and LEH share covariance is also shared to some extent by size, but that size does not covary with sex and LEH.

LEH weakly and uniquely explains femoral surface morphology. If the alpha were 0.10, $F(2,34) = 1.09$, $p < .10$, $R^2 = 0.03$. When site and LEH are considered together the R^2 value rises and the p value drops: with an alpha equal to 0.05, $F(2,34) = 1.50$, $p < .01$, $R^2 = 0.04$. When sex and LEH are considered with an alpha equal to 0.05, $F(2,34) = 1.87$, $p < .01$, $R^2 = 0.04$. Somewhat counterintuitively when site, sex,

and LEH are considered together the R^2 value drops and the p value rises so that at an alpha of 0.05, $F(2,34) = 0.81$, $p < .10$, $R^2 = 0.02$. When centroid size is considered with site and LEH at an alpha of 0.05, $F(2,34) = 0.76$, $p < .10$, $R^2 = 0.02$. When centroid size is considered with sex and LEH at an alpha of 0.05, $F(2,34) = 1.89$, $p < .01$, $R^2 = 0.02$. When all four IVs are considered together with an alpha of 0.05, $F(1,34) = 1.16$, $p < .05$, $R^2 = 0.01$. The prevalence of LEH effects femoral surface morphology but its effect appears to be dependent on population and sex. However population and sex when paired with LEH uniquely explain surface morphological variation. That is where LEH influences morphology, population and sex do not significantly covary. Size seems to help explain variance with LEH prevalence and sex, but to a lesser degree with LEH prevalence and population.

Cribra orbitalia did not uniquely explain humeral surface morphology. At an alpha of 0.05 only when centroid size, site and CO were considered together did they significantly explain humeral surface morphology ($F(2,65) = 1.33$, $p < .01$, $R^2 = 0.02$). Sex and CO considered together explain morphology at an alpha of 0.10 as do site, sex, and CO.

Femoral surface morphology was also not uniquely explained by presence or absence of CO, but significant R^2 and p values were returned for size and CO together, site and CO together, sex and CO together, as well as size site and CO together, and site, sex, and CO together (see Table 5.14).

Individuals with Schmorl's nodes were grouped within the rest of the population for humeri (Figure 5.20) and femora (Figure 5.21). Type III GLMs were – as with the previous tests – used to determine if IVs of size, site, sex, and presence or absence of Schmorl's nodes could explain the variance in the DV of surface morphology.

Humeral surface morphology was not uniquely explained by the presence or absence of Schmorl's nodes (see Table 5.17). However, when sex and Schmorl's nodes were considered together and alpha was equal to 0.05, $F(4,66) = 0.88$, $p < 0.05$, $R^2 = 0.03$. The R^2 value was smaller for all other statistically significant interactions but $p < 0.05$ when IVs size, sex, and presence or absence of Schmorl's nodes were considered together to explain humeral surface morphology. Additionally the p value was less than 0.01 when size, site, and Schmorl's nodes were considered together as well as when site, sex, and Schmorl's nodes were considered together. While the presence of Schmorl's nodes could not uniquely explain morphological variation, their presence or absence could explain morphology when they were considered in concert with other IVs.

Schmorl's nodes did not uniquely explain femoral surface morphology (see Table 5.18) however when site and Schmorl's nodes were considered together at an alpha of 0.05, $F(2,34) = 1.07$, $p < 0.05$, $R^2 = 0.03$. When size, site, and Schmorl's nodes were considered together at an alpha of 0.05, $F(2,34) = 1.28$, $p < 0.05$, $R^2 = 0.03$. When size, sex, and Schmorl's nodes were considered together at an alpha of 0.05, $F(1,34) = 0.98$, $p < 0.05$, $R^2 = 0.01$. When site, sex and Schmorl's nodes were considered together at an alpha of 0.05, $F(2,34) = 0.98$, $p < 0.05$, $R^2 = 0.02$. Where the presence of Schmorl's nodes may explain the variation in morphology for femoral surface morphology it covaries with the other IVs. That is morphology is affected by the presence of Schmorl's nodes, but how it is affected is also dependent upon size, population, and sex.

No visual pattern was found for humeri with any severity of OA or DJD of the proximal epiphysis in shape space (Figure 5.22).. Mild and severe cases of OA in the distal humeral epiphysis did tend towards the positive distribution of PC2 (see Figure 5.23), however, the paucity of individuals affected in addition to the spread of the distribution should be considered before drawing conclusions. There was no apparent trend for OA with femoral shape in the PC visualizations (Figure 5.24 and Figure 5.25). GLMs were used to quantitatively evaluate morphological variation by the severity of DJD and OA. Shape was used as the DV and DJD and OA severity along with sex, size, and site, and the interactions between all four were used as IVs. (R was unable to calculate some of the interactions between IVs in this case and therefore tables provided look different than those provided previously.)

Severity of OA and DJD in the proximal humeral epiphysis did uniquely explain morphological variation of the humeral surface (see Table 5.19). When alpha = 0.05, $F(5,54) = 1.04$, $p < 0.05$, $R^2 = 0.04$. Statistical significance in explaining variance in humeral surface morphological variation was also found for size and DJD severity considered together (at an alpha of 0.05, $F(4,54) = 0.89$, $p < 0.05$, $R^2 = 0.03$), for site and DJD severity considered together (at an alpha of 0.05, $F(8,54) = 1.15$, $p < 0.01$, $R^2 = 0.07$), for sex and DJD severity considered together (at an alpha of 0.05, $F(5,54) = 1.11$, $p < 0.01$, $R^2 = 0.04$), for size, site, and DJD severity considered together (at an alpha of 0.05, $F(4,54) = 1.12$, $p < 0.01$, $R^2 = 0.03$), for size, sex, and DJD severity considered together (at an alpha of 0.05, $F(2,54) = 1.26$, $p < 0.01$, $R^2 = 0.02$), and for size, sex, and DJD severity considered together (at an alpha of 0.05, $F(2,54) = 1.40$, $p < 0.01$, $R^2 = 0.02$). Therefore, humeral surface morphology is somewhat explained by DJD and OA severity at the proximal epiphysis and may be further explained when accounting for size, sex, and population.

Severity of OA and DJD in the distal humeral epiphysis did not uniquely explain morphological variation of the humeral surface (see Table 5.20), but several of the interactions with other IVs were

statistically significant suggesting that again the resultant shape is dependent on a multiplicity of factors and many of these IVs covary. When size and severity of OA and DJD were considered together at an alpha of 0.05, $F(4,57) = 1.38$, $p < 0.01$, $R^2 = 0.04$. When site and DJD severity were considered together at an alpha of 0.05, $F(8,57) = 1.35$, $p < 0.01$, $R^2 = 0.08$. When sex and DJD severity were considered together at an alpha of 0.05, $F(2,57) = 0.91$, $p < 0.05$, $R^2 = 0.01$. When size, site and DJD severity were considered together at an alpha of 0.05, $F(3,57) = 1.03$, $p < 0.01$, $R^2 = 0.02$. When site, sex and DJD severity were considered together at an alpha of 0.05, $F(2,57) = 1.19$, $p < 0.01$, $R^2 = 0.02$. And when all four IVs were considered together at an alpha of 0.05, $F(2,57) = 1.28$, $p < 0.01$, $R^2 = 0.02$. Morphology of the humeral surface then is explained by DJD and OA severity on the distal epiphysis particularly when other factors are considered.

GLM results for the relationship between DJD and OA severity and femoral surface morphology are provided in Table 5.21 and Table 5.22. Femoral surface morphology is uniquely explained by DJD and OA in the proximal epiphysis. When alpha is 0.05, $F(5,43) = 1.41$, $p < 0.01$, $R^2 = 0.08$. DJD and OA in the distal epiphysis also uniquely explained femoral surface morphology. At an alpha of 0.05, $F(5,22) = 1.51$, $p < 0.01$, $R^2 = 0.09$. When size, site, and sex are paired together with DJD severity the R^2 value only declines slightly and remains strongly statistically significant. When size, site, and DJD severity are considered together the p value remains at less than 0.01, but the R^2 value drops to 0.38. For all other tests involving DJD severity and two or more of the other IVs at once the R^2 value dropped further and the p value rose above 0.01 but remained statistically significant below 0.05. This underscores the point that DJD and OA severity uniquely explain femoral surface morphology.

When site and DJD severity in the distal epiphysis are considered together at an alpha of 0.05, $F(6,46) = 0.94$, $p < 0.05$, $R^2 = 0.07$. When sex and DJD severity at the distal epiphysis are considered together at an alpha of 0.05, $F(5,44) = 1.03$, $p < 0.05$, $R^2 = 0.06$. When size, site, and DJD severity at the distal epiphysis are considered together at an alpha of 0.05, $F(2,46) = 0.95$, $p < 0.05$, $R^2 = 0.02$. When size, sex, and DJD severity at the distal epiphysis are considered together at an alpha of 0.05, $F(3,44) = 1.44$, $p < 0.01$, $R^2 = 0.05$. DJD and OA severity explain femoral morphology without the input of any other factors. However, the relationship between DJD severity and morphology remains significant when factors like site, sex, and size are also considered. In this case however the R^2 value and therefore the best fit remains highest when DJD and OA severity are considered alone.

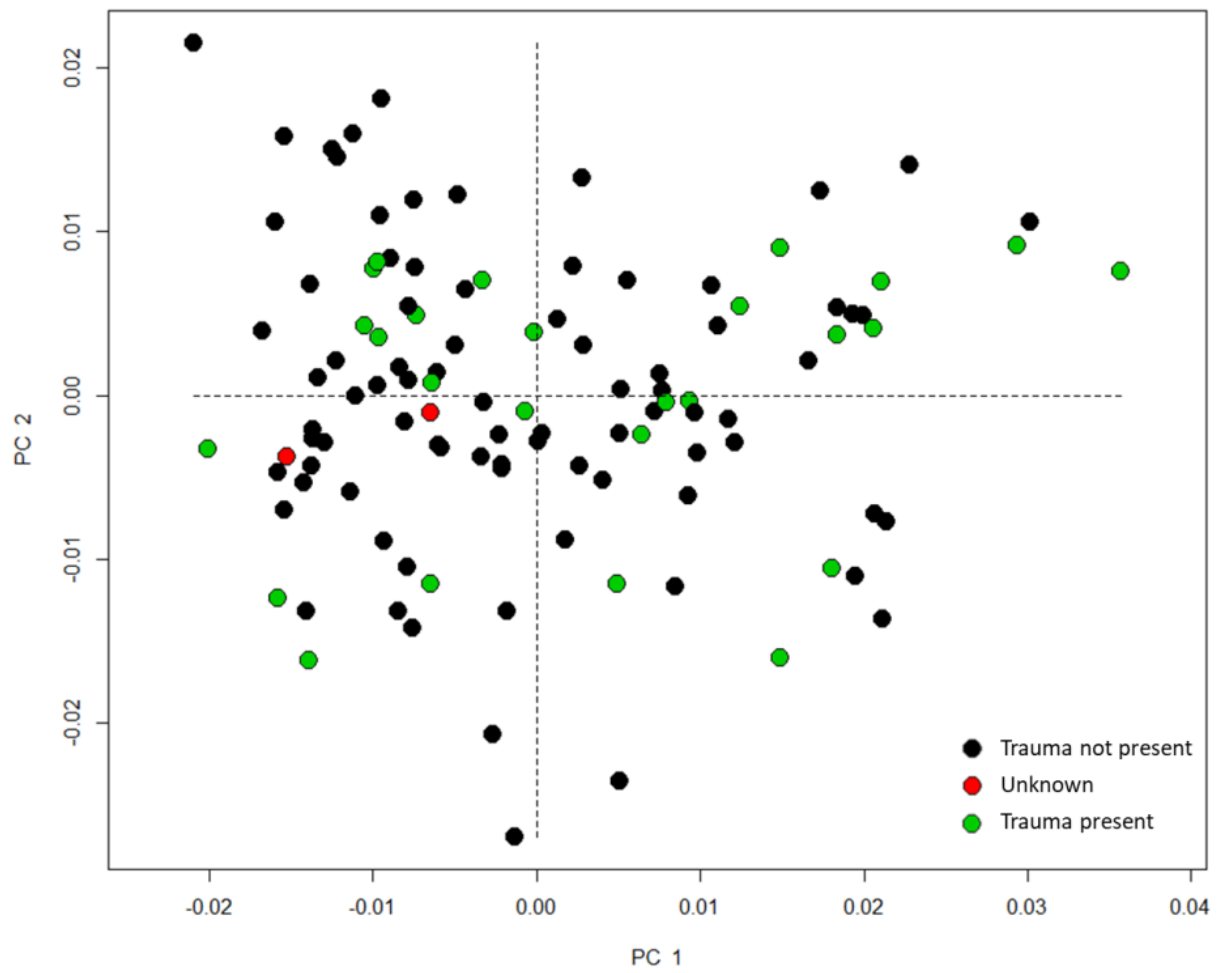


Figure 5.14 PC1 and PC2 humeri by trauma.

Table 5.11 GLM with interactions of humeral diaphyseal surface morphology by size, sex, and presence or absence of trauma.

	Df	SS	MS	Rsq	F	Z	Pr(>F)
Centroid Size	1	0.001207	0.0012067	0.018979	2.5802	2.3795	0.016
Site	3	0.011779	0.0039263	0.185254	8.3953	8.1885	0.001
Sex	4	0.001581	0.0003953	0.024868	0.8452	0.4055	0.336
trauma	2	0.000632	0.0003162	0.009945	0.676	-0.3887	0.642
Centroid Size x Site	3	0.001338	0.000446	0.021045	0.9537	1.1293	0.123
Centroid Size x Sex	4	0.001588	0.0003971	0.024981	0.8491	0.7536	0.23
Site x Sex	8	0.004547	0.0005684	0.071517	1.2154	3.2487	0.001
Centroid Size x trauma	1	0.000579	0.0005794	0.009112	1.2389	2.0399	0.025
Site x trauma	3	0.002079	0.0006929	0.032694	1.4816	3.7763	0.001
Sex x trauma	2	0.001026	0.0005128	0.01613	1.0965	2.2694	0.012
Centroid Size x Site x Sex	3	0.001515	0.0005049	0.023825	1.0797	2.8009	0.002
Centroid Size x Site x trauma	2	0.000811	0.0004054	0.012751	0.8667	1.6716	0.052
Centroid Size x Sex x trauma	1	0.000817	0.0008167	0.012845	1.7464	3.1422	0.002
Site x Sex x trauma	2	0.000821	0.0004104	0.012908	0.8774	1.8674	0.036
Centroid Size x Site x Sex x trauma	2	0.000993	0.0004964	0.015616	1.0615	2.3351	0.004
Residuals	69	0.03227	0.0004677				
Total	110	0.063582					

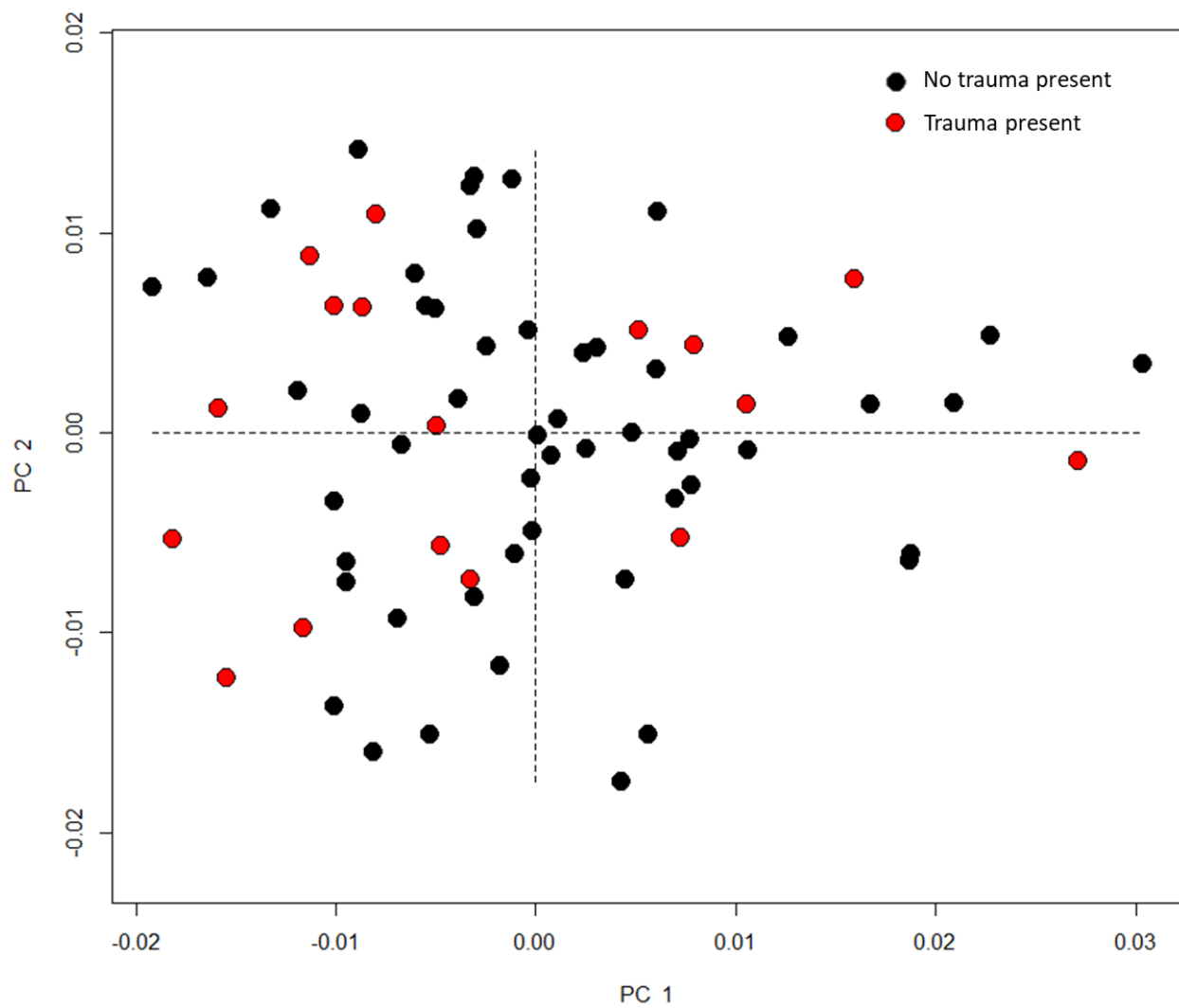


Figure 5.15 PC1 and PC2 of femur diaphyseal surface morphology organized by presence or absence of trauma.

Table 5.12 GLM with interactions of femoral diaphyseal surface morphology by presence or absence of trauma.

	Df	SS	MS	Rsqr	F	Z	Pr(>F)
Centroid Size	1	0.0016903	0.00169029	0.053904	4.4711	3.9934	0.001
Site	3	0.0037406	0.00124686	0.119289	3.2982	5.194	0.001
Sex	4	0.0019723	0.00049307	0.062896	1.3043	2.0281	0.023
trauma	1	0.0003762	0.00037623	0.011998	0.9952	0.8918	0.174
Centroid Size x Site	3	0.0009418	0.00031394	0.030035	0.8304	0.4172	0.33
Centroid Size x Sex	4	0.0014707	0.00036768	0.046902	0.9726	1.3065	0.096
Site x Sex	5	0.0024117	0.00048233	0.076909	1.2759	2.8447	0.002
Centroid Size x trauma	1	0.0003451	0.00034509	0.011005	0.9128	1.2435	0.108
Site x trauma	2	0.002085	0.00104249	0.066491	2.7576	5.4818	0.001
Sex x trauma	1	0.000285	0.00028505	0.00909	0.754	1.1423	0.133
Centroid Size x Site x Sex	2	0.0006484	0.00032422	0.020679	0.8576	1.9239	0.03
Centroid Size x Site x trauma	2	0.0007003	0.00035017	0.022334	0.9263	2.0299	0.029
Centroid Size x Sex x trauma	1	0.0002189	0.00021891	0.006981	0.5791	0.6357	0.257
Site x Sex x trauma	2	0.0006456	0.00032281	0.020589	0.8539	1.9051	0.038
Centroid Size x Site x Sex x trauma	1	0.0002158	0.00021576	0.006881	0.5707	0.7908	0.211
Residuals	36	0.0136097	0.00037805				
Total	69	0.0313574					

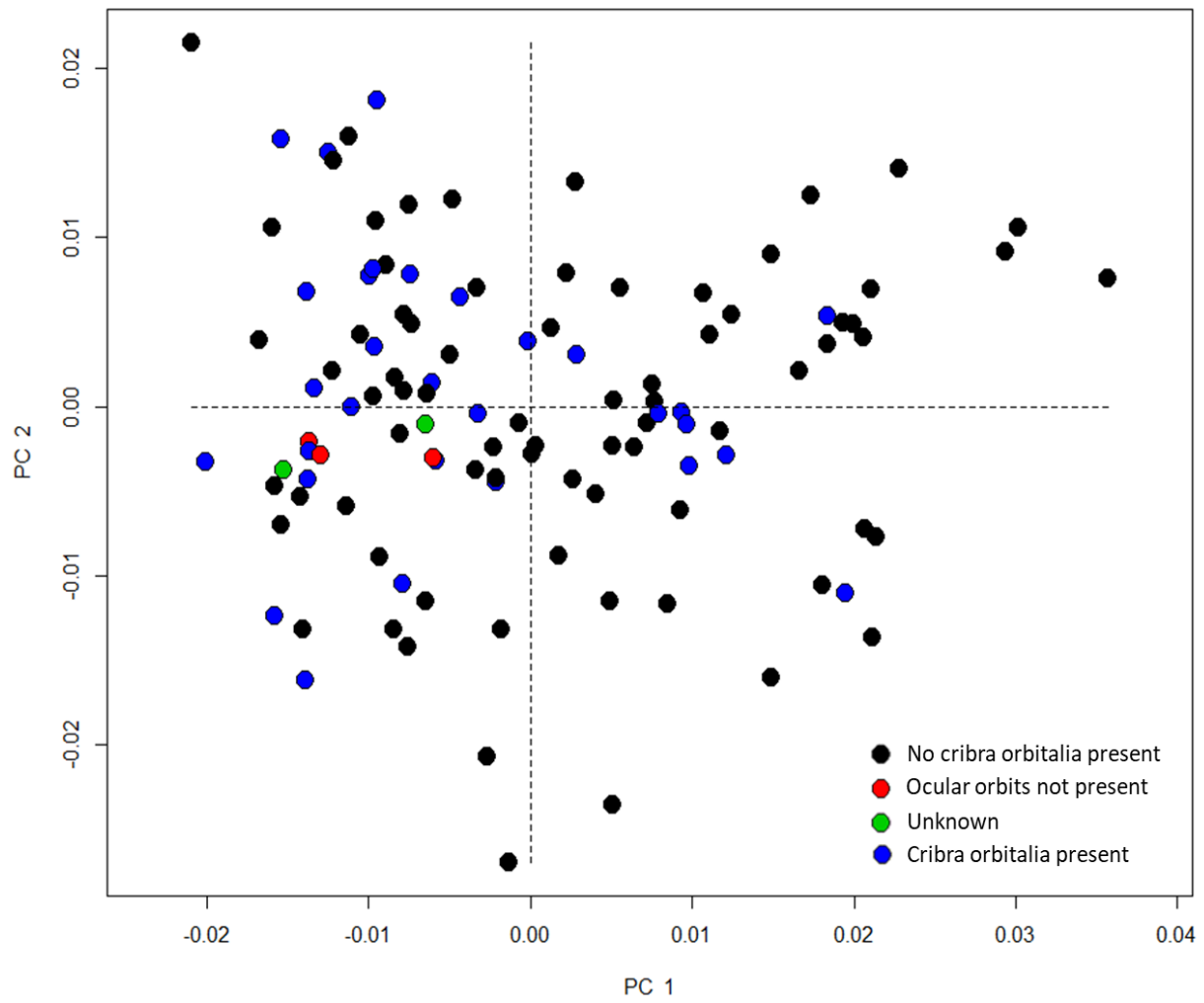


Figure 5.16 PC1 and PC2 humeri by cribra orbitalia.

Table 5.13 GLM with interactions of humeral diaphyseal surface morphology by presence or absence of cribra orbitalia.

	Df	SS	MS	Rsq	F	Z	Pr(>F)
Centroid Size	1	0.001207	0.0012067	0.018979	2.3939	2.1906	0.025
Site	3	0.011779	0.0039263	0.185254	7.7889	7.9337	0.001
Sex	4	0.001581	0.0003953	0.024868	0.7842	0.03	0.471
CO	3	0.001141	0.0003804	0.017949	0.7547	0.0228	0.464
Centroid Size x Site	3	0.001384	0.0004614	0.021773	0.9154	0.9952	0.156
Centroid Size x Sex	4	0.001724	0.000431	0.027116	0.8551	0.8414	0.206
Site x Sex	8	0.004322	0.0005403	0.06798	1.0718	2.5516	0.006
Centroid Size x CO	2	0.000763	0.0003814	0.011998	0.7567	0.7266	0.235
Site x CO	3	0.000888	0.0002959	0.013961	0.587	-0.1597	0.571
Sex x CO	3	0.001287	0.000429	0.02024	0.851	1.394	0.083
Centroid Size x Site x Sex	4	0.001588	0.0003969	0.024972	0.7875	1.3417	0.093
Centroid Size x Site x CO	2	0.001343	0.0006715	0.021122	1.3321	2.9845	0.003
Centroid Size x Sex x CO	1	0.000366	0.0003658	0.005754	0.7257	0.9903	0.173
Site x Sex x CO	2	0.000765	0.0003826	0.012036	0.7591	1.3502	0.097
Centroid Size x Site x Sex x CO	2	0.000678	0.0003392	0.01067	0.6729	0.8527	0.199
Residuals	65	0.032765	0.0005041				
Total	110	0.063582					

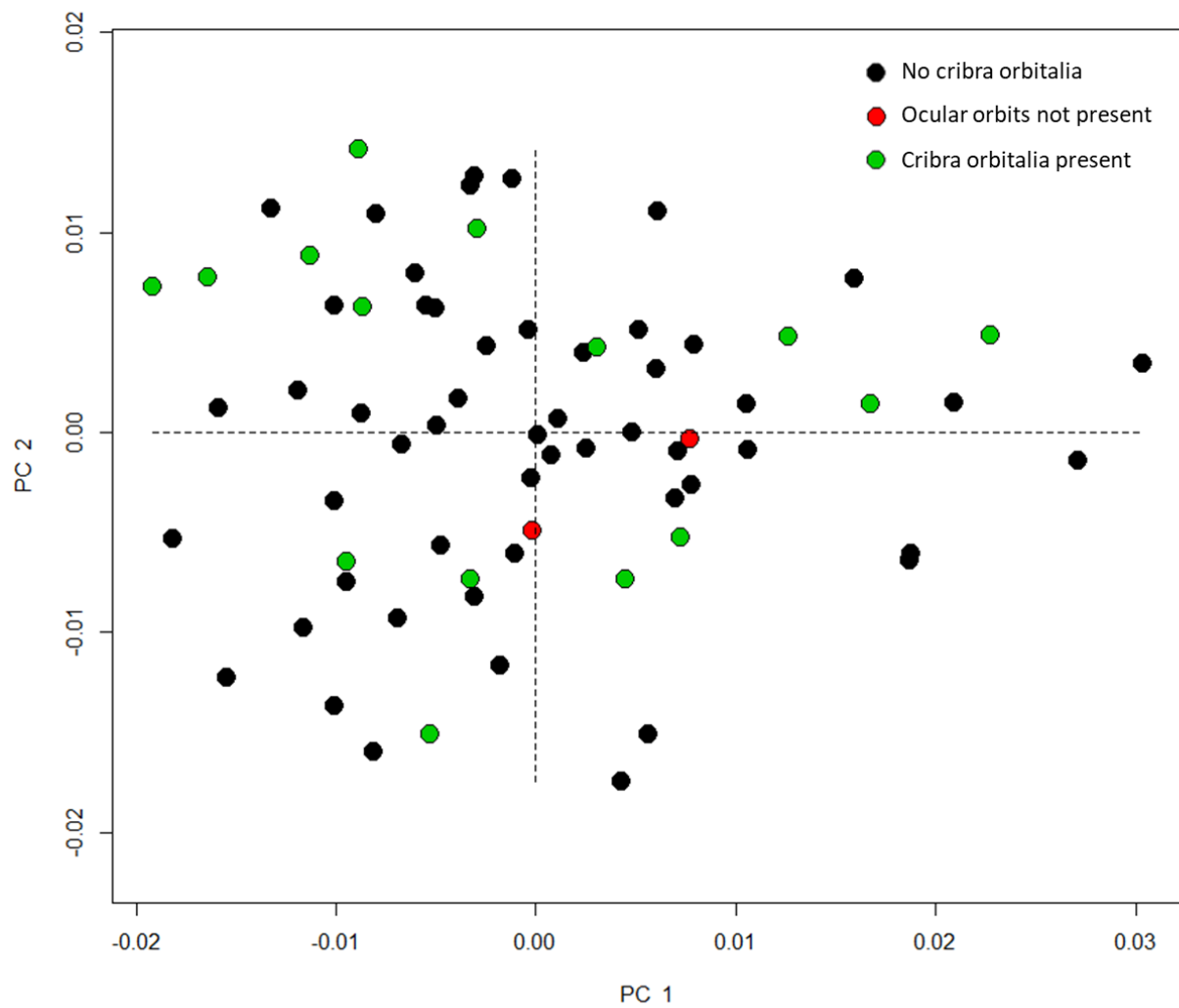


Figure 5.17 PC1 and PC2 of femur diaphyseal surface morphology organized by presence or absence of cribra orbitalia.

Table 5.14 GLM with interactions of femoral diaphyseal surface morphology by presence or absence of cribra orbitalia.

	Df	SS	MS	Rsq	F	Z	Pr(>F)
Centroid Size	1	0.0016903	0.00169029	0.053904	4.4942	4.0264	0.001
Site	3	0.0037406	0.00124686	0.119289	3.3152	5.1575	0.001
Sex	4	0.0019723	0.00049307	0.062896	1.311	2.054	0.025
CO	2	0.0005936	0.00029681	0.018931	0.7892	0.2763	0.363
Centroid Size x Site	3	0.0009502	0.00031674	0.030303	0.8422	0.5171	0.301
Centroid Size x Sex	4	0.001275	0.00031875	0.04066	0.8475	0.81	0.207
Site x Sex	5	0.0023292	0.00046585	0.07428	1.2386	2.7549	0.002
Centroid Size x CO	1	0.0006187	0.00061871	0.019731	1.645	2.7564	0.005
Site x CO	2	0.0007417	0.00037086	0.023653	0.986	1.6204	0.043
Sex x CO	2	0.0008238	0.00041189	0.026271	1.0951	1.949	0.014
Centroid Size x Site x Sex	2	0.0012417	0.00062086	0.039599	1.6507	3.7178	0.001
Centroid Size x Site x CO	1	0.0007637	0.00076371	0.024355	2.0306	3.5816	0.001
Centroid Size x Sex x CO	1	0.0002531	0.00025312	0.008072	0.673	1.1267	0.133
Site x Sex x CO	1	0.0004749	0.00047491	0.015145	1.2627	2.4356	0.005
Centroid Size x Site x Sex x CO	1	0.0003486	0.0003486	0.011117	0.9268	1.5803	0.052
Residuals	36	0.0135399	0.00037611				
Total	69	0.0313574					

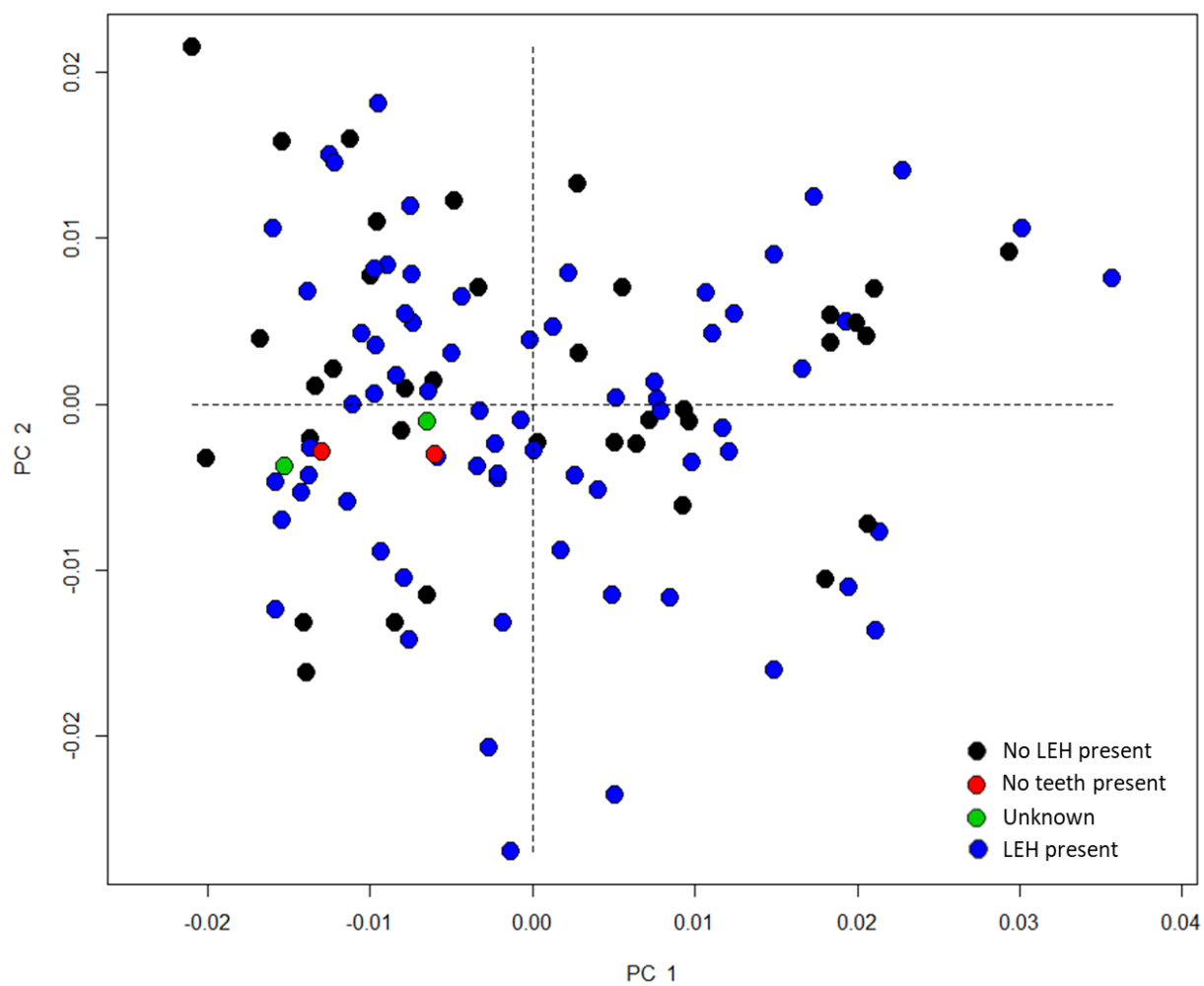


Figure 5.18 PC1 and PC2 humeri by LEH.

Table 5.15 GLM with interactions of humeral diaphyseal surface morphology by presence or absence of LEH.

	Df	SS	MS	Rsqr	F	Z	Pr(>F)
Centroid Size	1	0.001207	0.0012067	0.018979	2.4764	2.2687	0.022
Site	3	0.011779	0.0039263	0.185254	8.0573	8.0267	0.001
Sex	4	0.001581	0.0003953	0.024868	0.8112	0.1895	0.41
LEH	3	0.001033	0.0003442	0.016242	0.7064	-0.265	0.59
Centroid Size x Site	3	0.00138	0.00046	0.021703	0.9439	1.1102	0.127
Centroid Size x Sex	4	0.001671	0.0004177	0.026278	0.8572	0.8409	0.212
Site x Sex	8	0.004392	0.000549	0.069079	1.1267	2.84	0.003
Centroid Size x LEH	2	0.000644	0.0003222	0.010136	0.6613	0.279	0.374
Site x LEH	3	0.001345	0.0004484	0.021159	0.9203	1.8054	0.042
Sex x LEH	2	0.001101	0.0005506	0.01732	1.1299	2.2773	0.013
Centroid Size x Site x Sex	4	0.001496	0.000374	0.02353	0.7675	1.277	0.107
Centroid Size x Site x LEH	3	0.002407	0.0008023	0.037853	1.6464	4.1748	0.001
Centroid Size x Sex x LEH	1	0.000271	0.0002708	0.004259	0.5557	0.3353	0.361
Site x Sex x LEH	2	0.00084	0.0004198	0.013206	0.8615	1.6018	0.053
Centroid Size x Site x Sex x LEH	2	0.000761	0.0003807	0.011975	0.7813	1.4984	0.068
Residuals	65	0.031674	0.0004873				
Total	110	0.063582					

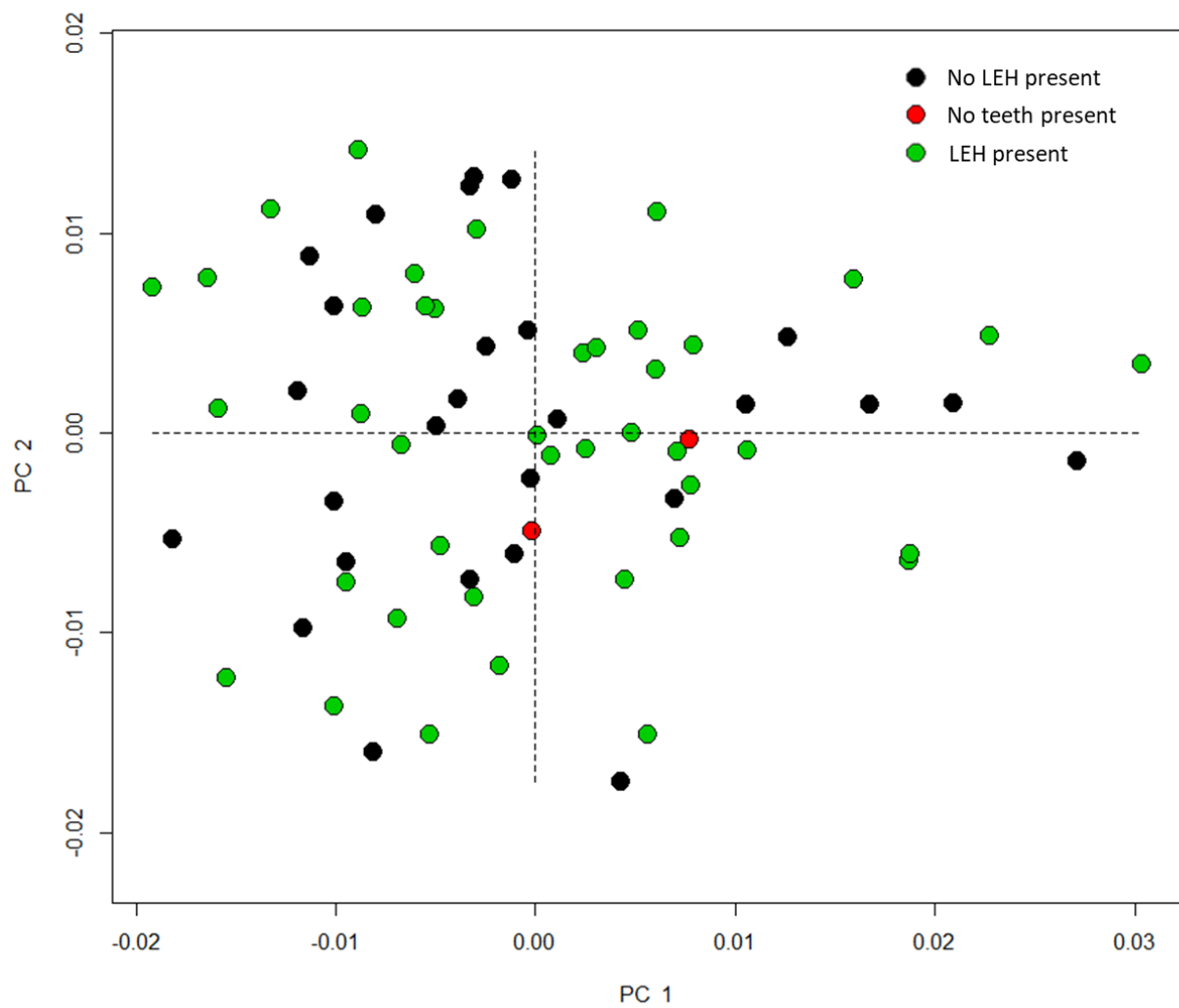


Figure 5.19 PC1 and PC2 of femur diaphyseal surface morphology organized by presence or absence of LEH.

Table 5.16 GLM with interactions of femoral diaphyseal surface morphology by presence or absence of LEH.

	Df	SS	MS	Rsqu	F	Z	Pr(>F)
Centroid Size	1	0.0016903	0.00169029	0.053904	4.5166	3.9998	0.001
Site	3	0.0037406	0.00124686	0.119289	3.3317	5.1753	0.001
Sex	4	0.0019723	0.00049307	0.062896	1.3175	2.04	0.023
LEH	2	0.0008192	0.00040961	0.026125	1.0945	1.3651	0.082
Centroid Size x Site	3	0.000968	0.00032266	0.030869	0.8622	0.6168	0.274
Centroid Size x Sex	4	0.0013042	0.00032605	0.041591	0.8712	0.9317	0.189
Site x Sex	5	0.0024263	0.00048525	0.077374	1.2966	2.9174	0.002
Centroid Size x LEH	1	0.0001706	0.00017063	0.005441	0.4559	-0.4474	0.659
Site x LEH	2	0.0011257	0.00056283	0.035898	1.5039	3.0716	0.002
Sex x LEH	2	0.001402	0.00070102	0.044712	1.8732	3.3682	0.001
Centroid Size x Site x Sex	2	0.0007025	0.00035124	0.022402	0.9385	2.1466	0.015
Centroid Size x Site x LEH	2	0.0005681	0.00028404	0.018116	0.759	1.5257	0.067
Centroid Size x Sex x LEH	1	0.0007076	0.00070757	0.022565	1.8907	3.0688	0.001
Site x Sex x LEH	2	0.0006036	0.00030179	0.019248	0.8064	1.5044	0.055
Centroid Size x Site x Sex x LEH	1	0.0004323	0.00043235	0.013788	1.1553	2.26	0.01
Residuals	34	0.0127243	0.00037424				
Total	69	0.0313574					

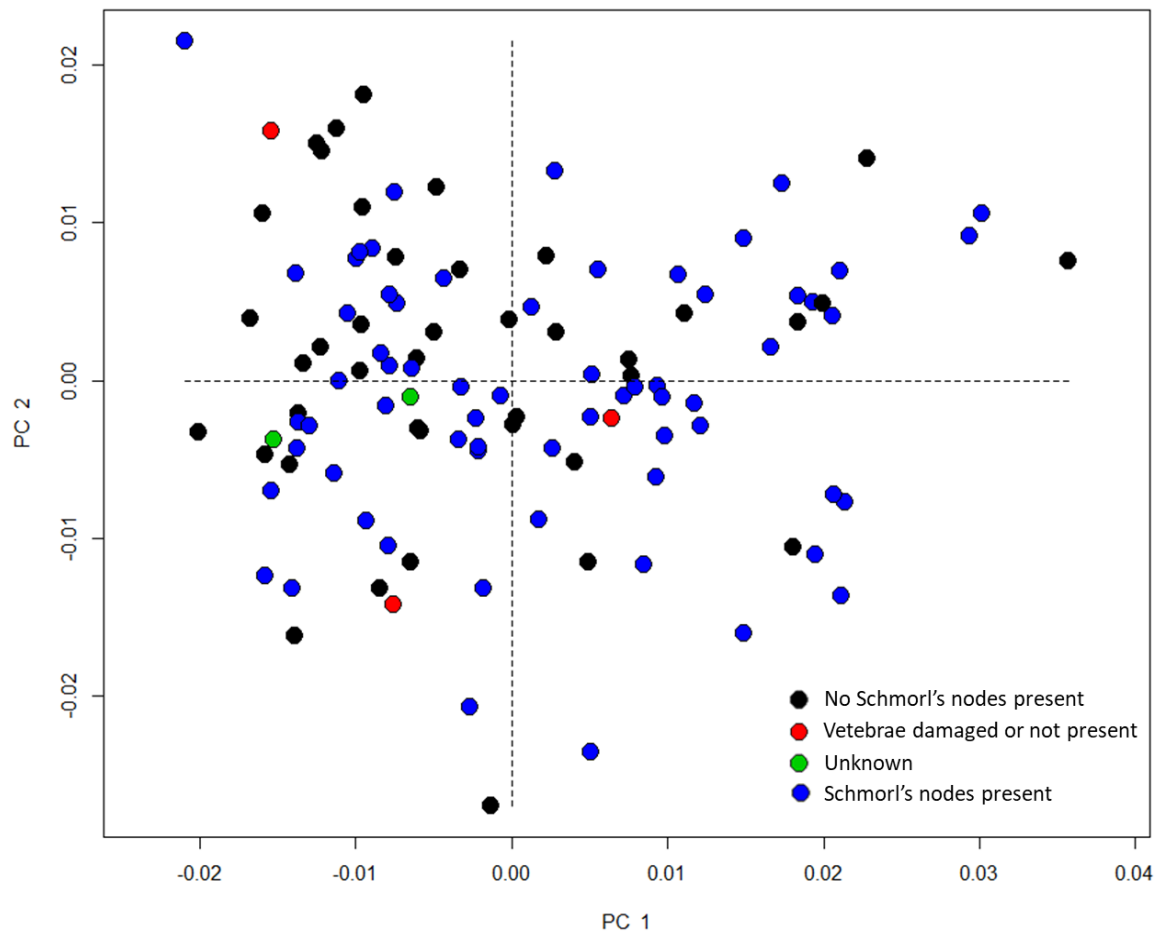


Figure 5.20 PC1 and PC2 humeri by Schmorl's nodes.

Table 5.17 GLM with interactions of humeral diaphyseal surface morphology by presence or absence of Schmorl's nodes.

	Df	SS	MS	Rsqu	F	Z	Pr(>F)
Centroid Size	1	0.001207	0.0012067	0.018979	2.4677	2.2721	0.019
Site	3	0.011779	0.0039263	0.185254	8.0292	7.9337	0.001
Sex	4	0.001581	0.0003953	0.024868	0.8084	0.1815	0.415
Schmorl's Nodes	3	0.00107	0.0003567	0.016829	0.7294	-0.149	0.553
Centroid Size x Site	3	0.001372	0.0004573	0.021578	0.9352	1.0824	0.137
Centroid Size x Sex	4	0.001636	0.000409	0.025731	0.8364	0.7186	0.251
Site x Sex	8	0.004519	0.0005649	0.071073	1.1552	3.0053	0.003
Centroid Size x Schmorl's Nodes	2	0.000948	0.0004741	0.014912	0.9695	1.5641	0.067
Site x Schmorl's Nodes	3	0.00125	0.0004167	0.019662	0.8522	1.4021	0.087
Sex x Schmorl's Nodes	4	0.001726	0.0004314	0.027142	0.8823	1.7823	0.04
Centroid Size x Site x Sex	3	0.000879	0.0002931	0.013828	0.5993	0.2488	0.416
Centroid Size x Site x Schmorl's Nodes	2	0.001051	0.0005253	0.016522	1.0742	2.4418	0.008
Centroid Size x Sex x Schmorl's Nodes	1	0.000527	0.000527	0.008288	1.0776	2.0319	0.016
Site x Sex x Schmorl's Nodes	2	0.001372	0.0006861	0.021583	1.4031	3.2243	0.002
Centroid Size x Site x Sex x Schmorl's Nodes	1	0.000391	0.0003914	0.006156	0.8005	0.9736	0.142
Residuals	66	0.032274	0.000489				
Total	110	0.063582					

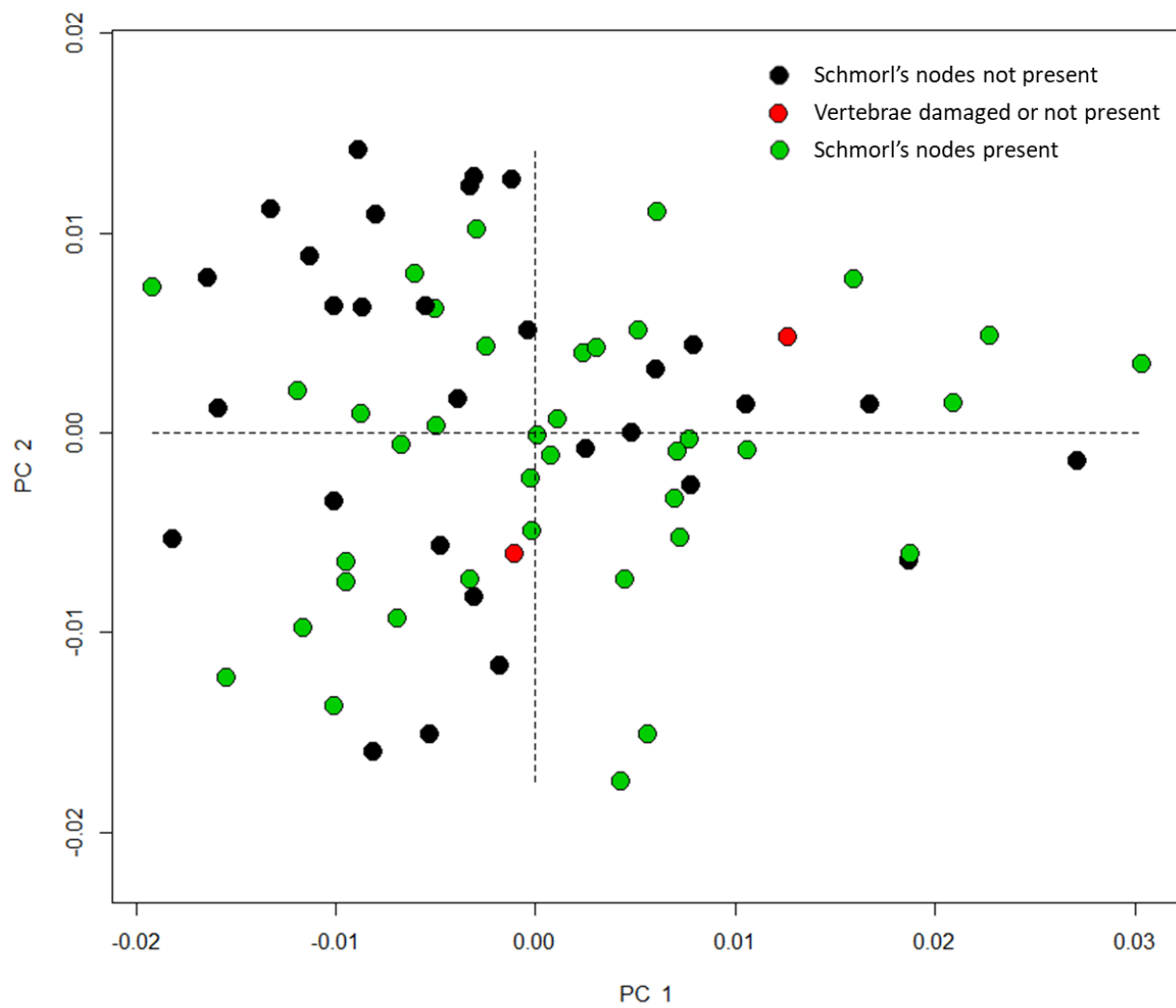


Figure 5.21 PC1 and PC2 of femur diaphyseal surface morphology by presence or absence of Schmorl's nodes.

Table 5.18 GLM with interactions of femoral diaphyseal surface morphology by presence or absence of Schmorl's nodes.

	Df	SS	MS	Rsq	F	Z	Pr(>F)
Centroid Size	1	0.0016903	0.00169029	0.053904	4.3392	3.8985	0.001
Site	3	0.0037406	0.00124686	0.119289	3.2008	5.0383	0.001
Sex	4	0.0019723	0.00049307	0.062896	1.2658	1.8718	0.033
Schmorl's Nodes	2	0.0008086	0.00040429	0.025786	1.0379	1.0645	0.141
Centroid Size x Site	3	0.0008995	0.00029984	0.028686	0.7697	0.209	0.402
Centroid Size x Sex	4	0.0014392	0.00035981	0.045897	0.9237	1.2105	0.111
Site x Sex	5	0.0023462	0.00046923	0.07482	1.2046	2.5591	0.005
Centroid Size x Schmorl's Nodes	2	0.0007504	0.00037522	0.023932	0.9632	1.48	0.077
Site x Schmorl's Nodes	2	0.000834	0.00041702	0.026598	1.0705	2.2051	0.013
Sex x Schmorl's Nodes	1	0.0001343	0.00013435	0.004284	0.3449	-0.8842	0.813
Centroid Size x Site x Sex	2	0.0011438	0.00057192	0.036478	1.4682	3.216	0.003
Centroid Size x Site x Schmorl's Nodes	2	0.0010007	0.00050036	0.031913	1.2845	2.52	0.01
Centroid Size x Sex x Schmorl's Nodes	1	0.0003803	0.00038026	0.012127	0.9762	1.9252	0.034
Site x Sex x Schmorl's Nodes	2	0.0007649	0.00038243	0.024391	0.9817	2.156	0.019
Centroid Size x Site x Sex x Schmorl's Nodes	1	0.0002079	0.00020788	0.006629	0.5336	0.6326	0.243
Residuals	34	0.0132444	0.00038954				
Total	69	0.0313574					

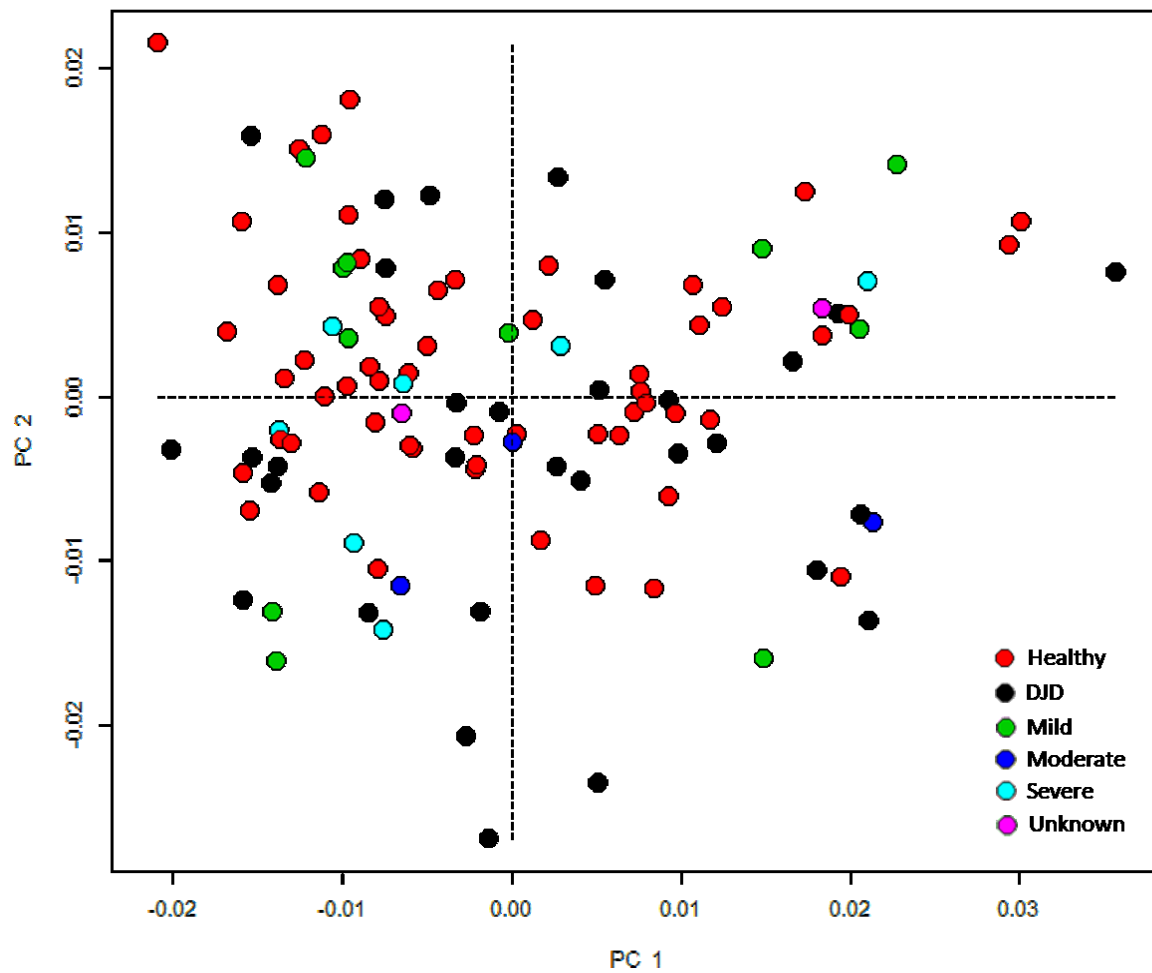


Figure 5.22 PC1 and PC2 humeri by DJD and OA severity at proximal epiphysis.

Table 5.19 GLM with interactions of humeral diaphyseal surface morphology by DJD and OA severity at proximal epiphysis.

	Df	SS	MS	Rsqr	F	Z	Pr(>F)
Centroid Size	1	0.001207	0.0012067	0.018979	2.6236	2.404	0.017
Site	3	0.011779	0.0039263	0.185254	8.5363	8.1823	0.001
Sex	4	0.001581	0.0003953	0.024868	0.8594	0.4806	0.314
DJD severity	5	0.002382	0.0004763	0.037459	1.0357	1.7712	0.035
Centroid Size x Site	3	0.001515	0.0005049	0.023823	1.0977	1.9565	0.029
Centroid Size x Sex	4	0.001807	0.0004517	0.028415	0.982	1.6981	0.044
Site x Sex	8	0.004577	0.0005721	0.071981	1.2438	3.538	0.001
Centroid Size x DJD severity	4	0.001634	0.0004084	0.025695	0.888	1.8193	0.04
Site x DJD severity	8	0.004231	0.0005289	0.066552	1.15	4.0187	0.001
Sex x DJD severity	5	0.002555	0.0005111	0.040189	1.1111	3.3791	0.001
Centroid Size x Site x Sex	2	0.000669	0.0003343	0.010517	0.7269	1.6176	0.07
Centroid Size x Site x DJD severity	4	0.002053	0.0005133	0.032291	1.116	3.7828	0.001
Centroid Size x Sex x DJD severity	2	0.00116	0.0005798	0.018238	1.2606	2.8255	0.001
Site x Sex x DJD severity	2	0.001285	0.0006427	0.020217	1.3974	3.033	0.001
Centroid Size x Site x Sex x DJD severity	1	0.000311	0.0003106	0.004886	0.6754	1.334	0.086
Residuals	54	0.024837	0.0004599				
Total	110	0.063582					

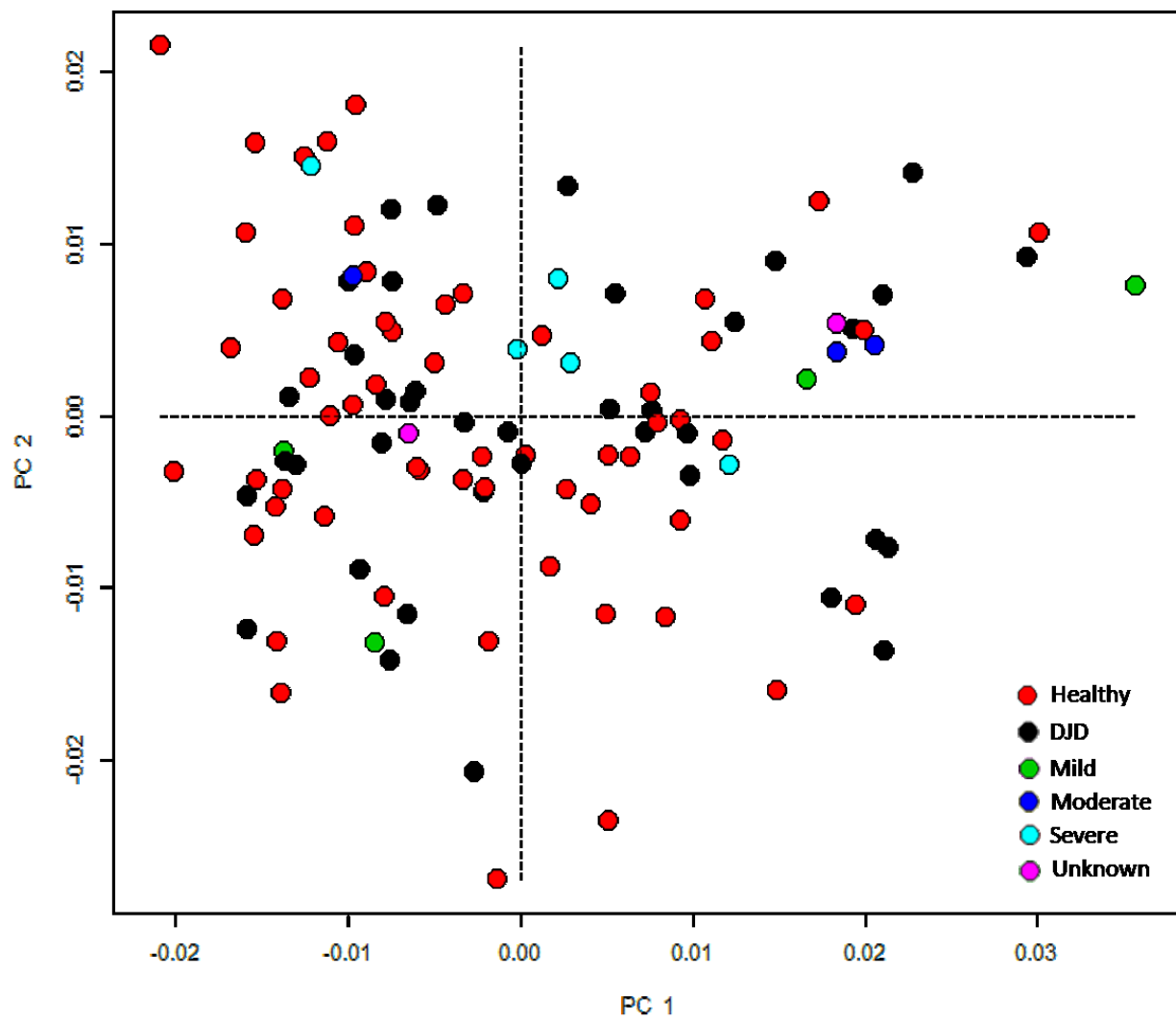


Figure 5.23 PC1 and PC2 humeri by DJD and OA severity at distal epiphysis.

Table 5.20 GLM with interactions of humeral diaphyseal surface morphology by DJD and OA severity at distal epiphysis.

	Df	SS	MS	Rsqr	F	Z	Pr(>F)
Centroid Size	1	0.001207	0.0012067	0.018979	2.6573	2.4293	0.017
Site	3	0.011779	0.0039263	0.185254	8.6459	8.1718	0.001
Sex	4	0.001581	0.0003953	0.024868	0.8704	0.5442	0.297
DJD severity	5	0.002128	0.0004255	0.033464	0.9371	1.1787	0.107
Centroid Size x Site	3	0.001321	0.0004404	0.020781	0.9698	1.3074	0.101
Centroid Size x Sex	4	0.001662	0.0004155	0.02614	0.915	1.2849	0.106
Site x Sex	8	0.004593	0.0005741	0.072239	1.2643	3.6503	0.001
Centroid Size x DJD severity	4	0.002501	0.0006252	0.039332	1.3767	3.8189	0.001
Site x DJD severity	8	0.004893	0.0006116	0.076957	1.3469	4.8741	0.001
Sex x DJD severity	2	0.000828	0.0004141	0.013027	0.912	1.9138	0.021
Centroid Size x Site x Sex	3	0.001229	0.0004098	0.019337	0.9025	2.5963	0.005
Centroid Size x Site x DJD severity	3	0.001398	0.0004661	0.021992	1.0264	3.0297	0.001
Centroid Size x Sex x DJD severity	1	0.000334	0.0003345	0.005261	0.7366	1.3445	0.092
Site x Sex x DJD severity	2	0.001084	0.0005419	0.017045	1.1933	3.1607	0.001
Centroid Size x Site x Sex x DJD severity	2	0.001158	0.0005791	0.018215	1.2752	3.2189	0.002
Residuals	57	0.025885	0.0004541				
Total	110	0.063582					

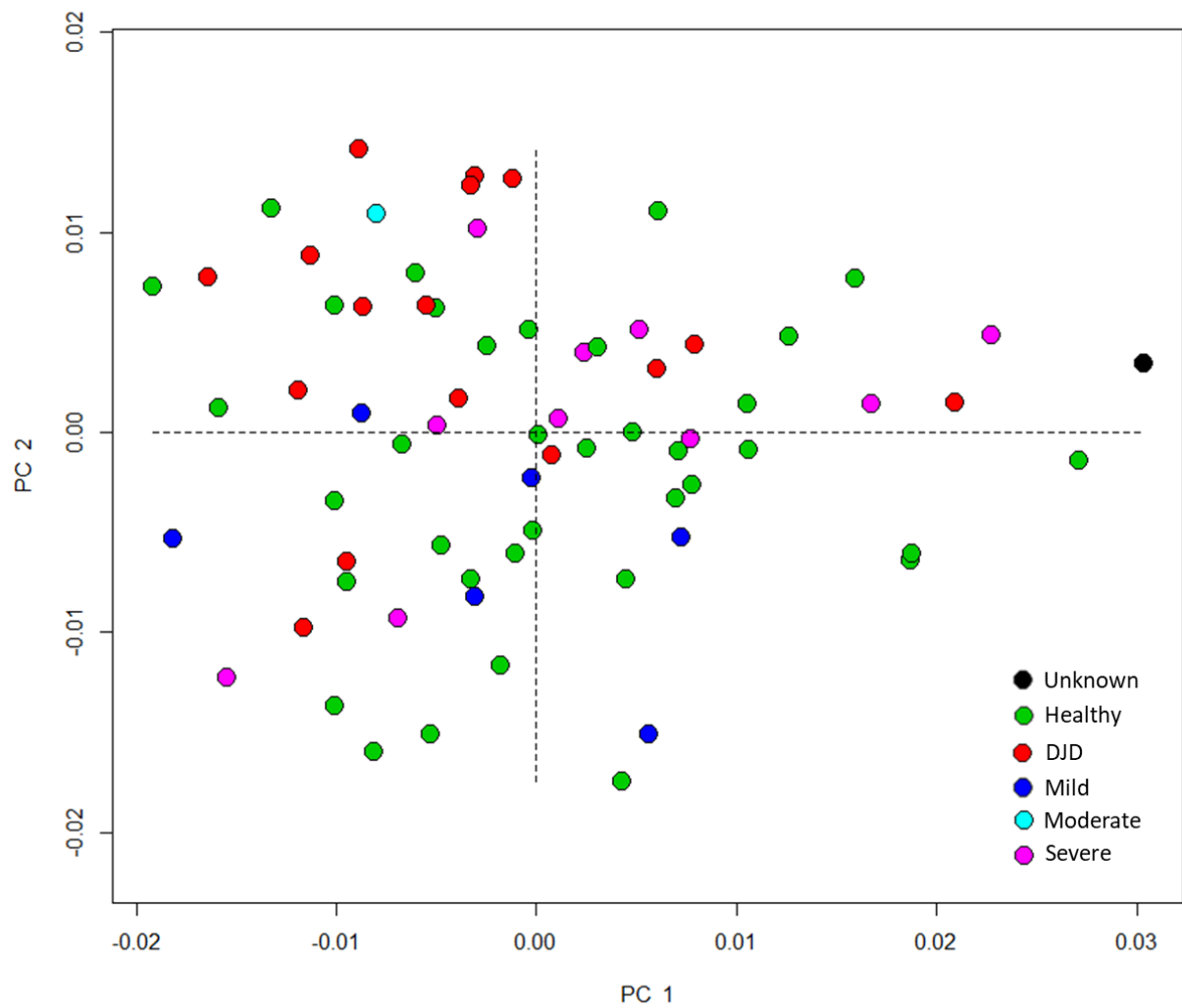


Figure 5.24 PC1 and PC2 of femur diaphyseal surface morphology by DJD and OA severity at proximal epiphysis..

Table 5.21 GLM with interactions of femoral diaphyseal surface morphology by DJD and OA severity at proximal epiphysis.

	Df	SS	MS	Rsqr	F	Z	Pr(>F)
Centroid Size	1	0.0016903	0.00169029	0.053904	4.5038	3.9175	0.001
Site	3	0.0037406	0.00124686	0.119289	3.3223	4.9238	0.001
Sex	4	0.0019723	0.00049307	0.062896	1.3138	1.9084	0.036
DJD severity	5	0.0028541	0.00057082	0.091018	1.521	3.1285	0.002
Centroid Size x Site	3	0.0008865	0.0002955	0.028271	0.7874	0.6613	0.235
Centroid Size x Sex	4	0.0014685	0.00036713	0.046831	0.9782	1.6307	0.052
Site x Sex	4	0.0014448	0.00036119	0.046074	0.9624	1.9581	0.028
Centroid Size x DJD severity	4	0.0015703	0.00039258	0.050078	1.046	2.6521	0.006
Site x DJD severity	7	0.0026361	0.00037659	0.084068	1.0034	3.0273	0.002
Sex x DJD severity	3	0.0016913	0.00056378	0.053937	1.5022	3.9329	0.001
Centroid Size x Site x Sex	2	0.0007061	0.00035305	0.022518	0.9407	2.6304	0.003
Centroid Size x Site x DJD severity	3	0.0011915	0.00039715	0.037996	1.0582	3.2573	0.001
Centroid Size x Sex x DJD severity	2	0.0005854	0.00029268	0.018667	0.7798	2.0115	0.015
Site x Sex x DJD severity	1	0.0003018	0.00030181	0.009625	0.8042	1.9972	0.014
Centroid Size x Site x Sex x DJD severity	1	0.0003612	0.00036119	0.011518	0.9624	2.1013	0.01
Residuals	22	0.0082567	0.0003753				
Total	69	0.0313574					

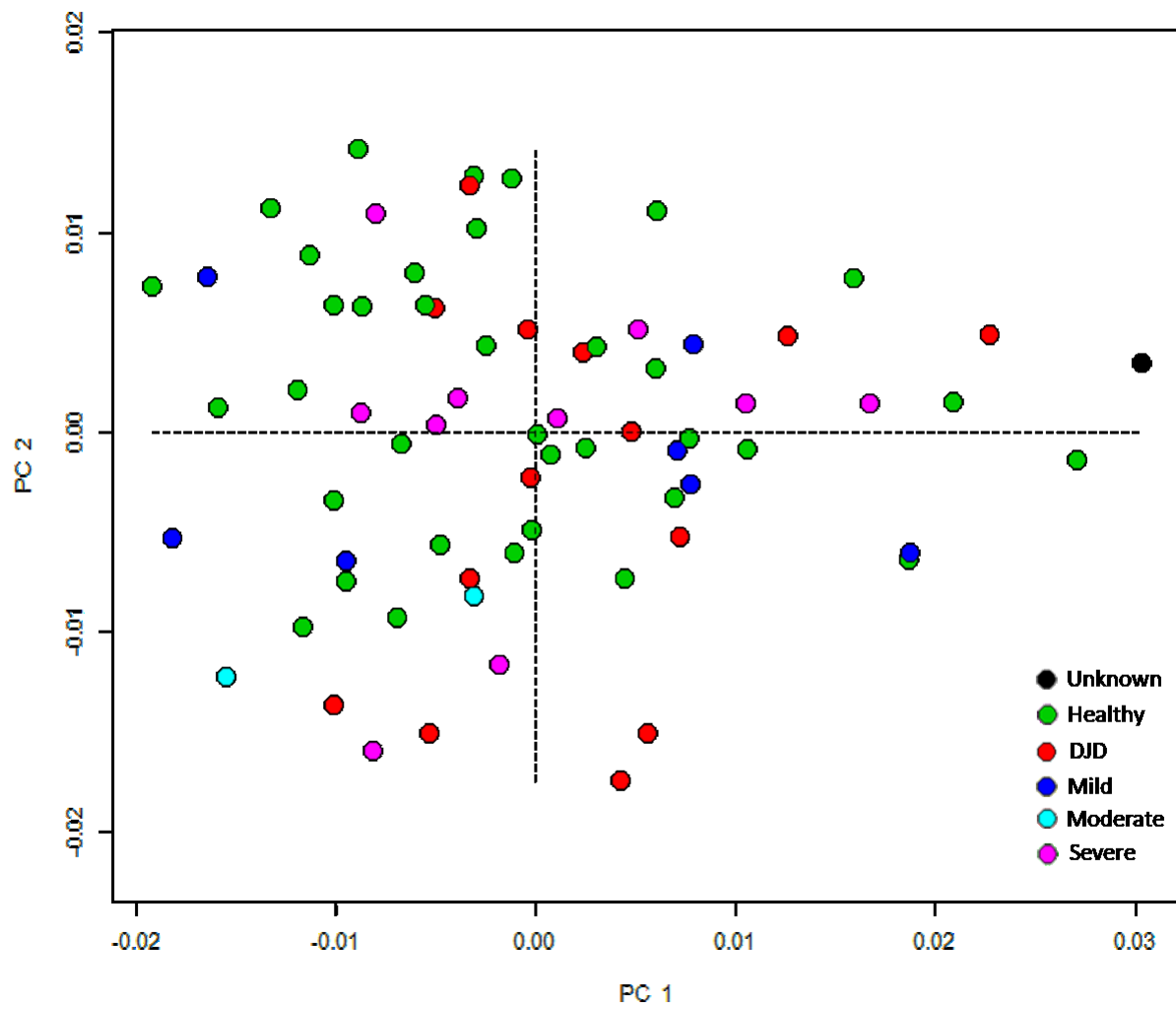


Figure 5.25 PC1 and PC2 of femur diaphyseal surface morphology by DJD and OA severity at distal epiphysis.

Table 5.22 GLM with interactions of femoral diaphyseal surface morphology by DJD and OA severity at distal epiphysis

	Df	SS	MS	Rsqr	F	Z	Pr(>F)
Centroid Size	1	0.0016903	0.00169029	0.053904	4.3077	3.8839	0.001
Site	3	0.0037406	0.00124686	0.119289	3.1776	5.0606	0.001
DJD severity	5	0.0029512	0.00059024	0.094114	1.5042	2.7071	0.005
Centroid Size x Site	3	0.0008153	0.00027177	0.026001	0.6926	-0.1082	0.523
Centroid Size x DJD severity	3	0.0011558	0.00038526	0.036858	0.9818	1.3082	0.102
Site x DJD severity	6	0.0022096	0.00036827	0.070465	0.9385	1.719	0.044
Centroid Size x Site x DJD severity	2	0.0007448	0.00037242	0.023753	0.9491	1.6061	0.048
Residuals	46	0.0180499	0.00039239				
Total	69	0.0313574					

	Df	SS	MS	Rsqr	F	Z	Pr(>F)
Centroid Size	1	0.0016903	0.00169029	0.053904	4.2654	3.8969	0.001
Sex	4	0.0022954	0.00057384	0.0732	1.4481	1.888	0.035
DJD severity	5	0.0030312	0.00060625	0.096668	1.5299	2.6067	0.007
Centroid Size x Sex	4	0.0019081	0.00047703	0.06085	1.2038	1.8948	0.034
Centroid Size x DJD severity	3	0.0012427	0.00041422	0.039629	1.0453	1.5288	0.065
Sex x DJD severity	5	0.0020369	0.00040737	0.064957	1.028	2.0195	0.032
Centroid Size x Sex x DJD severity	3	0.0017167	0.00057225	0.054747	1.4441	3.0291	0.001
Residuals	44	0.0174361	0.00039628				
Total	69	0.0313574					

5.2.2 Interpopulation

Humeral surface morphological variation by site is shown in Figure 5.26. Unlike with the previous IVs there is an obvious visual distinction in PC1 between the medieval English sites and the postmedieval Coach Lane and the medieval Sudanese site. For humeral morphology Coach Lane and 3-J-18 cluster together on the negative side of PC1 with Fishergate and Hereford clustering on the positive side. This suggests that for humeral morphology, there is more variation due to the temporal separation of Coach Lane from the other two English sites than due to the special variation from England to sub-Saharan Africa. Femoral surface morphology tells a slightly different tale in shape space with 3-J-18 occupying the negative aspect of PC1 and positive aspect of PC2 and the other sites occupying all other quadrants. For femoral variation the difference seems to be either population or environment.

Type III GLMs were conducted with shape as the DV and size, site, and sex as the IVs. Complete results for humeral surface morphology are available in Table 5.23 and results for the femoral surface morphology are available in Table 5.24. Site was found to uniquely explain humeral surface morphology, at an alpha of 0.05, $F(3,83) = 8.13$, $p < 0.01$, $R^2 = 0.19$. The only other statistically significant explanation of the DV was when site and sex were combined. When site and sex are combined and the alpha is 0.05, $F(8,83) = 1.16$, $p < 0.01$, $R^2 = 0.07$. The R^2 value for these two IVs combined was smaller than for site alone suggesting that site alone is a better explanation for humeral surface morphological variation.

Site was also found to uniquely explain femoral surface morphology, at an alpha of 0.05, $F(3,47) = 3.26$, $p < 0.01$, $R^2 = 0.12$. When site and sex are considered together at an alpha of 0.05, $F(5,47) = 1.25$, $p < 0.01$, $R^2 = 0.08$. When size site and sex are all considered together at an alpha of 0.05, $F(2,47) = 1.51$, $p < 0.01$, $R^2 = 0.04$. The decreasing R^2 value when IVs are combined suggests that for this test the most important explanation of femoral surface morphology is site.

The level of morphological distinction between Coach Lane and the other two English sites when the humeri are considered underscores the temporal divide. Fishergate and Hereford appear to be more similar to one another than either is to Coach Lane despite the fact that Hereford is much further from both, is more rural than both, and individuals at Hereford are more likely to be from privileged backgrounds whereas those from both Coach Lane and Fishergate House were not wealthy. The most likely cause of this morphological variation is the temporal disparity. That is, Coach Lane is a postmedieval cemetery and therefore the lifestyles of those interred there would have been more different from those interred at Fishergate or at Hereford than either of those two were from each other. As the humeral shape for Coach Lane and 3-J-18 are similar but the femoral shape shows the English populations pooling together regardless of temporal disparity possible explanations include similar diet or physical activity, terrain and possibly pathological load.

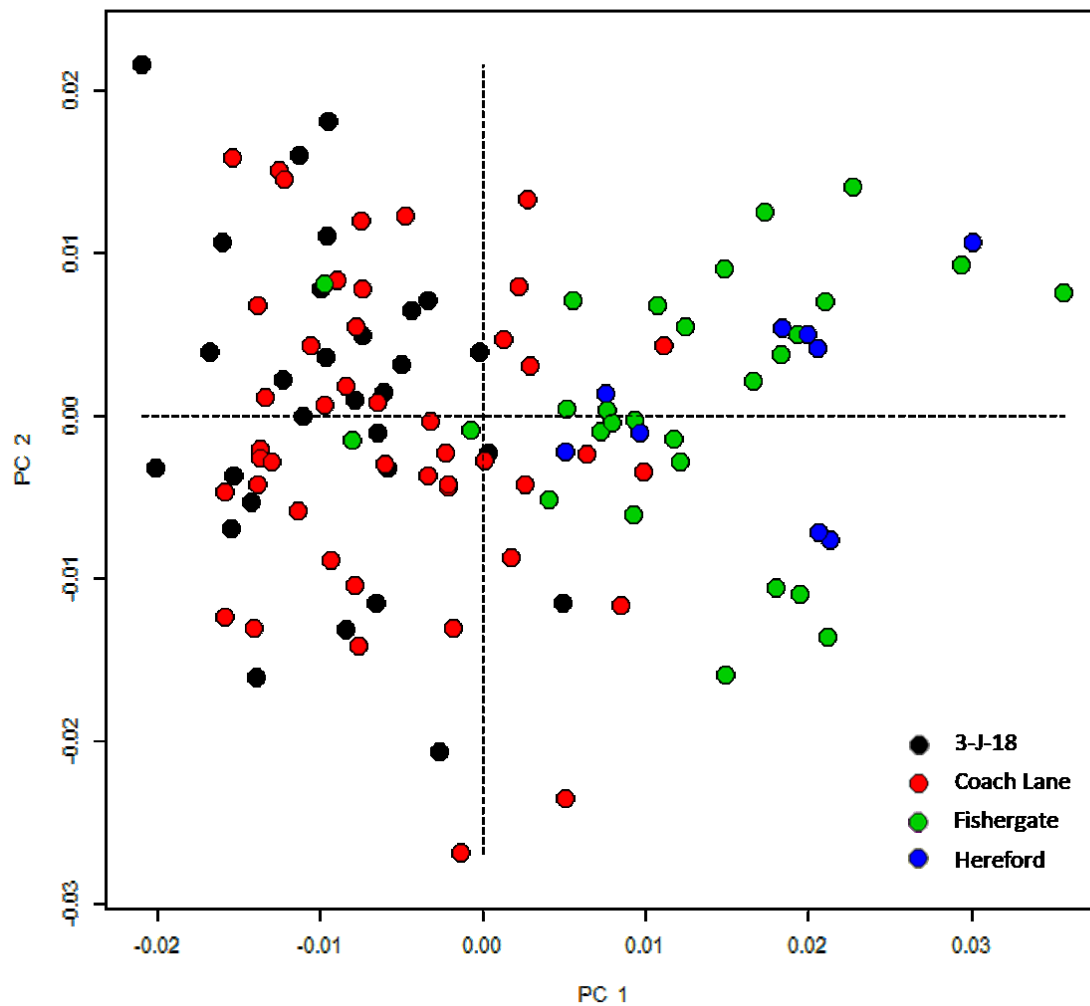


Figure 5.26 Humeral diaphyseal morphological variation in PC1 and PC2 for all sites.

Table 5.23 GLMs of humeral diaphyseal surface morphology by site.

	Df	SS	MS	Rsq	F	Z	Pr(>F)
Centroid Size	1	0.001207	0.0012067	0.018979	2.4992	2.3071	0.021
Site	3	0.011779	0.0039263	0.185254	8.1317	8.1267	0.001
Sex	4	0.001581	0.0003953	0.024868	0.8187	0.2547	0.398
Centroid Size x Site	3	0.001311	0.0004368	0.020612	0.9048	0.8578	0.189
Centroid Size x Sex	4	0.001617	0.0004042	0.025432	0.8372	0.6395	0.275
Site x Sex	8	0.004471	0.0005589	0.070322	1.1575	2.9363	0.003
Centroid Size x Site x Sex	4	0.001541	0.0003853	0.024242	0.7981	0.9977	0.158
Residuals	83	0.040075	0.0004828				
Total	110	0.063582					

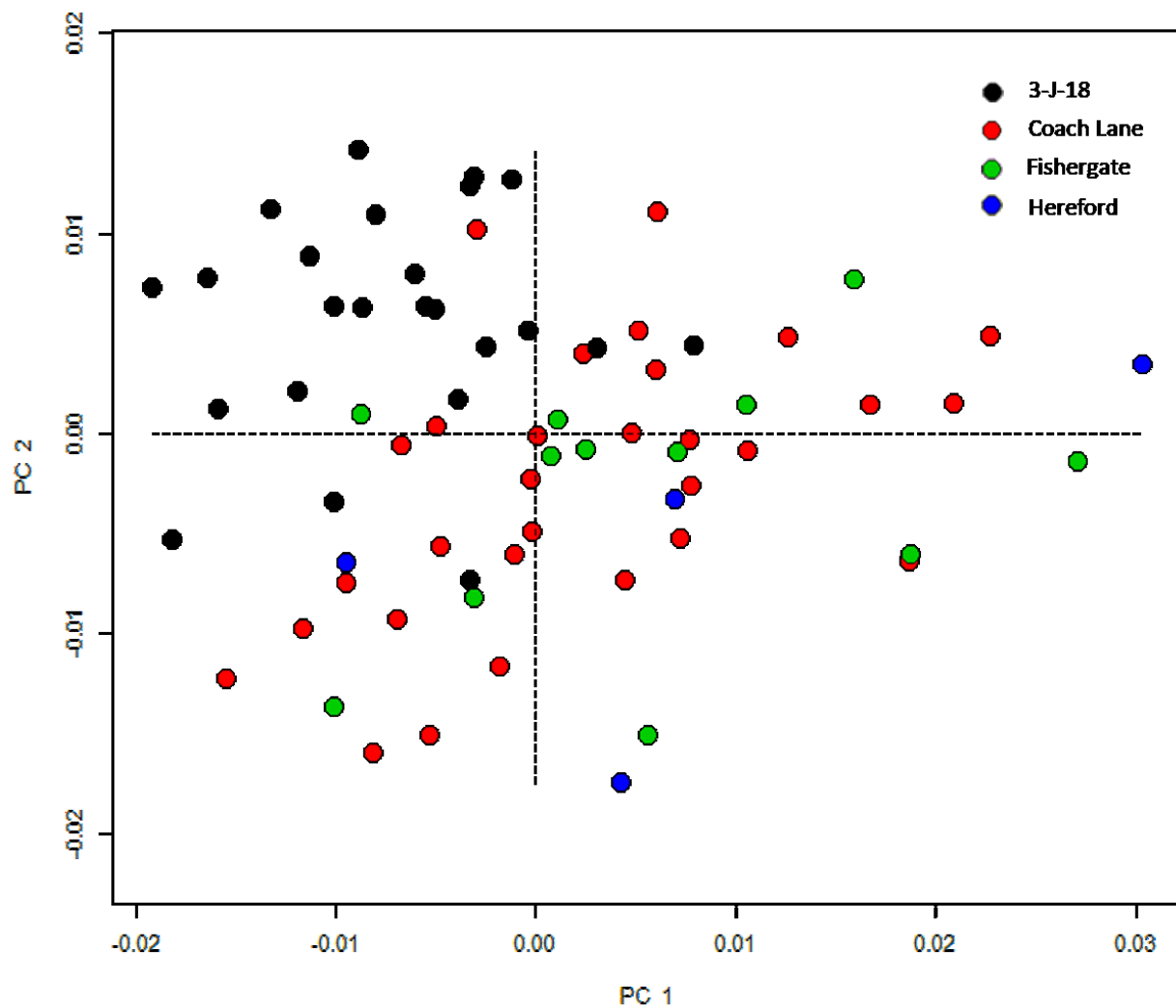


Figure 5.27 Femoral diaphyseal surface morphological variation in PC1 and PC2 for all sites.

Table 5.24 GLMs of humeral and femoral diaphyseal surface morphology by site.

	Df	SS	MS	Rsqr	F	Z	Pr(>F)
Centroid Size	1	0.0016903	0.00169029	0.053904	4.4158	4.0078	0.001
Site	3	0.0037406	0.00124686	0.119289	3.2573	5.1879	0.001
Sex	4	0.0019723	0.00049307	0.062896	1.2881	2.0327	0.025
Centroid Size x Site	3	0.0009557	0.00031856	0.030477	0.8322	0.381	0.349
Centroid Size x Sex	4	0.0014552	0.00036381	0.046408	0.9504	1.1829	0.123
Site x Sex	5	0.0023932	0.00047865	0.076321	1.2504	2.7378	0.004
Centroid Size x Site x Sex	2	0.0011592	0.00057958	0.036966	1.5141	3.1218	0.003
Residuals	47	0.017991	0.00038279				
Total	69	0.0313574					

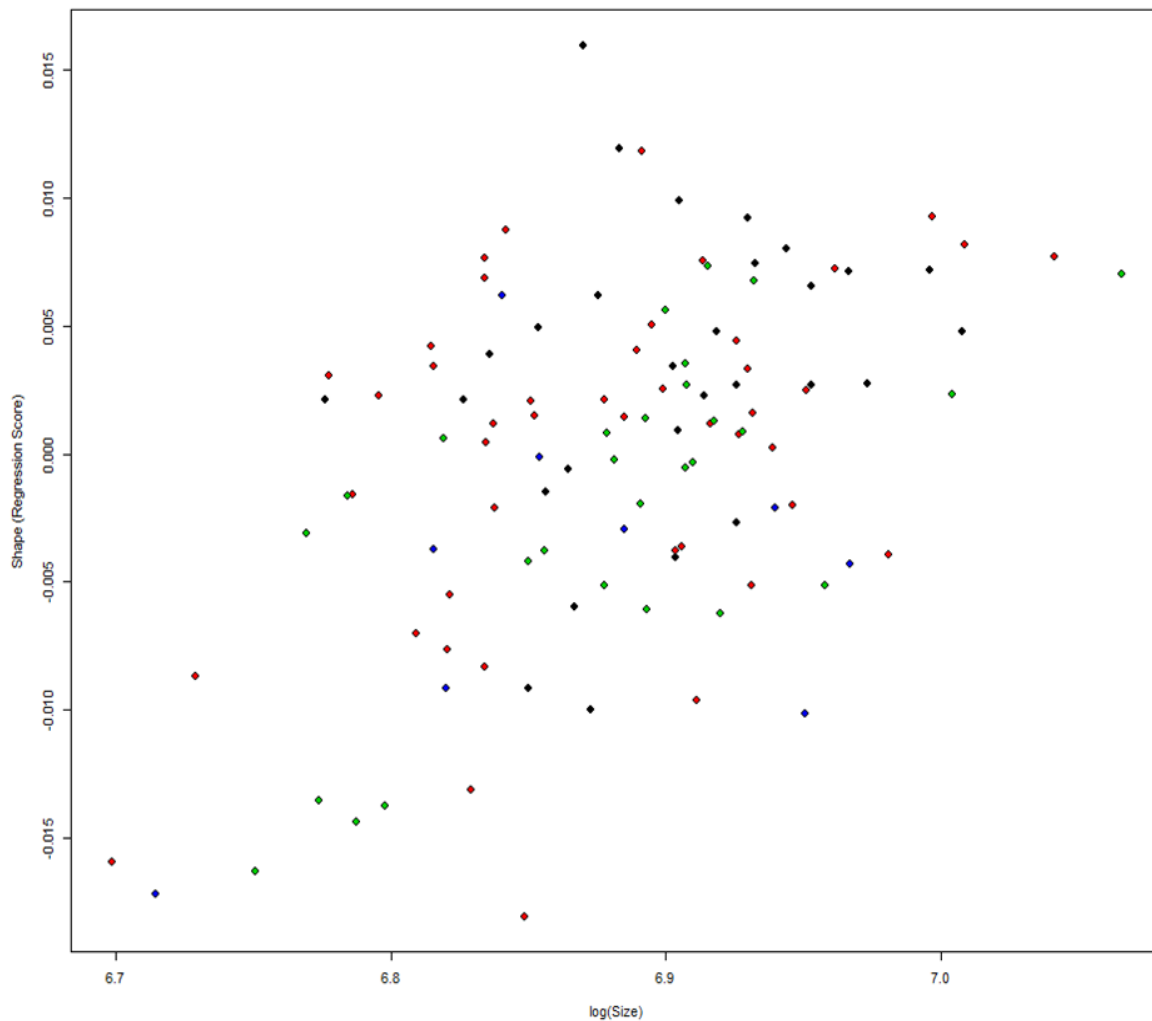


Figure 5.28 Humeral allometry by site. (black = 3-J-18, red = Coach Lane, blue = Fishergate, Blue = Hereford)

Table 5.25 Homogeneity of Slopes (top) and ANOVA (bottom) results for humeri by site.

Homogeneity of Slopes Test							
	Df	SEE	SS	Rsqr	F	Z	Pr(>F)
Common Allometry	106	0.050567					
Group Allometries	103	0.049351	0.0012159	0.019123	0.8459	0.40381	0.334

Type I (Sequential) Sums of Squares and Cross-products							
	Df	SS	MS	Rsqr	F	Z	Pr(>F)
log(size)	1	0.001262	0.0012623	0.019853	2.646	2.4549	0.014
Site	3	0.011752	0.0039174	0.184836	8.2117	8.2792	0.001
Residuals	106	0.050567	0.000477				
Total	110	0.063582					

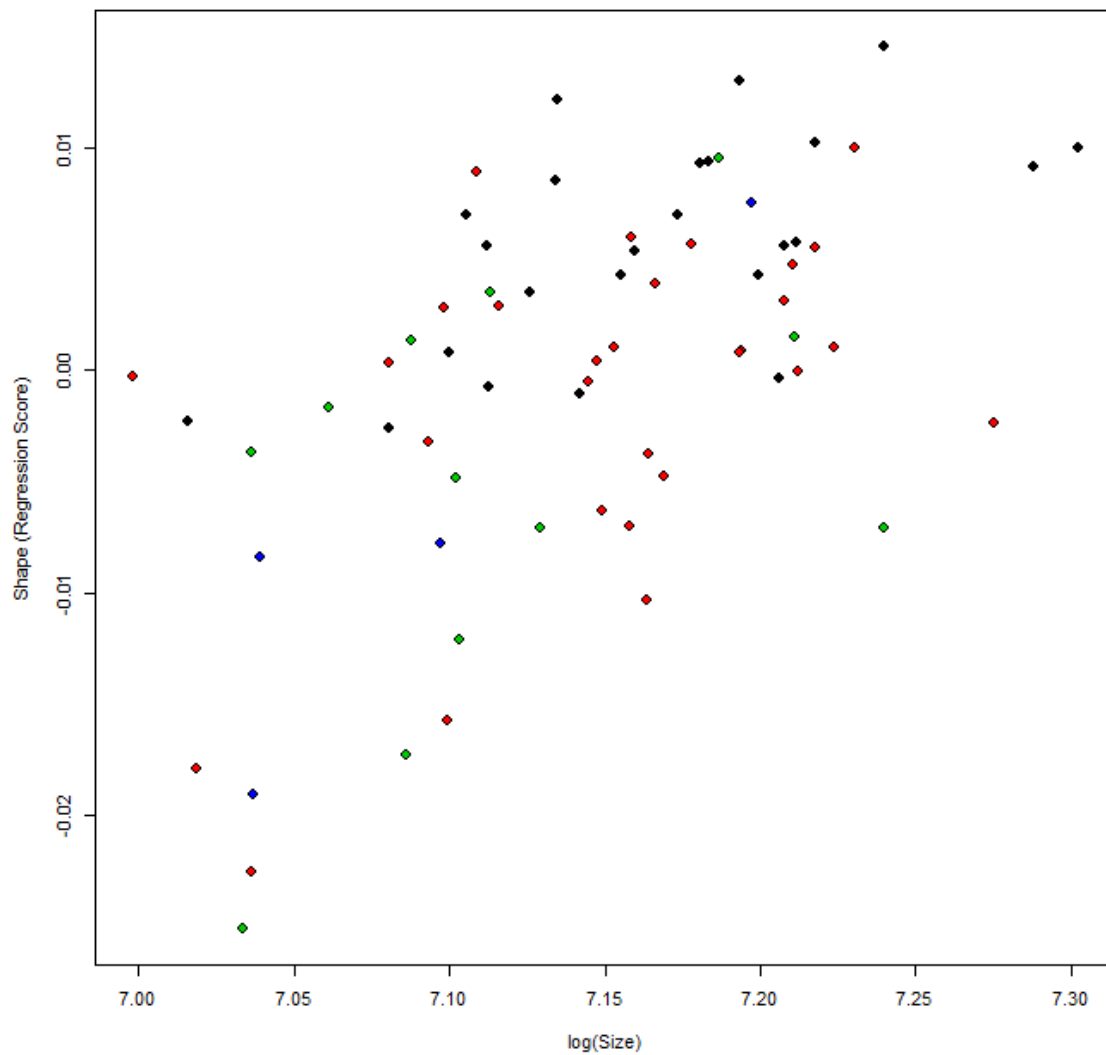


Figure 5.29 Femoral allometry by site. (black = 3-J-18, red = Coach Lane, blue = Fishergate, green = Hereford)

Table 5.26 Homogeneity of Slopes Test and GLM tests by site for femoral diaphyseal surface morphology.

Homogeneity of Slopes Test							
	Df	SSE	SS	Rsq	F	Z	Pr(>F)
Common Allometry	65	0.025896					
Group Allometries	62	0.024816	0.0010801	0.034446	0.8996	0.40049	0.348

Type III GLM							
	Df	SS	MS	Rsq	F	Z	Pr(>F)
log(size)	1	0.0017347	0.0017347	0.05532	4.3542	4.0045	0.001
Site	3	0.0037269	0.0012423	0.11885	3.1182	5.162	0.001
Residuals	65	0.0258959	0.0003984				
Total	69	0.0313575					

5.3 Discussion

Results for the present analysis were similar to those for the homologous points in that no clear pattern existed and variables which showed consistent variation with morphology in one population may not in another. Age and sex represented particularly strongly in the diaphyseal morphology of the English populations, but this was not strictly reflected in the Sudanese population. DJD varied with morphology fairly strongly in both populations, but in different ways.

5.3.1 Intrapopulation

5.3.1.1 *Sex*

As seen in Section 5.2.1.1 sexual dimorphism could explain some of the morphological variation seen in the diaphyseal surfaces of both the humerus and femur. In humeri, sex did not uniquely explain variation but when considered with population was statistically significant. For femora sex did uniquely explain variation and when combined with site or site and size explained morphological variation to a greater degree of confidence. However, while there was allometry seen in both humeri and femora it did not seem to correspond to sexual dimorphism.

Sexual dimorphism in humeral surface morphology exists, but only within rather than across populations. Sexual dimorphism in long bones has been shown to be site or population specific in other studies (İşcan et al., 1998; Robinson & Bidmos, 2009). This means that for the sites present there may have been separate sexually dimorphic ontogenetic trajectories, sexual dimorphism may have been expressed differently in the upper limb between populations, or labour and osteological response to labour varied between populations (Bulygina et al., 2006; Cobb & O'Higgins, 2007). If sexual dimorphism in humeral surface morphology had corresponded with allometry then it could be theorised that sexual dimorphism related to the relative level of force exerted on the bone. However, as this is not the case a more likely explanation to sexual dimorphism in the upper limb is the effect of hormones on the development of muscle possibly paired with sexual division of labour. As discussed in Section 5.1.1 sexual division of labour is difficult to prove and beyond the scope of this thesis. Hormones however, do influence the development of muscle and osteological response to stress in both the mechanical and biological sense (Cardoso & Henderson, 2010; Jurmain et al., 2012; Stock & Pfeiffer, 2004). Additionally, the humerus in humans is not typically a weight bearing bone. This means a greater degree of morphological variation is possible before survival is impaired.

The consistency of sexual dimorphism in femora across populations can possibly be attributed to a lower degree of possible morphological variation particularly in females. Bipedalism requires that certain morphological prerequisites be met. The femur must be robust enough to support the weight of the entire upper body and indeed multiplications of the weight of the upper body during locomotion. It must also host muscle attachments to balance as well as move and – if movement is to be efficient – must have a valgus angle. This means that when only locomotion is considered there will be a number of possible morphological variations that are not adaptive. What becomes crucial when considering sexual dimorphism of the femur in humans is the obstetric demands enacted when offspring has a relatively large cranial vault. This would suggest that the possible range of morphology for females would be narrower than that of males regardless of population. Males need only to walk. Females need to walk and survive maternity.

5.3.1.2 Age

Age may effect diaphyseal morphology as the change in hormone levels and fluctuation and possible different cultural expectations and nutrition may effect deposition and resorption particularly in the diaphysis (Bridges, 1989a; Stock & Pfeiffer, 2004). Deposition and resorption in the diaphysis varies by site on the bone, by individual, and with age, and may be either subperiosteal or endosteal. However, these results would support those of Ruff and Hayes (1982) who detected a pattern in diaphyseal morphology with age and sex. Remodeling of the diaphysis continues throughout the individual's adult life and slows with age – although it would peak in the early 30s (Rho et al., 2002). Activity and mobility may have some effect on the morphology of the diaphysis with age as cumulative degeneration or disease may limit mobility, and cultural impact may change the individual's role in society and therefore their daily activities.

Age did seem to explain surface morphology reasonably well. In neither humeri nor femora did age uniquely explain morphological variation but when combined with other variables it did. In humeri age and sex, age and site, size site and age, size sex and age, site sex and age, and size site sex and age all explained humeral surface morphological variation with a high degree of statistical certainty. Likewise in femora, size and age, sex and age, size site and age, size sex and age, site sex and age, and size site, sex and age explained femoral surface variation. This means that age interacts with these various factors to influence morphological variation.

Interaction between age and site with and without sex supports population based ontogenetic trajectories. It is also clear that sex and age do impact periosteal or surface morphology on the diaphysis. While most observations of the influence of sex on morphological shape have been based on cortical and endosteal variation (Mays, Ives, et al., 2009; O'Neill & Ruff, 2004; Ruff et al., 1994; Ruff & Hayes, 1982; Sparacello & Pearson, 2010) the observations her regarding diaphyseal surface morphology do lend further support to their work. However, where cortical morphology and rates of endosteal and periosteal resorption could be put down to hormonal variation between sexes and at different ages here there is the further complication of size and as emphasized by Ruff, Holt and Trinkaus (2006) loading history. It follows that if the bone is larger either due to genetics or previous loading history and impact on the bone causing a larger and more robust morphology the forces acted on the bone over time will cause the bone and body to react differently than it might if the bone were smaller and more gracile.

Age has inescapable effects on the morphology of the diaphysis both for humeri and femora but other factors mollify or enhance the impact. Shape is ultimately dependent not only on age and sex, but also population, size, and extrapolating from that last loading history.

5.3.1.3 Pathology

The shape of the humeral diaphysis appears far more reactive or related to the incidence of trauma than that of the femoral diaphysis. In no case did trauma alone explain morphological variation for either diaphysis, but in humeri when paired with size, site, sex, size and sex, site and sex, or size site and sex, trauma explained morphological variation with a reasonable degree of statistical certainty. For femora this was only true when trauma was paired with site, size and site, or site and sex. Trauma for this study was global trauma to the skeleton. That is the injury recorded could be to any element in the body and severity was not considered. The amount of morphological variation seen in relation to trauma could suggest that resources to bones were being biologically redistributed during the healing process. The relative lack of intervention in the femoral shape as compared to the humerus may be due to the fact that the femur is weight bearing. Injuries, even injuries which prevent most physical labour, only in severe cases render the individual unable to walk. Most of these individuals were probably relatively ambulatory during their convalescence and so while they may have limited their use of their upper limbs or avoided heavy lifting, they likely continued to bear weight on their legs unless they were entirely bedridden. However, for humeri it is much more likely that activity could have been limited or interrupted by trauma resulting in varying rates of resorption and deposition more relative to the individual's size, population, and sex than their activity level.

For both presence and absence of cribra orbitalia (CO) and linear enamel hypoplasia (LEH) femoral diaphyseal shape seemed slightly more sensitive than humeral diaphyseal shape but both were explained by CO and LEH when combined with some of the other variables present. In the case of CO, it could only explain humeral diaphyseal shape when considered with size and site. This is surprising considering that humeral shape could be explained by LEH when it was paired with site, sex, or size and site. CO is believed to be caused by prolonged and early hemoblastic anaemia (Stuart-Macadam, 1987b; P. L. Walker et al., 2009). If LEH can be indicative of major health issues throughout an individual's life, the effects associated with CO should be similarly extreme. However, some studies indicate a decline in the prevalence of CO with increasing age. The two theories to explain this are that individuals without CO live longer and increased age offers more time for the bone to heal. If the CO lesions themselves heal then so should the rest of the skeleton. This however does not explain why the presence or absence of CO can in part explain the morphology of femoral diaphysis. Something similar is observed in the presence or absence of LEH in relation to diaphyseal morphology. LEH better explains humeral morphology than CO, but the p value only drops under 0.01 when size and site are also considered. In femora, LEH paired with site, sex, size and sex, and size site and sex explains diaphyseal morphology with p values less than 0.01. Childhood stress seems to have a greater effect on the diaphyseal morphology of the lower limb than the upper limb. This could be due to juvenile weight and activity levels potentially setting the rates of cortical deposition and resorption for the rest of the individual's life or it could also have to do with the relative shape of the epiphysis and how that later influences the use of the rest of the bone (Frost, 1994; Hamrick, 1999; Ruff et al., 1994; Trinkaus et al., 1994).

Schmorl's Nodes appeared with greater prevalence in the English populations. This would tend to support Plomp and colleagues (2015) in that a population with a higher prevalence of a certain morphology to the neural arch and vertebral body would have a higher prevalence of Schmorl's nodes. Their conclusions might be further supported here if Schmorl's nodes explained femoral diaphyseal morphology better than humeral diaphyseal morphology because chronic pain in the lumbar region could be reasonably expected to limit or alter mobility. Schmorl's nodes when combined with site, size and site, size and sex, and site and sex do explain femoral morphology but not notably more so than they explain humeral diaphyseal morphology. These tests measure correlation not causation so while it is possible that Schmorl's nodes or any of the other IVs examined in this chapter cause variant morphologies in humeri or femora it is also possible that the observed morphologies were present for other reasons like genetic affinity and otherwise occur independent of one another. While the results here do not give outstandingly clear support to Plomp and colleagues (2015) they somewhat refute

Peng and colleagues' (2003) theory that Schmorl's nodes are a result of herniation. Herniation of the disk can be expected to impact mobility meaning for herniation to be the cause of Schmorl's nodes there also must be clear impact on the femoral diaphyseal shape more so than that of humeral diaphyseal shape.

DJD severity in all but the humeral distal epiphysis uniquely explained diaphyseal shape and in the femora the p values were less than 0.01. Other IVs combined with the severity of DJD also helped explain diaphyseal morphology with a high degree of statistical certainty. This set of results strongly suggests but does not prove a biomechanical aetiology to diaphyseal morphology in relation to DJD severity. Particularly in the weight-bearing femur, diaphyseal shape is being modified to mollify the effects of cartilaginous degeneration. The results further suggest that exactly how the diaphysis is reshaped is dependent on other variables like population, size, and sex. The latter two variables would introduce other biomechanical considerations, but genetics and hormones are also implicated. It seems unlikely that the statistical relationship between DJD severity and diaphyseal shape is coincidental.

5.3.2 Interpopulation

Predictably, populations were morphologically distinct. What was especially notable however was that for previous intrapopulation results morphological variation was indicated only in a statistical sense. In the case of interpopulation the variation was such that populations very nearly grouped in the PC charts (see for humeri Figure 5.26 and for femora Figure 5.27). This is somewhat typical for morphometric studies and rational in that groups of the same species that live in the same area under the same conditions and share genetic affinity might have morphologies more similar to one another than populations outside of their group (but see (Relethford, 2009) for discussion on population affinity). However, in Figure 5.26 the Coach Lane and Sudanese population seem to pool. Coach Lane was expected to be different from the other two English sites and the Sudanese population was expected to be different from all the English sites but the humeral diaphyseal shapes for the Sudan and Coach Lane are pooling in PC1. The postmedieval English site is more similar to the Sudanese site on the PC with the greatest amount of variation than it is to the medieval English sites.

The trend does not continue for femora. Populations remain clearly distinct but Figure 5.27 shows that the Sudanese site and Coach Lane no longer pool. In this case Coach Lane is more similar to the other English sites than it is to the Sudanese site. This set of results suggests that population affinity and environment are important components to understanding morphology. Population and genetics do not provide an unassailable roadmap to morphology. It could be argued that the Coach Lane population

bears similar femoral morphology to the other two English sites not due to population affinity but to the similarity of environment. Conversely, this would mean that relative humeral morphological similarity between Coach Lane and the 3-J-18 is due possibly to similar activity levels or types, nutrition, or pathological load. Regardless of cause the variation seen in humeral diaphyseal morphology relative to the other English sites underscores the impact of time on a population. Coach Lane may be a descendent population to particularly Fishergate, but it is as different from Hereford and Fishergate as they are from 3-J-18, a site roughly 7,000 kilometers removed.

5.4 Conclusion

Diaphyseal morphology of both the humerus and femur appear to correlate with inter and intrapopulation variation. Furthermore, the variables seem to explain diaphyseal morphology better than they do epiphyseal morphology. While it was rare for a variable to on its own uniquely explain diaphyseal morphology the R values tended to be higher than those seen in the previous chapter, and independent variables particularly DJD severity had a clearer relationship with morphology. This is likely due to the timing of formation for the epiphyses as opposed to the diaphysis as well as the continual remodelling of the endosteal and periosteal surfaces. That is, factors like DJD have a clearer effect on diaphyseal morphology because diaphyseal morphology may be altered roughly concurrently with the development of DJD whereas epiphyseal morphology is almost certain to be entirely defined before its onset.

Interpopulation variation was also arguably more pronounced in its relation to diaphyseal morphology. However, Coach Lane and 3-J-18 only pooled when considering humeral diaphyseal morphology. In all other measures epiphyseal and diaphyseal they were distinct with 3-J-18 distinguishing itself from the English populations and Coach Lane being only slightly different from Hereford and Fishergate. Notably, while 3-J-18 always clustered with itself and was generally distinct from the English populations in some of the epiphyseal charts the variation seen in 3-J-18 was contained within the expected range for the English populations, but in the diaphyseal charts 3-J-18 was always distinct.

Diaphyseal morphology is partially explained by intrapopulation variation. Usually independent variables must be combined to uniquely explain diaphyseal morphology for both the humerus and femur in all populations, but correlation between morphology and the independent variables was confirmed to various degrees of statistical certainty. For the first hypothesis the null hypothesis is

rejected. There is morphological variation in the diaphysis of the humerus and femur explained by intrapopulation variation. Several sub-hypotheses exist for the first hypothesis. For the first sub hypothesis predicting that there is correlation between diaphyseal morphology and sex we reject the null hypothesis. For humeral diaphyseal morphology there sex explained variation when paired with other variables and for femoral diaphyseal morphology sex could uniquely explain variation. The second sub-hypothesis states that age will be correlated with morphology. Here again the null hypothesis is rejected because when age and other variables are considered together for both humeral and femoral morphology they explain variation. The third hypothesis supposes that morphology will correlate with incidence of childhood stress. Humeral and femoral diaphyseal morphology are explained by CO and LEH when considered with other variables so the null hypothesis that there is no correlation is rejected. For the hypothesis suggesting a correlation between trauma and morphology the null hypothesis is rejected because trauma when considered with other variables did explain humeral and femoral morphology. The final hypothesis suggests a correlation between morphology and DJD severity. Here as well the null hypothesis is rejected because in both humeri and femora DJD severity in the proximal epiphysis uniquely explained diaphyseal morphology and DJD severity in both the distal and proximal epiphyses when paired with other variables explained diaphyseal morphology for all elements.

The second set of hypotheses pertains to inter population variation. The first sub-hypothesis cannot be answered here. The second sub-hypothesis suggests a correlation between site and morphology. Site uniquely explains both humeral and femoral diaphyseal morphology meaning that interpopulation variation exists between sites. For the second sub-hypothesis the null hypothesis is rejected. There is morphological variation between populations in the diaphysis for both the humerus and femur. The third sub-hypothesis suggests that there is more variation between populations than within populations. As the R^2 value for site for both the humeral and femoral diaphysis was the highest in all tests this null hypothesis is also rejected. Site best explains morphological variation.

The final hypothesis may not be entirely addressed here as only the epiphyseal and diaphyseal morphology have yet been addressed. However, the variation seen in the results for the epiphysis and diaphysis suggests that in this case as well the null hypothesis will be rejected. Different parts of the bone are more or less morphologically explained by different inter and intra population variation.

6 Cross-sectional semilandmarks

6.1 Introduction

The previous results chapters focused on epiphyseal morphology using homologous landmarks (Chapter 4) and diaphyseal morphology using surface semilandmarks (Chapter 5). This chapter will attempt to respond to the hypotheses regarding within population variation (1.1.1), between population variation (1.1.2), and morphological variation in different parts of the bone (1.1.3) in regards to the cross sections at midshaft. Whilst there are very few studies concerning strictly the morphology of the cross-sectional outline (L. A. B. Wilson & Humphrey, 2015) there are numerous studies which use cross-sectional geometry to describe diaphyseal shape (Lieberman et al., 2004; Marchi et al., 2006; O'Neill & Ruff, 2004; Shaw & Stock, 2009a; Sparacello et al., 2011b; Sparacello & Marchi, 2008; Stock & Pfeiffer, 2004; Yamanaka et al., 2005). This chapter will examine both the cross-sectional geometry and the morphology of its outline.

The results of previous research on cross-sectional morphology are primarily concerned with robusticity. In particular researchers have used methods included in cross-sectional research to suggest levels of mobility (Marchi et al., 2006; Ruff, Holt, Sládek, et al., 2006; Shaw & Stock, 2009b; Sparacello et al., 2011a; Sparacello & Marchi, 2008; Stock & Pfeiffer, 2004) or as Stock and Pfeiffer term it, “terrain dictated loading intensity,” (Stock & Pfeiffer, 2004, p. 1001). Higher degrees of loading (e.g. running or walking over uneven terrain) lead to anterior-posterior loading. Therefore the cross-section of a highly mobile individual's tibia or femur should be less circular than that of a more sedentary individual. Many studies also use the asymmetry in the upper limbs to investigate specialization or subsistence strategies or sexual division of labour (Sakaue, 1998; Sparacello et al., 2011a). It is possible to use cross-sectional geometry to draw conclusions about pathologies, trauma, nutritional deficiencies, and hormonal fluctuations. (For more information on these and other variables effect on diaphyseal and cross sectional morphology both periosteally and endosteally, please refer to Section 2.2.3.)

As seen in the methods detailed in section 3.5.2.2 this is not a traditional analysis of cross-sectional geometry, instead this study will examine the morphology of the cross-sectional outline. For comparison there will be a brief analysis of cross-sectional geometry from a biomechanical perspective (section 6.2.3), but this was conducted to determine the usefulness of obtaining cross-sectional outline morphology. Morphologically, this study only looks at the sub-periosteal surface, not the medullary

cavity or the endosteal shape or cortical thickness. This study also does not use standard AP and ML linear measurements (See section 3.5.2.3 for further information on how cross-sectional geometry was collected). The only determinate of size in this study is centroid size. Cross-sectional geometry here is a coordinate based assessment of the morphology rather than a linear measurement based assessment of geometry. The first justification for not using the typical AP ML measurements is a practical one. Imaging here was done via laser surface scan and only captures the shape of the outside of the bone. Obtaining a complete cross-section including not only the periosteal surface but the morphology of the medullary cavity and endosteal surface would require either cutting the bone or CT imaging. While some studies use these methods to good effect (Shaw & Stock, 2009a, 2009b) they can be prohibitively invasive or expensive. Several studies also use standard AP ML radiographs to calculate cortical morphology (O'Neill & Ruff, 2004; Weiss, 2005), however radiography on this scale was deemed beyond the scope of this study. The final traditional method for obtaining cross-sectional geometry is by creating moulds of the bone (Sparacello et al., 2011a, 2015; Sparacello & Marchi, 2008). The drawback to this method is that it only allows for data collection of the periosteal surface; however it is efficient and non-invasive. O'Neill and Ruff (2004) showed that simple elliptical approximations of cross-sections remained within a reasonable standard of error, but were not as accurate as the true cross-sections. The elliptical model considers only linear measurements and most evaluations of cross-sections are truly geometrical, but the less accurate estimation suggests that morphological data would be comparable. The method used here only looks at the periosteal morphology, but the other major alteration is that all of the studies mentioned above used analyses of geometry which include size. This study uses a coordinate system for which size may be included, but is not an integral part of the description of geometry.

As with the previous results chapters this chapter will investigate the first two hypotheses regarding intra and inter population variation. Cross-sectional data has a robust and long history of providing reasonably detailed and consistent information on past populations. However, the questions asked in this study particularly in regards to pathology are different from those usually applied to research involving cross-sectional geometry. Cross-sectional geometry and morphology is not expected to satisfactorily address the hypotheses in this study, but will show the furthest extents or limits of this research method. This inquiry begins to address the final research question regarding how discrete morphological variation may be in different parts of the bone (See 1.1.3).

6.1.1 Intrapopulation Variation: Cross-Sectional Morphological Variation at Midshaft with Sex

In addressing the first part of the first hypothesis (see sub-section 1.1.1.1) “morphological variation is significantly correlated with sex,” the answer will depend on how much centroid size and remodeling vary with sex. Cross-sectional variation with sex may be entirely determined by size. There may not be a purely morphological difference between males and females particularly at the midshaft. (Methodological choices for sampling only at the midshaft in this study are covered in Section 3.5.2.2. Using different methodologies, further research may be done on cross-sectional morphology and geometry, but this was considered outside the scope of this study.) While relative robusticity should be fairly obvious, gracility does not mean the individual is female nor does robusticity mean the individual is male. Additionally deposition and resorption do not occur at the same site in females and males. Ruff and Hayes (1982) observed that females deposit more bone in their proximal femurs than males. If females and males show differing levels of deposition and resorption at their midshaft consistently through their lifetimes then cross sectional geometry is likely to be sexually dimorphic both from a morphological perspective and a biomechanical one. However, shape will likely only consistently vary between females and males if groupings are also divided by size and age. The cross-sectional geometric values will likely show sexual variation because they already include size, but shape variation alone is unlikely to be sexually dimorphic.

Beyond size, hormones and hormonal effects over time or the metabolic effects of parturition, lactation, and menopause affect bone in general and the cortices in particular (Agarwal et al., 2004; Agarwal & Stout, 2004; Kaastad et al., 2000; Mays, 1996; Rho et al., 2002). This issue becomes inextricable with age and pathology because the resorption effects on women are only visible with increasing age and may be related to underlying pathology or in the case of osteoporosis simply need to reach a threshold before being considered pathological. Hormonal fluctuation however is also individually variable. A woman who does not have children will experience a different hormonal life history than a woman who does. Additionally, whilst breastfeeding is often discussed in terms of post-natal fetal neurological development age of weaning will have variable and diverse effects on cortical bone (Agarwal et al., 2004). Parturition and lactation effect on metabolic resorption particularly of the endosteum in women and that resorption will translate to subperiosteal deposition, but individual variation may outweigh sex variation in this case (Currey, 2003; Rho et al., 2002; Ruff & Hayes, 1982). Once again, this means that sex alone is unlikely to be a sufficient means to differentiate morphology. Hormonal effects on the bone are considerable but take time to alter the cross-sectional geometry and

occur over a lifetime. Therefore it is unlikely that morphology will vary with sex alone, but morphology should vary with age and sex considered together.

6.1.2 Intrapopulation Variation: Cross-Sectional Morphological Variation at Midshaft with Age

This section addresses the second part of the first hypothesis regarding age and morphological variation (see sub-section 1.1.1.2). There may be correlation between the morphological variation at midshaft and age, but it will likely be closely tied to sex, size and possibly pathology. The above section briefly discussed issues of endosteal resorption in women. Endosteal resorption and the development of osteopenia or even osteoporosis usually occur with age (although pathology and malnutrition can contribute to osteopenia in a young person). Conversely, osteogenic conditions may increase robusticity with age and in normal healthy people whose remodeling would not be termed osteopenic or osteogenic, robusticity will generally increase with age. Furthermore, endosteal resorption over time may contribute to subperiosteal expansion (Ruff & Hayes, 1982). This is logical as strong bone would have to continue to be in place particularly at muscle attachment sites regardless of growth, endosteal resorption, or medullary expansion (Currey, 2003). However, this means that subperiosteal expansion may be a good indicator of age – in both males and females it increases sharply between the ages of twenty and thirty and holds at a steady increase until about forty-five years of age – but following the age of forty-five females behave radically differently than males with a marked increase in subperiosteal deposition whilst males hold steady (Ruff & Hayes, 1982). Therefore, if morphological variation at the midshaft correlates with age it may well also be related to sex or there may be different morphological variation particularly for individuals in the 45+ age bracket.

Another possible factor in morphological variation at midshaft with age is microstructural ontogeny. Human bone does not reach its zenith of bone mineral content (BMC) until the approximate age of thirty-five. Younger adults will have bone with more “toughness,” elasticity, and ability to recover (Rho et al., 2002). While this does not speak directly to the morphology at midshaft and no similar pattern has been shown in the morphology of the epiphyses or diaphysis, were a morphological pattern to be found which differentiated young adults from older adults this could potentially be the reason.

It is possible that age alone may be determinate of morphology for both the coordinate based data which does not include size and the biomechanical data. The relationship will probably be stronger when grouping is determined by sex, but consideration of size is unlikely to affect the relationship. Age is expected to be most clearly related to shape in the cross-sectional outlines and when linked with sex.

6.1.3 Intrapopulation Variation: Cross-Sectional Morphological Variation at Midshaft with Pathology

The third part of the first hypothesis (see subsection 1.1.1.3) regards the relationship between childhood stress and morphological variation. Childhood stress in an osteological sense alone may result in adverse effects into adulthood. Severe stress may cause a disruption in development. While this has obvious effects particularly in limb ratio and overall height it may also affect the cortical bone. When bone ceases to develop, subperiosteal and endosteal bone are not deposited, but also osteocytes are not replaced. This last may lead to hypermineralization which along with the relatively thin walls of the cortices subjects the individual to a higher risk for micro-cracking and “creep,” where the bone deforms due to persistent stress (Currey, 2003). The issue may be compounded or possibly mediated for individuals with vitamin D deficiency as mineralization would be altered. While it is possible for particularly severe childhood stress to affect the cross-sectional morphology it is unlikely that that variation will be morphological alone. It is unlikely that any of the markers for childhood stress will create distinct morphological groupings particularly in the coordinate based data. As the cross-sectional geometry does include size it is possible that childhood stress markers will be determinate of groupings in that set, but the coordinate based set will likely require markers to interact with size and possibly sex before differentiating from entirely healthy individuals.

The fourth part of the first hypothesis (see subsection 1.1.1.4) seeks a correlation between degenerative disease and morphological variation. Various effects of osteoporosis or osteopenia have been discussed above (see section 6.1.1) and it is worth restating that endosteal resorption in cortical bone mass loss would result in subsequent sub-periosteal deposition and therefore could theoretically cause variation of the cross-sectional morphology with osteopenia or osteoporosis (Currey, 2003; Ruff & Hayes, 1982). Conversely, pathologies with osteogenic components like OA could also alter bone structures. In this case osteogenesis would cause deposition on the subperiosteal surface, but whether the osteogenesis caused the OA or the OA caused the osteogenesis would be a matter for debate. However, it is unlikely that osteogenic conditions will correlate with any morphological pattern as they do not correlate well with size and any changes they do cause may be quite subtle or inconsistent.

Trauma and morphological variation are central to the fifth part of the first hypothesis (see subsection 1.1.1.5) which theorises that there is a correlation between morphological variation and trauma. Trauma may be indirectly related to the morphological variation of the cross-section. As with previous chapters bones with fractures are not included for morphological or geometrical analysis.

Where trauma causes wasting or altered use, subperiosteal deposition will react to meet the new demands on the musculoskeletal system (Currey, 2003). From a less macro perspective, trauma may once again cause altered deposition, and can result in overall deformation of the bone with continued stress. Therefore, it is expected that trauma will have an effect on morphology. In this case stress caused by size will be relative to the individual's body mass. While size might affect remodeling it would affect each individual relative to their weight and so is not expected to have a statistically significant effect here. Remodeling during trauma could, however, be dependent on the hormonal response which suggests a possible link to sex in grouping by morphology.

Schmorl's nodes have been previously argued to be either a result of herniation of the disk (Peng et al., 2003) or morphology of the vertebral body (Plomp et al., 2012a, 2013; Plomp, Roberts, et al., 2015). Where traumatic or painful they might result in a at least temporary alteration of mobility patterns which could – if sustained – lead to an alteration in cross-sectional morphology or geometry. But Schmorl's nodes are not always associated with pain and are not associated with osteopenia or osteopenia and so are unlikely to offer a pattern consistent enough to detect in either morphology or geometry of the cross-sections.

6.1.4 Interpopulation Variation: Cross-Sectional Morphological Variation at Midshaft Between Populations

This section will address the second major hypothesis (section 1.1.2), which supposes that there is significant morphological variation between populations with emphasis on the second and third parts of that question (see sub-sections 1.1.2.2 and 1.1.2.3) concerning the degree of morphological variation between populations or demographics. In previous results chapters the most notable difference tended to be one of size between Coach Lane and Sudan on the extremes. I have hypothesised that this is likely due to the temporal division between the sites and a difference in sexual dimorphism between Coach Lane and the other two English sites. When the Sudanese skeletal set is compared to the English populations it diverges from the English populations in the same way that Coach Lane does, but to a greater degree. (However, the Sudanese population was generally smaller and more gracile than all the other populations considered whereas Coach Lane was generally larger and more robust.)

As noted in the introductory portion of this section (6.1) studies with methodologies that include cross-sectional geometry are frequently concerned with robusticity and mobility (Marchi et al., 2006; Ruff, Holt, Sládek, et al., 2006; Shaw & Stock, 2009b; Sparacello et al., 2011a; Sparacello & Marchi, 2008; Stock & Pfeiffer, 2004). This is because these are well reflected in cross-sectional geometry data

and should also be reflected in cross-sectional outline data. If individuals from the Coach Lane and Sudanese populations were generally more gracile or robust or had significantly different lifestyles than those from Fishergate or Hereford then there should be cross-sectional morphological variation correlated with population. This is expected to be the most obvious correlation for this morphological measure.

6.2 Results

For humeral cross-sections, ninety-five percent of variance is described in the first ten PCs, with ninety-nine percent described in the first nineteen PCs and all variation described in forty PCs (See Table 6.1). Figure 6.1, Figure 6.2, and Figure 6.3 show the distribution of humeral cross-sectional morphology along PC1, PC2, PC3 and includes warp grids describing shape extremes for the first three PCs. Shape change along the PC1 axis appears to be related to robusticity with the negative shape extreme being largely ovoid and the positive shape extreme being almost concave at the anterior aspect. In PC2 the negative shape extreme is longest along the medial lateral aspect but still mostly ovoid whereas the positive shape extreme appears to show more definition at the deltoid tuberosity with slight anterior concavity and its longest axis runs anterior-posterior. Shape change in PC3 is considerably more subtle with both extremes deviating only slightly from the mean as indicated by their warp grids. Both PC3 shape extremes describe ovoid to triangular shapes with the positive extreme of PC3 being the most defined with its longest axis running medial-laterally.

The degree of allometry was tested by comparing size and shape using a one-way ANOVA. Morphological variation with size was statistically significant at a level of 0.05. Figure 6.4 gives the regression of shape residuals against log CS, and Table 6.2 provides complete results for this ANOVA.

Table 6.1 Principal Component results for cross-sectional morphology of humerus at midshaft

	Standard deviation	Proportion of Variance	Cumulative Proportion
PC1	0.0384	33.9200%	33.9200%
PC2	0.03104	22.1580%	56.0720%
PC3	0.02533	14.7560%	70.8280%
PC4	0.01719	6.7950%	77.6240%
PC5	0.01648	6.2490%	83.8720%
PC6	0.01441	4.7760%	88.6480%
PC7	0.01001	2.3060%	90.9540%
PC8	0.009245	1.9660%	92.9200%

PC9	0.008252	1.5660%	94.4860%
PC10	0.00661	1.0050%	95.4910%
PC11	0.005972	0.8200%	96.3110%
PC12	0.005194	0.6210%	96.9320%
PC13	0.004422	0.4500%	97.3820%
PC14	0.004231	0.4120%	97.7930%
PC15	0.003854	0.3420%	98.1350%
PC16	0.003668	0.3090%	98.4440%
PC17	0.003128	0.2250%	98.6690%
PC18	0.002984	0.2050%	98.8740%
PC19	0.002683	0.1660%	99.0400%
PC20	0.002387	0.1310%	99.1710%
PC21	0.002374	0.1300%	99.3000%
PC22	0.002166	0.1080%	99.4080%
PC23	0.00212	0.1030%	99.5110%
PC24	0.002011	0.0930%	99.6040%
PC25	0.001819	0.0760%	99.6800%
PC26	0.001702	0.0670%	99.7470%
PC27	0.001587	0.0580%	99.8050%
PC28	0.001361	0.0430%	99.8480%
PC29	0.001195	0.0330%	99.8800%
PC30	0.001124	0.0290%	99.9100%
PC31	0.001028	0.0240%	99.9340%
PC32	0.000963	0.0210%	99.9550%
PC33	0.000793	0.0140%	99.9700%
PC34	0.000717	0.0120%	99.9810%
PC35	0.000686	0.0110%	99.9920%
PC36	0.00058	0.0080%	100.0000%
PC37	4.25E-17	0.0000%	100.0000%
PC38	3.16E-17	0.0000%	100.0000%
PC39	2.18E-17	0.0000%	100.0000%
PC40	2.10E-17	0.0000%	100.0000%

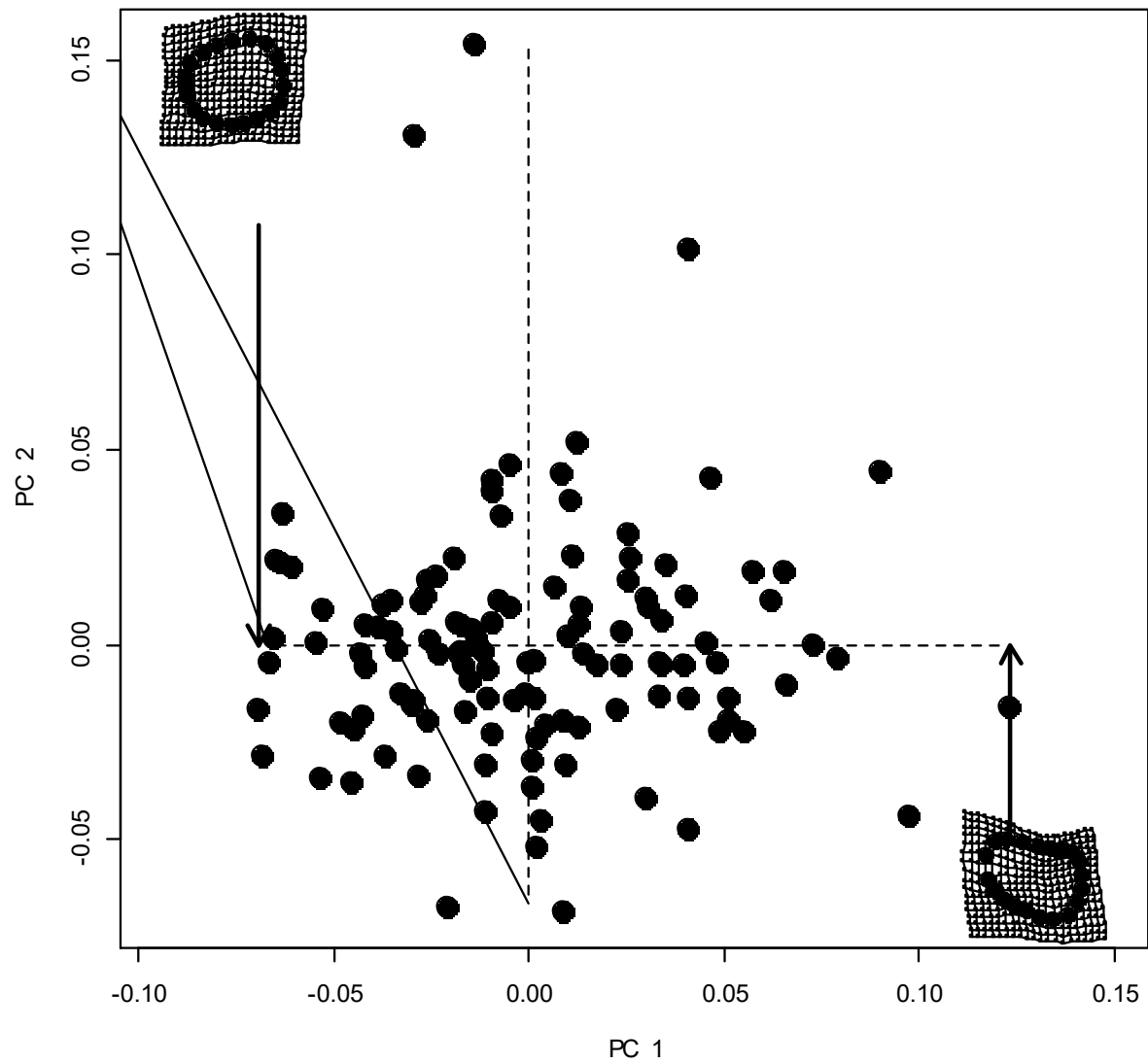


Figure 6.1 Visualisation of PC1 and PC2 for humeral cortical shape with warp grids for PC1 extremes.

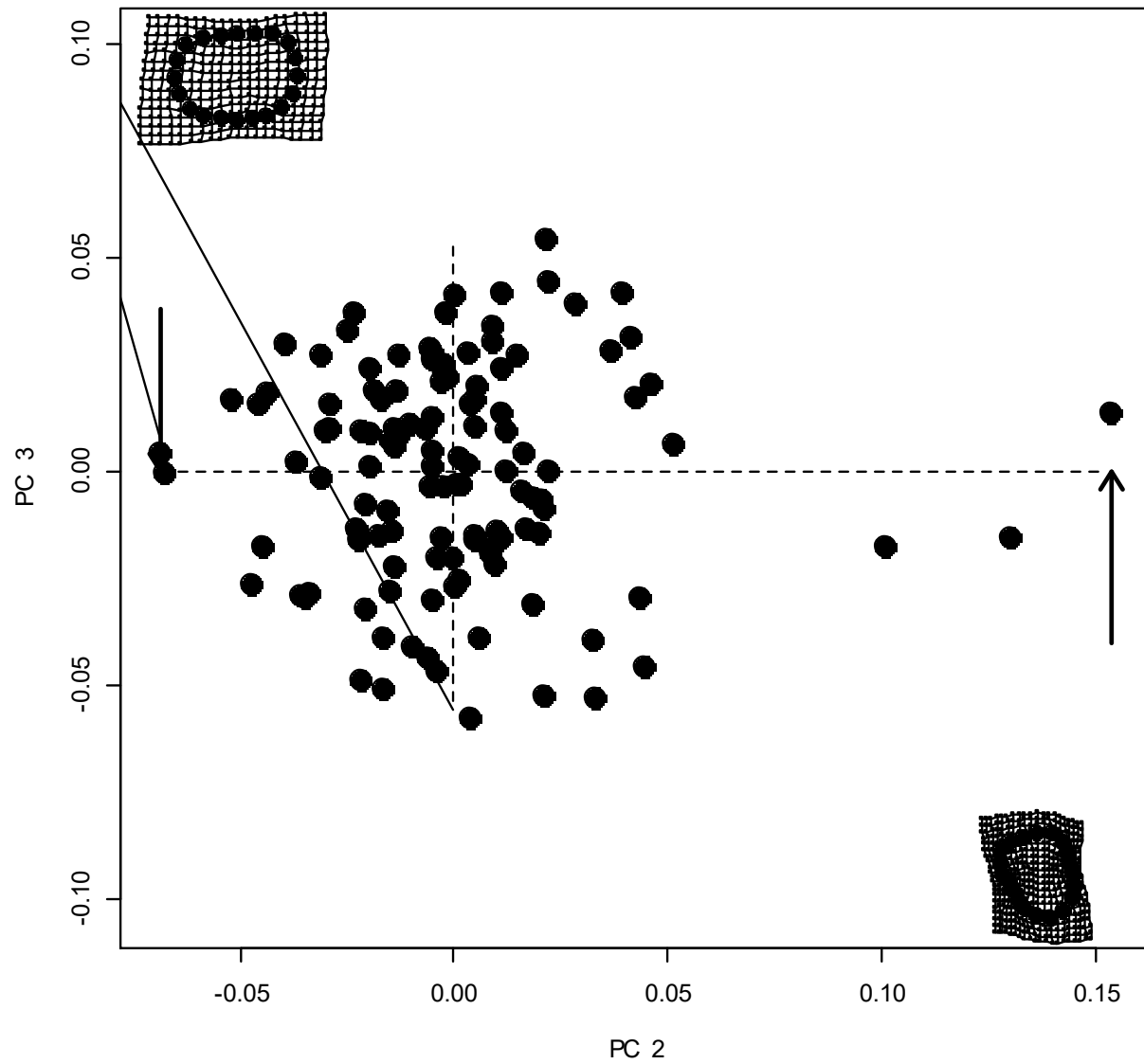


Figure 6.2 Visualisation of PC2 and PC3 for humeral cortical shape with warp grids for PC2 extremes.

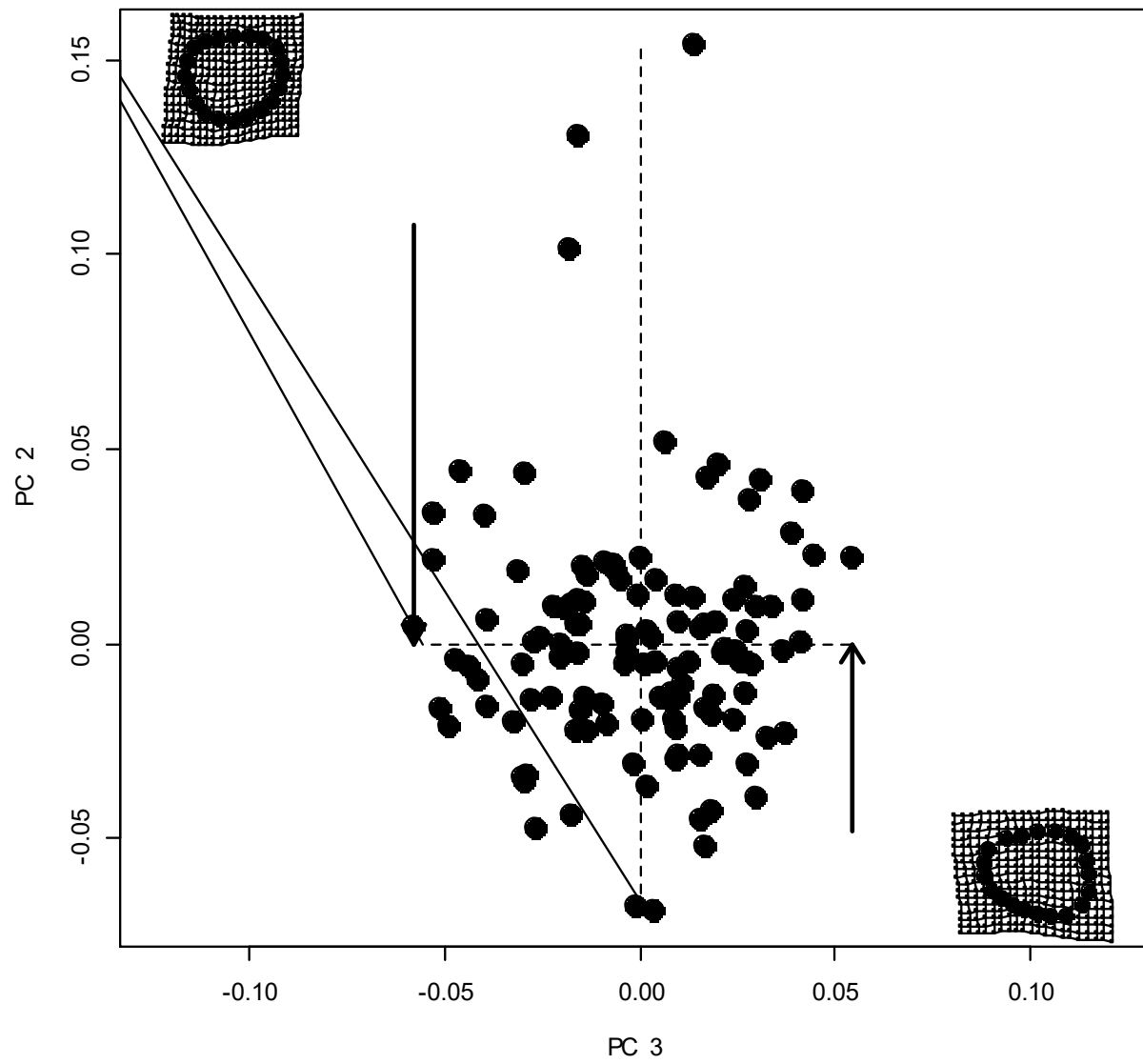


Figure 6.3 Visualisation of PC2 and PC3 for humeral cortical shape with warp grids for PC3 extremes.

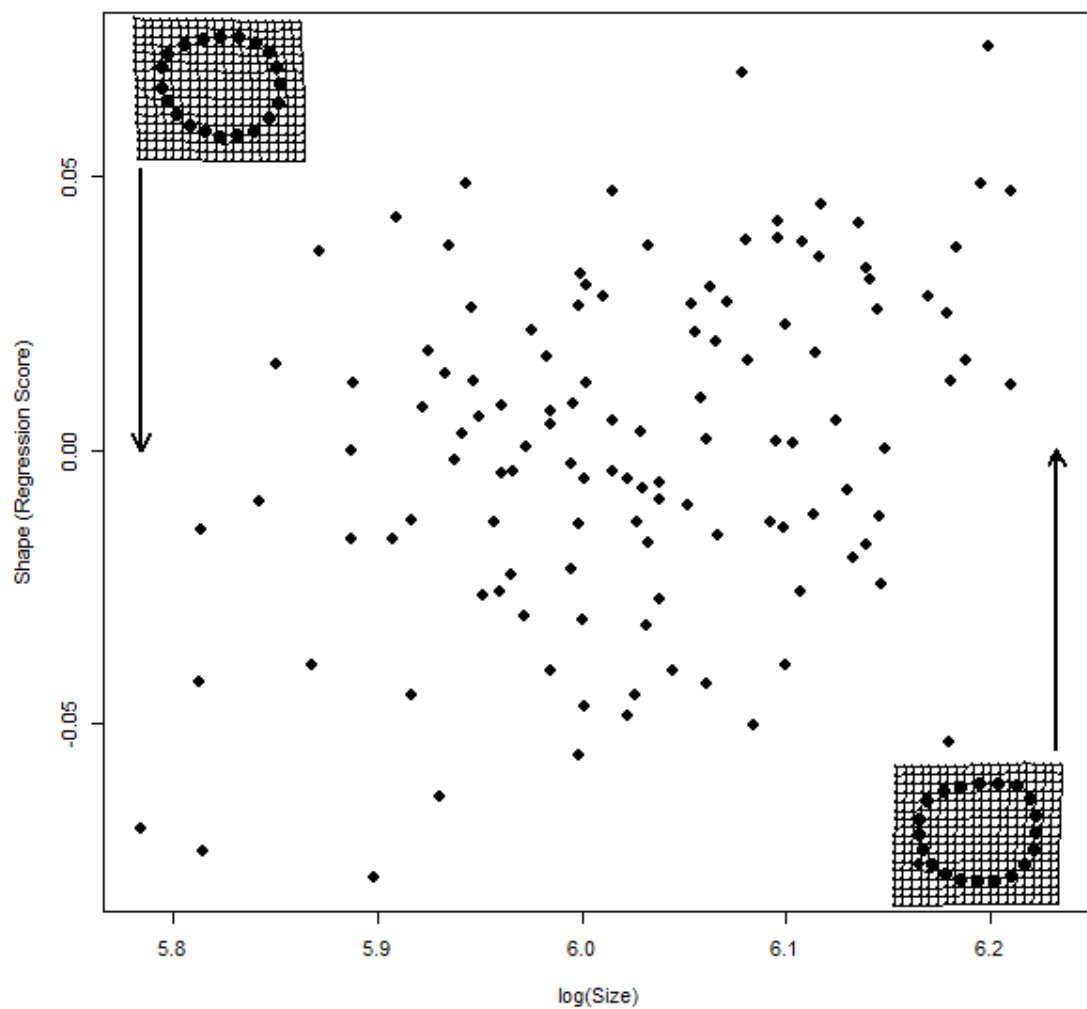


Figure 6.4 Allometry regression of log CS by Shape Regression Scores for humeral cross-sectional morphology. Warpgrids represent shape at size extremes.

Table 6.2 GLM Procrustes shape residuals compared to log(CS) for humeral cross-sectional morphology.

	Df	SS	MS	Rsq	F	Z	Pr(>F)
log(size)	1	0.0106	0.010596	0.020308	2.4668	2.0811	0.031
Residuals	119	0.51114	0.004295				
Total	120	0.52173					

For femoral cross-sections, ninety-five percent of variance is described in the first nine PCs with ninety-nine percent of variance described in the first sixteen PCs. All variation is described in forty PCs.

(See Table 6.3.) Figure 6.5 describes individual shape variation for the femoral cross-section at midshaft along PC1 and PC2. The negative shape extreme of PC1 is largely ovoid except for some definition at the *linea aspera*. The positive extreme is more asymmetrical with larger area between the lateral aspect and *linea aspera* than for the area between the medial aspect and *linea aspera*. Distribution of shapes and shape extremes for PC2 may be found in Figure 6.6. Here the main difference in shape appears to be the length of the anterior-posterior axis coupled with the definition of the *linea aspera*. The negative extreme shows a shape quite long in its anterior-posterior axis with a relatively defined *linea aspera*. In contrast, the positive extreme for PC2 is longer on the medial-lateral axis and the *linea aspera* is almost impossible to detect. Shape extremes for PC3 may be seen in Figure 6.7. Extremes in PC3 had less to do with the length of axes – although the positive extreme does have a longer anterior-posterior axis than the negative extreme shape – and more to do with the posterior-lateral shape. The negative shape extreme in PC3 remains convex until just before the *linea aspera*, but the positive extreme shape differentiates sharply between the lateral aspect and the posterior-lateral aspect via an area of slight but clear concavity.

Again, a one-way ANOVA comparing shape and log CS was used to determine whether or not allometry was present for femoral cross-sectional morphology. Shape varied with size at a statistical significance of 0.01. Full results for the ANOVA may be found in Table 6.4 and a regression of shape by log CS is displayed in Figure 6.8.

Table 6.3 Principal Component results for cross-sectional morphology of femora at midshaft.

	Standard deviation	Proportion of Variance	Cumulative Proportion
PC1	0.04212	34.9650%	34.9650%
PC2	0.0365	26.2500%	61.2200%
PC3	0.02368	11.0530%	72.2720%
PC4	0.02202	9.5540%	81.8250%
PC5	0.01639	5.2920%	87.1170%
PC6	0.01373	3.7130%	90.8300%
PC7	0.009774	1.8820%	92.7120%
PC8	0.009667	1.8410%	94.5530%
PC9	0.007574	1.1300%	95.6840%
PC10	0.006897	0.9370%	96.6210%
PC11	0.005992	0.7080%	97.3280%
PC12	0.005263	0.5460%	97.8740%

PC13	0.004597	0.4160%	98.2910%
PC14	0.00399	0.3140%	98.6040%
PC15	0.003354	0.2220%	98.8260%
PC16	0.003141	0.1940%	99.0200%
PC17	0.002984	0.1750%	99.1960%
PC18	0.002524	0.1260%	99.3210%
PC19	0.002472	0.1200%	99.4420%
PC20	0.002284	0.1030%	99.5440%
PC21	0.001973	0.0770%	99.6210%
PC22	0.00185	0.0670%	99.6890%
PC23	0.001626	0.0520%	99.7410%
PC24	0.001525	0.0460%	99.7870%
PC25	0.001511	0.0450%	99.8320%
PC26	0.001378	0.0370%	99.8690%
PC27	0.001329	0.0350%	99.9040%
PC28	0.001039	0.0210%	99.9250%
PC29	0.001001	0.0200%	99.9450%
PC30	0.000877	0.0150%	99.9600%
PC31	0.000831	0.0140%	99.9740%
PC32	0.000641	0.0080%	99.9820%
PC33	0.000619	0.0080%	99.9890%
PC34	0.000516	0.0050%	99.9940%
PC35	0.000413	0.0030%	99.9980%
PC36	0.000335	0.0020%	100.0000%
PC37	5.68E-17	0.0000%	100.0000%
PC38	2.70E-17	0.0000%	100.0000%
PC39	2.43E-17	0.0000%	100.0000%
PC40	2.36E-17	0.0000%	100.0000%

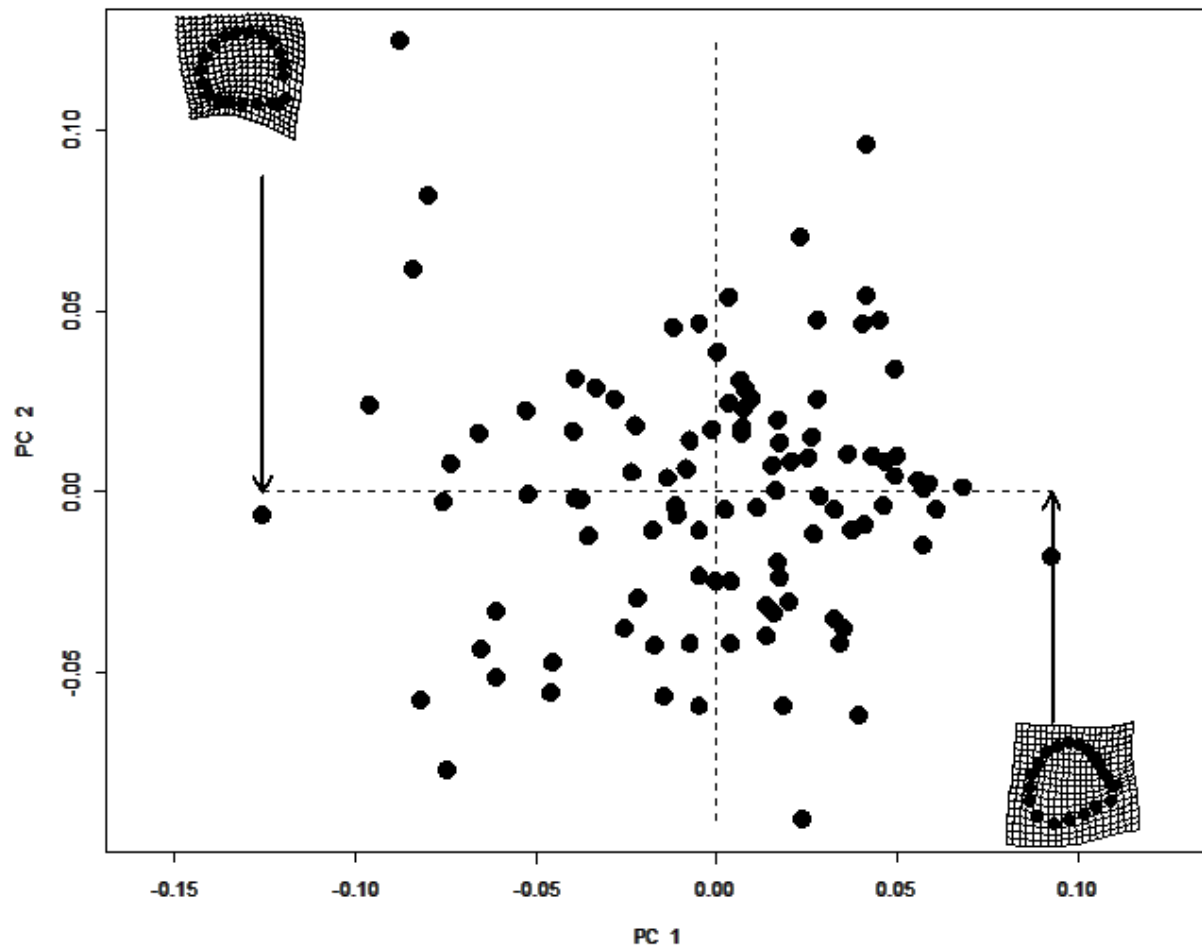


Figure 6.5 Visualisation of PC1 and PC2 for femoral cortical shape with warp grids for PC1 extremes.

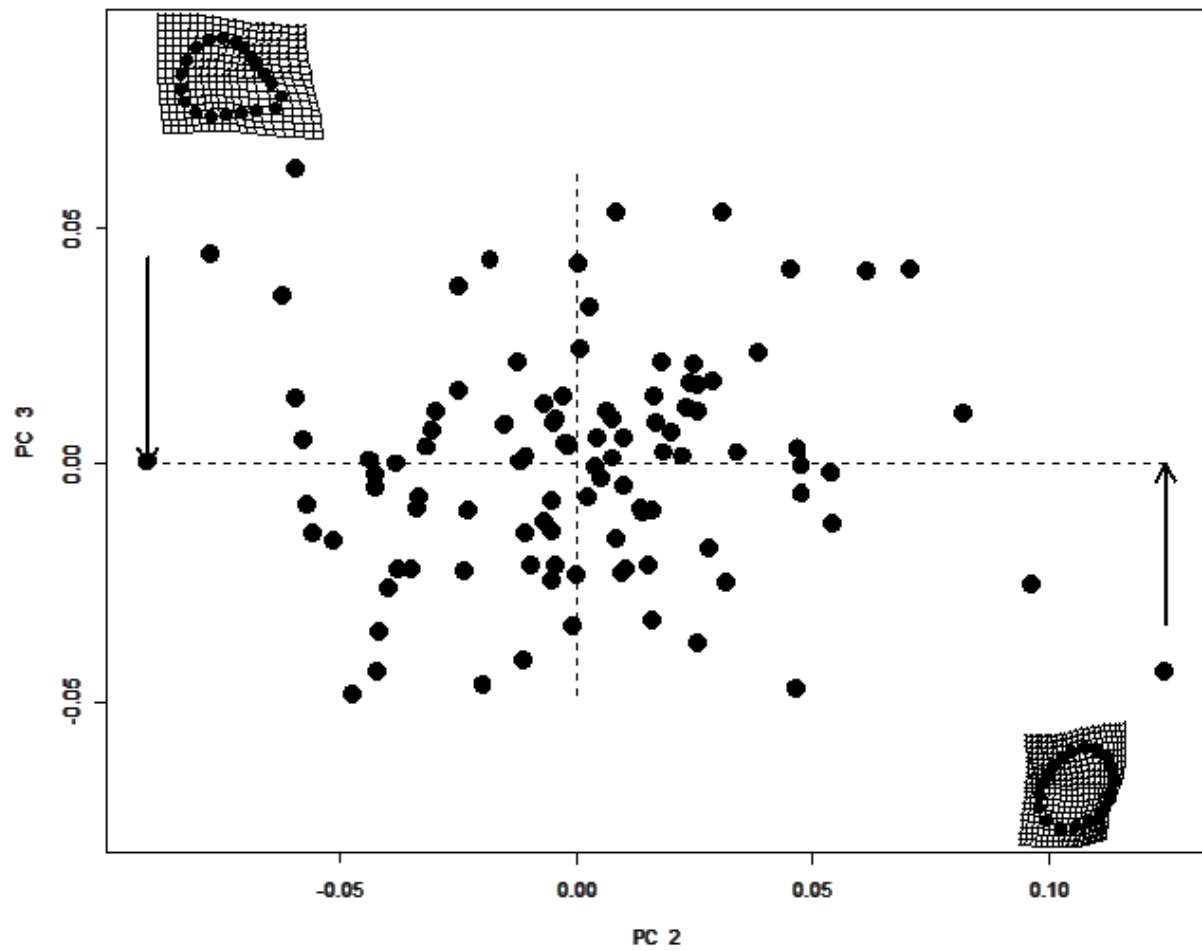


Figure 6.6 Visualisation of PC2 and PC3 for femoral cortical shape with warp grids for PC2 extremes.

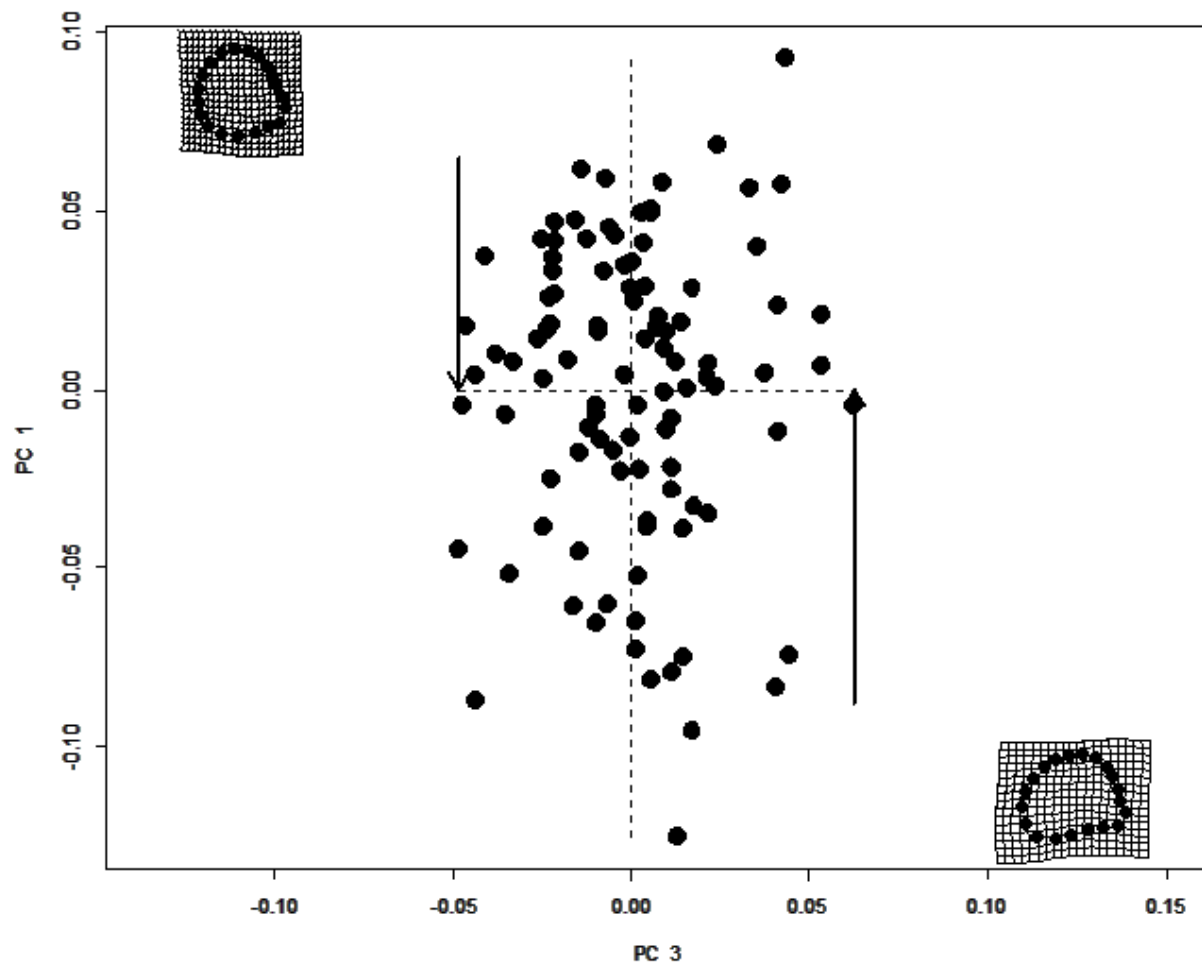


Figure 6.7 Visualisation of PC2 and PC3 for femoral cortical shape with warp grids for PC3 extremes.

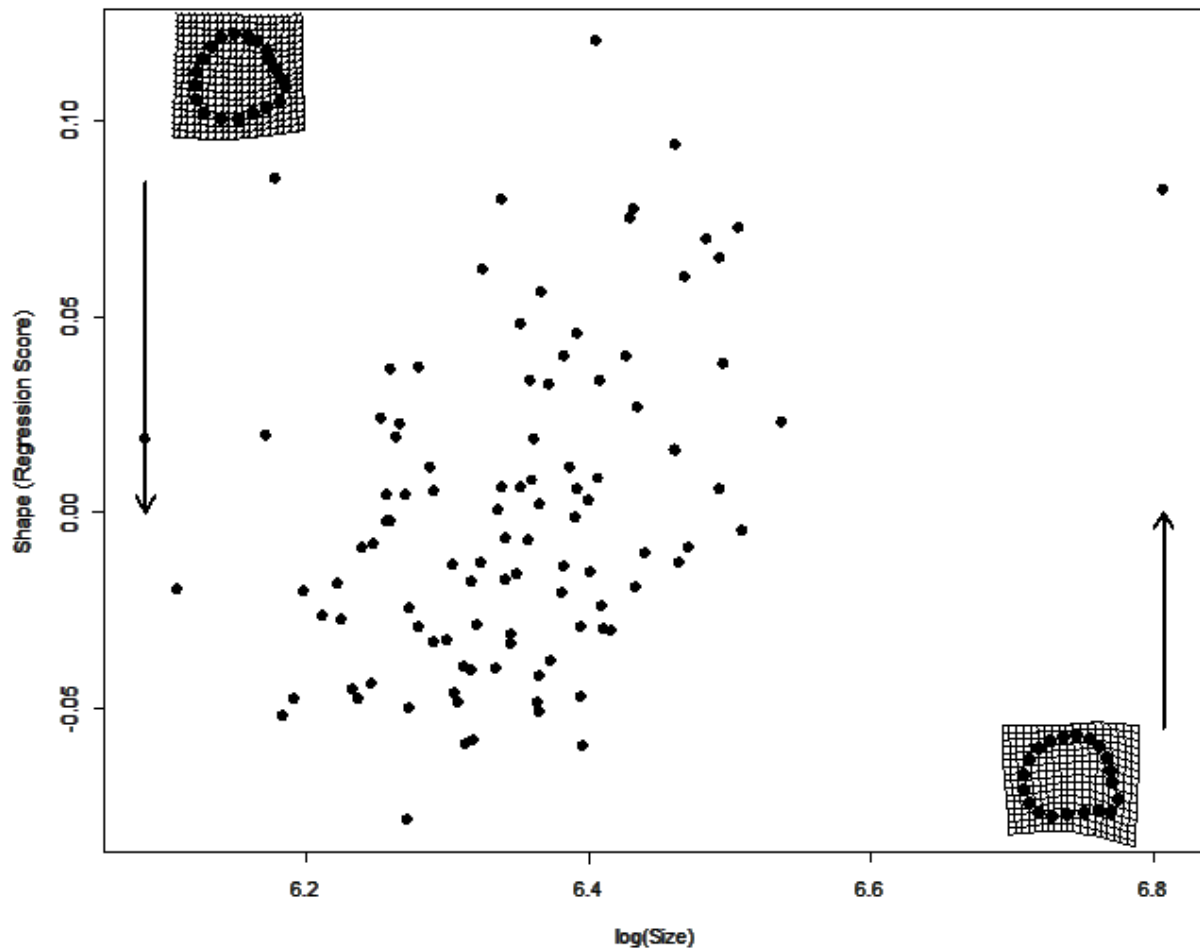


Figure 6.8 Allometry regression of log CS by Shape Regression Scores for femoral cross-sectional morphology.

Table 6.4 GLM Procrustes shape residuals compared to log(CS) for femoral cross-sectional morphology.

	Df	SS	MS	Rsq	F	Z	Pr(>F)
log(size)	1	0.02274	0.022737	0.044358	4.6417	3.7235	0.003
Residuals	100	0.48984	0.004898				
Total	101	0.51258					

Shape extremes for the three first PCs in no case completely matched shape variation seen with size. Humeral shape variation with size while remaining statistically significant shows the shapes at the extremity of sizes to both be somewhat ovoid. This is in contrast to the positive shape extremes in both PC1 and PC2. For the humerus while shape varied with size it is clear that allometric variation does not account entirely for shape variation in the upper PCs. Femoral cross-sectional shapes maintain this pattern, but to a lesser degree. PC1 appears to show an increase in robusticity towards the positive

extreme which might imply size. PC2 with its exaggerated *linea aspera* at the negative extreme and ovoid shape at the positive extreme also suggests a graduation although this time from robust to gracile. However, shapes represented at extreme sizes do not match those seen in the extremes of shape space and the largest and smallest projected extremes are different shapes, but not apparently in terms of gracility or robusticity. Allometry is present, but it is not clear that it represents all shape variation in the upper PCs.

6.2.1 Intrapopulation

6.2.1.1 Sex

Figure 6.9 and Table 6.5 show that sex does not uniquely explain variation in shape for humeral cross-sections. However, as noted in the previous section allometry is present as centroid size does uniquely account for morphological variation at a statistical confidence of 0.05. Figure 6.10 and Table 6.6 show that sex does not account for the allometry present in shape variation for humeral cross-sections.

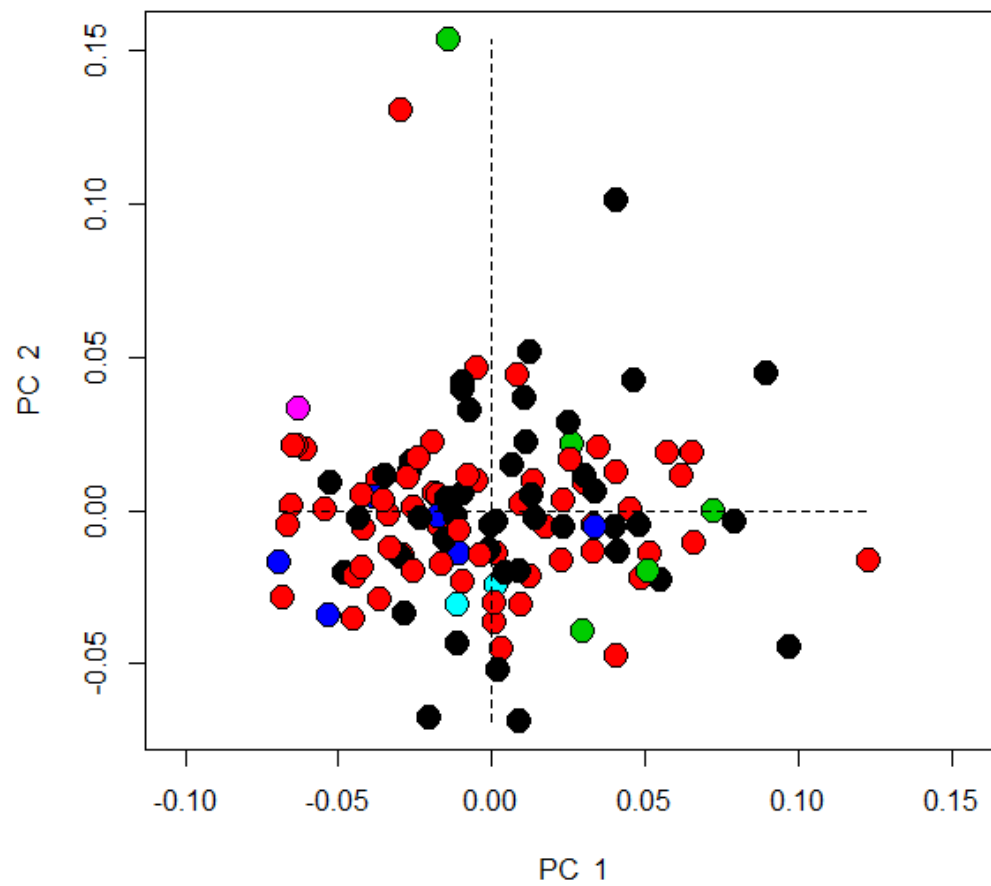


Figure 6.9 PC1 and PC2 of humeral cross-sectional morphology organized by sex. (black = female, red = male, green = possible female, blue = possible male, cyan = unknown, purple = unobservable)

Table 6.5 GLM with interactions of humeral cross-sectional morphology by sex and size.

	Df	SS	MS	Rsqr	F	Z	Pr(>F)
Centroid Size	1	0.01035	0.010355	0.019847	2.465	2.0392	0.034
sex	5	0.03018	0.006036	0.05784	1.4368	1.3266	0.111
Centroid Size x sex	4	0.01912	0.004781	0.036655	1.1381	1.1325	0.246
Residuals	110	0.46208	0.004201				
Total	120	0.52173					

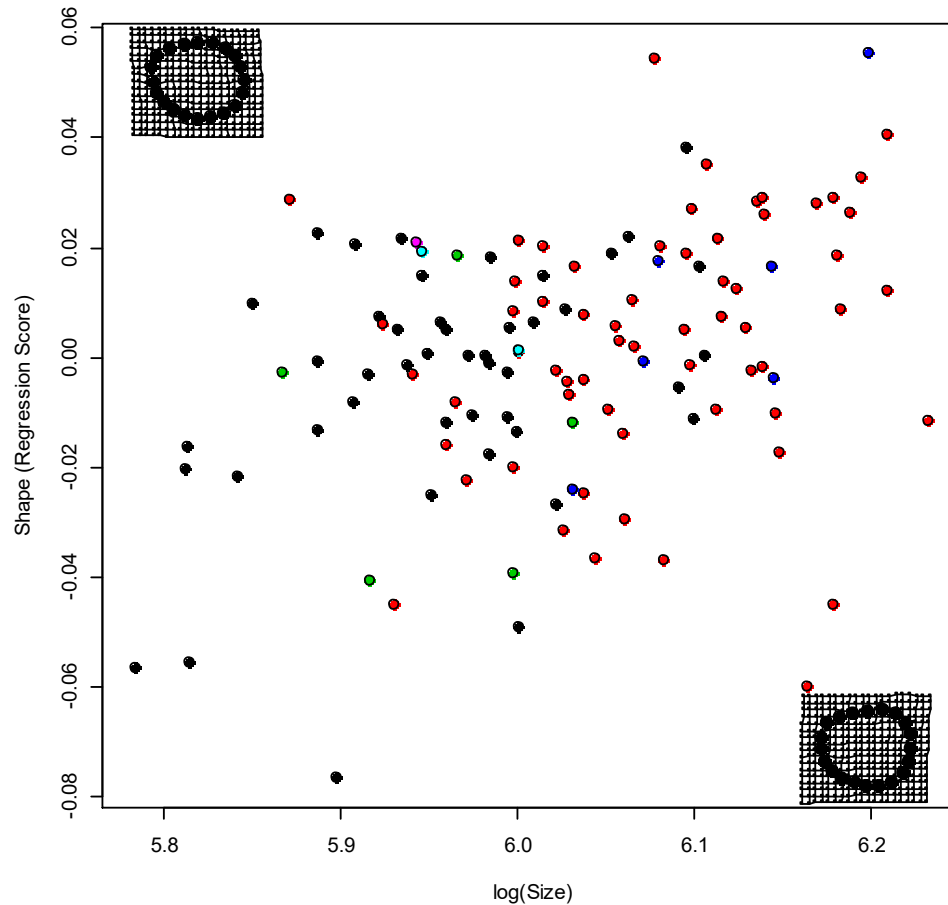


Figure 6.10 Allometry of humeral cross-sectional morphology at midshaft by sex. (black = female, red = male, green = possible female, blue = possible male, cyan = unknown, purple = unobservable)

Table 6.6 Homogeneity of Slopes Test and GLM tests by sex and by sex with size for humeral cross-sectional morphology at midshaft.

Homogeneity of Slopes Test

	Df	SSE	SS	Rsq	F	Z	Pr(>F)
Common Allometry	119	0.51114					
Group Allometries	110	0.4624	0.048736	0.093411	1.2882	1.225	0.14

Type III GLM

	Df	SS	MS	Rsq	F	Z	Pr(>F)
log(size)	1	0.0106	0.010596	0.020308	2.5108	2.0811	0.031
sex	5	0.03005	0.006011	0.057606	1.4244	1.3221	0.111
Residuals	114	0.48108	0.00422				
Total	120	0.52173					

For femoral cross-sections at midshaft the difference between sexes becomes somewhat more obvious both in shape space and when considering the results of the GLM. Figure 6.11 shows femoral cross sections organized in PC1 and PC2 by sex. Whilst there remains some overlap, there does appear to be a difference in intergroup variation particularly along the first PC. Notably, female femoral cross-sections (represented by the black dots) pool mostly in the positive areas of PC1 and PC2. Males (represented by the red dots) occupy most of the graph. They do not pool away from the female shapes, but they also pool into the negative portions of PC1 and PC2 suggesting that females have a narrower range of shape variation than males. However, as seen in Table 6.7 sex may only uniquely explain morphological variation of the femoral cross-section at a statistical significance of 0.10. There is allometry in the femoral cross-sectional morphology. Figure 6.12 shows femoral cross-sectional shape organized by sex and regressed shape against logCS. But as with shape space, the ANOVA and allometry tests reported in Table 6.8 show that although variation of shape by CS is significant at a significance level of 0.01, sex alone does not explain shape variation.

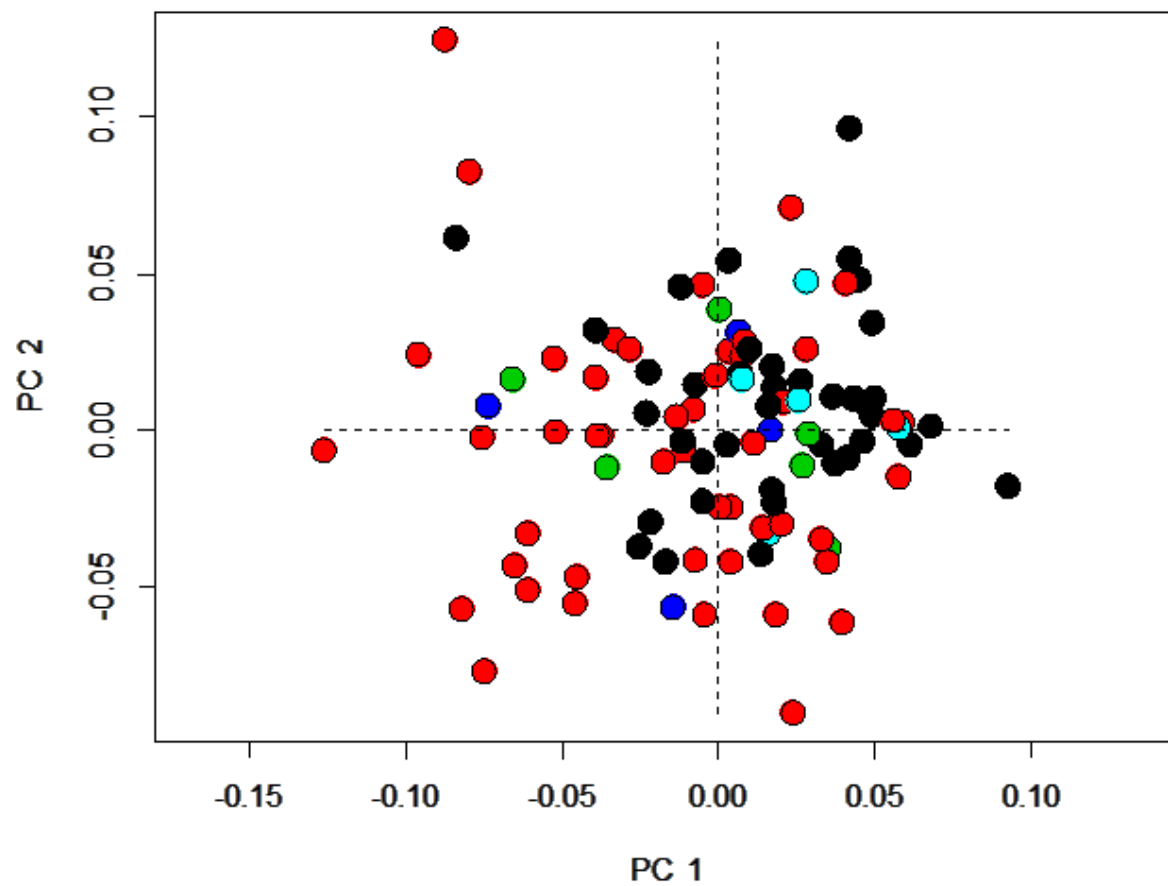


Figure 6.11 PC1 and PC2 of femoral cross-sectional morphology organized by sex. (black = female, red = male, green = possible female, blue = possible male, cyan = unknown)

Table 6.7 GLM with interactions of femoral cross-sectional morphology by sex and size.

	Df	SS	MS	Rsq	F	Z	Pr(>F)
Centroid Size	1	0.02463	0.024628	0.048047	5.1516	4.0457	0.002
sex	4	0.02841	0.007102	0.055424	1.4856	1.4096	0.065
Centroid Size by sex	4	0.01973	0.004932	0.038487	1.0316	1.035	0.334
Residuals	92	0.43981	0.004781				
Total	101	0.51258					

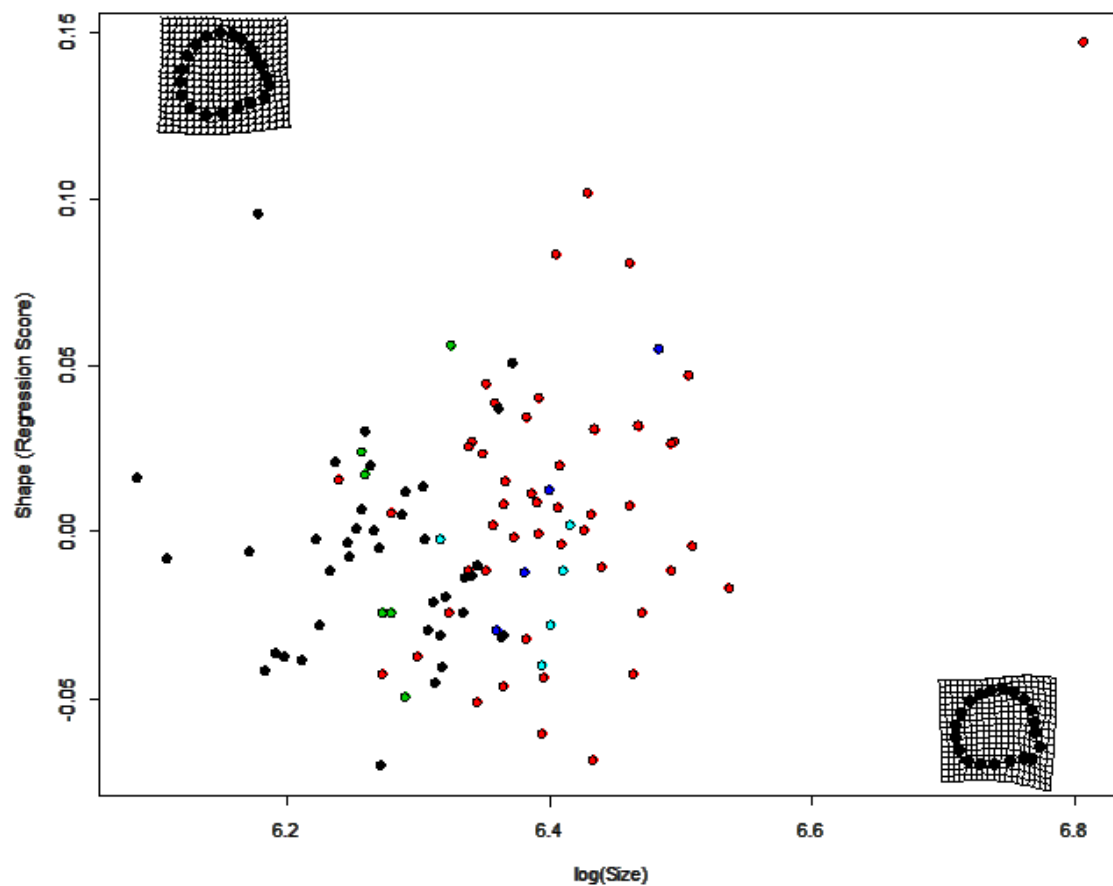


Figure 6.12 Allometry of femoral cross-sectional morphology at midshaft by sex. (black = female, red = male, green = possible female, blue = possible male, cyan = unknown)

Table 6.8 Homogeneity of Slopes Test for femoral cross-sections at midshaft and GLM tests of shape variation of femoral cross-sections by size and sex.

Homogeneity of Slopes Test

	Df	SSE	SS	Rsq	F	Z	Pr(>F)
Common Allometry	100	0.48984					
Group Allometries	92	0.44139	0.048452	0.094527	1.2624	1.2218	0.133

Type III GLM

	Df	SS	MS	Rsq	F	Z	Pr(>F)
log(size)	1	0.02274	0.022737	0.044358	4.7153	3.7235	0.003
sex	4	0.02693	0.006732	0.052535	1.3961	1.3317	0.106
Residuals	96	0.46291	0.004822				
Total	101	0.51258					

6.2.1.2 Age

Distribution of individuals by age group is shown in Figure 6.13 for humeral cross-sections at midshaft and Figure 6.14 for femoral cross-sections at midshaft. It may have been expected considering rates of deposition and remodeling those very young and very old adults might have been distinct from the rest of the group, but there is complete overlap of all age groups. Cross-sectional shape in humeri and femora does not seem to vary with age.

Three-way ANOVA tests were conducted to determine the relationship between the DV of shape against size, sex, age, and the interactions of those groups. For humeral cross sections (Table 6.9), sex could only uniquely explain morphology at a significance level of 0.10. However, age and sex together uniquely explained morphological variation at a significance of 0.05. The combination of size, sex, and age as well as site sex and age both uniquely and strongly ($p < 0.01$) explained morphological variation of the humeral cross-section at mid-shaft. Femoral cross-sectional morphology (Table 6.10) was weakly ($p < 0.10$) and uniquely explained by age. If site and age were considered together they accounted for femoral cross-sectional morphology at a statistical significance of 0.05. Size, sex and age together also explained femoral cross-sectional morphology at a significance of 0.05. When size, site, and age or site, sex, and age were considered together they explained morphological variation at a statistical significance of 0.01.

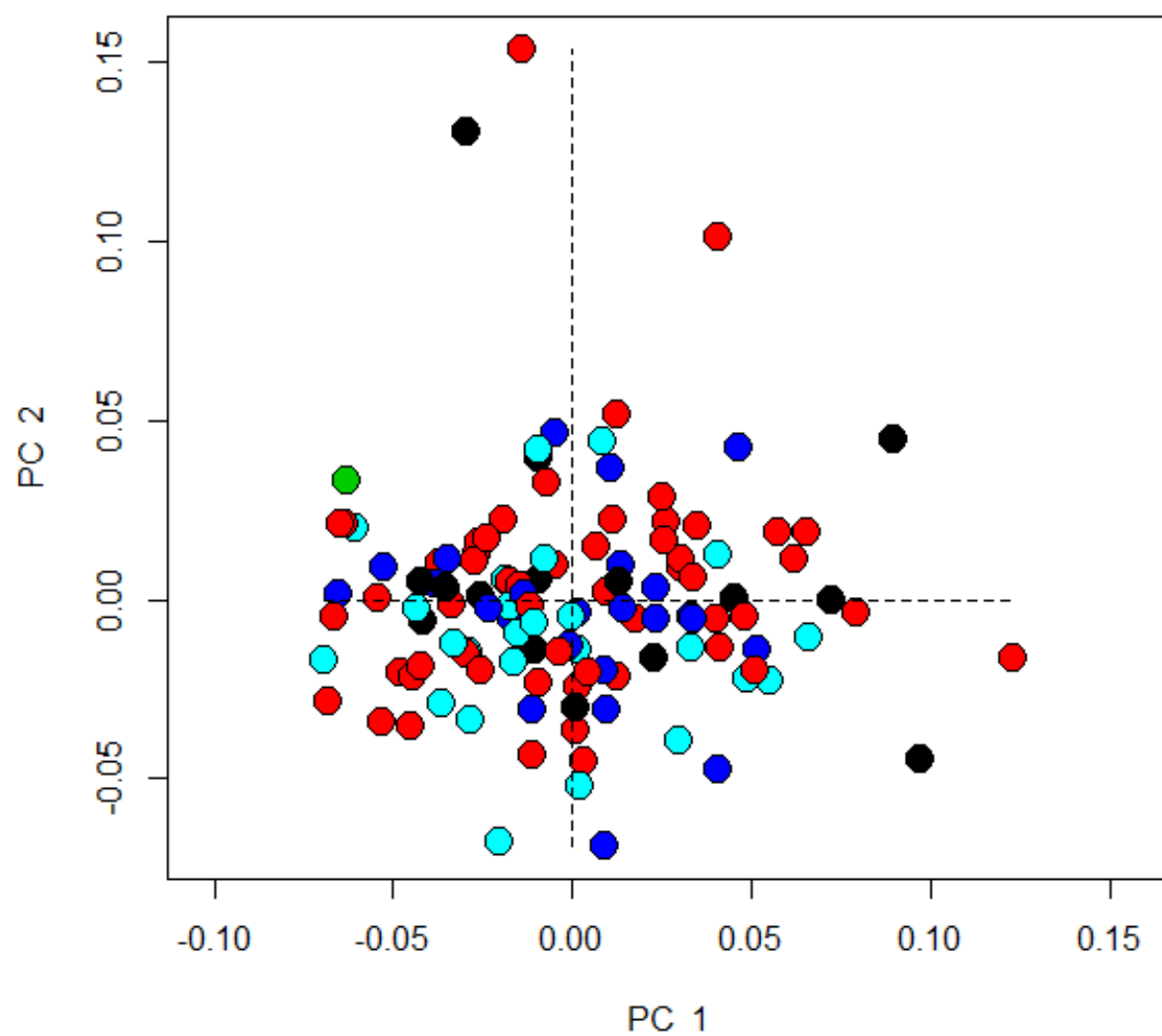


Figure 6.13 PC1 and PC2 of humeral morphology organized by age. (black= 35-45 years, red = 45+ years, green = unknown, blue = 17-25 years, cyan = 25-35 years)

Table 6.9 GLM with interactions of humeral cross-sectional morphology by size, sex, and age.

Type III GLM

	Df	SS	MS	Rsqr	F	Z	Pr(>F)
Centroid Size	1	0.01035	0.010355	0.019847	2.6919	2.0392	0.034
site	3	0.03019	0.010065	0.057872	2.6165	2.241	0.003
sex	5	0.03153	0.006305	0.060424	1.6391	1.4764	0.064
age	3	0.0131	0.004366	0.025102	1.1349	1.0929	0.283
Centroid Size x site	3	0.01333	0.004443	0.025546	1.155	1.1389	0.262
Centroid Size x sex	4	0.02025	0.005062	0.03881	1.316	1.3644	0.104
site x sex	7	0.03457	0.004939	0.066262	1.2839	1.4219	0.044
Centroid Size x age	3	0.01432	0.004772	0.027438	1.2405	1.4549	0.088
site x age	6	0.02189	0.003648	0.041952	0.9483	1.2099	0.157
sex x age	6	0.02901	0.004835	0.055606	1.257	1.6948	0.01
Centroid Size x site x sex	3	0.01079	0.003598	0.02069	0.9354	1.3355	0.128
Centroid Size x site x age	6	0.01399	0.002333	0.026823	0.6064	0.9117	0.51
Centroid Size x sex x age	3	0.02668	0.008894	0.051142	2.3122	3.5696	0.001
site x sex x age	6	0.02548	0.004247	0.048843	1.1041	1.9279	0.007
Centroid Size x site x sex x age	5	0.01084	0.002167	0.020769	0.5634	1.0637	0.296
Residuals	56	0.21541	0.003847				
Total	120	0.52173					

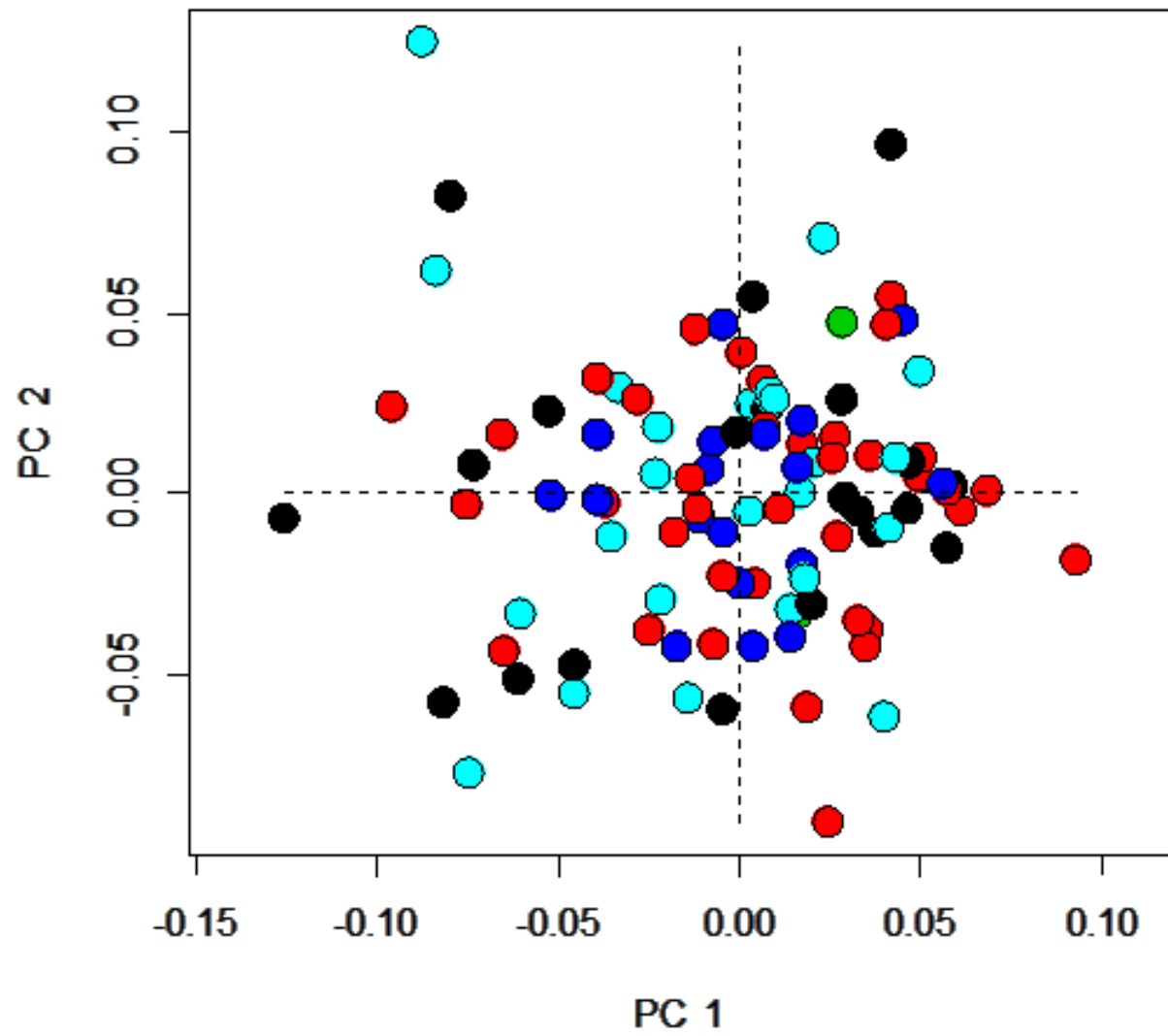


Figure 6.14 PC1 and PC2 of femur cortices organized by age. (black= 35-45 years, red = 45+ years, green = unknown, blue = 17-25 years, cyan = 25-35 years)

Table 6.10 GLM with interactions of femoral cross-sectional morphology by size, sex, and age.

Type III GLM

	Df	SS	MS	Rsqr	F	Z	Pr(>F)
Centroid Size	1	0.02463	0.024628	0.048047	5.9372	4.0457	0.002
site	3	0.04258	0.014192	0.083065	3.4215	2.6856	0.002
sex	4	0.02269	0.005672	0.044259	1.3673	1.2385	0.169
age	4	0.02606	0.006516	0.05085	1.5709	1.4921	0.05
Centroid Size by site	3	0.01867	0.006223	0.03642	1.5001	1.4661	0.075
Centroid Size by sex	4	0.0162	0.00405	0.031601	0.9762	1.027	0.352
site by sex	6	0.02381	0.003969	0.046461	0.9569	1.0741	0.293
Centroid Size by age	4	0.01448	0.003619	0.028245	0.8726	1.0377	0.335
site by age	8	0.0392	0.004899	0.076468	1.1812	1.4812	0.02
sex by age	5	0.01939	0.003879	0.037837	0.9351	1.323	0.1
Centroid Size by site by sex	2	0.01184	0.005921	0.023103	1.4274	2.0602	0.022
Centroid Size by site by age	7	0.03325	0.00475	0.064865	1.1451	1.8494	0.001
Centroid Size by sex by age	3	0.01171	0.003904	0.022852	0.9413	1.6742	0.04
site by sex by age	5	0.03464	0.006928	0.06758	1.6702	3.1928	0.001
Centroid Size by site by sex by age	1	0.00336	0.00336	0.006556	0.8101	1.5262	0.115
Residuals	41	0.17007	0.004148				
Total	101	0.51258					

6.2.1.3 Trauma and Pathology

Childhood stress indicators like LEH, and cribra orbitalia were not expected to have much effect on long bone cross-sectional morphology. While individuals who suffered childhood stress are expected to be smaller than individuals with no stress markers, remodeling of the diaphysis during adolescence and through adulthood could obscure any morphological impact childhood stress may have on cross-sectional geometry as seen with Harris lines. (Garn & Baby, 1969)

PC charts for humeral and femoral cross-sectional shape plotted by presence or absence of LEH (see Figure 6.15 and Figure 6.16) predictably show a complete overlap of individuals but possibly some between group variation. In a three-way GLM for humeri (Table 6.11) there is strong statistical significance ($p < 0.01$) indicating that the interaction of size and LEH explains morphological variation. However, no other factor related to the presence or absence of LEH explained morphological variation for the humeral cross-section. The three-way GLM for femoral cross-sections (Table 6.12) showed weak relationship with shape ($p < 0.1$) for the interaction of size, site, and presence or absence of LEH. Sex and

LEH considered together could uniquely explain morphological variation of femoral cross-sections at a statistical significance of 0.05.

Cribra orbitalia PC charts for humeral cross-sections (Figure 6.17) and femoral cross-sections (Figure 6.18) also show complete overlap for individuals with and without cribra orbitalia, but it is notable that variation does not appear to be the same. While individuals with cribra orbitalia fall within the normal range of shape variation they do cluster together particularly in the humeral cross-section PC views. This would suggest a cessation, delay, or possibly alteration in growth trajectory. Three-way GLM testing on humeral cross-sectional shape (see Table 6.13) shows no statistical relationship between humeral cross-sectional morphology and presence or absence of cribra orbitalia. Table 6.14 shows that while the presence or absence of cribra orbitalia does not uniquely explain femoral cross-sectional morphology if sex is also considered along with CO or if site and sex are considered together with CO, then morphological variation is explained at a statistical significance of 0.05. The statistical significance is stronger ($p < 0.01$) when all IVs – size, site, sex, and presence or absence of CO – are considered.

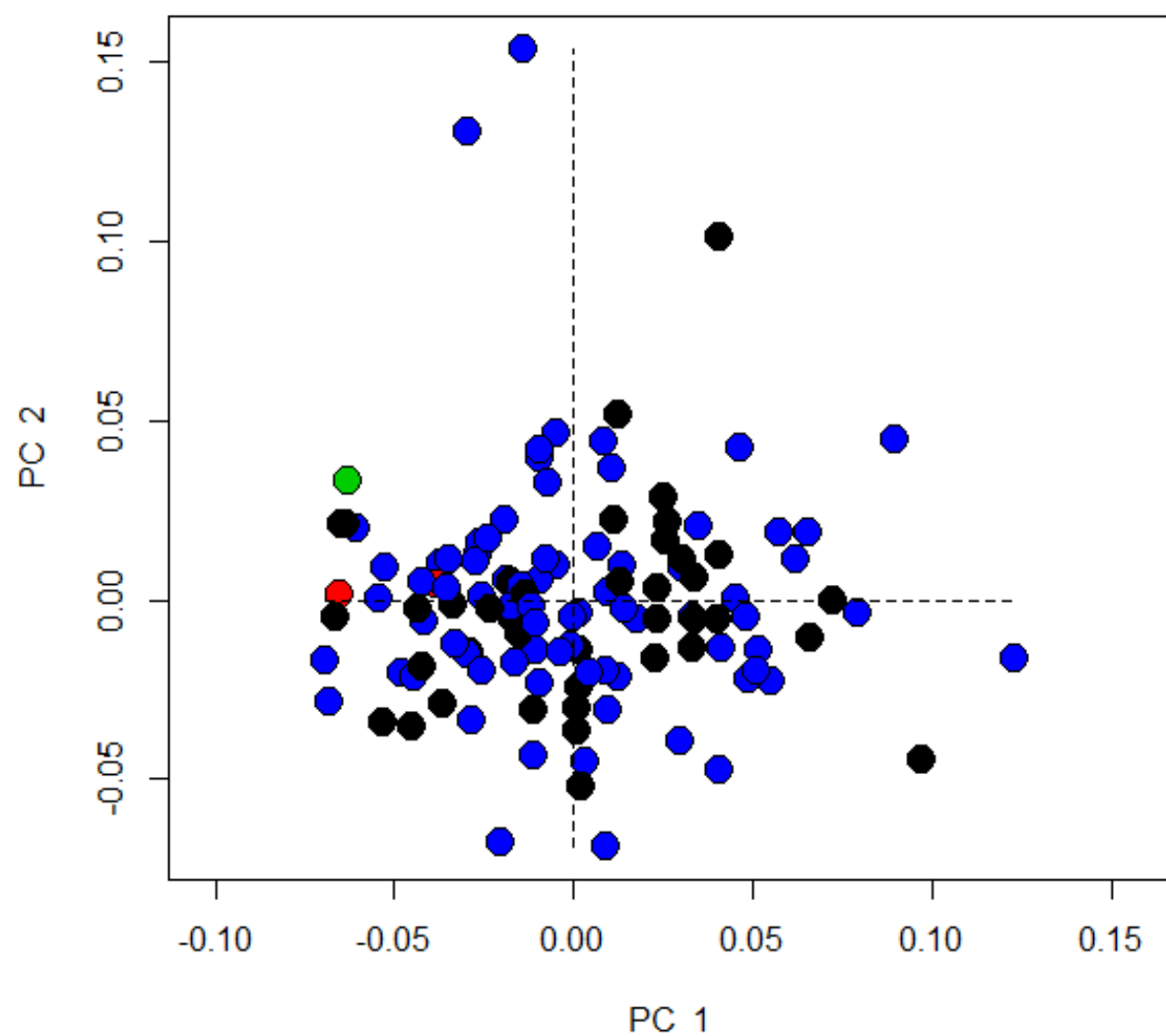


Figure 6.15 PC1 and PC2 of humerus cortices organized by LEH. (black = none, red = teeth not present, green = unknown, blue = LEH present)

Table 6.11 Three-way GLM of humeral cross-sectional morphology variation by size, sex, and presence or absence of LEH

Type III GLM

	Df	SS	MS	Rsqr	F	Z	Pr(>F)
Centroid Size	1	0.01035	0.010355	0.019847	2.6877	2.03924	0.034
site	3	0.03019	0.010065	0.057872	2.6124	2.24097	0.003
sex	5	0.03153	0.006305	0.060424	1.6365	1.47642	0.064
LEH	2	0.00836	0.004179	0.01602	1.0847	1.04745	0.312
Centroid Size x site	3	0.01233	0.004109	0.023627	1.0665	1.04048	0.327
Centroid Size x sex	4	0.02271	0.005678	0.043533	1.4738	1.51264	0.049
site x sex	7	0.03021	0.004316	0.057906	1.1203	1.23189	0.129
Centroid Size x LEH	2	0.01697	0.008486	0.032529	2.2026	2.45323	0.008
site x LEH	3	0.00704	0.002348	0.013502	0.6095	0.73953	0.695
sex x LEH	2	0.00391	0.001955	0.007494	0.5074	0.6013	0.757
Centroid Size x site x sex	4	0.03102	0.007756	0.05946	2.013	2.55457	0.001
Centroid Size x site x LEH	3	0.00914	0.003046	0.017516	0.7907	1.07082	0.293
Centroid Size x sex x LEH	1	0.00389	0.00389	0.007456	1.0097	1.26487	0.167
site x sex x LEH	2	0.00577	0.002887	0.011067	0.7494	1.02836	0.303
Centroid Size x site x sex x LEH	2	0.0055	0.00275	0.01054	0.7137	0.98945	0.331
Residuals	76	0.2928	0.003853				
Total	120	0.52173					

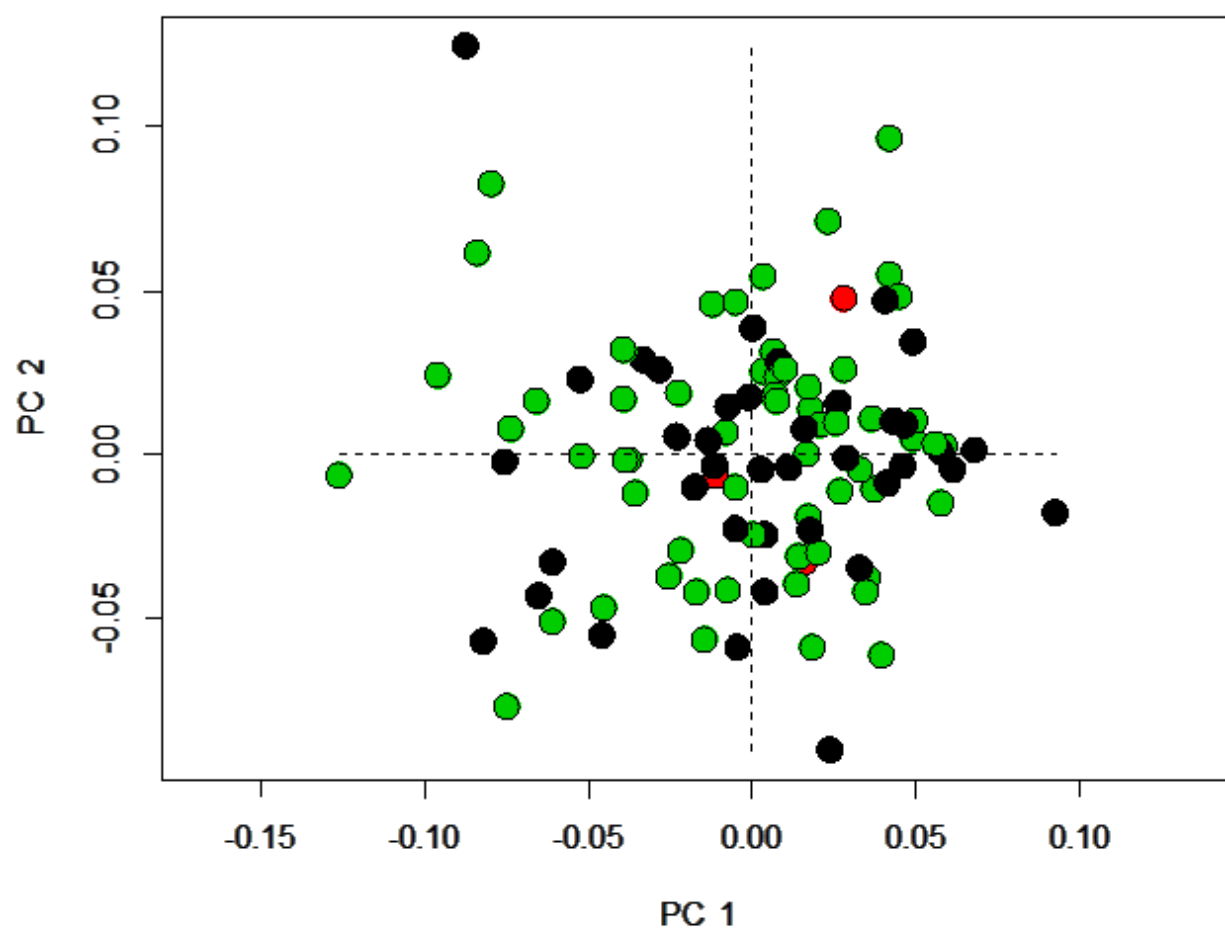


Figure 6.16 PC1 and PC2 of femur cortices organized by LEH. (black = none, red = teeth not present, green = LEH)

Table 6.12 GLM of femoral cross-sectional morphology variation by size, sex, and presence or absence of LEH.
Type III GLM

	Df	SS	MS	Rsq	F	Z	Pr(>F)
Centroid Size	1	0.02463	0.024628	0.048047	5.4082	4.0457	0.002
site	3	0.04258	0.014192	0.083065	3.1166	2.6856	0.002
sex	4	0.02269	0.005672	0.044259	1.2455	1.2385	0.169
LEH	2	0.0057	0.002848	0.011114	0.6255	0.6288	0.751
Centroid Size by site	3	0.0215	0.007165	0.041937	1.5735	1.6157	0.044
Centroid Size by sex	4	0.01691	0.004228	0.032993	0.9284	1.0283	0.342
site by sex	7	0.02413	0.003447	0.047068	0.7569	0.8924	0.588
Centroid Size by LEH	2	0.00738	0.003689	0.014395	0.8102	0.957	0.366
site by LEH	3	0.01147	0.003824	0.022379	0.8397	1.0561	0.304
sex by LEH	2	0.01596	0.00798	0.031136	1.7523	2.2379	0.013
Centroid Size by site by sex	2	0.01408	0.007041	0.027473	1.5462	2.0174	0.024
Centroid Size by site by LEH	2	0.01031	0.005155	0.020115	1.1321	1.5682	0.072
Centroid Size by sex by LEH	1	0.00228	0.002285	0.004457	0.5017	0.6504	0.562
site by sex by LEH	2	0.00871	0.004356	0.016995	0.9565	1.377	0.137
Centroid Size by site by sex by LEH	2	0.00648	0.00324	0.01264	0.7114	1.0317	0.308
Residuals	61	0.27778	0.004554				
Total	101	0.51258					

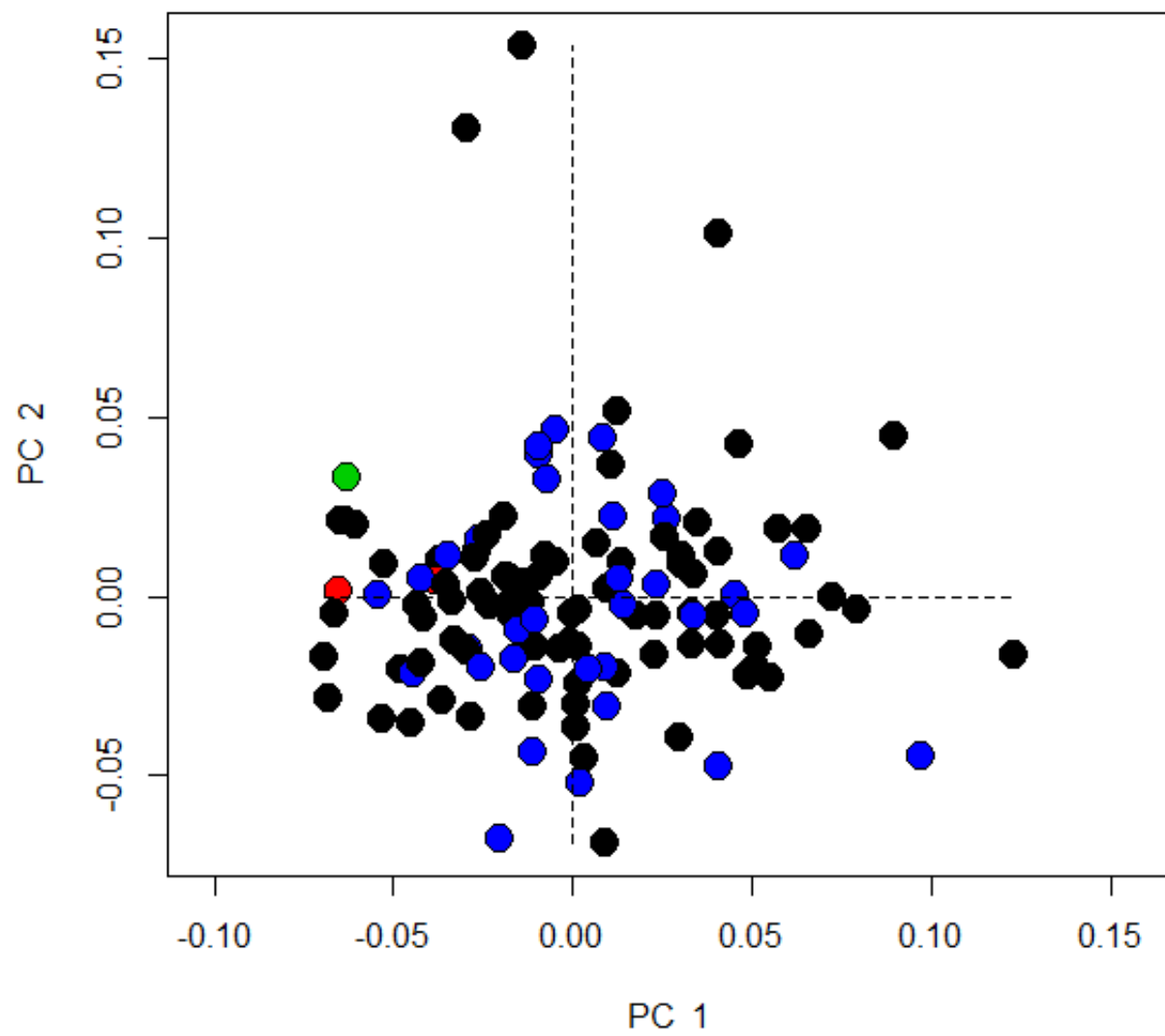


Figure 6.17 PC1 and PC2 of humerus cortices organized by cribra orbitalia. (black = none, red = orbits not present, green = unobservable, blue = cribra orbitalia present)

Table 6.13 GLM with interactions of humeral cross-sectional morphology by sex, size, and presence or absence of cribra orbitalia.

Type III GLM

	Df	SS	MS	Rsqr	F	Z	Pr(>F)
Centroid Size	1	0.01035	0.010355	0.019847	2.6618	2.03924	0.034
site	3	0.03019	0.010065	0.057872	2.5872	2.24097	0.003
sex	5	0.03153	0.006305	0.060424	1.6208	1.47642	0.064
CO	2	0.01038	0.00519	0.019894	1.3341	1.27433	0.161
Centroid Size x site	3	0.01174	0.003913	0.022499	1.0058	0.99914	0.372
Centroid Size x sex	4	0.02256	0.005639	0.043236	1.4497	1.50663	0.05
site x sex	7	0.02986	0.004266	0.057229	1.0965	1.22162	0.14
Centroid Size x CO	2	0.00807	0.004038	0.015477	1.0379	1.19743	0.197
site x CO	3	0.00903	0.003011	0.017313	0.774	0.90241	0.494
sex x CO	2	0.00887	0.004436	0.017003	1.1402	1.33963	0.15
Centroid Size x site x sex	4	0.02603	0.006508	0.049891	1.6728	2.10847	0.003
Centroid Size x site x CO	2	0.00807	0.004033	0.015458	1.0366	1.37088	0.132
Centroid Size x sex x CO	1	0.00077	0.000769	0.001473	0.1976	0.24598	0.95
site x sex x CO	2	0.00633	0.003163	0.012127	0.8132	1.07926	0.29
Centroid Size x site x sex x CO	2	0.00842	0.004208	0.016129	1.0816	1.44832	0.101
Residuals	77	0.29954	0.00389				
Total	120	0.52173					

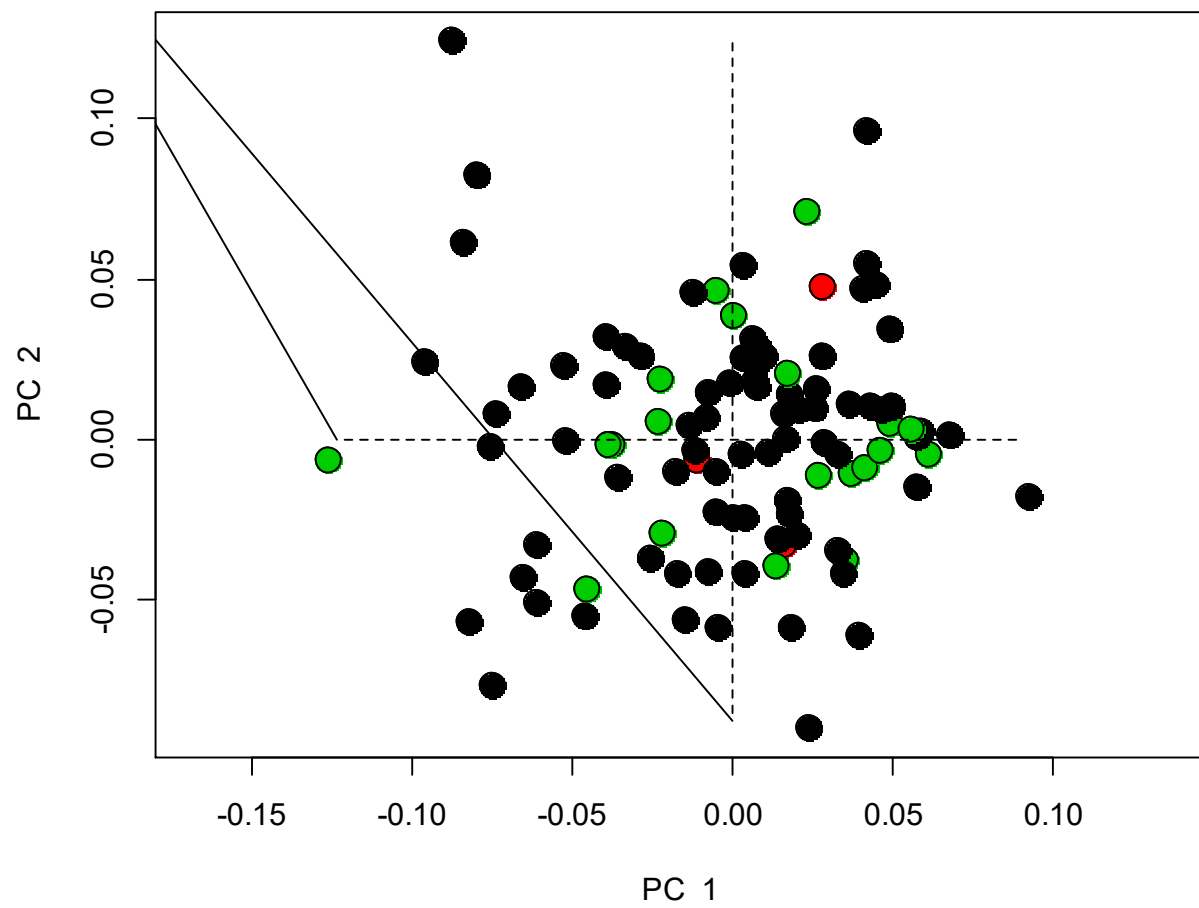


Figure 6.18 PC1 and PC2 of femur cortices organized by cribra orbitalia. (black = none, red = orbits not present, green = cribra orbitalia)

Table 6.14 ANOVA for femoral cross-sections grouped by presence or absence of cribra orbitalia.

Type III GLM							
	Df	SS	MS	Rsq	F	Z	Pr(>F)
Centroid Size	1	0.02463	0.024628	0.048047	5.4893	4.0457	0.002
site	3	0.04258	0.014192	0.083065	3.1633	2.6856	0.002
sex	4	0.02269	0.005672	0.044259	1.2641	1.2385	0.169
CO	2	0.004	0.001999	0.007799	0.4455	0.4345	0.931
Centroid Size by site	3	0.01918	0.006392	0.037412	1.4248	1.4305	0.084
Centroid Size by sex	4	0.01676	0.004191	0.032705	0.9341	1.0096	0.362
site by sex	7	0.02446	0.003494	0.047714	0.7787	0.8945	0.577
Centroid Size by CO	2	0.01286	0.006429	0.025087	1.4331	1.6518	0.06
site by CO	2	0.00218	0.001088	0.004244	0.2425	0.2843	0.979
sex by CO	2	0.01567	0.007837	0.030578	1.7467	2.0832	0.021
Centroid Size by site by sex	2	0.00954	0.004769	0.018608	1.0629	1.3458	0.132
Centroid Size by site by CO	1	0.00467	0.004669	0.009109	1.0407	1.282	0.174
Centroid Size by sex by CO	2	0.00809	0.004046	0.015785	0.9017	1.1706	0.225
site by sex by CO	1	0.00737	0.007373	0.014384	1.6434	2.0323	0.04
Centroid Size by site by sex by CO	1	0.01077	0.010773	0.021018	2.4013	2.872	0.008
Residuals	64	0.28714	0.004487				
Total	101	0.51258					

DJD severity refers to the level of DJD on a bone. Criteria for severity of DJD and OA are available in Table 3.19. PC charts for DJD severity for humeral cross-sectional shape (Figure 6.19) and femoral cross-sectional shape (Figure 6.21 for proximal DJD severity and Figure 6.22 for distal) seem to show complete overlap of all groups and similar variation.

GLM results for DJD and OA severity in the proximal humeral joint as compared to humeral cross-sectional morphology may be found in Table 6.15 with results for distal DJD severity in Table 6.16. Severity of DJD and OA in the proximal humeral joint uniquely explained morphology of the humeral cross section with a high degree of statistical confidence ($p < 0.01$). Three sets of interactions – DJD severity and site, DJD severity, site, and size, and DJD severity, site, and sex – also all explained humeral cross-sectional morphology with a high degree of statistical confidence ($p < 0.01$). DJD severity in the distal humeral joint also uniquely explained humeral cross-sectional variation, but this time at a statistical significance of 0.05. When sex and DJD severity of the distal joint were considered together they explained humeral cross-sectional morphological variation at a statistical significance of 0.01.

Results of three-way GLM test for DJD and OA severity as compared to femoral cross-sectional morphology may be found for the proximal joint in Table 6.17 and for the distal joint in Table 6.18. When considered together size and DJD severity in the proximal joint explained femoral morphological variation in the cross-section at a statistical significance of 0.05. Site considered with proximal DJD severity could explain cross-sectional morphological variation at a statistical significance of 0.01. DJD severity in the distal joint when paired with site explained cross-sectional morphological variation at a statistical significance of 0.05. When sex and distal DJD were combined they explained cross-sectional morphological variation of the femur at midshaft with a high degree of statistical confidence ($p < 0.01$).

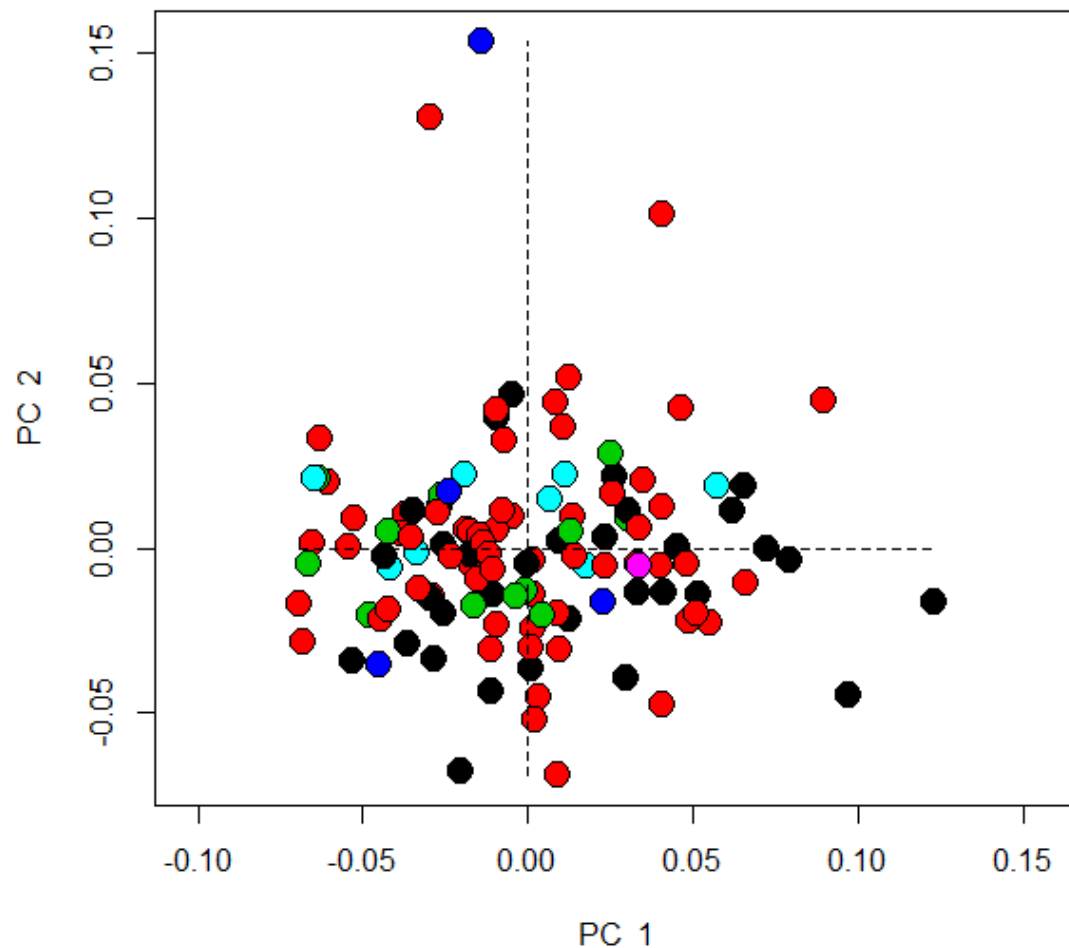


Figure 6.19 PC1 and PC2 of humeral cross-sectional morphology organized by DJD and OA severity at proximal joint. (black= DJD, red = healthy, green = mild, blue = moderate, cyan = severe, magenta = unknown)

Table 6.15 GLM with interactions of humeral cross-sectional morphology by size, sex, and DJD and severity of OA at the proximal joint.

Type III GLM

	Df	SS	MS	Rsq	F	Z	Pr(>F)
Centroid Size	1	0.01035	0.010355	0.019847	2.9663	2.0392	0.034
site	3	0.03019	0.010065	0.057872	2.8831	2.241	0.003
sex	5	0.03153	0.006305	0.060424	1.8062	1.4764	0.064
proximal DJD	5	0.03792	0.007584	0.072677	2.1725	1.9146	0.006
Centroid Size x site	3	0.0138	0.0046	0.026452	1.3179	1.2569	0.166
Centroid Size x sex	4	0.01655	0.004139	0.03173	1.1856	1.1874	0.198
site x sex	6	0.02666	0.004444	0.051107	1.2731	1.3534	0.073
Centroid Size x proximal DJD	4	0.01571	0.003927	0.030111	1.1251	1.2652	0.137
site x proximal DJD	9	0.04819	0.005354	0.092365	1.5339	1.8476	0.001
sex x proximal DJD	5	0.01667	0.003333	0.031945	0.9549	1.3216	0.109
Centroid Size x site x sex	2	0.00736	0.003682	0.014115	1.0548	1.4523	0.1
Centroid Size x site x proximal DJD	4	0.01858	0.004646	0.035621	1.331	1.9946	0.007
Centroid Size x sex x proximal DJD	3	0.00579	0.00193	0.011096	0.5528	0.8589	0.485
site x sex x proximal DJD	3	0.0223	0.007432	0.042734	2.129	3.4133	0.001
Centroid Size x site x sex x proximal DJD	1	0.00369	0.003692	0.007076	1.0575	1.5748	0.104
Residuals	62	0.21643	0.003491				
Total	120	0.52173					

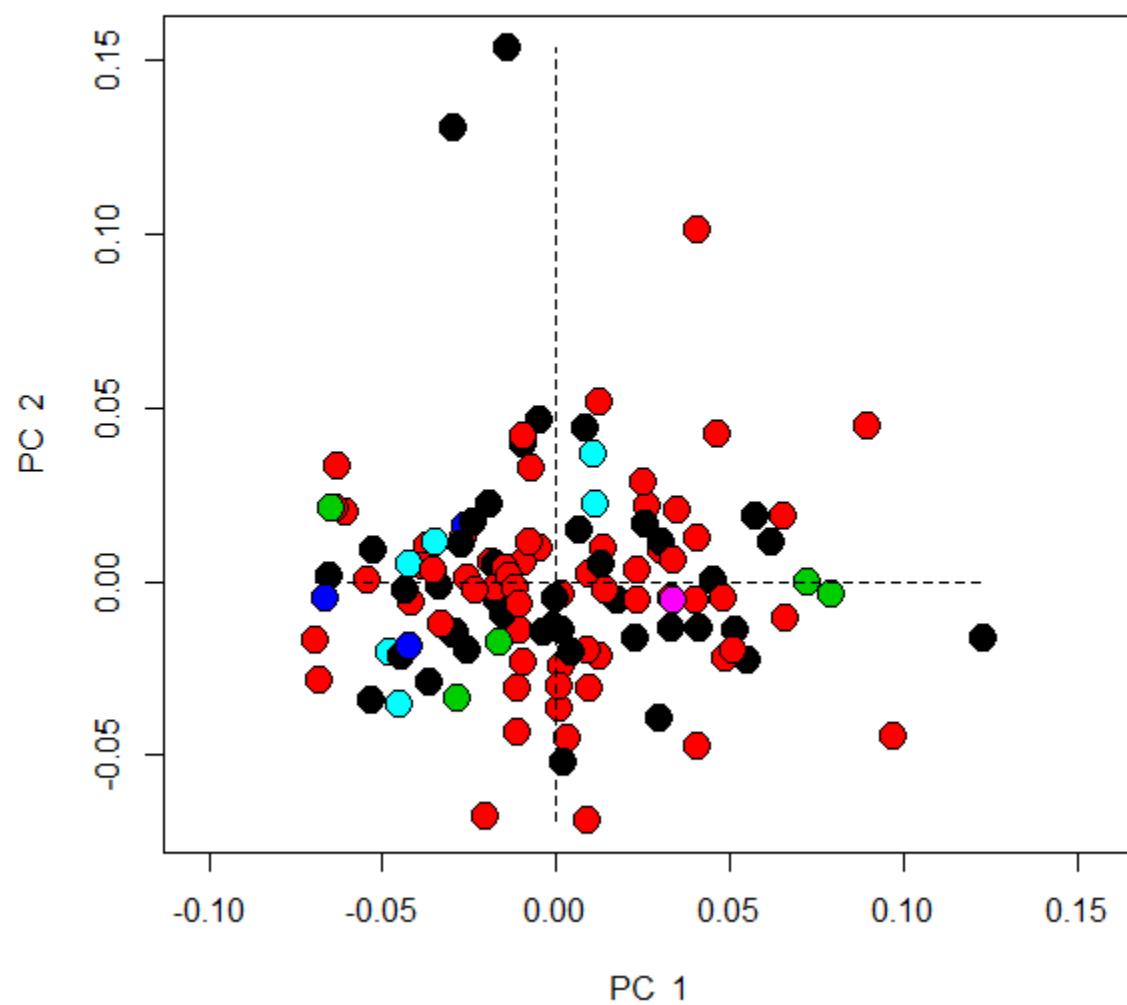


Figure 6.20 PC1 and PC2 of humeral cross-sectional morphology organized by DJD and OA severity at distal joint. (black= DJD, red = healthy, green = mild, blue = moderate, cyan = severe, magenta = unknown)

Table 6.16 GLM with interactions of humeral cross-sectional morphology by size, sex, and DJD and severity of OA at the distal joint.

	Df	SS	MS	Rsqr	F	Z	Pr(>F)
Centroid Size	1	0.01035	0.010355	0.019847	2.6471	2.03924	0.034
site	3	0.03019	0.010065	0.057872	2.5729	2.24097	0.003
sex	5	0.03153	0.006305	0.060424	1.6118	1.47642	0.064
distal DJD	5	0.03226	0.006452	0.061828	1.6493	1.6492	0.018
Centroid Size x site	3	0.0114	0.003799	0.021842	0.9711	1.03594	0.33
Centroid Size x sex	4	0.02115	0.005288	0.040539	1.3517	1.47945	0.06
site x sex	6	0.02531	0.004219	0.048519	1.0785	1.27979	0.115
Centroid Size x distal DJD	4	0.01411	0.003528	0.027044	0.9018	1.12466	0.254
site x distal DJD	8	0.02791	0.003489	0.053493	0.8918	1.17025	0.18
sex x distal DJD	3	0.02169	0.007229	0.041564	1.8479	2.39898	0.009
Centroid Size x site x sex	3	0.01286	0.004286	0.024643	1.0956	1.62746	0.056
Centroid Size x site x distal DJD	4	0.01087	0.002717	0.02083	0.6946	1.07573	0.304
Centroid Size x sex x distal DJD	1	0.00216	0.002164	0.004148	0.5532	0.67878	0.391
site x sex x distal DJD	2	0.00617	0.003085	0.011826	0.7886	1.22265	0.193
Centroid Size x site x sex x distal DJD	2	0.0056	0.0028	0.010732	0.7157	1.09477	0.214
Residuals	66	0.25818	0.003912				
Total	120	0.52173					

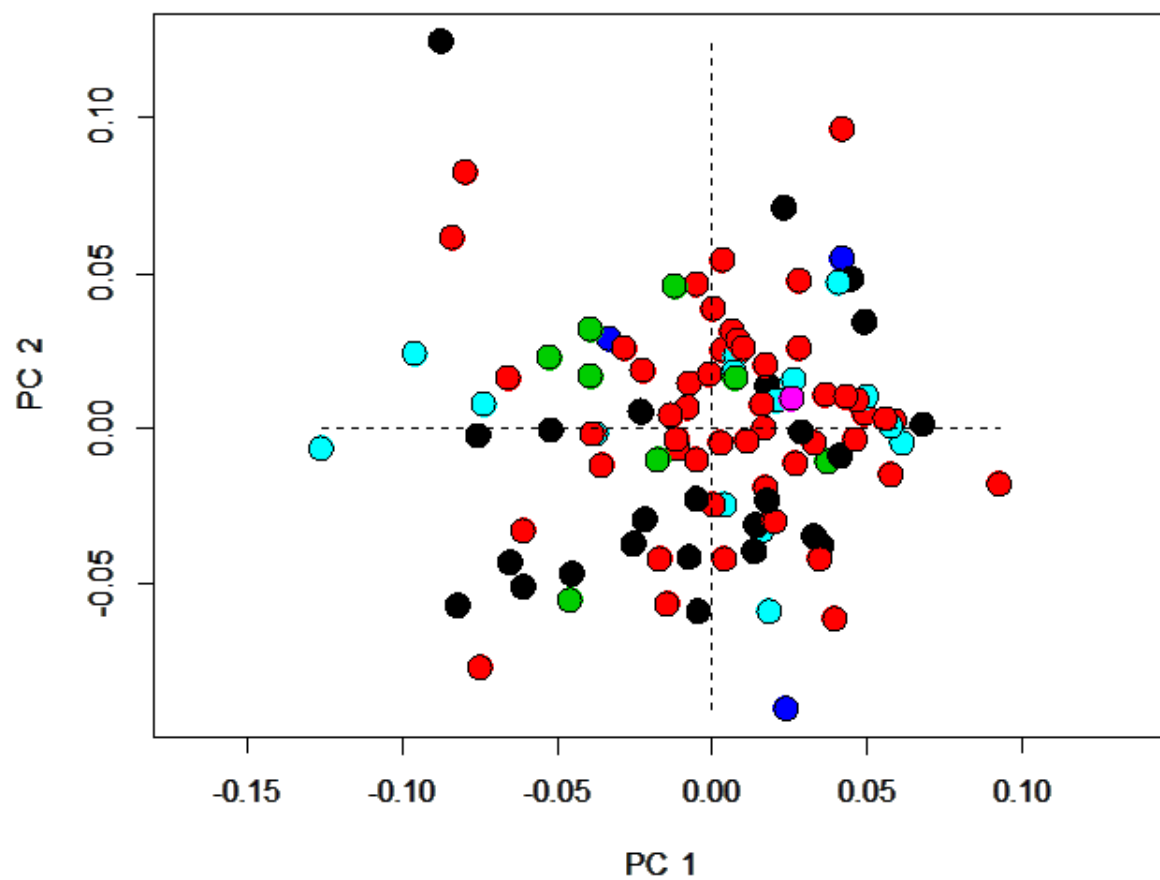


Figure 6.21 PC1 and PC2 of femoral cross-sectional morphology organized by DJD and OA severity at proximal joint. (black= DJD, red = healthy, green = mild, blue = moderate, cyan = severe, magenta = unknown)

Table 6.17 GLM with interactions of femoral cross-sectional morphology by size, sex, and DJD and severity of OA at the proximal joint.

Type III GLM

	Df	SS	MS	Rsqr	F	Z	Pr(>F)
Centroid Size	1	0.02463	0.024628	0.048047	5.3208	4.0457	0.002
site	3	0.04258	0.014192	0.083065	3.0663	2.6856	0.002
sex	4	0.02269	0.005672	0.044259	1.2253	1.2385	0.169
proximal DJD	5	0.01859	0.003719	0.036274	0.8034	0.8548	0.632
Centroid Size by site	3	0.02115	0.007049	0.041259	1.523	1.6358	0.049
Centroid Size by sex	4	0.01773	0.004432	0.034584	0.9575	1.108	0.256
site by sex	7	0.02755	0.003936	0.053752	0.8504	1.0572	0.331
Centroid Size by proximal DJD	4	0.02512	0.006281	0.049015	1.357	1.8206	0.011
site by proximal DJD	7	0.04353	0.006219	0.08493	1.3436	1.9159	0.002
sex by proximal DJD	5	0.02102	0.004204	0.04101	0.9083	1.5123	0.055
Centroid Size by site by sex	2	0.00581	0.002904	0.01133	0.6274	1.0728	0.276
Centroid Size by site by proximal DJD	4	0.01331	0.003328	0.025969	0.719	1.3141	0.131
Centroid Size by sex by proximal DJD	3	0.00933	0.003111	0.01821	0.6722	1.2727	0.15
site by sex by proximal DJD	2	0.00666	0.003332	0.012999	0.7198	1.3248	0.149
Centroid Size by site by sex by proximal DJD	2	0.00458	0.002292	0.008944	0.4953	0.9071	0.373
Residuals	45	0.20829	0.004629				
Total	101	0.51258					

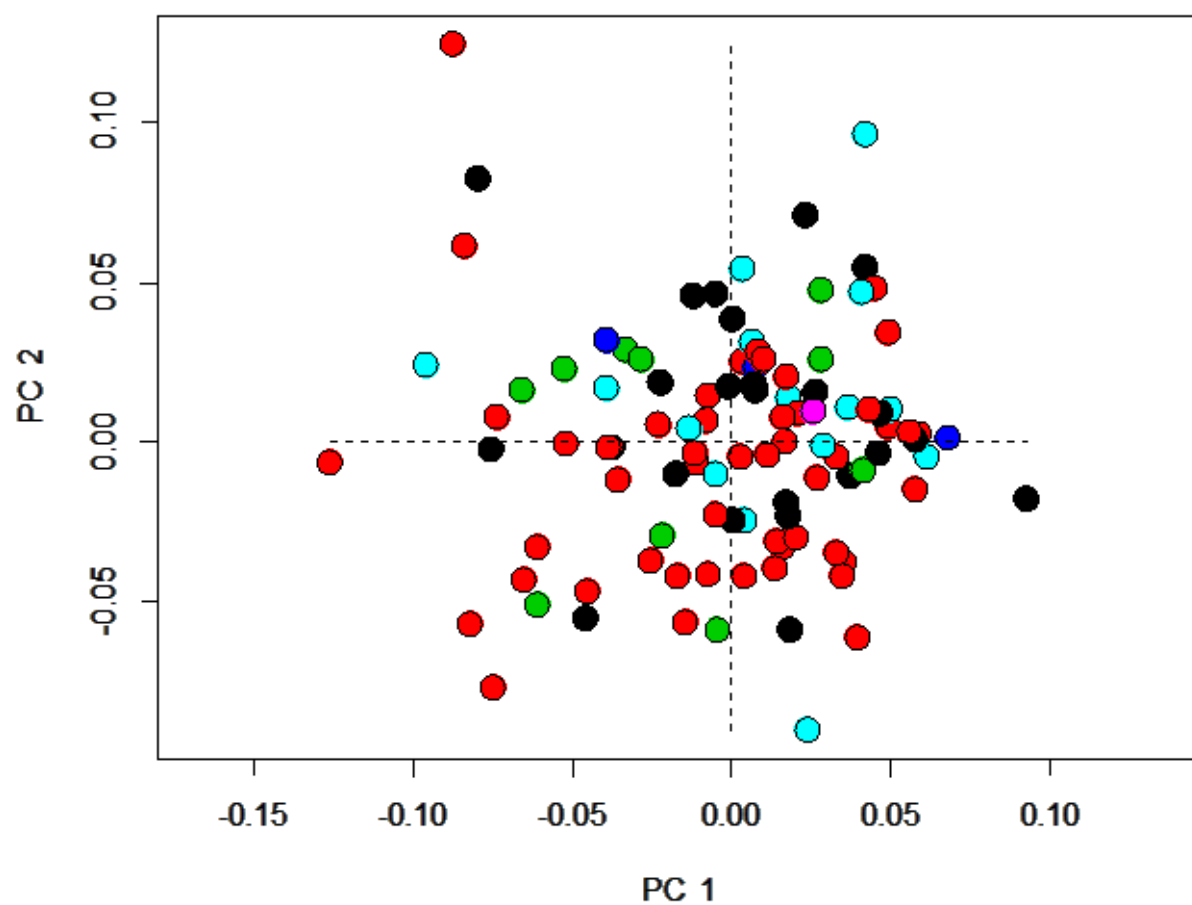


Figure 6.22 PC1 and PC2 of femoral cross-sectional morphology organized by DJD and OA severity at distal joint. (black= DJD, red = healthy, green = mild, blue = moderate, cyan = severe, magenta = unknown)

Table 6.18 GLM with interactions of femoral cross-sectional morphology by size, sex, and DJD and severity of OA at the distal joint.

	Df	SS	MS	Rsq	F	Z	Pr(>F)
Centroid Size	1	0.02463	0.024628	0.048047	5.0535	4.0457	0.002
site	3	0.04258	0.014192	0.083065	2.9122	2.6856	0.002
sex	4	0.02269	0.005672	0.044259	1.1638	1.2385	0.169
distal DJD	5	0.02119	0.004239	0.041346	0.8697	0.9761	0.42
Centroid Size by site	3	0.0203	0.006767	0.039608	1.3886	1.5704	0.052
Centroid Size by sex	4	0.01596	0.003991	0.031143	0.8189	1.0015	0.359
site by sex	7	0.02544	0.003634	0.04963	0.7457	0.9734	0.453
Centroid Size by distal DJD	4	0.01764	0.00441	0.034415	0.9049	1.2191	0.184
site by distal DJD	9	0.04192	0.004658	0.081777	0.9557	1.4198	0.03
sex by distal DJD	5	0.02939	0.005878	0.057337	1.2061	2.0458	0.006
Centroid Size by site by sex	2	0.00415	0.002076	0.008099	0.4259	0.748	0.576
Centroid Size by site by distal DJD	4	0.01343	0.003357	0.026196	0.6888	1.2789	0.158
Centroid Size by sex by distal DJD	2	0.00434	0.002172	0.008473	0.4456	0.8298	0.454
site by sex by distal DJD	3	0.00666	0.002221	0.013	0.4558	0.898	0.432
Centroid Size by site by sex by distal DJD	2	0.0127	0.00635	0.024775	1.3029	2.4765	0.015
Residuals	43	0.20956	0.004873				
Total	101	0.51258					

PC charts for trauma across humeral cross-sections (Figure 6.23) and femoral cross-sections (Figure 6.24) show no distinct grouping or variation as expected. In the GLM (Table 6.19) for the humeral cross section size and incidence of trauma considered together and size, site and incidence of trauma considered together could explain morphological variation at a statistical significance of 0.05. In the GLM for femoral cross-sections when site and trauma were considered together they explained morphology at a statistical significance of 0.05. When size, site, sex, and trauma were all considered together they explained morphology with a strong statistical confidence ($p < 0.01$).

PC charts for humeral cross-sections by Schmorl's Nodes (Figure 6.25) and femoral cross-sections by Schmorl's Nodes (Figure 6.26) show once again, no distinction between groups and little obvious distinction between variation between groups. GLM results for the humeral cross-sections (Table 6.21) show that when interactions between size, sex, and Schmorl's Nodes were considered together they explain morphological variation at a significance level of 0.01. For femoral cross-sectional

morphology GLM results showed no variation between groups when Schmorl's nodes were considered (see Table 6.22).

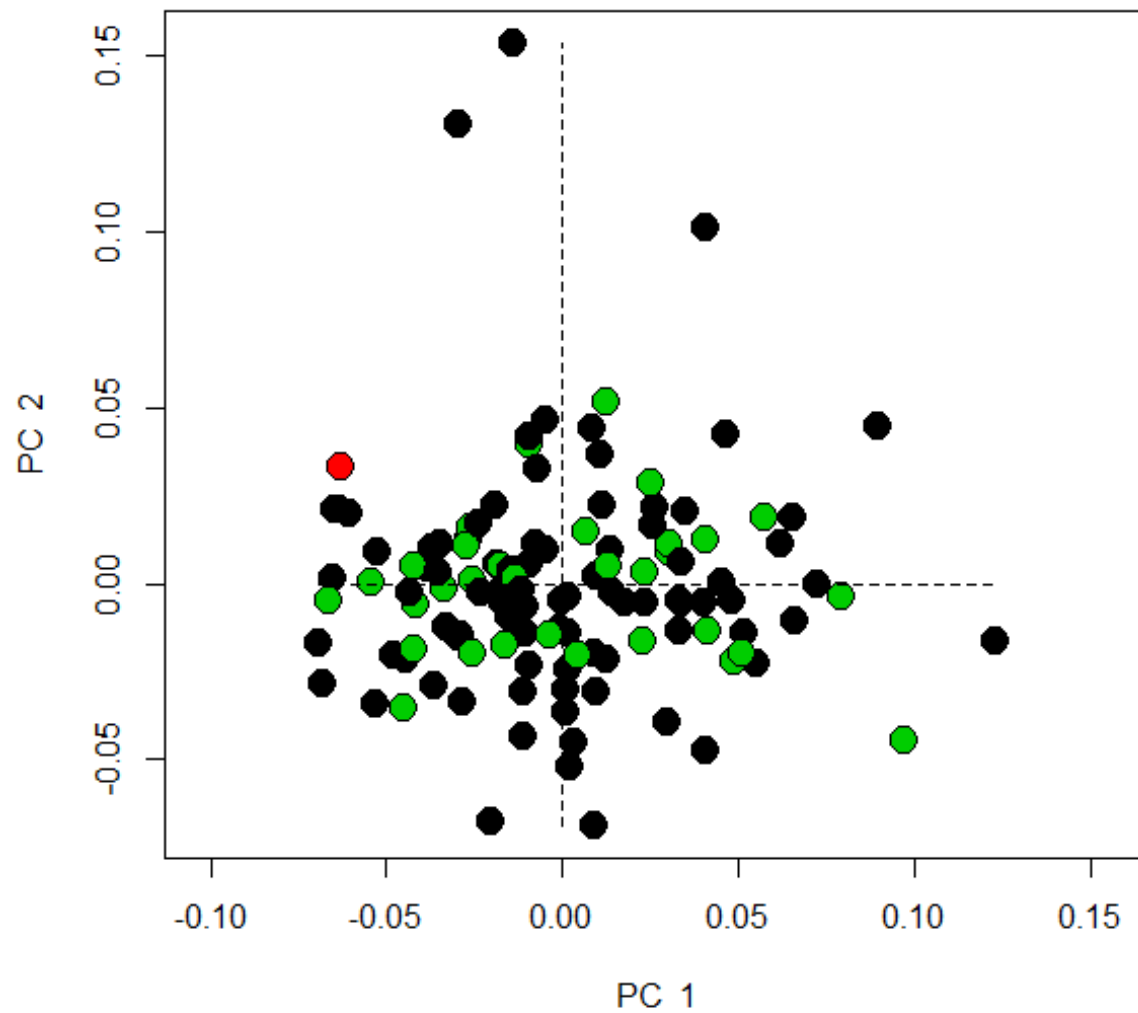


Figure 6.23 PC1 and PC2 of humeral cross-sectional morphology organized by presence or absence of trauma. (black= trauma absent red = trauma unobservable, green = trauma present)

Table 6.19 GLM with interactions of humeral cross sectional morphology by size, sex, and presence or absence of trauma.

	Df	SS	MS	Rsq	F	Z	Pr(>F)
Centroid Size	1	0.01035	0.010355	0.019847	2.693	2.03924	0.034
site	3	0.03019	0.010065	0.057872	2.6175	2.24097	0.003
sex	5	0.03153	0.006305	0.060424	1.6397	1.47642	0.064
trauma	1	0.00188	0.001881	0.003605	0.4891	0.45102	0.793
Centroid Size x site	3	0.01286	0.004286	0.024643	1.1146	1.07398	0.304
Centroid Size x sex	4	0.02162	0.005406	0.041442	1.4058	1.42268	0.081
site x sex	7	0.03542	0.00506	0.067882	1.3158	1.41935	0.043
Centroid Size x trauma	1	0.00814	0.008145	0.015611	2.1182	2.22744	0.024
site x trauma	3	0.00749	0.002498	0.014364	0.6497	0.76119	0.648
sex x trauma	2	0.00622	0.003112	0.011929	0.8093	0.94259	0.379
Centroid Size x site x sex	3	0.01662	0.005542	0.031864	1.4412	1.76497	0.025
Centroid Size x site x trauma	2	0.01448	0.007242	0.027761	1.8834	2.31136	0.011
Centroid Size x sex x trauma	1	0.00433	0.004332	0.008304	1.1267	1.33377	0.159
site x sex x trauma	2	0.00407	0.002034	0.007798	0.529	0.69204	0.641
Centroid Size x site x sex x trauma	2	0.0089	0.004451	0.017063	1.1576	1.4971	0.088
Residuals	80	0.30761	0.003845				
Total	120	0.52173					

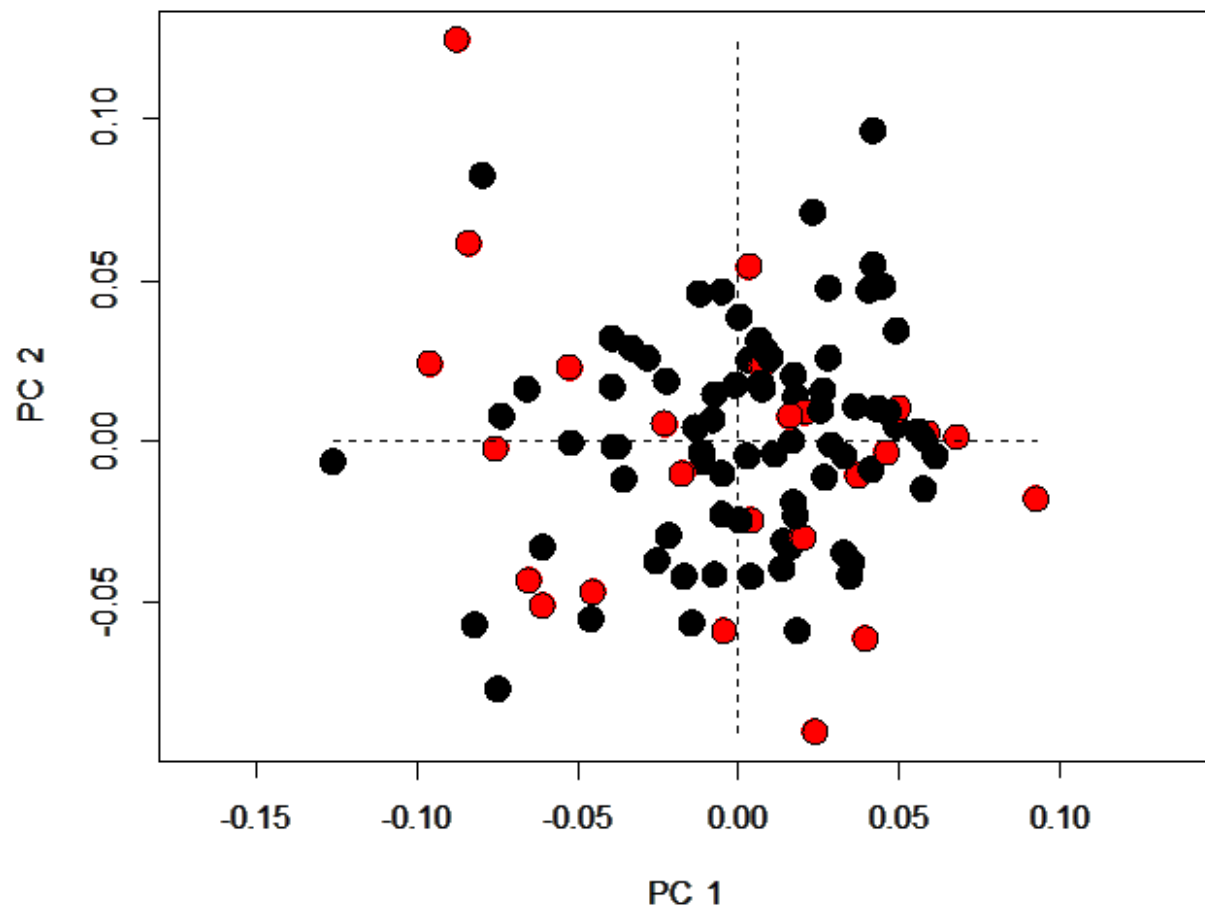


Figure 6.24 PC1 and PC2 of femoral cross-sectional morphology organized by presence or absence of trauma. (black= trauma absent red = trauma present)

Table 6.20 GLM with interactions of femoral cross-sectional morphology by size, sex, and presence or absence of trauma.

Type III GLM

Centroid Size	1	0.02463	0.024628	0.048047	5.7414	4.0457	0.002
site	3	0.04258	0.014192	0.083065	3.3087	2.6856	0.002
sex	4	0.02269	0.005672	0.044259	1.3222	1.2385	0.169
trauma	1	0.00404	0.004038	0.007878	0.9413	0.8103	0.416
Centroid Size by site	3	0.01835	0.006117	0.035804	1.4261	1.3654	0.103
Centroid Size by sex	4	0.01606	0.004015	0.031328	0.9359	0.9672	0.394
site by sex	7	0.02593	0.003705	0.050597	0.8637	0.9435	0.507
Centroid Size by trauma	1	0.00553	0.005527	0.010783	1.2885	1.3506	0.151
site by trauma	2	0.0133	0.006649	0.025943	1.5501	1.7199	0.045
sex by trauma	1	0.00581	0.005814	0.011342	1.3554	1.435	0.125
Centroid Size by site by sex	3	0.01858	0.006193	0.036244	1.4437	1.7817	0.023
Centroid Size by site by trauma	2	0.00766	0.00383	0.014946	0.893	1.1051	0.267
Centroid Size by sex by trauma	1	0.00515	0.005153	0.010053	1.2013	1.3461	0.145
site by sex by trauma	2	0.01052	0.00526	0.020522	1.2261	1.5964	0.073
Centroid Size by site by sex by trauma	2	0.01723	0.008613	0.033608	2.008	2.6546	0.005
Residuals	64	0.27453	0.00429				
Total	101	0.51258					

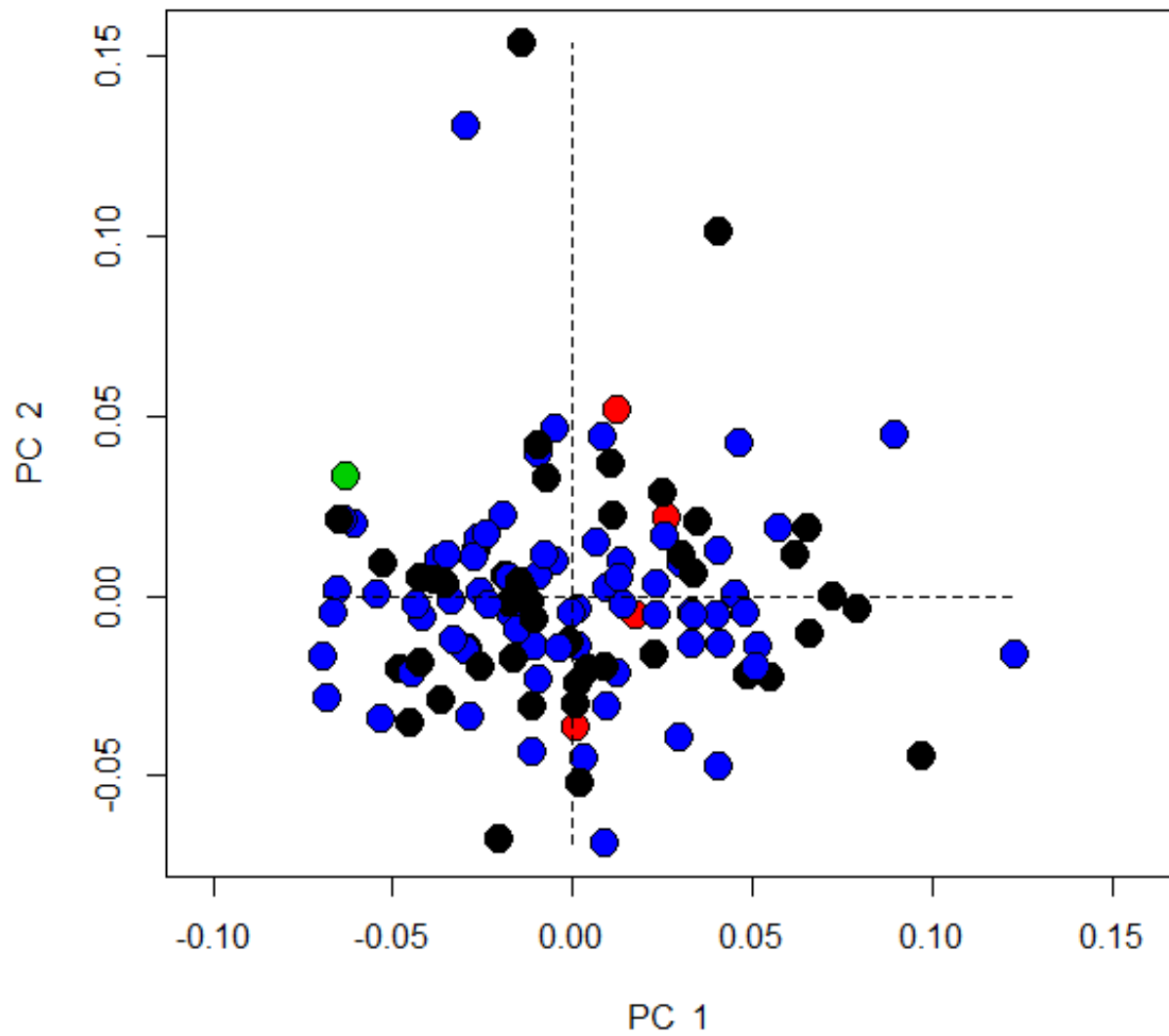


Figure 6.25 PC1 and PC2 of humeral cross-sectional morphology organized by presence or absence of Schmorl's nodes. (black= no Schmorl's nodes, red = vertebrae not present, green = unobservable, blue = Schmorl's nodes present)

Table 6.21 GLM with interactions of humeral cross-sectional morphology by size, sex, and presence or absence of Schmorl's nodes.

	Df	SS	MS	Rsq	F	Z	Pr(>F)
Centroid Size	1	0.01035	0.010355	0.019847	2.6812	2.0392	0.034
site	3	0.03019	0.010065	0.057872	2.606	2.241	0.003
sex	5	0.03153	0.006305	0.060424	1.6326	1.4764	0.064
Schmorl's nodes	2	0.0054	0.002698	0.010343	0.6986	0.6633	0.705
Centroid Size x site	3	0.01212	0.004041	0.023233	1.0462	1.0213	0.351
Centroid Size x sex	4	0.02056	0.005139	0.0394	1.3307	1.3687	0.101
site x sex	7	0.03407	0.004868	0.065307	1.2604	1.3753	0.058
Centroid Size x Schmorl's nodes	2	0.01042	0.005211	0.019975	1.3492	1.5148	0.091
site x Schmorl's nodes	3	0.00822	0.00274	0.015753	0.7094	0.8462	0.539
sex x Schmorl's nodes	5	0.02193	0.004385	0.042025	1.1355	1.4025	0.082
Centroid Size x site x sex	3	0.01479	0.004929	0.028343	1.2763	1.6433	0.044
Centroid Size x site x Schmorl's nodes	3	0.0119	0.003966	0.022802	1.0268	1.3449	0.125
Centroid Size x sex x Schmorl's nodes	1	0.01048	0.010478	0.020084	2.7132	3.3412	0.006
site x sex x Schmorl's nodes	2	0.00604	0.003022	0.011583	0.7824	1.0899	0.27
Centroid Size x site x sex x Schmorl's nodes	2	0.00795	0.003975	0.015236	1.0292	1.4442	0.114
Residuals	74	0.28579	0.003862				
Total	120	0.52173					

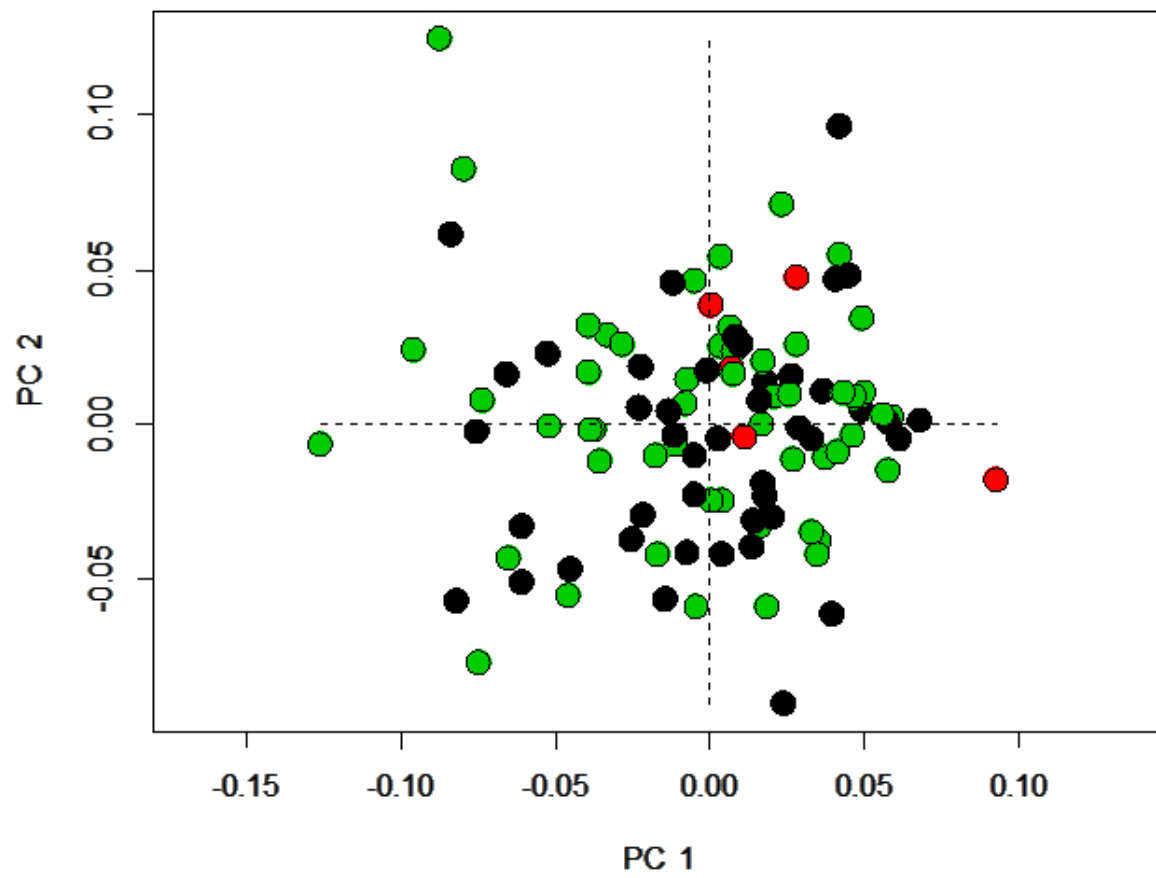


Figure 6.26 PC1 and PC2 of femoral cross-sectional morphology organized by presence or absence of Schmorl's nodes. (black= no Schmorl's nodes, red = vertebrae not present, green = Schmorl's nodes present)

Table 6.22 GLM with interactions of femoral cross-sectional morphology by size, sex, and presence or absence of Schmorl's nodes.

Type III GLM

	Df	SS	MS	Rsq	F	Z	Pr(>F)
Centroid Size	1	0.02463	0.024628	0.048047	5.3745	4.0457	0.002
site	3	0.04258	0.014192	0.083065	3.0972	2.6856	0.002
sex	4	0.02269	0.005672	0.044259	1.2377	1.2385	0.169
Schmorl's nodes	2	0.01276	0.00638	0.024896	1.3924	1.4006	0.111
Centroid Size by site	3	0.01941	0.006469	0.037863	1.4118	1.4736	0.076
Centroid Size by sex	4	0.01365	0.003412	0.026629	0.7447	0.8434	0.579
site by sex	7	0.02817	0.004025	0.05496	0.8783	1.048	0.331
Centroid Size by Schmorl's nodes	2	0.01158	0.00579	0.022593	1.2636	1.5039	0.094
site by Schmorl's nodes	3	0.01311	0.004369	0.025573	0.9535	1.2247	0.183
sex by Schmorl's nodes	5	0.02371	0.004742	0.046256	1.0348	1.4079	0.09
Centroid Size by site by sex	2	0.01172	0.00586	0.022865	1.2788	1.7954	0.031
Centroid Size by site by Schmorl's nodes	3	0.00757	0.002523	0.014766	0.5506	0.8184	0.58
Centroid Size by sex by Schmorl's nodes	1	0.00271	0.002712	0.005291	0.5919	0.815	0.399
site by sex by Schmorl's nodes	2	0.00895	0.004473	0.017452	0.9761	1.4651	0.108
Centroid Size by site by sex by Schmorl's nodes	2	0.00816	0.004078	0.015912	0.8899	1.3413	0.151
Residuals	57	0.26119	0.004582				
Total	101	0.51258					

6.2.2 Interpopulation

Previous chapters suggest that elements from Coach Lane Skeletons have larger CS than those from all other populations sampled. Figure 6.27 shows humeral cross-sectional shape space. In shape space there is an overlap of all populations, but Coach Lane and 3-J-18 seem to have the most dispersion over PC1 and PC2. This could point to genetic or social heterogeneity in these populations or more obtusely may be indicative of better health in these populations allowing them to complete their various ontogenetic trajectories (Baab, McNulty, et al., 2012; Klingenberg, 1998; Meiri et al., 2004, 2006). To observe what relationship site might have with size and shape an allometry test and a GLM were run. A relationship between site and log CS is not clear in Figure 6.28 which plots allometry for humeral cross-sectional shape by site. The Homogeneity of Slopes and ANOVA along with the Type III GLM (Table 6.23) for humeral cross sections however prove that allometry exists and that site explains allometric variation. The GLM shows that site uniquely explains humeral cross-section morphology with a high

($p < 0.01$) degree of confidence. When site and sex are considered together they also explain morphology at a statistical confidence of 0.05.

Femoral cross-sectional morphology plotted in shape space for PC1 and PC2 (Figure 6.29) shows very little pattern by site. The regression plot shows no clear pattern for sites (Figure 6.30). Once again however, the Homogeneity of Slopes Test, ANOVA and GLM (Table 6.24) show strong group allometry. Site uniquely explains femoral cross-section allometry at a statistical confidence of 0.01 and size and site considered together explain morphology at a confidence of 0.05. Considering the GLM test alone size uniquely explains morphological variation with a with a confidence level of 0.01.

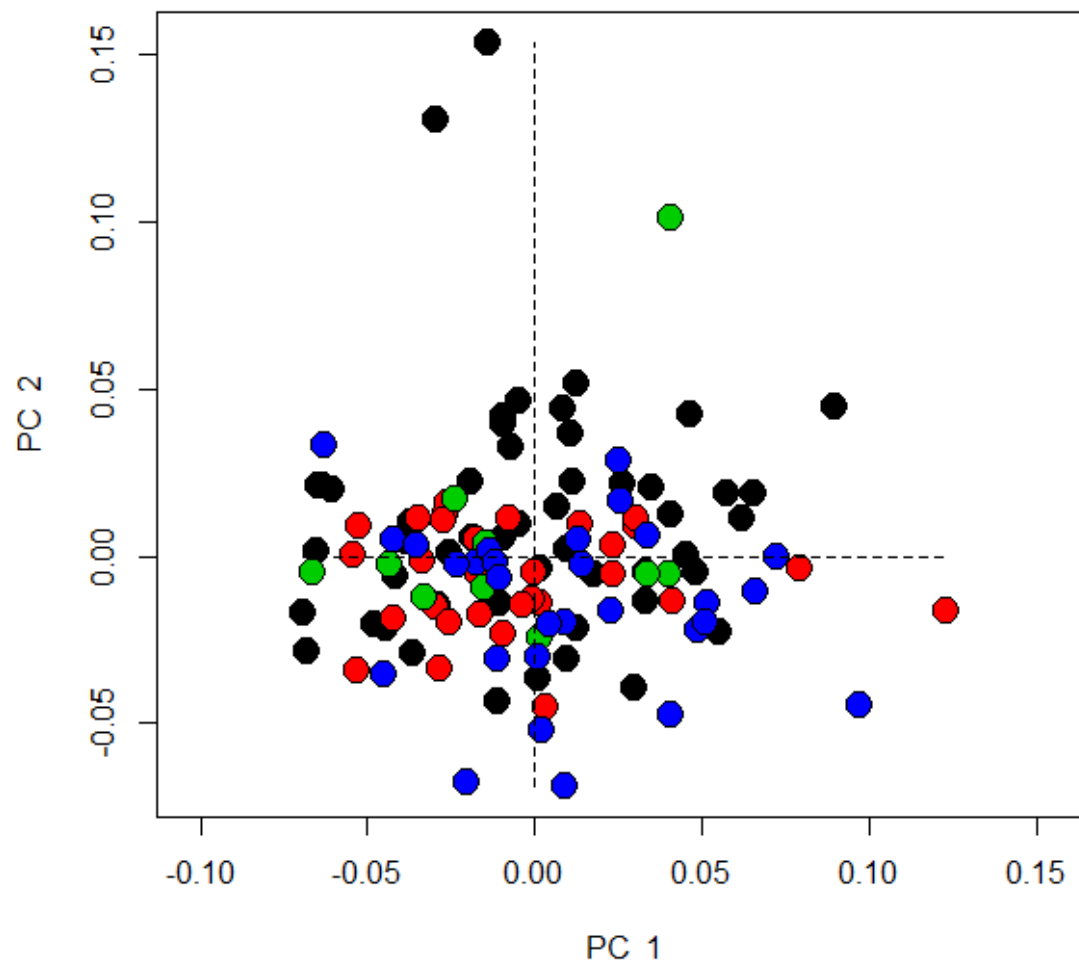


Figure 6.27 PC1 through PC3 of humeral cross-sectional morphology by site. (black = Coach Lane, red = Fishergate, green= Hereford, blue = 3-J-18)

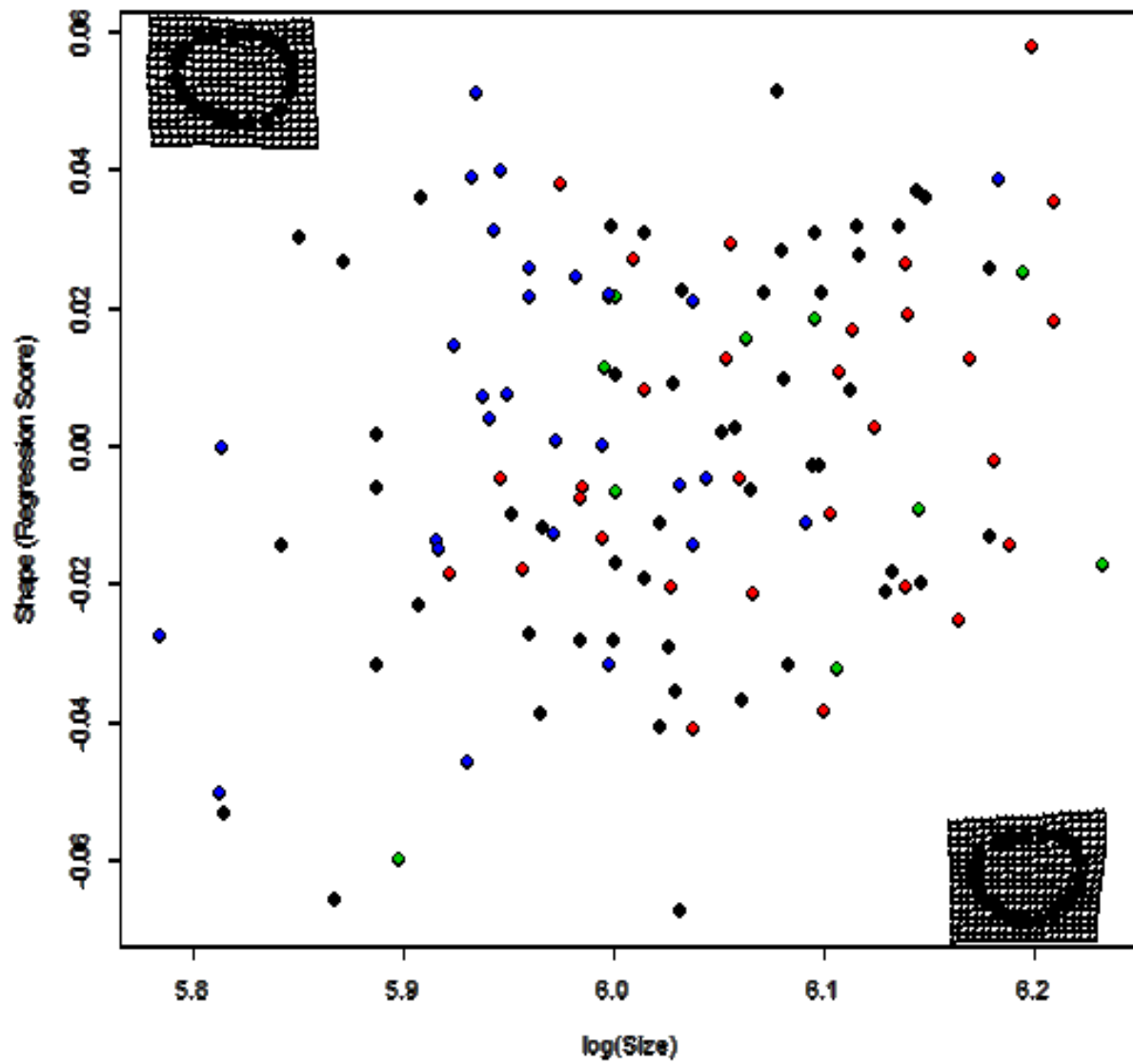


Figure 6.28 Allometry of humeral cross-section at midshaft by site. (black = Coach Lane, red = Fishergate, green= Hereford, blue = 3-J-18)

Table 6.23 GLMs for humerus cross-section at midshaft by log(CS), site, and sex.

Homogeneity of Slopes Test

	Df	SSE	SS	Rsqr	F	Z	Pr(>F)
Common Allometry	119	0.51114					
Group Allometries	113	0.46971	0.041429	0.079406	1.6611	1.578	0.014

Type III GLM with size and sex

	Df	SS	MS	Rsqr	F	Z	Pr(>F)
log(size)	1	0.0106	0.010596	0.020308	2.549	2.08113	0.031
site	3	0.02998	0.009993	0.057462	2.4041	2.226	0.003
log(size):site	3	0.01145	0.003816	0.021944	0.9181	0.90139	0.476
Residuals	113	0.46971	0.004157				
Total	120	0.52173					

Type III GLM with size by site and sex

	Df	SS	MS	Rsqr	F	Z	Pr(>F)
Centroid Size	1	0.01035	0.010355	0.019847	2.6657	2.0392	0.034
site	3	0.03019	0.010065	0.057872	2.5909	2.241	0.003
sex	5	0.03153	0.006305	0.060424	1.6231	1.4764	0.064
Centroid Size x site	3	0.0126	0.004199	0.024146	1.081	1.0477	0.331
Centroid Size x sex	4	0.02122	0.005306	0.040677	1.3659	1.389	0.093
site x sex	7	0.0351	0.005014	0.067273	1.2908	1.3998	0.047
Centroid Size x site x sex	4	0.01948	0.00487	0.037336	1.2536	1.4649	0.073
Residuals	93	0.36126	0.003885				
Total	120	0.52173					

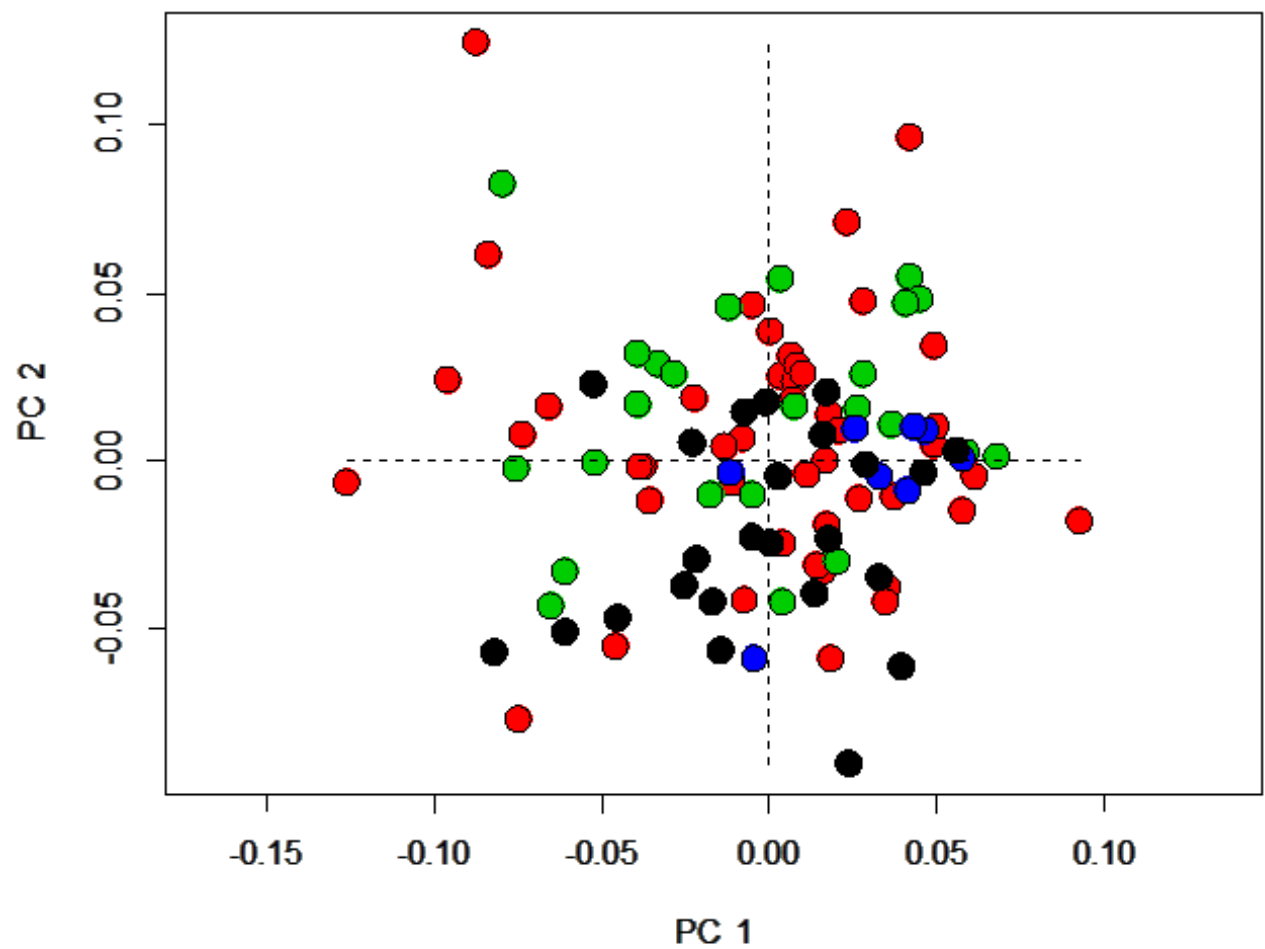


Figure 6.29 PC1 and PC2 of femoral cross-sectional morphology by site. (black = 3-J-18, red = Coach Lane, green= Fishergate, blue = Hereford)

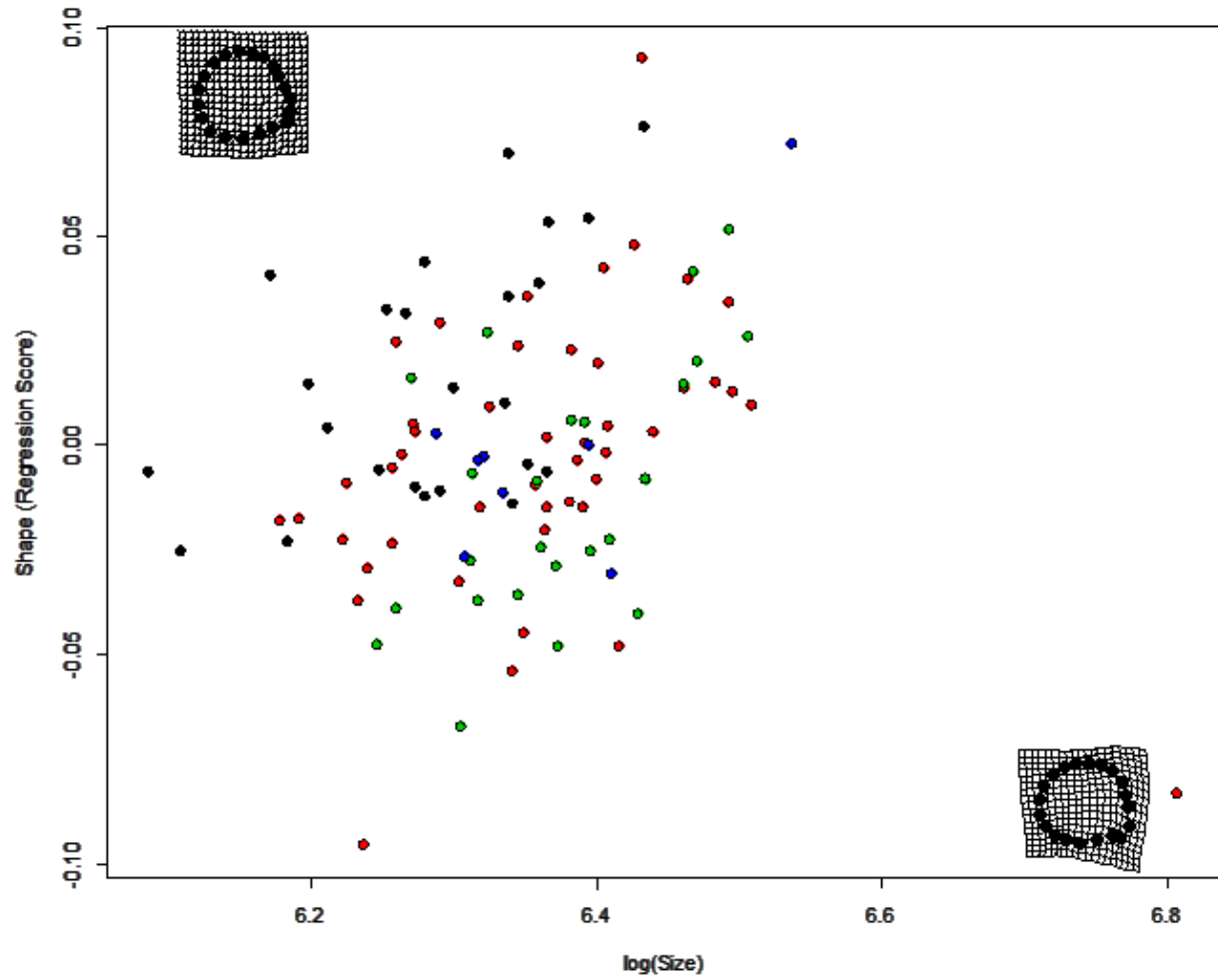


Figure 6.30 Allometry of femoral cross-section at midshaft by site. (black = 3-J-18, red = Coach Lane, green= Fishergate, blue = Hereford)

Table 6.24 Homogeneity of Slopes Test, ANOVA and GLM for femoral cross-section at midshaft by log(CS), site, and sex.

Homogeneity of Slopes Test

	Df	SSE	SS	Rsq	F	Z	Pr(>F)
Common Allometry	100	0.48984					
Group Allometries	94	0.42272	0.067114	0.13093	2.4873	2.1877	0.001

Type III ANOVA with size and site

	Df	SS	MS	Rsq	F	Z	Pr(>F)
log(size)	1	0.02274	0.022737	0.044358	5.056	3.7235	0.003
site	3	0.04414	0.014715	0.086124	3.2721	2.7767	0.002
log(size):site	3	0.02297	0.007656	0.044811	1.7025	1.5972	0.047
Residuals	94	0.42272	0.004497				
Total	101	0.51258					

Type III GLM with size by site and sex

	Df	SS	MS	Rsq	F	Z	Pr(>F)
Centroid Size	1	0.02463	0.024628	0.048047	5.4441	4.0457	0.002
site	3	0.04258	0.014192	0.083065	3.1373	2.6856	0.002
sex	4	0.02269	0.005672	0.044259	1.2537	1.2385	0.169
Centroid Size by site	3	0.01965	0.006549	0.038327	1.4476	1.4515	0.082
Centroid Size by sex	4	0.01563	0.003908	0.0305	0.864	0.9349	0.448
site by sex	7	0.02587	0.003695	0.050462	0.8168	0.9353	0.522
Centroid Size by site by sex	3	0.01774	0.005912	0.034602	1.3069	1.5604	0.064
Residuals	76	0.3438	0.004524				
Total	101	0.51258					

6.2.3 Biomechanics

Descriptive statistics are provided below for the humerus and femur at 40% and 50% of the length in Table 6.25, Table 6.26, Table 6.27, and Table 6.28. ANOVA were conducted to determine between group variance. P-values are provided in Table 6.29 for humeral biomechanical properties and in Table 6.30 for femoral biomechanical properties. Tukey's HSD test was used to determine where the variation between groups was strongest, and adjusted p-values for Tukey's HSD tests conducted on IVs which showed an alpha of 0.05 or lower are available for humeri in Table 6.31 and for femora in Table 6.32.

Site and sex variation could be seen in humeral cross-sectional geometry at a p level of 0.01 for TA, I_{max} , I_{min} , and J. Tukey's HSD tests show that site variation occurs with strong statistical significance ($p < 0.01$) when comparing 3-J-18 to any other population but not when comparing other populations to one another. This shows that for humeral cross-sectional geometry the Sudanese population is significantly different from the English populations, but the English populations are not significantly different from one another. As there were five categories for sex a Tukey's HSD test was reasonable and showed that variation was strongly significant between females and males, females and possible males, and possible females and possible males for TA, I_{max} , I_{min} , and J. There was also strongly significant variation ($p < 0.01$) between possible females and males for TA, I_{min} , and J and simply significant variation ($p < 0.05$) for I_{max} . There was statistically significant variation between individuals whose sex was indeterminate and possible males when considering TA, I_{max} , I_{min} , and J.

ANOVA tests showed significant ($p < 0.05$) variation when proximal DJD and OA severity were compared to TA, I_{min} , and J for humeral cross sections, however when Tukey's HSD post-hoc test was applied no consistent difference was seen when simply comparing DJD and OA severity. Only when sex was also considered were significant differences shown.

For femoral cross-sectional geometry, site explained TA and I_x/I_y with strong statistical significance ($p < 0.01$) and I_{min} with statistical significance ($p < 0.05$). Sex explained cross-sectional geometry with strong statistical significance for all but I_x/I_y . Trauma explained TA, I_{max} , I_{min} , and J at an alpha level of 0.05. The presence or absence of Schmorl's nodes explained I_x/I_y with strong statistical significance. Tukey's HSD post-hoc tests were not performed for the presence or absence of trauma or Schmorl's nodes because those are binary. Tukey's HSD was performed for site and sex. TA and I_x/I_y were both explained with strong statistical significance by the comparison of Coach Lane and 3-J-18 and Fishergate and 3-J-18. The comparison of Coach Lane and 3-J-18 also explained I_{min} at an alpha of 0.05. For femoral cross-sections TA, I_{max} , I_{min} , and J were explained with strong statistical significance (0.01) by the comparison of females to males. TA was explained by the comparison of possible females to males at an alpha of 0.05.

Table 6.25 Average values for Total Area (TA), J, I_{\max} , and I_{\min} at humeral cross-sections at 40%.

	TA at 40%	J at 40%	I_{\max} at 40%	I_{\min} at 40%	I_x/I_y at 40%
All					
Mean	273.315	12832.87	7239.311	5593.561	1.223315
Standard Error	5.415842	446.2089	249.9462	204.2858	0.016714
Total	120	120	120	120	120
Coach Lane					
Mean	288.8782	14018.94	7922.929	6096.01	1.276166
Standard Error	7.290879	664.1086	353.3345	319.5284	0.02676
Total	52	52	52	52	52
Fishergate					
Mean	294.3021	14454.84	8138.063	6316.774	1.21533
Standard Error	8.689721	843.7554	470.7006	382.3567	0.029174
Total	30	30	30	30	30
Hereford					
Mean	287.1991	13938.47	7918.177	6020.296	1.269621
Standard Error	19.0063	1861.295	1084.162	807.2245	0.061219
Total	10	10	10	10	10
3-J-18					
Mean	226.7282	8497.499	4764.335	3733.164	1.119132
Standard Error	5.29937	383.1594	212.586	178.5726	0.026969
Total	28	28	28	28	29
Female (female and possible female)					
Mean	234.1851	9171.813	5320.718	3851.095	1.260331
Standard Error	4.832538	375.4447	220.7782	163.0664	0.03214
Total	50	50	50	50	50
Male (male and possible male)					
Mean	307.2317	15635.42	8710.509	6924.91	1.19836
Standard Error	5.46559	541.3296	307.8767	242.3286	0.017552
Total	68	68	68	68	68

Table 6.26 Average values for Total Area (TA), J, I_{\max} , and I_{\min} at humeral cross-sections at midshaft.

	TA at 50%	J at 50%	I_{\max} at 50%	I_{\min} at 50%	I_x/I_y at 50%
All					
Mean	296.8536	15134.86	9167.827	5967.035	1.01374
Standard Error	5.622127	555.2932	339.1435	221.8777	0.014606
Total	120	120	120	120	120
Coach Lane					
Mean	310.9487	16393.46	9823.416	6570.046	0.994234
Standard Error	7.826246	782.614	479.3978	314.4714	0.023283
Total	52	52	52	52	52
Fishergate					
Mean	320.8982	17516.84	10736.1	6780.74	0.995183
Standard Error	10.13855	1121.394	723.1122	408.2385	0.025727
Total	30	30	30	30	30
Hereford					
Mean	318.5022	17315.97	10404.73	6911.237	1.007314
Standard Error	21.02728	2194.86	1261.3	944.1335	0.05742
Total	10	10	10	10	10
3-J-18					
Mean	237.1833	9466.375	5828.26	3638.114	1.072143
Standard Error	5.747942	439.34	249.8056	200.1779	0.02864
Total	28	28	28	28	28
Female (female and possible female)					
Mean	252.7886	10847.53	6634.499	4213.028	1.0597
Standard Error	5.752998	491.0815	300.363	200.512	0.022749
Total	50	50	50	50	50
Male (male and possible male)					
Mean	330.7731	18437.12	11113.18	7323.942	0.979859
Standard Error	6.443176	695.9174	436.1515	270.0762	0.019022
Total	68	68	68	68	68

Table 6.27 Average values for Total Area (TA), J, I_{\max} , and I_{\min} at femoral cross-sections at 40%.

	TA at 40%	J at 40%	I_{\max} at 40%	I_{\min} at 40%	I_x/I_y at 40%
All					
Mean	553.4457	53120.17	29251.27	23868.9	1.010265
Standard Error	14.0081	4007.959	2179.702	1839.753	0.016221
Total	102	102	102	102	102
Coach Lane					
Mean	571.1961	58354.35	32164.53	26189.82	0.984129
Standard Error	26.88987	8417.065	4546.41	3884.964	0.025446
Total	46	46	46	46	46
Fishergate					
Mean	581.4647	56036.29	30657.51	25378.78	0.95636
Standard Error	16.65651	3232.049	1781.619	1478.262	0.029437
Total	24	24	24	24	24
Hereford					
Mean	573.4552	55048.71	30010.95	25037.75	0.996313
Standard Error	32.08859	6996.216	4516.261	2562.614	0.026515
Total	8	8	8	8	8
3-J-18					
Mean	484.7352	39529.05	22008.06	17520.99	1.118916
Standard Error	16.3264	2709.454	1815.209	948.0904	0.040927
Total	24	24	24	24	24
Female (female and possible female)					
Mean	471.9352	36792.25	19918.71	16873.54	0.987878
Standard Error	9.397505	1428.436	755.0258	691.1709	0.021432
Total	45	45	45	45	45
Male (male and possible male)					
Mean	619.398	66702.33	37102.52	29599.81	1.032051
Standard Error	22.15017	7249.214	3911.089	3356.367	0.025269
Total	52	52	52	52	52

Table 6.28 Average values for Total Area (TA), J, I_{\max} , and I_{\min} at femoral cross-sections at midshaft.

	TA at 50%	J at 50%	I_{\max} at 50%	I_{\min} at 50%	I_x/I_y at 50%
All					
Mean	535.5438	49611.49	28308.01	21303.48	0.994891
Standard Error	12.03522	2908.931	1732.834	1193.838	0.018951
Total	102	102	102	102	102
Coach Lane					
Mean	554.0474	54021.37	30909.47	23111.9	0.961445
Standard Error	21.99187	5831.061	3445.246	2402.905	0.027062
Total	46	46	46	46	46
Fishergate					
Mean	563.1599	52966.94	29690.18	23276.76	0.942557
Standard Error	15.98006	3080.045	1846.429	1272.835	0.036101
Total	24	24	24	24	24
Hereford					
Mean	551.5298	51554.75	29092.65	22462.1	0.97251
Standard Error	31.21318	6793.326	4716.781	2200.766	0.029968
Total	8	8	8	8	8
3-J-18					
Mean	467.1339	37156.04	21678.18	15477.86	1.118789
Standard Error	16.3264	2709.454	1815.209	948.0904	0.040927
Total	24	24	24	24	24
Female (female and possible female)					
Mean	456.2789	34570.07	19143.59	15426.48	0.961152
Standard Error	8.507676	1245.208	667.1506	604.4077	0.024199
Total	45	45	45	45	45
Male (male and possible male)					
Mean	600.0923	62135.95	36059.69	26076.26	1.027874
Standard Error	22.15017	7249.214	3911.089	3356.367	0.025269
Total	52	52	52	52	52

Table 6.29 P-values for ANOVA tests of biomechanics of humeral cross-sections at midshaft. Rows are for the DVs and columns are for the IVs. Light purple highlighting indicates $p < 0.1$. Green highlighting indicates $p < 0.05$. Blue highlighting indicates $p < 0.01$.

Humeral cross-sections at midshaft	TA	I_{\max}	I_{\min}	J	I_x/I_y
Site	3.9200E-14	4.2800E-11	1.2600E-13	1.8900E-12	0.1816
Sex	8.1200E-15	3.3100E-12	5.9000E-15	1.0600E-13	0.2201
Age	0.4040	0.3137	0.2286	0.2628	0.1471
Trauma	0.8440	0.9547	0.6648	0.8967	0.0844
LEH	0.2300	0.1533	0.1756	0.1497	0.1914
Cribra Orbitalia	0.1980	0.3239	0.2908	0.2993	0.8188
Schmorl's Nodes	0.1600	0.1668	0.1795	0.1605	0.6310
DJD severity at proximal joint	0.0370	0.0634	0.0144	0.0325	0.4769
DJD severity at distal joint	0.5650	0.6555	0.4503	0.5638	0.9221

Table 6.30 P-values for ANOVA tests of biomechanics of femoral cross-sections at midshaft. Rows are for the DVs and columns are for the IVs. Light purple highlighting indicates $p < 0.1$. Green highlighting indicates $p < 0.05$. Blue highlighting indicates $p < 0.01$.

Femoral cross-sections at midshaft	TA	I_{\max}	I_{\min}	J	I_x/I_y
Site	2.5800E-03	0.1393	0.0444	0.0883	0.0013
Sex	2.9000E-07	0.0003	0.0028	0.0008	0.1870
Age	0.5216	0.6850	0.7884	0.7277	0.2764
Trauma	0.0104	0.0131	0.0308	0.0186	0.7519
LEH	0.6579	0.5639	0.5476	0.5975	0.4196
Cribra Orbitalia	0.8400	0.8811	0.9447	0.9199	0.7859
Schmorl's Nodes	0.6200	0.7242	0.6083	0.6787	0.0045
DJD severity at proximal joint	0.4896	0.3649	0.5237	0.4394	0.1348
DJD severity at distal joint	0.9695	0.9673	0.9767	0.9746	0.1563

Table 6.31 Adjusted p-value results for post-hoc (Tukey's HSD) tests of previous ANOVA tests for humeral cross-sections. Light purple highlighting indicates $p < 0.1$. Green highlighting indicates $p < 0.05$. Blue highlighting indicates $p < 0.01$. (Note: Where only two groups exist there was no need for post-hoc tests and results with no significant post-hoc results were excluded.)

Humerus				
Site	TA	I_{\max}	I_{\min}	J
Coach Lane-3-J-18	0	0	0	0
Fishergate-3-J-18	0	0	0	0
Hereford-3-J-18	4.00E-07	1.38E-05	3.00E-07	2.10E-06
Fishergate-Coach Lane	0.665871	0.382035	0.93025	0.595201
Hereford-Coach Lane	0.939484	0.905422	0.91512	0.903423
Hereford-Fishergate	0.998169	0.98326	0.995386	0.999002
Sex	TA	I_{\max}	I_{\min}	J
m-f	0	0	0	0
pf-f	0.999911	0.9996	0.993445	1
pm-f	6.2E-06	0.000008	6.1E-06	4.8E-06
uk-f	0.999277	0.999953	0.99283	0.9992
pf-m	0.003536	0.02566	0.001508	0.007565
pm-m	0.519636	0.365326	0.494622	0.395063
uk-m	0.094268	0.183836	0.062502	0.112789
pm-pf	0.00146	0.004256	0.000666	0.001662
uk-pf	0.999941	0.999483	0.999925	0.999708
uk-pm	0.024548	0.035984	0.014973	0.022092

Table 6.32 Adjusted p-value results for post-hoc (Tukey's HSD) tests of previous ANOVA tests for femoral cross-sections. Light purple highlighting indicates $p < 0.1$. Green highlighting indicates $p < 0.05$. Blue highlighting indicates $p < 0.01$. (Note: Where only two groups exist there was no need for post-hoc tests and results with no significant post-hoc results were excluded.)

Femur					
<u>Site</u>	TA	I_{\max}	I_{\min}	J	I_x/I_y
Coach Lane-3-J-18	0.004212	N/A	0.040273	0.071724	0.004517
Fishergate-3-J-18	0.006261	N/A	0.082612	0.188343	0.0058
Hereford-3-J-18	1.65E-01	N/A	4.26E-01	5.65E-01	2.01E-01
Fishergate-Coach Lane	0.983175	N/A	0.999928	0.998676	0.975595
Hereford-Coach Lane	0.999894	N/A	0.998755	0.995246	0.998525
Hereford-Fishergate	0.991631	N/A	0.997979	0.999251	0.977095
<u>Sex</u>	TA	I_{\max}	I_{\min}	J	I_x/I_y
m-f	1E-07	6.04E-05	0.000529	0.000133	N/A
pf-f	0.999997	1	1	1	N/A
pm-f	0.13543	0.568441	0.637633	0.589841	N/A
uk-f	0.318903	0.845233	0.737405	0.798957	N/A
unknown-f	0.608715	0.938308	0.894477	0.919708	N/A
pf-m	0.027069	0.172997	0.265824	0.201628	N/A
pm-m	0.999964	0.998998	0.999874	0.999511	N/A
uk-m	0.987869	0.957141	0.998505	0.984646	N/A
unknown-m	0.999961	0.999996	0.999993	1	N/A
pm-pf	0.376821	0.785265	0.80893	0.790373	N/A
uk-pf	0.604133	0.941403	0.870624	0.913832	N/A
unknown-pf	0.701846	0.95835	0.918039	0.94214	N/A
uk-pm	0.999473	0.999295	0.999997	0.999846	N/A
unknown-pm	0.999821	1	0.999891	0.999993	N/A
unknown-uk	0.997002	0.999732	0.999579	0.999664	N/A

6.3 Discussion and Conclusion

In section 6.1.1 the prediction was made that sex would only be notable in cross-sectional morphology and geometry in the guise of size. This did not entirely bear out. For morphology (results available in section 6.2.1.1) size uniquely explained morphological variation for both humeral and femoral cross-sections, but sex never did. However for cross-sectional geometry sex uniquely explained variation in the TA, I_{max} , I_{min} , and J values for both the humeral and femoral cross-sections with strong statistical significance. The relevant hypothesis for these results references morphology and so H0 “Morphological variation is not significantly correlated with sex,” is accepted. In this case size matters. Based on these results it is more useful to use cross-sectional geometry than morphology for research questions regarding sex.

Sexual dimorphism was likely more clear in cross-sectional geometry than morphology as the former incorporates size and robusticity (Klingenberg & Nijhout, 1999; Sakaue, 1998; Wilczak, 1998). This suggests that females and males in all populations had similar levels of gracility and robusticity, but did vary consistently in size. As the cross-sections in this study only included sections taken at 40% and 50% conclusions cannot be drawn regarding sex linked resorption and deposition ((Currey, 2003; Rho et al., 2002; Ruff & Hayes, 1982)) or hormonal effects due to life history of particularly female individuals (Agarwal et al., 2004; Agarwal & Stout, 2004; Kaastad et al., 2000; Mays, 1996).

In section 6.1.2 I hypothesised that age might explain particularly morphological variation at the midshaft but would be likely to do so more prevalently when considered with sex. In this case that prediction proved largely true meaning that for morphology variation is significantly correlated with age. We can therefore reject the null hypothesis. In the humerus age alone did not uniquely explain morphological variation at the midshaft, but when age and sex were considered together they could explain variation. For femoral cross-sections at midshaft morphological variation was uniquely explained by age alone and when paired with other interactions or sets of interactions these continued to explain variation. However, sex and age considered together did not explain morphological variation at the femoral midshaft. Conversely, cross-sectional geometry was not explained by age. This seems to suggest that age is related to morphology of the cross section at midshaft but not to size or that if size plays a role in morphological variation with age it is at least somewhat separate. Additionally, while for sex cross-sectional geometry proved to be a better method, for age morphology is more telling.

This study included only adults meaning any discussion of ontogeny refers to the individuals' biological history as opposed to their conditions and health at the time of their death. Therefore, it follows that morphology would be a better indicator of adult age than any value associated with size. Although relative levels of gracility and robusticity would correspond with size they would not necessarily be consistent with age for several reasons. In this study the oldest age group is 45+. Osteopenia and osteoporosis were and continue to be health issues for the elderly, but were an individual archaeological or modern to show signs of osteoporosis before the age of about 50 it may be considered "early onset." This means that in the oldest age group of this study there are likely individuals who are, statistically speaking, too young to show notable decline in BMC (Riis et al., 1996). Peak BMC reached somewhere between 25 and 35 years of age could have some morphological impact but likely not impact on size (Rho et al., 2002). The subsequent increase in subperiosteal deposition particularly at the muscle attachment sites with age would have a morphological effect on the bone (Currey, 2003; Jurmain et al., 2012; Ruff & Hayes, 1982).

Predictions regarding the relationship between cross-sectional morphology and geometry and pathologies including childhood stress, trauma, and degenerative diseases may be found in section 6.1.3. Childhood stress was not expected to correlate in any way with cross-sectional morphology but was expected to in some way explain cross-sectional geometry. In summary the opposite was true. There was no relationship between either LEH or CO with cross-sectional geometry. LEH and CO also never uniquely explained cross-sectional morphology for the humerus or femur. However when LEH and centroid size were considered together they did explain humeral cross-sectional morphology. Sex and LEH together also explained femoral cross-sectional morphology. CO and sex together as well as the groupings of site, sex, and CO and size, site, sex and CO explained femoral cross-sectional morphology.

The dichotomy between the predictions and reality between childhood stress markers and cross-sectional morphology and geometry could be in part due to catch-up growth. The delay in deposition could have resulted in the morphological equivalent of LEH. That is bone deposition ceased due to stress and then resumed as if nothing adverse had occurred. Later catch-up growth would not deposit bone in the same pattern as seen for healthy individuals resulting in a slightly different morphology (Gowland, 2015; Hughes-Morey, 2016; McDade et al., 2008; McEwan et al., 2005; Primeau et al., 2015; Ruff et al., 1994). In extreme cases of congenital anaemia there is alteration of the bone architecture and morphology (P. L. Walker et al., 2009) possibly acquired anaemia or prolonged pathogen load also results in morphological changes to a lesser degree. Furthermore the difference in the cortices may be

entirely or almost entirely endosteal meaning that the cortices of these individuals may be thinner, but the subperiosteal size would be relatively similar to that of individuals with no stress markers. Additionally, as childhood stress markers were linked to size or site or sex to explain morphology, genetic, environmental, hormonal, and biomechanical influences would explain the morphology of the cross-sections. In this case, contrary to expectations, cross-sectional morphology was a better means of researching the effects of childhood stress than cross-sectional geometry.

DJD and OA were in section 6.1.3 hypothesised to show no relationship with cross-sectional geometry or morphology as it was argued the related deposition of bone would be too random to contribute to a pattern. Where the null hypothesis is 'variation is not significantly correlated with the severity of DJD' we must reject the null hypothesis. Proximal and distal DJD severity did uniquely explain humeral morphology as well as the values for TA, I_{min} , and J. In the femur DJD severity did not explain any of the values from the cross-sectional geometry but when proximal DJD and site or proximal DJD and size or distal DJD and sex or distal DJD and site were considered together they explained femoral cross-sectional morphology. It is notable that the pattern between severity of DJD and morphology was most obvious in the humerus. This would support the notion that DJD occurs more in joints which are underused (Solovieva et al., 2005). In general DJD influencing shape suggests that the osteogenic component of DJD and OA is consistent and does effect subperiosteal deposition. It remains uncertain whether or not osteogenesis is caused by or causes DJD. For research into DJD these results would suggest that use of the cross-sectional morphology or geometry could both be valid depending on the research question.

Trauma was expected to have an effect on morphology, but not on cross-sectional geometry. The reason given was that the effect on the individual's mobility would correlate to their size and therefore cancel out any size differences. That proved entirely incorrect because where incidence of trauma explained morphology in the cross-sections of the humerus and femur it was often paired with size and incidence of trauma explained femoral values of TA, I_{max} , I_{min} , and J. This means that trauma's effect on morphology is likely due to mobility and that size impacts how healing occurs.

Incidence of Schmorl's nodes was predicted to have no effect on cross-sectional morphology or geometry. There was no relationship between cross-sectional morphology and Schmorl's nodes in the femur. For humeral cross-sectional morphology if incidence of Schmorl's nodes was considered with size and sex then they did explain humeral morphology. Additionally in the cross-sectional geometry incidence of Schmorl's nodes did explain femoral values for I_x/I_y . Schmorl's nodes have been correlated

with a young age at mortality (Šlaus, 2000) and reduced neural canal space which may lead to lumbar pain (Plomp et al., 2012b). It has been speculated that they may also be related to heavy loading but they have been shown to occur in gorillas which are unlikely to experience loading in a manner similar to humans (Jurmain, 1999). Even so, the variation of I_x/I_y with incidence of Schmorl's nodes suggests the results for femoral cross-sectional geometry are related to mobility. A lower value of I_x/I_y suggests a more athletic profile for the cortex meaning if the individual in question was highly mobile and had the right vertebral morphology they would be at a higher risk for Schmorl's nodes (Peng et al., 2003; Plomp et al., 2012a; Shaw & Stock, 2009a, 2009b; Stock & Shaw, 2007). Why this was not reflected in the morphology of the femoral cross section suggests that in this case size is crucial. Humeral morphology could be explained by incidence of Schmorl's nodes, but only with size and sex also considered. This points to the hormonal effects of sex and possibly sexual dimorphism and size being crucial in the understanding of morphology with the incidence of this type of lesion.

In section 6.1.4 I predicted that populations would show variation in cross-sectional morphology and geometry. This prediction is supported by the evidence. We can reject the null hypothesis that populations are not morphologically distinct. For both the humerus and femur cross-sectional morphology uniquely explained site. When a post-hoc test was applied to the geometric values it was found that the greatest differences were between 3-J-18 and any other site. 3-J-18 was the only non-English site included which suggests that the Sudanese population was more different than the differences between the English sites. This is possible, however it must be noted that the Sudanese population was also much smaller and in general more gracile than any of the English sites. The sites are demonstrably different but that may be due in large part to size more than shape. It is interesting that despite being bigger and in other morphological measures differentiating itself to some degree from the other English site Coach Lane did not stand out here. Only the Sudanese individuals were significantly different. This could be due to their relative size or genetic effect on shape, but it could also be due to relative mobility and lifestyle. The Sudanese population occupied rougher terrain and were less urban and likely more active than any of the English populations. The only rural English population studied here were from Hereford where most individuals would have enjoyed a privileged and sedentary lifestyle. The other two English populations were urban and while they must have engaged in some physical labour and activity it might not have been to the degree that the Sudanese population did. While it is likely some of the population differences seen here are down to the populations being different, cross-sectional geometry is particularly good at detecting robusticity and mobility and it is likely that here mobility is a function of interpopulation variation (Marchi et al., 2006; Ruff, Holt, Sládek,

et al., 2006; Shaw & Stock, 2009b; Sparacello et al., 2011a; Sparacello & Marchi, 2008; Stock & Pfeiffer, 2004).

This chapter was not only interested in determining relative levels of variation with different factors, but also with determining the strengths and weaknesses of a morphological method as opposed to a geometrical method which includes size. As might have been predicted factors which are dependent on or result in size differences were notable in the geometric method at least as well as they were in the morphological method. Likewise when size was not a theoretically relevant factor morphology performed at least as well or better than the geometric method. Consistent with how it has been used in prior studies cross-sectional geometry was effective at determining site and sex (Lieberman et al., 2004; Marchi et al., 2006; O'Neill & Ruff, 2004; Shaw & Stock, 2009a; Sparacello et al., 2011b; Sparacello & Marchi, 2008; Stock & Pfeiffer, 2004; Yamanaka et al., 2005). It was also useful in interpreting rates of DJD and trauma. Morphology of the cross section was useful for site, age, childhood stress, and trauma, but could not determine age at all. In some of these results one of the methods gave results which were more significant than the other suggesting that even where both are effective one might be slightly better depending on the research question. The results here suggest that in general when using cross-sections to ask questions about pathology, stress, and trauma examining the morphology is best, but when asking questions regarding population demography cross-sectional geometry is the best method. Additionally, in studies where pathologies are related to robusticity size and shape information would be equally important and size information for these purposes is best collected using cross-sectional geometry.

7 Discussion and Conclusion

7.1 Introduction

This thesis was originally conceived and informed by the work of Charlotte Henderson in reference to enthesal changes (Cardoso & Henderson, 2010; C. Y. Henderson, 2009; Jurmain et al., 2012), Davina Craps' work on osteoarthritis (Craps, 2015), and Kimberly Plomp's demonstration of the relation of vertebral morphology to the presence of Schmorl's nodes (Plomp et al., 2012b; Plomp, Roberts, et al., 2015; Plomp, Viðarsdóttir, et al., 2015). The aim was to link skeletal morphology with incidence of osteoarthritis. In spite of Jurmain's and Henderson's warnings (Jurmain et al., 2012) another initial aim was to try to link morphology to activity. This last was quickly abandoned. Plomp's PhD thesis

looked at several pathologies and lesions including Hansen's disease and osteoarthritis as well as Schmorl's nodes in relationship to morphology (Plomp, 2013). Plomp used homologous points at the epiphysis to try to show a relationship between the incidence of OA and morphology but found none. Therefore the inclusion of the epiphysis in this study was meant to replicate Plomp's results and contrast to sections on different measures of morphology. As will be explored further below, the results of this study did not entirely match Plomp's but there are many possible reasons for this.

Due to Plomp's results and the multiple etiologies of OA it was not expected that there would be a link between OA and morphology in any of the parts of the bone. To account for this and due to many researchers linking DJD and OA to population stress (Gawri et al., 2014; Klaus et al., 2009; Novak & Šlaus, 2011; Šlaus, 2000; Sofaer-Derevenski, 2000), other skeletal lesions were included. This was done partly to see if any of these lesions or pathologies could be linked to morphology, but also if any did, to help explain why that was the case. Particularly, given the interrelatedness of auto-immune disorders and spondyloarthropathies and their tendency towards co-morbidity and hormonal or endocrinal involvement it was my belief that inclusion of other factors which could possibly explain in particular epigenetic activation due to fetal or early childhood conditions which would in turn influence long bone morphology and degenerative disorders (Klaus, 2014; Samsel et al., 2014). Morphological variation was best described by the severity of DJD and OA rather than any other pathological lesion or condition measured. The results were unexpected but not inexplicable.

It was also important to ensure that the demographic profile of the individuals was understood in relationship to their morphological and to a lesser degree pathological variation. Previous studies on DJD and OA which use GMM as a methodology have found a relationship between population or sex and morphology and pathology (Stevens & Viðarsdóttir, 2008). Sexual dimorphism, population variation, and allometry were all expected to contribute to morphological variation. Specifically it was expected that allometry would correspond to some sexual dimorphism and population variation. This was not entirely the case and in actuality, of these demographic factors only site reliably explained morphological variation.

7.2 Summary of results

Detailed results may be found in the results sections of their respective chapters. This section will serve as a cursory glance at all the results within this study as they relate to the stated hypotheses and one another. Very generally stated the two IVs which consistently explained morphological variation

were site and DJD and OA severity. The morphology most effectively explained by the IVs in this study was diaphyseal surface morphology.

7.2.1 Within population variation

A secondary aim of this thesis as to show that GMM is useful in research into within population variation as well as between population variation. The goal was to show that sex, age, and pathology may influence morphology. In some respects associated with some measures of morphology they do. This section will discuss which morphological measures were explained by within population variation and in what way. Why these results are seen and how they relate to other literature will be discussed in Section 7.3.1.

7.2.1.1 Epiphysis

Epiphyseal morphological variation using GMM has already been studied particularly in relation to the incidence and severity of DJD and OA (Plomp, 2013; Stevens & Viðarsdóttir, 2008). Both of these studies found very little relationship between epiphyseal shape and within population variation (Stevens and Viðarsdóttir (2008) were able to show some relationship when considering multiple factors). Additionally, when Anderson and Trinkaus (1998) examined the angle of the femoral neck they found interesting results regarding activity level, but they did not find a relation to the angle of the femoral neck and sex. Due to these previous studies, epiphyseal morphology was not expected to be explained easily by within population heterogeneity.

7.2.1.1.1 Sexual dimorphism and morphological variation

Sex does not uniquely explain epiphyseal morphology for the humerus or femur at any of the epiphyses. Sex and site together can explain the morphology of the proximal femoral epiphysis. Sex also did not explain allometry in any of the epiphyses.

7.2.1.1.2 Age and morphological variation

Age alone does not uniquely explain epiphyseal morphology. When linked with sex site and size as well the pair or group of factors may explain epiphyseal morphology particularly in the proximal femur. This could point to sexual dimorphism in aging, but here again the null hypothesis that age does not explain morphology is accepted.

7.2.1.1.3 Childhood stress indicators and morphological variation

Childhood stress indicators could not uniquely explain epiphyseal morphological variation.

When linked with other IVs or groups of IVs the groupings could explain epiphyseal morphology. The null hypothesis that childhood stress indicators do not explain morphology is accepted.

7.2.1.1.4 Degenerative Joint Disease and morphological variation

DJD and OA severity uniquely explained femoral proximal epiphyseal morphology. When linked with other IVs DJD and OA severity could explain distal femoral epiphyseal morphology as well as humeral epiphyseal morphology. However with the exception of the proximal femoral epiphysis the null hypothesis that DJD and OA do not explain morphology is accepted.

7.2.1.1.5 Trauma and morphological variation

Incidence of trauma does not uniquely explain epiphyseal morphological variation. Various groupings of trauma with other IVs do explain morphological variation in all epiphyses. Here the null hypothesis that trauma does not explain morphological variation is accepted.

Schmorl's nodes uniquely explained femoral proximal and distal morphology, but not that of the humeral epiphyses. In all cases when linked with various other IVs or groupings of IVs morphology was explained with Schmorl's nodes. For the femoral epiphyses the null hypothesis that the presence or absence of Schmorl's nodes does not explain morphological variation should be rejected. However for the humeral epiphyses, the null hypothesis is accepted.

7.2.1.2 Diaphysis

Diaphyseal surface morphological variation has only previously been examined with GMM in one study which was methodological rather than interested in the heterogeneous influences to shape (Frelat et al., 2012). Other examinations of diaphyseal shape (beyond cross-sectional geometry) do exist (De Groote, 2011a; Shackelford & Trinkaus, 2002; Yamanaka et al., 2005) but the paucity of studies on the subject, likely due to the computational necessities of the technique, suggest there may be information to be found in this area of study. Additionally, particularly when femoral curvature is in question the basis of the study is on robusticity, mobility, and biomechanics rather than within population variation. Therefore the questions of within population variation as applied to diaphyseal surface morphology were the most relevant of the study.

Additionally, allometry was present in the diaphyses, but did not necessarily correspond with sex or age. Size was linked to other factors to be discussed below, but could be related more to relative gracility or possibly activity and mobility rather than any of the factors mapped here.

7.2.1.2.1 Sexual dimorphism and morphological variation

Sex was able to explain diaphyseal surface morphological variation in femora and in the humerus when site and sex were linked they explained variation. In the femora the sexual dimorphism could be related to primary sexual characteristics as the valgus angle would have to be resolved by the diaphysis. (Previous studies (Shackelford & Trinkaus, 2002; Stevens & Viðarsdóttir, 2008) have shown that the resolution of the presumably disparate valgus angle in females and males is not seen at the femoral neck or knee – which is logical from an ontological and developmental perspective (Frost, 1999; Ruff, 2003) – so the remaining variation must exist in the diaphysis.) Humeral sexual dimorphism is likely to be more complex and is demonstrably heterogeneous in its morphological etiologies. Here the null hypothesis that sex does not explain morphological variation of the diaphyseal surface is rejected.

7.2.1.2.2 Age and morphological variation

Age was not able to explain diaphyseal surface morphological variation for either the humerus or the femora unless paired with size, sex, or both. This underscores Ruff and Hayes' (Ruff & Hayes, 1982) study on the relationship of sex with age related changes in cross-sectional geometry. However in general the null hypothesis that age does not explain morphological variation of the diaphyseal surface is accepted.

7.2.1.2.3 Childhood stress indicators and morphological variation

Childhood stress indicators could not uniquely explain diaphyseal surface morphological variation for either element. Humeral morphological variation could be explained by CO linked with both size and site. Femoral morphology could be explained by CO linked with sex, size, or site. LEH similarly could explain humeral and femoral morphology but only when linked with some combination of size, site, or sex. Overall this means that it is still possible that childhood stress indicators could impact morphology of the diaphysis but not without the influence of other factors. In this case the null hypothesis that childhood stress does not explain morphological variation of the diaphyseal surface is accepted.

7.2.1.2.4 Degenerative Joint Disease and morphological variation

Severity of DJD and OA in the proximal humerus, proximal femur and distal femur was able to uniquely explain diaphyseal surface morphological variation for both the humerus and the femur. DJD

and OA in the distal humerus could also explain morphological variation when linked with size, site, or sex. This means that the null hypothesis that DJD and OA do not explain morphological variation is rejected.

7.2.1.2.5 Trauma and morphological variation

Neither the incidence of trauma nor Schmorl's nodes could uniquely explain diaphyseal morphology in either the humerus or femur. Both when linked with size, site, or sex or some combination of those factors could explain morphological variation. Where trauma was considered among the IVs, humeral diaphyseal shape was explained more often than femoral. The null hypothesis that the incidence of trauma does not explain morphological variation in the diaphysis is accepted. Likewise, the null hypothesis that the incidence of Schmorl's nodes does not explain morphological variation in the diaphysis is also accepted.

7.2.1.3 Cross-Section

Cross-sectional morphology and geometry was included for similar reasons as epiphyseal morphology. Cross-sectional geometry studies are usually focused on mobility or activity related change (Lieberman et al., 2004; Mays, 2001; Rhodes & Knüsel, 2005; Shaw & Stock, 2009a, 2009b; Sparacello et al., 2011a; Sparacello & Marchi, 2008; Stock & Pfeiffer, 2004; Stock & Shaw, 2007). Where morphology was a major and discrete component of the study (L. A. B. Wilson & Humphrey, 2015; Yamanaka et al., 2005), mobility and activity remained the focus. It therefore follows that within population variation as examined here would be unlikely to be related to cross-sectional geometry or morphology. This study made no attempt to identify more or less active individuals or divide the populations by occupation which could indicate their relative level of mobility. However, the wealth of literature available on this subject made it necessary to examine if for nothing more than comparative reasons. The results were somewhat predictable, but provide some interesting insights. Allometry was clearly present in the cross-sectional morphology for both humeri and femora, but it did not relate to sexual dimorphism.

7.2.1.3.1 Sexual dimorphism and morphological variation

Sex alone could not explain cross-sectional morphological variation, but it did explain cross-sectional geometrical variation for both humeri and femora. This suggests that size and sex together should explain morphological variation, but again, that is not the case. There exists geometrical sexual dimorphism that is not being captured or represented morphologically. This means the null hypothesis that sex does not explain cross-sectional morphological variation is accepted while the null hypothesis that sex does not explain cross-sectional geometric variation is rejected.

7.2.1.3.2 Age and morphological variation

Age alone did not uniquely explain humeral cross-sectional morphology, but it did explain femoral cross-sectional morphology. Furthermore, when age is considered with sex or sex and size it can explain humeral cross-sectional morphology. However, age does not explain cross-sectional geometry at all. This largely supports the results of Ruff and Hayes (1982) in that we are seeing a clear relationship between sex, age, and cross-sectional shape if not form. The reason it is not entirely as clear is that Ruff and Hayes took cross sections across the entirety of the diaphysis whereas this study only looks at the cross-section at midshaft. For morphology we can reasonably reject the null hypothesis that age does not explain cross-sectional morphology. However, we must accept the null hypothesis that age does not explain cross-sectional geometry.

7.2.1.3.3 Childhood stress indicators and morphological variation

Incidence of childhood stress indicators did not uniquely explain cross-sectional morphology or geometry. When combined with size, sex, or site LEH and CO could explain morphology somewhat. However, here we must accept the null hypotheses that childhood stress indicators do not explain cross-sectional morphology or geometry.

7.2.1.3.4 Degenerative Joint Disease and morphological variation

DJD and OA severity uniquely explained humeral morphological variation but did not uniquely explain femoral morphological variation. Additionally, DJD and OA severity in the proximal humerus explained cross-sectional geometry in the humerus, but distal humeral DJD and OA did not and neither DJD in the proximal or distal femur explained femoral cross-sectional geometry. If, as previous studies would indicate cross-sectional morphology and geometry are related to mobility and activity related use and robusticity then this has interesting implications for DJD and OA. However, regarding results, in the humerus the null hypotheses that DJD and OA do not uniquely explain cross-sectional morphology or geometry is rejected and in reference to the femur the null hypotheses are accepted.

7.2.1.3.5 Trauma and morphological variation

Trauma did not uniquely explain humeral or femoral cross-sectional morphology. When other factors like site, size, or sex were considered cross-sectional morphology in reference to the incidence of trauma was explained for both the humerus and femur. Humeral cross-sectional geometry could also not be uniquely explained by the incidence of trauma, but femoral cross-sectional geometry could. Once again, this suggests that if cross-sectional geometry is particularly sensitive to mobility patterns these incidents of trauma might have caused a change or temporary cessation in locomotion. For cross-

sectional morphology we must accept the null hypothesis that trauma does not explain morphology. However we also must reject the null hypothesis that trauma does not explain cross-sectional geometry.

The incidence of Schmorl's nodes did not uniquely explain humeral or femoral cross-sectional morphology or geometry with the notable exception of I_x/I_y in the femur. With this in mind for the most part we can accept the null hypotheses that the incidence of Schmorl's nodes explains humeral or femoral cross-sectional morphology or geometry.

7.2.2 Between population variation

GMM is often used to determine the level of between population variation. In cases where only humans or only one species or clade is considered it has been used to determine levels of migration and heterogeneity or adaption to a particular environment (Cardini, Thorington, et al., 2007; Claude et al., 2004; Gunz, 2012; von Cramon-Taubadel & Lycett, 2014). Between species it may be used to understand degree of speciation as well as functional adaptation (Bonnar, 2007; Cardini, Jansson, et al., 2007; De Groote, 2011b; Di Vincenzo et al., 2012; O'Higgins et al., 2012; Young, 2008). GMM is an ideal method for determining variation between populations and as this method has a longer established history than using GMM to show intrapopulation variation, it is important to show in this study how between population variation appears.

The populations themselves are also variable. Further discussion of this may be found in section 7.3.2, however three of the four populations are from England and one is from what is now the Sudan. Coach Lane is a later site than the other three and all of the sites had arguably variable socioeconomic statuses between them. Socio-economic status of the Sudanese site is arguably not comparable to the English sites but this makes the variation between populations more rather than less relevant.

7.2.2.1 Pathological rates between populations

Incidence of pathology between populations was not a primary concern of this research, but it is important information to have in order to contextualize the results and understand how pathology might interact with morphology.

Table 7.1 Demographic information by site.

Sudan	Sex	Age			
		18-25	25-35	35-45	45+
3-J-18	34	10	9	8	7
Female	18	6	4	3	5

% of pop.	52.94%	17.65%	11.76%	8.82%	14.71%
Male	15	3	5	5	2
% of pop.	44.12%	8.82%	14.71%	14.71%	5.88%
Unknown	1	1	0	0	0
% of pop.	2.94%	2.94%	0.00%	0.00%	0.00%

Coach Lane	Sex	Age			
		18-25	25-35	35-45	45+
Total	50	6	11	9	22
Female	20	1	3	4	12
% of pop.	40.00%	2.00%	6.00%	8.00%	24.00%
Male	28	5	8	5	10
% of pop.	56.00%	10.00%	16.00%	10.00%	20.00%
Unknown	2	0	0	0	0
% of pop.	4.00%	0.00%	0.00%	0.00%	0.00%

Fishergate House	Sex	Age			
		18-25	25-35	35-45	45+
Total	27	5	3	5	14
Female	13	1	2	1	9
% of pop.	48.15%	3.70%	7.41%	3.70%	33.33%
Male	14	4	1	4	5
% of pop.	51.85%	14.81%	3.70%	14.81%	18.52%
Unknown	0	0	0	0	0
% of pop.	0.00%	0.00%	0.00%	0.00%	0.00%

Hereford	Sex	Age			
		18-25	25-35	35-45	45+
Total	12	1	3	4	4
Female	5	0	2	2	1
% of pop.	41.67%	0.00%	16.67%	16.67%	8.33%
Male	4	1	1	1	1
% of pop.	33.33%	8.33%	8.33%	8.33%	8.33%
Unknown	3	0	0	1	2
% of pop.	25.00%	0.00%	0.00%	8.33%	16.67%

Table 7.2 Childhood stress indicators by site.

Sudan	Cribra Orbitalia			LEH		
	CO present	CO absent	orbitals not present	LEH present	LEH absent	teeth not present
3-J-18	11	23	0	16	18	0
Female	8	10	0	7	11	0
% of pop.	23.53%	29.41%	0.00%	20.59%	32.35%	0.00%
Male	3	12	0	9	6	0
% of pop.	8.82%	35.29%	0.00%	26.47%	17.65%	0.00%
Unknown	0	1	0	0	1	0
% of pop.	0.00%	2.94%	0.00%	0.00%	2.94%	0.00%

Coach Lane	Cribra Orbitalia			LEH		
	CO present	CO absent	orbitals not present	LEH present	LEH absent	teeth not present
Total	14	31	5	40	5	5
Female	9	11	0	17	3	0
% of pop.	18.00%	22.00%	0.00%	34.00%	6.00%	0.00%
Male	5	20	3	23	2	3
% of pop.	10.00%	40.00%	6.00%	46.00%	4.00%	6.00%
Unknown	0	0	2	0	0	2
% of pop.	0.00%	0.00%	4.00%	0.00%	0.00%	4.00%

Fishergate House	Cribra Orbitalia			LEH		
	CO present	CO absent	orbitals not present	LEH present	LEH absent	teeth not present
Total	3	24	0	17	10	0
Female	1	12	0	11	2	0
% of pop.	3.70%	44.44%	0.00%	40.74%	7.41%	0.00%
Male	2	12	0	6	8	0
% of pop.	7.41%	44.44%	0.00%	22.22%	29.63%	0.00%
Unknown	0	0	0	0	0	0
% of pop.	0.00%	0.00%	0.00%	0.00%	0.00%	0.00%

Hereford	Cribra Orbitalia			LEH		
	CO present	CO absent	orbitals not present	LEH present	LEH absent	teeth not present
Total	2	10	0	4	8	0
Female	1	4	0	1	4	0
% of pop.	8.33%	33.33%	0.00%	8.33%	33.33%	0.00%
Male	1	3	0	2	2	0
% of pop.	8.33%	25.00%	0.00%	16.67%	16.67%	0.00%
Unknown	0	3	0	1	2	0
% of pop.	0.00%	25.00%	0.00%	8.33%	16.67%	0.00%

Table 7.3 Trauma and Schmorl's nodes by site.

Sudan	Trauma		Schmorl's Nodes		
	Trauma Present	Trauma Absent	Schmorl's Nodes Present	Schmorl's Nodes Absent	Vertebrae not present
3-J-18	11	23	9	25	0
Female	6	12	5	13	0
% of pop.	17.65%	35.29%	14.71%	38.24%	0.00%
Male	5	10	4	11	0
% of pop.	14.71%	29.41%	11.76%	32.35%	0.00%
Unknown	0	1	0	1	0
% of pop.	0.00%	2.94%	0.00%	2.94%	0.00%

Coach Lane	Trauma		Schmorl's Nodes		
	Trauma Present	Trauma Absent	Schmorl's Nodes Present	Schmorl's Nodes Absent	Vertebrae not present
Total	8	42	33	12	5
Female	3	17	11	7	2
% of pop.	6.00%	34.00%	22.00%	14.00%	4.00%
Male	5	23	21	5	2
% of pop.	10.00%	46.00%	42.00%	10.00%	4.00%
Unknown	0	2	1	0	1
% of pop.	0.00%	4.00%	2.00%	0.00%	2.00%

Fishergate House	Trauma		Schmorl's Nodes		
	Trauma Present	Trauma Absent	Schmorl's Nodes Present	Schmorl's Nodes Absent	Vertebrae not present
Total	10	17	18	9	0
Female	4	9	6	7	0
% of pop.	14.81%	33.33%	22.22%	25.93%	0.00%
Male	6	8	12	2	0
% of pop.	22.22%	29.63%	44.44%	7.41%	0.00%
Unknown	0	0	0	0	0
% of pop.	0.00%	0.00%	0.00%	0.00%	0.00%

Hereford	Trauma		Schmorl's Nodes		
	Trauma Present	Trauma Absent	Schmorl's Nodes Present	Schmorl's Nodes Absent	Vertebrae not present
Total	1	11	8	4	0
Female	0	5	3	2	0
% of pop.	0.00%	41.67%	25.00%	16.67%	0.00%
Male	1	3	4	0	0
% of pop.	8.33%	25.00%	33.33%	0.00%	0.00%
Unknown	0	3	1	2	0
% of pop.	0.00%	25.00%	8.33%	16.67%	0.00%

Table 7.4 DJD and OA severity by site.

Sudan	DJD Severity				
	Healthy	DJD	Mild	Moderate	Severe
Proximal Humerus	11	2	0	0	0
Distal Humerus	11	1	0	1	0
Proximal Femur	4	8	0	0	0
Distal Femur	9	1	0	1	1

Coach Lane	DJD Severity				
	Healthy	DJD	Mild	Moderate	Severe
Proximal Humerus	29	16	0	2	8
Distal Humerus	31	18	1	1	4
Proximal Femur	28	7	1	2	12
Distal Femur	27	12	2	1	8

Fishergate House	DJD Severity				
	Healthy	DJD	Mild	Moderate	Severe
Proximal Humerus	11	13	4	2	1
Distal Humerus	9	15	4	1	2
Proximal Femur	11	4	3	4	3
Distal Femur	7	7	2	3	5

Hereford	DJD Severity				
	Healthy	DJD	Mild	Moderate	Severe
Proximal Humerus	7	1	1	1	0
Distal Humerus	6	3	1	0	0
Proximal Femur	5	2	0	0	1
Distal Femur	4	2	2	0	0

7.2.2.2 Epiphysis

Epiphyseal union for different epiphyses happens at different points during development and does exhibit sexually distinctive rates of development with girls developing earlier than boys (see Figure 2.1 and Figure 2.2.) (Scheuer & Black, 2000). The degree of development and union of the epiphyses is a good indicator of age in subadult skeletons. Parts of the epiphysis begin developing in utero and the general morphology of the epiphysis may be influenced by childhood body mass and activity patterns, but is more or less set well before adulthood (Frost, 1999; Hamrick, 1996). Other parts of the skeleton such as the craniofacial structure are predetermined in infancy with little to no environmental influence (Viðarsdóttir et al., 2002b). With such a narrow window in which morphology could be altered it was expected that interpopulation variation might be present but would be the result of influences prior to adulthood and even adolescence.

7.2.2.2.1 Interpopulation variation

Site uniquely explains epiphyseal morphological variation. However, site does not help to explain epiphyseal morphological variation in relation to other factors. This suggests that epiphyseal morphology is strictly controlled by genetic and epigenetic determinants or at least that symptoms relating to the lesions and factors examined here are expressed in ways that do not affect epiphyseal morphology. However, that site and childhood indicators of stress did not consistently explain epiphyseal morphology in relationship to site is noteworthy. This means either all individuals studied

reacted relatively similar to childhood stress or that predetermined morphology guided by genetic and epigenetic factors was so strong that stress had no effect on epiphyseal morphology.

7.2.2.3 Diaphysis

Diaphyses are demonstrably complex in their development. Childhood health and stress do play a role in determining overall length, shape, and possible robusticity of the diaphysis (Lewis et al., 2016; McEwan et al., 2005; O. M. Pearson & Lieberman, 2004; Schug & Goldman, 2014; Sekiyama et al., 2015; Zioupos & Currey, 1998). In stressed individuals a period of “catch-up” growth may occur in late adolescence and early adulthood where additional rapid growth allows them to achieve genetically predetermined stature that was not achieved during childhood (Lewis et al., 2016; Ruff et al., 1994; Sekiyama et al., 2015). However, this “catch-up” growth may not allow sufficient time or deposition to the subperiosteal or endosteal bone. McEwan and colleagues (2005) show that the best determination of childhood stress and “catch-up” growth is not Harris Lines but bone mineral density. Regardless of when diaphyseal modelling is complete, remodeling occurs throughout the individual’s life based on weight-bearing activities (Ruff et al., 2013; Ruff, Holt, & Trinkaus, 2006; Wallace et al., 2012). The diaphyseal morphology then was expected to be very sensitive to any and all environmental impact.

7.2.2.3.1 Interpopulation variation

Site uniquely explains diaphyseal morphological variation. Site was also an important secondary factor in explaining diaphyseal morphological variation in the context of sex, age, trauma, Schmorl’s nodes, CO, LEH, and DJD. It is possible that this variation is due to genetic or epigenetically programmed reactions to these other factors, but it is likely due to the frequency with which the diaphysis remodels that this interplay is more environmental. Individuals at each site who share certain life experiences or pathological lesions are showing similarity in their diaphyseal shape not necessarily due to genetic affinity but to shared terrain, climate, nutrition, and activity.

7.2.2.3.2 Comparison of intra and interpopulation variation

Diaphyses are arguably the most sensitive morphologies to the extrinsic and intrinsic factors measured. DJD severity uniquely explained diaphyseal morphology as did site, sex, and size. However, the R squared value for site was consistently higher than these other factors meaning that while the other factors seem to explain and possibly influence diaphyseal morphology site best explains it. The R squared values are still quite low, but they describe less variation around the best fit line than is shown by other independent variables.

7.2.2.4 Cross-Section

Similar to the diaphysis, the cross-section may experience stress related low bone mineral content or density, but also will remodel throughout life in reaction to weight bearing activities (Drapeau & Streeter, 2006; Ruff, 2000; Ruff et al., 1994). If individuals engage in intense physical activity from early childhood their cortices can be expected to be much thicker than sedentary individuals, and even those who do practice intense physical activity but started later in life (Shaw & Stock, 2009a, 2009b). This variation in cortical thickness is reflected in the general outline of the cross-section. Robusticity of the cross-section is reflected in its general morphology. The cross-section however is also sensitive to hormonal and age related changes (Ruff & Hayes, 1982). Once again, the cross-section should be sensitive to its surrounding environment.

7.2.2.4.1 Interpopulation variation

Site could uniquely explain cross-sectional morphological and geometric variation. However, site did not help explain morphological variation when paired with most factors. So while site itself was an important determinant of cross-sectional and geometric variation, cross-sectional shape and form do not seem to interact differently with other IVs based on site. In particular post-hoc tests done on cross-sectional geometry showed that the difference found in cross-sectional geometry between sites was largely between the Sudanese site and the three European ones. Although the cross-sections are behaving in a statistically different manner to the diaphysis, this set of data seems to suggest once again that the differences seen in the diaphysis and cross-section are not genetic or epigenetically predetermined phenotypes but instead dependent on the surrounding environment. The lack of other IV's impact on cross-sectional morphology or geometry is likely due to cross-sectional sampling only occurring at the midshaft in this study.

7.2.2.4.2 Comparison of intra and interpopulation variation

While site uniquely explained both morphological and geometric variation in the cross-section it did not consistently help explain variation when paired with other factors. Unlike the results seen for diaphyseal morphology the R-squared value was also not consistently higher than any other R-squared value. The R-squared value was also lower than seen previously for site meaning much more variation was seen. Cross-sectional robusticity easily points towards weight-bearing activity and could in turn point to a difference in terrain between sites. This would be supported by the cross-sectional geometric post-hoc results. However, severity of DJD and OA in the proximal humerus especially has a lower p-

value and higher R-squared value than site which would mean in this case site does not best explain morphological variation of the humeral cross-section.

7.2.3 Morphological variation in different parts of the bone

All morphological variation with different IVs was not created equal. The diaphyseal surface proved to be the most sensitive to factors other than site. In the diaphysis sex, size, and most incidents of DJD and OA were readily reflected in the morphology. This was the only part of the bone where a multiplicity of IVs could uniquely explain morphology. However, it is notable that cross-sectional morphology and epiphyseal morphology could be explained by IVs provided other factors were taken into account. It is also very noteworthy that the proximal epiphyseal morphology of the femur could be uniquely explained by Schmorl's nodes and DJD severity.

7.3 Interpretation of Results

7.3.1 Within population

7.3.1.1 *Sex and adult long bone morphology*

When speaking about sex in human biology or osteoarchaeology there is a point at which the conversation ceases to regard strictly sex and begins to address gender. Broadly speaking, there are two ways sex and gender may influence skeletal morphology these being sexual dimorphism and sexual division of labour. This thesis has intentionally skirted the latter. These two factors also have an overlap in that sex will influence how and to what degree any gendered activity may influence biological systems. Sexual dimorphism will account for some of the morphological variation found in this study. However, this variation may be further magnified by a possible sexual division of labour. Additionally, sex specific hormones will determine how the skeletal system metabolically responds to varying degrees of culturally informed activity.

Other studies have used GMM, osteometric, or other morphometric techniques in an attempt to better understand human sexual dimorphism (Alunni-Perret et al., 2008; J. Y. Anderson & Trinkaus, 1998; Bigoni et al., 2010; K. M. Brown, 2015; Bulygina et al., 2006; Coquerelle et al., 2011; González et al., 2007; Green & Curnoe, 2009; İçsan et al., 1998; Kranioti, Bastir, et al., 2009; Kranioti & Michalodimitrakis, 2009; Mall et al., 2000; Patriquin et al., 2003; Pretorius et al., 2006; Robinson & Bidmos, 2009; Sakaue, 2004; Scholtz et al., 2010; Srivastava et al., 2013; Velemínská et al., 2012; P. L. Walker, 2008). Many of these studies do examine the morphology of skeletal elements which would be the sites of primary sex characteristics, like the pelvis and its structures (K. M. Brown, 2015; González et al., 2007; Patriquin et

al., 2003, 2005; Pretorius et al., 2006), or secondary sex characteristics such as the craniofacial complex and mandible (Bigoni et al., 2010; Bulygina et al., 2006; Coquerelle et al., 2011; Green & Curnoe, 2009; Robinson & Bidmos, 2009; Velemínská et al., 2012; P. L. Walker, 2008). The rest however examine skeletal elements less obviously linked with sexual dimorphism including the femur, humerus, ulna, and scapula.

Two major themes have developed from this research. Sexual dimorphism is often found to be dependent upon population and sexual dimorphism is directly related to ontogeny. Many of the above studies regardless of the skeletal element chosen include a stipulation that their findings may only necessarily be applied to the populations included in that study and those which conducted research on multiple populations often showed that sexual dimorphism varied between populations (Bulygina et al., 2006; İşcan et al., 1998; Robinson & Bidmos, 2009). Studies which attempted to prove sexual dimorphism based on long bone morphology often simply restricted themselves to one population (Kranioti, Bastir, et al., 2009; Sakaue, 2004; Srivastava et al., 2013). These studies could all prove sexual dimorphism with reasonable certainty regardless of the apparent outlandishness of their choice in skeletal element, but sexual dimorphism in all elements including pelves and skulls was consistently population dependent. Sakaue (2004) demonstrated the presence of sexual dimorphism in long bones of recent Yamato Japanese. In a somewhat similar study İşcan and colleagues (1998) showed population dependent sexual dimorphism in the humeri of Japanese, Chinese, and Thai populations.

The ontogenetic effects on sexual dimorphism are related with both population and age. Viðarsdóttir, and colleagues (2002b) showed population linked ontogeny starting in infants and Bulygina and colleagues (2006) expanded upon this concept by demonstrating that ontogeny was not only population specific but also population specific for sexual dimorphism. Other authors have shown ontogenetic effects on sexual dimorphism in other primates and point in general to two theories on ontogeny (Cobb & O'Higgins, 2007; Mitteroecker et al., 2005; Mitteroecker, Gunz, Bernhard, et al., 2004). That is sexual dimorphism may derive either from an early cessation in morphological development or a wholly different ontogenetic trajectory. As the net widens to include multiple populations of the same species or multiple species with some shared evolutionary history heterochrony in regionality (skeletal and geographical), speciation, and sexual dimorphism becomes increasingly impactful (Klingenberg, 1998; Lieberman et al., 2007; McNulty, 2009; Shea, 1989).

Sexual dimorphism is therefore clearly population dependent; a result indirectly upheld by this study. Sex could explain femoral diaphyseal surface shape, but in other morphologies often needed to

be linked with site. However, all this points towards the question of environmental and cultural effect on morphology. Genetics and the biological effects of sex impact how a biological system will respond to external influence, but then how did the external environment and cultural practices of these disparate populations effect the skeletal morphology of the individuals within them? Only a few authors concerned with sexual division of labour are included in this thesis because sexual division of labour was not a primary research question here (Bridges, 1989a; Havelková et al., 2011; Marchi et al., 2006; Meyer et al., 2011; Molnar et al., 2011; Novak & Šlaus, 2011; Sparacello et al., 2011b; Wilczak, 1998). For most of these authors sexual division of labour was incidental to the rest of their study. That is in studies regarding enthesal changes, osteoarthritis, or cortical thickness they found variations between females and males and enough additional evidence to support that these variations may be due to a sexual division of labour. However, most of these authors also note the biological overlay of effects on the skeleton that could possibly negate that argument. Males being slightly larger are more likely to have more robust cortices, osteoarthritis may be due to global hormonal fluctuations, and enthesal changes are more common in older men (C. Y. Henderson, 2009) and Rabey and colleagues (2015) show they may not even be well related to activity at all. With these stipulations in mind it is still possible that sexual dimorphism is in part due to culturally gendered practices, activities, or culturally encouraged sedentism. Sparacello and colleagues (2011b) found marked sexual dimorphism in rates of upper limb asymmetry which they suggest may be linked to weapons training. Conversely Havelková and colleagues (2011) showed a high rate of enthesal changes in hinterland males as expected, but also a high rate of enthesal changes in castle females relative to castle males meaning that not only were castle females doing enough work to develop enthesal changes but they were doing so much relative to their male counterparts that they developed enthesal changes in spite of being biologically less likely to do so.

This study looked at three different populations one from a radically different environment and all likely practicing different amounts and types of physical labour. If sexual dimorphism in proximal long bones were entirely genetically predetermined throughout our species then sex would have always uniquely explained morphology. Sex did explain morphology but was only started to be consistent when linked with site. This supports research where sexual dimorphism is population dependent but suggests there are also additional factors which may explain sexual dimorphism.

7.3.1.2 Age

The previous section touched on ontogeny and its influence on adult shape, but as this study was concerned only with adult skeletons the effect of age on morphology was expected to be quite

weak. In this study age had to be linked to other IVs to explain any of the morphology studied. Adult age is still important in understanding the processes which influence skeletal morphology. Age estimation in adults after fusion of the medial clavicle is largely based on degenerative changes particularly (but not exclusively) in the pubic symphysis (Katz & Suchey, 1986; Mays, 2015b; Samworth & Gowland, 2007; Suchey & Katz, 1997), auricular surface (C O Lovejoy et al., 1985; Osborne et al., 2004), and sternal rib ends (Loth et al., 1994). This means that degenerative changes either pathological or incidental may be expected in the rest of the skeleton (Agarwal & Grynpas, 2009; Ruff & Hayes, 1982). Age also interacts with sex in the formation of enthesal changes (Cardoso & Henderson, 2010; Jurmain et al., 2012; Niinimäki, 2011) and to an arguably lesser degree loss of bone mineral content (Agarwal, 2008; Agarwal & Stout, 2004; F. H. Anderson et al., 1996; J. B. Anderson & Garner, 1998; Brickley, 2002).

Given this and previous research it is likely that the most telling effect of age on the skeleton is in bone mineral content coupled in particular with medullary expansion. In particular trabecular and endosteal bone would be affected (Agarwal et al., 2004; K Kennedy, 1989; Mays, 2001; Vedi et al., 1996; Zaki et al., 2009) but the only morphological effects that might be picked up from the methodologies utilised in this study would be those associated with enthesal changes.

7.3.1.3 Pathologies

7.3.1.3.1 Childhood Stress

At no point in this research could childhood stress indicators uniquely explain any part of proximal long bone morphology, but when linked with the other IVs they were related with some consistency. This might be expected particularly for epiphyses when linked to site because it would point towards the influence of childhood stress on structures which develop during childhood in relation to genetic predisposition or epigenetically encoded reactions to stress (Agarwal, 2016; Frost, 1994). It is more surprising that a similar pattern is found in the diaphysis which continually remodels throughout life and in fact does not complete development at least microscopically or in regards to bone mineral content until somewhere between twenty-five to thirty-five years of age (Currey, 2003, 2004; Rho et al., 2002). This points to childhood stress being less a unique life event from which an individual might catch up and recover but a trigger for or even symptom of an epigenetic switch which influences the individual's response to their environment for the rest of their life.

The first point that should be made here is that the individuals studied were all from medieval sites with the exception of those from Coach Lane who lived in postmedieval northern England. These are not individuals who can be said to have had a “modern” lifestyle nor can they be said to have had a

strictly “traditional” lifestyle as those two extremes are characterized in Bindon and Baker’s (1997) paper on the subject. Even the Sudanese population who appear to have been largely pastoralists likely did not meet the activity threshold to be considered “traditional,” and their rate of childhood stress indicators especially when factoring in the higher likelihood of parasitic infection is comparable with the English rates suggesting they were not any more nutritionally stressed. Additionally, as archaeological aging techniques are not generally considered reliable after forty-five to fifty years of age (Gowland, 2006, 2007; Samworth & Gowland, 2007), (although see (Osborne et al., 2004)) there is no way of knowing whether the individuals in these sites are experiencing shorter life-spans due to activation of epigenetic traits in utero in response to stressful environments. In considering this question of stress, survival, and quality of life the Osteological Paradox is very much in play. The only evidentially based claim that can be made in this context is that individuals with childhood stress indicators and a range of other independent variables often have similar morphologies. It is – without assuming one of the theoretical explanations regarding stress markers and survival – impossible to say if those with stress indicators actually represent a more stressed group than those without or whether they had the “thrifty gene” and it was “switched on,” and it can also not be said whether or not they died early and of conditions related to or caused by childhood stress (Armelagos et al., 2009, 2011; DeWitte & Stojanowski, 2015; Kinnally, 2014; Neel, 1962; Temple & Goodman, 2014; Wood et al., 1992). These are not questions which can be sufficiently answered with the evidence gathered in this research.

Wood and colleagues (1992) also suggest as a less plausible theory that the very lesions used to determine childhood stress might themselves heal casting further doubt on the relationship between nutritional or pathological stress and skeletal lesions. This suggestion that in particular cribra orbitalia and hyperostosis may heal or alternatively may once formed be continually re-colonized by bone marrow during episodes of nutritional stress has been echoed by other authors (Šlaus, 2000; Stuart-Macadam, 1989; P. L. Walker et al., 2009; Wapler et al., 2004). Linear enamel hypoplasia seems biologically impossible to heal or exacerbate in any manner beyond carious lesions, but it has been suggested that Schmorl’s nodes (not strictly related to stress but often predominant in younger individuals) may also heal (Jurmain, 1999; Novak & Šlaus, 2011). Additionally, epigenetic triggering of stress and in fact most epigenetic triggering appears to occur in utero. Stress during childhood alone may not cause an activation of the “thrifty gene” even where it is present. Individuals genetically predisposed to survival in specifically adverse conditions may not develop childhood stress indicators because their phenotypic response was determined by conditions in utero or even to their mother in her own childhood (Gowland, 2015; Klaus, 2014).

What does seem clear is that whatever portion of the population is or is not stressed, they are all reacting morphologically in a predictable manner provided other impacts and influences on their skeletal system. This means that “catch up growth” does not completely erase the effects of early stress and while an individual may still reach their genetically predetermined stature the architecture and morphology of their long bones will be permanently if only subtly altered (Hughes-Morey, 2016; Ruff et al., 1994). A question which could in part be addressed using data from this study is whether or not a pattern exists for non-survivors in the young adult age category as that relates to the presence or absence of childhood stress indicators. Assuming early stress predisposes an individual to adverse immune reactions and complications from pathology they would be most vulnerable during their late adolescence and early adulthood when “catch up growth” occurs. This is reflected in Dewitte’s (2014) analysis of age and stress during the “black death” epidemic (also see (DeWitte & Stojanowski, 2015)). Childhood stress could contribute to or explain the typical mortuary profile which sees an increase in mortality in early adulthood. Those deceased individuals may also have a variant long bone morphology which was an additional symptom of their stressed state.

7.3.1.3.2 Trauma

Trauma, unlike all of the other IVs considered is episodic and temporary. The biological reaction and healing time will be dependent on the severity of the injury, the individual’s health and nutrition at the time as well as their ability to rest and be cared for and trauma may cause the onset of DJD or OA or even limit future mobility, but most injuries eventually heal. Trauma was only able to uniquely explain cross-sectional femoral geometry and the proximal femoral epiphysis in the Sudanese population. However, for something as temporary as trauma, that it has lasting effects particularly on the morphology of the femoral epiphysis is notable.

There are three possible explanations for why trauma is so significant. Early trauma may lead to continual traumatic incidents. That is an individual injured particularly in early childhood may have permanent mobility issues or in the case of head trauma might have difficulty with motor control or culturally have a higher likelihood of being targeted in interpersonal violence. The morphology of their epiphyses could then be impacted by the initial trauma which heals and disappears, but other traumatic incidents continue to occur throughout the individual’s life. In the second scenario the trauma and skeletal morphology are caused by the individual’s social status. That is trauma is incidental to or symptomatic of stress caused by low status which also happens to have ontogenetic effect on skeletogenesis (Klaus, 2014). The final explanation is that the individual survives the trauma long

enough for diaphyseal morphology to modify, but not long enough to heal either due to protracted convalescence or additional complications.

There are two notable ways trauma might influence morphological change in uninjured bones. First, trauma particularly trauma which involves the bone either via fracture or injury to the tendon or ligament will trigger inflammation. Inflammation triggers a release of cortisol and other hormones that under ideal circumstances promote osteoblastic activity, fight infection, and heal the injury (DeWitte, 2014; Waldron, 2009). However, particularly in biologically stressed individuals threshold levels for activation may be too high to be triggered with the normal release of biochemicals. This will cause a delayed response to healing and more of these chemicals to be released causing them to have a higher likelihood of activating other stress responses throughout the body.

The second way trauma might influence uninjured bones is by causing a significant alteration or cessation in activity. In an extreme case, trauma can lead to paralysis causing the effected limb or limbs to wither and therefore resulting in particular in endosteal and trabecular resorption. Even where the injury does not cause paralysis it may cause a temporary loss of activity particularly in the lower limbs. This was well reflected in data here as trauma's effect on morphology was most notable in the femur. This suggests that people when injured spend enough time recovering and sufficiently change their ambulatory practices relative to the rest of their population to alter the morphology of their bones. This means that in understanding the relationship between trauma and skeletal morphology the question is not simply how long a bone might take to heal, but how long it takes for bone to start experiencing resorption or wasting and how long it takes for a person who has sufficiently healed to become ambulatory again to regain enough bone mass to render them statistically indistinguishable from the rest of their population.

7.3.1.3.3 DJD

DJD and OA have multiple etiologies. They may be acquired due to trauma, overuse, underuse, hormonal reaction, complications from disease or poor diet, auto-immune disorder, or genetic predisposition (Frost, 1999; Grenier et al., 2014; Jurmain, 1999; Jurmain et al., 2012; Laiguillon et al., 2014; Reginato & Olsen, 2002; J. Rogers & Waldron, 1989; Weiss & Jurmain, 2007; Zhang et al., 2014). To fully explore the aetiology of osteoarthritis and how the diagnosis of OA and the understanding of OA patterning in particular have informed osteoarchaeology is well beyond the reach of this thesis. What this thesis has shown is that there exists some relationship between appendicular DJD and OA and proximal long bone morphology particularly in the diaphysis.

As suggested by the shotgun style list of possible aetiologies above and as stressed by multiple authors most notably Jurmain (1999; Jurmain et al., 2012) the presence or absence or patterning of DJD and OA is not sufficient to characterize activity patterns. However, DJD and OA could be influenced biomechanically by skeletal morphology or morphology and DJD or OA could result from similar aetiologies particularly where DJD and OA are related to hormones, or activity or lack of activity. The relationship here is likely to be one of correlation rather than causation. Even with this stipulation taken into account many of the aetiologies likely responsible for some DJD and OA could also relate to morphology including level of biological stress and genetic predisposition.

Another notable and relevant aspect of DJD and OA is they are continual once acquired. DJD and OA never heal. Once osteophytes are formed or cartilage is damaged the effects are permanent. Cartilage being avascular and its matrix being extracellular repair requires subchondral vascularization (porosity) which in and of itself may interfere with the cartilage (Frost, 1999; Laiguillon et al., 2014; Siebelt et al., 2014). Conversely, Rothschild (1997) could not find a correlation between porosity and OA. Treatment of and medical research regarding OA largely focuses on understanding chemical pathways and reducing further damage to the cartilage rather than attempting to repair it (Finnegan et al., 2014; Gawri et al., 2014; Laiguillon et al., 2014; McQueen et al., 2014; Shin et al., 2014; Siebelt et al., 2014; Toumi et al., 2014; Willett et al., 2014; Zhang et al., 2014). This means the inflammation incited by damage to the joint would become chronic and have lasting although likely subtle repercussions on the hormonal and endocrine system. Even if the individual does not suffer sufficient chronic pain to limit locomotion or activity once acquired, DJD and OA would cause continual release of stress related hormones as a result of the continual damage to the joint cartilage. In one of the more surprising results of this study proximal femoral epiphyseal morphology could be explained both by Schmorl's nodes and by DJD and OA severity. There are several possible explanations for this, but a genetically predetermined morphology or high levels of stress hormones from an early age seem to be the best supported.

Literature also shows a direct relationship between DJD and OA and joint surface morphology. In considering force distribution it is straightforward to assume that the greater the force applied to a joint surface, the larger and flatter that joint surface should be to distribute the force and avoid damage in the course of normal compression (Frost, 1999; Hamrick, 1996; Organ & Ward, 2006). During development then body mass helps determine the final shape and form of a joint to ensure that cartilaginous capsules experience enough compression to remain healthy but not so much as to damage them. However, juvenile activity and body mass may not be predictive of adult activity and weight. As

diaphyses continue to reform throughout life, it is possible their specific morphology in relation to DJD and OA severity is related to an attempt by the biological system to limit damage to the joint capsule in relation to weight bearing activity.

7.3.2 Population differences

Every measure of morphology examined in this research was uniquely explained by site. Given previous uses of GMM this is not surprising (Claude et al., 2004; Viðarsdóttir et al., 2002b; Viscosi & Cardini, 2011). Geometric Morphometrics is very useful for determining between population morphological differences. The question however is why those morphological differences exist. This research only included adult humans from medieval and postmedieval sites. While some morphological variation was expected and observed these individuals were all more alike than different (Relethford, 2009, 2010; Relethford & Harpending, 1994; Relethford & Lees, 1982). What do these between site morphological variations mean and why does site impact other IVs and their effect on long bone morphology.

This study included four sites and each of these sites had major differences from the other three. If population variation were based solely on geographical distance then 3-J-18, the site from Sudan, would always have been the most different from the other three sites which were from England. If population variation were based solely on temporal distance then Coach Lane, the lone postmedieval site would have been the most different from the other three medieval sites. If socioeconomic status were the primary means of difference Hereford as the most elite site would have been most different and if urban or rural living was the sole arbitrator of morphological distinction then Coach Lane and Fishergate would have been different from 3-J-18 and Hereford. In fact what we have in the results is a more complex situation than any of those scenarios. Post-hoc results for cross-sectional geometry show a clear distinction between the Sudanese and English sites. But when looking at PC1 in the epiphyseal results Coach Lane is often the most different and will pool with 3-J-18. 3-J-18 also is not consistently morphologically distinct from Hereford and Fishergate.

As outlined above variations in site profiles which could have influence on morphology are as follows: terrain, climate, subsistence or nutrition, temporality, socio-economic background, pathogen and parasite load, and activity level (Blom et al., 2005; Cardini, Jansson, et al., 2007; Frost, 1994; Gowland, 2015; Meiri & Dayan, 2003; Millien et al., 2006; Ruff, Holt, & Trinkaus, 2006; Sullivan, 2005; Vercellotti et al., 2014). Particularly given the archaeological nature of this study these variables may not

be separated, and will influence one another as well as morphology, pathology, biological stress, and likelihood of trauma.

Coach Lane, Hereford, and Fishergate were all English sites with 3-J-18 the only site located outside of England. Here Bergman's rule seems to apply as the individuals in 3-J-18 were anecdotally smaller than those from the English sites who would have been born, lived, and died in a much colder climate (Bindon & Baker, 1997; Cardini, Jansson, et al., 2007; Meiri & Dayan, 2003; Millien et al., 2006). However, allometric results show that the Sudanese population is not always or consistently the smallest and most gracile. Bindon and Baker (1997) attempt to demonstrate how activation of the "thrifty gene" may explain the failure of Bergman's rule to consistently apply to human populations. However, there are several other possibilities for why the Sudanese population who lived in a much warmer climate are so close in size to their English counterparts thousands of miles from the equator. The Sudanese population enjoyed year round sunshine which only cultural practice could inhibit meaning that they likely had better vitamin D levels than the English populations which in turn likely gave them an immunological, nutritional, and growth advantage over their English counterparts (Ives & Brickley, 2014; Mays, Brickley, et al., 2009; Sakamoto et al., 2013).

Diet is also important and related to climate and environment. Contemporary documentation reports that people living in this area of Sudan raised cattle for beef and dairy which means while their diets could have been low in folic acid and vitamin C, their B₁₂ and calcium intake, both of which are implicated in development and growth particularly in reference to osteological health, should have been optimal (Ginns, 2006; Honkanen et al., 1996; López et al., 1996; Sullivan, 2005; P. L. Walker et al., 2009). Conversely, and possibly the cause of the comparable cribra orbitalia observed in both the English and Sudanese populations the individuals examined from 3-J-18 lived in an environment where tropical parasites and pathogens can survive. While their diet may have been high in meat and dairy, some of these parasites particularly malaria can inhibit absorption of B₁₂ and calcium therefore inhibiting development and impacting general health (Gowland & Western, 2012; Smith-Guzmán, 2015; Sullivan, 2005). Those from the English sites particularly Fishergate – due to its proximity to a very polluted water source – would have been similarly at risk from parasitic infection particularly from the ingestion of fish – an important component of the English Christian diet – but they would not have been at risk from malaria (Sullivan, 2005).

Cultural moors including the European traditions regarding Christian fasting would have dictated nutrition in particular for the English sites. (The individuals at 3-J-18 are buried in a Church yard and are

presumably Christian, but the Christianity they practiced varied significantly from Catholicism or Protestantism and in fact may not be correctly characterized as Coptic Christianity. Inferences regarding European dietary restrictions in reference to religious practice therefore do not apply (Edwards, 2004).) This is especially true for Hereford which was a medieval cemetery attached to a monastery. Many of those there interred might have been monks, and while they enjoyed an apparently sedentary lifestyle, they likely observed traditions of fasting (Barrow, 1999; D. Walker, 1964). Fasting in medieval Christianity usually means substituting fish for beef or pork, but some historical individuals were noted for taking fasting to extremes for reasons either regarding their own interpretation of religion or that of those around them. It is not apparent or noted that that is the case for any of those included in this study, but it is notable and in extreme cases would cause at least endosteal resorption (Šlaus, 2000).

Social status would have dictated diet throughout life including variety and quality of food. It also would have had impact on stress, physical activity, and medical care or ability to avoid pathogens (Havelková et al., 2011; Mays, Ives, et al., 2009; Sullivan, 2005). These factors all may not directly alter the morphology of the bone, but they do impact adult stature, longevity, and amount of physical labour or weight-bearing activity all of which will have at least indirect morphological impact (Angel et al., 1987; Currey, 2003; Hughes-Morey, 2016; Ruff et al., 2013; Watts, 2015). Social status is however difficult to unravel. Hereford probably housed the richest individuals with the lowest amount of physiological stress, but as monks while it is likely many of these individuals came from wealthy backgrounds they may not all have done so. Coach Lane and 3-J-18, are sufficiently culturally removed from both Fishergate and Hereford that it is not useful to speculate on how they may be relatively placed on a socio-economic scale. Coach Lane individuals likely lived in polluted conditions and the individuals from 3-J-18 have comparable rates of traumatic injury to those from Fishergate. But as they were from completely different places and times where they were socially relative to those from Fishergate and Hereford is unknown. This variation or similarity in their status however probably contributes to their final skeletal morphology as it would have dictated how long and how hard they worked, how much physical danger they were susceptible to, nutrition, and medical care.

Population differences very clearly play into morphological variation. However given available population size and multiple variables likely to influence morphology at death no clear cause-effect relationships should be made. Studying additional populations in similar ways may increase understanding of these complex influences, but this is an area unlikely to provide a straightforward answer.

7.4 Research Limitations

Several limitations came up in the course of this study and even while selecting materials and methodology which might impact how results should be understood. Some of these issues could be potentially addressed in future research, others might be selectively corrected by choosing different or additional methods, and others – like the osteological paradox – were unavoidable and demand an educated theoretical approach. These are detailed below.

7.4.1 Sample size

This research required complete and relatively undamaged long bones from an archaeological context. (In the case of 3-J-18 preservation was so excellent that some individuals or some bones had to be excluded due to desiccated soft tissue obscuring the surface of the bone) The methodology was also time consuming and required dedicated use of a 3D laser scanner. Each bone took on average two hours to scan. These two issues severely reduced the number of individuals and the number of their bones which could be included in this study. In the case of Hereford where preservation is relatively good nineteen individuals make up the collection but only twelve met the requirements for this study. Due to institutional time constraints only thirty individuals from 3-J-18 could be included. Additionally, archaeological sites do not consistently lend large numbers of individuals and Klaus (2014) correctly cautions that sites should not be considered complete populations. I have previously explained how my choice of statistical methods escapes the issue of having more variables than samples (in this case bones or individuals), but this has the limitation that there are statistical questions that may not be asked of this data. In some cases this could be overcome by gathering more, but where the question is applied to a given site this is insurmountable as no more individuals from that site will meet the requirements for this research.

7.4.2 Osteological paradox

No study of health of individuals in an archaeological context would be complete without a discussion of the Osteological Paradox and how it applies. Beyond the simple interpretation that deceased individuals are dead and therefore not a representative sample of the living there are certain aspects of the paradox which apply directly to this research. Wood and colleagues (1992) discuss how hidden heterogeneity influences risk of death and therefore not only makes demographics difficult to interpret without the application of theoretical models, but also how risk of death or lesions should be

interpreted as they interact with other factors which are likely unknown to the archaeologist. This study seems like it might escape those issues but in fact due to what is known about the impact of in particular, stress and its relationship to size, shape, longevity, and development there is no aspect of this study that should not be understood within the theoretical limits of the Osteological Paradox.

Between population variation was not a major concern of this research and examined to understand the impact of that type of variation on other factors. However, the contrast of the individuals from various sites relies somewhat on the very assumption this research is meant to combat: that populations are homogenous and stationary, and that the selection of deceased individuals examined in the study are sufficiently representative of the population as they were when they were alive. In addition to Wood and colleagues (1992), the theoretical complications of this implicit assumption is suggested or outright stated by other authors examining similar themes (DeWitte & Stojanowski, 2015; Klaus, 2014). The solution to this is fairly straightforward; understand samples of deceased individuals as members of a population who did not survive. But this then impacts comparison with individuals from other populations as their health profile would likely be different, and even within population comparison particularly when trying to determine age (Gowland, 2007; C O Lovejoy et al., 1985; Osborne et al., 2004).

Populations in this study did show differing rates of pathology. Individuals from Fishergate and 3-J-18 showed more trauma than those from Hereford and Coach Lane. Additionally, Sudanese population showed higher rates of cribra orbitalia than all but Coach Lane. As they lived in a hot environment with rough terrain and there are historical accounts of them raising cattle for meat and dairy their trauma may be associated with the rough terrain and dangers of working with large animals and their cribra orbitalia is likely a result of malaria (Edwards, 2004; Ginns, 2006; Gowland & Western, 2012; Soler, 2012). The English populations show higher rates of LEH, Schmorl's nodes, and DJD. Their terrain was more forgiving, but England is famously temperate to cold and it is reasonable to assume that most individuals in the English populations were likely vitamin D deficient which would have left them at risk for developing immunological disorders, exacerbating their chances of a hormonal or endocrinal response which would lead to DJD, and made them more susceptible to infectious disease (Mays, Brickley, et al., 2009; Mays, Ives, et al., 2009; McDade, 2003; Sorensen et al., 2009). Two of the three English populations were also urban meaning they would have been exposed to parasites and pollutants daily. Conversely both of the two urban populations studied existed after the Black Death

meaning that these individuals survived or descended from survivors and would not have the epigenetic or genetic frailties associated with plague victims (Dewitte, 2014).

According to Wood and colleagues (1992) there are two possibilities for populations with lesions. They could represent stressed individuals who succumbed to the disease before the lesion healed or they could represent stronger individuals who survived long enough for the lesion to form. All cemeteries sampled in this study show some individuals with each of the lesions examined (and the Sudanese population also shows signs of Hansen's disease in some individuals), but what this says for the comparison of health profiles between the populations is harder to pinpoint. A final point regarding the inherent selection bias of individuals in this study is that each of the cemeteries sampled were associated with a specific Church meaning all the individuals in this study were or belonged to families who were sufficiently known by the Church and community that they could gain entrance to the cemetery at death. For 3-J-18 this is particularly significant as space was limited by the geology of the area, but even for Fishergate where individuals might have joined only because the tithe was low, there still existed basic community requirements for inclusion (Ginns, 2006; Soler, 2012). This underscores that the deceased individuals examined cannot stand as surrogates for the entirety of their living community.

DJD and OA – which correspond well with morphological variation in almost all areas of the proximal long bones – themselves are not directly life threatening, but many authors regard them as indicators of population stress (Jurmain, 1977; KAR Kennedy, 1998; Klaus, 2014; Lovell, 1994; Šlaus, 2000; Sofaer-Derevenski, 2000; Weiss et al., 2012). It should be noted that most of these publications refer to axial rather than appendicular osteoarthritis. Stature, and therefore long bone form if not shape has long been noted as related to stress during development (Angel et al., 1987; Benjamin Miller Auerbach, 2008; Currey, 2003; Ruff et al., 1994). Frost (1994) and Hamrick (1999) also directly link childhood activity and conditions to auricular development. With all this considered adding in the context of the Osteological Paradox there are two overarching scenarios for how DJD and OA might develop and correspond with specific morphological profiles. In one scenario stressed or frail versus unstressed or resilient individuals have different and distinct morphological profiles and the stressed or frail individuals due to the morphology of their long bones are more at risk for trauma or microtrauma that would lead to DJD and OA whereas an unstressed or resilient individuals due to consistent uninterrupted development throughout their childhood have morphologies better equipped to avoid micro-traumas and other inciting incidents. Morphology causes DJD and OA. In the second scenario

stressed or frail individuals have disparate morphology due to interruptions in their development, but also have stressed immune systems more prone to having adverse reactions or needing higher activation levels in the event of any assault on the system meaning for these individuals DJD and OA might develop even without micro-trauma simply due to an immune or endocrinal response. Morphology is incidental to DJD and OA. In both cases DJD and OA may be mechanically induced meaning that unstressed or resilient individuals are still at risk, but the aetiology is different.

7.4.3 What GMM does not capture

GMM has the advantage of allowing discussion of morphology in a numerical or statistical fashion without immediately introducing size. However, one should understand the limitations of the method. GMM can discuss size, but shape change with size or allometry is not immediately obvious. Somewhat related to this GMM works to algebraically calculate mean shape which means selection of points could cause statistically morphological artifacts if only one or a few points vary particularly if they do so far from the centroid (Pinocchio effect (Bookstein, 2016; Klingenberg, 2013; Klingenberg & McIntyre, 1998; Viscosi & Cardini, 2011; J. A. Walker, 2000)). GMM is largely reliant upon homology which as Bookstein is wont to remind us (Bookstein, 1991, 2000, 2009; K. Schaefer & Bookstein, 2009) is basically never satisfied in biological systems. GMM being based on landmarks is also unable to capture otherwise notable features like lesions, enthesal changes, and non-metric traits unless those are specifically accounted for. GMM can be a very useful means of discussing shape and its impact on biological systems, ontogeny, evolution and speciation, population variation, sexual dimorphism, and increasingly biomechanics and pathology. However, while this study attempted to collect pertinent shape data to the research questions posed, this same shape data may not be useful in other studies, nor does it describe even the entirety of the bones studied.

It is tempting to view semilandmarks as an escape from the tyranny of the wireframe but there are two issues. Semilandmarks are just a more complex wireframe and their algebraic components are meant to eradicate irregularities (Bookstein, 2000; Gunz et al., 2005b). Semilandmarks are algebraically designed to “slide” to the position that causes the least amount of morphological disparity within the line or surface. This does escape the necessity of homologous points and eliminates user error or statistical artifacts due to even spacing, but it means semilandmarks cannot capture small subtle differences that biologically speaking might be crucial. Furthermore, it is possible in some cases that semilandmarks actually introduce error into the sample as Benazzi and colleagues could not replicate results using semilandmarks (2011). This does not nullify the results from studies like this one which

utilise semilandmarks, but it does underscore the importance of checking for error, and replication in scientific studies.

This research attempted to contextualize results within a broader understanding of stress. Biologically speaking however, stress often begins in utero or during childhood and so stress can and has been linked to stature, limb proportions, and research generally concerned with size (Angel et al., 1987; Benjamin Miller Auerbach, 2008; Hughes-Morey, 2016; Ruff et al., 2005; Ruff, Holt, Sládek, et al., 2006; Shaw & Stock, 2011). In this research size and its consequences (allometry) were only briefly considered (Klingenberg, 1998, 2016; Klingenberg & Zimmermann, 1992; Lieberman et al., 2007; Mitteroecker et al., 2013c). In this study allometry was directly examined in the context of sex and population, although results showed that centroid size could often be linked with multiple factors to explain morphology. GMM can be used to contextualize shape and is especially useful for studies of ontogeny and sexual dimorphism. These are logical outshoots from this research. Other obvious size related GMM studies which could be undertaken from data in this study include an examination of in particular the knee joint in relation to size and in reference to the biomechanical necessities of bipedal locomotion within different terrains (Organ & Ward, 2006; Rabey et al., 2015; Shackelford & Trinkaus, 2002; Stevens & Viðarsdóttir, 2008) and an examination of diaphyseal surface morphology within the context of Frelat and colleagues note regarding distortion of shape due to the length of the z axis in GMM studies of long bones (Frelat et al., 2012).

Finally, it is important to bring up one final issue with Geometric Morphometrics. Kendall's shape space exists to allow objects to be understood in a non-Euclidean manner. However, this strictly means that once projected back into Euclidean space there is distortion because shape space is curved. In biological studies this is not considered problematic because biological structures are never so morphologically anomalous that this distortion would become notable (Mitteroecker & Huttegger, 2009). Provided the research is not on two functionally disparate but homologous structures such as Bookstein's example of a human and fish mandibles, no statistical issues arise from the distortion of projection from Kendall's shape space to Euclidean space (Bookstein, 2000; Kendall, 1989).

7.4.4 Number of cross-sections and ability to use morphometrics on all of them

The cross-sections examined morphologically and geometrically in this study came only from the midshaft. There were two reasons for this. For one, this study did not focus exclusively on cross-sections and that part of the study was meant as a comparative measure to the other morphological tests. For another particularly in regards to the humeral cross-section which is usually sampled at 40% of the

diaphysis rather than 50% to avoid the deltoid tuberosity, morphological examinations of in particular the distal diaphyses would have required the additional development or adaptation of methodology (Ruff, 2002). Cross-sections from the distal portion of the humeral and femoral diaphysis can be very round and featureless in shape particularly in gracile individuals. While semilandmarks do not mathematically require bordering homologous points, the methodology is facilitated by homologous points (Bookstein, 2000; Gunz et al., 2005a). Wilson and Humphrey (2015) escape this issue by not using semilandmarks at all and adjusting the process of Procrustes rotation and translation. This is an area for future research because as Wilson and Humphrey discuss, there are issues with interpreting data from semilandmarks as they slide and therefore do not always reflect the same morphology and because simply placing homologous points around a largely featureless outline also produces statistical artifacts. Wilson and Humphrey's argument on this point of the methodology are based on a study which compared homologous and semilandmark shape data (Benazzi et al., 2011), but which also is at odds with earlier work on the same subject (Gunz et al., 2005a). Which approach is best will depend on how data is collected and analysed.

Despite the methodological issues involved, this is an important area to expand into. Midshaft cross-sectional geometry and morphology only addresses the midshaft. This study showed the reactivity of the surface of the diaphysis and other studies have addressed at least with cross-sectional geometry cross-sections throughout the bone (Ruff & Hayes, 1982; L. A. B. Wilson & Humphrey, 2015; Yamanaka et al., 2005). At present the data here may be prepared to studies which only look at the midsection, but to be truly comparative, the sample should be expanded.

7.5 Future Research

Some direct questions arose from this research particularly in reference to the limitations in particular of sample size. The number of individuals included in this research is so small as to make the results easily impeachable. Particularly to draw conclusions regarding diaphyseal and cross sectional morphology as they stand further individuals and sites should be studied. However, the results are sufficient to suggest that for both diaphyseal and cross-sectional morphology there may be correlations to be found especially in regards to pathology. As most studies conclude, there should be more work done in this area. Another similar area of potential future research brought up frequently is adding a morphological analysis of cross-sections beyond just the midshaft. This would require some methodological development, however other authors have published on this vein (L. A. B. Wilson &

Humphrey, 2015; Yamanaka et al., 2005) and the usefulness of sampling along the entirety of the diaphysis has long been established (Ruff & Hayes, 1982). However these are not the only potential future research questions that could be inspired by this study. Further ideas will be discussed below.

7.5.1 Surface morphology of articular surfaces

Articular surfaces were explicitly avoided in this study due to the hypotheses made and the desire to include osteoarthritis as an independent variable. However, morphology of the articular surfaces is important in the context of activity and mobility research as well as research into the development or evolution of bipedal locomotion (Organ & Ward, 2006; Sylvester & Pfisterer, 2012; Weber et al., 2001). Aspects of the epiphysis and articular surface have already been attempted using homologous GMM studies. Particularly for evolutionary and primate studies, an exploration of the surface of the joint itself using semi landmarks might be more elucidating when considering weight-bearing and arborealism.

7.5.2 Internal architecture of the bone

This study did not examine any of the internal structure of the bone either the endosteum, the trabecular internal structures, or any of the microscopic structures. Examination of the latter using GMM might not be elucidating given that current research regarding microstructures and shape refers more to the interruption of Haversian canals by lamellar structures than an overall consistency of morphology, but the microstructure itself remains important for the understanding of structural integrity (Agarwal et al., 2004; Boel et al., 2007; Drapeau & Streeter, 2006; Rho et al., 2002; Vedi et al., 1996). Additionally, a combined microscopic and macroscopic understanding of morphology and remodeling both under normal or ideal conditions and in the process of reaction to pathological or traumatic incursion is useful for understanding how bone behaves within the system of a living individual and how that individual presents in the archaeological record. This sort of research would likely be destructive as imaging the microstructure of bone requires taking slices, but it would yield information that could be applied archaeologically and possibly medically.

There has been in this thesis some discussion of endosteal deposition and architecture particularly in relation to discussions of the cross-sections and diaphyses. O'Neil and Ruff (2004) demonstrated that latex cast modelling reasonably and non-invasively replicated cross-sectional results. Crucially however this method requires calculating the endosteal width from a radiograph. The information in this study only concerned the outer shape and form of the cross-section at midshaft and radiographs were not collected. Endosteal deposition and resorption is a useful indicator of health,

mobility, and the aging process (K Kennedy, 1989; Mays, 2000, 2001; O. M. Pearson & Lieberman, 2004; Ruff et al., 1994; Sparacello & Pearson, 2010). Additionally, in living individuals the medullary cavity is not empty but serves as a space for bone marrow. Understanding the shape and space of the medullary cavity in relation to the general health of the individual may explain nutritional stress and in some cases disease processes both in the form of anaemias and neoplastic disease.

If the endosteum is important then so is the trabecular structure of the bone. Jang and Kim (2008, 2010) have taken the biomechanical importance of trabecular bone to its logical extreme using computational models to determine the ideal cortical and trabecular structure in relation to biomechanical strain. However, they acknowledge that their approach only considers the mechanical aspect of bone and that a biological system is subject to complex signaling which will not always be mechanically ideal. Other authors also have examined trabeculae from an organizational and biomechanical perspective using experimental or theoretical methodology (Barak et al., 2011; Biewener et al., 1996; Boyle & Kim, 2011a; Van Lenthe & Huiskes, 2002). Insofar as this research was interested in Wolff's Law, research towards biomechanical optimization of the trabecular structure in relation to cortical bone is a reasonable continuation especially if paired with morphological studies of the articular surfaces. Speaking further to Jang and Kim's concerns regarding the biological system, Agarwal and colleagues (2004) examined the trabecular structure of vertebrae in relation to osteopenia. As with the endosteum it is tempting to understand the internal structure of the bone in a purely mechanical sense, but as a part of a biological system the trabeculae will remodel in response to hormonal activation, metabolic necessities, and pathological process in addition to biomechanical strain. Osteopenia and osteoporotic fractures are related to bone loss mostly in the trabeculae (Brickley, 2002; Riis et al., 1996; Vainionpää et al., 2005). This researched was informed by an interest in morphological reactions to osteopenia but ultimately failed to address questions in this area because the internal structure of the bone was not examined. This underscores the usefulness of pursuing studies of the internal architecture of the bone in reference to external morphology both from a biomechanical perspective and within the context of age related osteopenia or pathology.

7.5.3 Distal long bones

This study examined the humerus and femur because these being two of the largest long bones in the human body they were more likely to survive intact. Their size also facilitated 3D surface capture. At the outset of this study the surface morphology of smaller long bones particularly the ulna and radius could not be captured using the equipment available. These two problems of availability and

methodology are not insurmountable. There do exist skeletal collections with intact ulnae and radii (in fact 3-J-18 from this study is one such collection), and 3D images can be collected using white light techniques or a micro CT scanner. Distal long bones are interesting because they contextualize data gathered from the proximal long bones. For example in this study incidence of Schmorl's nodes was recorded but correlation between Schmorl's nodes and long bone morphology was dependent on numerous additional factors. However, Schmorl's nodes are very clearly related to the morphology of vertebrae (Plomp et al., 2013; Plomp, Viðarsdóttir, et al., 2015). Some pathologies or demographic factors may similarly be better correlated with the morphologies of distal long bones.

Distal long bones are also more sensitive particularly cortically to various impacts including metabolic issues accompanying osteopenia and biomechanical stress and strain. It is in fact somewhat *de rigueur* to examine the distal long bones in relation to these research questions (Drapeau & Streeter, 2006; Kohrt et al., 1997; Shaw & Stock, 2009a; Vainionpää et al., 2005). Drapeau and Streeter (2006) explain that humans may be considered sufficiently cursorial that our distal long bones particularly in our legs are costly to move and therefore must be light, but are also subject to tremendous stress and potential for injury in the natural course of bipedal movement. As a result the morphology of in particular the tibia is especially vulnerable or reactive to changes in activity and the environment. Shaw and Stock (2009a) show that roughly the opposite is true for the upper limb except where weight bearing activities directly impact the distal portion of the lower limb. In individuals who do not use their forearms regularly in weight-bearing activities, these smaller long bones are more susceptible or reactive to osteoporosis. (It then follows that weight-training is a useful means of preventing osteoporotic fractures in older women (Sievänen et al., 1996).) Assuming the equipment and collections to efficiently examine the distal long bones this is a natural progression for the research questions posed in this study.

7.5.4 Robusticity and Pathology

Emerging research is showing increasing relationship between development and robusticity and pathology. Sparacello and colleagues (2016) examined two Neolithic skeletons with tuberculosis lesions in relation to other contemporary skeletons. Their findings were that these two skeletons were comparatively gracile, but not outside of the normal distribution and concluded that this points towards a similar progression of disease for tuberculosis in the Neolithic and presently. This helps to further explain and support the observation that children with metabolic insults whether those are pathological

or nutritional experience delayed or stunted growth (Benjamin Miller Auerbach, 2008; Ruff et al., 2013; Schug & Goldman, 2014; Vercellotti et al., 2014).

Sparacello and colleagues (2016) further noticed a disparity in the patterning of cortical deposition in both individuals with tuberculosis and in their arms and legs. One of these individuals seems to have been mostly unable to walk around while the other appears to have been clearly ambulatory. Varying patterns seen in deposition for two individuals with the same disease suggests a multiplicity of differing individual morphological and cortical reactions with the additional study of other pathologies. Alternatively, tuberculosis causes wasting which while demonstrably within normal variation in regards to size, could cause slightly different morphologies in long bone diaphyseal surfaces.

7.5.5 Childhood Development and Ontogeny

This study suffered from a small sample size contributed to by the fact that many of the sites included were also small or had such degrees of taphonomy that the number of individuals who could be included in the study was quite low. It would thereby be statistically naïve to discuss interpopulation variation on the basis of morphological heterogeneity (Cardini & Elton, 2007). However, the sites were morphologically distinct. Viðarsdóttir and O'Higgins (Viðarsdóttir et al., 2002b) showed morphological cranial variation between populations was present in infants and that ontogenetic trajectories were population specific. Long bones and the post crania have considerably different functions, but if they show interpopulation morphological variation it follows that there may also be population specific ontogenetic trajectories in the post-crania. Furthermore, in this study – like much past research - sexual dimorphism was site specific (Bulygina et al., 2006; Işcan et al., 1998; Patriquin et al., 2005; Robinson & Bidmos, 2009; P. L. Walker, 2008). Particularly in reference to Cobb and O'Higgins (2007) observations of divergent ontogenetic trajectories for sexual dimorphism in great apes it is very likely that sexual dimorphism and its morphological effects on post-cranial morphology may be explained by these allometric and ontogenetic trajectories.

Another question which arose in this study was in regards to the morphology of the femoral epiphyses being explained by severity of DJD or the presence or absence of Schmorl's nodes. In Chapter 4 I posited that there were two likely explanations for this. Epiphyseal morphology and DJD or epiphyseal morphology and Schmorl's nodes could all be symptoms of the same underlying condition likely prolonged biological stress causing over activation of the immune system. Alternatively, studies have shown that the vertebrae of individuals with Schmorl's nodes are morphologically distinct from those without and that that morphology bears some similarity to that of earlier hominids (Plomp,

Viðarsdóttir, et al., 2015). Particularly because the epiphyseal morphology evincing variation with the presence or absence of Schmorl's nodes is in the hip and knee – both which describe the valgus angle, a key component in morphological adaption to bipedal locomotion – the vertebral morphology linked to Schmorl's nodes may be due to the same genetic cause that creates the femoral epiphyseal morphologies. That is, bipedal locomotion is not only impeded by the shape of the vertebrae; the hip and knee are affected as well. Alternatively, the hip and knee could be adapting against the morphology of the vertebrae to facilitate bipedal locomotion. However, both DJD and Schmorl's nodes generally have their onset in adulthood so were this to be researched it would have to be done via a longitudinal study imaging individuals throughout their lives.

In this study, childhood indicators of stress could not uniquely explain morphology. This suggests that observed variation in cortical deposition, longitudinal growth, and alterations in BMC are only reflected in those measurements (Bridges, 1989a; Mays, Ives, et al., 2009). However, as this study was only of adults it is possible that children with nutritional or pathological stress experience a different ontogenetic trajectory than their healthy counterparts. If that ontogenetic trajectory were delayed or development stopped early for some individuals this morphological variation may not be clear especially if individuals have different amounts of biological stress and react differently to the stress. Morphological variation with biological stress might only be clear by studying infants and children. This sort of study could be done longitudinally with imaging, although the ethics are questionable. It could also be researched in dry bone. The issue with the latter is that skeletonized individuals without indications of pathological infection are still deceased and by definition not healthy. When no lesions are present that may mean that the individual died for other reasons or it could mean that they died before any biological reaction was seen in the bone (Temple & Goodman, 2014; Wood et al., 1992).

7.6 Concluding Remarks

This study was interested in whether or not intra and interpopulation variation would be morphologically discernable in the proximal long bones. Another aim was to determine whether or not morphological analysis of the diaphyseal surface was useful to science and which parts of the bone were useful in understanding questions regarding pathology, sexual dimorphism, biological stress, and population affinity. The current scientific literature as it stands includes studies of long bone morphology using GMM, but most of these studies concern epiphyseal or cortical morphology, or use only homologous points (Bonnan, 2004, 2007; Bonnan et al., 2008; De Groote, 2011a, 2011b; De Groote

et al., 2010; Frelat et al., 2012; Kranioti, Bastir, et al., 2009; Vance & Steyn, 2013; L. A. B. Wilson & Humphrey, 2015). De Groote (2011b) uses two-dimensional semilandmarks along the diaphysis which allowed her to make conclusions regarding forearm muscle use in Neanderthals relative to humans. This on its own suggests that the morphology of the diaphysis itself contains important information. Frelat and colleagues (2012) provided an arithmetic means of overcoming the length of long bones where landmarking is such that shape variation is dominated by the length of the bone over all other elements. In the context of these prior studies, this research attempted to prove that diaphyseal three-dimensional surface shape could be linked to inter and intra population variation. It can. Diaphyseal surface shape has been shown in this study to be uniquely explained by site as well as DJD and OA severity. This study also showed that DJD and OA had the greatest effect on diaphyseal surface shape meaning that pathologies and degeneration do have some sort of morphological relationship with the diaphysis. As Sherrat (2015) and Adams (D. C. Adams & Otarola-Castillo, 2013a) continue to develop means by which archaeologists, osteoarchaeologists, evolutionary anthropologists, and paleontologists may study the morphology of deceased individuals and extinct species, and as De Groote, Bonnan, and Wilson prove the applicability of semilandmarks to diaphyseal morphology in particular it becomes incumbent upon particularly early career researchers to expand inquiry into these areas (Bonnan, 2004, 2007; Bonnan et al., 2008; De Groote, 2011a, 2011b; De Groote et al., 2010; L. A. B. Wilson & Humphrey, 2015).

The questions asked in this study were very general and the results were not expected to be positive. Yet, there were exciting revelations. Diaphyseal morphology is explained by degenerative conditions in the joint, and the proximal femoral epiphyseal morphology is uniquely explained by Schmorl's nodes as well as DJD and OA. This opens up new avenues of research. I have postulated on, but not answered why the proximal femur behaves in this manner. And if DJD and OA explains diaphyseal morphology in the proximal long bone, is the same true of the distal long bones? Could other conditions be linked to diaphyseal morphology? What can the relative thickness of the cortices say in relation to diaphyseal surface morphology? What roles do biomechanical and biological stress play? What is the role of hormones in ontogeny? Does modularity in ontogeny explain some of these results?

One of the most interesting and unexpected results was the relationship between the presence and absence of Schmorl's nodes and the proximal femur. Vertebral morphology, pelvic morphology, and the valgus angle at the femoral neck and at the knee allow for the bipedal locomotion central to human evolution and encephalization. Anderson and Trinkaus (1998) showed that femoral neck angle is related

to sedentism. With this developmental plasticity in mind, is the shape of the femoral head then in part dictated by the morphology of the vertebrae?

This study underscores the importance of choosing an informative morphological set appropriate to the research question as I have shown that some IVs better explain different parts of the bone than others. However, it also has shown the benefit of being somewhat exploratory. The diaphyseal surface is highly plastic particularly relative to the epiphyses, but it does not necessarily follow that cross-sectional geometry and morphology would provide different answers. This study has shown that it does. Additionally, the kind of landmarks chosen – homologous, 2D semilandmarks, 3D semilandmarks – are all likely to give different but useful information. The overall shape must also be considered as the selection of points will influence what aspects of morphological variation will be visible within a set. Different sets of points will emphasise different aspects of morphology. Additionally, the methodology used must be statistically appropriate to the research question and sample size. Some GMM statistical methodologies were not applied to this study because they did not answer the research questions, or the subdivided number of individuals was too small to support them. These methodologies and landmark selections will, however, be applicable to future research.

Diaphyseal plasticity and reactivity is underscored here. Digital techniques now exist where researchers can fully investigate questions regarding three-dimensional surfaces with increasing ease. This study has also created new questions about the effects of biological stress on morphology and pathology as well as the timing of development and ontogeny. Future research will, as always, elucidate these questions and bring more to bear.

8 Bibliography

- Adams, C. J. (2006). An Animal Manifesto Gender, Identity, and Vegan-Feminism in the Twenty-First Century. *Parallax*, 12(1), 120–128. <http://doi.org/10.1080/13534640500448791>
- Adams, D. C., & Otarola-Castillo, E. (2013a). geomorph: an R package for the collection and analysis of geometric morphometric shape data. *Methods in Ecology and Evolution*, 4(4), 393–399.
- Adams, D. C., & Otarola-Castillo, E. (2013b). Package “geomorph.”
- Adams, D. C., Rohlf, F. J., & Slice, D. E. (2004). Geometric morphometrics: Ten years of progress following the “revolution.” *Italian Journal of Zoology*, 71(1), 5–16. <http://doi.org/10.1080/11250000409356545>
- Adams, D. C., Rohlf, F. J., & Slice, D. E. (2013). A field comes of age: Geometric morphometrics in the 21st century. *Hystrix*, 24(1). <http://doi.org/10.4404/hystrix-24.1-6283>
- Aerssens, J., Boonen, S., Lowet, G., & Dequeker, J. (1998). Interspecies Differences in Bone Composition, Density, and Quality: Potential Implications for in Vivo Bone Research. *Endocrinology*, 139(2), 663–670.
- Agarwal, S. C. (2008). Light and Broken Bones: Examining and Interpreting Bone Loss and Osteoporosis in Past Populations. In M. A. Katzenberg & S. R. Saunders (Eds.), *Biological Anthropology of the Human Skeleton* (Second Edi, pp. 387–410). John Wiley & Sons, Inc.
- Agarwal, S. C. (2016). Bone Morphologies and Histories : Life Course Approaches in Bioarchaeology. *Yearbook of Physical Anthropology*, 159, 130–149. <http://doi.org/10.1002/ajpa.22905>
- Agarwal, S. C., Dumitriu, M., Tomlinson, G. A. a, & Gryn timer, M. D. D. (2004). Medieval trabecular bone architecture: the influence of age, sex, and lifestyle. *American Journal of Physical Anthropology*, 124(1), 33–44. <http://doi.org/10.1002/ajpa.10335>
- Agarwal, S. C., & Gryn timer, M. D. (2009). Measuring and Interpreting Age-related Loss of Vertebral Bone Mineral Density in a Medieval Population. *American Journal of Physical Anthropology*, 139, 244–252. <http://doi.org/10.1002/ajpa.20977>
- Agarwal, S. C., & Stout, S. D. (Eds.). (2004). *Bone Loss and Osteoporosis: An Anthropological Perspective. Bone Loss and Osteoporosis*. Kluwer Plenum Academic Press.
- Albanese, J., Cardoso, H. F. V, & Saunders, S. R. (2005). Universal methodology for developing univariate sample-specific sex determination methods: An example using the epicondylar breadth of the humerus. *Journal of Archaeological Science*, 32(1), 143–152. <http://doi.org/10.1016/j.jas.2004.08.003>
- Alunni-Perret, V., Staccini, P., & Quatrehomme, G. (2008). Sex determination from the distal part of the femur in a French contemporary population. *Forensic Science International*, 175(2–3), 113–117. <http://doi.org/10.1016/j.forsciint.2007.05.018>
- Anderson, F. H., Francis, R. M., & Faulkner, K. (1996). Androgen supplementation in eugonadal men with osteoporosis-effects of 6 months of treatment on bone mineral density and cardiovascular risk factors. *Bone*, 18(2), 171–177. [http://doi.org/10.1016/8756-3282\(95\)00441-6](http://doi.org/10.1016/8756-3282(95)00441-6)

- Anderson, J. B., & Garner, S. C. (1998). Phytoestrogens and bone. *Bailliere's Clinical Endocrinology and Metabolism*, 12(4), 543–557.
- Anderson, J. Y., & Trinkaus, E. (1998). Patterns of sexual, bilateral and interpopulational variation in human femoral neck-shaft angles. *Journal of Anatomy*, 192, 279–285.
- Angel, J. L., Kelley, J. O., Parrington, M., & Pinter, S. (1987). Life stresses of the free black community as represented by the First African Baptist Church, Philadelphia, 1823-1841. *American Journal of Physical Anthropology*, 74(2), 213–29. <http://doi.org/10.1002/ajpa.1330740209>
- Armelagos, G. J., Goodman, A. H., Harper, K. N., & Blakey, M. L. (2009). Enamel hypoplasia and early mortality: Bioarcheological support for the Barker hypothesis. *Evolutionary Anthropology*, 18(6), 261–271. <http://doi.org/10.1002/evan.20239>
- Armelagos, G. J., Goodman, A. H., & Jacobs, K. H. (2011). The Origins of Agriculture : Population Growth during a Period of Declining Health The Origins of Agriculture : Population Growth During a Period of Declining Health, 13(1), 9–22.
- Ashby, S., & Spall, C. (2005). Artefact and Environmental Evidence: Bone, Antler, Ivory and Horn Objects. In C. Spall & N. Toop (Eds.), *Blue Bridge Lane & Fishergate York.: Report on Excavations; July 2000 to July 2002*.
- Auerbach, B. M. (2008). Human skeletal variation in the New World during the Holocene: Effects of climate and subsistence across geography and time - Part I, 3295793, 1107.
- Auerbach, B. M., & Ruff, C. B. (2006). Limb bone bilateral asymmetry: variability and commonality among modern humans. *Journal of Human Evolution*, 50(2), 203–218. <http://doi.org/10.1016/j.jhevol.2005.09.004>
- Baab, K. L., McNulty, K. P., & Rohlf, F. J. (2012). The shape of human evolution: A geometric morphometrics perspective. *Evolutionary Anthropology*, 21(4), 151–165. <http://doi.org/10.1002/evan.21320>
- Baab, K. L., McNulty, K. P., & Rohlf, F. J. (2012). The shape of human evolution: a geometric morphometrics perspective. *Evolutionary Anthropology*, 21(4), 151–65. <http://doi.org/10.1002/evan.21320>
- Bacon, A. M. (2000). Principal components analysis of distal humeral shape in pliocene to recent African hominids: The contribution of geometric morphometrics. *American Journal of Physical Anthropology*, 111(4), 479–487. [http://doi.org/10.1002/\(SICI\)1096-8644\(200004\)111:4<479::AID-AJPA4>3.0.CO;2-#](http://doi.org/10.1002/(SICI)1096-8644(200004)111:4<479::AID-AJPA4>3.0.CO;2-#)
- Barak, M. M., Lieberman, D. E., & Hublin, J. J. (2011). A Wolff in sheep's clothing: Trabecular bone adaptation in response to changes in joint loading orientation. *Bone*, 49(6), 1141–1151. <http://doi.org/10.1016/j.bone.2011.08.020>
- Barker, D. J. P. (2003). Editorial: The Developmental Origins of Adult Disease, 18(8), 733–736.
- Barker, D. J. P. (2004). The developmental origins of well-being. *Philosophical Transactions: Biological Sciences*, 359(1449), 1359–1366. <http://doi.org/10.1098/rstb.2004.1518>

- Barrow, J. (1999). The Canons and Citizens of Hereford c. 1160 - c.1240. *Midland History*, 24(1), 1–23. <http://doi.org/10.1179/mdh.1999.24.1.1>
- Bašić, Ž., Anterić, I., Vilović, K., Petaros, A., Bosnar, A., Madžar, T., ... Anđelinović, Š. (2013). Sex determination in skeletal remains from the medieval Eastern Adriatic coast - discriminant function analysis of humeri. *Croatian Medical Journal*, 54, 272–8. <http://doi.org/10.3325/cmj.2013.54.272>
- Benazzi, S., Fiorenza, L., Katina, S., Bruner, E., & Kullmer, O. (2011). Quantitative assessment of interproximal wear facet outlines for the association of isolated molars. *American Journal of Physical Anthropology*, 144(2), 309–16. <http://doi.org/10.1002/ajpa.21413>
- Benítez, H. a., Lemic, D., Bažok, R., Gallardo-Araya, C. M., & Mikac, K. M. (2014). Evolutionary directional asymmetry and shape variation in *Diabrotica virgifera virgifera* (Coleoptera: Chrysomelidae): An example using hind wings. *Biological Journal of the Linnean Society*, 111(1), 110–118. <http://doi.org/10.1111/bij.12194>
- Biewener, A. A., Fazzalari, N. L., Konieczynski, D. D., & Baudinette, R. V. (1996). Adaptive changes in trabecular architecture in relation to functional strain patterns and disuse. *Bone*, 19(1), 1–8. [http://doi.org/10.1016/8756-3282\(96\)00116-0](http://doi.org/10.1016/8756-3282(96)00116-0)
- Bigoni, L., Velemínská, J., & Brůžek, J. (2010). Three-dimensional geometric morphometric analysis of cranio-facial sexual dimorphism in a Central European sample of known sex. *HOMO- Journal of Comparative Human Biology*, 61(1), 16–32. <http://doi.org/10.1016/j.jchb.2009.09.004>
- Bilezikian, J. P., Raisz, L. G., & Martin, T. J. (Eds.). (2008). *Principles of Bone Biology* (3rd ed.). Academic Press, Inc.
- Bindon, J. R., & Baker, P. T. (1997). Bergmann's Rule and the Thrifty Genotype. *American Journal of Physical Anthropology*, 210, 201–210.
- Blom, D. E., Buikstra, J. E., Keng, L., Tomczak, P. D., Shoreman, E., & Stevens-Tuttle, D. (2005). Anemia and childhood mortality: Latitudinal patterning along the coast of pre-Columbian Peru. *American Journal of Physical Anthropology*, 127(2), 152–169. <http://doi.org/10.1002/ajpa.10431>
- Boel, L. W., Boldsen, J. L., & Melsen, F. (2007). Double lamellae in trabecular osteons: Towards a new method for age estimation by bone microscopy. *HOMO- Journal of Comparative Human Biology*, 58(4), 269–277. <http://doi.org/10.1016/j.jchb.2006.08.007>
- Bogin, B. (1999). *Patterns of Human Growth. Journal of anatomy* (Second, Vol. 165). Cambridge University Press.
- Boldsen, J. L. (2007). Early childhood stress and adult age mortality—A study of dental enamel hypoplasia in the medieval Danish village of Tirup. *American Journal of Physical Anthropology*, 132(1), 59–66. <http://doi.org/10.1002/ajpa.20467>
- Boldsen, J. L., Milner, G. R., & Boldsen, S. K. (2015). Sex estimation from modern American humeri and femora, accounting for sample variance structure. *American Journal of Physical Anthropology*, 750(February), n/a-n/a. <http://doi.org/10.1002/ajpa.22812>
- Bonnan, M. F. (2004). Morphometric analysis of humerus and femur shape in Morrison sauropods: implications for functional morphology and paleobiology. *Paleobiology*, 30(3), 444–470.

[http://doi.org/10.1666/0094-8373\(2004\)030<0444:MAOHAF>2.0.CO;2](http://doi.org/10.1666/0094-8373(2004)030<0444:MAOHAF>2.0.CO;2)

- Bonnan, M. F. (2007). Linear and geometric morphometric analysis of long bone scaling patterns in jurassic neosauropod dinosaurs: Their functional and paleobiological implications. *Anatomical Record*, 290(9), 1089–1111. <http://doi.org/10.1002/ar.20578>
- Bonnan, M. F., Farlow, J. O., & Masters, S. L. (2008). Using Linear and Geometric Morphometrics To Detect Intraspecific Variability and Sexual Dimorphism In Femoral Shape In Alligator mississippiensis and Its Implications For Sexing Fossil Archosaurs. *The Society of Vertebrate Paleontology*, 28(2), 422–431. [http://doi.org/http://dx.doi.org/10.1671/0272-4634\(2008\)28\[422:ULAGMT\]2.0.CO;2](http://doi.org/http://dx.doi.org/10.1671/0272-4634(2008)28[422:ULAGMT]2.0.CO;2)
- Bookstein, F. L. (1991). *Morphometric tools for landmark data*. Cambridge: Cambridge University Press.
- Bookstein, F. L. (2000). Morphometrics, 1–11.
- Bookstein, F. L. (2009). Measurement, explanation, and biology: Lessons from a long century. *Biological Theory*, 4(1), 6–20.
- Bookstein, F. L. (2016). The Inappropriate Symmetries of Multivariate Statistical Analysis in Geometric Morphometrics. *Evolutionary Biology*, 1–37. <http://doi.org/10.1007/s11692-016-9382-7>
- Bord, S., Horner, A., Hembry, R. M., Reynolds, J. J., & Compston, J. E. (1996). Production of collagenase by human osteoblasts and osteoclasts in vivo. *Bone*, 19(1), 35–40. [http://doi.org/10.1016/8756-3282\(96\)00106-8](http://doi.org/10.1016/8756-3282(96)00106-8)
- Boyle, C., & Kim, I. Y. (2011a). Computational Simulation of Bone Remodeling using Design Space Topology Optimization. *Pamm*, 11(1), 97–98. <http://doi.org/10.1002/pamm.201110040>
- Boyle, C., & Kim, I. Y. (2011b). Three-dimensional micro-level computational study of Wolff's law via trabecular bone remodeling in the human proximal femur using design space topology optimization. *Journal of Biomechanics*, 44(5), 935–942. <http://doi.org/10.1016/j.jbiomech.2010.11.029>
- Brickley, M. (2002). An investigation of historical and archaeological evidence for age-related bone loss and osteoporosis. *International Journal of Osteoarchaeology*, 12(5), 364–371. <http://doi.org/10.1002/oa.635>
- Brickley, M., Mays, S. A., & Ives, R. (2005). Skeletal manifestations of vitamin D deficiency osteomalacia in documented historical collections. *International Journal of Osteoarchaeology*, 15(6), 389–403. <http://doi.org/10.1002/oa.794>
- Brickley, M., Mays, S. A., & Ives, R. (2007). An investigation of skeletal indicators of vitamin D deficiency in adults: Effective markers for interpreting past living conditions and pollution levels in 18th and 19th century Birmingham, England. *American Journal of Physical Anthropology*, 132(1), 67–79. <http://doi.org/10.1002/ajpa.20491>
- Brickley, M., & McKinley, J. I. (Eds.). (2004). *Guidelines to the Standards for Recording Human Remains*. Southampton: BABAO, IFA and individual authors.
- Bridges, P. (1989a). Changes in activities with the shift to agriculture in the southeastern United States.

Current Anthropology, 30(3), 385–394.

Bridges, P. (1989b). Spondylolysis and its relationship to degenerative joint disease in the prehistoric southeastern United States. *American Journal of Physical Anthropology*, 79, 321–329.

Bridges, P. (1991). Degenerative joint disease in hunter–gatherers and agriculturalists from the southeastern United States. *American Journal of Physical Anthropology*, 85, 379–391.

Bridges, P. (1994). Vertebral arthritis and physical activities in the prehistoric southeastern United States. *American Journal of Physical Anthropology*, 93, 83–93.

Brooks, S., & Suchey, J. M. (1990). Skeletal age determination based on the os pubis: a comparison of the Acsádi-Nemeskéri and Suchey-Brooks methods. *Human Evolution*, 5(3), 227–238.

Brothwell, D. R. (Ed.). (1963). *Dental Anthropology* (Vol. V). London: Pergamon Press LTD.

Brothwell, D. R. (1989). Relationship of tooth wear to ageing. In M. Y. Iscan (Ed.), *Age markers in the human skeleton* (pp. 303–316). Springfield, IL: Charles C Thomas.

Brown, K. M. (2015). Selective pressures in the human bony pelvis: Decoupling sexual dimorphism in the anterior and posterior spaces. *American Journal of Physical Anthropology*, 157(3), 428–440. <http://doi.org/10.1002/ajpa.22734>

Brown, K. R., Pollintine, P., & Adams, M. A. (2008). Biomechanical implications of degenerative joint disease in the apophyseal joints of human thoracic and lumbar vertebrae. *American Journal of Physical Anthropology*, 136(3), 318–26. <http://doi.org/10.1002/ajpa.20814>

Buikstra, J. A., & Ubelaker, D. H. (Eds.). (1994). *Standards for Data Collection from Human Skeletal Remains: Proceedings of a Seminar at the Field Museum of Natural History (Arkansas Archeological Report Research Series)*. Arkansas Archaeological Survey.

Bulygina, E., Mitteroecker, P., & Aiello, L. C. (2006). Ontogeny of facial dimorphism and patterns of individual development within one human population. *American Journal of Physical Anthropology*, 131(3), 432–43. <http://doi.org/10.1002/ajpa.20317>

Burr, D. B. (1980). The Relationships Among Physical, Geometrical and Mechanical Properties of Bone, With a Note on the Properties of Nonhuman Primate Bone. *Yearbook of Physical Anthropology*, 23, 109–146.

Cardini, A., & Elton, S. (2007). Sample size and sampling error in geometric morphometric studies of size and shape. *Zoomorphology*, 126(2), 121–134. <http://doi.org/10.1007/s00435-007-0036-2>

Cardini, A., & Elton, S. (2008a). Variation in guenon skulls (I): species divergence, ecological and genetic differences. *Journal of Human Evolution*, 54(5), 615–37. <http://doi.org/10.1016/j.jhevol.2007.09.022>

Cardini, A., & Elton, S. (2008b). Variation in guenon skulls (II): sexual dimorphism. *Journal of Human Evolution*, 54(5), 638–647. <http://doi.org/10.1016/j.jhevol.2007.09.023>

Cardini, A., Jansson, A.-U., & Elton, S. (2007). A geometric morphometric approach to the study of ecogeographical and clinal variation in vervet monkeys. *Journal of Biogeography*, 34(10), 1663–1678. <http://doi.org/10.1111/j.1365-2699.2007.01731.x>

- Cardini, A., Thorington, R. W., & Polly, P. D. (2007). Evolutionary acceleration in the most endangered mammal of Canada: speciation and divergence in the Vancouver Island marmot (Rodentia, Sciuridae). *Journal of Evolutionary Biology*, 20(5), 1833–46. <http://doi.org/10.1111/j.1420-9101.2007.01398.x>
- Cardoso, F. A., & Henderson, C. Y. (2010). Enthesopathy formation in the humerus: Data from known age-at-death and known occupation skeletal collections. *American Journal of Physical Anthropology*, 141(4), 550–60. <http://doi.org/10.1002/ajpa.21171>
- Chamberlain, A. T. (2006). *Demography in archaeology*. Cambridge University Press. <http://doi.org/10.1017/CBO9780511607165>
- Chen, J. H., Liu, C., You, L., & Simmons, C. A. (2010). Boning up on Wolff's Law: Mechanical regulation of the cells that make and maintain bone. *Journal of Biomechanics*, 43(1), 108–118. <http://doi.org/10.1016/j.jbiomech.2009.09.016>
- Christie, N. (2002). Medieval Britain and Ireland in 2001. *Medieval Archaeology*, 46(1), 125–264. <http://doi.org/10.1179/med.2002.46.1.125>
- Churchill, S. E., & Morris, A. G. (1998). Muscle marking morphology and labour intensity in prehistoric Khoisan foragers. *International Journal of Osteoarchaeology*, 8(5), 390–411. [http://doi.org/10.1002/\(SICI\)1099-1212\(1998090\)8:5<390::AID-OA435>3.0.CO;2-N](http://doi.org/10.1002/(SICI)1099-1212(1998090)8:5<390::AID-OA435>3.0.CO;2-N)
- Cignoni, P., & Ranzuglia, G. (2014). MeshLab. Visual Computing Lab - ISTI - CNR.
- Claude, J., Pritchard, P., Tong, H., Paradis, E., & Auffray, J.-C. (2004). Ecological correlates and evolutionary divergence in the skull of turtles: a geometric morphometric assessment. *Systematic Biology*, 53(6), 933–48. <http://doi.org/10.1080/10635150490889498>
- Cobb, S. N., & O'Higgins, P. (2007). The ontogeny of sexual dimorphism in the facial skeleton of the African apes. *Journal of Human Evolution*, 53(2), 176–90. <http://doi.org/10.1016/j.jhevol.2007.03.006>
- Confavreux, C. B., Levine, R. L., & Karsenty, G. (2009). A paradigm of integrative physiology, the crosstalk between bone and energy metabolisms. *Molecular and Cellular Endocrinology*, 310(1–2), 21–29. <http://doi.org/10.1016/j.mce.2009.04.004>
- Cooper, C., Javaid, M. K., Taylor, P., Walker-Bone, K., Dennison, E., & Arden, N. (2002). The Fetal Origins of Osteoporotic Fracture. *Calcified Tissue International*, 70, 391–394. <http://doi.org/10.1007/s00223-001-0044-z>
- Coquerelle, M., Bookstein, F. L., Braga, J., Halazonetis, D. J., Weber, G. W., & Mitteroecker, P. (2011). Sexual dimorphism of the human mandible and its association with dental development. *American Journal of Physical Anthropology*, 145(2), 192–202. <http://doi.org/10.1002/ajpa.21485>
- Cox, M. (2000). Ageing adults form the skeleton. In M. Cox & S. Mays (Eds.), *Human osteology in archaeology and forensic science* (pp. 61–81). London: Greenwich Medical Media.
- Craps, D. D. (2015). *Exploring New Research Avenues for Osteoarthritis and Rheumatoid Arthritis in Palaeopathology : Interdisciplinary Approaches Focusing on Methodological Techniques*. Durham University.

- Cucina, A., Vargiu, R., Mancinelli, D., Ricci, R., Santandrea, E., Catalano, P., & Coppa, A. (2006). The necropolis of Vallerano (Rome, 2nd-3rd century AD): An anthropological perspective on the ancient Romans in the Suburbium. *International Journal of Osteoarchaeology*, 16(2), 104–117. <http://doi.org/10.1002/oa.808>
- Currey, J. D. (2003). The many adaptations of bone. *Journal of Biomechanics*, 36(10), 1487–1495. [http://doi.org/10.1016/S0021-9290\(03\)00124-6](http://doi.org/10.1016/S0021-9290(03)00124-6)
- Currey, J. D. (2004). Tensile yield in compact bone is determined by strain, post-yield behaviour by mineral content. *Journal of Biomechanics*, 37(4), 549–556. <http://doi.org/10.1016/j.jbiomech.2003.08.008>
- Currey, J. D., Brear, K., & Zioupos, P. (1996). The Effects of Ageing and Changes in Mineral Content in Degrading the Toughness of Human Femora. *Journal of Biomechanics*, 29(2), 257–260. <http://doi.org/10.1227/01.NEU.0000297048.04906.5B0>
- Davies, T. G., Shaw, C. N., & Stock, J. T. (2012). A test of a new method and software for the rapid estimation of cross-sectional geometric properties of long bone diaphyses from 3D laser surface scans. *Archaeological and Anthropological Sciences*, 4(4), 277–290. <http://doi.org/10.1007/s12520-012-0101-8>
- De Groote, I. (2011a). Femoral curvature in Neanderthals and modern humans: A 3D geometric morphometric analysis. *Journal of Human Evolution*, 60(5), 540–548. <http://doi.org/10.1016/j.jhevol.2010.09.009>
- De Groote, I. (2011b). The Neanderthal lower arm. *Journal of Human Evolution*, 61(4), 396–410. <http://doi.org/10.1016/j.jhevol.2011.05.007>
- De Groote, I., Lockwood, C. a, & Aiello, L. C. (2010). Technical note: A new method for measuring long bone curvature using 3D landmarks and semi-landmarks. *American Journal of Physical Anthropology*, 141(4), 658–64. <http://doi.org/10.1002/ajpa.21225>
- Dewitte, S. N. (2014). Health in Post-Black Death London (1350 – 1538): Age Patterns of Periosteal New Bone Formation in a Post-Epidemic Population. *American Journal of Physical Anthropology*, 155, 260–267. <http://doi.org/10.1002/ajpa.22510>
- DeWitte, S. N. (2014). Differential survival among individuals with active and healed periosteal new bone formation. *International Journal of Paleopathology*, 7, 38–44. <http://doi.org/10.1016/j.ijpp.2014.06.001>
- DeWitte, S. N., & Stojanowski, C. M. (2015). The Osteological Paradox 20 Years Later: Past Perspectives, Future Directions. *Journal of Archaeological Research*, 23(4), 397–450. <http://doi.org/10.1007/s10814-015-9084-1>
- Di Vincenzo, F., Churchill, S. E., & Manzi, G. (2012). The Vindija Neanderthal scapular glenoid fossa: Comparative shape analysis suggests evo-devo changes among Neanderthals. *Journal of Human Evolution*, 62(2), 274–285. <http://doi.org/10.1016/j.jhevol.2011.11.010>
- Djuric, M., Milovanovic, P., Janovic, A., Draskovic, M., Djukic, K., & Milenkovic, P. (2008). Porotic Lesions in Immature Skeletons from Stara Torina, Late Medieval Serbia. *International Journal of Osteoarchaeology*, 18, 458–475. <http://doi.org/10.1002/oa>

- Dohar, W. J. (1987). *Pastoral Care after the Black Death: the Diocese of Hereford, 1327-1404*. University of Toronto.
- Drapeau, M. S. M., & Streeter, M. a. (2006). Modeling and remodeling responses to normal loading in the human lower limb. *American Journal of Physical Anthropology*, 129(3), 403–9. <http://doi.org/10.1002/ajpa.20336>
- Duray, S. M. (1996). Dental indicators of stress and reduced age at death in prehistoric native Americans. *American Journal of Physical Anthropology*, 99(2), 275–286. [http://doi.org/10.1002/\(SICI\)1096-8644\(199602\)99:2<275::AID-AJPA5>3.0.CO;2-Y](http://doi.org/10.1002/(SICI)1096-8644(199602)99:2<275::AID-AJPA5>3.0.CO;2-Y)
- Eden, J. (1998). Phytoestrogens and the menopause. *Bailliere's Clinical Endocrinology and Metabolism*, 12(4), 581–587. [http://doi.org/10.1016/S0950-351X\(98\)80005-0](http://doi.org/10.1016/S0950-351X(98)80005-0)
- Edwards, D. N. (2004). *The Nubian Past: An Archaeology of the Sudan*. London: Routledge.
- Eerkens, J. W., Barfod, G. H., Jorgenson, G. a., & Peske, C. (2014). Tracing the mobility of individuals using stable isotope signatures in biological tissues: “locals” and “non-locals” in an ancient case of violent death from Central California. *Journal of Archaeological Science*, 41, 474–481. <http://doi.org/10.1016/j.jas.2013.09.014>
- Erickson, D., Thompson, T. J. U., & Rankin, B. W. J. (2014). The application of 3D visualization of osteological trauma for the courtroom: A critical review. *Journal of Forensic Radiology and Imaging*, 2(3), 132–137. <http://doi.org/10.1016/j.jofri.2014.04.002>
- Falk, D. (1980). Hominid Brain Evolution : The Approach From Paleoneurology. *Yearbook of Physical Anthropology*, 23, 93–107.
- Finnegan, S., Robson, J., Scaife, C., McAllister, C., Pennington, S. R., Gibson, D. S., & Rooney, M. E. (2014). Synovial membrane protein expression differs between juvenile idiopathic arthritis subtypes in early disease. *Arthritis Research & Therapy*, 16(1), R8. <http://doi.org/10.1186/ar4434>
- Foster, A., Buckley, H., & Tayles, N. (2014). Using Enthesis Robusticity to Infer Activity in the Past: A Review. *Journal of Archaeological Method and Theory*, 21(3), 511–533. <http://doi.org/10.1007/s10816-012-9156-1>
- Frassica, F. J., Inoue, N., Virolainen, P., & Chao, E. Y. S. (1997). Skeletal system: Biomechanical concepts and relationships to normal and abnormal conditions. *Seminars in Nuclear Medicine*, 27(4), 321–327. [http://doi.org/10.1016/S0001-2998\(97\)80004-9](http://doi.org/10.1016/S0001-2998(97)80004-9)
- Frelat, M. a, Katina, S., Weber, G. W., & Bookstein, F. L. (2012). Technical note: A novel geometric morphometric approach to the study of long bone shape variation. *American Journal of Physical Anthropology*, 0(February), 1–11. <http://doi.org/10.1002/ajpa.22177>
- Frost, H. M. (1994). Wolff's Law and bone's structural adaptations to mechanical usage: an overview for clinicians. *Angle Orthodontist*, 64(3), 175–188. [http://doi.org/10.1043/0003-3219\(1994\)064<0175:WLABSA>2.0.CO;2](http://doi.org/10.1043/0003-3219(1994)064<0175:WLABSA>2.0.CO;2)
- Frost, H. M. (1999). Joint anatomy, design, and arthroses: insights of the Utah paradigm. *The Anatomical Record*, 255(2), 162–74.

- Gaimster, M. (2011). *Post-medieval fieldwork in Britain, Northern Ireland and the Channel Isles in 2010*. *Post-Medieval Archaeology* (Vol. 45). <http://doi.org/10.1179/174581311X13135030529593>
- Gaimster, M., & O'Connor, K. (2006). Notes and News. *Medieval Archaeology*, 50(1), 243–400. <http://doi.org/10.1179/174581706x124266>
- Garn, S. M., & Baby, R. S. (1969). Bilateral Symmetry in Finer Lines of Increased Density. *American Journal of Physical Anthropology*, 31(1), 89–92.
- Gawri, R., Rosenzweig, D. H., Krock, E., Ouellet, J. a, Stone, L. S., Quinn, T. M., & Haglund, L. (2014). High mechanical strain of primary intervertebral disc cells promotes secretion of inflammatory factors associated with disc degeneration and pain. *Arthritis Research & Therapy*, 16(1), R21. <http://doi.org/10.1186/ar4449>
- Ginns, A. (2006). Preliminary Report on the Excavations Conducted on Mis Island (AKSC), 2005-2006. *Sudan & Nubia*, 10, 13–19.
- Ginns, A. (2007). *Preliminary Report on the Second Season of Excavations conducted on Mis Island (AKSC)*.
- Goldberg, P. J. P. (1992). *Women, work, and life cycle in a Medieval economy : women in York and Yorkshire c.1300-1520*. Oxford University Press.
- González, P. N., Bernal, V., Ivan Perez, S., & Barrientos, G. (2007). Analysis of dimorphic structures of the human pelvis: its implications for sex estimation in samples without reference collections. *Journal of Archaeological Science*, 34(10), 1720–1730. <http://doi.org/10.1016/j.jas.2006.12.013>
- Gonzalez, P. N., Bernal, V., & Perez, S. I. (2009). Geometric morphometric approach to sex estimation of human pelvis. *Forensic Science International*, 189(1–3), 68–74. <http://doi.org/10.1016/j.forsciint.2009.04.012>
- Goodman, A. H. (1991). Health, adaptation, and maladaptation in past societies. In H. Bush & M. Zvelebil (Eds.), *Health in past societies* (p. p 31–38). Oxford: Tempus Reparatum.
- Goodman, A. H., & Armelagos, G. J. (1985). Factors affecting the distribution of enamel hypoplasias within the human permanent dentition. *American Journal of Physical Anthropology*, 68, 479–493. <http://doi.org/10.1002/ajpa.1330680404>
- Goodman, A. H., & Rose, J. C. (1990). Assessment of systemic physiological perturbations from dental enamel hypoplasias and associated histological structures. *American Journal of Physical Anthropology*, 33(S11), 59–110. <http://doi.org/10.1002/ajpa.1330330506>
- Gowland, R. L. (2006). Aging in the past: examining age identity from funerary evidence. In R. L. Gowland & C. Knüsel (Eds.), *Social Archaeology of Funerary Remains* (pp. 143–154). Oxford: Oxbow.
- Gowland, R. L. (2007). Age, ageism and osteological bias: the evidence from late Roman Britain. *Journal of Roman Archaeology; Supplementary Series*, 65(November), 153–169.
- Gowland, R. L. (2015). Entangled lives: Implications of the developmental origins of health and disease hypothesis for bioarchaeology and the life course. *American Journal of Physical Anthropology*, 158(August), 530–540. <http://doi.org/10.1002/ajpa.22820>

- Gowland, R. L., & Western, A. G. (2012). Morbidity in the marshes: Using spatial epidemiology to investigate skeletal evidence for malaria in Anglo-Saxon England (AD 410-1050). *American Journal of Physical Anthropology*, 147(2), 301–311. <http://doi.org/10.1002/ajpa.21648>
- Gray, H. (1974). *Gray's Anatomy: Anatomy of the Human Body*. (C. M. Goss, Ed.) (Twenty-Nin). Philadelphia: Lea & Febiger.
- Green, H., & Curnoe, D. (2009). Sexual dimorphism in Southeast Asian crania: A geometric morphometric approach. *HOMO- Journal of Comparative Human Biology*, 60(6), 517–534. <http://doi.org/10.1016/j.jchb.2009.09.001>
- Green Swiontkowski, N. M. (1998). *Skeletal Trauma in Children, Third Edition*.
- Grenier, S., Bhargava, M. M., & Torzilli, P. a. (2014). An in vitro model for the pathological degradation of articular cartilage in osteoarthritis. *Journal of Biomechanics*, 47(3), 645–52. <http://doi.org/10.1016/j.jbiomech.2013.11.050>
- Guide, Q., & Sherratt, E. (2015). Quick Guide to Geomorph v.2. 1 . 3, (March), 1–71.
- Gunz, P. (2012). Evolutionary Relationships Among Robust and Gracile Australopiths: An “Evo-devo” Perspective. *Evolutionary Biology*, 39(4), 472–487. <http://doi.org/10.1007/s11692-012-9185-4>
- Gunz, P., & Mitteroecker, P. (2013). Semilandmarks: a method for quantifying curves and surfaces. *Hystrix, the Italian ...*, (May). <http://doi.org/10.4404/hystrix-24.1-6292>
- Gunz, P., Mitteroecker, P., & Bookstein, F. L. (2005a). Semilandmarks in Three Dimensions. In *Modern Morphometrics in Physical Anthropology* (pp. 73–98). http://doi.org/10.1007/0-387-27614-9_3
- Gunz, P., Mitteroecker, P., & Bookstein, F. L. (2005b). Semilandmarks in Three Dimensions. In *Modern Morphometrics in Physical Anthropology* (pp. 73–98). http://doi.org/10.1007/0-387-27614-9_3
- Haduch, E., Szczepanek, A., Skrzat, J., Środek, R., & Brzegowy, P. (2009). Residual Rickets or Osteomalacia: A Case Dating from the 16–18th Centuries from Krosno Odrzańskie, Poland. *International Journal of Osteoarchaeology*, 19, 593–612. <http://doi.org/10.1002/oa>
- Hamrick, M. W. (1996). Articular size and curvature as determinants of carpal joint mobility and stability in strepsirhine primates. *Journal of Morphology*, 230(2), 113–27. [http://doi.org/10.1002/\(SICI\)1097-4687\(199611\)230:2<113::AID-JMOR1>3.0.CO;2-I](http://doi.org/10.1002/(SICI)1097-4687(199611)230:2<113::AID-JMOR1>3.0.CO;2-I)
- Hamrick, M. W. (1999). A chondral modeling theory revisited. *Journal of Theoretical Biology*, 201(3), 201–8. <http://doi.org/10.1006/jtbi.1999.1025>
- Hanihara, T. (1992). Negritos, Australian Aborigines, and the “proto-sundadont” dental pattern: The basic populations in East Asia, V. *American Journal of Physical Anthropology*, 88(2), 183–196. <http://doi.org/10.1002/ajpa.1330880206>
- Hanihara, T. (1996). Comparison of craniofacial features of major human groups. *American Journal of Physical Anthropology*, 99(3), 389–412. [http://doi.org/10.1002/\(SICI\)1096-8644\(199603\)99:3<389::AID-AJPA3>3.0.CO;2-S](http://doi.org/10.1002/(SICI)1096-8644(199603)99:3<389::AID-AJPA3>3.0.CO;2-S)
- Hanihara, T. (2000). Frontal and facial flatness of major human populations. *American Journal of Physical Anthropology*, 111(1), 105–134. [http://doi.org/10.1002/\(SICI\)1096-8644\(200001\)111:1<105::AID-](http://doi.org/10.1002/(SICI)1096-8644(200001)111:1<105::AID-)

- Hanihara, T. (2008). Morphological variation of major human populations based on nonmetric dental traits. *American Journal of Physical Anthropology*, 136(2), 169–182.
<http://doi.org/10.1002/ajpa.20792>
- Hanihara, T., & Ishida, H. (2001). Frequency variations of discrete cranial traits in major human populations. I. Supernumerary ossicle variations. *Journal of Anatomy*, 198(6), 689–706.
<http://doi.org/10.1046/j.1469-7580.2001.19930251.x>
- Hanihara, T., & Ishida, H. (2009). Regional differences in craniofacial diversity and the population history of Jomon Japan. *American Journal of Physical Anthropology*, 139(3), 311–322.
<http://doi.org/10.1002/ajpa.20985>
- Harmon, E. H. (2007). The shape of the hominoid proximal femur: A geometric morphometric analysis. *Journal of Anatomy*, 210(2), 170–185. <http://doi.org/10.1111/j.1469-7580.2006.00688.x>
- Harmon, E. H. (2009). The shape of the early hominin proximal femur. *American Journal of Physical Anthropology*, 139(2), 154–71. <http://doi.org/10.1002/ajpa.20966>
- Harrigan, T. P., & Hamilton, J. J. (1992). Optimality conditions for finite element simulation of adaptive bone remodeling. *International Journal of Solids and Structures*, 29(23), 2897–2906.
[http://doi.org/10.1016/0020-7683\(92\)90147-L](http://doi.org/10.1016/0020-7683(92)90147-L)
- Harvati, K. (2009). Into Eurasia : A geometric morphometric re-assessment of the Upper Cave (Zhoukoudian) specimens. *Journal of Human Evolution*, 57(6), 751–762.
<http://doi.org/10.1016/j.jhevol.2009.07.008>
- Havelková, P., Villotte, S., Velemínský, P., Poláček, L., & Dobisíková, M. (2011). Enthesopathies and activity patterns in the Early Medieval Great Moravian population: Evidence of division of labour. *International Journal of Osteoarchaeology*, 21(4), 487–504. <http://doi.org/10.1002/oa.1164>
- Hawkes, K. (2003). Grandmothers and the evolution of human longevity. *American Journal of Human Biology*, 15(3), 380–400. <http://doi.org/10.1002/ajhb.10156>
- Hawkey, D. E. (1998). Disability, compassion and the skeletal record: using musculoskeletal stress markers (MSM) to construct an osteobiography from early New Mexico. *International Journal of Osteoarchaeology*, 8(5), 326–340. [http://doi.org/10.1002/\(SICI\)1099-1212\(1998090\)8:5<326::AID-OA437>3.0.CO;2-W](http://doi.org/10.1002/(SICI)1099-1212(1998090)8:5<326::AID-OA437>3.0.CO;2-W)
- Henderson, C. Y. (2009). *Musculo-Skeletal Stress Markers in Bioarchaeology: Indicators of Activity Levels or Human Variation? A re-analysis and Interpretation*. University of Durham.
- Henderson, P. H., Sowers, M., Kutzko, K. E., & Jannausch, M. L. (2000). Bone mineral density in grand multiparous women with extended lactation. *American Journal of Obstetrics and Gynecology*, 182(6), 1371–1377. <http://doi.org/10.1067/mob.2000.107468>
- Hennessy, R. J., Lane, A., Kinsella, A., Larkin, C., O’Callaghan, E., & Waddington, J. L. (2004). 3D morphometrics of craniofacial dysmorphology reveals sex-specific asymmetries in schizophrenia. *Schizophrenia Research*, 67(2–3), 261–8. <http://doi.org/10.1016/j.schres.2003.08.003>

- Hennessy, R. J., & Stringer, C. B. (2002). Geometric morphometric study of the regional variation of modern human craniofacial form. *American Journal of Physical Anthropology*, 117(1), 37–48. <http://doi.org/10.1002/ajpa.10005>
- Herrera, B., Hanihara, T., & Godde, K. (2014). Comparability of multiple data types from the bering strait region: Cranial and dental metrics and nonmetrics, mtDNA, and Y-chromosome DNA. *American Journal of Physical Anthropology*, 154(3), 334–348. <http://doi.org/10.1002/ajpa.22513>
- Herring, D. A., Saunders, S. R., & Katzenberg, M. A. (1998). Investigating the weaning process in past populations. *American Journal of Physical Anthropology*, 105(4), 425–439. [http://doi.org/10.1002/\(SICI\)1096-8644\(199804\)105:4<425::AID-AJPA3>3.0.CO;2-N](http://doi.org/10.1002/(SICI)1096-8644(199804)105:4<425::AID-AJPA3>3.0.CO;2-N)
- Hillson, S. (2005a). *Teeth* (2nd ed.). Cambridge: Cambridge University Press.
- Hillson, S. (2005b). *Teeth* (Second Edi). Cambridge University Press. [http://doi.org/10.1002/1521-3773\(20010316\)40:6<9823::AID-ANIE9823>3.3.CO;2-C](http://doi.org/10.1002/1521-3773(20010316)40:6<9823::AID-ANIE9823>3.3.CO;2-C)
- Hillson, S., & Bond, S. (1997). Relationship of enamel hypoplasia to the pattern of tooth crown growth: A discussion. *American Journal of Physical Anthropology*, 104(1), 89–103. [http://doi.org/10.1002/\(SICI\)1096-8644\(199709\)104:1<89::AID-AJPA6>3.0.CO;2-8](http://doi.org/10.1002/(SICI)1096-8644(199709)104:1<89::AID-AJPA6>3.0.CO;2-8)
- Hillson, S., Grigson, C., & Bond, S. (1998). Dental defects of congenital syphilis. *American Journal of Physical Anthropology*, 107(1), 25–40. [http://doi.org/10.1002/\(SICI\)1096-8644\(199809\)107:1<25::AID-AJPA3>3.0.CO;2-C](http://doi.org/10.1002/(SICI)1096-8644(199809)107:1<25::AID-AJPA3>3.0.CO;2-C)
- Holst, M. R. (2005). *Fishergate House Artefacts and Environmental Evidence: The Human Bone*. York.
- Honkanen, R., Pulkkinen, P., Järvinen, R., Kröger, H., Lindstedt, K., Tuppurainen, M., & Uusitupa, M. (1996). Does lactose intolerance predispose to low bone density? A population-based study of perimenopausal Finnish women. *Bone*, 19(1), 23–28. [http://doi.org/10.1016/8756-3282\(96\)00107-X](http://doi.org/10.1016/8756-3282(96)00107-X)
- Hughes-Morey, G. (2016). Interpreting adult stature in industrial London. *American Journal of Physical Anthropology*, 159(1), 126–134. <http://doi.org/10.1002/ajpa.22840>
- Humphries, A. L., Maxwell, A. B., Ross, A. H., & Ubelaker, D. H. (2015). A Geometric Morphometric Study of Regional Craniofacial Variation in Mexico. *International Journal of Osteoarchaeology*, 25(6), 795–804. <http://doi.org/10.1002/oa.2345>
- Hunter, J., & Cox, M. (2005). *Forensic Archaeology: Advances in the Theory and Practice*. <http://doi.org/10.4324/9780203970300>
- Introna Jr, F., Di Vella, G., & Campobasso, C. Pietro. (1998). Sex Determination by Discriminant Analysis of patella measurements. *Forensic Science International*, 95, 39–45.
- İşcan, M. Y., Loth, S. R., King, C. A., Shihai, D., & Yoshino, M. (1998). Sexual dimorphism in the humerus: a comparative analysis of Chinese, Japanese and Thais. *Forensic Science International*, 98, 17–29. [http://doi.org/10.1016/S0379-0738\(98\)00119-4](http://doi.org/10.1016/S0379-0738(98)00119-4)
- İşcan, M. Y., Loth, S. R., & Wright, R. (1984). Age estimation from the rib by phase analysis: white males. *Journal of Forensic Sciences*, 29(4), 1094–1104.

- İşcan, M. Y., Loth, S. R., & Wright, R. (1985). Age estimation from the rib by phase analysis: white females. *Journal of Forensic Sciences*, 30(3), 853–863.
- Ives, R., & Brickley, M. (2014). New findings in the identification of adult vitamin D deficiency osteomalacia: Results from a large-scale study. *International Journal of Paleopathology*, 7, 45–56. <http://doi.org/10.1016/j.ijpp.2014.06.004>
- Jacobs, C. R., Levenston, M. E., Beaupré, G. S., Simo, J. C., & Carter, D. R. (1995). Numerical instabilities in bone remodeling simulations: The advantages of a node-based finite element approach. *Journal of Biomechanics*, 28(4). [http://doi.org/10.1016/0021-9290\(94\)00087-K](http://doi.org/10.1016/0021-9290(94)00087-K)
- Jang, I. G., & Kim, I. Y. (2008). Computational study of Wolff's law with trabecular architecture in the human proximal femur using topology optimization. *Journal of Biomechanics*, 41(11), 2353–2361. <http://doi.org/10.1016/j.jbiomech.2008.05.037>
- Jang, I. G., & Kim, I. Y. (2010). Computational simulation of simultaneous cortical and trabecular bone change in human proximal femur during bone remodeling. *Journal of Biomechanics*, 43(2), 294–301. <http://doi.org/10.1016/j.jbiomech.2009.08.012>
- Jurmain, R. D. (1977). Stress and the etiology of osteoarthritis. *American Journal of Physical Anthropology*, 46, 353–366.
- Jurmain, R. D. (1980). The pattern of involvement of appendicular degenerative joint disease. *American Journal of Physical Anthropology*, 53, 143–150.
- Jurmain, R. D. (1999). *Stories from the skeleton. Behavioral reconstruction in human osteology*. Williston, VT,: Gordon and Breach Publishers.
- Jurmain, R. D., Cardoso, F. A., Henderson, C. Y., & Villotte, S. (2012). Bioarchaeology's Holy Grail: the Reconstruction of Activity. In A. L. Grauer (Ed.), *A Companion to Paleopathology* (pp. 531–552). Wiley-Blackwell.
- Kaastad, T. S., Huiskes, R., Reikeras, O., & Nordsletten, L. (2000). Effects of hormonal conditions and drugs on both muscle and bone strength can be assessed in a single rat test. *Bone*, 26(4), 355–60. [http://doi.org/10.1016/S8756-3282\(00\)00240-4](http://doi.org/10.1016/S8756-3282(00)00240-4)
- Kachel, A. F., & Premo, L. S. (2012). Disentangling the Evolution of Early and Late Life History Traits in Humans. *Evolutionary Biology*, 39(4), 638–649. <http://doi.org/10.1007/s11692-012-9169-4>
- Kamegai, T., Kruragano, S., & Hanihara, K. (1982). Secular change of dentofacial morphology during Japanese historic ages. *Journal of Anthropology Society Nippon*, 90(3), 303–314.
- Karapanou, O., & Papadimitriou, A. (2010). Determinants of menarche. *Reproductive Biology and Endocrinology : RB&E*, 8, 115. <http://doi.org/10.1186/1477-7827-8-115>
- Katz, D., & Suchey, J. M. (1986). Age Determination of the Male Os Pubis. *American Journal of Physical Anthropology*, 69, 427–435.
- Katzenberg, M. A., Herring, D. A., & Saunders, S. R. (1996). Weaning and infant mortality: evaluating the skeletal evidence. *Yearbook of Physical Anthropology*, 39, 177–199. [http://doi.org/10.1002/\(SICI\)1096-8644\(1996\)23+<177::AID-AJPA7>3.0.CO;2-2](http://doi.org/10.1002/(SICI)1096-8644(1996)23+<177::AID-AJPA7>3.0.CO;2-2)

- Kendall, D. (1989). A survey of the statistical theory of shape. *Statistical Science*, 4(2), 87–99.
- Kennedy, K. (1989). Skeletal Markers of Occupational Stress. In Y. Iscan & K. A. R. Kennedy (Eds.), *Reconstruction of Life From the Skeleton* (pp. 129–160). New York: Wiley-Liss.
- Kennedy, K. (1998). Markers of occupational stress: conspectus and prognosis of research. *International Journal of Osteoarchaeology*, 8(July), 305–310.
- King, G., & Henderson, C. Y. (2014). Living cheek by jowl: The pathoecology of medieval York. *Quaternary International*, 341, 131–142. <http://doi.org/10.1016/j.quaint.2013.07.032>
- Kinnally, E. L. (2014). Epigenetic Plasticity Following Early Stress Predicts Long-Term Health Outcomes in Rhesus Macaques, 155, 192–199. <http://doi.org/10.1002/ajpa.22565>
- Klaus, H. D. (2014). Frontiers in the Bioarchaeology of Stress and Disease : Cross-Disciplinary Perspectives From Pathophysiology , Human Biology , and Epidemiology , 155, 294–308. <http://doi.org/10.1002/ajpa.22574>
- Klaus, H. D., Larsen, C. S., & Tam, M. E. (2009). Economic Intensification and Degenerative Joint Disease : Life and Labor on the Postcontact North Coast of Peru, 139(October 2008), 204–221. <http://doi.org/10.1002/ajpa.20973>
- Klingenberg, C. P. (1998). Heterochrony and allometry: the analysis of evolutionary change in ontogeny. *Biological Reviews of the Cambridge Philosophical Society*, 73(1), 79–123.
- Klingenberg, C. P. (2013). Visualizations in geometric morphometrics: How to read and how to make graphs showing shape changes. *Hystrix*, 24(1), 1–10. <http://doi.org/10.4404/hystrix-24.1-7691>
- Klingenberg, C. P. (2015). Analyzing Fluctuating Asymmetry with Geometric Morphometrics: Concepts, Methods, and Applications. *Symmetry*, 7, 843–934. <http://doi.org/10.3390/sym7020843>
- Klingenberg, C. P. (2016). Size, shape and form: concepts of allometry in geometric morphometrics. *Development Genes and Evolution*, (April), 1–25. <http://doi.org/10.1007/s00427-016-0539-2>
- Klingenberg, C. P., Barluenga, M., & Meyer, A. (2002). Shape analysis of symmetric structures: quantifying variation among individuals and asymmetry. *Evolution; International Journal of Organic Evolution*, 56(10), 1909–20.
- Klingenberg, C. P., & McIntyre, G. (1998). Geometric morphometrics of developmental instability: analyzing patterns of fluctuating asymmetry with Procrustes methods. *Evolution*, 52(5), 1363–1375.
- Klingenberg, C. P., & McIntyre, G. S. (1998). Geometric Morphometrics of Developmental Instability : Analyzing Patterns of Fluctuating Asymmetry with Procrustes Methods. *Evolution*, 52(5), 1363–1375.
- Klingenberg, C. P., & Nijhout, H. F. (1999). Genetics of Fluctuating Asymmetry: A Developmental Model of Developmental Instability. *Evolution*, 53(2), 358–375.
- Klingenberg, C. P., & Zimmermann, M. (1992). Static, ontogenetic, and evolutionary allometry: a multivariate comparison in nine species of water striders. *American Naturalist*, 140(4), 601–20.

- Knüsel, C. J., Goggel, S., & Lucy, D. (1997). Comparative degenerative joint disease of the vertebral column in the medieval monastic cemetery of the Gilbertine Priory of St. Andrew, Fishergate, York,. *American Journal of Physical ...*, (103), 481–495.
- Koehler, K., Braun, H., Achtzehn, S., Hildebrand, U., Predel, H. G., Mester, J., & Schänzer, W. (2012). Iron status in elite young athletes: Gender-dependent influences of diet and exercise. *European Journal of Applied Physiology*, 112(2), 513–523. <http://doi.org/10.1007/s00421-011-2002-4>
- Kohrt, W. M., Ehsani, A. A., & Birge, S. J. (1997). Effects of Exercise Involving Predominantly Either Joint-Reaction or Ground-Reaction Forces on Bone Mineral Density in Older Women. *J Bone Miner Res*, 12(8), 1253–1261. <http://doi.org/10.1359/jbmr.1997.12.8.1253>
- Kranioti, E. F., Bastir, M., Sánchez-Meseguer, A., & Rosas, A. (2009). A geometric-morphometric study of the cretan humerus for sex identification. *Forensic Science International*, 189(1–3), 2–9. <http://doi.org/10.1016/j.forsciint.2009.04.013>
- Kranioti, E. F., & Michalodimitrakis, M. (2009). Sexual dimorphism of the humerus in contemporary cretans - A population-specific study and a review of the literature. *Journal of Forensic Sciences*, 54(5), 996–1000. <http://doi.org/10.1111/j.1556-4029.2009.01103.x>
- Kranioti, E. F., Vorniotakis, N., Galiatsou, C., İşcan, M. Y., & Michalodimitrakis, M. (2009). Sex identification and software development using digital femoral head radiographs. *Forensic Science International*, 189(1–3). <http://doi.org/10.1016/j.forsciint.2009.04.014>
- Laiguillon, M.-C., Houard, X., Bougault, C., Gosset, M., Nourissat, G., Sautet, A., ... Sellam, J. (2014). Expression and function of visfatin (Nampt), an adipokine-enzyme involved in inflammatory pathways of osteoarthritis. *Arthritis Research & Therapy*, 16(1), R38. <http://doi.org/10.1186/ar4467>
- Langthorn, J. Y. (n.d.). *Assessment of the human remains from Coach Lane, North Shields, North Tyneside, Tyne and Wear, COL10*.
- Larsen, C. S. (1997). *Bioarchaeology*. Cambridge: Cambridge University Press.
- Larsen, C. S. (2002). Bioarchaeology : The Lives and Lifestyles of Past People. *Journal of Archaeological Research*, 10(2), 119–166.
- Lee, N. K., & Karsenty, G. (2008). Reciprocal regulation of bone and energy metabolism. *Trends in Endocrinology and Metabolism*, 19(5), 161–166. <http://doi.org/10.1016/j.tem.2008.02.006>
- Lee, N. K., Sowa, H., Hinoi, E., Ferron, M., Ahn, J. D., Confavreux, C., ... Karsenty, G. (2007). Endocrine Regulation of Energy Metabolism by the Skeleton. *Cell*, 130(3), 456–469. <http://doi.org/10.1016/j.cell.2007.05.047>
- Leiberman, D. E., Devlin, M. J., & Pearson, O. M. (2001). Articular area response to mechanical loading: effects of exercise, age, and skeletal location. *American Journal of Physical Anthropology*, 116(June 2000), 266–277.
- Leigh, S. R. (2006). Cranial ontogeny of Papio baboons (Papio hamadryas). *American Journal of Physical Anthropology*, 130(1), 71–84. <http://doi.org/10.1002/ajpa.20319>

- Lele, S. R., & Richtsmeier, J. T. (2001a). *An invariant approach to statistical analysis of shapes*. London: Chapman and Hall-CRC Press.
- Lele, S. R., & Richtsmeier, J. T. (2001b). *An Invariant Approach to Statistical Analysis of Shapes*. Boca Raton, London, New York, Washington D.C.: Chapman & Hall/CRC.
- Lewis, M. E. (2006). *The Bioarchaeology of Children*. *New England Journal of Medicine* (Vol. 323). <http://doi.org/10.1017/CBO9780511542473>
- Lewis, M. E., Shapland, F., & Watts, R. (2016). The influence of chronic conditions and the environment on pubertal development: An example from medieval England. *International Journal of Paleopathology*, 12, 1–10. <http://doi.org/10.1016/j.ijpp.2015.10.004>
- Lieberman, D. E., Carlo, J., Ponce de León, M., & Zollikofer, C. P. (2007). A geometric morphometric analysis of heterochrony in the cranium of chimpanzees and bonobos. *Journal of Human Evolution*, 52(6), 647–662. <http://doi.org/10.1016/j.jhevol.2006.12.005>
- Lieberman, D. E., Polk, J. D., & Demes, B. (2004). Predicting long bone loading from cross-sectional geometry. *American Journal of Physical Anthropology*, 123(2), 156–171. <http://doi.org/10.1002/ajpa.10316>
- Linkhart, T. A., Mohan, S., & Baylink, D. J. (1996). Growth factors for bone growth and repair: IGF, TGF?? and BMP. *Bone*, 19(1 SUPPL.). [http://doi.org/10.1016/S8756-3282\(96\)00138-X](http://doi.org/10.1016/S8756-3282(96)00138-X)
- López, J. M., González, G., Reyes, V., Campino, C., & Díaz, S. (1996). Bone turnover and density in healthy women during breastfeeding and after weaning. *Osteoporosis International*, 6(2), 153–159. <http://doi.org/10.1007/BF01623940>
- Loth, S. R., İşcan, M. Y., & Scheuerman, E. H. (1994). Intercostal variation at the sternal end of the rib. *Forensic Science International*, 65(2), 135–143. [http://doi.org/10.1016/0379-0738\(94\)90268-2](http://doi.org/10.1016/0379-0738(94)90268-2)
- Lovejoy, C. O., Heiple, K. G., & Burstein, a H. (1973). The gait of Australopithecus. *American Journal of Physical Anthropology*, 38(3), 757–779. <http://doi.org/10.1002/ajpa.1330380315>
- Lovejoy, C. O., McCollum, M. a., Reno, P. L., & Rosenman, B. a. (2003). Developmental Biology and Human Evolution. *Annual Review of Anthropology*, 32, 85–109. <http://doi.org/doi:10.1146/annurev.anthro.32.061002.093223>
- Lovejoy, C. O., Meindl, R. S., Ohman, J. C., Heiple, K. G., & White, T. D. (2002). The Maka Femur and Its Bearing on the Antiquity of Human Walking : Applying Contemporary Concepts of Morphogenesis to the Human Fossil Record. *American Journal of Physical Anthropology*, 119, 97–133. <http://doi.org/10.1002/ajpa.10111>
- Lovejoy, C. O., Meindl, R. S., Pryzbeck, T. R., & Mensforth, R. P. (1985). Chronological metamorphosis of the auricular surface of the ilium: a new method for the determination of adult skeletal age at death. *American Journal of Physical Anthropology*, 68(1), 15–28. <http://doi.org/10.1002/ajpa.1330680103>
- Lovell, N. (1994). Spinal arthritis and physical stress at Bronze Age Harappa. *American Journal of Physical Anthropology*, 93, 149–164.

- Low, F. M., Gluckman, P. D., & Hanson, M. a. (2012). Developmental Plasticity, Epigenetics and Human Health. *Evolutionary Biology*, 39(4), 650–665. <http://doi.org/10.1007/s11692-011-9157-0>
- Lycett, S. J., & von Cramon-Taubadel, N. (2013). Understanding the comparative catarrhine context of human pelvic form: A 3D geometric morphometric analysis. *Journal of Human Evolution*, 64(4), 300–310. <http://doi.org/10.1016/j.jhevol.2013.01.011>
- Mall, G., Graw, M., Gehring, K. D., & Hubig, M. (2000). Determination of sex from femora. *Forensic Science International*, 113(1–3), 315–321. [http://doi.org/10.1016/S0379-0738\(00\)00240-1](http://doi.org/10.1016/S0379-0738(00)00240-1)
- Manica, A., Amos, W., Balloux, F., & Hanihara, T. (2007). The effect of ancient population bottlenecks on human phenotypic variation. *Nature*, 448(7151), 346–8. <http://doi.org/10.1038/nature05951>
- Marchi, D. (2015). Using the morphology of the hominoid distal fibula to interpret arboreality in *Australopithecus afarensis*. *Journal of Human Evolution*, 85, 136–148. <http://doi.org/10.1016/j.jhevol.2015.06.002>
- Marchi, D., Sparacello, V. S., Holt, B. M., & Formicola, V. (2006). Biomechanical approach to the reconstruction of activity patterns in Neolithic Western Liguria, Italy. *American Journal of Physical Anthropology*, 131(4), 447–455. <http://doi.org/10.1002/ajpa.20449>
- Márquez-Grant, N. (2015). An overview of age estimation in forensic anthropology: perspectives and practical considerations. *Annals of Human Biology*, 42(4), 308–322. <http://doi.org/10.3109/03014460.2015.1048288>
- Martin, R. B. (2003). Bones: structure and mechanics. *Journal of Biomechanics*. [http://doi.org/10.1016/S0021-9290\(03\)00033-2](http://doi.org/10.1016/S0021-9290(03)00033-2)
- May, R. L., Goodman, A. H., & Meindl, R. S. (1993). Response of bone and enamel formation to nutritional supplementation and morbidity among malnourished Guatemalan children. *American Journal of Physical Anthropology*, 92(1), 37–51. <http://doi.org/10.1002/ajpa.1330920104>
- Mays, S. A. (1985). The relationship between harris line formation and bone growth and development. *Journal of Archaeological Science*, 12(3), 207–220. [http://doi.org/10.1016/0305-4403\(85\)90021-4](http://doi.org/10.1016/0305-4403(85)90021-4)
- Mays, S. A. (1995). The Relationship between Harris Lines and other Aspects of Skeletal Development in Adults and Juveniles. *Journal of Archaeological Science*, 22, 511–520. <http://doi.org/10.1006/jasc.1995.0049>
- Mays, S. A. (1996). Age-dependent cortical bone loss in a medieval population. *International Journal of Osteoarchaeology*, 6(May 1995), 144–154.
- Mays, S. A. (2000). Age-dependent cortical bone loss in women from 18th and early 19th century London. *American Journal of Physical Anthropology*, 112(3), 349–361. [http://doi.org/10.1002/1096-8644\(200007\)112:3<349::AID-AJPA6>3.0.CO;2-0](http://doi.org/10.1002/1096-8644(200007)112:3<349::AID-AJPA6>3.0.CO;2-0)
- Mays, S. A. (2001). Effects of age and occupation on cortical bone in a group of 18th-19th century British men. *American Journal of Physical Anthropology*, 116(1), 34–44. <http://doi.org/10.1002/ajpa.1099>
- Mays, S. A. (2010). The Effects of Infant Feeding Practices on Infant and Maternal Health in a Medieval Community. *Childhood in the Past: An International Journal*, 3(1), 63–78.

<http://doi.org/10.1179/cip.2010.3.1.63>

- Mays, S. A. (2015a). Bone-formers and bone-losers in an archaeological population. *American Journal of Physical Anthropology*, 0(October), n/a-n/a. <http://doi.org/10.1002/ajpa.22912>
- Mays, S. A. (2015b). The effect of factors other than age upon skeletal age indicators in the adult. *Annals of Anatomy*, 42(4), 332–341. <http://doi.org/10.3109/03014460.2015.1044470>
- Mays, S. A., Brickley, M., & Ives, R. (2009). Growth and Vitamin D Deficiency in a Population from 19th Century Birmingham, England. *International Journal of Osteoarchaeology*, 19, 406–415. <http://doi.org/10.1002/oa.976>
- Mays, S. A., & Cox, M. (2000). Sex determination in skeletal remains. In M. Cox & S. A. Mays (Eds.), *Human osteology in archaeology and forensic science* (pp. 117–129). London: Greenwich Medical Media.
- Mays, S. A., Ives, R., & Brickley, M. (2009). The effects of socioeconomic status on endochondral and appositional bone growth, and acquisition of cortical bone in children from 19th century Birmingham, England. *American Journal of Physical Anthropology*, 140(3), 410–416. <http://doi.org/10.1002/ajpa.21076>
- McCane, B. (2013). Shape variation in outline shapes. *Systematic Biology*, 62(1), 134–46. <http://doi.org/10.1093/sysbio/sys080>
- McDade, T. W. (2003). Life history theory and the immune system: steps toward a human ecological immunology. *American Journal of Physical Anthropology, Suppl* 37(46), 100–25. <http://doi.org/10.1002/ajpa.10398>
- McDade, T. W., Reyes-García, V., Tanner, S., Huanca, T., & Leonard, W. R. (2008). Maintenance versus growth: Investigating the costs of immune activation among children in lowland Bolivia. *American Journal of Physical Anthropology*, 136(4), 478–484. <http://doi.org/10.1002/ajpa.20831>
- McEwan, J. M., Mays, S. A., & Blake, G. M. (2005). The relationship of bone mineral density and other growth parameters to stress indicators in a medieval juvenile population. *International Journal of Osteoarchaeology*, 15(3), 155–163. <http://doi.org/10.1002/oa.750>
- McNulty, K. P. (2006). Studying Ontogeny with Geometric Morphometrics.
- McNulty, K. P. (2009). Computing singular warps from Procrustes aligned coordinates. *Journal of Human Evolution*, 57(2), 191–4. <http://doi.org/10.1016/j.jhevol.2009.05.008>
- McNulty, K. P. (2012). Evolutionary Development in *Australopithecus africanus*. *Evolutionary Biology*, 39(4), 488–498. <http://doi.org/10.1007/s11692-012-9172-9>
- McNulty, K. P., Frost, S. R., & Strait, D. S. (2006). Examining affinities of the Taung child by developmental simulation. *Journal of Human Evolution*, 51(3), 274–96. <http://doi.org/10.1016/j.jhevol.2006.04.005>
- McQueen, F. M., McHaffie, A., Clarke, A., Lee, A. C., Reeves, Q., Curteis, B., & Dalbeth, N. (2014). MRI osteitis predicts cartilage damage at the wrist in RA: a three year prospective 3T- MRI study examining cartilage damage. *Arthritis Research & Therapy*, 16(1), R33.

<http://doi.org/10.1186/ar4462>

- Meindl, R. S., & Lovejoy, C. O. (1985). Ectocranial suture closure: a revised method for the determination of skeletal age at death based on the lateral-anterior sutures. *American Journal of Physical Anthropology*, 68(1), 57–66. <http://doi.org/10.1002/ajpa.1330680106>
- Meiri, S., & Dayan, T. (2003). On the validity of Bergmann's rule. *Journal of Biogeography*, 30(3), 331–351. <http://doi.org/10.1046/j.1365-2699.2003.00837.x>
- Meiri, S., Dayan, T., & Simberloff, D. (2004). Body size of insular carnivores: little support for the island rule. *The American Naturalist*, 163(3), 469–479. <http://doi.org/10.1086/382229>
- Meiri, S., Dayan, T., & Simberloff, D. (2006). The generality of the island rule reexamined. *Journal of Biogeography*, 33(9), 1571–1577. <http://doi.org/10.1111/j.1365-2699.2006.01523.x>
- Merbs, C. F. (2002). Asymmetrical spondylolysis. *American Journal of Physical Anthropology*, 119(2), 156–174. <http://doi.org/10.1002/ajpa.10100>
- Meyer, C., Nicklisch, N., Held, P., Fritsch, B., & Alt, K. W. (2011). Tracing patterns of activity in the human skeleton: an overview of methods, problems, and limits of interpretation. *Homo : Internationale Zeitschrift Für Die Vergleichende Forschung Am Menschen*, 62(3), 202–17. <http://doi.org/10.1016/j.jchb.2011.03.003>
- Miles, A. E. W. (1962). Assessment of the Ages of a Population of Anglo-Saxons from Their Dentitions. *Proceedings of the Royal Society of Medicine*, 55(October), 881–886.
- Miles, A. E. W. (2001). The Miles Method of Assessing Age from Tooth Wear Revisited. *Journal of Archaeological Science*, 28, 973–982. <http://doi.org/10.1006/jasc.2000.0652>
- Millien, V., Kathleen Lyons, S., Olson, L., Smith, F. A., Wilson, A. B., & Yom-Tov, Y. (2006). Ecotypic variation in the context of global climate change: Revisiting the rules. *Ecology Letters*, 9(7), 853–869. <http://doi.org/10.1111/j.1461-0248.2006.00928.x>
- Milne, N., Vizcaíno, S. F., & Fernicola, J. C. (2009). A 3D geometric morphometric analysis of digging ability in the extant and fossil cingulate humerus. *Journal of Zoology*, 278(1), 48–56. <http://doi.org/10.1111/j.1469-7998.2008.00548.x>
- Mitteroecker, P., & Gunz, P. (2009). Advances in Geometric Morphometrics. *Evolutionary Biology*, 36(2), 235–247. <http://doi.org/10.1007/s11692-009-9055-x>
- Mitteroecker, P., Gunz, P., Bernhard, M., Schaefer, K., & Bookstein, F. L. (2004). Comparison of cranial ontogenetic trajectories among great apes and humans. *Journal of Human Evolution*, 46(6), 679–698. <http://doi.org/10.1016/j.jhevol.2004.03.006>
- Mitteroecker, P., Gunz, P., & Bookstein, F. L. (2005). Heterochrony and geometric morphometrics: a comparison of cranial growth in *Pan paniscus* versus *Pan troglodytes*. *Evolution & Development*, 7(3), 244–58. <http://doi.org/10.1111/j.1525-142X.2005.05027.x>
- Mitteroecker, P., Gunz, P., Weber, G. W., & Bookstein, F. L. (2004). Regional dissociated heterochrony in multivariate analysis. *Annals of Anatomy*, 186(5–6), 463–470. [http://doi.org/10.1016/S0940-9602\(04\)80085-2](http://doi.org/10.1016/S0940-9602(04)80085-2)

- Mitteroecker, P., Gunz, P., Windhager, S., & Schaefer, K. (2013a). A brief review of shape, form, and allometry in geometric morphometrics, with applications to human facial morphology. *Hystrix*, 24(1), 59–66. <http://doi.org/10.4404/hystrix-24.1-6369>
- Mitteroecker, P., Gunz, P., Windhager, S., & Schaefer, K. (2013b). A brief review of shape, form, and allometry in geometric morphometrics, with applications to human facial morphology. *Hystrix*, 24(1), 59–66. <http://doi.org/10.4404/hystrix-24.1-6369>
- Mitteroecker, P., Gunz, P., Windhager, S., & Schaefer, K. (2013c). A brief review of shape, form, and allometry in geometric morphometrics, with applications to human facial morphology. *Hystrix*, 24(1), 59–66. <http://doi.org/10.4404/hystrix-24.1-6369>
- Mitteroecker, P., & Huttegger, S. (2009). The concept of morphospaces in evolutionary and developmental biology: Mathematics and metaphors. *Biological Theory*, 4(1), 54–67.
- Molnar, P., Ahlstrom, T. P., & Leden, I. (2011). Osteoarthritis and activity-an analysis of the relationship between eburnation, Musculoskeletal Stress Markers (MSM) and age in two Neolithic hunter-gatherer populations from Gotland, Sweden. *International Journal of Osteoarchaeology*, 21(3), 283–291. <http://doi.org/10.1002/oa.1131>
- MorphoJ, version 1.06b. (n.d.). Oracle Corporation.
- Neel, J. V. (1962). Diabetes Mellitus : A “Thrifty” Genotype Rendered Detrimental by “Progress”? *American Journal of Human Genetics*, (1949), 353–362.
- Neubauer, S., & Hublin, J.-J. (2012). The Evolution of Human Brain Development. *Evolutionary Biology*, 39(4), 568–586. <http://doi.org/10.1007/s11692-011-9156-1>
- NextEngine Scan Studio HD: Scan, Align, Fuse, Polish and Export Version 1.3.2. (2010). Shape Tools LLC and NextEngine, Inc.
- Niinimäki, S. (2011). What do muscle marker ruggedness scores actually tell us? *International Journal of Osteoarchaeology*, 21(3), 292–299. <http://doi.org/10.1002/oa.1134>
- Niinimäki, S. (2012). The relationship between musculoskeletal stress markers and biomechanical properties of the humeral diaphysis. *American Journal of Physical Anthropology*, 147(4), 618–628. <http://doi.org/10.1002/ajpa.22023>
- Nolte, M., & Wilczak, C. A. (2012). Three-dimensional Surface Area of the Distal Biceps Enthesis, Relationship to Body Size Sex, Age, and Secular Changes in a 20 th Century American Sample. *International Journal of Osteoarchaeology*, n/a-n/a. <http://doi.org/10.1002/oa.2292>
- Novak, M., & Šlaus, M. (2011). Vertebral pathologies in two early modern period (16th–19th century) populations from Croatia. *American Journal of Physical Anthropology*, 145(July 2010), 270–281. <http://doi.org/10.1002/ajpa.21491>
- Nowak, O., & Piontek, J. (2002). Does the occurrence of Harris lines affect the morphology of human long bones? *Homo : Internationale Zeitschrift Für Die Vergleichende Forschung Am Menschen*, 52(3), 254–76. <http://doi.org/10.1078/0018-442X-00033>
- O’Higgins, P. (2000a). The study of morphological variation in the hominid fossil record: biology,

- landmarks and geometry. *Journal of Anatomy*, 197 (Pt 1, 103–20.
- O'Higgins, P. (2000b). The study of morphological variation in the hominid fossil record: biology, landmarks and geometry. *Journal of Anatomy*, 197 (Pt 1, 103–20.
- O'Higgins, P., Cobb, S. N., Fitton, L. C., Gröning, F., Phillips, R., Liu, J., & Fagan, M. J. (2011). Combining geometric morphometrics and functional simulation: an emerging toolkit for virtual functional analyses. *Journal of Anatomy*, 218(1), 3–15. <http://doi.org/10.1111/j.1469-7580.2010.01301.x>
- O'Higgins, P., Fitton, L. C., Phillips, R., Shi, J., Liu, J., Gröning, F., ... Fagan, M. J. (2012). Virtual Functional Morphology: Novel Approaches to the Study of Craniofacial Form and Function. *Evolutionary Biology*, 39(4), 521–535. <http://doi.org/10.1007/s11692-012-9173-8>
- O'Higgins, P., & Jones, N. (1998). Facial growth in *Cercocebus torquatus*: an application of three-dimensional geometric morphometric techniques to the study of morphological variation. *Journal of Anatomy*, 193, 251–72.
- O'Neill, M. C., & Ruff, C. B. (2004). Estimating human long bone cross-sectional geometric properties: a comparison of noninvasive methods. *Journal of Human Evolution*, 47(4), 221–235. <http://doi.org/10.1016/j.jhevol.2004.07.002>
- Organ, J. M., & Ward, C. V. (2006). Contours of the hominoid lateral tibial condyle with implications for *Australopithecus*. *Journal of Human Evolution*, 51(2), 113–27. <http://doi.org/10.1016/j.jhevol.2006.01.007>
- Ortner, D. J., & Mays, S. A. (1998). Dry-bone Manifestations of Rickets in Infancy and Early Childhood. *International Journal of Osteoarchaeology*, 8, 45–55.
- Ortner, D., & Putschar, W. G. J. (1981). *Identification of pathological conditions in human skeletal remains*. Washinton: Smithsonian Institution Press.
- Osborne, D. L., Simmons, T. L., & Nawrocki, S. P. (2004). Reconsidering the auricular surface as an indicator of age at death. *Journal of Forensic Sciences*, 49(5), 905–911. <http://doi.org/10.1520/JFS2003348>
- Özener, B. (2010). Fluctuating and directional asymmetry in young human males: Effect of heavy working condition and socioeconomic status. *American Journal of Physical Anthropology*, 143(1), 112–120. <http://doi.org/10.1002/ajpa.21300>
- Pálfi, G. (1992). Traces des activités sur les squelettes des anciens Hongrois. *Bulletins et Mémoires de La Société D'anthropologie de Paris*, 4(3), 209–231. <http://doi.org/10.3406/bmsap.1992.2318>
- Pálfi, G. (1997). Maladies dans l'Antiquité et au Moyen-Âge. Paléopathologie comparée des anciens Gallo-Romains et Hongrois. *Bulletins et Mémoires de La Société D'anthropologie de Paris*, 9(1), 1–205. <http://doi.org/10.3406/bmsap.1997.2472>
- Palliser, D. M. (1973). Epidemics in Tudor York. *Northern History*, 8(1), 45–63. <http://doi.org/10.1179/nhi.1973.8.1.45>
- Palliser, D. M. (2014). *Medieval York: 600-1540* (Illustrate). Oxford: OUP Oxford.
- Parr, W. C. H., Wroe, S., Chamoli, U., Richards, H. S., McCurry, M. R., Clausen, P. D., & McHenry, C.

- (2012). Toward integration of geometric morphometrics and computational biomechanics: New methods for 3D virtual reconstruction and quantitative analysis of Finite Element Models. *Journal of Theoretical Biology*, 301, 1–14. <http://doi.org/10.1016/j.jtbi.2012.01.030>
- Patriquin, M. L., Loth, S. R., & Steyn, M. (2003). Sexually dimorphic pelvic morphology in South African whites and blacks. *Homo : Internationale Zeitschrift Fur Die Vergleichende Forschung Am Menschen*, 53(3), 255–262. <http://doi.org/10.1078/0018-442X-00049>
- Patriquin, M. L., Steyn, M., & Loth, S. R. (2005). Metric analysis of sex differences in South African black and white pelvis. *Forensic Science International*, 147(2–3 SPEC.ISS.), 119–127. <http://doi.org/10.1016/j.forsciint.2004.09.074>
- Pearson, A., Groves, C., & Cardini, A. (2015). The “temporal effect” in hominids : Reinvestigating the nature of support for a chimp-human clade in bone morphology. *Journal of Human Evolution*, 88, 146–159. <http://doi.org/10.1016/j.jhevol.2015.06.012>
- Pearson, O. M., & Lieberman, D. E. (2004). The aging of Wolff’s “law”: ontogeny and responses to mechanical loading in cortical bone. *American Journal of Physical Anthropology*, 125(S39), 63–99. <http://doi.org/10.1002/ajpa.20155>
- Peng, B., Wu, W., Hou, S., Shang, W., Wang, X., & Yang, Y. (2003). The pathogenesis of Schmorl’s nodes. *The Journal of Bone and Joint Surgery. British Volume*, 85(6), 879–882. <http://doi.org/10.1302/0301-620X.85B6.13555>
- Perez, S. I., Bernal, V., & Gonzalez, P. N. (2006). Differences between sliding semi-landmark methods in geometric morphometrics, with an application to human craniofacial and dental variation. *Journal of Anatomy*, 208(6), 769–84. <http://doi.org/10.1111/j.1469-7580.2006.00576.x>
- Peterson, J. (1998). The Natufian hunting conundrum: spears, atlatls, or bows? musculoskeletal and armature evidence. *International Journal of Osteoarchaeology*, 8(5), 378–389. [http://doi.org/10.1002/\(SICI\)1099-1212\(1998090\)8:5<378::AID-OA436>3.0.CO;2-I](http://doi.org/10.1002/(SICI)1099-1212(1998090)8:5<378::AID-OA436>3.0.CO;2-I)
- Pinhasi, R., & Mays, S. A. (2007). *Advances in Human Palaeopathology. Advances in Human Palaeopathology*. <http://doi.org/10.1002/9780470724187>
- Plomp, K. A. (2013). *Quantifying Palaeopathology using Geometric Morphometrics*. Durham University.
- Plomp, K. A., Roberts, C. A., & Viðarsdóttir, U. S. (2012a). Vertebral morphology influences the development of Schmorl’s nodes in the lower thoracic vertebrae. *American Journal of ...*, 149(October), 572–582. <http://doi.org/10.1002/ajpa.22168>
- Plomp, K. A., Roberts, C. A., & Viðarsdóttir, U. S. (2012b). Vertebral morphology influences the development of Schmorl’s nodes in the lower thoracic vertebrae. *American Journal of Physical Anthropology*, 149(4), 572–582. <http://doi.org/10.1002/ajpa.22168>
- Plomp, K. A., Roberts, C. A., & Viðarsdóttir, U. S. (2015). Does the correlation between schmorl’s nodes and vertebral morphology extend into the lumbar spine? *American Journal of Physical Anthropology*, 157(3), 526–534. <http://doi.org/10.1002/ajpa.22730>
- Plomp, K. A., Viðarsdóttir, U. S., & Roberts, C. A. (2013). Three Dimensional Shape Analysis and Quantitative Description of Rhinomaxillary Syndrome.

- Plomp, K. A., Viðarsdóttir, U. S., Weston, D. A., Dobney, K., & Collard, M. (2015). The ancestral shape hypothesis: an evolutionary explanation for the occurrence of intervertebral disc herniation in humans. *BMC Evolutionary Biology*, 15(1), 68. <http://doi.org/10.1186/s12862-015-0336-y>
- Pomeroy, E., & Zakrzewski, S. R. (2009). Sexual dimorphism in diaphyseal cross-sectional shape in the medieval Muslim population of Écija, Spain, and Anglo-Saxon Great Chesterford, UK. *International Journal of Osteoarchaeology*, 19(1), 50–65. <http://doi.org/10.1002/oa.981>
- Ponce de León, M. S., & Zollikofer, C. P. (2001). Neanderthal cranial ontogeny and its implications for late hominid diversity. *Nature*, 412(6846), 534–8. <http://doi.org/10.1038/35087573>
- Porcu, E., Venturoli, S., Fabbri, R., Paradisi, R., Longhi, M., Sganga, E., & Flamigni, C. (1994). Skeletal maturation and hormonal levels after the menarche. *Archives of Gynecology and Obstetrics*, 255, 43–46.
- Post, J. B. (1971). Ages at menarche and menopause: Some mediaeval authorities. *Population Studies*, 25(1), 83–87. <http://doi.org/10.1080/00324728.1971.10405785>
- Pretorius, E., Steyn, M., & Scholtz, Y. (2006). Investigation into the usability of geometric morphometric analysis in assessment of sexual dimorphism. *American Journal of Physical Anthropology*, 129(1), 64–70. <http://doi.org/10.1002/ajpa.20251>
- Primeau, C., Friis, L., Sejrsen, B., & Lynnerup, N. (2015). A method for estimating age of medieval sub-adults from infancy to adulthood based on long bone length. *American Journal of Physical Anthropology*, 145(April 2015), n/a-n/a. <http://doi.org/10.1002/ajpa.22860>
- Proctor, D., Broadfield, D., & Proctor, K. (2008). Quantitative three-dimensional shape analysis of the proximal hallucial metatarsal articular surface in Homo, Pan, Gorilla, and Hylobates. *American Journal of ...*, 135(August 2007), 216–224. <http://doi.org/10.1002/ajpa>
- Pujol, A., Rissech, C., Ventura, J., & Turbón, D. (2016). Ontogeny of the male femur: Geometric morphometric analysis applied to a contemporary Spanish population. *American Journal of Physical Anthropology*, 159(1), 146–163. <http://doi.org/10.1002/ajpa.22846>
- Rabey, K. N., Green, D. J., Taylor, A. B., Begun, D. R., Richmond, B. G., & McFarlin, S. C. (2015). Locomotor activity influences muscle architecture and bone growth but not muscle attachment site morphology. *Journal of Human Evolution*, 78, 91–102. <http://doi.org/10.1016/j.jhevol.2014.10.010>
- R Development Core Team. 2008. R: a language and environment for statistical computing. R Foundation for Statistical Computing. (n.d.). Vienna.
- Reginato, A. M., & Olsen, B. R. (2002). The role of structural genes in the pathogenesis of osteoarthritic disorders. *Arthritis Research*, 4(6), 337–345. <http://doi.org/10.1186/ar595>
- Reilly, G. C., & Currey, J. D. (2000). The effects of damage and microcracking on the impact strength of bone. *Journal of Biomechanics*, 33(3), 337–343. [http://doi.org/10.1016/S0021-9290\(99\)00167-0](http://doi.org/10.1016/S0021-9290(99)00167-0)
- Reitsema, L. J., & McIlvaine, B. K. (2014). Reconciling “Stress” and “Health” in Physical Anthropology : What Can Bioarchaeologists Learn From the Other Subdisciplines ?, 185(July), 181–185. <http://doi.org/10.1002/ajpa.22596>

- Relethford, J. H. (2009). Race and global patterns of phenotypic variation. *American Journal of Physical Anthropology*, 139(1), 16–22. <http://doi.org/10.1002/ajpa.20900>
- Relethford, J. H. (2010). Population-specific deviations of global human craniometric variation from a neutral model. *American Journal of Physical Anthropology*, 142(1), 105–111. <http://doi.org/10.1002/ajpa.21207>
- Relethford, J. H., & Harpending, H. C. (1994). Craniometric variation, genetic theory, and modern human origins. *American Journal of Physical Anthropology*, 95(3), 249–270. <http://doi.org/10.1002/ajpa.1330950302>
- Relethford, J. H., & Lees, F. C. (1982). The use of quantitative traits in the study of human population structure. *Yrbk. Phys. Anthropol*, 25, 113–132.
- Rho, J. Y., Zioupos, P., Currey, J. D., & Pharr, G. M. (2002). Microstructural elasticity and regional heterogeneity in human femoral bone of various ages examined by nano-indentation. *Journal of Biomechanics*, 35(2), 189–198. [http://doi.org/10.1016/S0021-9290\(01\)00199-3](http://doi.org/10.1016/S0021-9290(01)00199-3)
- Rhodes, J., & Knüsel, C. J. (2005). Activity-related skeletal change in medieval humeri: Cross-sectional and architectural alterations. *American Journal of Physical ...*, 128, 536–546. <http://doi.org/10.1002/ajpa.20147>
- Ribot, I., & Roberts, C. A. (1996). A Study of Non-specific Stress Indicators and Skeletal Growth in Two Mediaeval Subadult Populations. *Journal of Archaeological Science*, 23(1), 67–79. <http://doi.org/10.1006/jasc.1996.0006>
- Riis, B. J., Hansen, M. A., Jensen, A. M., Overgaard, K., & Christiansen, C. (1996). Low bone mass and fast rate of bone loss at menopause: Equal risk factors for future fracture: A 15-year follow-up study. *Bone*, 19(1), 9–12. [http://doi.org/10.1016/8756-3282\(96\)00102-0](http://doi.org/10.1016/8756-3282(96)00102-0)
- Robb, J. (1998). The interpretation of skeletal muscle sites: a statistical approach. *International Journal of Osteoarchaeology*, 8(June), 363–377.
- Roberts, C. A. (n.d.). *Hereford Skeletal Report*.
- Roberts, C. A. (2007). A bioarcheological study of maxillary sinusitis. *American Journal of Physical Anthropology*, 133(2), 792–807. <http://doi.org/10.1002/ajpa.20601>
- Roberts, C. A., & Manchester, K. (2010). *The Archaeology of Disease* (3rd ed.). Stroud, Gloucestershire: The History Press.
- Robinson, M. S., & Bidmos, M. A. (2009). The skull and humerus in the determination of sex: Reliability of discriminant function equations. *Forensic Science International*, 186(1–3), 1–5. <http://doi.org/10.1016/j.forsciint.2009.01.003>
- Rogers, J., Shepstone, L., & Dieppe, P. (1997). Bone formers: osteophyte and enthesophyte formation are positively associated. *Annals of the Rheumatic Diseases*, 56(November), 85–90. <http://doi.org/10.1136/ard.56.2.85>
- Rogers, J., & Waldron, T. (1989). Infections in palaeopathology: the basis of classification according to most probable cause. *Journal of Archaeological Science*, 16(6), 611–625.

[http://doi.org/10.1016/0305-4403\(89\)90026-5](http://doi.org/10.1016/0305-4403(89)90026-5)

- Rogers, T. L. (2009). Sex determination of adolescent skeletons using the distal humerus. *American Journal of Physical Anthropology*, 140(1), 143–148. <http://doi.org/10.1002/ajpa.21060>
- Rohlf, F. J. (2015). The tps series of software. *Hystrix, the Italian Journal of Mammalogy*, 26(1), 9–12.
- Rohlf, F. J., & Slice, D. E. (1990). Extensions of the Procrustes method for the optimal superimposition of landmarks. *Systematic Zoology*, 39(1), 40–59.
- Rothschild, B. M. (1997). Porosity: A curiosity without diagnostic significance. *American Journal of Physical Anthropology*, 104(4), 529–533. [http://doi.org/10.1002/\(SICI\)1096-8644\(199712\)104:4<529::AID-AJPA7>3.0.CO;2-M](http://doi.org/10.1002/(SICI)1096-8644(199712)104:4<529::AID-AJPA7>3.0.CO;2-M)
- Rozzi, F. V. R., Gonzalez-Jose, R., & Pucciarelli, H. M. (2005). Cranial growth in normal and low-protein-fed Saimiri . An environmental heterochrony. *Journal of Human Evolution*, 49, 505–535. <http://doi.org/10.1016/j.jhevol.2005.06.002>
- Ruff, C. B. (1988). Hindlimb articular surface allometry in hominoidea and Macaca, with comparisons to diaphyseal scaling. *Journal of Human Evolution*, 17(7), 687–714. [http://doi.org/10.1016/0047-2484\(88\)90025-5](http://doi.org/10.1016/0047-2484(88)90025-5)
- Ruff, C. B. (1994). Morphological Adaptation to Climate in Modern and Fossil Hominids. *Yearbook of Physical Anthropology*, 37, 65–107.
- Ruff, C. B. (2000). Body size, body shape, and long bone strength in modern humans. *Journal of Human Evolution*, 38(2), 269–290. <http://doi.org/10.1006/jhevol.1999.0322>
- Ruff, C. B. (2002). Long bone articular and diaphyseal structure in old world monkeys and apes. I: Locomotor effects. *American Journal of Physical Anthropology*, 119(4), 305–342. <http://doi.org/10.1002/ajpa.10117>
- Ruff, C. B. (2003). Ontogenetic adaptation to bipedalism: age changes in femoral to humeral length and strength proportions in humans, with a comparison to baboons. *Journal of Human Evolution*, 45(4), 317–349. <http://doi.org/10.1016/j.jhevol.2003.08.006>
- Ruff, C. B. (2005). Mechanical determinants of bone form: Insights from skeletal remains. *Journal of Musculoskeletal Neuronal Interactions*, 5(3), 202–212.
- Ruff, C. B., Garofalo, E., & Holmes, M. a. (2013). Interpreting skeletal growth in the past from a functional and physiological perspective. *American Journal of Physical Anthropology*, 150(1), 29–37. <http://doi.org/10.1002/ajpa.22120>
- Ruff, C. B., & Hayes, W. C. (1982). Subperiosteal Expansion and Cortical Remodeling of the Human Femur and Tibia with Aging. *Science*, 217(4563), 945–948.
- Ruff, C. B., Holt, B. M., Sládek, V., Berner, M., Murphy, W. a., zur Nedden, D., ... Recheis, W. (2006). Body size, body proportions, and mobility in the Tyrolean “Iceman.” *Journal of Human Evolution*, 51(1), 91–101. <http://doi.org/10.1016/j.jhevol.2006.02.001>
- Ruff, C. B., Holt, B., & Trinkaus, E. (2006). Who’s afraid of the big bad Wolff?: “Wolff’s law” and bone functional adaptation. *American Journal of Physical Anthropology*, 129(4), 484–498.

<http://doi.org/10.1002/ajpa.20371>

- Ruff, C. B., Niskanen, M., Junno, J.-A., & Jamison, P. (2005). Body mass prediction from stature and bi-iliac breadth in two high latitude populations, with application to earlier higher latitude humans. *Journal of Human Evolution*, 48(4), 381–392. <http://doi.org/10.1016/j.jhevol.2004.11.009>
- Ruff, C. B., Walker, A., & Trinkaus, E. (1994). Postcranial robusticity in homo. III: Ontogeny. *American Journal of Physical Anthropology*, 93(1), 35–54. <http://doi.org/10.1002/ajpa.1330930103>
- Sakamoto, R., Jaceldo-Siegl, K., Haddad, E., Oda, K., Fraser, G. E., & Tonstad, S. (2013). Relationship of vitamin D levels to blood pressure in a biethnic population. *Nutrition, Metabolism and Cardiovascular Diseases*, 23(8), 7760–784. <http://doi.org/10.1016/j.numecd.2012.04.014>
- Sakaue, K. (1998). Bilateral Asymmetry of the Humerus in Jomon People and Modern Japanese. *Anthropological Science*, 105(4), 231–246.
- Sakaue, K. (2004). Sexual determination of long bones in recent Japanese. *Anthropological Science*, 112(1), 75–81. <http://doi.org/10.1537/ase.00067>
- Samsel, M., Kacki, S., & Villotte, S. (2014). Palaeopathological diagnosis of spondyloarthropathies: Insights from the biomedical literature. *International Journal of Paleopathology*, 7, 70–75. <http://doi.org/10.1016/j.ijpp.2014.07.002>
- Samworth, R., & Gowland, R. L. (2007). Estimation of adult skeletal age-at-death: Statistical assumptions and applications. *International Journal of Osteoarchaeology*, 17(2), 174–188. <http://doi.org/10.1002/oa.867>
- Schaefer, K., & Bookstein, F. L. (2009). Does geometric morphometrics serve the needs of plasticity research? *Journal of Biosciences*, 34(4), 589–599. <http://doi.org/10.1007/s12038-009-0076-5>
- Schaefer, M., Black, S., & Scheuer, L. (2009a). *Juvenile Osteology. Juvenile Osteology*. <http://doi.org/10.1016/B978-0-12-374635-1.00001-1>
- Schaefer, M., Black, S., & Scheuer, L. (2009b). *Juvenile Osteology: A Laboratory and Field Manual*. Academic Press.
- Schattmann, A., Bertrand, B., Vatteoni, S., & Brickley, M. (2016). Approaches to co-occurrence: Scurvy and rickets in infants and young children of 16–18th century Douai, France. *International Journal of Paleopathology*, 12, 63–75. <http://doi.org/10.1016/j.ijpp.2015.12.002>
- Scheuer, L., & Black, S. (2000). *Developmental juvenile osteology*. London: Academic Press.
- Scheuer, L., & Black, S. (Eds.). (2004). *The Juvenile Skeleton*. London: Elsevier Ltd.
- Scholtz, Y., Steyn, M., & Pretorius, E. (2010). A geometric morphometric study into the sexual dimorphism of the human scapula. *HOMO- Journal of Comparative Human Biology*, 61(4), 253–270. <http://doi.org/10.1016/j.jchb.2010.01.048>
- Schug, G. R., & Goldman, H. M. (2014). Birth Is But Our Death Begun : A Bioarchaeological Assessment of Skeletal Emaciation in Immature Human Skeletons in the Context of Environmental , Social , and Subsistence Transition, 259(February), 243–259. <http://doi.org/10.1002/ajpa.22536>

- Schwartz, a G., Lipner, J. H., Pasteris, J. D., Genin, G. M., & Thomopoulos, S. (2013). Muscle loading is necessary for the formation of a functional tendon enthesis. *Bone*, 55(1), 44–51. <http://doi.org/10.1016/j.bone.2013.03.010>
- Sekiya, M., Roosita, K., & Ohtsuka, R. (2015). Developmental stage-dependent influence of environmental factors on growth of rural Sundanese children in West Java, Indonesia. *American Journal of Physical Anthropology*, 157(1), 94–106. <http://doi.org/10.1002/ajpa.22692>
- Shackelford, L. L., & Trinkaus, E. (2002). Late pleistocene human femoral diaphyseal curvature. *American Journal of Physical Anthropology*, 118(4), 359–70. <http://doi.org/10.1002/ajpa.10093>
- Shanb, A., & Youssef, E. (2014). The impact of adding weight-bearing exercise versus nonweight bearing programs to the medical treatment of elderly patients with osteoporosis. *Journal of Family and Community Medicine*, 21(3), 176. <http://doi.org/10.4103/2230-8229.142972>
- Shaw, C. N., & Stock, J. T. (2009a). Habitual throwing and swimming correspond with upper limb diaphyseal strength and shape in modern human athletes. *American Journal of Physical Anthropology*, 140(1), 160–72. <http://doi.org/10.1002/ajpa.21063>
- Shaw, C. N., & Stock, J. T. (2009b). Intensity, repetitiveness, and directionality of habitual adolescent mobility patterns influence the tibial diaphysis morphology of athletes. *American Journal of Physical Anthropology*, 140(1), 149–59. <http://doi.org/10.1002/ajpa.21064>
- Shaw, C. N., & Stock, J. T. (2011). The influence of body proportions on femoral and tibial midshaft shape in hunter-gatherers. *American Journal of Physical Anthropology*, 144(1), 22–29. <http://doi.org/10.1002/ajpa.21363>
- Shea, B. T. (1983). Paedomorphosis and neoteny in the pygmy chimpanzee. *Science*, 222(4623), 521–522.
- Shea, B. T. (1989). Heterochrony in human evolution: the case for neoteny reconsidered. *American Journal of Physical Anthropology*, 32, 69–101.
- Shin, Y., Huh, Y. H., Kim, K., Kim, S., Park, K. H., Koh, J.-T., ... Ryu, J.-H. (2014). Low-density lipoprotein receptor-related protein 5 governs Wnt-mediated osteoarthritic cartilage destruction. *Arthritis Research & Therapy*, 16(1), R37. <http://doi.org/10.1186/ar4466>
- Short Notices. (1908). *The English Historical Review*, 23(91), 604–624.
- Sicotte, N. L., Kern, K. C., Giesser, B. S., Arshanapalli, a, Schultz, a, Montag, M., ... Bookheimer, S. Y. (2008). Regional hippocampal atrophy in multiple sclerosis. *Brain : A Journal of Neurology*, 131(Pt 4), 1134–41. <http://doi.org/10.1093/brain/awn030>
- Siebelt, M., Groen, H. C., Koelewijn, S. J., de Blois, E., Sandker, M., Waarsing, J. H., ... Weinans, H. (2014). Increased physical activity severely induces osteoarthritic changes in knee joints with papain induced sulphate-glycosaminoglycan depleted cartilage. *Arthritis Research & Therapy*, 16(1), R32. <http://doi.org/10.1186/ar4461>
- Sievänen, H., Heinonen, A., & Kannus, P. (1996). Adaptation of bone to altered loading environment: A biomechanical approach using X-ray absorptiometric data from the patella of a young woman. *Bone*, 19(1), 55–59. [http://doi.org/10.1016/8756-3282\(96\)00111-1](http://doi.org/10.1016/8756-3282(96)00111-1)

- Singleton, M. (2002). Patterns of cranial shape variation in the Papionini (Primates: Cercopithecinae). *Journal of Human Evolution*, 42(5), 547–578. <http://doi.org/10.1006/jhev.2001.0539>
- Šlaus, M. (2000). Biocultural Analysis of Sex Differences in Mortality Profiles and Stress Levels in the Late Medieval Population From Nova Rača , Croatia. *American Journal of Physical Anthropology*, 111(September 1999), 193–209.
- Šlaus, M. (2008). Osteological and dental markers of health in the transition from the Late Antique to the Early Medieval period in Croatia. *American Journal of Physical Anthropology*, 136(4), 455–469. <http://doi.org/10.1002/ajpa.20829>
- Slice, D. E. (2005). Modern morphometrics. In D. E. Slice (Ed.), *Modern morphometrics in physical anthropology* (pp. 1–46). New York: Kluwer Academic/Plenum Publishers.
- Smith-Guzmán, N. E. (2015). The skeletal manifestation of malaria: An epidemiological approach using documented skeletal collections. *American Journal of Physical Anthropology*, 158(February), 624–635. <http://doi.org/10.1002/ajpa.22819>
- Sofaer-Derevenski, J. R. (2000). Sex differences in activity-related osseous change in the spine and the gendered division of labor at Ensay and Wharram Percy, UK. *American Journal of Physical Anthropology*, 111(December 1998), 333–354.
- Soler, A. (2012). *LIFE AND DEATH IN A MEDIEVAL NUBIAN FARMING COMMUNITY : THE EXPERIENCE AT MIS ISLAND*. Michigan State University.
- Solovieva, S., Vehmas, T., Riihima, H., Luoma, K., & Leino-Arjas, P. (2005). Hand use and patterns of joint involvement in osteoarthritis . A comparison of female dentists and teachers. *Rheumatology*, 44, 521–528. <http://doi.org/10.1093/rheumatology/keh534>
- Somerville, A. D., Goldstein, P. S., Baitzel, S. I., Bruwelheide, K. L., Dahlstedt, A. C., Yzardiaga, L., ... Schoeninger, M. J. (2015). Diet and gender in the Tiwanaku colonies: Stable isotope analysis of human bone collagen and apatite from Moquegua, Peru. *American Journal of Physical Anthropology*, 158(3), 408–422. <http://doi.org/10.1002/ajpa.22795>
- Sorensen, M. V., Snodgrass, J. J., Leonard, W. R., McDade, T. W., Tarskaya, L. a., Ivanov, K. I., ... Alekseev, V. P. (2009). Lifestyle incongruity, stress and immune function in indigenous siberians: The health impacts of rapid social and economic change. *American Journal of Physical Anthropology*, 138(1), 62–69. <http://doi.org/10.1002/ajpa.20899>
- Sparacello, V. S., d’Ercole, V., & Coppa, A. (2015). A bioarchaeological approach to the reconstruction of changes in military organization among Iron Age Samnites (Vestini) From Abruzzo, Central Italy. *American Journal of Physical Anthropology*, 156(3), 305–316. <http://doi.org/10.1002/ajpa.22650>
- Sparacello, V. S., & Marchi, D. (2008). Mobility and subsistence economy: A diachronic comparison between two groups settled in the same geographical area (Liguria, Italy). *American Journal of Physical Anthropology*, 136(4), 485–495. <http://doi.org/10.1002/ajpa.20832>
- Sparacello, V. S., & Pearson, O. M. (2010). The importance of accounting for the area of the medullary cavity in cross-sectional geometry: A test based on the femoral midshaft. *American Journal of Physical Anthropology*, 143(4), 612–624. <http://doi.org/10.1002/ajpa.21361>

- Sparacello, V. S., Pearson, O. M., Coppa, A., & Marchi, D. (2011a). Changes in skeletal robusticity in an iron age agropastoral group: The samnites from the Alfedena necropolis (Abruzzo, Central Italy). *American Journal of Physical Anthropology*, 144(1), 119–130. <http://doi.org/10.1002/ajpa.21377>
- Sparacello, V. S., Pearson, O. M., Coppa, A., & Marchi, D. (2011b). Changes in skeletal robusticity in an iron age agropastoral group: the Samnites from the Alfedena necropolis (Abruzzo, Central Italy). *American Journal of Physical Anthropology*, 144(1), 119–30. <http://doi.org/10.1002/ajpa.21377>
- Sparacello, V. S., Roberts, C. A., Canci, A., Moggi-Cecchi, J., & Marchi, D. (2016). Insights on the paleoepidemiology of ancient tuberculosis from the structural analysis of postcranial remains from the Ligurian Neolithic (northwestern Italy). *International Journal of Paleopathology*, 15, 50–64.
- Squyres, N., & DeLeon, V. B. (2015). Clavicular curvature and locomotion in anthropoid primates: A 3D geometric morphometric analysis. *American Journal of Physical Anthropology*, 158(2), 257–268. <http://doi.org/10.1002/ajpa.22785>
- Srivastava, R., Saini, V., Rai, R. K., Pandey, S., Singh, T. B., Tripathi, S. K., & Pandey, A. K. (2013). Sexual dimorphism in ulna: an osteometric study from India. *Journal of Forensic Sciences*, 58(5), 1251–6. <http://doi.org/10.1111/1556-4029.12158>
- Steckel, R. H., Rose, J. C., Larsen, C. S., & Walker, P. L. (2002). Skeletal Health in the Western Hemisphere from 4000 B.C. to the Present. *Evolutionary Anthropology*, 11(4), 142–155. <http://doi.org/10.1002/evan.10030>
- Steele, J. (2000). Skeletal Indicators of Handedness. In M. Cox & S. Mays (Eds.), *Human osteology in archaeology and forensic science* (pp. 307–323). London: Greenwich Medical Media.
- Stevens, S., & Viðarsdóttir, U. S. (2008). the shape of the non- \square pathological bony knee joint with age: a morphometric analysis of the distal femur and proximal tibia in three populations of known age at death. *International Journal of ...*, 18(December 2007), 352–371. <http://doi.org/10.1002/oa>
- Stirland, A. J. (1998). Musculoskeletal evidence for activity: problems of evaluation. *International Journal of Osteoarchaeology*, 8(5), 354–362. [http://doi.org/10.1002/\(SICI\)1099-1212\(1998090\)8:5<354::AID-OA432>3.0.CO;2-3](http://doi.org/10.1002/(SICI)1099-1212(1998090)8:5<354::AID-OA432>3.0.CO;2-3)
- Stock, J. T., & Pfeiffer, S. (2004). Long bone robusticity and subsistence behaviour among Later Stone Age foragers of the forest and fynbos biomes of South Africa. *Journal of Archaeological Science*, 31, 999–1013. <http://doi.org/10.1016/j.jas.2003.12.012>
- Stock, J. T., & Shaw, C. N. (2007). Which Measures of Diaphyseal Robusticity Are Robust ? A Comparison of External Methods of Quantifying the Strength of Long Bone Diaphyses to Cross-Sectional Geometric Properties. *American Journal of Physical Anthropology*, 134(July), 412–423. <http://doi.org/10.1002/ajpa>
- Stock, J. T., Shirley, M. K., Sarringhaus, L. a., Davies, T. G., & Shaw, C. N. (2013). Skeletal evidence for variable patterns of handedness in chimpanzees, human hunter-gatherers, and recent British populations. *Annals of the New York Academy of Sciences*, 1288(1), 86–99. <http://doi.org/10.1111/nyas.12067>
- Stuart-Macadam, P. (1985). Porotic Hyperostosis : Representative of a Childhood Condition. *American Journal of Physical Anthropology*, 66, 391–398.

- Stuart-Macadam, P. (1987a). A Radiographic Study of Porotic Hyperostosis. *American Journal of Physical Anthropology*, 74, 511–520.
- Stuart-Macadam, P. (1987b). Porotic hyperostosis: new evidence to support the anemia theory. *American Journal of Physical Anthropology*, 74(4), 521–526. <http://doi.org/10.1002/ajpa.1330740410>
- Stuart-Macadam, P. (1989). Porotic hyperostosis: relationship between orbital and vault lesions. *American Journal of Physical Anthropology*, 80, 187–193. <http://doi.org/10.1002/ajpa.1330800206>
- Stuart-Macadam, P. (1991). Anaemia in Roman Britain. In H. Bush & M. Zvelebil (Eds.), *Health in past societies* (pp. 101–103). Oxford: Tempus Reparatum.
- Stuart-Macadam, P. (1992). Anemia in Past Human Populations. In P. Stuart-macadam & S. Kent (Eds.), *Diet, Demography, and Disease: Changing Perspectives on Anemia* (pp. 151–170). New York: Aldine de Gruyter, Inc.
- Suchey, J. M., & Katz, D. (1997). Applications of pubic age determination in a forensic setting. In *Forensic Osteology* (pp. 204–236).
- Sullivan, A. (2005). Prevalence and etiology of acquired anemia in Medieval York, England. *American Journal of Physical Anthropology*, 128(2), 252–272. <http://doi.org/10.1002/ajpa.20026>
- Suzuki, H., Hayashi, T., Tanabe, G., & Sakura, H. (1956). *Characteristics of the skulls of the Medieval Kamakura people in Medieval Japanese skeletons from the burial site at Zaimokuza, Kamakura City*. Iwanami Tokyo: Anthropological Society of Nippon.
- Swiderski, D. (2003). Separating size from allometry: analysis of lower jaw morphology in the fox squirrel, *Sciurus niger*. *Journal of Mammalogy*, 84(3), 861–876.
- Sylvester, A. D., & Pfisterer, T. (2012). Quantifying lateral femoral condyle ellipticalness in chimpanzees, gorillas, and humans. *American Journal of Physical Anthropology*, 149(3), 458–67. <http://doi.org/10.1002/ajpa.22144>
- Temple, D. H. (2014). Plasticity and constraint in response to early-life stressors among late/final jomon period foragers from Japan: Evidence for life history trade-offs from incremental microstructures of enamel. *American Journal of Physical Anthropology*, 155(4), 537–545. <http://doi.org/10.1002/ajpa.22606>
- Temple, D. H., & Goodman, A. H. (2014). Bioarcheology has a “health” problem: Conceptualizing “stress” and “health” in bioarcheological research. *American Journal of Physical Anthropology*, 155(2), 186–191. <http://doi.org/10.1002/ajpa.22602>
- Temple, D. H., Kusaka, S., & Sciulli, P. W. (2011). Patterns of social identity in relation to tooth ablation among prehistoric Jomon foragers from the Yoshigo site, Aichi prefecture, Japan. *International Journal of Osteoarchaeology*, 21(3), 323–335. <http://doi.org/10.1002/oa.1146>
- Thomas, M. A. (2016). Are vegans the same as vegetarians? The effect of diet on perceptions of masculinity. *Appetite*, 97, 79–86. <http://doi.org/10.1016/j.appet.2015.11.021>
- Toumi, H., Best, T. M., Mazor, M., Coursier, R., Pinti, A., & Lespessailles, E. (2014). Association between

- individual quadriceps muscle volume/enthesis and patello femoral joint cartilage morphology. *Arthritis Research & Therapy*, 16(1), R1. <http://doi.org/10.1186/ar4426>
- Trinkaus, E., Churchill, S. E., & Ruff, C. B. (1994). Postcranial robusticity in Homo. II: Humeral bilateral asymmetry and bone plasticity. *American Journal of Physical Anthropology*, 93(1), 1–34. <http://doi.org/10.1002/ajpa.1330930102>
- Ubelaker, D. H. (1989). Estimation of age at death from immature human bone. In M. Y. İşcan (Ed.), *Age markers in the human skeleton* (pp. 55–70). Springfield, IL: Charles C Thomas.
- Vainionpää, A., Korpelainen, R., Leppäluoto, J., & Jämsä, T. (2005). Effects of high-impact exercise on bone mineral density: A randomized controlled trial in premenopausal women. *Osteoporosis International*, 16(2), 191–197. <http://doi.org/10.1007/s00198-004-1659-5>
- Van Lenthe, G. H., & Huiskes, R. (2002). How morphology predicts mechanical properties of trabecular structures depends on intra-specimen trabecular thickness variations. *Journal of Biomechanics*, 35(9), 1191–1197. [http://doi.org/10.1016/S0021-9290\(02\)00081-7](http://doi.org/10.1016/S0021-9290(02)00081-7)
- Vance, V. L., & Steyn, M. (2013). Geometric morphometric assessment of sexually dimorphic characteristics of the distal humerus. *HOMO- Journal of Comparative Human Biology*, 64(5), 329–340. <http://doi.org/10.1016/j.jchb.2013.04.003>
- Vedi, S., Croucher, P. I., Garrahan, N. J., & Compston, J. E. (1996). Effects of hormone replacement therapy on cancellous bone microstructure in postmenopausal women. *Bone*, 19(1), 69–72. [http://doi.org/10.1016/8756-3282\(96\)00108-1](http://doi.org/10.1016/8756-3282(96)00108-1)
- Velemínská, J., Bigoni, L., Krajíček, V., Borský, J., Šmahelová, D., Cagáňová, V., & Peterka, M. (2012). Surface facial modelling and allometry in relation to sexual dimorphism. *HOMO- Journal of Comparative Human Biology*, 63(2), 81–93. <http://doi.org/10.1016/j.jchb.2012.02.002>
- Vercellotti, G., Piperata, B. A., Agnew, A. M., Wilson, W. M., Dufour, D. L., Reina, J. C., ... Sciulli, P. W. (2014). Exploring the Multidimensionality of Stature Variation in the Past Through Comparisons of Archaeological and Living Populations. *American Journal of Physical Anthropology*, 155, 229–242. <http://doi.org/10.1002/ajpa.22552>
- Viðarsdóttir, U. S., & Cobb, S. (2004). Inter- and intra-specific variation in the ontogeny of the hominoid facial skeleton: testing assumptions of ontogenetic variability. *Annals of Anatomy*, 186, 423–428.
- Viðarsdóttir, U. S., O'Higgins, P., & Stringer, C. (2002a). A geometric morphometric study of regional differences in the ontogeny of the modern human facial skeleton. *Journal of Anatomy*, 201(3), 211–29.
- Viðarsdóttir, U. S., O'Higgins, P., & Stringer, C. (2002b). A geometric morphometric study of regional differences in the ontogeny of the modern human facial skeleton+. *Journal of Anatomy*, 201(3), 211–29. <http://doi.org/10.1046/j.1469-7580.2002.00092.x>
- Viguet-Carrin, S., Garnero, P., & Delmas, P. D. (2006). The role of collagen in bone strength. *Osteoporosis International*, 17, 319–336. <http://doi.org/10.1007/s00198-005-2035-9>
- Villamor, E., Marin, C., Mora-plazas, M., & Baylin, A. (2011). Vitamin D deficiency and age at menarche : a prospective study 1 – 3. *American Journal of Clinical Nutrition*, (C), 1–6.

<http://doi.org/10.3945/ajcn.111.018168.1>

- Viscosi, V., & Cardini, A. (2011). Leaf morphology, taxonomy and geometric morphometrics: a simplified protocol for beginners. *PLoS One*, 6(10), e25630. <http://doi.org/10.1371/journal.pone.0025630>
- von Cramon-Taubadel, N., Frazier, B. C., & Lahr, M. M. (2007). The problem of assessing landmark error in geometric morphometrics: Theory, methods, and modifications. *American Journal of Physical Anthropology*, 134(1), 24–35. <http://doi.org/10.1002/ajpa.20616>
- Von Cramon-Taubadel, N., Frazier, B. C., & Lahr, M. M. (2007). The problem of assessing landmark error in geometric morphometrics: Theory, methods, and modifications. *American Journal of Physical Anthropology*, 134(1), 24–35. <http://doi.org/10.1002/ajpa.20616>
- von Cramon-Taubadel, N., & Lycett, S. J. (2014). A comparison of catarrhine genetic distances with pelvic and cranial morphology: Implications for determining hominin phylogeny. *Journal of Human Evolution*, 77, 179–186. <http://doi.org/10.1016/j.jhevol.2014.06.009>
- Waldron, T. (2009). *Palaeopathology*. Cambridge: Cambridge University Press. <http://doi.org/10.1017/CBO9781107415324.004>
- Waldron, T., & Rogers, J. (1991). Inter-observer variation in coding osteoarthritis in human skeletal remains. *International Journal of Osteoarchaeology*, 1, 49–56.
- Walker, D. (1964). I Charters of the Earldom of Hereford, 1095–1201. *Camden Fourth Series*, 1, 1–75. <http://doi.org/10.1017/S0068690500002701>
- Walker, J. A. (2000). Ability of geometric morphometric methods to estimate a known covariance matrix. *Systematic Biology*, 49(4), 686–96.
- Walker, P. L. (1986). Porotic hyperostosis in a marine-dependent California Indian population. *American Journal of Physical Anthropology*, 69, 345–354. <http://doi.org/10.1002/ajpa.1330690307>
- Walker, P. L. (2005). Greater sciatic notch morphology: Sex, age, and population differences. *American Journal of Physical Anthropology*, 127(4), 385–391. <http://doi.org/10.1002/ajpa.10422>
- Walker, P. L. (2008). Sexing skulls using discriminant function analysis of visually assessed traits. *American Journal of Physical Anthropology*, 136(1), 39–50. <http://doi.org/10.1002/ajpa.20776>
- Walker, P. L., Bathurst, R. R., Richman, R., Gjerdrum, T., & Andrushko, V. A. (2009). The causes of porotic hyperostosis and cribra orbitalia: A reappraisal of the iron-deficiency-anemia hypothesis. *American Journal of Physical Anthropology*, 139(2), 109–125. <http://doi.org/10.1002/ajpa.21031>
- Wallace, I. J., Tommasini, S. M., Judex, S., Garland, T., & Demes, B. (2012). Genetic variations and physical activity as determinants of limb bone morphology: An experimental approach using a mouse model. *American Journal of Physical Anthropology*, 148(1), 24–35. <http://doi.org/10.1002/ajpa.22028>
- Wapler, U., Crubézy, E., & Schultz, M. (2004). Is Cribra Orbitalia Synonymous with Anemia? Analysis and Interpretation of Cranial Pathology in Sudan. *American Journal of Physical Anthropology*, 123(4), 333–339. <http://doi.org/10.1002/ajpa.10321>
- Watts, R. (2015). The long-term impact of developmental stress. Evidence from later medieval and post-

- medieval London (AD1117-1853). *American Journal of Physical Anthropology*, 158, 569–580. <http://doi.org/10.1002/ajpa.22810>
- Weber, G., Schäfer, K., Prossinger, H., Gunz, P., Mitteroecker, P., & Seidler, H. (2001). Virtual Anthropology: The Digital Evolution in Anthropological Sciences. *Journal of Physiological Anthropology and Applied Human Science*, 20(2), 69–80.
- Wei, J., & Ducy, P. (2010). Co-dependence of bone and energy metabolisms. *Archives of Biochemistry and Biophysics*, 503(1), 35–40. <http://doi.org/10.1016/j.abb.2010.05.021>
- Weiss, E. (2003). Understanding muscle markers: aggregation and construct validity. *American Journal of Physical Anthropology*, 121(3), 230–40. <http://doi.org/10.1002/ajpa.10226>
- Weiss, E. (2005). Humeral cross-sectional morphology from 18th century Quebec prisoners of war: Limits to activity reconstruction. *American Journal of Physical Anthropology*, 126(July 2004), 311–317. <http://doi.org/10.1002/ajpa.20069>
- Weiss, E., Corona, L., & Schultz, B. (2012). Sex differences in musculoskeletal stress markers: Problems with activity pattern reconstructions. *International Journal of Osteoarchaeology*, 22(1), 70–80. <http://doi.org/10.1002/oa.1183>
- Weiss, E., & Jurmain, R. D. (2007). Osteoarthritis revisited: a contemporary review of aetiology. *International Journal of Osteoarchaeology*, 17(5), 437–450. <http://doi.org/10.1002/oa>
- Welsby, D. A. (2002). *The Medieval Kingdoms of Nuba: Pagans, Christians and Muslims along the Middle Nile*. London: The British Museum Press.
- Wentz, R., & Grummond, N. De. (2009). Life on horseback: palaeopathology of two Scythian skeletons from Alexandropol, Ukraine. *International Journal of Osteoarchaeology*, 115(April 2008), 107–115. <http://doi.org/10.1002/oa>
- White, T. D., & Folkens, P. A. (2000). *Human Osteology* (2nd ed.). San Diego: Academic Press.
- White, T. D., & Folkens, P. A. (2005). *The Human Bone Manual* (Vol. 50). San Diego: Elsevier Academic Press. <http://doi.org/10.1016/B978-0-12-088467-4.50022-3>
- WHO scientific group on the assessment of osteoporosis at primary health care level. (2004). *Summary meeting report*.
- Whyte, M. P., & Thakker, R. V. (2013). Rickets and osteomalacia. *Medicine (United Kingdom)*, 41(10), 594–599. <http://doi.org/10.1016/j.mpmed.2013.07.012>
- Wilczak, C. A. (1998). Consideration of sexual dimorphism, age, and asymmetry in quantitative measurements of muscle insertion sites. *International Journal of Osteoarchaeology*, 8(June), 311–325.
- Willett, N. J., Thote, T., Lin, A. S., Moran, S., Raji, Y., Sridaran, S., ... Guldberg, R. E. (2014). Intra-articular injection of micronized dehydrated human amnion/chorion membrane attenuates osteoarthritis development. *Arthritis Research & Therapy*, 16(1), R47. <http://doi.org/10.1186/ar4476>
- Wilson, L. A. B., & Humphrey, L. T. (2015). A Virtual geometric morphometric approach to the quantification of long bone bilateral asymmetry and cross-sectional shape. *American Journal of*

- Physical Anthropology*, 556(July), 541–556. <http://doi.org/10.1002/ajpa.22809>
- Wilson, W. (2005). *An Explanation for the Onset of Mechanically Induced Cartilage Damage*. Eindhoven, Eindhoven, Netherlands: Universiteitsdrukkerij TU.
- Winet, H. (1996). The role of microvasculature in normal and perturbed bone healing as revealed by intravital microscopy. *Bone*, 19(1), 39S–57S.
- Wolff, J. (1986). *The Law of Bone Remodelling*. Berlin, Heidelberg: Springer Berlin Heidelberg. <http://doi.org/10.1007/978-3-642-71031-5>
- Wood, J. W., Milner, G. R., Harpending, H. C., Weiss, K. M., Cohen, N., Eisenberg, L. E., ... Wilkinson, R. G. (1992). The Osteological Paradox: Problems of Inferring Prehistoric Health from Skeletal Samples. *Current Anthropology*, 33(4), 343–370. <http://doi.org/papers2://publication/uuid/3AD1960D-AE51-4550-BE94-EBED5FB00559>
- World Health Organization UNICEF. (2003). *Global strategy for infant and young child feeding*. World Health Organization.
- Wright, L., & Adams, C. J. (2015). *Vegan Studies Project*. University of Georgia Press.
- Yamanaka, A., Gunji, H., & Ishida, H. (2005). Curvature, length, and cross-sectional geometry of the femur and humerus in anthropoid primates. *American Journal of Physical Anthropology*, 127(1), 46–57. <http://doi.org/10.1002/ajpa.10439>
- Young, N. M. (2008). A comparison of the ontogeny of shape variation in the anthropoid scapula: Functional and phylogenetic signal. *American Journal of Physical Anthropology*, 136(3), 247–264. <http://doi.org/10.1002/ajpa.20799>
- Zaki, M. E., Hussien, F. H., & Abd El-shafy El Banna, R. (2009). Osteoporosis Among Ancient Egyptians. *International Journal of Osteoarchaeology*, 19, 78–89. <http://doi.org/10.1002/oa>
- Zelditch, M. L., Swiderski, D. L., Sheets, H. D., & Fink, W. L. (2004). *Geometric morphometrics for biologists: a primer*. Elsevier Academic Press.
- Zeng, Q. Q., Jee, W. S. S., Bigornia, A. E., King, J. G., D'Souza, S. M., Li, X. J., ... Wechter, W. J. (1996). Time responses of cancellous and cortical bones to sciatic neurectomy in growing female rats. *Bone*, 19(1), 13–21. [http://doi.org/10.1016/8756-3282\(96\)00112-3](http://doi.org/10.1016/8756-3282(96)00112-3)
- Zhang, K. Y., Kedgley, A. E., Donoghue, C. R., Rueckert, D., & Bull, A. M. (2014). The relationship between lateral meniscus shape and joint contact parameters in the knee: a study using data from the Osteoarthritis Initiative. *Arthritis Research & Therapy*, 16(1), R27. <http://doi.org/10.1186/ar4455>
- Zioupou, P., & Currey, J. D. (1998). Changes in the Stiffness, Strength, and Toughness of Human Cortical Bone With Age. *Bone*, 22(1), 57–66.
- Zioupou, P., Hansen, U., & Currey, J. D. (2008). Microcracking damage and the fracture process in relation to strain rate in human cortical bone tensile failure. *Journal of Biomechanics*, 41(14), 2932–2939. <http://doi.org/10.1016/j.jbiomech.2008.07.025>
- Zioupou, P., Wang, X. T., & Currey, J. D. (1996). Experimental and theoretical quantification of the development of damage in fatigue tests of bone and antler. *Journal of Biomechanics*, 29(8), 989–

1002. [http://doi.org/10.1016/0021-9290\(96\)00001-2](http://doi.org/10.1016/0021-9290(96)00001-2)

Zollikofer, C. P., & Ponce de León, M. S. (2004). Kinematics of Cranial Ontogeny: Heterotopy, Heterochrony, and Geometric Morphometric Analysis of Growth Models. *Journal of Experimental Zoology. Part B, Molecular and Developmental Evolution*, 302B, 322–340. <http://doi.org/10.1002/jez.b.21006>

Zumwalt, A. (2005). A new method for quantifying the complexity of muscle attachment sites. *Anatomical Record. Part B, New Anatomist*, 286(1), 21–8. <http://doi.org/10.1002/ar.b.20075>

Zumwalt, A. (2006). The effect of endurance exercise on the morphology of muscle attachment sites. *The Journal of Experimental Biology*, 209(3), 444–54. <http://doi.org/10.1242/jeb.02028>